NASA CR-112145

FINAL REPORT

INTEGRATED DYNAMIC ANALYSIS SIMULATION OF SPACE STATIONS WITH CONTROLLABLE SOLAR ARRAYS (SUPPLEMENTAL DATA AND ANALYSES)

By

Joseph A. Heinrichs
Fairchild Industries, Inc.

Joseph J. Fee
Wolf Research and Development Corp.

Prepared Under Contract No. NAS1-10155

By

FAIRCHILD

Fairchild Industries
Germantown, Maryland 20767

For

NATIONAL AERONAUTICS AND SPACE ADMINISTRATION

September 1972

NASA CR-112145

FINAL REPORT

INTEGRATED DYNAMIC ANALYSIS SIMULATION OF SPACE STATIONS WITH CONTROLLABLE SOLAR ARRAYS (SUPPLEMENTAL DATA AND ANALYSES)

By

Joseph A. Heinrichs
Fairchild Industries, Inc.

Joseph J. Fee
Wolf Research and Development Corp.

Prepared Under Contract No. NAS1-10155

By

FAIRCHILD

Fairchild Industries
Germantown, Maryland 20767

For

NATIONAL AERONAUTICS AND SPACE ADMINISTRATION

September 1972

TABLE OF CONTENTS

(TABLE OF CONTENTS - CONTINUED)

1.0 INTRODUCTION

This volume of the final report presents space station and solar array data and the analyses which were performed in support of the integrated dynamic analysis study. It is intended to supplement the information included in NASA CR-112118.

The presented analysis methods and the formulated digital simulation were developed by the combined efforts of Fairchild Industries and its associate, Wolf Research and Development Corporation.

Section 2 of this volume presents the space station and solar array configurations which were considered during the course of this study. These are resulting configurations from studies performed by various aerospace companies. Control systems for space station altitude control and solar array orientation control (Report Section 3) include generic type control systems. These systems have been digitally coded and included in the simulation.

Report Section 4 presents the detailed analytical formulations which were derived and digitally simulated to provide an automated method of dynamic analysis. These formulations and corresponding simulations were derived for two study phases. The first study phase considered only the rigid body dynamics of the space station; while the second study phase included the flexible body dynamics of space station as well as the rigid and flexible dynamics of spinning space stations. Required input to the simulation includes the vibration mode data associated with the controllable and non-controllable appendages, and the space station. Therefore, extensive structural analyses were performed on the structures in support of the study work and analyses results are presented in Report Section 5. Appendix A presents detailed information and structural analyses data associated with the models utilized.

Verification analyses performed with the simulation are presented in Report Section 6. These analyses used simple structural configurations for the subsequent comparison with the simulation. Numerous documents were written during the course of this study which present interim study results and user information for the simulations.

2. SPACE STATION/SOLAR ARRAY STRUCTURAL CONFIGURATIONS

The formulation of an interaction analysis method for the determination of solar array structural requirement required structural concept definitions for purposes of providing analytical baselines. By direction from NASA/LRC, two solar array configurations were specified as analytical baselines for this study. One configuration consisted of the flexible rollup array studied by the Lockheed Missile and Space Company (Reference 2.1) and is sized to meet a 100 kilowatt power requirement. An initial version of the fully extended array and space station configurations is shown in Figure 2-1. The other solar array configuration which was used in this study was the foldout panel concept shown in Figure 2-2. The structural configuration of this array is based upon a Boeing Aircraft Corporation design which was proposed for a Mars mission vehicle. This design was updated to meet the 100 kw power requirement and to meet the geometrical constraints of the space station's shroud for the launch phase of powered flight. These two array configurations were utilized to derive structural vibration mode data which are required in the implementation of the dynamic interactions analysis.

A space station configuration concept utilized was that presented by the North American Rockwell Corporation (NAR) in Reference 2.2. The configuration is comprised of one or more modules which can be assembled in space in "cruciform" and "bar bell" arrangements. Typical arrangements are depicted in Figure 2-3. The specific arrangement of modules analyzed for vibration mode properties, is that given in Figure 2-4. It is comprised of a power boom, a core module, and eight attached modules arranged in a cruciform configuration. An artificial "G" space station configuration was also chosen and analyzed and is shown in Figure 2-5.

An updated version of the rollup solar array configuration was also analyzed. This design was configured by Lockheed under Contract NAS9-11039. A review of their study is given in Reference 2.3 and a sketch of the array is shown in

Figure 2-6. It is comprised of a series of 10 flexible solar cell substrates deployed with a center boom and tensioned between an inner and outer boom. During a proposed artificial "G" mode of operation, the roll up array configuration is changed to that shown in Figure 2-7. All array configurations were analyzed for cantilever vibration mode properties.

REFERENCES

Reference 2.1 - "Space Station Solar Array Technology Program Mid-Term Review", Lockheed Missile and Space Company, May 1971.

Reference 2.2 - "Modular Space Station - Phase B Extension, First Quarterly Review", North American Rockwell, Space Division, PDS-71-2, May 1971.

Reference 2.3 - "Space Array Technology Evaluation Program, Second Topical Report", Lockheed Missile and Space Company (LMSC-A981486), November 1971.

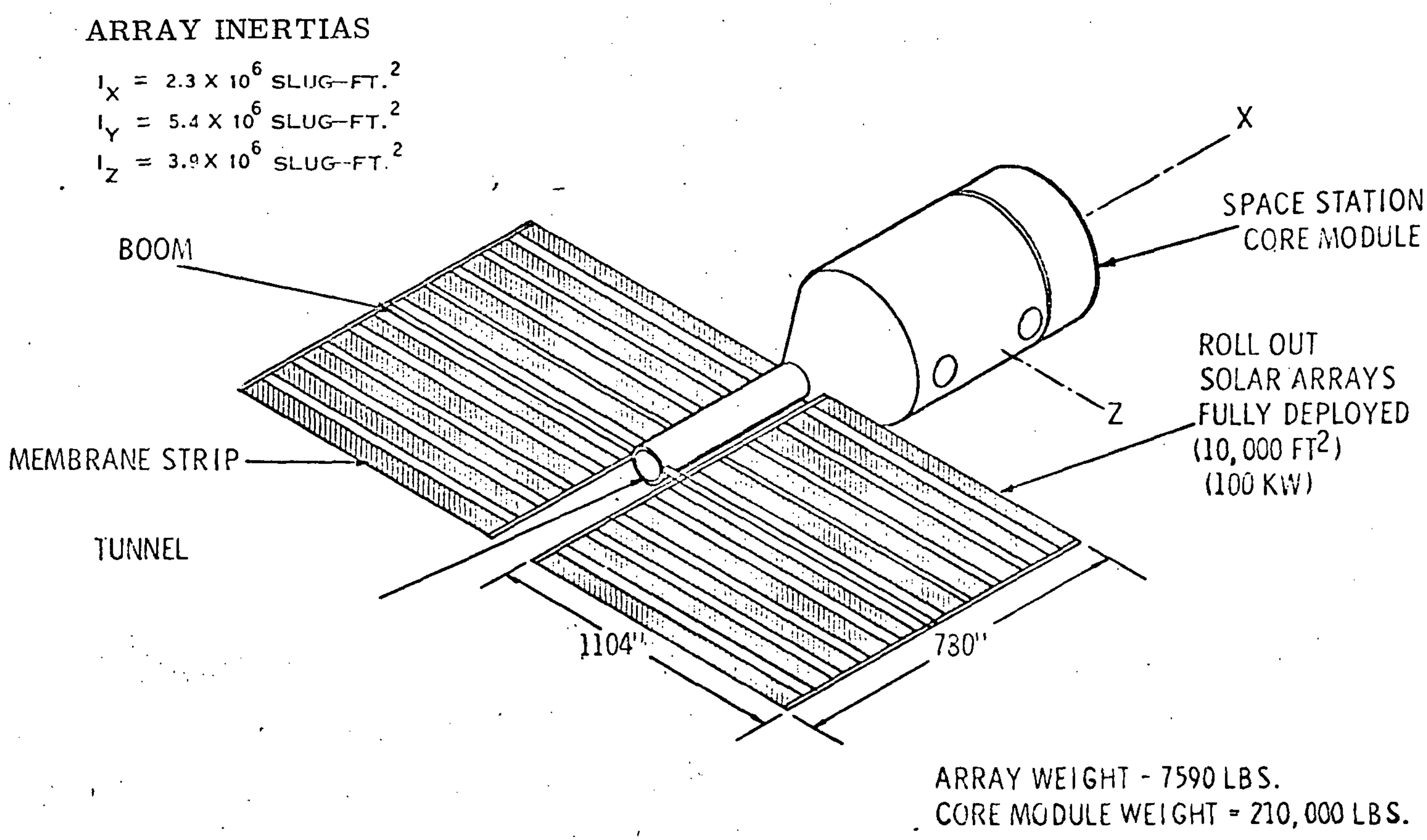

Figure 2-1. Space Station/Rollup Flexible Array

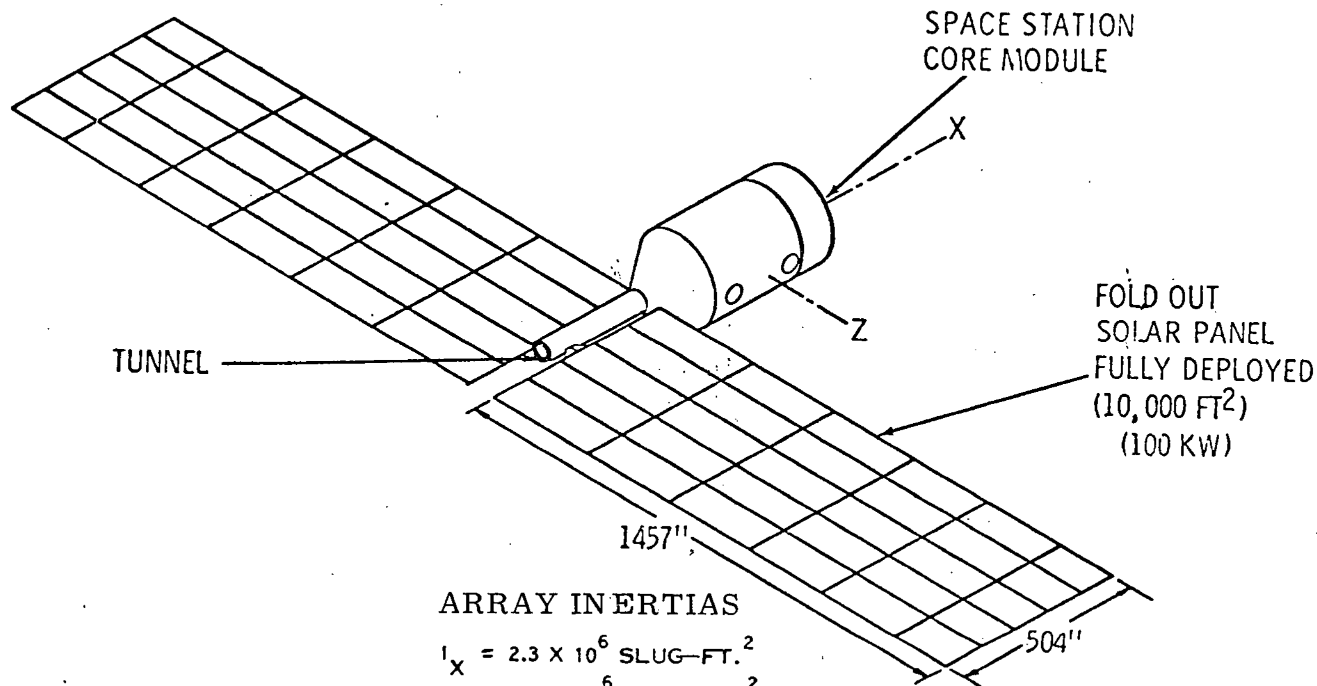

ARRAY INERTIAS

$I_X = 2.3 \times 10^6$ SLUG–FT.^{2}

$I_Y = 5.4 \times 10^6$ SLUG–FT.^{2}

$I_Z = 3.9 \times 10^6$ SLUG–FT.^{2}

ARRAY WEIGHT - 6090 LBS.
CORE MODULE WEIGHT = 210,000 LBS.

Figure 2-2. Space Station/Foldout Panel Array

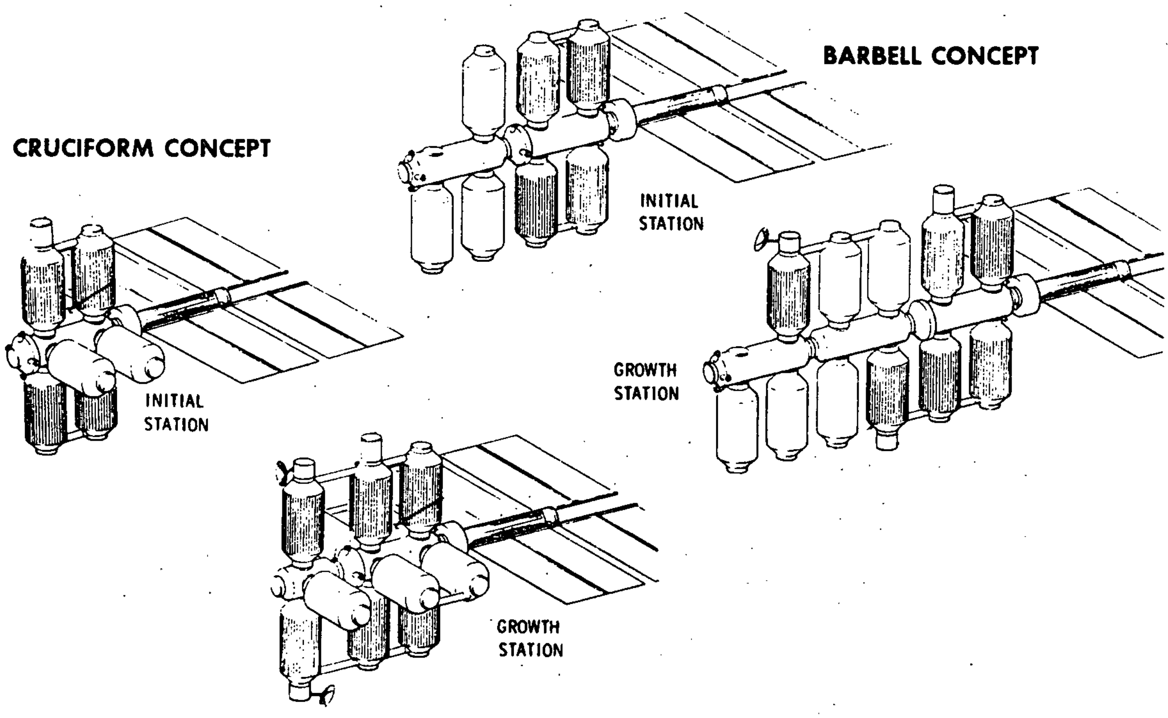

Figure 2-3. Space Station - Modular Concept

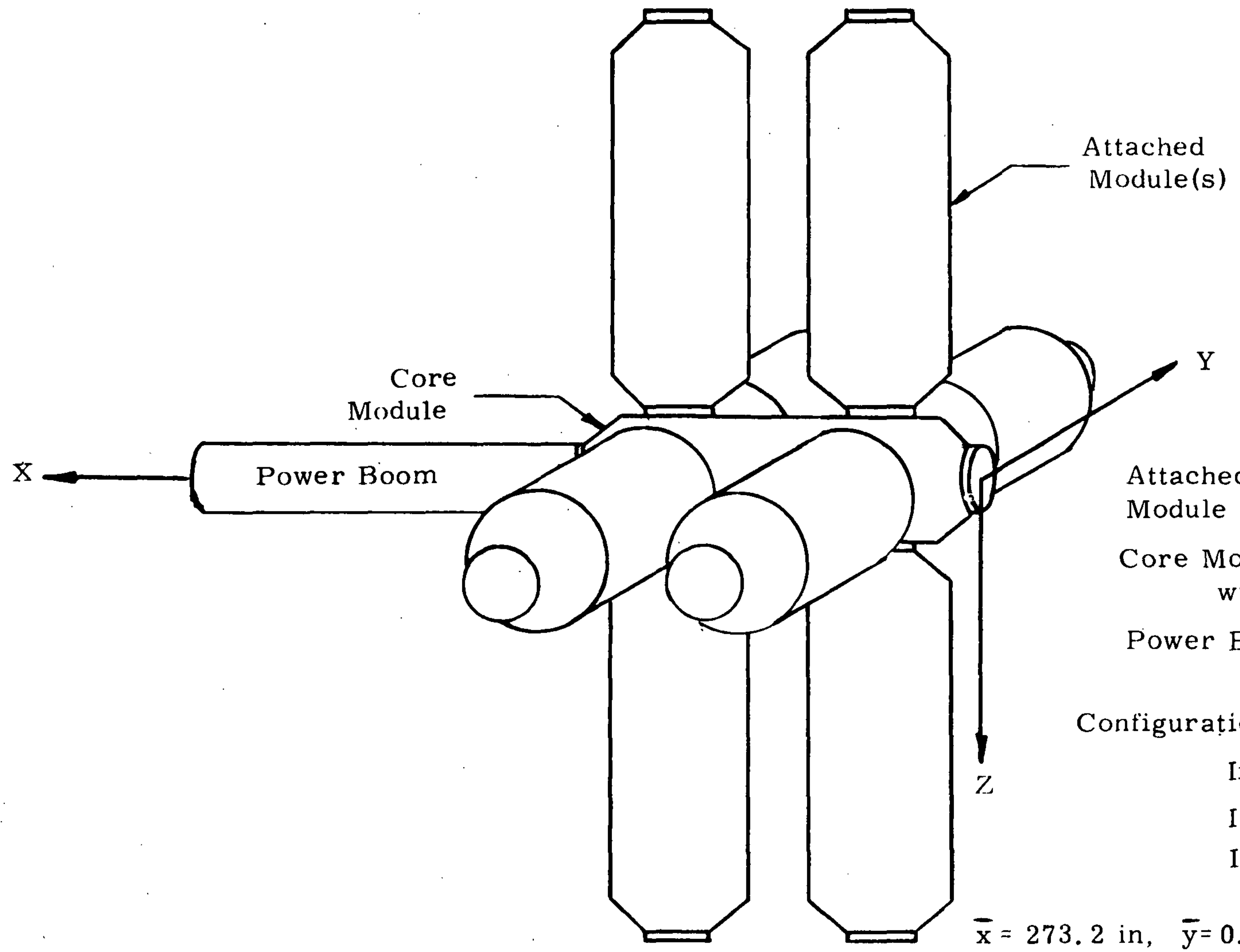

Attached Module wt. = 25,000 lb/ Module

Core Module wt. = 25,000 lb.

Power Boom wt. = 17,500 lb.

Configuration Wt. = 242,500 lb.

$I_x = 6.0 \times 10^7$ lb.-in-sec^2

$I_y = 10.0 \times 10^7$ lb-in-sec^2

$I_z = 10.0 \times 10^7$ lb-in-sec^2

$\bar{x} = 273.2$ in, $\bar{y} = 0.$ in., $\bar{z} = .0$ in.

Figure 2-4 Zero "G" Space Station Configuration

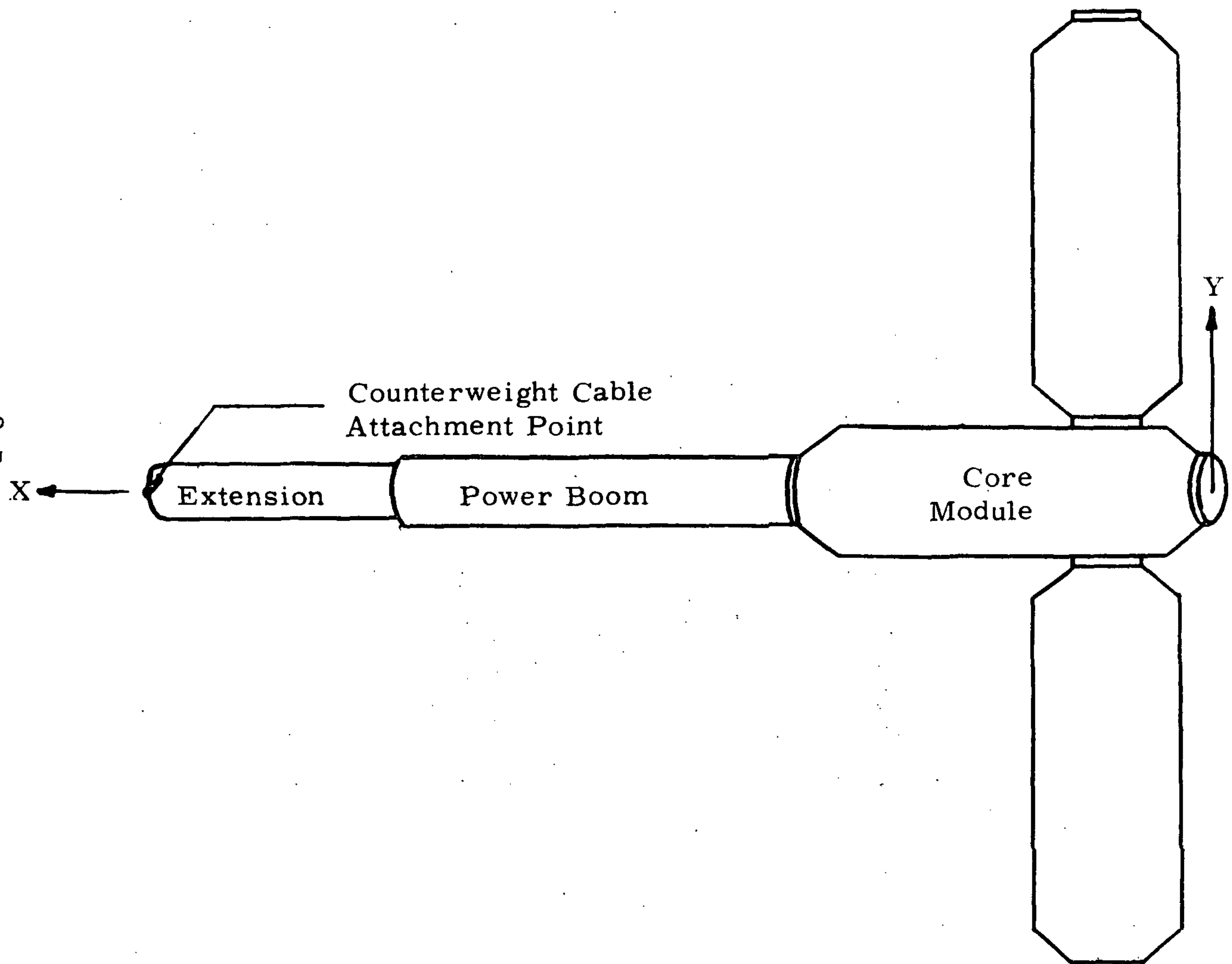

Configuration Wt. = 92, 500 lb.

I_x = 1. 56 x 10^7 lb-in-sec^2

I_y = 3. 0 x 10^7 lb-in-sec^2

I_z = 4. 5 x 10^7 lb-in-sec^2

$\bar{x}$ - 249. 5 in. , $\bar{y}$ = 0. in. , $\bar{z}$ = 0. in.

Figure 2-5 Artificial "G" Space Station Configuration

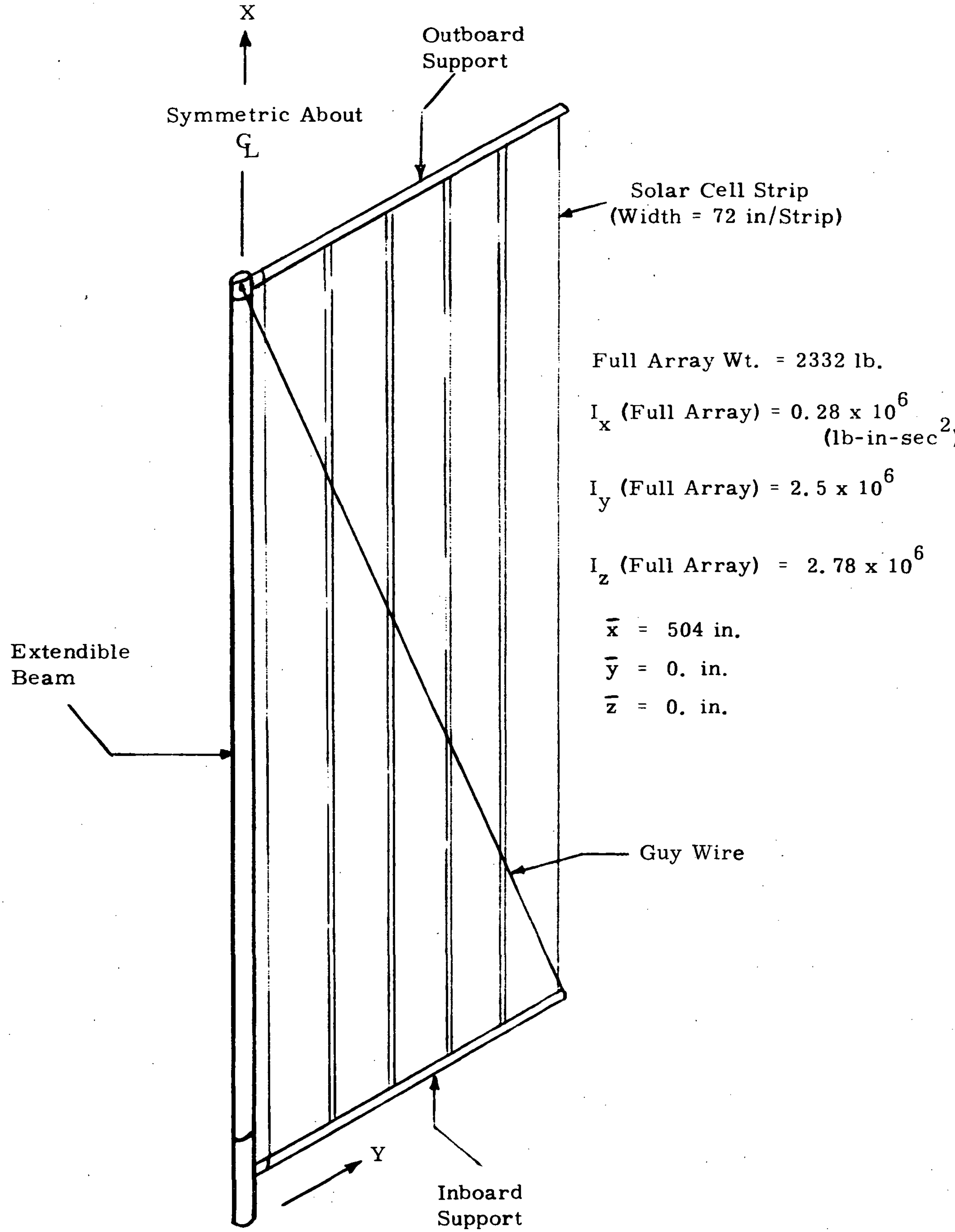

Figure 2-6 Zero "G" Roll-Up Solar Array Configuration

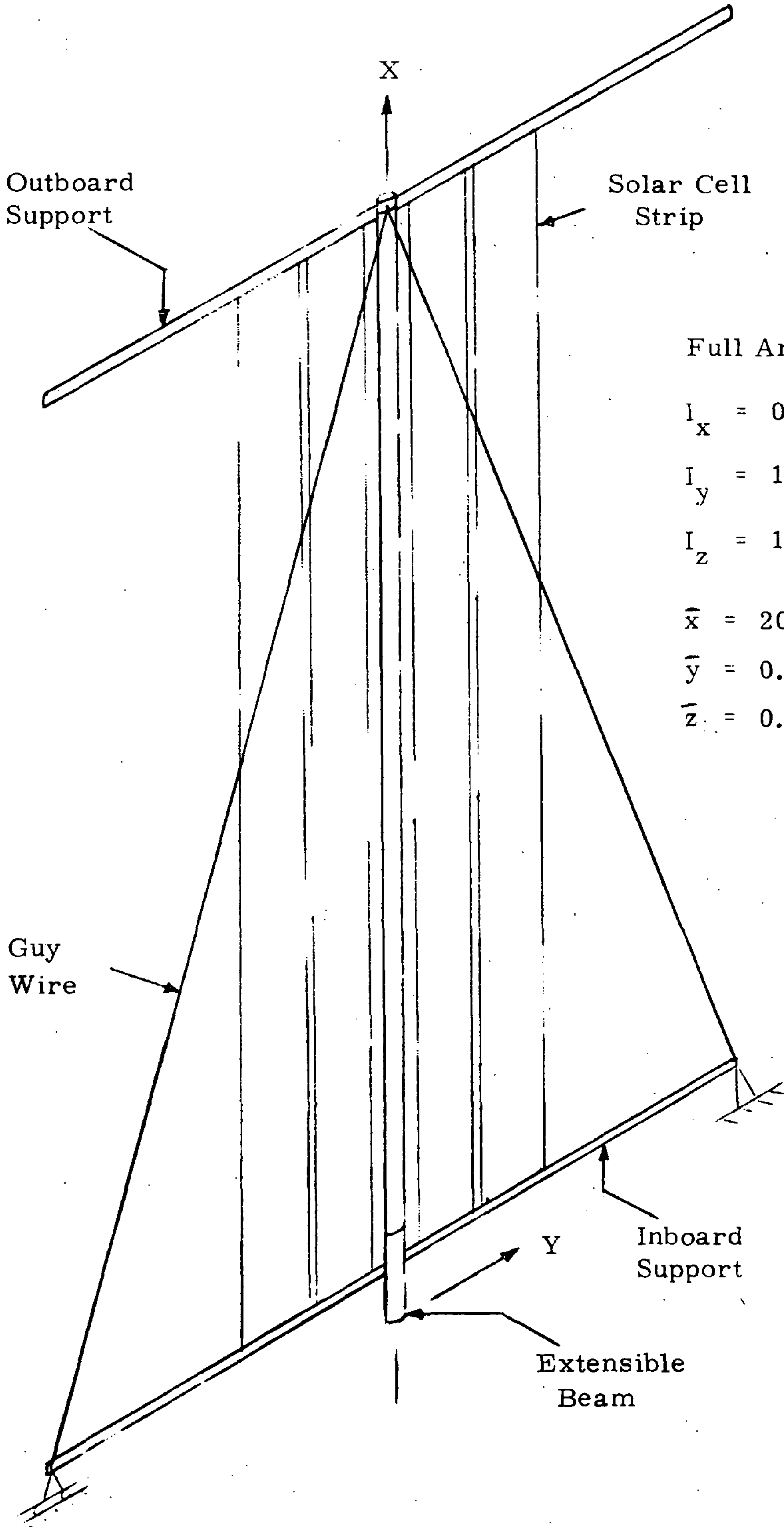

Full Array Wt. = 2044 lbs.

I_x = 0.16×10^6 lb-in-sec^2

I_y = 1.34×10^6 lb-in-sec^2

I_z = 1.5×10^6 lb-in-sec^2

$\bar{x}$ = 205. in.

$\bar{y}$ = 0. in.

$\bar{z}$ = 0. in.

Figure 2-7 Artificial "G" Rollup Solar Array Configuration

3. GUIDANCE AND CONTROL SYSTEM CONSIDERATIONS

3.1 SPACE STATION ATTITUDE CONTROL SYSTEM

The guidance and control system for the North American space station incorporates two generic types of control laws/torquers for attitude control. A control moment gyro (CMG) control system is used for precision attitude stabilization without the need for propellant expenditure. A reaction jet control system (RCS) is used for reference attitude acquisition maneuvers and for momentum desaturation, as required, for the CMG system.

The attitude control requirements as given in Reference 3.1 during zero G operations are as follows:

- Stabilization of the Station, prior to manning, to an accuracy of ±5 degrees
- Stabilization during initial docking to an accuracy of ±1 degree
- Stabilization during routine experiment operations to a ±0.25 degree attitude tolerance, and with angular rate excursions below 0.05 degree per second.

3.1.1 CMG CONTROL SYSTEM

The CMG control system has been designed by the General Electric Company for North American.

A simulation model has been developed and is based upon a number of reports provided by G. E. A block diagram of this simulation model as given in Reference 3.2 is presented in Figure 3-1. The detailed equations for the control law are in accordance with the system selected by GE, which can be characterized as follows. It consists of three two-degree-of-freedom control moment gyros with parallel outer gimbals and with their momentum vectors initially equally spaced in the orbit plane. This configuration permits simpler steering laws and a planar, rather than three dimensional, anti-hangup law.

Reference 3.1 indicates that this control system has a natural frequency of 1.414 Hz and a damping ratio of 0.707. It was found that during the performance of various digital simulations, that a relatively small numerical integration interval ($\Delta t = .005$ second) was required to stabilize solutions to motion equations when the CMG was chosen as the active control system. This was due to high frequencies of inner control loops. Since small integration time steps were required for stability of solution with the CMG of Reference 3.2, a simpler system for the control structural motions was also derived to represent CMG controlling torques. This system which was suggested by NAR, produces a more efficient computer simulation time to real time ratio when the CMG is chosen as the active control. It is programmed in the simulation as represented by the diagram shown in Figure 3-2. It is comprised of a lead-lag compensator, a constant multiplying the moment of inertia properties of the spacecraft under investigation and an output torque limiter. The time constants of the lead-lag compensator, the constant multiplying spacecraft inertia and the limiting torque are allowed as input quantities to the control subroutine in the simulation. This simplified representation thus allows a certain degree of flexibility when analyzing general space station configurations. The commanded position angle is obtained from parameters calculated within the computer program (Reference 3.3). The actual angle is calculated within the program logic and is comprised of rigid plus flexible spacecraft body structural motions. Since space station structural flexibility is considered in the feedback control loop, the position of angle sensors and angular rate within the structural system is allowed to be specified. In like manner, the position of the control torque is specified so that generalized modal torques produced by the control system can be considered as input to modal degrees of freedom.

A simple wobble damper control representation is included in the simulation for control of spinning structural configurations. It consists of a single degree-of-freedom control moment gyro with its gimbal axis along the nominal spin axis and its momentum vector normal to that axis. With reference to Figure 3-3, the spinning structural system is considered to be about the X axis. The control moment gyro is torqued so that its momentum vector $\bar{h}$ always lags the wobble rate, ω_T, by 90^o. A correction torque is applied to the space station which is equal to the following.

$$T_C = -(\omega_S + \dot{\alpha}) \times \bar{h}$$

An increase in the nominal spin rate also occurs to the correction wobble torque and is given as

$$\bar{T}_S = - \bar{\omega}_T \times \bar{h}$$

The magnitudes of parameters associated with the wobble damper control system are an option when performing the simulation of a spinning space station.

3.1.2 REACTION JET CONTROL SYSTEM (RCS)

The reaction jet control system (RCS) is used for reference attitude acquisition maneuvers, momentum unloading of the control moment gyro, and as an alternate to the CMG for controlling the attitude of the space station. A RCS is composed of four thruster modules and each module has four thrusters. The modules are located at the periphery of a space station, as shown in Figure 3-4. All sixteen thrusters compose a fully redundant three axes attitude control system.

A jet thrust level is indicated in Reference 3.1 to be 10 pounds in order to provide the same torque magnitude with the RCS as with the CMG control system. Reference 3.1 further states that this small jet size requires significant pulse durations for most maneuvers and thus should minimize the need for a minimum impulse provision which was a major problem area for Apollo. Expected orbit makeup (correction) firing times are indicated to range from 7 to 14 seconds. Reference 3.1 indicates that the preprocessing electronics for the RCS sums the outer loop attitude and rate signals with any attitude maneuver command signals. It also includes the phase-plane deadband logic which then feeds the jet drive electronics.

Based upon the foregoing information, a suitable model of the RCS for the North American space station should be as depicted in Figure 3-5. Because of the indicated comparable torque levels of the CMG control system and the RCS (and the low thrust levels and relatively long firing times) the former will represent a dynamic excitation element for the space station/array that is comparable to the latter. All maneuvers using the RCS are performed by firing two thrusters as a couple. The primary thrusters for each maneuver are selected by choosing the pair of thrusters with the longest lever arm.

The torque equations in the simulation of a rigid space station, and based upon the block diagram in Figure 3-5, are

$$\begin{bmatrix} T_R \\ T_P \\ T_Y \end{bmatrix} = \begin{bmatrix} B_R \\ B_P \\ B_Y \end{bmatrix} \begin{bmatrix} K_\theta \; \phi_e + K_{\dot\theta} \; \dot\phi \\ K_\theta \; \theta_e + K_{\dot\theta} \; \dot\theta \\ K_\theta \; \psi_e + K_{\dot\theta} \; \dot\psi \end{bmatrix}$$

where

T_R, T_P, T_Y are the torques applied to the space station about the roll, pitch and yaw axes respectively.

B_R, B_P, B_Y are the torque dead bands for each axis

K_θ is the gain proportional to the space station angle error

$K_{\dot\theta}$ is the gain proportional to the space station rate about each axis

$\phi_\epsilon, \theta_\epsilon, \psi_\epsilon$ are the angle errors in roll, pitch and yaw respectively

$\dot\phi, \dot\theta, \dot\psi$ are the space station rates in roll, pitch and yaw.

These equations are used in the RCS digital subroutine in the simulation to develop the control torques for the thruster system. This proportional control system, when used as an alternate to the CMG control system, will permit more economical computation of the interaction dynamics.

Since the computerized method of simulating space station motions was modified in Phase II study efforts to account for space station flexibility, the reaction jet control system in the simulation consists of six individual constant-thrust-magnitude thrusters at specified structural locations to control the three angular rigid body motions. Location of each thruster, thrust magnitude and thrust direction, are allowed to be specified prior to performing a simulation. Program logic computes the generalized forces into space station modal degrees of freedom using other appropriate input structural mode constants. The typical applied torque equation is

$$T = K \bullet 1 (E_C - E_{DB})$$

where

T = output torque of the reaction jets at any given time for which the computed "error" is E_C.

K = torque capability of the reaction jets

$1(\ )$ = unit step function having the value zero for negative or zero arguments and the value unity for positive arguments.

E_C = computed equivalent attitude/rate error of the space station determined by

$$E_C = K_1(K_2 \phi - \omega)$$

where K_1 and K_2 are input constants and ϕ and ω are attitude and rate errors of the space station respectively.

E_{DB} = deadband threshold level for equivalent attitude/rate error which determines when the reaction jets are active.

3.2 SOLAR ARRAY ORIENTATION CONTROL SYSTEM (OCS)

The operating characteristics of the Orientation Control System (OCS) for the solar arrays being considered in this study effort can have a major impact on the latter's design requirements. Hence, in developing an analysis method to evaluate the design of such arrays, the significant dynamic characteristics of the OCS must be properly modeled. Two generic types of OCS drive systems have been considered and are characterized by the following:

- The continuous array drive system
- The non-linear (bang-bang) drive system.

3.2.1 CONTINUOUS ARRAY DRIVE SYSTEM

A block diagram of the continuous OCS is shown in Figure 3-6. The difference between the commanded array angle and actual array angle are used to generate the angle error signal. This error signal is then filtered by the provided compensation in the control loop. The array angular rate $\dot{\theta}$ is multiplied by the back EMF coefficient K_B and added (negatively) to the filtered error signal. This gives the effective drive signal for the motor. The drive motor is modeled as a first order lag with K_M as the torque gain of the motor and τ_M as the motor time constant. The output torque of the motor is reduced by the friction in the reduction gear unit as shown by the K_F feedback loop. The effective torque of the motor is increased by the ratio of the reduction gear and delivered to the solar array. To determine the stability of the OCS, the solar array is assumed to be rigid and have an inertia I_A about is axis of rotation.

To assess the effects of the two rate feedback loops in Figure 3-6 the value of $K_F\dot{\theta}$ and T_M were compared for $\dot{\theta}$ equalto orbital rate. The results showed $K_F\dot{\theta}$ to be significantly smaller than T_M and hence the K_F feedback loop can be dropped from the simulation without any loss of generality. This is generally expected to occur for this class of control systems. With one of the feedback loops removed, the OCS continuous drive model can be simplified. The drive mechanism can then be modeled by two first order filters to smooth the array angle error and rate signals. The two signals are weighted by the appropriate gains and added together. The sum is then filtered by a third first order filter (i.e., the motor) where the gain of the filter is the product of the torque gain of the motor and the gear ratio of the drive system. This is shown schematically in Figure 3-7.

To evaluate the stability of the continuous drive OCS, the T-2170 Inland torque motor is assumed as the prime mover in the system. The characteristics of this motor are generally representative of the class of DC torque motors that would be suitable for the array drive system. These characteristics are:

$L_M = 3 \times 10^{-3}$ Henrys
$K_T = 18.9$ oz-in/amp
$R_T = 3.3$ ohms
$K_B = 1.3$ volts/rad/sec

The motor gain and time constant are defined as

$$K_M = K_T / R_T = 5.727 \text{ oz-in/volt}$$

$$\tau_M = L_M / R_T = 0.00091 \text{ sec.}$$

A larger torque motor than required was chosen to allow the motor to operate near its rated speed without an unusually high gear reduction ratio. The chosen motor requires the use of a 6800:1 reduction gear.

The open loop transfer function of the simplified continuous drive OCS is given by equation 1.

$$\frac{\theta}{\theta_c} = G(S) = \frac{K_\theta K_M K_G}{S\left\{\tau_\theta \tau_M I_A S^3 + I_A (\tau_\theta + \tau_M) S^2 + (K_M K_G^2 K \tau_\theta + I_A) S + K_M K_G^2 K_\beta\right\}} \quad \text{(Equation 1)}$$

The steady state hang off error for the system when following a velocity input (orbit rate) is given by equation 2.

$$e_{ss} = \frac{\dot{\Theta}_c}{\lim\limits_{S \to O} S\, G\,(S)} \qquad \text{(Equation 2)}$$

Hence, by selecting a suitable steady state following error, the value of K_Θ can be determined. The steady state error is chosen to be 1 degree for the determination of K_Θ . This is somewhat tighter than required but it allows for other components in the system to contribute to the steady state error without exceeding the desired overall system value. Substituting equation 1 into equation 2 gives an expression for K_Θ in terms of known quantities.

$$K_\Theta = \frac{K_B\, K_G\, \dot{\Theta}}{e_{ss}} \qquad \text{(Equation 3)}$$

Using the values for K_B, K_G, and e_{ss} previously given and assuming an orbit period of 100 minutes, the gain of the loop compensation is

$$K_\Theta = 530$$

The time constant for the loop compensation is selected by restricting the maximum overshoot to be less than 1 db. Using the characteristics of the T-2170 torque motor and an array inertia of 77,000 slug ft^2, Equation 1 reduces to

$$G(s) = \frac{{}^{1}/166.8\, T_\Theta}{S\,(S + \frac{1}{T_\Theta})} \qquad \text{(Equation 4)}$$

when all small terms are neglected. An appropriate time constant for equation 4 is

$T_\Theta \approx 0.01$ sec.

The values presented in this section are considered representative of the continuous drive control system. If other values are desired, provisions are available to include them in the digital simulation.

3.2.2 NON-LINEAR DRIVE SYSTEM

The non-linear drive OCS is similar to the continuous drive system with the exception that the control logic is operated in an on-off manner. When the error signal exceeds some pre-selected threshold value, the motor is turned on until the array is driven to the null position at which point the motor is switched off. The time that the motor takes to reach its running speed when switched on is very small compared to the total time that the motor is operated to drive the array back to the null position. Similarly, the time the motor takes to coast to a stop when the power is turned off is small compared to its total on-time. This would allow the motor to be modeled as a square wave rate generator, i.e., when the motor is commanded on, the array begins rotating at a constant velocity and when the motor is commanded off the array stops rotating.

A non-linear orientation control drive system has been formulated by the Ball Brothers Research Corporation (Reference 3. 4), and this system is included as a control subroutine in the simulation. It is represented by the diagram shown in Figure 3-8. Values of the various constants shown are those received as representative of the BBRC system. In order that simulations could be performed with the many constants varied as parameters, the following were allowed to be input variables to the program subroutine representing this system.

- Deadband angle
- Bus Voltage Generator time constant,
- Bus Voltage Generator amplification constant, A
- Motor Gain ($K_T N/R$)
- Coulomb Friction
- Scaling constant, G

- Gear Ratio, K_G
- Back EMF

The relative velocity vector and angular error are computed by the simulation program for the space station rigid body and flexible degrees of freedom and the solar array degrees of freedom.

3.3 REFERENCES

Reference 3.1. "Solar-Powered Space Station Preliminary Design," Vol. III, Guidance and Control Subsystem, North American Rockwell, July 1970.

Reference 3.2. "Preliminary Synthesis and Simulation of the Selected CMG Attitude Control System," G.E. Report EL-506-D, 5 March 1970.

Reference 3.3. "Small Eccentricities or Inclinations in the Brower Theory of the Artificial Satellite," R.H. Lyddane, Astronomical Journal, Vol. 68, No. 8, Octiber 1963, pg. 555.

Reference 3.4. "Space Station Solar Array Technology Evaluation Program," Second Topical Report, Lockheed Missile and Space Company (LMSC-A981486), November 1971.

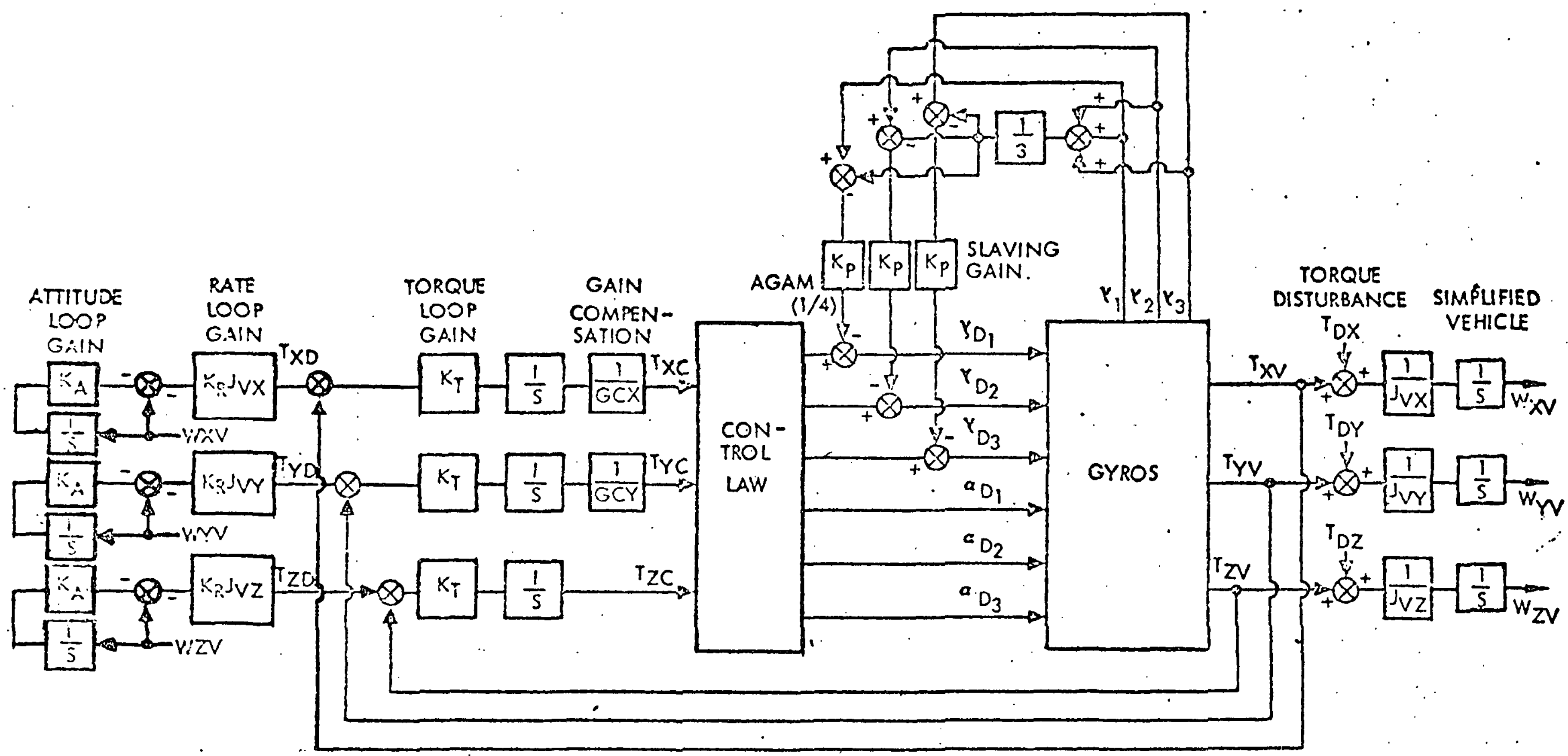

FOR TRANSPOSE CONTROL LAW:

$$GCX = \cos^3\theta_1 + \cos^2\theta_2 + \cos^2\theta_3$$

$$GCY = \sin^2\theta_1 + \sin^2\theta_2 + \sin^2\theta_3$$

$$\gamma D_i = T_{ZC}/3H \cos\gamma$$

$$\alpha D_i = (T_{XC}\cos\theta_i + T_{YC}\sin\theta_i)/H\cos\gamma_1$$

Figure 3.1 Simulation Diagram - CMG Control System

CMG CONTROL SYSTEM

(Simplified)

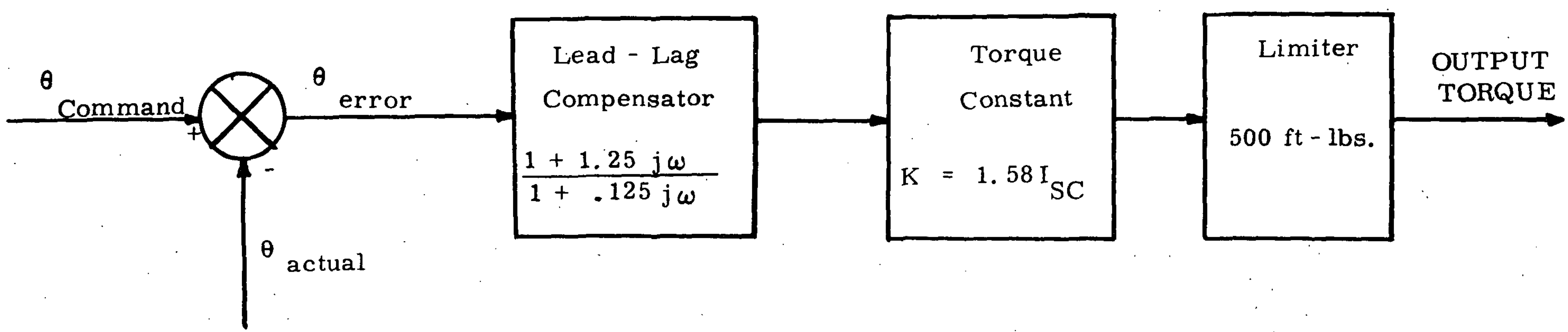

FIGURE 3-2

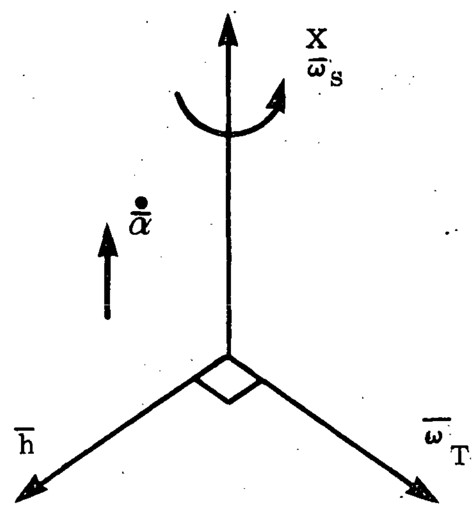

$\dot{\alpha}$ - Gimbal Rate of CMG

$\bar{h}$ - Momentum Vector

ω_s - Spin Axis Component of Spin Rate

ω_T - Transverse Component of Spin Rate

Applied Torques

$\bar{T}_c = -(\overline{\omega_s + \dot{\alpha}}) \times \bar{h}$ (opposes $\bar{\omega}_T$)

$\bar{T}s = -\bar{\omega}_T \times \bar{h}$ (increases spin rate)

FIGURE 3-3 Wobble Damper Control Torques

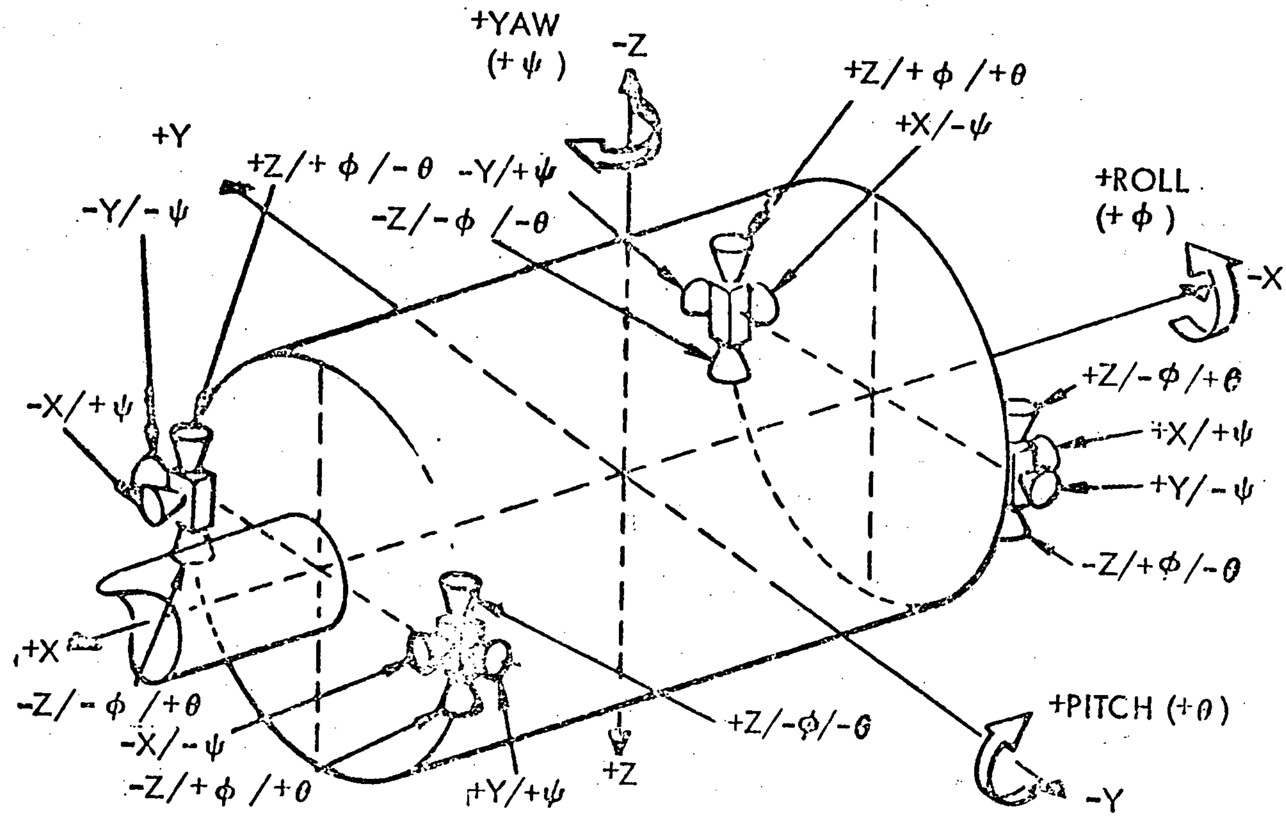

Figure 3-4 RCS Jet Location/Function

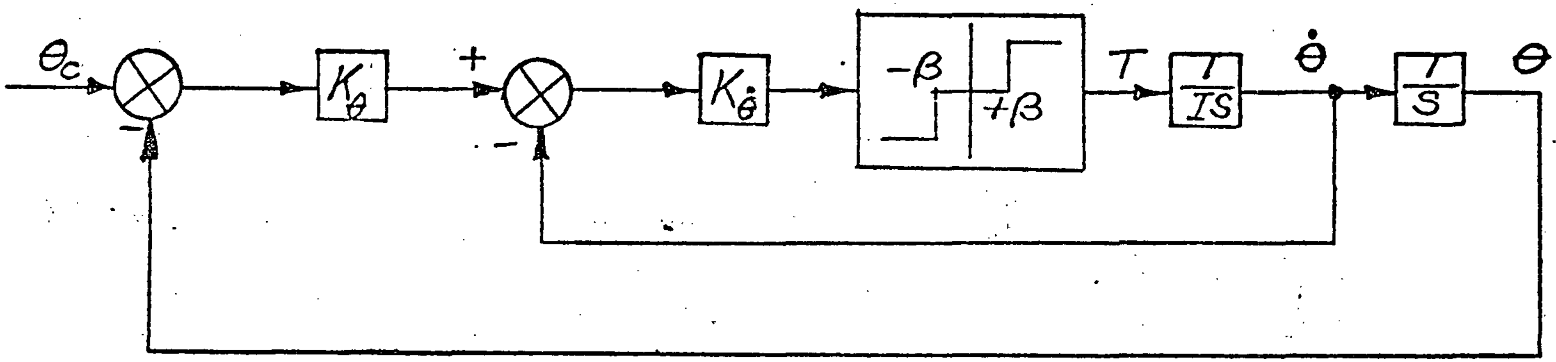

LEGEND

θ_c = Commanded Attitude Angle
$\theta, \dot\theta$ = Attitude Angle, Rate
$K_\theta, K_{\dot\theta}$ = Attitude Angle Gain, Rate Gain
β = Control Loop Deadband
T = RCS Torque Level
I = Space Station Moment of Inertia

Figure 3-5. RCS Model

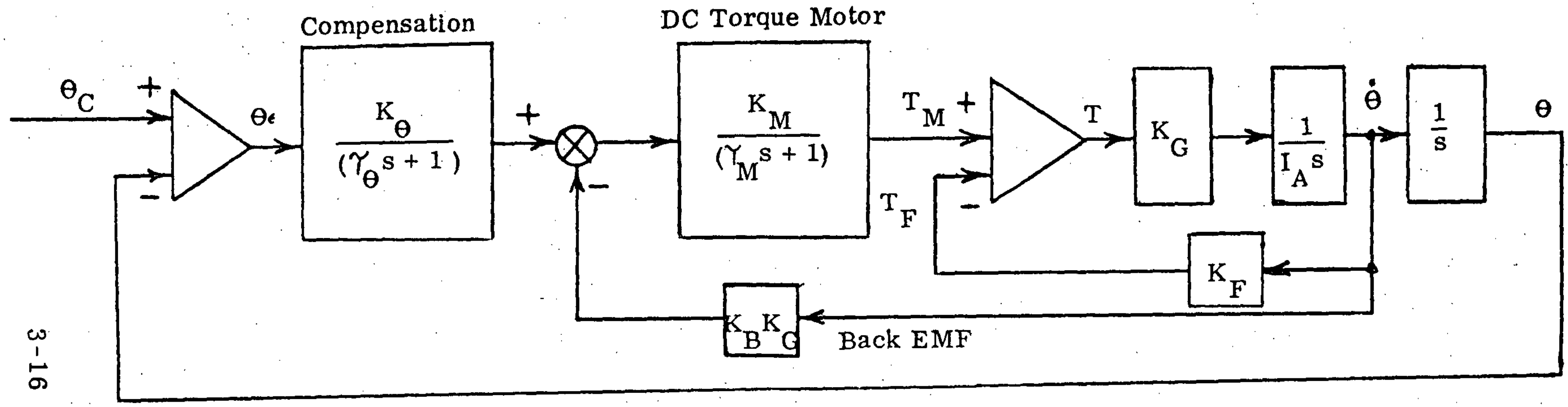

Figure 3-6. Model for Continuous Drive OCS for Solar Arrays
(one continuous motion axis)

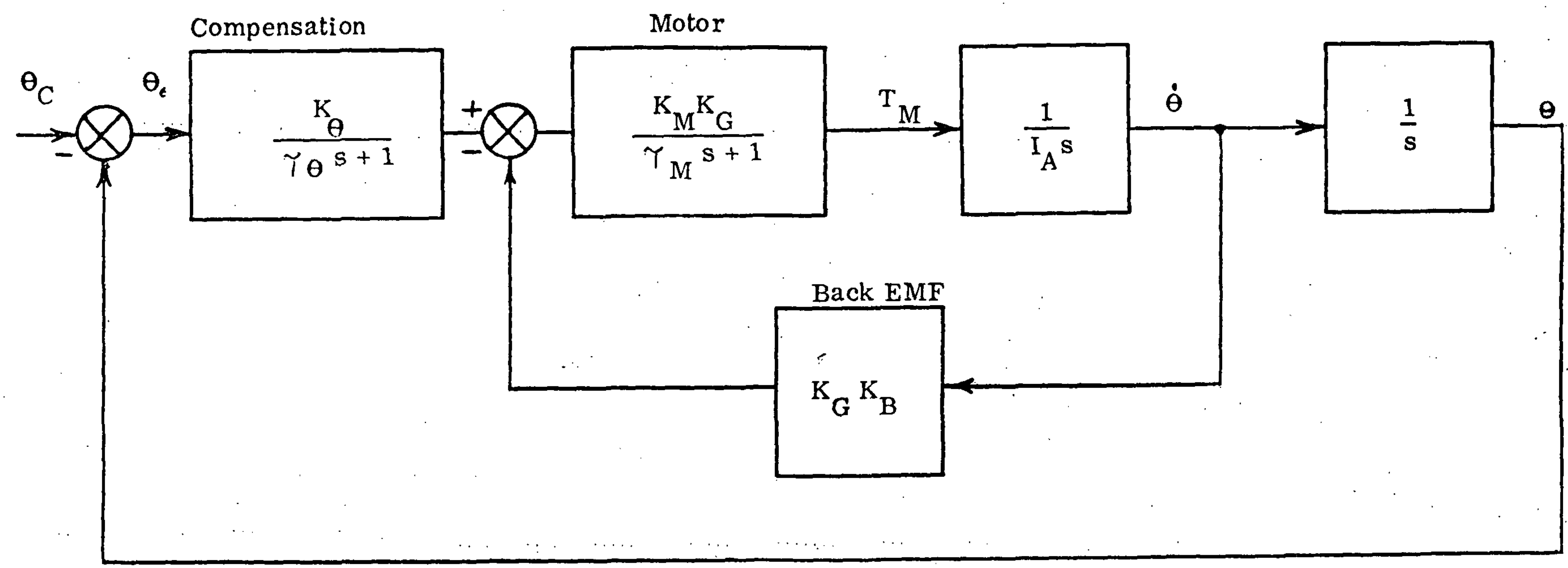

Figure 3-7. Simplified Continuous Drive OCS Model

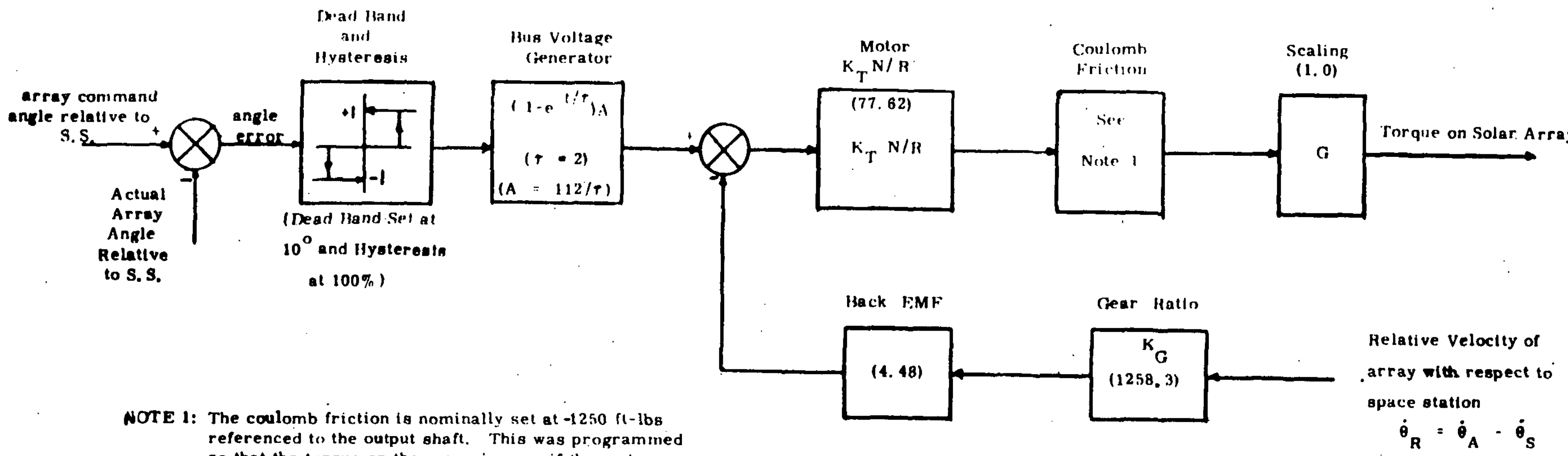

NOTE 1: The coulomb friction is nominally set at -1250 ft-lbs referenced to the output shaft. This was programmed so that the torque on the array is zero if the motor torque is less than 1250 ft-lbs when the array is not moving relative to the space station. When the array is moving and the motor torque is less than 1250 ft-lbs, the torque on the array is the coulomb torque minus the motor torque. When the motor torque is greater than 1250 ft-lbs, the torque on the array is the difference between the motor torque and coulomb torque.

Figure 3-8. Non-Linear Orientation Control System

4. DYNAMIC INTERACTIONS ANALYSIS FORMULATION AND DIGITAL SIMULATION

Three phases of interaction analysis formulations and corresponding simulations resulted during the study period. Separate digital simulations and the associated user information were derived on the basis of each analytical formulation. The formulations are categorized by the following:

- Rigid space station with two flexible controllable appendages in a zero "G" orbit environment
- Flexible space station with two flexible controllable appendages and four flexible non-controllable appendages in a zero "G" orbital environment
- Flexible space station with four flexible non-controllable appendages in an artificial "G" orbital environment.

A detailed description and derivation of each of the formulations that were digitally programmed are contained in the following report subsections.

4.1 RIGID SPACE STATION/FLEXIBLE CONTROLLED APPENDAGES

The interaction dynamics study simulation is designed to determine the effects of important solar array structural characteristics on the motion of an orbiting space station. Two flexible solar arrays are connected to the space station by means of rigid driver assemblies which are totally constrained in translation and allowed two rotational degrees of freedom for each driver about the attachment point. The array drivers are rotated to obtain the desired sun/solar array aspect. The space station is attitude stabilized by a Control Moment Gyro System (CMG) which is augmented by a reaction control system to provide maneuver capability and "momentum dumping". The simulation model utilized for this system is described below:

- The space station and the two rigid array drivers are each modeled as rigid bodies with each of the rigid drivers permitted to rotate about the spacecraft attachment points along an axis parallel to the spacecraft roll axis and an axis normal to that in the plane of the solar array. The rigid array driver rotation may be additionally constrained in rotational freedom by user input to the digital simulation.
- The flexible array is modeled by the synthetic modes technique of Likins (Reference 4.1), i.e., the array is modeled in terms of a finite number of orthogonal cantilever modes suitably augmented by six synthetic modes to assure that the steady state (rigid) conditions for constant acceleration are met. The appendage equation is an exact formulation which includes all accelerations of the appendage base. In accord with the synthetic modes approach, the effect of the two flexible arrays upon the rigid body system is obtained in the form of the equivalent force and torque exerted by the flexible arrays upon the system by the modal accelerations. The effects of the rigid system motion upon the flexible arrays is accounted for by system acceleration in the appendage equation of each array.
- Maneuver and attitude control of the space station together with the solar array orientation control are modeled in terms of the appropriate time varying forces and torques produced by closed loop guidance equations. The guidance and steering commands are computed external to the dynamics section and provide the space station with a fixed orientation relative to orbit coordinates.

Formulation of these equations is given in the Command and Control description.

- The array driver gear train for the axis parallel to the space station roll axis is modeled as an ideal mechanical transformer referenced to the spacecraft side of the gear train. The other driver axis is directly driven. Either axis of both drivers may be locked.
- The simulation orbit generator uses Lyddane's method for near earth orbits which may be circular. (Ref. 4.2).

A block diagram representation of the simulation program is presented in the following where important logical switches and function interconnection have been delineated (Figures 4-1 thru 4-5).

4.1.1 CONVENTIONS AND COORDINATE SYSTEMS

The coordinate systems given below represent the main computational frames utilized in the simulation.

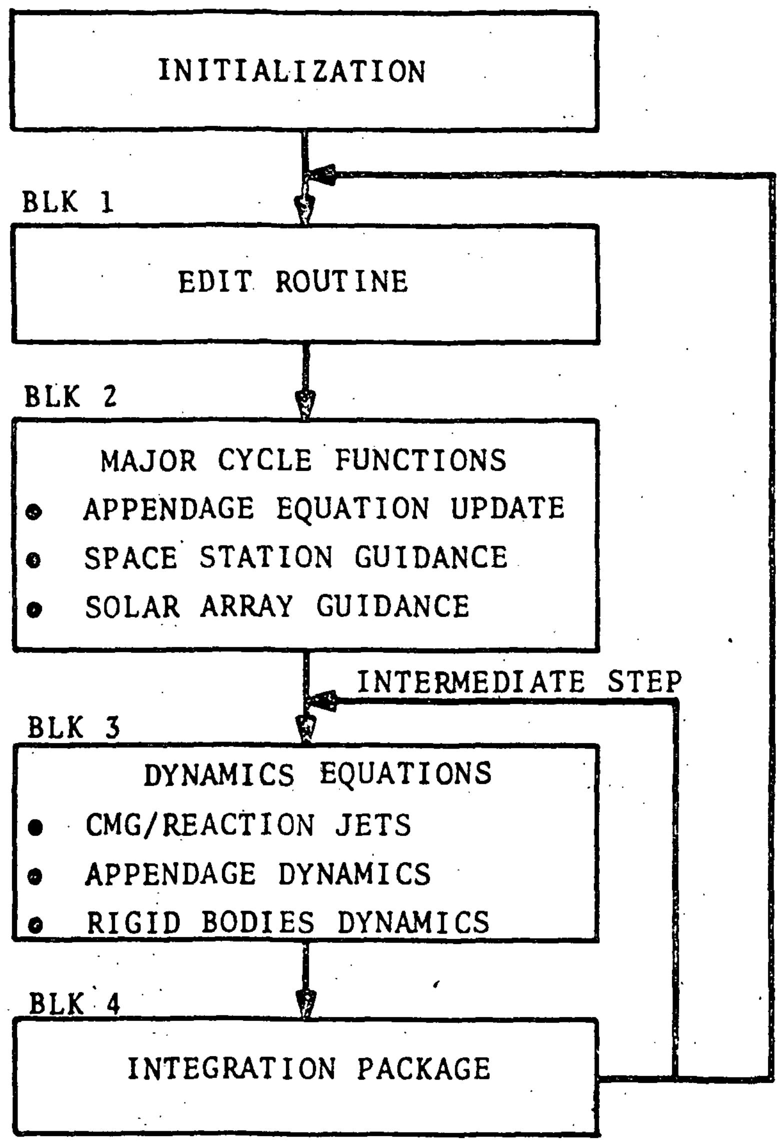

Figure 4-1 Overall Flow Chart

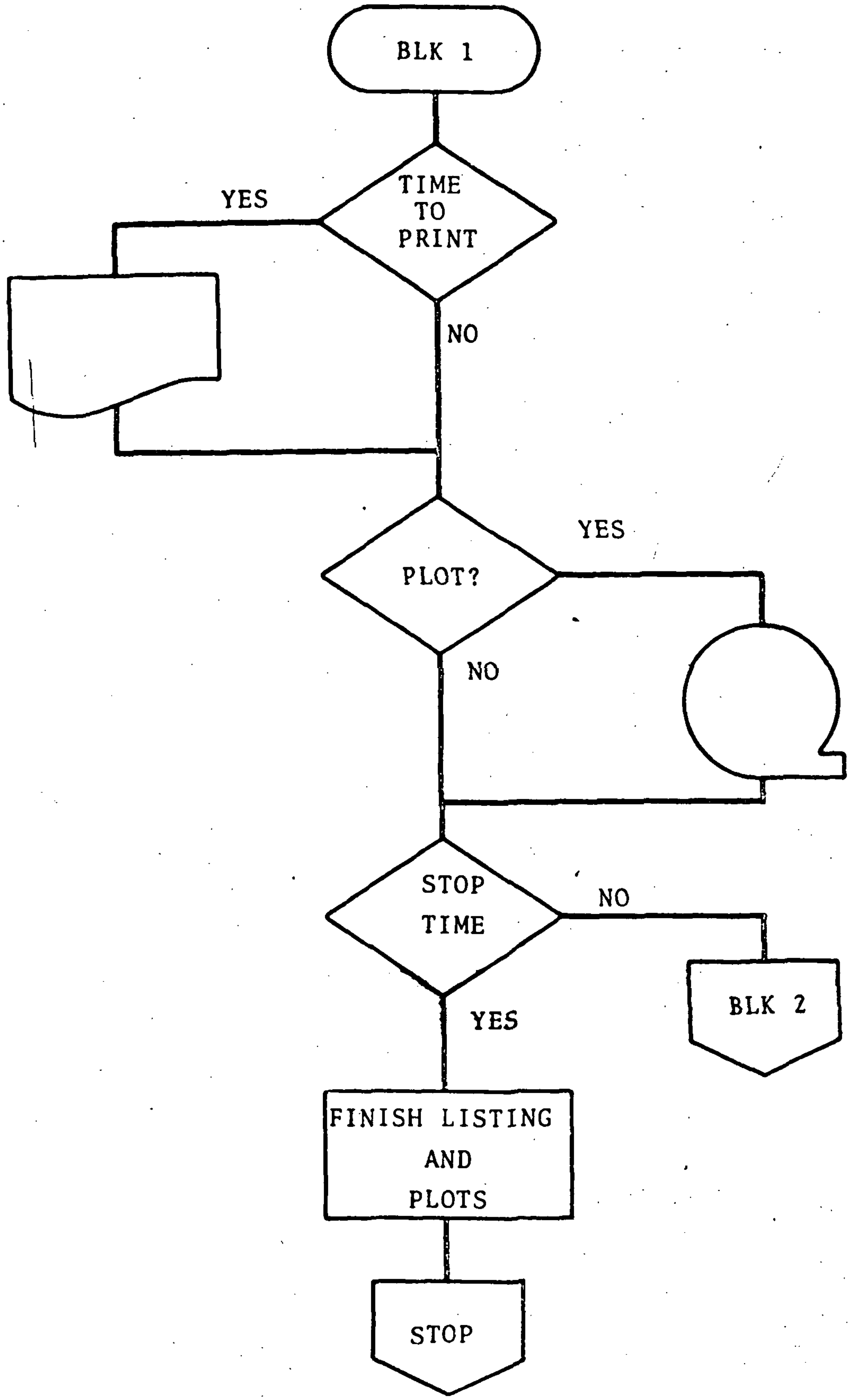

Figure 4-2 Blk 1 Edit Routine Flow Chart

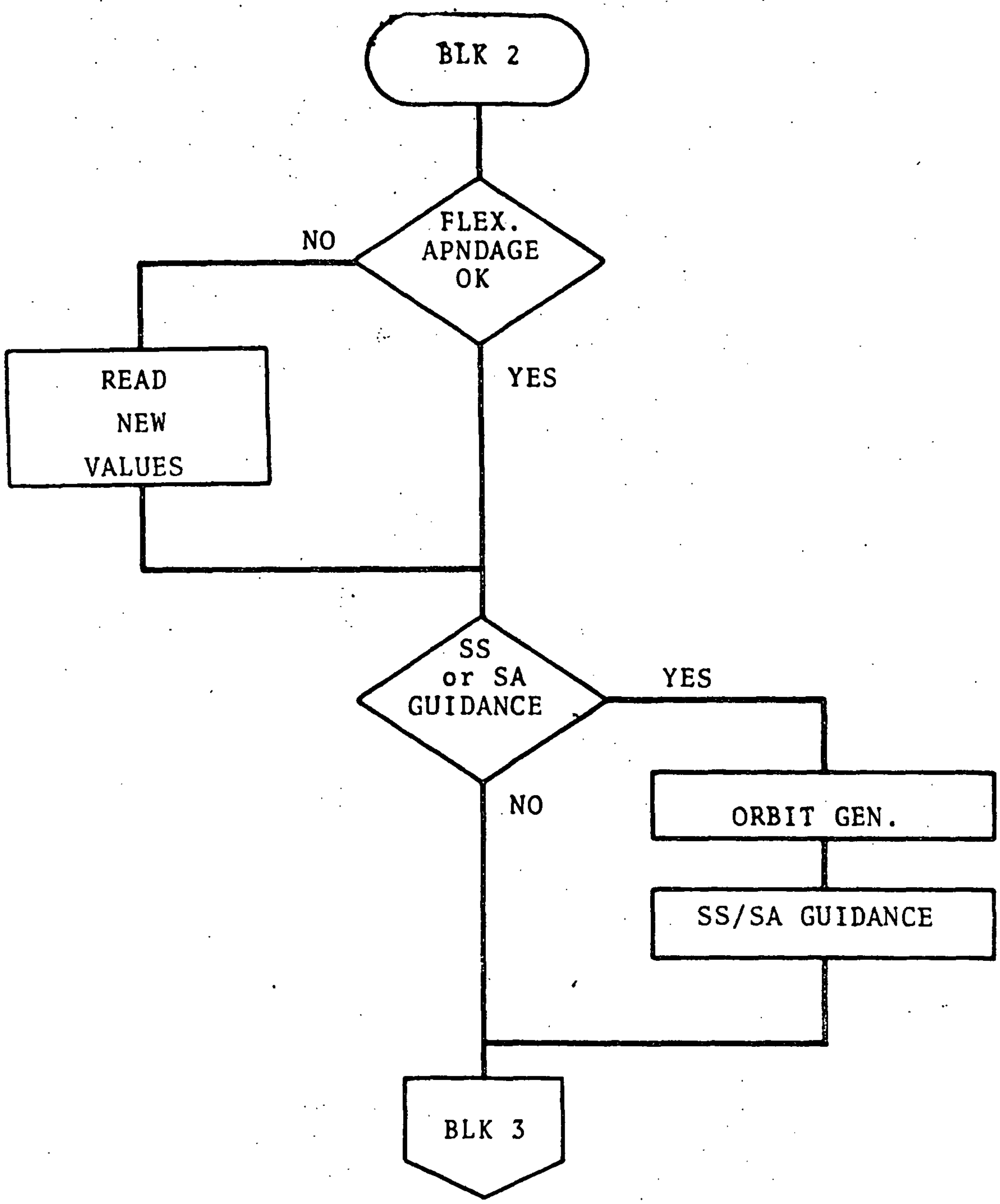

Figure 4-3 Blk 2 - Major Cycle Flow Chart

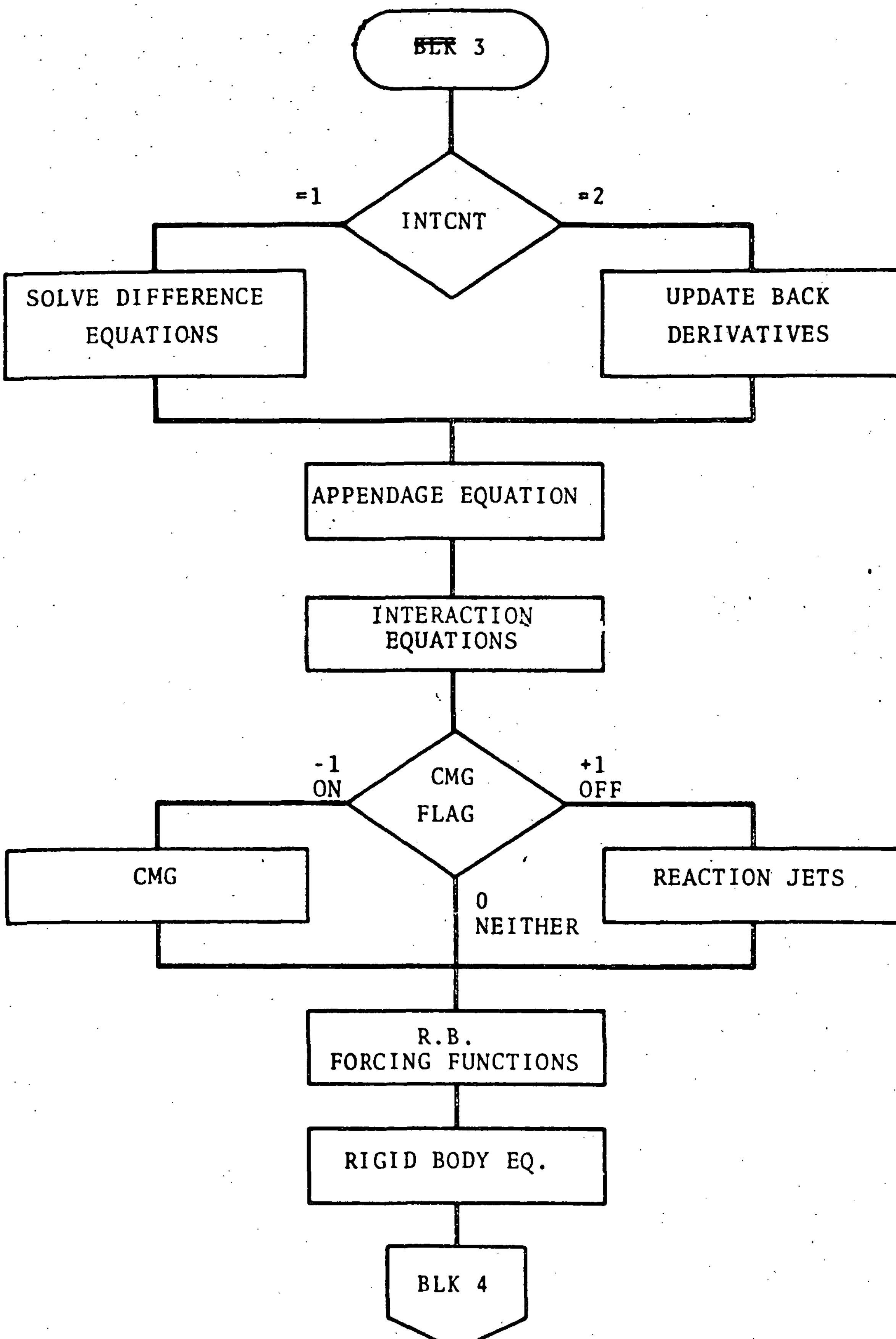

Figure 4-4 Blk 3 - Dynamics Equations Flow Chart

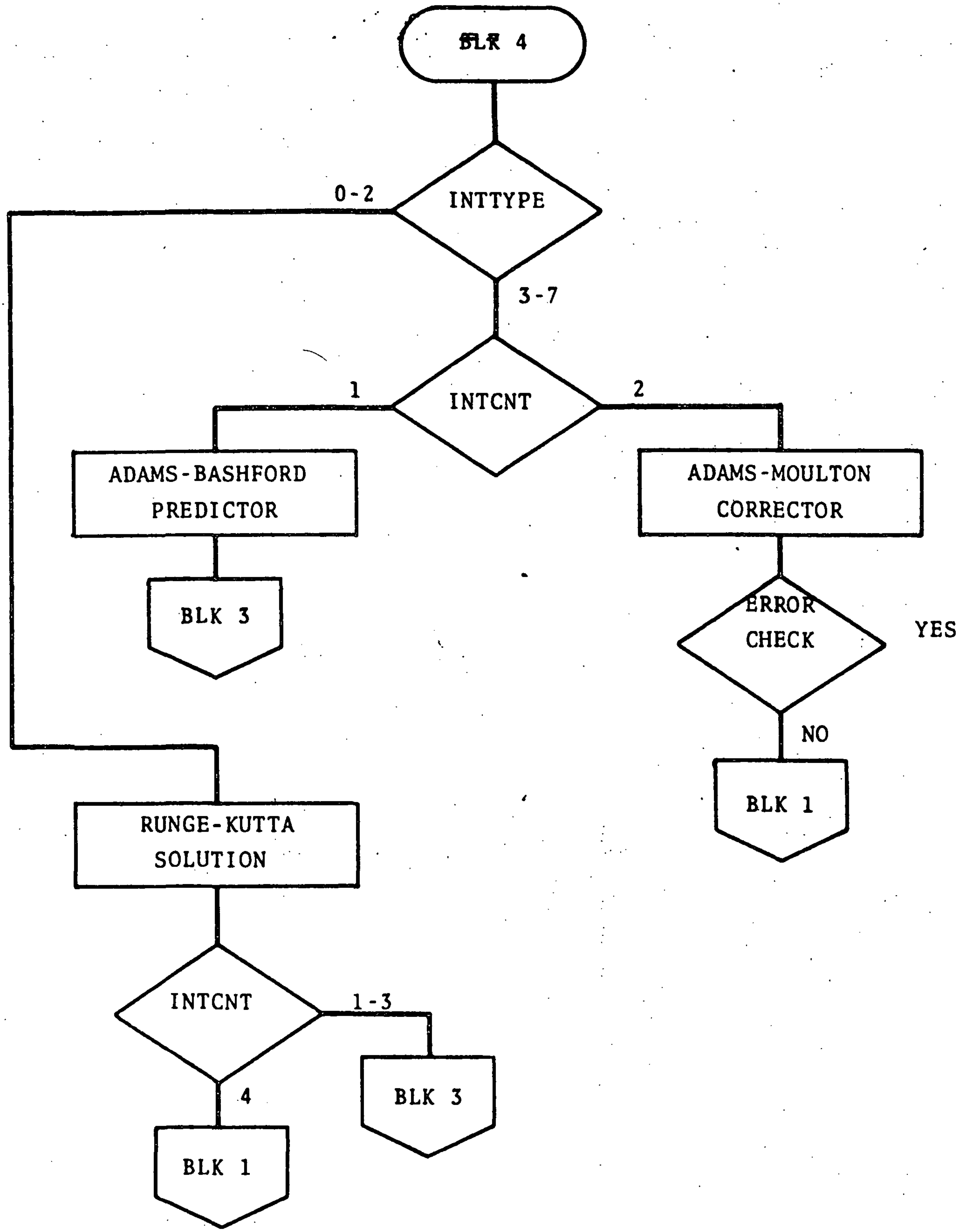

Figure 4-5 Blk 4 - Integration Package Flow Chart

4.1.1.1 COORDINATE FRAME 1

Earth Centered Inertial (ECI) Coordinates

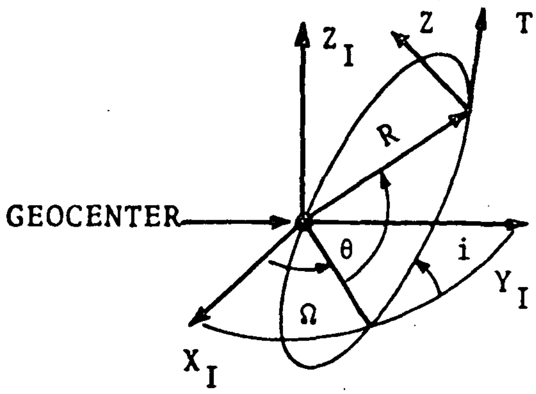

X_I - In equatorial plane pointing at Aries

Z_I - Points to geocentric north pole

Y_I - Provides right handed set in order X_I, Y_I, Z_I

4.1.1.2 COORDINATE FRAME 2

Local Level (RTN) Coordinate

$$\begin{bmatrix} R \\ T \\ N \end{bmatrix} = \begin{bmatrix} C\theta & S\theta & 0 \\ -S\theta & C\theta & 0 \\ 0 & 0 & 1 \end{bmatrix} \begin{bmatrix} 1 & 0 & 0 \\ 0 & Ci & Si \\ 0 & -Si & Ci \end{bmatrix} \begin{bmatrix} C\Omega & S\Omega & 0 \\ -S\Omega & C\Omega & 0 \\ 0 & 0 & 1 \end{bmatrix} \begin{bmatrix} X_I \\ Y_I \\ Z_I \end{bmatrix}$$

R - directed along geocenter to space station radius vector

N - normal to orbit plane

T - completes right handed set (R, T, N)

where Ω - longitude of ascending node

i - orbital inclination

θ - sum of argument of perigee (ω), plus the true anomaly (ν)

C,S - cosine and sine functions

As indicated above, the Euler rotations are about the Z_I, the X_I' and the N axis where X_I' is the X_I axis after rotation through Ω.

4.1.1.3 COORDINATE FRAME 3

Commanded Space Station Coordinates

The desired space station orientation X_c, Y_c, Z_c represent, in order, the commanded orientation of the space station roll, pitch and yaw axes. The vehicle command orientation is related to the R, T, N set by means of three Euler rotations:

α_c about T axis

β_c about N' axis

γ_c about X_c (commanded roll) axis

where N' is the N axis after rotation by α_c

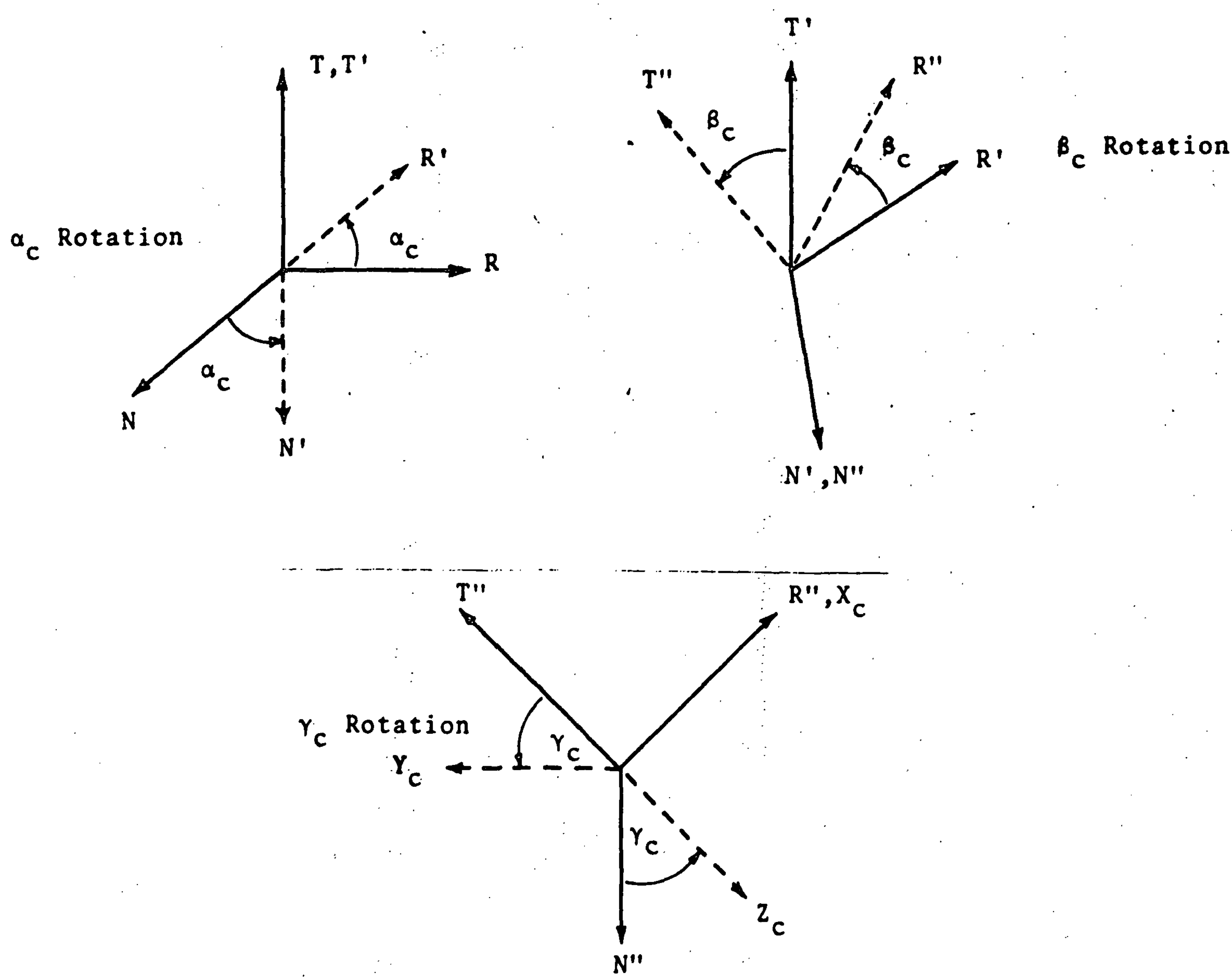

4.1.1.4 COORDINATE FRAME 4

Actual Space Station Coordinates

The actual orientation of the space station is similarly related to the RTN frame by a set of Euler angles α, β, γ. The order of rotations is the same as for the command angles and the resultant direction cosine matrix is given below in expanded form

$$\begin{bmatrix} X_s \\ Y_s \\ Z_s \end{bmatrix} = \begin{bmatrix} 1 & 0 & 0 \\ 0 & C\gamma & S\gamma \\ 0 & -S\gamma & C\gamma \end{bmatrix} \begin{bmatrix} C\beta & S\beta & 0 \\ -S\beta & C\beta & 0 \\ 0 & 0 & 1 \end{bmatrix} \begin{bmatrix} C\alpha & 0 & -S\alpha \\ 0 & 1 & 0 \\ S\alpha & 0 & C\alpha \end{bmatrix} \begin{bmatrix} R \\ T \\ N \end{bmatrix}$$

X_s, Y_s, Z_s - actual roll, pitch, and yaw axes of the space station.

α, β, γ - Euler angles

in more condensed form

$$\begin{bmatrix} X_s \\ Y_s \\ Z_s \end{bmatrix} = \begin{bmatrix} C_A \end{bmatrix} \begin{bmatrix} R \\ T \\ N \end{bmatrix}$$

4.1.1.5 COORDINATE FRAME 5

Solar Array Driver Coordinates

Each rigid solar array driver is constrained to rotate about an axis parallel to the space station roll (X_s) axis and about the array vane (Z_{A_i}) axis where the resultant set of axes for the first driver are X_{A_1}, Y_{A_1} and Z_{A_1} as shown below.

The resultant direction cosine relation is in expanded form

$$\begin{bmatrix} X_c \\ Y_c \\ Z_c \end{bmatrix} = \begin{bmatrix} 1 & 0 & 0 \\ 0 & C\gamma_c & S\gamma_c \\ 0 & -S\gamma_c & C\gamma_c \end{bmatrix} \begin{bmatrix} C\beta_c & S\beta_c & 0 \\ -S\beta_c & C\beta_c & 0 \\ 0 & 0 & 1 \end{bmatrix} \begin{bmatrix} C\alpha_c & 0 & -S\alpha_c \\ 0 & 1 & 0 \\ S\alpha_c & 0 & C\alpha_c \end{bmatrix} \begin{bmatrix} R \\ T \\ N \end{bmatrix}$$

X_c - commanded roll axis

Y_c - commanded pitch axis

Z_c - commanded yaw axis

$\alpha_c, \beta_c, \gamma_c$ - commanded Euler angles

or in more condensed fashion

$$\begin{bmatrix} X_c \\ Y_c \\ Z_c \end{bmatrix} = \begin{bmatrix} C_{A_c} \end{bmatrix} \begin{bmatrix} R \\ T \\ N \end{bmatrix}$$

Rotation ϕ_A about X_s

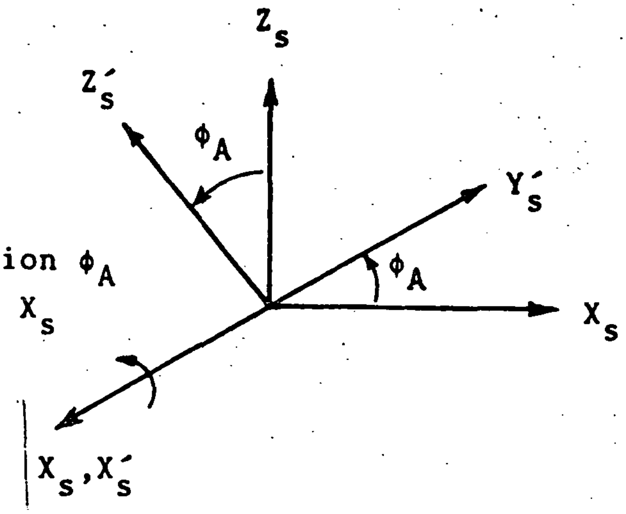

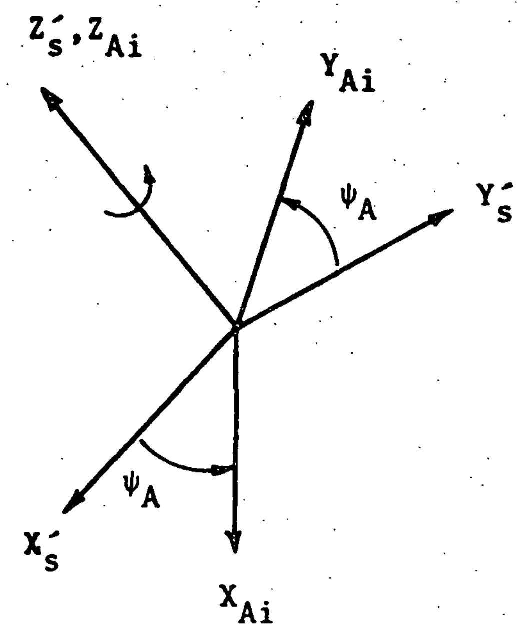

$$\begin{bmatrix} X_A \\ Y_A \\ Z_A \end{bmatrix} = \begin{bmatrix} \cos\psi_A & \sin\psi_A & 0 \\ -\sin\psi_A & \cos\psi_A & 0 \\ 0 & 0 & 1 \end{bmatrix} \cdot \begin{bmatrix} 1 & 0 & 0 \\ 0 & \cos\phi_A & \sin\phi_A \\ 0 & -\sin\phi_A & \cos\phi_A \end{bmatrix} \begin{bmatrix} X_s \\ Y_s \\ Z_s \end{bmatrix}$$

In condensed form

$$\begin{bmatrix} X_{A_1} \\ Y_{A_1} \\ Z_{A_1} \end{bmatrix} = \begin{bmatrix} C_1 \end{bmatrix} \begin{bmatrix} X_s \\ Y_s \\ Z_s \end{bmatrix}$$

The second rigid driver nominally has the same Y_A axis as the first and the remaining axes are reversed.

$$\begin{bmatrix} X_{A_2} \\ Y_{A_2} \\ Z_{A_2} \end{bmatrix} = \begin{bmatrix} -1 & 0 & 0 \\ 0 & 1 & 0 \\ 0 & 0 & -1 \end{bmatrix} \begin{bmatrix} C_1 \end{bmatrix} \begin{bmatrix} X_s \\ Y_s \\ Z_s \end{bmatrix}$$

$$\begin{bmatrix} C_2 \end{bmatrix} = \begin{bmatrix} -1 & 0 & 0 \\ 0 & 1 & 0 \\ 0 & 0 & -1 \end{bmatrix} \begin{bmatrix} C_1 \end{bmatrix}$$

$$\begin{bmatrix} X_{A_2} \\ Y_{A_2} \\ Z_{A_2} \end{bmatrix} = \begin{bmatrix} C_2 \end{bmatrix} \begin{bmatrix} X_s \\ Y_s \\ Z_s \end{bmatrix}$$

where

$Y_{A(1,2)}$ is normal to the plane of the (1, 2) array and is pointed to the sun.

$Z_{A(1,2)}$ is normal to the space station roll axis and in the plane of the array. The Z_A axis provides the seasonal adjustment and is referred to as the vane axis.

$X_{A(1,2)}$ makes X_A, Y_A, Z_A a right handed set.

4.1.1.6 COORDINATE FRAME 6

Control Moment Gyro Orientation

The Control Moment Gyro is oriented with respect to the spacecraft axes in the following manner:

$$\begin{bmatrix} X_G \\ Y_G \\ Z_G \end{bmatrix}_{\substack{\text{Outer} \\ \text{Gimbal}}} = \begin{bmatrix} 0 & 1 & 0 \\ 0 & 0 & 1 \\ 1 & 0 & 0 \end{bmatrix} \begin{bmatrix} X_s \\ Y_s \\ Z_s \end{bmatrix}$$

or

$$\begin{bmatrix} X_G \\ Y_G \\ Z_G \end{bmatrix} = \begin{bmatrix} C_G \end{bmatrix} \begin{bmatrix} X_s \\ Y_s \\ Z_s \end{bmatrix}$$

Transformation from outer gimbal axes to inner gimbal axes is treated in the discussion of CMG dynamics.

Direction Cosine Identities

$$\begin{bmatrix} X_s \\ Y_s \\ Z_s \end{bmatrix} = \begin{bmatrix} C_o \end{bmatrix}^T \begin{bmatrix} X_I \\ Y_I \\ Z_I \end{bmatrix}$$

$$\begin{bmatrix} C_o \end{bmatrix}^T = \begin{bmatrix} C_A \end{bmatrix} \begin{bmatrix} C_s \end{bmatrix}$$

$$\begin{bmatrix} C_A \end{bmatrix} = \begin{bmatrix} C_o \end{bmatrix}^T \begin{bmatrix} C_s \end{bmatrix}^T$$

$$\alpha = \tan^{-1}\left(\frac{-C_{A\ 13}}{C_{A\ 11}}\right)$$

$$\beta = \sin^{-1}\left(C_{A\ 12}\right)$$

$$\gamma = \tan^{-1}\left(\frac{-C_{A\ 32}}{C_{A\ 22}}\right)$$

$$\begin{bmatrix} \dot{C}_i \end{bmatrix} = \begin{bmatrix} C_i \end{bmatrix} \begin{bmatrix} 0 & -w_{i3} & w_{i2} \\ w_{i3} & 0 & -w_{i1} \\ -w_{i2} & w_{i1} & 0 \end{bmatrix}$$

i = i^{TH} coordinate frame

0 - space station basis

1,2 - driver bases

w_i = rotation of i^{TH} rigid body about its C of G.

4.1.2 INITIALIZATION PROCEDURES

4.1.2.1 GENERAL INITIALIZATION PROCEDURES

The program is capable of initializing the simulation with any of the integrals or key parameters to user specified values. The input will utilize the Namelist feature of FORTRAN IV and the default (no input data) will be to use the values given in the Data Statements. Such a procedure will assure that any run will not fail because of omitted data and is at the same time extremely flexible.

4.1.2.2 DIRECTION COSINE INITIALIZATION

Space Station Commanded Attitude (C_c)

The basic philosophy used for space station orientation is "belly down" or earth pointing attitude control. Therefore the desired orientation can be specified in terms of the three Euler angles given in Section 1, α_c about T, β_c about N' and γ_c about R'' (or yaw). Specification of these three commanded angles will give any desired space station attitude with respect to the (R, T, N) orbit unit vector set. The steps in computing (C_c), the direction cosine matrix of desired space station orientation are as follows:

A. Computation of Inertial to RTN Direction Cosine Matrix (C_s)

$$\hat{R} = \frac{\bar{R} \cdot \bar{R}}{|R^2|}$$

$$\hat{V} = \frac{\bar{V} \cdot \bar{V}}{|V^2|}$$

where $\bar{R}$ is the vector position of the orbiting space station in EC1 coordinates and $\bar{V}$ is the vector velocity.

$$\hat{N} = \frac{\hat{R} \times \hat{V}}{|\hat{R} \times \hat{V}|}$$

$$\hat{T} = \hat{N} \times \hat{R}$$

$$[C_s]_{\text{Initial}} = \begin{bmatrix} \hat{R}_1 & \hat{R}_2 & \hat{R}_3 \\ \hat{T}_1 & \hat{T}_2 & \hat{T}_3 \\ \hat{N}_1 & \hat{N}_2 & \hat{N}_3 \end{bmatrix}_{\text{Initial}}$$

$$(\text{RTN} \leftarrow \text{ECI})$$

Note that $[C_s]$ is computed throughout the simulation.

B. Computation of the Commanded Attitude Matrix (C_{Ac})

Performing the multiplications in the order indicated in Section 4.1.3 we find:

$$[C_{Ac}] = \begin{bmatrix} C\beta_c \; C\alpha_c & S\beta_c & -S\alpha_c \; C\beta_c \\ \begin{pmatrix} S\gamma_c \; S\alpha_c \\ -C\gamma_c \; S\beta_c \; C\alpha_c \end{pmatrix} & C\gamma_c \; C\beta_c & \begin{matrix} C\gamma_c \; S\beta_c \; S\alpha_c \\ + C\alpha_c \; S\gamma_c \end{matrix} \\ \begin{matrix} S\gamma_c \; S\beta_c \; C\alpha_c \\ C\gamma_c \; S\alpha_c \end{matrix} & -S\gamma_c \; C\beta_c & \begin{matrix} -S\gamma_c \; S\beta_c \; S\alpha_c \\ C\gamma_c \; C\alpha_c \end{matrix} \end{bmatrix}$$

$$(\text{Command S/S} \leftarrow \text{RTN})$$

where

C and S imply cosine and sine respectively. (C_{Ac}) is computed once, at the start of the simulation.

C. Computation of the Command Direction Cosine Matrix (C_c)

$$\left|C_c\right| = \left|C_{Ac}\right| \left|C_s\right|$$

($[C_c]$ is computed throughout the simulation) in which the commanded roll axis unit vector and commanded pitch axis unit vector are respectively:

$$\bar{R}_{o_c}\Big|_{ECI} = (C_c(11),\ C_c(12),\ C_c(13))$$

$$\bar{P}_{i_c}\Big|_{ECI} = (C_c(21),\ C_c(22),\ C_c(23))$$

<u>Space Station Attitude</u> (C_o)

$$\left[C_o\right]^T_{\text{Initial}} = \left[C_A\right]\left[C_s\right]_{\text{Initial}}$$

where $[C_A]$ is the direction cosine matrix of actual space station attitude relative to the RTN set. This matrix is identical in structure to the $[C_{Ac}]$ matrix except that α, β and γ are used in place of α_c, β_c, and γ_c respectively. $[C_o]^T$ is defined as the transpose of $[C_o]$ matrix.

SOLAR ARRAY

The solar array drivers are allowed to rotate about an axis parallel to the roll axis and about the array vane axis. In addition, the two vane axes are 180 degrees apart and the two axes normal to the arrays are parallel. Therefore only two angles are needed to specify the direction cosines of both arrays relative to the spacecraft. ϕ_{A_o} is the rotation of the vane axis of Driver 1 about the space station roll axis. ψ_{A_o} is the rotation of the solar array about the vane axis.

$$\begin{bmatrix} X_{A1} \\ Y_{A1} \\ Z_{A1} \end{bmatrix} = \begin{bmatrix} C\psi_{A_o} & S\psi_{A_o} & 0 \\ S\psi_{A_o} & C\psi_{A_o} & 0 \\ 0 & 0 & 1 \end{bmatrix} \begin{bmatrix} 1 & 0 & 0 \\ 0 & C\phi_{A_o} & S\phi_{A_o} \\ 0 & -S\phi_{A_o} & C\phi_{A_o} \end{bmatrix} \begin{bmatrix} X_s \\ Y_s \\ Z_s \end{bmatrix}$$

or

$$\begin{bmatrix} X_{A1} \\ Y_{A1} \\ Z_{A1} \end{bmatrix} = \begin{bmatrix} C_1 \end{bmatrix}_{\text{Initial}} \begin{bmatrix} X_s \\ Y_s \\ Z_s \end{bmatrix}$$

and

$$\begin{bmatrix} X_{A2} \\ Y_{A2} \\ Z_{A2} \end{bmatrix} = \begin{bmatrix} -1 & 0 & 0 \\ 0 & 1 & 0 \\ 0 & 0 & -1 \end{bmatrix} \begin{bmatrix} X_{A1} \\ Y_{A1} \\ Z_{A1} \end{bmatrix}$$

$$
\left[C_2\right]_{\text{Initial}} = \begin{bmatrix} -C_{1(11)} & -C_{1(12)} & -C_{1(13)} \\ C_{1(21)} & C_{1(22)} & C_{1(23)} \\ -C_{1(31)} & -C_{1(32)} & -C_{1(33)} \end{bmatrix}
$$

4.1.3 RIGID BODY EQUATIONS OF MOTION

4.1.3.1 GENERAL RIGID BODY DYNAMICS FORMULATION

The space station and the rigid array drivers are modeled as a subsystem of interconnected rigid bodies whose motion is described by the Newton-Euler equations of motion. This is shown in Figure 4.6. As stated earlier the effect of appendage dynamics is modeled as an external force and torque. The pertinent equations are given below:

- System Force

$$
m_T \left. \frac{d^2(\bar{R}_0+\bar{C})}{dt^2} \right|_I = \bar{F}_{A_J} + \bar{F}_R
$$

- Space Station Moment

$$
\left. \frac{d}{dt} (\bar{L}_0 \ (CG_{ss})) \right|_I = (\bar{C}-\bar{\ell}_R) \times \bar{F}_R - \sum_J \bar{r}_J' \times \bar{F}_{H_J} - \sum_J T_J + T_{AC} + \bar{T}_{CMG}
$$

- Hinged Body Moment

$$
\left. \frac{d}{dt} (\bar{L}_J \ (CG_J)) \right|_I = \bar{T}_{AJ} + T_J + \bar{r}_J \times \bar{F}_{H_J}
$$

J	-	Index of solar array. J is equal to 1 or 2
$\bar{F}_{A_J}$, $\bar{T}_{A_J}$	-	are the force and torque exerted by the flexible array on each rigid driver
$\bar{T}_{A_C}$	-	torque exerted on spacecraft by rigid driver along constrained axes
m_T	-	total system mass
O_N	-	Newtonian reference point
O_B	-	Spacecraft reference point
$CG_{S.S.}$	-	Space Station center of gravity
CG_{SYS}	-	Center of gravity for the entire rigid body system
CG_J	-	Center of gravity for the J^{TH} rigid driver
$\bar{R}_0$	-	Distance space station has moved from unperturbed orbital position
$\bar{F}_R$	-	External force applied by reaction control system
$\bar{L}_J$	-	Angular Momentum of J^{TH} rigid body

$J = 0,1,2$

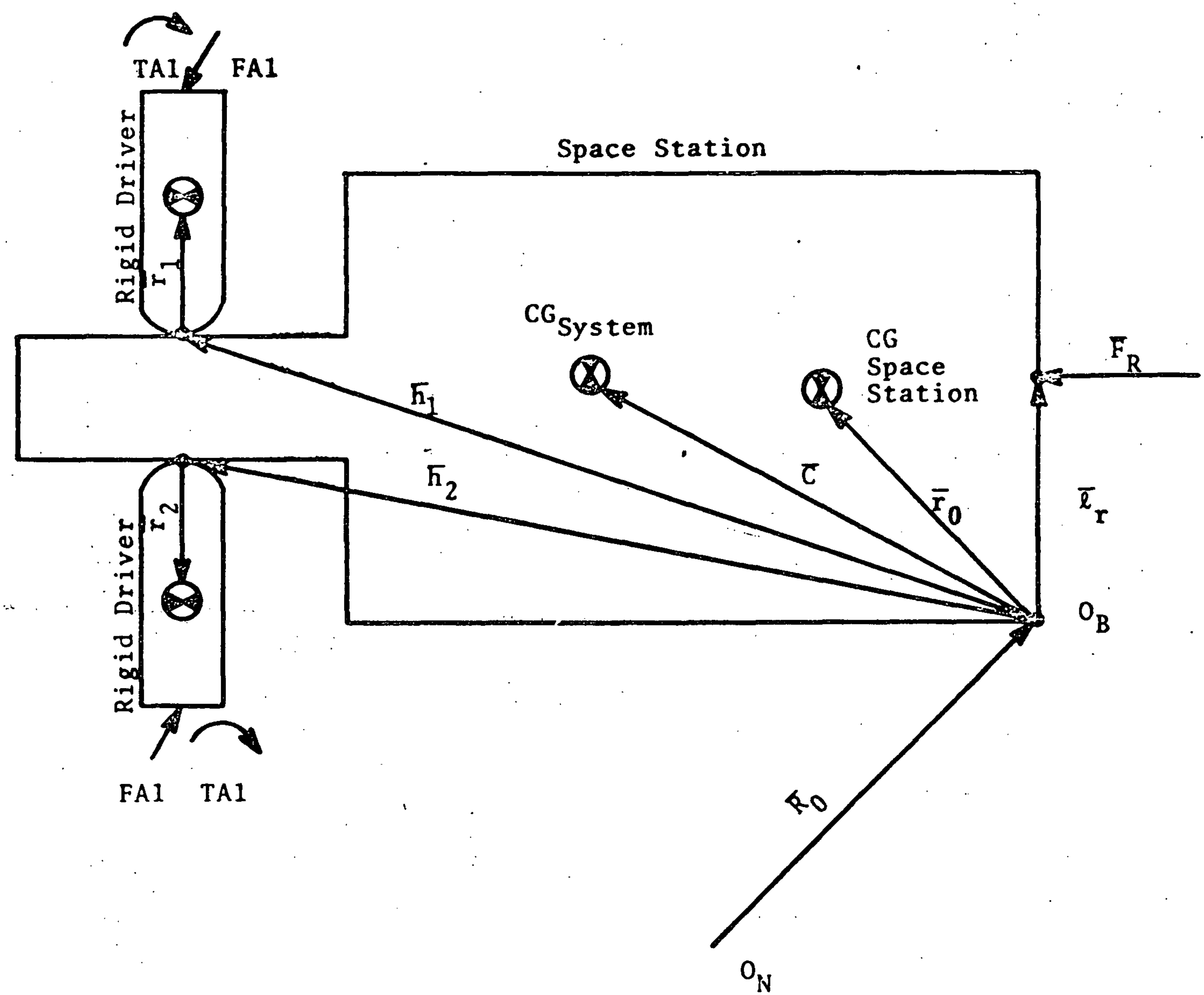

Figure 4-6 Rigid Body System Geometry

$\bar{h}_J$ - Vector from space station reference point to hinge point for rigid drivers and CMG package

$\bar{r}_J$ - vector from the respective hinge point to the J^{TH} rigid body (on space station)

$\bar{\ell}_R$ - vector from space station reference point to rocket location

$\bar{C}$ - vector from space station reference to rigid system CG

$\bar{T}_J$ - hinge torque <u>on</u> J^{TH} driver produced by control system

$\bar{r}_J$ - $(\bar{r}_o - \bar{h}_J)$ hinge force moment arm

$\bar{F}_{H_J}$ - hinge force exerted <u>by</u> space station <u>on</u> J^{TH} body

$\left.\frac{d}{dt}(\ )\right|_I$ - implies differentiation w.r.t. an inertial reference frame

$\bar{T}_{C_{M_G}}$ - control torque exerted by the control moment gyros

Before proceeding further, it is instructive to present the principal coordinate frames and direction cosine identities to be utilized in the matrix formulation of these equations.

$$\left\{X_s\right\} = \left[C_0\right]^T \left\{X_I\right\}$$

$$\left\{X_{A_1}\right\} = \left[C_1\right]^T \left\{X_s\right\}$$

$$\left\{X_{A_2}\right\} = \left[C_2\right]^T \left\{X_s\right\}$$

where

$\left\{X_I\right\}$ is the vector basis defined by unit vectors in the X_I, Y_I, Z_I directions

$\left\{X_s\right\}$ is the vector basis defined by unit vectors along X_s, Y_s and Z_s directions

$\left\{X_{A_i}\right\}$ is the vector basis for the i^{TH} solar array

$\left[\quad\right]^T$ indicates that the transpose of the matrix is required.

We have previously shown how the C_0, C_1 and C_2 matrices are initialized in terms of Euler angles. The updating of these time varying matrices during the course of the simulation will be performed by the following equation.

$$\left[\dot{C}_i\right] = \left[C_i\right]\begin{bmatrix} 0 & -w_{i3} & w_{i2} \\ w_{i3} & 0 & -w_{i1} \\ -w_{i2} & w_{i1} & 0 \end{bmatrix}$$

$$= \left[C_1\right]\left[\tilde{w}_i\right]$$

where

$$\left.\begin{matrix} w_{i1} \\ w_{i2} \\ w_{i3} \end{matrix}\right]$$ are the rotational rates about i^{TH} coordinate frame axes ($i = 0,1,2$). For i equals zero, these rates are the spacecraft roll, pitch and yaw rates.

This equation is derived in Section 4.1.7. The four vector equations presented may now be formulated as a matrix equation in a convenient coordinate frame. In the equations that follow the space station frame was chosen for the system force and space station moment equations. Each driver moment equation is written in terms of driver coordinates.

In the following formulation the square brackets used to denote a matrix are dropped and it is assumed that all quantities given are in matrix format. A few useful identities are given below.

$$A \times B \rightarrow \tilde{A}B$$

$$\tilde{A}B \equiv -\tilde{B}A$$

$$m_T \left[\begin{array}{l} \ddot{R}_0 + 2\,\tilde{w}_0\,\dot{R}_0 + (\tilde{w}_0\,\tilde{w}_0 + \dot{\tilde{w}}_0)\,R_0 \\ + (\tilde{w}_0\,\tilde{w}_0 + \dot{\tilde{w}}_0)\,(\mu_0\,r_o + \sum_J \mu_J\,(h_J + C_J\,r_J)) \\ + \sum_J \mu_J \left(\begin{array}{l} C_J(\tilde{w}_J\,\tilde{w}_J + \dot{\tilde{w}}_J)\,r_J \\ + 2\,\tilde{w}_0\,C_J\,\tilde{w}_J\,r_J \end{array} \right) \end{array} \right] = F_R + \sum_{J=1}^{2} C_J\,F_{A_J}$$

(SYSTEM FORCE)

$$\bar{\bar{I}}_0\,\dot{w}_0 + \tilde{w}_0\,\bar{\bar{I}}_0\,w_0 = \tilde{\ell}_R\,F_R - \sum_{J=1}^{2} T_J + T_{CMG} - \sum_{J=1}^{2} \tilde{r}_J\,F_{H_J} + T_{AC}$$

(SPACE STATION MOMENT)

$$\begin{array}{l} \bar{\bar{I}}_J\,(C_J^T\,\dot{w}_0 + \dot{w}_J + (C_J^T\,w_0)^{\sim}\,w_J) \\ + (C_J^T\,w_0 + w_J)^{\sim}\,\bar{\bar{I}}_J\,(w_J + C_J^T\,w_0) \end{array} = \begin{array}{l} T_{A_J} + C_J^T\,T_J \\ + \tilde{r}_J\,C_J^T\,F_{H_J} \end{array}$$

$J = 1,2$

(RIGID DRIVER MOMENT)

where

$$F_{H_J} = m_J \left[\begin{array}{l} (\tilde{w}_0\,\tilde{w}_0 + \dot{\tilde{w}}_0)\,(R_0 + h_J) + 2\tilde{w}_0\,\dot{R}_0 + \ddot{R}_0 \\ + (2\tilde{w}_0\,C_J\,\tilde{w}_i + \tilde{w}_0\,\tilde{w}_0\,C_J + \dot{\tilde{w}}_0\,C_J)\,r_J \\ + C_J\,(\tilde{w}_J\,\tilde{w}_J + \dot{\tilde{w}}_J)\,r_J \end{array} \right] - C_J\,F_{A_J}$$

(HINGE FORCE)

where

$\ddot{R}_0$, $\dot{R}_0$ and R_0 (3x1 matrix)	-	The "apparent" (space station referenced) acceleration of the space station reference point and its first two integrals.
μ_J (scalar)	-	$^{m_J}/_{m_T}$
$\bar{\bar{I}}_J$ (3x3 matrices)	-	Inertia tensor of the J^{TH} rigid driver referenced to the driver basis and center of gravity.
$\bar{\bar{I}}_0$ (3x3 matrix)	-	Space station inertia tensor referenced to the space station basis and center of gravity.
$\dot{w}_0$, w_0 (3x1 matrix)	-	Space station angular acceleration and rate.
$\dot{w}_1$, w_1 (3x1 matrix)		Driver angular accelerations and rates.
$\dot{w}_2$, w_2 (3x1 matrix)		

4.1.3.2 MATRIX FORMULATION OF RIGID BODY DYNAMICS

The equations developed must now be rearranged in a form suitable for solution. This involves formulating the problem in terms of coefficients of $\ddot{R}_0$, $\dot{w}_0$, $\dot{w}_1$ and $\dot{w}_2$ and then inverting the coefficient matrix to obtain these derivatives.

In addition some changes are required in the form of the equations to obtain the following model requirements:

- The rotational motion of the rigid solar array drivers is constrained to motion about an axis parallel to the spacecraft roll axis and an axis in the plane of the solar array normal to the space station roll axis.
- The gear ratio for the array rotation in the roll direction is explicitly incorporated into the moment equations by considering all array driver rotation on the space station side of the gear train.

In effect, this reduces the three equations for each rigid driver to two, the first of which is solved for the scalar variable $\hat{\dot{w}}_{Ai}$ which is the driver rotation referred to the space station side of the gear box. The roll axis rotation of the driver is taken to be the orbit adjustment while the rotation about the array axis of symmetry is considered nominally to be the seasonal adjustment.

In addition the effect of the constrained axis of driver rotation (rotation about an axis normal to the roll axis and the vane or Z_A axis) must be included in the Space Station Moment Equation. This is done by solving for the constraint torque in terms of $\ddot{R}_0$ and $\dot{w}_0$ and adding the terms in these variables to the equation of space station moment to obtain the set of ten scalar equations presented on the following page in matrix form.

2

RIGID BODY DYNAMICS MATRIX

$$
\begin{bmatrix}
[A_1] & [A_5] & [A_9] & [A_{13}] \\
[A_2] & [A_6] & [A_{10}] & [A_{14}] \\
[A_3] & [A_7] & [A_{11}] & [A_{15}] \\
[A_4] & [A_8] & [A_{12}] & [A_{16}]
\end{bmatrix}
\begin{bmatrix}
\ddot{R}_{0_1} \\ \ddot{R}_{0_2} \\ \ddot{R}_{0_3} \\ \dot{w}_{0_1} \\ \dot{w}_{0_2} \\ \dot{w}_{0_3} \\ \dot{\hat{w}}_{A_{11}} \\ \dot{w}_{A_{12}} \\ \dot{\hat{w}}_{A_{21}} \\ w_{A_{22}}
\end{bmatrix}
=
\begin{bmatrix}
F_1 \\ F_2 \\ F_3 \\ F_4
\end{bmatrix}
$$

Definitions -

C_1, $\left[C_2\right]$	-	Direction cosine matrix (3x3) relating driver bases to space station basis

$$\begin{bmatrix} X_s \\ Y_s \\ Z_s \end{bmatrix} = \begin{bmatrix} C_i \end{bmatrix} \begin{bmatrix} X_{Ai} \\ Y_{Ai} \\ Z_{Ai} \end{bmatrix}$$

C_1^*, C_2^*	-	direction cosines relating array basis to normally unconstrained axes
C_1^{**}, C_1^{**}	-	direction cosines relating array basis to normally constrained axes
h_1, h_2	-	3x1 vectors in space station basis giving hinge position from reference point
I_0, I_1, I_2	-	inertia matrices of space station, driver 1 and driver 2 respectively. Each is expressed in its own basis
K_G	-	gear ratio for array driver orbit adjust mechanism
l_1, l_2	-	vector from driver CG to appendage connection point given in the driver basis
m_1, m_2, m_T	-	masses of array drivers and total system respectively

R_0 - vector from Newtonian reference to space station reference point in space station basis

r_o - vector from reference point to space station CG in space station basis

r_1, r_2 - vectors from hinge point to driver CG in the driver basis

r_1', r_2' - vectors from hinge point to space station CG

w_0 - rotation rate of space station

w_1, w_2 - rotation rate of rigid driver (on array side of gear train)

$\hat{w}_{A1}$, w_{A2} - rotation rate of rigid driver on space station side of gear box

$\tilde{[\ ]}$ - matrix equivalent of vector cross product

μ_1, μ_2 - mass fractions $\mu_1 = \dfrac{m_1}{m_2}$ $\mu_2 = \dfrac{m_2}{m_T}$

Equation Set I - System Translation

$$[A_1]\ \ddot{R}_0] + [A_5]\ \dot{w}_o] + [A_9]\ \dot{w}_{A1}] + [A_{13}]\ \dot{w}_{A2}] = F_1]$$

$$[A_1] = m_T\ [I]$$

$$[A_5] = -m_T\left([\tilde{R}_0] + \mu_0\ [\tilde{r}_0] + \mu_1\ \left(h_1] + [C_1]\ r_1]\right)^{\sim} + \mu_2\ \left(h_2] + [C_2]\ r_2]\right)^{\sim}\right)$$

$$[A_9] = -m_T\ \mu_1\ [C_1]\ [\tilde{r}_1]\ [C_1{*}]^T \begin{bmatrix} \frac{1}{KG} & 0 \\ 0 & 1 \end{bmatrix}$$

$$[A_{13}] = -m_T\ \mu_2\ [C_2]\ [\tilde{r}_2]\ [C_2{*}]^T \begin{bmatrix} \frac{1}{KG} & 0 \\ 0 & 1 \end{bmatrix}$$

$$\begin{aligned} F_1] = {} & F_R] + [C_1]\ F_{A1}] + [C_2]\ F_{A2}] \\ & -m_T \Bigg(2\ [\tilde{w}_0]\ \dot{R}_0] + [\tilde{w}_0]\ [\tilde{w}_0]\ \left(R_0] + [\mu_0\ r_0]\right) \\ & + [\tilde{w}_0]\ [\tilde{w}_0]\ \left(\left(h_1] + [C_1]\ r_1]\right)\mu_1 + \left(h_2] + [C_2]\ r_2]\right)\mu_2\right) \\ & + \mu_1\ \left([C_1]\ [\tilde{w}_1]\ [\tilde{w}_1]\ r_1] + 2\ [\tilde{w}_0]\ [C_1]\ [\tilde{w}_1]\ r_1]\right) \\ & + \mu_2\ \left([C_2]\ [\tilde{w}_2]\ [\tilde{w}_2]\ r_2] + 2\ [\tilde{w}_0]\ [C_2]\ [\tilde{w}_2]\ r_2]\right) \Bigg) \end{aligned}$$

where

$[I\ ]$ is the identity matrix,

$[\tilde{\ \ }]$ and $(\ \ )^{\sim}$ indicate that the cross product form is required

$$\begin{bmatrix} X_1 \\ X_2 \\ X_3 \end{bmatrix}^{\sim} \qquad \begin{bmatrix} 0 & -X_3 & X_2 \\ X_3 & 0 & -X_1 \\ -X_2 & X_1 & 0 \end{bmatrix}$$

KG is the gear ratio for the array driver

$[C_i{*}]^T$ = transforms $\hat{w}_{Ai}$ to array basis $\left(X_{Ai},\ Y'_{Ai},\ Z_{Ai}\right)$

$$[C_i{*}]^T = \begin{bmatrix} C_{i1} & 0 \\ C_{i2} & 0 \\ 0 & 1 \end{bmatrix}$$

C_{i1} is the direction cosine between the X_s space station axis (roll) and X_{Ai}

C_{i2} is the direction cosine relating X_s and Y_{Ai}

$$\left.w_i\right] = \begin{bmatrix} C_{i1} & 0 \\ C_{i2} & 0 \\ 0 & 1 \end{bmatrix} \begin{bmatrix} 1/KG & 0 \\ 0 & 1 \end{bmatrix} \begin{bmatrix} \hat{w}_{Ai1} \\ w_{Ai2} \end{bmatrix}$$

Equation Set II - Space Station Rotation

$$[A_2]\ \ddot{R}_0] + [A_6]\ \dot{w}_0] + [A_{10}]\ \dot{w}_{A1}] + [A_{14}]\ \dot{w}_{A2}] = F_2]$$

$$[A_2] = m_1 \left(-[\tilde{r}_1'] + [C_1^{**}]\ [\tilde{r}_1]\ [C_1]^T\right) + m_2 \left(-[\tilde{r}_2'] + [C_2^{**}]\ [\tilde{r}_2]\ [C_2]^T\right)$$

$$\begin{aligned}[A_6] = {} & [I_0] + m_1 [\tilde{\tilde{r}}_1'] \left(R_0] + h_1] + [C_1]\ r_1]\right)^{\sim} \\ & + m_2 [\tilde{r}_2'] \left(R_0] + h_2] + [C_2]\ r_2]\right)^{\sim} \\ & + [C_1^{**}] \left([I_1]\ [C_1]^T - m_1 [\tilde{r}_1]\ [C_1]^T \left(R_0] + h_1] + [C_1]\ r_1]\right)^{\sim}\right) \\ & + [C_2^{**}] \left([I_2]\ [C_2]^T - m_2 [\tilde{r}_2]\ [C_2]^T \left(R_0] + h_2] + [C_2]\ r_2]\right)^{\sim}\right)\end{aligned}$$

$$[A_{10}] = + m_1 [\tilde{r}_1']\ [C_1]\ [\tilde{r}_1]\ [C_1^*]^T \begin{bmatrix} 1/KG^2 & 0 \\ 0 & 1 \end{bmatrix}$$

$$[A_{14}] = + m_2 [r_2']\ [C_2]\ [\tilde{r}_2]\ [C_2^*]^T \begin{bmatrix} 1/KG^2 & 0 \\ 0 & 1 \end{bmatrix}$$

$$[F_2] = -[\tilde{\ell}_r]\ F_R] - T_1] - T_2]$$

$$-[\tilde{w}_0]\ [I_0]\ w_0] + \begin{bmatrix} 1/KG & 0 & 0 \\ 0 & 1 & 0 \\ 0 & 0 & 1 \end{bmatrix} [\tilde{r}_1']\ F_{H1}']$$

$$+ \begin{bmatrix} 1/KG & 0 & 0 \\ 0 & 1 & 0 \\ 0 & 0 & 1 \end{bmatrix} [\tilde{r}_2']\ F_{H2}'] + T_{CMG}]$$

$$+ C_1^{**} \left(T_{A1}] - \left([C_1]^T\ w_0] \right)^{\sim} [I_1]\ [C_1]\ w_0] - [\tilde{r}_1]\ [C_1]^T\ F_{H1}'] \right)$$

$$+ C_2^{**} \left(T_{A2}] - \left([C_2]\ w_0] \right)^{\sim} [I_2]\ [C_2]\ w_0] - [\tilde{r}_2]\ [C_2]^T\ F_{H2}'] \right)$$

and

$$F_{H1}'\Big] = m_1 \begin{bmatrix} [\tilde{w}_0]\ [\tilde{w}_0]\ \left(R_0] + h_1] \right) + 2\ [\tilde{w}_0]\ \dot{R}_0] \\ \left(2\ [\tilde{w}_0]\ [C_1]\ [\tilde{w}_1] + [\tilde{w}_0]\ [\tilde{w}_0]\ [C_1] \right) r_1] + \\ [C_1]\ [\tilde{w}_1]\ [\tilde{w}_1]\ r_1] \end{bmatrix} + [C_1]\ F_{A1}]$$

$$F_{H2}'\Big] = m_2 \begin{bmatrix} [\tilde{w}_0]\ [\tilde{w}_0]\ \left(R_0] + h_2] \right) + 2\ [\tilde{w}_0]\ \dot{R}_0] \\ \left(2\ [\tilde{w}_0]\ [C_2]\ [\tilde{w}_2] + [\tilde{w}_0]\ [\tilde{w}_0]\ [C_2] \right) r_2] + \\ [C_2]\ [\tilde{w}_2]\ [\tilde{w}_2]\ r_2] \end{bmatrix} + [C_2]\ F_{A2}]$$

where

$$r_i'] = r_0] - h_i]$$

$F_{H1}']$ & $F_{H2}']$ - are the hinge force equations less the linear terms in $\ddot{R}_0$, $\dot{w}_0$, and $\dot{w}_i$

The terms in C_i^{**} represent the effect of the normally constrained rigid driver axis moment on the space station moment equation

$$C_i^{**} = [C_i] \begin{bmatrix} +C_{i12} \\ -C_{i11} \\ 0 \end{bmatrix} \lfloor C_{i12} \; - C_{i11} \; 0 \rfloor$$

$i = 1,2$ gives the projection of constrained axis component of the i^{TH} driver variables onto the space station axes.

Equation Set III - Rigid Driver 1 Dynamics

The dynamics of the X_{A1} and Y_{A1} axes are restricted to rotation about the X_s direction.

$$[A_3]\ \ddot{R}_0] + [A_7]\ \dot{w}_0] + [A_{11}]\ \dot{w}_{A1}] + [A_{15}]\ \dot{w}_{A2}] = F_3]$$

$$[A_3] = + [C_1^*]\ [m_1]\ [\tilde{r}_1]\ [C_1]^T$$

$$[A_7] = \begin{bmatrix} 1/KG & 0 \\ 0 & 1 \end{bmatrix} \left[[C_1^*]\ [I_1]\ [C_1]^T - m_1\ [\tilde{r}_1]\ [C_1]^T\ (R_0] + h_1] + [C_1]\ r_1])^{\sim} \right]$$

$$[A_{11}] = \begin{bmatrix} 1/KG^2 & 0 \\ 0 & 1 \end{bmatrix} [C_1^*]\ ([I_1] - m_1\ [\tilde{r}_1]\ [\tilde{r}_1])\ [C_1^*]^T$$

$$[A_{15}] = 0$$

$$F_3] = \begin{bmatrix} 1/KG & 0 \\ 0 & 1 \end{bmatrix} [C_1^*] \begin{bmatrix} T_{A1}] + \left([C_1]^T\ T_1]\right)\ KG \\ - [I_1]\ ([C_1]^T\ w_0])^{\sim}\ w_1] \\ - \left(([C_1]^T\ w_0])^{\sim} + [\tilde{w}_1] \right) [I_1]\ (w_1] + [C_1]^T\ w_0]) \\ - [\tilde{r}_1]\ [C_1]^T\ F'_{H1}] \end{bmatrix}$$

Equation Set IV - Rigid Driver 2 Dynamics

$$[A_4]\ \ddot{R}_0] + [A_8]\ \dot{w}_0] + [A_{12}]\ \dot{w}_{A1}] + [A_{16}]\ \dot{w}_{A2}] = F_4]$$

$$[A_4] = + [C_2^*]\ m_2\ [\tilde{r}_2]\ [C_2]^T$$

$$[A_8] = \begin{bmatrix} 1/KG & 0 \\ 0 & 1 \end{bmatrix} \left[[C_2^*]\ [I_2]\ [C_2]^T - m_2\ [\tilde{r}_2]\ [C_2]^T\ (R_0] + h_2] + [C_2]\ r_2])^{\sim} \right]$$

$$[A_{12}] = 0$$

$$[A_{16}] = \begin{bmatrix} 1/KG^2 & 0 \\ 0 & 1 \end{bmatrix} [C_2^*]\ ([I_2] - m_2\ [\tilde{r}_2]\ [\tilde{r}_2])\ [C_2^*]^T$$

$$F_4] = \begin{bmatrix} 1/KG & 0 \\ 0 & 1 \end{bmatrix} [C_2^*] \left[\begin{array}{l} T_{A2}] + \left([C_2]^T\ T_2]\right) KG \\ -[I_2]\ ([C_2]^T\ w_0])^{\sim}\ w_2] - [\tilde{r}_2]\ [C_2]^T\ F'_{H2}] \\ -\left(([C_2]^T\ w_0])^{\sim} + [\tilde{w}_2]\right) \cdot [I_2]\ (w_2] + [C_2]^T\ w_0]) \end{array} \right]$$

where

$$w_1] = [C_1^*]^T \begin{bmatrix} 1/KG & 0 \\ 0 & 1 \end{bmatrix} \begin{matrix} \hat{w}_{A11} \\ \hat{w}_{A12} \end{matrix}\Bigg]$$

$$w_2] = [C_2^*]^T \begin{bmatrix} 1/KG & 0 \\ 0 & 1 \end{bmatrix} \begin{matrix} \hat{w}_{A21} \\ \hat{w}_{A22} \end{matrix}\Bigg]$$

and

$$[\dot{C}_1] = [C_1] \quad [\tilde{w}_1]$$

$$[\dot{C}_2] = [C_2] \quad [\tilde{w}_2]$$

4.1.3.3 APPLICATION OF ADDITIONAL CONSTRAINTS

The constraint torque imposed by the rigid driver axis simultaneously normal to the roll axis and the array vane axis has been incorporated into simulation by:

- Solving the driver equations for the constraint torque about the locked axis.

  $T_{Con} = f\,(\ddot{R}_0, \dot{w}_0, w_0, T_{A_i}, F_{H_i})$

- The moment applied to the space station is the negative of this constraint torque which is applied by combining the terms in $\ddot{R}_0$ and $\dot{w}_0$ with those of A_2 and A_6 for the unconstrained case and adding the remaining terms to F_2.

This results, as we have previously noted, in the addition of a set of terms preceded by C_i^{**} which is the direction cosine matrix relating the normally constrained driver axis to the space station axes.

We could perform the same procedure for additional constraints imposed by the user and solve a further reduced matrix. However, since the values of these constraints are of real interest for engineering analysis an alternative scheme is utilized:

- The matrix equation for the affected axis is changed from an equation in $\ddot{R}_0$, $\dot{w}_0$ and $\dot{w}_A$ to an equation in $\ddot{R}_0$, $\dot{w}_0$ and T_C, the constraint torque. In other words, we now solve for the constraint torque instead of the rotational acceleration.

  In terms of matrix changes the appropriate row of matrix A_{11} and A_{16} is changed to $\lfloor -1 \;\; 0 \rfloor$ if the axis parallel to the roll axis is constrained or $\lfloor 0 \;\; -1 \rfloor$ if the vane axis is constrained.

- Since the affected matrix variable is now constraint torque, the columns of A_{10} and A_{14} are changed to give the projection of the negative of constraint torque in space station coordinates. If the vane axis is constrained, the second column of these matrices become

$$\left.\begin{matrix} C_{i31} \\ C_{i32} \\ C_{i33} \end{matrix}\right] \qquad i = 1,2$$

If the other axis is constrained the first column is changed to

$$\left.\begin{matrix} 1 \\ 0 \\ 0 \end{matrix}\right]$$

and both are changed accordingly if the drivers are completly locked.

4.1.4 FLEXIBLE ARRAY DYNAMICS

4.1.4.1 GENERAL FORMULATION OF A FLEXIBLE APPENDAGE EQUATION

The model for the flexible array dynamics is adapted from the synthetic modes approach developed by Likens in Reference 4.1. The utilization of orthogonal modes augmented by a set of synthetic modes is an attractive approach for simulating the dynamics of large, driven, flexible structures from both a modeling and a computational efficiency viewpoint. The geometry of the system considered is shown in Figure 4-7.

Major Assumptions and Conventions

- Each flexible array utilizes the basis associated with the rigid driver to which it is fixed. This is the basis in which the equations are solved.
- The particle masses have negligible inertias about their respective CG's
- The appendage deflections are sufficiently small that conventional structural analysis is valid; i.e., the system is linear.

Force on i^{TH} Particle

$$F_i = m_i \frac{d^2}{dt^2} \left(\bar{R}_0 + \bar{h}_J + \bar{\ell}_J + \bar{r}_i + U_i\right)\Bigg|_I$$

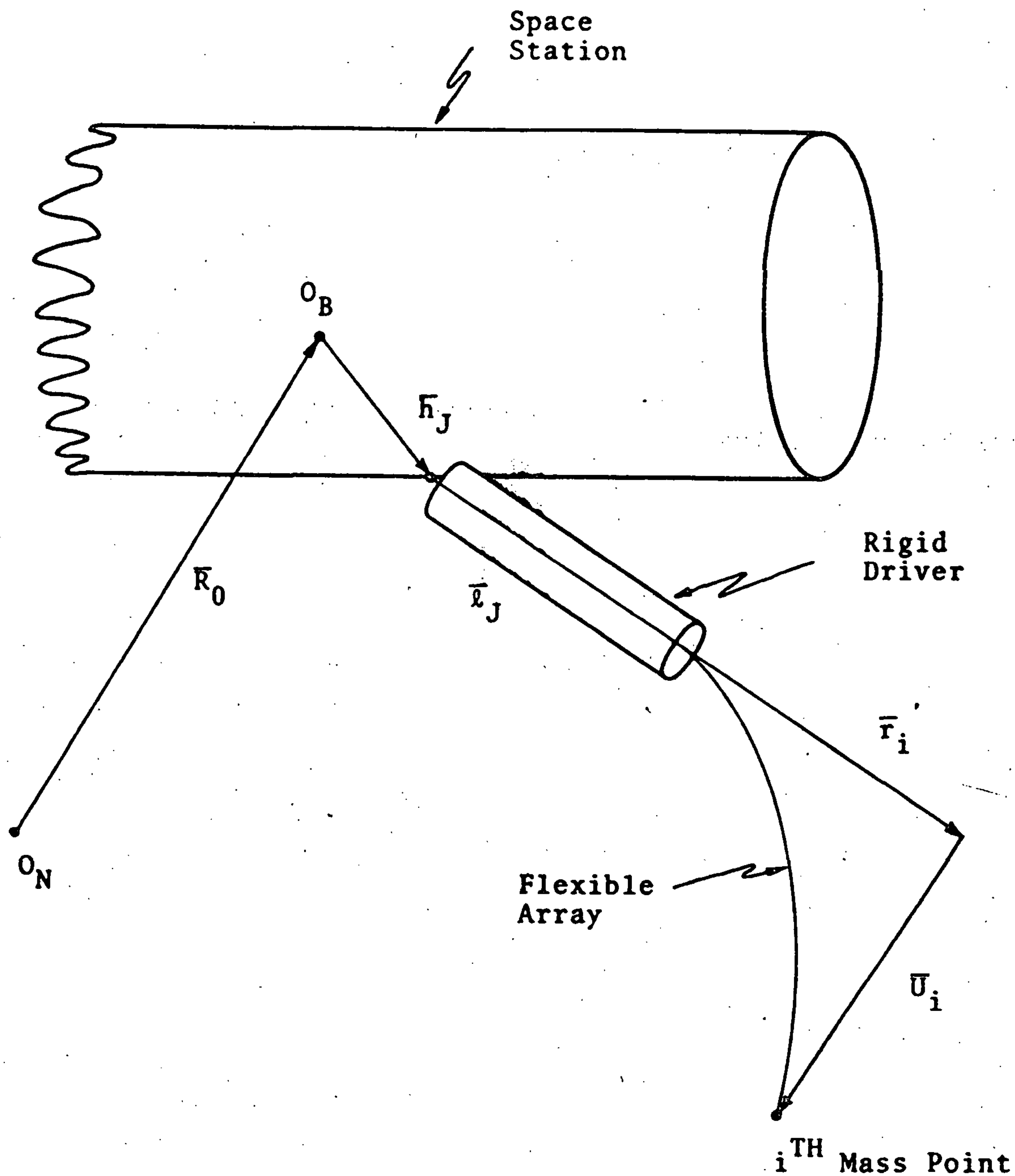

$$\bar{P}_i = \bar{R}_0 + \bar{h}_J + \bar{\ell}_J + \bar{r}_i + \bar{U}_i$$

$\bar{P}_i$ - vector position of i^{TH} mass particle of flexible appendage J

$\bar{r}_i$ - vector position of i^{TH} mass particle for undeformed appendage

$\bar{U}_i$ - vector deflection of mass particle

Figure 4-7 Flexible Array Geometry

In order to simplify the notation in the following list:

$$\underline{R_0} = C_J^T R_0$$

$$\underline{w_0} = C_J^T w_0 C_J$$

$$F_i = m_i \left[\begin{array}{l} \ddot{\underline{R_0}} + 2\underline{\tilde{w}_0} \, \dot{\underline{R_0}} + (\dot{\underline{\tilde{w}_0}} + \underline{\tilde{w}_0}\,\underline{\tilde{w}_0})(\underline{R_0} + \underline{h_J} + \ell_J + r_i + U_i) \\ + (\dot{\tilde{w}}_J + \tilde{w}_J \tilde{w}_J)(\ell_J + r_i + U_i) + 2\underline{\tilde{w}_0}\,\tilde{w}_J (\ell_J + r_i + U_i) \\ + 2(\underline{\tilde{w}_0} + w_J)\dot{U}_i + \ddot{U}_i \end{array} \right]$$

$J=1,2 \quad i=1,2....n$

Because of the linear elastic properties of the flexible array the force F_J is also related to the deformation of the array and the applied loads:

$$[M]\, q + [K]\, q = -\, [G]\, q - [B]\, q + L$$

where

$$q = [U_1^{\,1} \;\; U_2^{\,1} \;\; U_3^{\,1} \;\; U_1^{\,2} \;\; U_2^{\,2} \;\; U_3^{\,2} \; - - - \; U_1^{\,N} \;\; U_2^{\,N} \;\; U_3^{\,N}]$$

K is the symmetric stiffness matrix

L is the matrix of applied loads and rigid body forcing functions.

$$M = \begin{bmatrix} m_1 & 0 & 0 & 0 & 0 & 0 \\ 0 & m_2 & 0 & 0 & 0 & 0 \\ 0 & 0 & m_3 & 0 & 0 & 0 \\ 0 & 0 & 0 & m_4 & 0 & 0 \\ 0 & 0 & 0 & 0 & \ddots & \end{bmatrix}$$

$3n \times 3n$

$$G = \begin{bmatrix} \underset{3\times3}{2\tilde{w}_T\, m_1} & 0 & 0 & 0 & 0 \\ 0 & 2\tilde{w}_T m_2 & 0 & 0 & 0 \\ 0 & 0 & 2\tilde{w}_T m_3 & 0 & 0 \\ 0 & 0 & 0 & \ddots & \end{bmatrix}$$

$3n \times 3n$

$$w_T = \underline{w_0} + w_J$$

$$
B = \begin{bmatrix}
\underset{3\times3}{m_1\,\dot{\underline{\Omega}}} & 0 & 0 & 0 & 0 \\
0 & \underset{3\times3}{m_2\,\dot{\underline{\Omega}}} & 0 & 0 & 0 \\
0 & 0 & m_3\,\dot{\underline{\Omega}} & 0 & 0 \\
 & & & \ddots &
\end{bmatrix}
$$

$$
\begin{aligned}
\dot{\underline{\Omega}} &= \dot{\tilde{w}}_T + \underline{\tilde{w}_0}\;\underline{\tilde{w}_0} + \tilde{w}_J\,\tilde{w}_J + 2\,\underline{\tilde{w}_0}\,\tilde{w}_J \\
&= \dot{\tilde{w}}_T + \tilde{w}_T\,\tilde{w}_T
\end{aligned}
$$

Before formulating the expression for the L term the following identities are useful

$$
\sum_E = \begin{bmatrix} \underset{3\times3}{E} & \vdots & \underset{3\times3}{E} & \vdots & \cdots\cdots\cdots & E \end{bmatrix}^T
$$

$$
\hat{\sum}_{EO} \begin{bmatrix} \underset{3\times3}{E} & \vdots & \underset{3\times3}{0} \end{bmatrix}^T
$$

$$
\hat{\sum}_{OE} \begin{bmatrix} \underset{3\times3}{0} & \vdots & \underset{3\times3}{E} \end{bmatrix}^T
$$

where

$$\begin{bmatrix} E \\ 3x3 \end{bmatrix} = \begin{bmatrix} 1 & 0 & 0 \\ 0 & 1 & 0 \\ 0 & 0 & 1 \end{bmatrix}$$

$$\bar{r} = [r_1 \; r_2 \; r_3 \; - - - - \; r_n]^T$$

$$\tilde{A}B = -\tilde{B}A$$

$$\ddot{R}_J = \underline{\ddot{R}_0} - (\widetilde{R_0 + h_J}) \; \underline{\dot{w}_0}$$

$$w_T = \underline{w_0} + w_J$$

$$L = -M \sum_E [\ddot{R}_J - \widetilde{\ell_J'} \; \dot{w}_T] + M \tilde{r} \dot{w}_T$$

$$-M \sum_E C - M D \bar{r} + \lambda$$

where

$$\tilde{r} = \underset{3n \times 3n}{\begin{bmatrix} \underset{3x3}{\tilde{r}_1} & 0 & 0 & 0 \\ & \underset{3x3}{\tilde{r}_2} & 0 & 0 \\ & & & 0 \\ \text{SYMMETRIC} & & & \end{bmatrix}}, \qquad \lambda = \underset{3n \; x1}{\begin{bmatrix} \lambda_1 \\ \lambda_2 \\ \vdots \\ \lambda_{3n} \end{bmatrix}}$$

$$[C] = 2\,\underline{w_0}\,\underline{\dot{R}_0} + \underline{\tilde{w}_0}\,\underline{\tilde{w}_0}\,(\underline{R_0}+\underline{h_J}) + \tilde{w}_T\,w_T\,\ell_J + \tilde{r}_J\,\dot{w}_T$$

$$\underset{3n\times3n}{\left[\,D\,\right]} = \begin{bmatrix} \left(\sum_E \underline{w_0}\right)^{\sim}\left(\sum_E \underline{w_0}\right)^{\sim} + \left(\sum_E w_J\right)^{\sim}\left(\sum_E w_J\right)^{\sim} \\ + 2\left(\sum_E \underline{w_0}\right)^{\sim}\left(\sum_E w_J\right)^{\sim} \end{bmatrix}$$

$$\left(\sum_E w\right)^{\sim} = \begin{bmatrix} \tilde{w} & 0 & 0 & 0 \\ 0 & \tilde{w} & 0 & 0 \\ 0 & 0 & \tilde{w} & 0 \\ 0 & 0 & 0 & \tilde{W} \end{bmatrix}$$

Let

$$\ddot{U} = \begin{matrix} \ddot{R}_J \\ \dot{w}_T \end{matrix}\Bigg]$$

$$L = -M\left(\sum_E \hat{\sum}^T_{EO} - \left(\sum_E \tilde{\ell}'_J - \tilde{r}\right)\hat{\sum}^T_{OE}\right)\ddot{U}$$

$$- M\left(\sum_E C + D\,\overline{r}\right) + \lambda$$

where

$$\ell'_J = \ell_J - r_J$$

Conversion to Normal Coordinates

There exists a unique orthogonal transformation which has the following properties:

a. $\phi^T M \phi = [E]$

b. $\phi^T K \phi = \begin{bmatrix} \sigma_1^2 & & & \\ & \sigma_2^2 & & \\ & & \ddots & \\ & & & \sigma_N^2 \end{bmatrix} = \overline{\sigma^2}$

such that

$$q\,(R,t) = \phi(R)\,\eta(t)$$

A finite number of cantilever modes ($\overline{\phi}$) satisfying (a) and (b) are utilized to transform the appendage equation:

$$M\overline{\Phi}\ddot{\eta} + K\phi\eta = -G\phi\dot{\eta} - B\phi\eta + L$$

Premultiplying by $\overline{\phi}^T$ we have

$$\ddot{\overline{\eta}} + 2\xi\overline{\sigma}\,\dot{\overline{\eta}} + \overline{\sigma}^2\,\eta = \overline{\phi}^T G\overline{\phi}\,\dot{\overline{\eta}} - \phi^T B\overline{\phi}\,\eta + \overline{\phi}^T L$$

$\bar{\eta}, \dot{\bar{\eta}}, \ddot{\bar{\eta}}$ are N x 1 matrices where

N is the number of cantilevered modes utilized. Note that a modal damping term has been arbitrarily inserted in the classic manner of structural analysis.

Now since the appendage mass, mode shape, and geometry are all known a priori and remain invariant, the appendage equation can be reformulated to reduce the required computational effort

$$\ddot{\bar{\eta}} + 2\xi\bar{\sigma}\dot{\bar{\eta}} + \bar{\sigma}^2 \eta = -A_1 \dot{\bar{\eta}} - A_3 \bar{\eta}$$
$$-A_4 C - A_5$$
$$-\Delta' \ddot{U} + \phi^T L$$

where

$\ddot{\bar{\eta}}, \dot{\bar{\eta}}, \bar{\eta}$ are N x 1 vectors

4.1.4.2 ADDITION OF SYNTHETIC MODES

A particularly important term in the Appendage Equation is the next to the last term $\Delta' \ddot{U}$ where

$$\Delta' = -\bar{\phi}^T M \left(\sum_E \hat{\sum}_{EO}^T - \sum_E \hat{\sum}_{OE} \tilde{\ell}'_J - \tilde{r} \hat{\sum}_{OE} \right)$$

If we define $\Delta = \lim\limits_{N \to \infty} \Delta'$ it can be shown that

$$\Delta^T \Delta = \left[\begin{array}{c|c} \underset{3x3}{M_A} & \underset{3x3}{-P_A M_A} \\ \hline P_A M_A & I_A \end{array} \right]$$

where

M_A - Appendage mass

I_A - Apendage inertia

P_A - Centroid vector for appendage relative to attachment point.

Since $\Delta'^T \Delta' \neq \Delta^T \Delta$, the rigid or steady state representation of the appendage is inaccurate. In order to circumvent this difficulty, synthetic modes may be added in terms of additional rows for Δ'.

$$\text{Let } \Delta = \begin{bmatrix} \Delta' \\ \Delta'' \end{bmatrix}$$

The synthetic modes are then defined as

$$\ddot{\bar{\eta}}_s + 2\,\bar{\xi}_s \bar{\sigma}_s \dot{\bar{\eta}}_s + \bar{\sigma}_s^2\, \eta_s = \Delta''\, \ddot{U}_J$$

To avoid impacting the frequency range of interest the following procedures is utilized:

$$(\sigma_s)_{MIN} >> \sigma_{MAX}$$

$$\xi_s > .71.$$

The synthetic modes are computed in terms of a difference equation to avoid potential integration instability:

$$\eta_s(NT) = a\Delta''\ddot{U}(NT) + b\Delta''\ddot{U}(NT-T)$$

$$-d\,\eta_s(NT-T) \;-e\,\eta_s(NT-2T)$$

for each synthetic mode.

Six synthetic modes will be employed, each one will be chosen to satisfy the constraints for a given column and thus the first synthetic mode will have six coefficients, the second will have five and so forth, until the sixth mode which has only one coefficient.

The capability of using a steady state mode function is also included in this case

where

$$\eta_s(NT) = K\Delta''\ddot{U}(NT)$$

$$K = \frac{a+b}{1+d+e}$$

Forces and Torques Induced by the Flexible Appendage (from Likins)

$$f' = \sum_E^T M\phi\sigma^2\eta$$

$$l' = \left(\sum_E^T \tilde{r} + \tilde{\ell}_J' \sum_E^T\right) M\phi\sigma^2\eta$$

where f' and l' are respectively, the force and torque upon the rigid driver.

Let

$$\Lambda' = \begin{bmatrix} f' \\ l' \end{bmatrix}$$

$$\Lambda' = \left(\hat{\sum}_{EO} \sum_E + \hat{\sum}_{OE} \left(\hat{\sum}_E^T \tilde{r}+\tilde{\ell}_J \sum_E^T\right)\right) M\phi\sigma^2\eta$$

$$\Lambda' = -\Delta^T \sigma^2 \eta \text{ (for ideal } \Delta^T)$$

For the case where Δ is approximated by a finite number of cantilever modes augmented by the synthetic modes as discussed earlier

$$\Lambda' = -\bar{\Delta}^T \bar{\sigma}^{2} \bar{\eta}$$

$$\bar{\Delta}^T = [\bar{\Delta}_1 \ \bar{\Delta}_2]^T$$

where

$\bar{\Delta}_1^T \bar{\sigma}^2 \bar{\eta}$ - external force impressed upon J^{TH} rigid driver (F_{AJ})

$\bar{\Delta}_2^T \bar{\sigma}^2 \bar{\eta}$ - external torque impressed upon J^{TH} rigid driver (T_J)

Difference Equation Formulation for Synthetic Modes

Given an equation of the form

$$\ddot{q} + a\dot{q} + b\,q = F(t),$$

A difference equation formulation utilizing a staircase step representation of F(t) can be readily obtained by the use of Z transform theory. The equivalent block diagram corresponding to this approach is shown in the following figure.

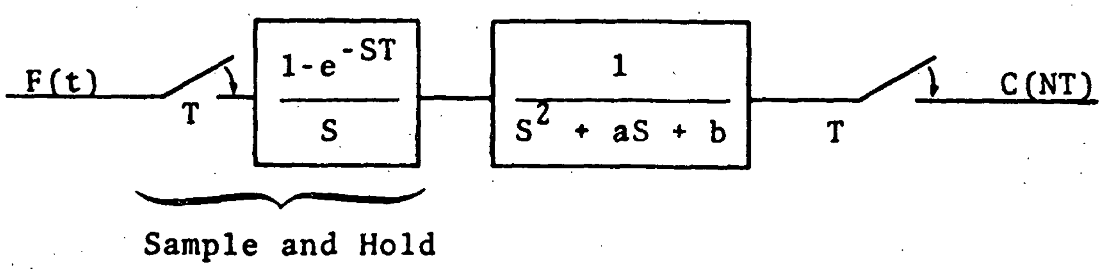

C(NT)	-	Output of system to staircase step representation of F(t) at t = NT
T	-	Sampling interval
S	-	LaPlace transform variable

In terms of the sampled data Z transform:

$$\frac{C(Z)}{F(Z)} = \frac{Z-1}{Z}\,\mathcal{Z}\left(\frac{1}{S(S^2+aS+b)}\right)$$

Let

$\mathcal{Z}$ = Z transformation

$\alpha = a/2$

$\beta^2 = b - \alpha^2$

$$\frac{1}{S[(S+\alpha)^2+\beta^2]} = \left[\frac{1}{S} - \frac{S+\alpha}{(S+\alpha)^2+\beta^2} - \frac{\alpha}{(S+\alpha)^2+\beta^2}\right]\left[\frac{1}{\alpha^2+\beta^2}\right]$$

Laplace Transform	Z Transform
$1/S$	$Z/Z-1$
$-(S+\alpha)/[(S+\alpha)^2 + \beta^2]$	$-\dfrac{(Z^2 - Ze^{-\alpha T}\cos\beta T)}{(Z^2 - 2Ze^{-\alpha T}\cos\beta T + e^{-2\alpha T})}$
$-\alpha/[(S+\alpha)^2 + \beta^2]$	$-\dfrac{\alpha}{\beta}\dfrac{(Ze^{-\alpha T}\sin\beta T)}{(Z^2 - 2Ze^{-\alpha T}\cos\beta T + e^{-2\alpha T})}$

$$\frac{C(Z)}{F(Z)} = \frac{Z-1}{Z}\,\frac{1}{b}\left[\frac{\begin{array}{l} Z^3 - 2Z^2\,e^{-\alpha T}\cos\beta T + e^{-2\alpha T}\,Z \\ -Z^3 + Z^2\,(e^{-\alpha T}\cos\beta T - \frac{\alpha}{\beta}\,e^{-\alpha T}\sin\beta T) \\ +Z^2 - Ze^{-\alpha T}\cos\beta T + \frac{\alpha}{\beta}\,Ze^{-\alpha T}\sin\beta T) \end{array}}{(Z-1)\,(Z^2 - 2Ze^{-\alpha T}\cos\beta T + e^{-2\alpha T})}\right]$$

$$= \frac{1}{b}\left[\frac{\begin{array}{l} Z\,(1-e^{-\alpha T}\cos\beta T - \alpha/\beta e^{-\alpha T}\sin\beta T) \\ +\,(e^{-2\alpha T} - e^{\alpha T}\cos\beta T + \frac{\alpha}{\beta}\,e^{-\alpha T}\sin\beta T) \end{array}}{Z^2 - 2Ze^{-\alpha T}\cos\beta T + e^{-2\alpha T}}\right]$$

The equivalent difference equation is:

$$C(NT) = a_1 \, F\,(NT-T) + a_2 \, F\,(NT-2T)$$
$$-a_3 \, C\,(NT-T) - a_4 \, C\,(NT-2T)$$

where

$$a_1 = (1-e^{-\alpha T} \cos \beta T - \alpha/\beta \; e^{-\alpha T} \sin \beta T)$$

$$a_2 = (e^{-2\alpha T} - e^{-\alpha T} \cos \beta T + \alpha/\beta e^{-\alpha T} \sin \beta T)$$

$$a_3 = -2e^{-\alpha T} \cos \beta T$$

$$a_4 = e^{-2\alpha T}$$

$X(NT)$ - present sampled value of X

$X(NT-T)$ - previous sampled value of X

4.1.4.3 PRESIMULATION COMPUTATIONS

The form of the appendage equation given in the preceding section is:

$$\ddot{\bar{\eta}} + 2\xi\sigma\,\dot{\bar{\eta}} + \sigma^2\,\bar{\eta} = -A_1\dot{\bar{\eta}} - A_3\bar{\eta} - A_4C - A_5 - \Delta\ddot{U}$$

In their most general form these equations require the multiplication of 3nx3n matrices where n is the number of mass points used to define the appendage. The form of the mass matrix employed allows considerable simplification of the computation and permits the calculation of a set of coefficients of much reduced order prior to the actual simulation.

<u>Computation of A_2, A_4, A_6</u>

From the preceding equation we can define the A_1 and A_3 matrices in terms of rigid body rotation parameters and A_2, a constant matrix:

$$A_{1_{\ell m}} = \sum_{i=1}^{3}\sum_{J=1}^{3} 2\,\tilde{w}_{T_{iJ}}\,A_{2_{iJ\ell m}}$$

$$A_{3_{\ell m}} = \sum_{i=1}^{3}\sum_{J=1}^{3} \dot{\tilde{\Omega}}_{iJ}\,A_{2_{iJ\ell m}}$$

where

$$A_{2_{IJ\ell m}} = \sum_{k=1}^{n} \phi^{m}_{kJ}\,\phi^{\ell}_{ki}\,m_k$$

ℓ, m	-	cantilever mode numbers $(0 < \ell,m \leq N)$
k	-	mass point number $(0 < k \leq n)$
i, J	-	identify the three components of the n mode shape displacements $(0 < i,J \leq 3)$
m_k	-	k^{TH} mass element $(0 < k \leq n)$

A_4 is an Nx3 matrix which multiplies the 3x1 C matrix which is a summation of rigid acceleration terms

$$A_{4_{\ell i}} = \sum_{k=1}^{n} \phi_{ki}^{\ell} \, m_k$$

ℓ - cantilever mode number $(0 < \ell \leq N)$

i - component identifier $(0 < i \leq 3)$

The A_5 matrix can be reduced to the product of a constant matrix and a matrix of rigid angular accelerations:

$$A_{5_\ell} = \sum_{J=1}^{3} \sum_{i=1}^{3} d_{Ji} \, A_{6_{Ji\ell}}$$

where

$$A_{6_{Ji\ell}} = \sum_{k=1}^{n} m_k \, \phi_{ki}^{\ell} \, r_{ki}$$

where

d_{Ji} are rigid acceleration terms

r_{ki} are the coordinates of the undeflected mass points relative to the attachment point.

Computation of the Δ Matrix

The Δ matrix is an (N+6x6) matrix which is composed entirely of constant parameters. It is formed by calculating the unaugmented Δ matrix Δ′ (Nx6) shown below and augmenting this matrix to obtain the desired $\Delta^T\Delta$ product.

$$\Delta' = -\phi^T M \begin{pmatrix} \sum\limits_{E} \hat{\Sigma}^T_{EO} \cdot \tilde{b}_i & \sum\limits_{E} \hat{\Sigma}^T_{OE} \end{pmatrix}$$

where each $\tilde{b}_i$ is a 3 x 3 matrix formed by $\tilde{b}_i = (r_i + 1'_J)$

The matrix multiplication may be performed yielding the general formula for Δ′, an (Nx6) matrix shown below:

$$\text{a)} \quad \Delta'_{lm} = \sum_{i=1}^{n} m_i \ \phi^1_{im}$$

for ℓ and m such that $1 \leq \ell \leq N$ and $1 \leq m \leq 3$

$$\text{b)} \quad \Delta'_{lm} = \sum_{i=1}^{n} m_i \left(\phi^1_{ik}\, b_{ij} - \phi^1_{ij}\, b_{ik} \right)$$

for ℓ and m such that $1 \leq \ell \leq N$ and $4 \leq m \leq 6$
where the J's and k's are related to m by:

m	j	k
4	2	3
5	3	1
6	1	2

Six rows will be added to the Δ' matrix to form the Δ matrix. These rows will be added in such a manner so that the new Δ matrix will represent the real world. This is accomplished by performing the multiplication $\Delta^T\Delta$. This multiplication should equal.

$$\underset{\text{(ideal)}}{\Delta^T\Delta} = \begin{bmatrix} M_A & 0 & 0 & 0 & P_{A3}M_A & -P_{A2}M_A \\ 0 & M_A & 0 & -P_{A3}M_A & 0 & P_{A1}M_A \\ 0 & 0 & M_A & P_{A2}M_A & -P_{A1}M_A & 0 \\ 0 & -P_{A3}M_A & P_{A2}M_A & I_{A11} & I_{A12} & I_{A13} \\ P_{A3}M_A & 0 & -P_{A1}M_A & I_{A21} & I_{A22} & I_{A23} \\ -P_{A2}M_A & P_{A1}M_A & 0 & I_{A31} & I_{A32} & I_{A33} \end{bmatrix}$$

where

a. M_A is the total mass of the flexible appendage

b. $P_{A_{1,2,3}}$ is the coordinates of the appendage mass centroid, with respect to the attachment point.

$$P_{Ai} = \left[\sum_{k=1}^{n} (r_{ki} + 1_{,})\, m_k\right] / M_A$$

c. I_A is the moment of inertia with respect to the attachment point.

$$I_A = -\sum_{k=1}^{n} m_k \tilde{b}_k^{\,2}$$

Since every element of the $\Delta^T\Delta$ product has the form:

$$(\Delta^T\Delta)_{iJ} = \Delta_{1i}\,\Delta_{1J} + \Delta_{2i}\,\Delta_{2y} \text{------} \Delta_{Ni} + \Delta_{NJ}$$

We can add a row of augmenting Δ's to obtain a perfect row in the $\Delta^T\Delta$ matrix; e.g., add

$\Delta_{N+1,1}$ $\Delta_{N+1,1}$ to idealize 1, 1 element

$\Delta_{N+1,1}$ $\Delta_{N+1,2}$ to idealize 1, 2 element

and so forth.

We can perform the same function for the second row and by making its first entry zero, avoid changing the previously obtained result. This process continues until six rows of augmenting Δ's have been developed. (The last row is a single element.)

The six augmenting Δ rows are defined by the following set of equations:

$$\Delta_{(N+1)1} = \left[M_A - \sum_{i=1}^{N} \Delta_{i1}\, \Delta_{i1} \right]^{1/2}$$

$$\Delta_{(N+1)j} = -\left(\sum_{i=1}^{N} \Delta_{ij}\, \Delta_{i1} \right) / \Delta_{(N+1)1} \qquad j = 2,3,4$$

$$\Delta_{(N+1)5} = \left(P_{A3} M_A - \sum_{i=1}^{N} \Delta_{i5}\, \Delta_{i1} \right) / \Delta_{(N+1)1}$$

$$\Delta_{(N+1)6} = \left(-P_{A2} M_A - \sum_{i=1}^{N} \Delta_{i6}\, \Delta_{i1} \right) / \Delta_{(N+1)1}$$

$$\Delta_{ij} = 0 \qquad \begin{aligned} i &= N+k \\ j &= 1,2,\ldots k-1 \\ k &= 2,3,4,5,6 \end{aligned}$$

$$\Delta_{(N+2)2} = \left[M_A - \sum_{i=1}^{N+1} \Delta_{i2}\, \Delta_{i2} \right]^{1/2}$$

$$\Delta_{(N+2)j} = -\left(\sum_{i=1}^{N+1} \Delta_{ij}\, \Delta_{i2} \right) / \Delta_{(N+2)2} \qquad J = 3,5$$

$$\Delta_{(N+2)4} = -P_{A3}M_A \sum_{i=1}^{N+1} \Delta_{i4}\,\Delta_{i2}\,/\Delta_{(N+2)2}$$

$$\Delta_{(N+2)6} = P_{A1}M_A - \sum_{i=1}^{N+1} \Delta_{i4}\,\Delta_{i2}\,/\Delta_{(N+2)2}$$

$$\Delta_{(N+3)3} = \left[M_A - \sum_{i=1}^{N+2} \Delta_{i3}\,\Delta_{i3}\right]^{1/2}$$

$$\Delta_{(N+3)4} = P_{A2}M_A - \sum_{i=1}^{N+2} \Delta_{14}\,\Delta_{i3}\,/\Delta_{(N+3)3}$$

$$\Delta_{(N+3)5} = P_{A2}M_A - \sum_{i=1}^{N+2} \Delta_{i5}\,\Delta_{i3}\,/\Delta_{(N+3)3}$$

$$\Delta_{(N+3)6} = P_{A2}M_A - \sum_{i=1}^{N+2} \Delta_{i6}\,\Delta_{i3}\,/\Delta_{(N+3)3}$$

$$\Delta_{(N+4)4} = \left[I_{A11} - \sum_{i=1}^{N+3} \Delta_{i4}\,\Delta_{i4}\right]^{1/2}$$

$$\Delta_{(N+4)5} = I_{A21} - \sum_{i=1}^{N+3} \Delta_{i5}\,\Delta_{14}\,/\Delta_{(N+4)4}$$

$$\Delta_{(N+4)5} = I_{A21} - \sum_{i=1}^{N+3} \Delta_{i5}\,\Delta_{14} \;/\Delta_{(N+4)4}$$

$$\Delta_{(N+4)6} = I_{A31} - \sum_{i=1}^{N+3} \Delta_{i6}\,\Delta_{i4} \;/\Delta_{(N+4)6}$$

$$\Delta_{(N+5)5} = \left[I_{A22} - \sum_{i=1}^{N+4} \Delta_{i5}\,\Delta_{i5} \right]^{1/2}$$

$$\Delta_{(N+5)6} = I_{A23} - \sum_{i=1}^{N+4} \Delta_{i6}\,\Delta_{i5} \;/\Delta_{(N+5)5}$$

$$\Delta_{(N+6)6} = \left[I_{A33} - \sum_{i=1}^{N+5} \Delta_{i6}\,\Delta_{i6} \right]^{1/2}$$

As we have shown the equations, the inertial quantities not absorbed by the modal representation are accounted for by the synthetic modes representation. For the specific case which we are considering, the allocation of some of the mass and inertia to the rigid body driver is advisable. This requires that biased values of mass, moment of inertia and centroid location be used in lieu of the values now used.

4.1.5 GUIDANCE AND CONTROL

The STRISS simulation has two principal guidance and control functions:

- The space station is to be oriented with the roll axis normal to the orbit plane and yaw axis along the negative of the radius vector from the geocenter to the spacecraft.
- The two solar arrays are driven normal to the space station to sun line within the limits of permissible array motion.

4.1.5.1 SPACE STATION GUIDANCE

Since the commanded attitude is fixed relative to the R, T, N frame, computation of the space station commands consist of updating the (C_s) matrix as a function of orbit position and then multiplying by the constant (C_{Ac}) matrix to obtain the current value of $\overline{R}_{0_c}$ and $\overline{P}_{i_c}$.

$$[C_c] = [C_{Ac}]\ [C_s]$$

$$\overline{R}_{0_c} = \text{row 1 of } [C_c] \quad \text{(Commanded roll axis)}$$

$$\overline{P}_{i_c} = \text{row 2 of } [C_c] \quad \text{(Commanded pitch axis)}$$

where the vectors given above are expressed in inertial coordinates. For the nominal case where the roll axis is normal to the orbit plane and yaw is along the $-\overline{R}$ direction, the required Euler angle commands are:

$$\alpha_c = -90°$$

$$\beta_c = \gamma_c = 0$$

4.1.5.2 SOLAR ARRAY GUIDANCE

Orientation commands for the solar array drivers are obtained by using the cross product of the array Y_A axis and the earth-to-sun unit vector as an error signal. When the Y_A axis, which is normal to the plane of the solar array, is pointing toward the sun the error is null. Other orientations result in an error signal of proper sign being generated. The components of the error signal along the permitted axes of notation are then input to the array driver control equations.

Earth-to-Sun Unit Vector

$$\hat{S}\Big|_{EC1} = \begin{bmatrix} C\Gamma \\ S\Gamma \; C\Delta \\ S\Gamma \; S\Delta \end{bmatrix}$$

Γ - rotation of sun in ecliptic plane

Δ - deflection of ecliptic

$$\hat{S}\Big|_{ss} = [C_0]^T \; \hat{S}\Big|_{ECI}$$

Cross Product Law

$$\hat{E}1 = \hat{Y}_{A1} \times \hat{S}\Big|_{ss}$$

$$\hat{E}2 = \hat{Y}_{A2} \times \hat{S}\Big|_{ss}$$

$$\phi_{AE1} = \hat{E}1(1)$$

$$\phi_{AE2} = -\hat{E}2(1)$$

$$\psi_{AE1} = \hat{1}_{\psi 1} \cdot \hat{E}_1$$

$$\psi_{AE2} = \hat{1}_{\psi 2} \cdot E_2$$

where

$$\hat{i}_{\psi 1} = \begin{bmatrix} 0 \\ -S\phi_{A1} \\ C\phi_{A1} \end{bmatrix}$$

$$\hat{i}_{\psi 2} = \begin{bmatrix} 0 \\ -S\phi_{A2} \\ C\phi_{A2} \end{bmatrix}$$

ϕ_{AEi} and ψ_{AEi} are the solar array error components along the axes of allowable rotation for the i^{TH} driver.

4.1.5.3 SPACE STATION CONTROL

The space station attitude controls are affected by one of two methods:

- Control Moment Gyro (CMG)
- Reaction Control System

The program permits the selection of one or the other by setting a logical flag.

4.1.5.3.1 Control Moment Gyro (CMG) Dynamics

The CMG modelled in the simulation is the Three Parallel Mount (3 PM) configuration shown in Figure 4-8. This CMG and the mathematical description utilized were developed by the General Electric Company Defense Electronics Division (References 4.3 through 4.5) and utilizes three individual two degree of freedom CMG's mounted with their outer gimbal axes parallel. The CMG is mounted in the spacecraft with the parallel outer gimbal axes aligned with the space station axis of minimum moment of inertia which is, in the present case, the roll axis.

CMG COORDINATE FRAMES

The CMG will be mounted in the space station with the following orientation of the Outer Gimbal basis relative to the space station axes.

$$\begin{bmatrix} X_G \\ Y_G \\ Z_G \end{bmatrix}_{\substack{\text{Outer}\\\text{Gimbal}}} = \begin{bmatrix} 0 & 1 & 0 \\ 0 & 0 & 1 \\ 1 & 0 & 0 \end{bmatrix} \begin{bmatrix} X_s \\ Y_s \\ Z_s \end{bmatrix}$$

This orientation assumes that minimum momentum requirement is along the X_s (roll) spacecraft axis where

$$\begin{bmatrix} X_s \\ Y_s \\ Z_s \end{bmatrix} \quad \begin{Bmatrix} \text{roll} \\ \text{pitch} \\ \text{yaw} \end{Bmatrix} \quad \begin{Bmatrix} w_{ro} \\ w_{pi} \\ w_{ya} \end{Bmatrix} \quad \begin{Bmatrix} \phi \\ \theta \\ \psi \end{Bmatrix}$$

The I^{TH} CMG Inner Gimbal axis is defined by the following transformation

$$\begin{bmatrix} X \\ Y \\ Z \end{bmatrix}_{\substack{\text{Inner}\\ \text{Gimbal}}} = \begin{bmatrix} \cos\theta_i & \sin\theta_i & 0 \\ -\sin\theta_i & \cos\theta_i & 0 \\ 0 & 0 & 1 \end{bmatrix} \begin{bmatrix} X \\ Y \\ Z \end{bmatrix}_{\substack{\text{Outer}\\ \text{Gimbel}}}$$

$$\theta_i = \alpha_i + \delta_i$$

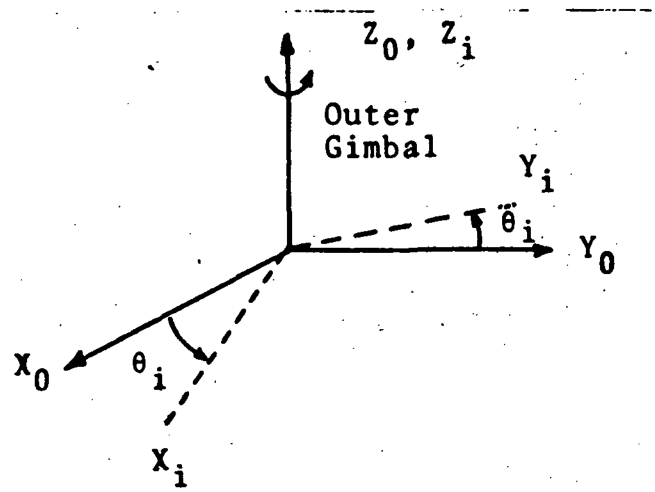

where $\delta_1 = 0$

$\delta_2 = 120°$

$\delta_3 = 240°$

and the δ's are fixed

α_i is the outer gimbal angle

In the parallel mount configuration employed there are three individual CMG gyros.

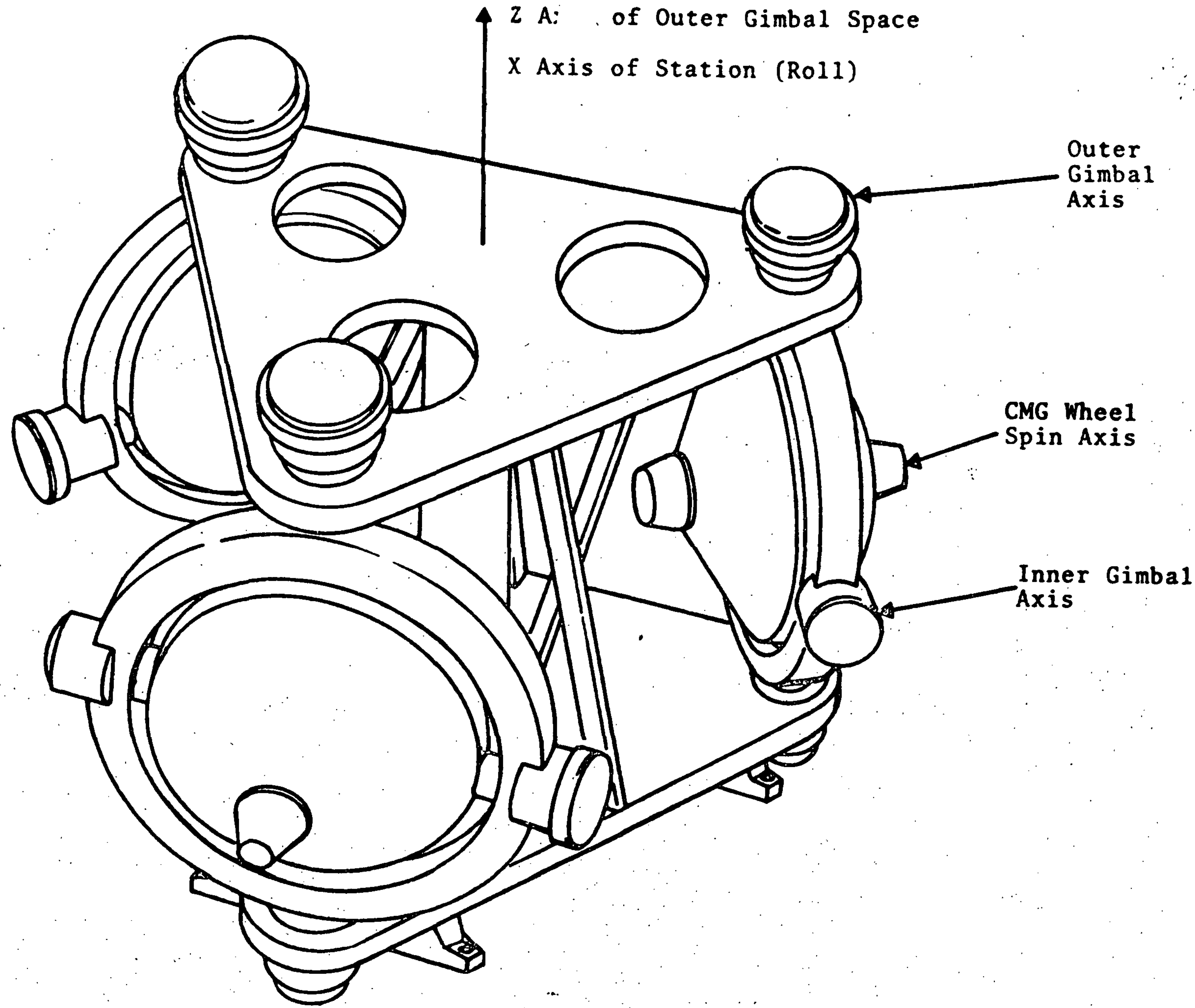

Figure 4-8 3 PM Control Moment Gyro Array

The I^{TH} CMG wheel momentum vector, $\bar{h}$, in the inner gimbal space is

$$h_{x_i} = 0$$
$$h_{y_i} = h \cos \gamma_i$$
$$h_{z_i} = h \sin \gamma_i$$

h - magnitude of each CMG momentum

γ_i - inner gimbal angle of I^{TH} CMG

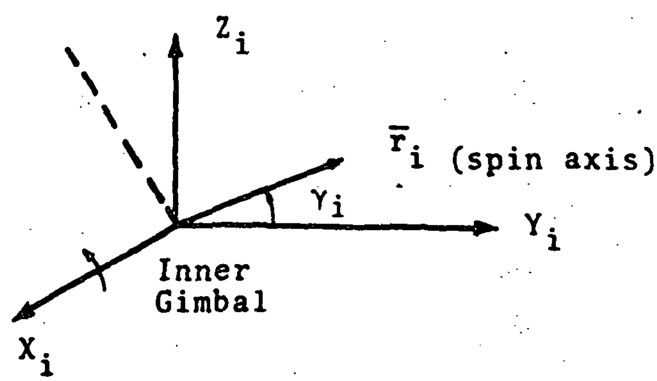

The CMG momentum wheel vector is, in Outer Gimbal space:

$$\begin{matrix} h_{xo} \\ h_{yo} \\ h_{zo} \end{matrix} = \begin{matrix} -\, h \cos \gamma_i \sin \theta_i \\ h \cos \gamma_i \cos \theta_i \\ h \sin \gamma_i \end{matrix}$$

The ITH CMG Inner Gimbal axis is defined by the following transformation

$$\begin{bmatrix} X \\ Y \\ Z \end{bmatrix}_{\substack{\text{Inner}\\\text{Gimbal}}} = \begin{bmatrix} \cos\theta_i & \sin\theta_i & 0 \\ -\sin\theta_i & \cos\theta_i & 0 \\ 0 & 0 & 1 \end{bmatrix} \begin{bmatrix} X \\ Y \\ Z \end{bmatrix}_{\substack{\text{Outer}\\\text{Gimbel}}}$$

$$\theta_i = \alpha_i + \delta_i$$

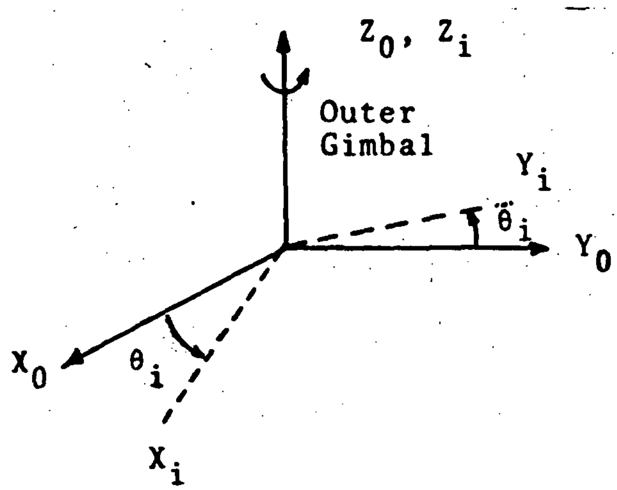

where $\delta_1 = 0$

$\delta_2 = 120°$

$\delta_3 = 240°$

and the δ's are fixed

α_i is the outer gimbal angle

In the parallel mount configuration employed there are three individual CMG gyros.

CMG TORQUE EQUATIONS

$$T_g = \dot{\bar{H}}_g = \mathring{\bar{H}} + \bar{w}_g \times \bar{H} \quad \text{(Torque Equation)}$$

where

T_g - external torque exerted <u>on</u> CMG

$\mathring{\bar{H}}_g$ - change in magnitude of momentum vector in CMG coordinates

$\bar{w}_g$ - rotation rate of CMG in inertial space

$\bar{H}$ - CMG momentum vector

$$\bar{H} = \bar{h}_{wheel} + \bar{\bar{I}}_{Gimbal} \; \bar{w}_g$$

$$\mathring{\bar{H}} = \cancelto{0}{\mathring{\bar{h}}} + \bar{\bar{I}}_{Gimbal} \; \mathring{\bar{w}}_g$$

$$\bar{w}_g \times \bar{H} \approx \bar{w}_g \times \bar{h}$$

where

$\bar{\bar{I}}_{Gimbal}$ is the CMG moment of inertia matrix (inertia tensor)

- ● implies the derivative with respect to inertial coordinates
- o implies the derivative with respect to CMG coordinates

Initial Conditions

Initially the CMG's have, for the nominal case, zero inner and outer gimbal angles. Thus we have

$$\theta_1 = 0°$$

$$\theta_2 = 120°$$

$$\theta_3 = 240°$$

and the net momentum of the system is identically zero.

The torque on the space station is equal to $-T_G$

$$T_{out} = -\left(\bar{\bar{I}}_{Gimbal} \cdot \overset{o}{\bar{w}}_g + \bar{w}_g \times \bar{h}\right)$$

Performing all computations in the Inner Gimbal space we have

$$T_{out_{xi}} = -I_{Gi} \ddot{\gamma}_i + w_{zi} h \cos \gamma - w_{yi} h \sin \gamma$$

$$T_{out_{yi}} = w_{xi} h \sin \gamma$$

$$T_{out_{zi}} = -I_{Go} \ddot{\alpha} - w_{xi} h \cos \gamma$$

where

w_i is the total inertial rate of the i^{TH} CMG gyro with respect to inertial space

$$w_{xi} = \dot{\gamma} + \Omega_{xi}$$

$$w_{yi} = \Omega_{yi}$$

$$w_{zi} = \dot{\alpha} + \Omega_{zi}$$

where Ω is defined as:

$$\begin{bmatrix} \Omega_{xi} \\ \Omega_{yi} \\ \Omega_{zi} \end{bmatrix} = \begin{bmatrix} \cos\theta_i & \sin\theta_i & 0 \\ -\sin\theta_i & \cos\theta_i & 0 \\ 0 & 0 & 1 \end{bmatrix} \begin{bmatrix} 0 & 1 & 0 \\ 0 & 0 & 1 \\ 1 & 0 & 0 \end{bmatrix} \begin{bmatrix} w_{ro} \\ w_{pi} \\ w_{ya} \end{bmatrix}$$

$\begin{bmatrix} \Omega_{xi} \\ \Omega_{yi} \\ \Omega_{zi} \end{bmatrix}$ is the rotation rate of vehicle transformed to inner gimbal space

and

$\dot{\alpha}, \dot{\gamma}; \ddot{\alpha}, \ddot{\gamma}$ are the scalar derivatives of outer and inner gimbal angles and gimbal rates, respectively.

Therefore,

$$T_{out\,(i^{TH}CMG)} = \begin{bmatrix} x_i = I_{Gi}\ddot{\gamma} + (\dot{\alpha} + w_{ro})\, h \cos\gamma - \Omega_{yi}\, h \sin\gamma \\ y_i = (\dot{\gamma} + \Omega_{xi})\, h \sin\gamma \\ zi = I_{Go}\ddot{\alpha} - (\dot{\gamma} + \Omega_{xi})\, h \cos\gamma \end{bmatrix}$$

$$I_{Gi} = J_{Gi}$$

$$I_{Go} = J_{Go} + J_{Gi(Z)} \cos^2 \gamma + J_{Gi(Y)} \sin^2 \gamma$$

let

$$\dot{\alpha}_I = \dot{\alpha} + w_{ro}$$

$$\dot{\gamma}_I = \dot{\gamma} + \Omega_{xi}$$

$$\left.\begin{matrix} T_{out} \\ (i^{TH}CMG) \end{matrix}\right] \begin{matrix} x_i \\ y_i \\ z_i \end{matrix} = \begin{matrix} I_{G1} \ddot{\gamma} + \dot{\alpha}_I h \cos \gamma - \Omega_{yi} h \sin \gamma \\ \dot{\gamma}_I h \sin \gamma \\ I_{Go} \ddot{\alpha} - \dot{\gamma}_I h \cos \gamma \end{matrix}$$

where

I_{Gi} - inertia tensor of inner gimbal expressed in the inner gimbal coordinate frame

J_{Gi} - inertia matrix of inner gimbal in inner gimbal coordinate

I_{Go} - inertia tensor of outer gimbal plus inner gimbal (suitably transformed) expressed in inner gimbal coordinates

J_{Go} - inertia matrix of outer gimbal in inner gimbal coordinates

CMG MOTOR TORQUE CONTROL LAW

$$T_{M1} = \left(\dot{\gamma}_{pi} - \dot{\gamma}_i - \frac{\dot{\alpha}_i \, H \cos \gamma}{K_{M1}} + \gamma_{Ai}\right) K_{M1}$$

$$T_{M2} = \left(\dot{\alpha}_{pi} - \dot{\alpha}_i + \frac{\dot{\gamma} \, H \cos \gamma}{K_{M2}}\right) K_{M2}$$

are the equations for the motor torque for inner and outer gimbals respectively, where the terms divided by KM1 and KM2 are used to decouple the torque motor dynamics between gimbals in a given CMG. KM1 and KM2 are, respectively, the inner and outer torque motor gains. If the motor torque exceeds the stiction torque plus the reaction torque produced by the CMG motion, the gimbal accelerates

$$\bar{T}_{GIMBAL} = \bar{T}_{M1_i} - \bar{T}_{REACT1} - \bar{T}_{RUN1}.$$

if

$$(\bar{T}_{M1_i} - \bar{T}_{REACT1} - \bar{T}_{STICK1}) > 0$$

otherwise

$$T_{\substack{GIMBAL \\ (INNER)}} = 0$$

Similarly for

$$T_{\substack{GIMBAL \\ (OUTER)}}$$

where

$$\bar{T}_{REACT1} = T_{OUT_{xi}} - I_{Gi}\,\ddot{\gamma}$$

in other words, T_{REACT} is the torque exerted by the gyro about the inner gimbal axis when the gimbal is not accelerated.

$$T_{REACT2} = T_{OUT_{3i}} - I_{Go}\,\ddot{\alpha}$$

T_{STICK} is the stiction torque

T_{RUN} is the running torque

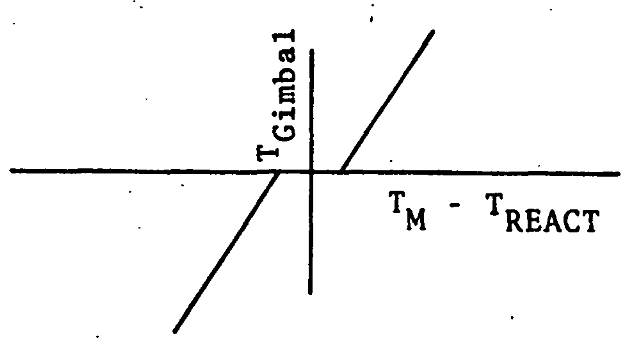

$\gamma = T_{Gimbal_i} / J_{Gi}$ $\ddot{\alpha} = T_{Gimbal_0}/J_{G0}$

If $T_{GIMBAL} = 0$, it is necessary to set the gimbal rates about the affected axes to the component of body rate on the axis, e.g.

$$T_{\substack{GIMBAL \\ (INNER)}} = 0 \quad \dot{\gamma}_I = \Omega_{xi} \quad , \quad \ddot{\gamma} = 0$$

$$T_{\substack{GIMBAL \\ (OUTER)}} = 0 \quad \dot{\alpha}_1 = \Omega_{zi} \quad , \quad \ddot{\alpha} = 0$$

COMPUTATION OF CMG GIMBAL COMMAND RATES

The terms $\dot{\gamma}_{pi}$ and $\dot{\alpha}_{pi}$ represent the commanded gimbal rates and are obtained from the following computation:

$$T_{xc} = \int (T_{xe} - T_{xv})\, dt$$

$$T_{yc} = \int (T_{ye} - T_{yv})\, dt$$

$$T_{zc} = \int (T_{ze} - T_{zv})\, dt$$

where

$T_{(\ )e}$ is the disturbance torque applied to the CMG by the control law.

$T_{(\ )v}$ is the torque presently applied by the gyro to the vehicle

$$\dot{\gamma}_{pi} = -T_{zc}/3h \cos \gamma$$

$$\dot{\alpha}_{pi} = T_{xc} \cos \theta_i + T_{yc} \sin \theta_i + T_{AH_i}$$

The last term in the second equation represents the torque term to eliminate "hang-up" or antiparallelism.

Another term

$$\gamma_{A1} = [(\gamma_1 + \gamma_2 + \gamma_3)/3 - \gamma_i] \cdot K_p$$

is added to the inner gimbal commanded angle to assure an equal distribution of orientation and reduce the possibility of gimbal limits being encountered

$$\begin{matrix} T_{xe} \\ T_{ye} \\ T_{ze} \end{matrix} = \begin{bmatrix} 0 & 1 & 0 \\ 0 & 0 & 1 \\ 1 & 0 & 0 \end{bmatrix} \begin{matrix} (K_D \phi_\varepsilon - K_R w_{ro}) \\ (K_D \theta_\varepsilon - K_R w_{pi}) \\ (K_D \psi_\varepsilon - K_R w_{ya}) \end{matrix}$$

where ϕ_ε, θ_ε, and ψ_ε are the space station attitude errors.

ATTITUDE ERROR EQUATIONS

$$\overline{E1} = \overline{R}_0 \times \overline{R}_{0C}$$

$$\theta_\varepsilon = \begin{bmatrix} 0 & 0 & 0 \\ 0 & 1 & 0 \\ 0 & 0 & 0 \end{bmatrix} \begin{bmatrix} C_0 \end{bmatrix}^T \quad E_1]$$

$$\overline{E2} = \overline{P}_i \times \overline{P}_{iC}$$

$$\begin{matrix} \phi_\varepsilon \\ \psi_\varepsilon \end{matrix} = \begin{bmatrix} 1 & 0 & 0 \\ 0 & 0 & 1 \end{bmatrix} \begin{bmatrix} C_0 \end{bmatrix}^T \quad E_2]$$

where

$\overline{R}_0$, $\overline{P}_i$ - unit vectors of roll and pitch axes in inertial coordinates

$\overline{R}_{0C}$, $\overline{P}_{iC}$ - unit vectors of roll and pitch axes in in inertial coordinates

$\overline{E}_1$, $\overline{E}_2$ - error vectors in inertial coordinates

$E_1]$, $E_2]$ - 3x1 matrix representation of $\overline{E}_1$ and $\overline{E}_2$

and $[C_0{}^T]$ is used to transform the attitude errors into the space station frame.

CMG CONTROL TORQUE

The computation of the CMG control torque involves the transformation of the output torque of each CMG to the space station basis followed by the summation of the three torque terms:

$$\left.\begin{matrix} To_i \\ (i^{TH}\ \text{CMG}) \end{matrix}\right]_{ss} = \begin{bmatrix} \cos\theta_i & -\sin\theta_i & 0 \\ \sin\theta_i & +\cos\theta_i & 0 \\ 0 & 0 & 1 \end{bmatrix} \left.\begin{matrix} To \\ (i^{TH}\ \text{CMG}) \end{matrix}\right]_{\substack{\text{Inner} \\ \text{Gimbal}}}$$

$$\left.\begin{matrix} To \\ (\text{TOTAL}) \end{matrix}\right]_{ss} = \left.To_1\right]_{ss} + \left.To_2\right]_{ss} + \left.To_3\right]_{ss}$$

4.1.5.3.2 Reaction Control System

A perfect proportional control system is modelled as an alternative to the Control Moment Gyro. The utilization of this alternative control system will permit more economical computation of the interaction dynamics.

$$\left[To \right] = \begin{bmatrix} I_{o(11)} & & \\ & I_{o(22)} & \\ & & I_{o(33)} \end{bmatrix} \begin{bmatrix} (K\theta \ \phi_\varepsilon + K\dot{\theta} \ w_{ro}) \\ (K\theta \ \theta_\varepsilon + K\dot{\theta} \ w_{pi}) \\ (K\theta \ \psi_\varepsilon + K\dot{\theta} \ w_{ya}) \end{bmatrix}$$

$K\theta$, $K\dot{\theta}$ are control gains chosen to satisfy frequency and damping characteristics.

ϕ_ε, θ_ε, and ψ_ε are computed in identical fashion to that presented in the previous section.

4.1.5.4 SOLAR ARRAY CONTROL EQUATIONS

The solar array drive controller mechanism consists of two first order filters which smooth the attitude error and driver rate signals. The two signals are weighted by appropriate gains, added together and then the sum is filtered by a third first order lag filter. The control system equations are adaptive with respect to driver inertia and roll axis gear ratio.

Filter Input Signals

$$\hat{w}_{11} = b_{11}\, w_{11} + a_{11}\, \hat{w}_{11_{-1}}$$
$$\hat{w}_{12} = b_{12}\, w_{12} + a_{12}\, \hat{w}_{12_{-1}}$$
$$\hat{w}_{21} = b_{21}\, \hat{w}_{21} + a_{21}\, \hat{w}_{21_{-1}}$$
$$\hat{w}_{22} = b_{22}\, w_{22} + a_{22}\, \hat{w}_{22_{-1}}$$
$$\hat{\phi}_{AE1} = b_{11}\, \phi_{AE1} + a_{11}\, \hat{\phi}_{AE1_{-1}}$$
$$\hat{\psi}_{AE1} = b_{12}\, \psi_{AE1} + a_{12}\, \hat{\psi}_{AE1_{-1}}$$
$$\hat{\phi}_{AE2} = b_{21}\, \phi_{AE2} + a_{21}\, \hat{\phi}_{AE2_{-1}}$$
$$\hat{\psi}_{AE2} = b_{22}\, \psi_{AE2} + a_{22}\, \hat{\psi}_{AE2_{-1}}$$

where

w_{iJ} - J^{TH} component of i^{TH} driver rotation rate

ϕ_{AEi} - roll axis error of i^{TH} driver

ψ_{AEi} - vane axis error of i^{TH} driver

$\hat{X}$ - implies "smoothed" or filtered value of X

X_{-1} - implies immediately previous value of X

a_{iJ} - difference equation coefficient $a_{iJ}=\exp\left(\frac{\text{INT.STEP}}{\tau_{iJ}}\right)$

b_{iJ} - $1 - a_{iJ}$

τ_{iJ} - filter time constant

Computation of Hinge Torque

$$T_{C11} = K\theta_A \cdot I_{1(R0)} \cdot \hat{\phi}_{AE1} + K\dot{\theta}_A \cdot I_{1(R0)} \cdot \hat{w}_{11}$$

$$T_{C12} = K\theta_A \cdot I_{1(33)} \cdot \hat{\psi}_{AE1} + K\dot{\theta}_A \cdot I_{1(33)} \cdot \hat{w}_{12}$$

$$T_{C21} = K\theta_A \cdot I_{2(R0)} \cdot \hat{\phi}_{AE2} + K\dot{\theta}_A \cdot I_{2(R0)} \cdot \hat{w}_{21}$$

$$T_{C22} = K\theta_A \cdot I_{2(33)} \cdot \hat{\psi}_{AE2} + K\dot{\theta}_A \cdot I_{2(33)} \cdot \hat{w}_{22}$$

Filtered Hinge Torque

$$\hat{T}_{C11} = b_{13}\, T_{C11} + a_{13}\, \hat{T}_{C11_{-1}}$$

$$\hat{T}_{C12} = b_{13}\, T_{C12} + a_{13}\, \hat{T}_{C12_{-1}}$$

$$\hat{T}_{C21} = b_{13}\, T_{C21} + a_{13}\, \hat{T}_{C21_{-1}}$$

$$\hat{T}_{C22} = b_{13}\, T_{C22} + a_{13}\, \hat{T}_{C22_{-1}}$$

where

$K\theta_A$, $K\dot{\theta}_A$ - displacement and rate gains

$I_{J(R0)}$ - root sum square (RSS) of 11 and 22 elements of the J^{TH} inertia matrix divided by KG

$I_{J(33)}$ - vane axis moment of inertia for J^{TH} rigid driver

a_{13} - $\exp\left(\frac{\text{Integration Step}}{\tau_{13}}\right)$

b_{13} - $1 - a_{13}$

4.1.6 ORBIT GENERATOR

The calculation of the space station orbit is required to perform the previously specified guidance functions. Lyddane's method is employed in this simulation to obtain the desired orbital state vector. This method provides a closed form of solution and is much more efficient and economical than numerical integration techniques. WOLF R & D has developed a standardized Lyddane's method subroutine which will be utilized in the simulation. A complete analytic treatment is presented in Reference 4.2 and will not be repeated here. Lyddane's method is an extension of Brouwer's theory which provides closed form solution of orbits from mean orbital elements. A brief exposition of the method is given below.

- Brouwer/Lyddane Theory

  Brouwer's theory utilizes the standard elliptic elements a, e, I, , w, M. The end product is typified by

$$w_{osc_{t-t_o}} = w'' + (t-t_o)\, f_1\, (a'',e'',I'') + f_2\, (a'',e'',I'',\ '',w'',M'')$$

where

$w_{osc_{t-t_o}}$ = "real world" or "osculating" value of the argument of perigee at time $t-t_o$.

w'' = "mean" value of the argument of perigee at time t_o. These "mean" values are related to the constants of integration of the differential equations of motion. They do not represent real world values, but are required for the prediction of osculating elements.

The difficulty with Brouwer's theory is that the function f_2 involves terms with e" and sin I" in the denominator, and for very small values of e" and/or I", these terms present a situation which violates the basic foundations of "small perturbation" theory.

3

In order to overcome these difficulties, Lyddane used a different set of parameters, which were first suggested in the 1800's by Poincare'. These variables, which do not produce divisions by e or sin I, are:

a

$e\ (\sin M)$

$e\ (\cos M)$

$(\sin I)\ (\sin \Omega)$

$(\sin I)\ (\cos \Omega)$

$w + \Omega + M$

With these parameters, numerical values are computed for each of the above six quantities from equations similar to those given by Brouwer. Then the individual values for e and M are obtained from

$$e^2 = (e \sin M)^2 + (e \cos M)^2$$

$$\operatorname{Tan} M = \frac{e\ (\sin M)}{e\ (\cos M)}$$

Similar Procedures are performed for I and , and finally, w is computed from

$$w = (w + \Omega + M) - \Omega - M$$

4.1.7 EQUATIONS OF CONSTRAINED MOTION FOR A SYSTEM OF THREE RIGID BODIES

Case A - Unconstrained Rotation

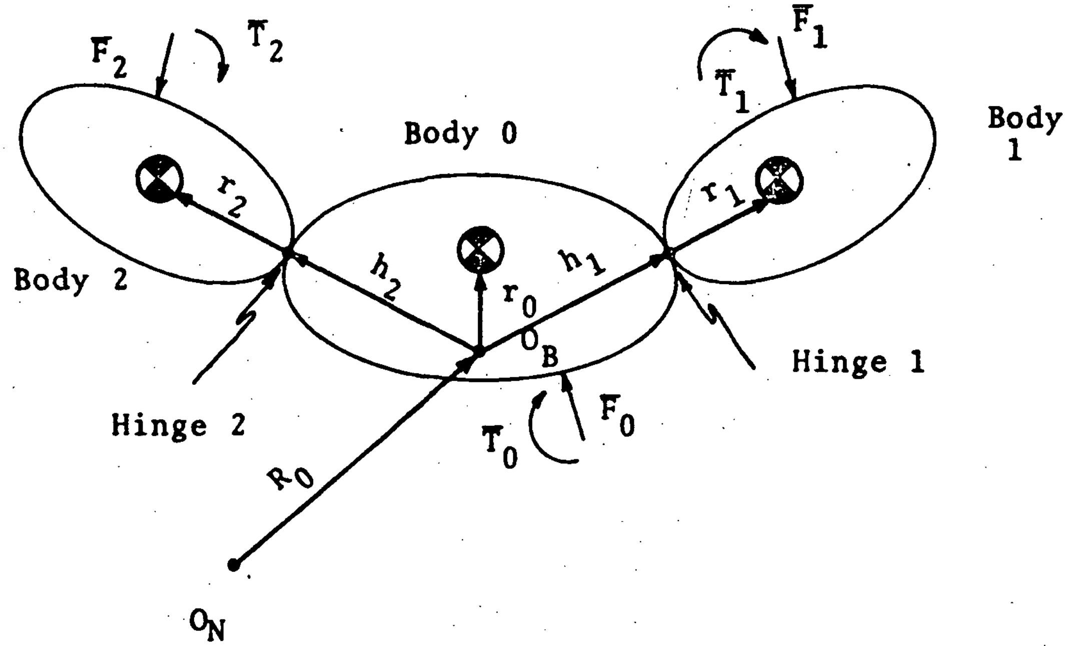

Consider the three body system presented above in which bodies one and two have unconstrained rotation about the two hinge points and neither of the two bodies can have translational motion with respect to the central (zero) body.

Definitions:

O_N - Newtonian reference point

O_B - Zero body reference point

R_0 - Distance of body reference point from Newtonian reference

r_o - Distance of zero body CG from body reference point

h_i, $i=1,2$ - Distance between body reference point and i^{TH} hinge point

r_i, $i=1,2$ - distance between i^{TH} hinge point and i^{TH} body center of gravity

$\bar{F}_0$, $\bar{T}_0$ - Vector force and torque applied to body zero

$\bar{F}_1$, $\bar{T}_1$ - Vector force and torque applied to body one

$\bar{F}_2$, $\bar{T}_2$ - Vector force and torque applied to body two

Coordinate Frames and Relationships

$\{I\}$ - Inertially fixed coordinate basis

$\{X\}$ - Coordinate basis fixed to body zero

$\{x_1\}$ - Coordinate basis fixed to body one

$\{x_2\}$ - Coordinate basis fixed to body two

where {I} can be represented as the unity matrix and each of the others as a triad of orthogonal unit vectors in the form of a 3x3 matrix.

$$\{I\} = C_0 \{X\} \; ; \; \{I\}^T = \{X\}^T C_0^T$$

$$\{X\} = C_1 \{x_1\} \; ; \; \{X\}^T = \{x_1\}^T C_1^T$$

$$\{X\} = C_2 \{x_2\} \; ; \; \{X\}^T = \{x_2\}^T C_2^T$$

where

C_i are the direction cosine matrices

$i=0,1,2$

Vector Representation of Variables

Each of the variables defined as distances represent the scalar magnitude of the related vector quantity. Each of the vectors defined below is given in a "convenient" frame and choice of basis is, of course, arbitrary.

$$\bar{R}_0 = \{X\}^T R_0$$

$$\bar{r}_o = \{X\}^T r_0$$

$$\bar{h}_i = \{X\}^T h_i$$

$$\bar{r}_i = \{x_i\} \quad r_i$$

where the bars designate a vector quantity.

The following identity is offered

$$\dot{C}_i = C_i \tilde{w}_i \qquad i = 0,1,2$$

where

$$\tilde{w}_i = \begin{bmatrix} 0 & -w_{i3} & w_{i2} \\ w_{i3} & 0 & -w_{i1} \\ -w_{i2} & w_{i1} & 0 \end{bmatrix}$$

EQUATIONS OF MOTION

1. Acceleration of the System Mass Center

$$m_T \frac{d^2}{dt^2} \left(\bar{R}_0 + \bar{C}\right)\Big|_I = \bar{F}_1 + \bar{F}_2 \; \left(\begin{array}{l}\text{Forces external to the} \\ \text{System}\end{array}\right)$$

m_T = total system mass

m_0 = mass of body zero

m_1 = mass of body one

m_2 = mass of body two

$$\bar{C} = \frac{m_0 \; \bar{r}_0 + m_1 \; (\bar{h}_1 + \bar{r}_1) + m_2 \; (\bar{h}_2 + \bar{r}_2)}{m_T}$$

C is the system mass center relative to O_B

$$m_T \; \frac{d^2 \; \bar{R}_0}{dt^2}\Big|_I + m_0 \; \frac{d^2 \; \bar{r}_0}{dt^2}\Big|_I$$

$$+ \; m_1 \; \frac{d^2 \; (\bar{h}_1 + \bar{r}_1)}{dt^2}\Big|_I + \frac{m_2 \; d^2 \; (\bar{h}_2 + \bar{r}_2)}{dt^2}\Big|_I = \bar{F}_1 + \bar{F}_2$$

Noting that $\bar{F}_1$ is in body one coordinates and $\bar{F}_2$ in those of body two, we have in the inertial basis $(\frac{d}{dt}\{I\} \equiv 0)$:

$$
\left.
\begin{aligned}
& m_T \frac{d^2}{dt^2} \left(\{\bar{I}\}^T \hat{C}_0 \hat{R}_0\right) \\
& + m_0 \frac{d^2}{dt^2} \left(\{\bar{I}\}^T \hat{C}_0 \hat{r}_0\right) \\
& + m_1 \frac{d^2}{dt^2} \left(\{\bar{I}\}^T \left(\hat{C}_0 \hat{h}_1 + \hat{C}_0 \hat{C}_1 \hat{r}_1\right)\right) \\
& + m_2 \frac{d^2}{dt^2} \left(\{\bar{I}\}^T \left(\hat{C}_0 \hat{h}_2 + \hat{C}_0 \hat{C}_2 \hat{r}_1\right)\right)
\end{aligned}
\right\}
= \{\bar{I}\}^T \begin{pmatrix} \hat{C}_0 \hat{C}_1 \bar{F}_1 \\ + \hat{C}_0 \hat{C}_2 \bar{F}_2 \end{pmatrix}
$$

where

$$\frac{d}{dt} \left(\{\bar{I}\}^T \hat{C}_0 \hat{R}_0\right) = \{\bar{I}\}^T \hat{C}_0 \left(\dot{\hat{R}}_0 + \tilde{w}_0 \hat{R}_0\right)$$

$$\frac{d^2}{dt^2} \left(\{\bar{I}\} \hat{C}_0 \hat{R}_0\right) = \{\bar{I}\}^T \hat{C}_0 \left(\ddot{\hat{R}}_0 + 2\tilde{w}_0 \dot{\hat{R}}_0 + \tilde{w}_0 \tilde{w}_0 \hat{R}_0 + \dot{\tilde{w}}_0 \hat{R}\right)$$

$$= \{\bar{X}\}^T \left(\ddot{\hat{R}}_0 + 2\tilde{w}_0 \dot{\hat{R}}_0 + \tilde{w}_0 \tilde{w}_0 \hat{R}_0 + \dot{\tilde{w}}_0 \hat{R}\right)$$

and

$$\frac{d}{dt} \left(\{I\} C_0 \hat{C}_1 \hat{r}_1\right) = \{\bar{I}\}^T \left(\hat{C}_0 \hat{C}_1 \dot{\hat{r}}_1 + \hat{C}_0 \tilde{w}_0 \hat{C}_1 \hat{r}_1 + \hat{C}_0 \hat{C}_1 \tilde{w}_1 \hat{r}\right.$$

$$
\frac{d^2}{dt^2}\left(\{I\}\, C_0\, C_1\, r_1\right) = \{I\}^T \left[\begin{array}{l} C_0\, \tilde{w}_0\, \tilde{w}_0\, C_1\, r_1 + C_0\, \tilde{w}_0\, C_1\, \tilde{w}_1\, r_1 \\ + C_0\, \tilde{w}_0\, C_1\, \tilde{w}_1\, r_1 + C_0\, C_1\, \tilde{w}_1\, \tilde{w}_1\, r_1 \\ + C_0\, \tilde{\dot{w}}_0\, C_1\, r_1 + C_0\, C_1\, \tilde{\dot{w}}_1\, r_1 \end{array} \right]
$$

$$
= \{X\}^T \left(\begin{array}{r} \tilde{w}_0\, \tilde{w}_0\, C_1\, r_1 + 2\tilde{w}_0\, C_1\, \tilde{w}_1\, r_1 \\ + C_1\, \tilde{w}_1\, \tilde{w}_1\, r_1 \\ + \tilde{\dot{w}}_0\, C_1\, r_1 + C_1\, \dot{w}_1\, \dot{r}_1 \end{array} \right)
$$

This gives us, in the body zero basis

$$m_T\{X\}^T \begin{bmatrix} \ddot{R}_0 + 2\tilde{w}_0 \dot{R}_0 + \tilde{w}_0 \tilde{w}_0 R_0 + \dot{\tilde{w}}_0 R_0 \\ + \mu_0 (\tilde{w}_0 \tilde{w}_0 + \dot{\tilde{w}}_0) r_0 \\ + \mu_1 \begin{bmatrix} (\tilde{w}_0 \tilde{w}_0 + \dot{\tilde{w}}_0)(h_1 + C_1 r_1) \\ + 2\tilde{w}_0 C_1 \tilde{w}_1 r_1 + C_1 \dot{\tilde{w}}_1 r_1 \\ + C_1 \tilde{w}_1 \tilde{w}_1 r_1 \end{bmatrix} \\ + \mu_2 \begin{bmatrix} (\tilde{w}_0 \tilde{w}_0 + \dot{\tilde{w}}_0)(h_2 + C_2 r_2) \\ + 2\tilde{w}_0 C_2 \tilde{w}_2 r_2 \\ + C_2 \tilde{w}_2 \tilde{w}_2 r_2 \\ + C_2 \dot{\tilde{w}}_2 r_2 \end{bmatrix} \end{bmatrix} = \{X\}^T \begin{bmatrix} C_1 F_1 \\ + \\ C_2 F_2 \\ + F_0 \end{bmatrix}$$

$$\mu_0 = \frac{m_0}{m_T}$$

$$\mu_1 = \frac{m_1}{m_T}$$

$$\mu_2 = \frac{m_2}{m_T}$$

2. Hinge Force Applied To The i^{TH} Body

$(i = 1,2)$

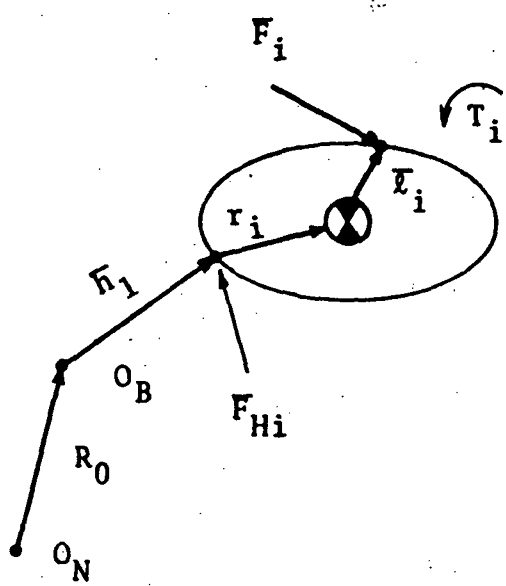

F_{Hi}, the hinge force, is given in the body zero, $\{X\}$, basis

$$m_i \; \{I\}^T \frac{d^2}{dt} \left(C_0 \; (R_0 + h_i) + C_0 \; C_i \; r_i \right) = \{I\}^T \; C_0 \; (F_{Hi} + C_i \; F_i)$$

$$\{X\}^T \; F_{Hi} = \{X\}^T \; m_i \left[\begin{array}{ll} \ddot{R}_0 + 2w_0 \; \dot{R}_0 & \\ + (\tilde{w}_0 \; \tilde{w}_0 + \dot{\tilde{w}}_0) \; (R_0 + h_i + C_i \; r_i) & \\ + 2\tilde{w}_0 \; C_i \; \tilde{w}_i \; r_i & - C_i \; F_i \\ + C_i \; (\tilde{w}_i \; \tilde{w}_i + \dot{\tilde{w}}_i) \; r_i & \end{array} \right]$$

3. Torque Equation For The i^{TH} Body

$$\frac{d}{dt} \bar{L}_i \Big|_I = \bar{T}_i + \tilde{\ell}_i \bar{F}_i$$

$$- \tilde{r}_i \bar{F}_{Hi} + \bar{T}_{Hi}$$

$\bar{L}_i$ - Angular momentum about CG of i^{TH} Body

$$\bar{L}_i - \{x_i\}^T \underset{3x3}{[I_i]} \{x_i\} \cdot \left[\{x_i\}^T w_i + \{X\}^T w_0\right]$$

T_{Hi} - hinge torque

$$\frac{d}{dt} \bar{L}_i \Big|_I = \frac{d}{dt} \{I\}^T C_0 C_i [I_i] C_i^T C_0^T \{I\} \left(\{I\}^T (C_0 C_i w_i + C_0 w_0)\right)$$

$$= \{I\}^T (C_0 \tilde{w}_0 C_i + C_0 C_i \tilde{w}_i) [I_i] \{x_i\}.\{x_i\}^T \left(w_i + C_i^T w_0\right)$$

$$+ \{x_i\}^T [I_i] \left(\tilde{w}_i^T C_i^T C_0^T + C_i^T \tilde{w}_0^T C_0^T\right) \{I\}.\{I\}^T \left(C_0 C_i w_i + C_0 w_0\right)$$

$$+ \{x_i\}^T [I_i] \{x_i\}.\{I\}^T \left(C_0 \tilde{w}_0 C_i w_i + C_0 C_i \tilde{w}_i w_i + C_0 \tilde{w}_0 w_0 + C_0 C_i \dot{w}_i + C_0 \dot{w}_0\right)$$

noting that $\{x\} \cdot \{x\}^T$ equals the identity matrix

$$\frac{d}{dt} L_i \bigg|_I = \{x_i\}^T \left(C_i^T \tilde{w}_0 C_i + \tilde{w}_i\right) [I_i] \left(w_i + C_i^T w_0\right)$$

$$+ \{x_i\}^T [I_i] \left(\tilde{w}_i^T - C_i^T \tilde{w}_0 C_i\right) \left(w_i + C_i^T w_0\right)$$

$$+ \{x_i\}^T [I_i] \left(C_i^T \tilde{w}_0 C_i w_i + \dot{w}_i + C_i^T \dot{w}_0\right)$$

$$= \{x_i\}^T \left(C_i^T \tilde{w}_0 C_i + \tilde{w}_i\right) [I_i] \left(w_i + C_i^T w_0\right)$$

$$+ \{x_i\}^T [I_i] \left(\dot{w}_i + C_i^T \dot{w}_0\right)$$

$$+ \{x_i\}^T [I_i] \begin{pmatrix} \tilde{w}_i^T C_i^T w_0 - C_i^T \tilde{w}_0 C_i w_i \\ + C_i^T \tilde{w}_0 C_i w_i \end{pmatrix}$$

We note that

$$(C_i w_0)^{\sim} = C_i \tilde{w}_0 C_i^T$$

$$\tilde{A} B = - \tilde{B} A$$

$$\tilde{A}^T = - \tilde{A}$$

$$\tilde{w}_i^T C_i^T w_0 = -\tilde{w}_i C_i^T w_0 = C_i^T \tilde{w}_0 C_i w_i$$

∴ Two of the terms cancel giving

$$\{x_i\}^T \begin{bmatrix} \left(\left(C_i^T w_0\right)^{\sim} + \tilde{w}_i\right) [I_i] \left(w_i^T C_i^T w_0\right) \\ + [I_i] \; \dot{w}_i + C_i^T \dot{w}_0 \\ + [I_i] \; C_i^T \tilde{w}_0 C_i w_i \end{bmatrix} = \{x_i\}^T \begin{bmatrix} C_i^T T_{Hi} \\ -\tilde{r}_i \; C_i^T F_{Hi} \\ \tilde{\ell}_i \; F_i + T_i \end{bmatrix}$$

where T_{Hi} and F_{Hi} are given in the zero body basis and T_i, F_i are in the i^{TH} body basis.

4. Torque Equation for Body Zero

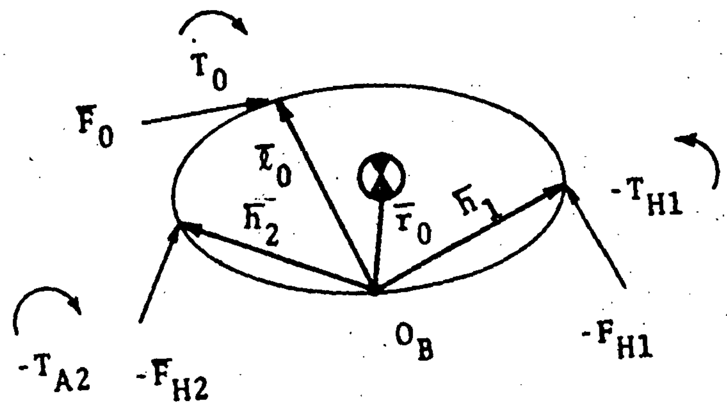

External Moments on Body Zero

$(-r_0 + h_1)^{\sim}$ $\quad -F_{H1} \quad -T_{H1}$

$(-r_0 + h_2)^{\sim}$ $\quad -F_{H2} \quad -T_{H2}$

$(-r_0 + \ell_0)^{\sim}$ $\quad F_0 \quad +T_0$

Reaction Torque

$$\left.\frac{d\,\bar{L}_0}{dt}\right|_I = \{X\}^T \begin{bmatrix} \tilde{w}_0\ [I_0]\ w_0 \\ [I_0]\ \dot{w}_0 \end{bmatrix}$$

$$\{X\}^T \begin{bmatrix} \tilde{w}_0\ [I_0]\ w_0 \\ [I_0]\ \dot{w}_0 \\ \end{bmatrix} = \begin{bmatrix} (r_0 + h_1)^{\sim}\ F_{H1} \\ (-r_0 + h_2)^{\sim}\ F_{H2} \\ (-r_0 + \ell_0)^{\sim}\ F_0 \end{bmatrix} + T_0 - T_{H1} - T_{H2}$$

Matrix Equations

Since $\{x\} \cdot \{x\}^T$ is equal to the identity matrix we can obtain a set of scalar matrix equations from the preceding by formally taking this product on both sides of the equation. For purposes of computer solution we shall also require a formulation of the form

$$[A] \; \dot{X}] = B$$

$$\dot{X}]^T = \lfloor \ddot{R}_0, \dot{w}_0, \dot{w}_1, \dot{w}_2 \rfloor$$

and B is a function of external forces and terms in w_0, w_1, w_2, $\dot{R}_0$ and R_0. Noting the identity

$$X\tilde{Y} = -\tilde{Y}X$$

System Acceleration Equation

L.H.S.

$$m_T \ddot{R}_0] - m_T \left(R_0]^{\sim} + N_0\, r_0]^{\sim} + N_1 (h_1] + C_1\, r_1])^{\sim} + N_2\, (h_2] + C_2\, r_2])^{\sim} \right) \dot{w}_0$$

$$- m_1\, C_1\, \tilde{r}_1\, \dot{w}_1 - m_2\, C_2\, \tilde{r}_2\, \dot{w}_2$$

R.H.S.

$$- m_T\, (2\tilde{w}_0\, \dot{R}_0 + \tilde{w}_0\, \tilde{w}_0\, R_0)$$

$$- m_0\, \tilde{w}_0\, \tilde{w}_0\, r_0 - m_1\, \tilde{w}_0\, \tilde{w}_0\, (h_1 + C_1\, r_1)$$

$$- m_1\, (2\tilde{w}_0\, C_1\, \tilde{w}_1\, r_1 + C_1\, \tilde{w}_1\, \tilde{w}_1\, r_1)$$

$$- m_2 \left(\tilde{w}_0\, \tilde{w}_0\, (h_2 + C_2\, r_2) - 2\tilde{w}_0\, C_2\, \tilde{w}_2\, r_2 \right)$$

$$- m_2\, (C_2\, \tilde{w}_2\, \tilde{w}_2\, r_2)$$

$$+ C_1\, F_1 + C_2\, F_2 + F_0$$

NOTE: L.H.S. - implies "lefthand side"

R.H.S. - implies "righthand side"

I^{TH} Body Torque Equation

L.H.S

$$m_i \tilde{r}_i C_i^T \ddot{R}_0 + \left[[I_i] C_i^T - m_i \tilde{r}_i C_i^T (R_0 + h_i + C_i r_i)^{\sim} \right] \dot{w}_0$$

$$+ ([I_i] - m_i \tilde{r}_i \tilde{r}_i) \dot{w}_i$$

R.H.S.

$$-m_i \tilde{r}_i C_i^T \left(\begin{array}{l} \ddot{R}_0 + 2\tilde{w}_0 \dot{R}_0 + \tilde{w}_0 \tilde{w}_0 (R_0 + h_i + C_i r_i) \\ + 2\tilde{w}_0 C_i \tilde{w}_i r_i + C_i \tilde{w}_i \tilde{w}_i r_i \end{array} \right)$$

$$- \left[\left(C_i^T w_0\right)^{\sim} + \tilde{w}_i \right] [I_i] \left(w_i + C_i^T w_0\right)$$

$$- [I_i] \left(C_i^T \tilde{w}_0 C_i w_i\right) + C_i^T T_{Hi}$$

$$+ \tilde{\ell}_i F_i + T_i$$

$$+ m_i \tilde{r}_i F_i$$

Body Zero Torque Equation

L.H.S.

Terms in $\ddot{R}_0$

$$\left(m_1 \; (-r_0 + h_1)^{\sim} + m_2 \; (-r_0 + h_2)^{\sim} \right)$$

Terms in $\dot{w}_0$

$$\left(\begin{array}{l} -m_1 \; (-r_0 + h_1)^{\sim} \quad (R_0 + h_1 + C_1 \; r_1)^{\sim} \\ \\ -m_2 \; (-r_0 + h_2)^{\sim} \quad (R_0 + h_2 + C_2 \; r_2)^{\sim} \end{array} + [I_0] \right)$$

Terms in $\dot{w}_i + \dot{w}_2$

$$\left(-m_1 \; (-r_0 + h_1)^{\sim} \; C_1 \; \tilde{r}_1 \right) \dot{w}_1 \quad \left(-m_2 \; (-r_0 + h_2)^{\sim} \; C_2 \; \tilde{r}_2 \right) \dot{w}_2$$

R.H.S.

$$-m_1\ (-r_0+h_1)^{\sim} \begin{bmatrix} 2\tilde{w}_0 \qquad 0\ \tilde{w}_0\ (R_0 + h_1 + C_1\ r_1) \\ \\ +\ 2\tilde{w}_0\ C_1\ \tilde{w}_1\ r_1 + C_1\ \tilde{w}_1\ \tilde{w}_1\ r_1 \end{bmatrix}$$

$$-m_2\ (-r_0+h_2)^{\sim} \begin{bmatrix} 2\tilde{w}_0\ \dot{R}_0 + \tilde{w}_0\ \tilde{w}_0\ (R_0 + h_2 + C_2\ r_2) \\ \\ +\ 2\tilde{w}_0\ C_1\ \tilde{w}_1\ r_1 + C_1\ \tilde{w}_1\ \tilde{w}_1\ r_1 \end{bmatrix}$$

$$-\ (-r_0 + \ell_0)^{\sim}\ F_0 - \tilde{w}_0\ [I_0]\ w_0$$

$$-T_{H1}\quad -T_{H2}\quad +T_0$$

$$+\ m_1\ (-r_0 + h_1)^{\sim}\ C_1\ F_1$$

$$+\ m_2\ (-r_0 + h_1)^{\sim}\ C_2\ F_2$$

Case B - Constrained Rotation

In the previous case the hinge torques were assumed to be arbitrary functions which completely accounted for the rotational interaction between the bodies 1 and 2 and the central element. In general, one or more axes of rotation may be constrained and the equations given previously must be modified to handle the rotational constraints.

- Modification to the Driver Moment Equation

  If we consider the constrained axes in terms of unit vectors, the modification procedure is easily visualized:

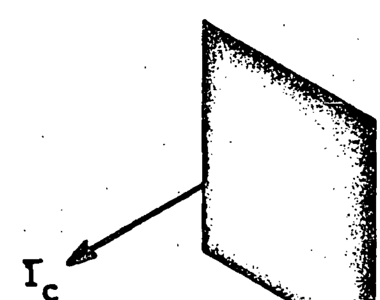

Consider the unit vector of constraint shown above. The remaining two degrees of rotation must be about mutually orthogonal axes lying in the plane normal to $\hat{1}_c$. An additional constraint, if it exists, must lie within the plane and for this case the single degree of rotational freedom is about the unit vector normal to both of the constraint axes.

The moment equation is altered by the elimination of constrained degree of freedom. This can most easily be done by taking the dot product of the unconstrained equations with unit vectors along the axes of allowable rotation. The reduction in dimension may be utilized advantageously by then reformulating the equations in terms of the new driver rotational acceleration components thereby eliminating a variable for each constraint.

Modification of the Zero Body Moment Equation

The constraint application effects this equation in two ways:

1. The negative of the constraint torque which nulls the outer body rotation about the axis of constraint must be applied to body zero.

2. If the driver moment equations are written in terms of the reduced set of variables the zero body moment equation must be modified appropriately.

Computation of the constraint torque is simply the reaction torque of the outer body minus the external outer body torque; this difference projected onto the constrained axis. The implementation of this computation can be done in either of two ways.

1. The constraint torque can be solved for formally and the terms in $\ddot{R}_0$ and $\dot{w}_0$ added to the L.H.S. of the zero body moment equation while all other terms are added to the R.H.S. of the equation.

2. The scalar equation of the outer body rotational acceleration about the constrained axis can be changed to an equation in terms of constraint torque (with suitable coupling to the zero body moment equation).

The former is recommended for constraints which are always applied while the latter is useful if the application of constraints is optional.

4.2 FLEXIBLE SPACE STATION/FLEXIBLE APPENDAGE, ZERO "G" CONDITION

The flexible body considerations used in the initial study phase have been extended to include the space station as a non-rigid structure and in addition, the capability of simulating the flexible dynamics of four non-controlled appendages has also been included. Extension of the initial digital simulation to include the capability of modeling the space station as a flexible structure necessitated a major revision of the systems dynamic equations which had been previously derived. Basically, appendage and array base motion must now include translation and rotation due to space station flexibility. Likewise, space station flexible modes must be excited by external forces and torques, and appendage and array interaction forces and torques. However, much of the philosophy and equation development techniques established in Section 4.1 are still applicable. Space station guidance and orbital motion, solar array guidance, ability to constrain solar array motions and so forth remain essentially unchanged from those descriptions given in Section 4.1.

The equation derivations logically fall into four separate categories:

1. Modal analysis of a freely translating and rotating space station.
2. Modal analysis of an appendage rigidly fixed to a base which is arbitrarily moving in space.
3. Modal analysis of appendage hinged to a base which is moving arbitrarily in space.
4. Total system equation which can be simultaneously solved for both rigid and flexible motions of a flexible space station with a maximum of two hinged arrays and up to four rigidly attached appendages.

4.2.1 MODAL ANALYSIS OF A FREELY TRANSLATING AND ROTATING SPACE STATION*

The space station, taken as a rigid body, rotates with an angular velocity $\bar{\omega}_o$ with respect to inertial space. Its translation is measured by $\bar{R}_o$, a vector from O_N, the origin of an inertial coordinate frame, to point O_B, a point fixed on the space station. This "rigid body" motion is conveniently described by a coordinate frame X_s fixed in the space station with origin at point O_B.

Determination of the flexible motion of the space station assumes that the station may be described by a collection of n discrete rigid bodies interconnected by massless elastic constraints. This system is idealized as initially undamped. The flexible motion of each discrete rigid body is measured relative to the X_s coordinate frame defined in the preceding paragraph. Thus, for example, the i^{th} rigid body's center of mass is located by the vector

$$\vec{p}_i = \vec{q}_i + \vec{x}_i$$

where

$\vec{p}_i$ - center of mass of i^{th} rigid body P_i

$\vec{q}_i$ - vector fixed in X_s; it accommodates in its changes of orientation the motion of P_i due to "rigid body" motion of the space station (Figure 4-9).

$\vec{x}_i$ - describes small deformations of system at P_i

Likewise, the i^{th} rigid body's angular velocity - measured in its own principal axes frame - is $\vec{\omega}_{b_i}$ with respect to the X_s coordinate system. Thus flexible motion of the i^{th} body may be represented by the variables x_{i_1}, x_{i_2}, x_{i_3}, θ_{i_1}, θ_{i_2}, θ_{i_3}, and their respective derivatives.

*See Reference 4.6.

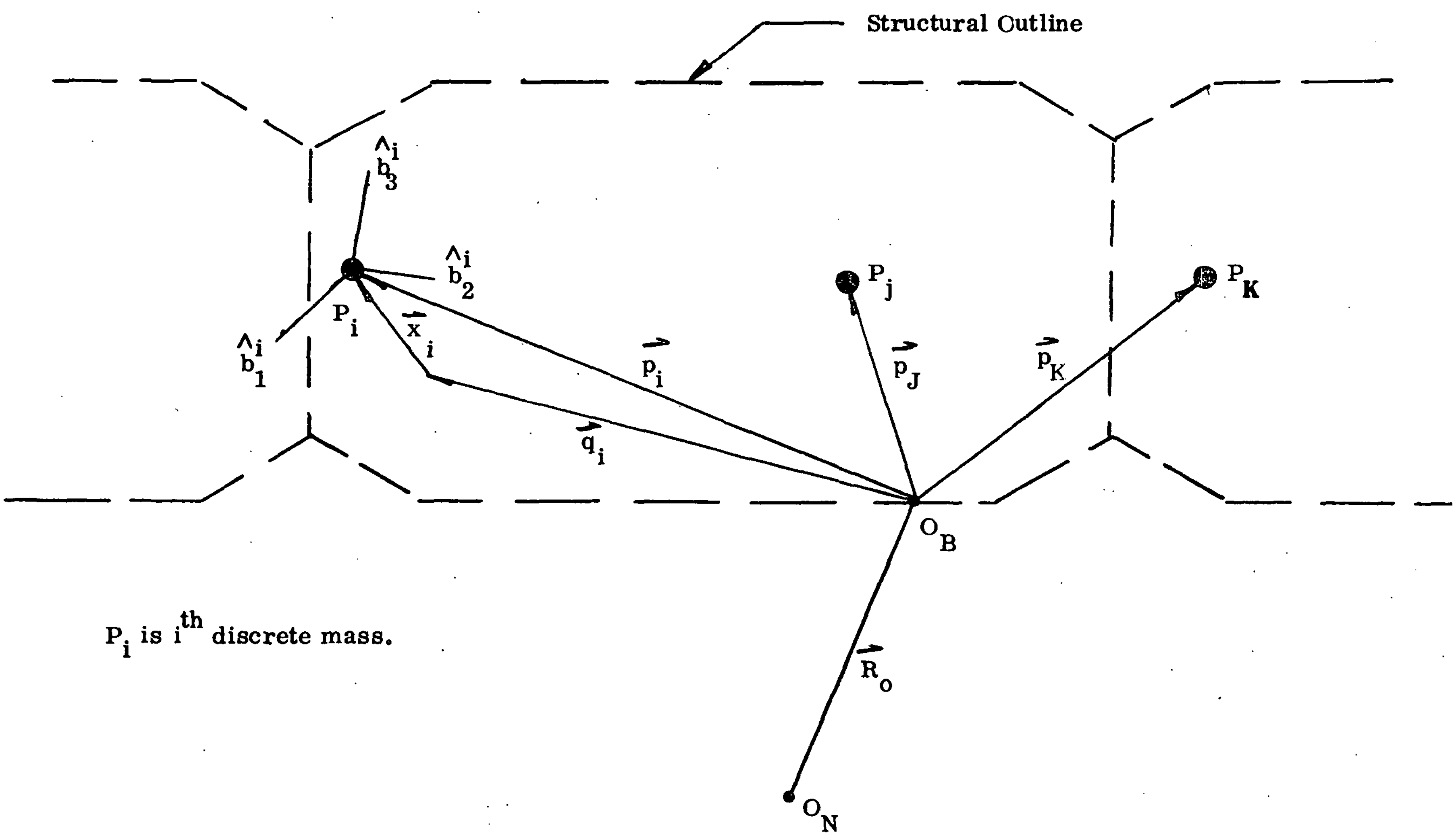

FIGURE 4-9 SPACE STATION COORDINATE SYSTEM

4.2.1.1 Coordinate Frames and Relationships

$[I]$ - inertially fixed coordinates

$[X_s]$ - coordinate basis fixed to and moving with the space station taken as a rigid body (origin at O_B, angular velocity $\bar{\omega}_o$ with respect to inertial space)

$[B_i]$ - coordinate basis with origin at the center of mass of the i^{th} elastically connected rigid body used to define space station flexible motion (angular velocity Ω^i with respect to inertial space). This basis is initially oriented along $[X_s]$.

The relationships between these frames are defined by the following direction cosine matrices:

$$[I] = C_O \, [X_s]$$

$$[X_s] = C_{B_i} \, [B_i] \qquad i = 1, 2, --, n$$

where

$$C_{B_i} \cong \begin{bmatrix} 1 & \theta_{i_3} & -\theta_{i_2} \\ -\theta_{i_3} & 1 & \theta_{i_1} \\ \theta_{i_2} & -\theta_{i_1} & 1 \end{bmatrix} = E - \tilde{\theta}_i$$

E is the identity matrix. The $\sim$ operation is basically used in cross product calculations and is defined by

$$\tilde{y} = \widetilde{\begin{bmatrix} y_1 \\ y_2 \\ y_3 \end{bmatrix}} = \begin{bmatrix} 0 & -y_3 & y_2 \\ y_3 & 0 & -y_1 \\ -y_2 & y_1 & 0 \end{bmatrix}$$

As shown in Section 4.1

$$\dot{C}_o = C_o \tilde{\omega}_o$$

$$\dot{C}_{B_i} = C_{B_i} \tilde{\omega}_{b_i}, \quad \dot{C}_{b_i}^T = -\tilde{\omega}_{b_i} C_{b_i}^T$$

4.2.1.2 <u>Equation Derivation</u>

Using D'Alembert's principle, the total external force acting on the i^{th} rigid body is

$$F_i = m_i \frac{d^2}{dt^2} \left[\vec{R}_o + \vec{q}_i + \vec{x}_i \right]_I$$

Defining $\vec{R}_o$, $\vec{q}_i$, and $\vec{x}_i$, in the X_s frame, and derivation in Reference 4.1, representative calculations are

$$\frac{d}{dt} (\vec{R}_o)_I = \frac{d}{dt} \left[I^T C_o R_o \right] = I^T (C_o \tilde{\omega}_o R_o + C_o \dot{R}_o)$$

$$\frac{d^2}{dt^2} (\vec{R}_o)_I = I^T \left[C_o \tilde{\omega}_o \dot{R}_o + C_o \ddot{R}_o + C_o \tilde{\omega}_o \tilde{\omega}_o R_o \right.$$

$$\left. + C_o \dot{\tilde{\omega}}_o R_o + C_o \tilde{\omega}_o \dot{R}_o \right]$$

$$= X_s^T \left[\tilde{\omega}_o \tilde{\omega}_o R_o + 2 \tilde{\omega}_o \dot{R}_o + \dot{\tilde{\omega}}_o R_o + \ddot{R}_o \right]$$

Therefore, remembering that $\vec{q}_i$ does not vary with respect to time in the X_s frame, the translational equation of motion for the i^{th} rigid body becomes

$$\left\{ F_i \right\} = m_i X_S^T \left[\tilde{\omega}_o \tilde{\omega}_o (R_o + q_i \quad x_i) + 2 \tilde{\omega}_o (\dot{R}_o + \dot{x}_i) \right. \tag{4.1}$$

$$\left. + \dot{\tilde{\omega}}_o (R_o + q_i + x_i) + \ddot{R}_o + \ddot{x}_i \right]$$

Thus F_i must be expressed in $\left\{X_s\right\}$ frame.

Rotational motion of the rigid body in the $\left[B_i\right]$ frame is expressed by Euler's equation for principal axes

$$\left\{T_i\right\}_B = \left[I^i\right] \left\{\dot{\Omega}^i\right\} + \tilde{\Omega}^i \left[I^i\right] \left\{\Omega^i\right\} \tag{4.2}$$

where

$$\left[I^i\right] = \begin{bmatrix} I_1^i & 0 & 0 \\ 0 & I_2^i & 0 \\ 0 & 0 & I_3^i \end{bmatrix} \equiv \text{inertia matrix for } i^{th} \text{ rigid body}$$

$\left\{\Omega^i\right\}$ - angular velocity of i^{th} body with respect to inertial space.

$\left\{\Omega^i\right\} = \left\{\omega_{bi}\right\} + C_{b_i} \left\{\omega_o\right\}$ in the $\left[B_i\right]$ frame. Therefore, substitution into equation (4.2) gives

$$\begin{aligned} \left\{T_i\right\}_B = {} & \left[I^i\right] \left\{\dot{\omega}_{bi}\right\} - \left[I^i\right] \tilde{\omega}_{b_i} C_{b_i}^T \left\{\omega_o\right\} + \left[I^i\right] C_{bi}^T \left\{\dot{\omega}_o\right\} \\ & + \tilde{\omega}_{bi} \left[I^i\right] \left\{\omega_{bi}\right\} + \tilde{\omega}_{bi} \left[I^i\right] C_{bi}^T \left\{\omega_o\right\} + \left[\widetilde{C_{bi}^T \left\{\omega_o\right\}}\right]\left[I^i\right]\left\{\omega_{bi}\right\} \\ & + \left[\widetilde{C_{bi}^T \left\{\omega_o\right\}}\right] \left[I^i\right] C_{bi}^T \left\{\omega_o\right\} \end{aligned} \tag{4.3}$$

For small flexible rotations of the i^{th} rigid body $C_{bi}^T \cong E + \tilde{\theta}_i$ as shown above. Substituting this along with the simplification

$$\left[\widetilde{C_{bi}^T \left\{\omega_o\right\}}\right] \cong \tilde{\omega}_o + \left[\widetilde{\tilde{\theta}^i \left\{\omega_o\right\}}\right]$$

into equation (4.3) gives

$$
\begin{aligned}
\left\{T_i\right\}_B = {} & \left[I^i\right]\left\{\dot{\omega}_{bi}\right\} - \left[I^i\right]\tilde{\omega}_{bi}\left\{\omega_o\right\} - \cancel{\left[I^i\right]\tilde{\theta}^i\tilde{\omega}_{bi}\left\{\omega_o\right\}} \\
& + \left[I^i\right]\left\{\dot{\omega}_o\right\} + \left[I^i\right]\tilde{\theta}^i\left\{\dot{\omega}_o\right\} + \cancel{\tilde{\omega}_{bi}\left[I^i\right]\left\{\omega_{bi}\right\}} + \tilde{\omega}_{bi}\left[I^i\right]\left\{\omega_o\right\} \\
& + \cancel{\tilde{\omega}_{bi}\left[I^i\right]\tilde{\theta}^i\left\{\omega_o\right\}} + \tilde{\omega}_o\left[I^i\right]\left\{\omega_{bi}\right\} - \cancel{\left[\widetilde{\tilde{\theta}^i\left\{\omega_o\right\}}\right]\left[I^i\right]\left\{\omega_{bi}\right\}} \\
& + \tilde{\omega}_o\left[I^i\right]\left\{\omega_o\right\} - \tilde{\omega}_o\left[I^i\right]\tilde{\theta}^i\left\{\omega_o\right\} + \left[\widetilde{\tilde{\theta}^i\left\{\omega_o\right\}}\right]\left[I^i\right]\left\{\omega_o\right\} \\
& + \cancel{\left[\widetilde{\tilde{\theta}^i\left\{\omega_o\right\}}\right]\left[I^i\right]\tilde{\theta}^i\left\{\omega_o\right\}}
\end{aligned}
\qquad (4.4)
$$

Note that linearization of the above equation has been assumed since terms containing products of small variables have been neglected.

The force equation is written in the X_s coordinate basis. Transforming Equation 4.4 to the X_s frame involves multiplication by $C_{b_i}^T \cong E - \tilde{\theta}^i$. This procedure results in Equation 4.5.

$$
\begin{aligned}
\left\{T_i\right\} = {} & \left[I^i\right]\left\{\dot{\omega}_{bi}\right\} - \cancel{\tilde{\theta}^i\left[I^i\right]\left\{\dot{\omega}_{bi}\right\}} - \left[I^i\right]\tilde{\omega}_{bi}\left\{\omega_o\right\} \\
& + \cancel{\tilde{\theta}^i\left[I^i\right]\tilde{\omega}_{bi}\left\{\omega_o\right\}} + \left[I^i\right]\left\{\dot{\omega}_o\right\} - \tilde{\theta}^i\left[I^i\right]\left\{\dot{\omega}_o\right\} - \left[I^i\right]\tilde{\theta}^i\left\{\dot{\omega}_o\right\} \\
& - \cancel{\tilde{\theta}^i\left[I^i\right]\tilde{\theta}^i\left\{\dot{\omega}_o\right\}} + \tilde{\omega}_{bi}\left[I^i\right]\left\{\omega_o\right\} - \cancel{\tilde{\theta}^i\tilde{\omega}_{bi}\left[I^i\right]\left\{\omega_o\right\}} \\
& + \tilde{\omega}_o\left[I^i\right]\left\{\omega_{bi}\right\} - \cancel{\tilde{\theta}^i\tilde{\omega}_o\left[I^i\right]\left\{\omega_{bi}\right\}} + \tilde{\omega}_o\left[I^i\right]\left\{\omega_o\right\} \\
& - \tilde{\theta}^i\tilde{\omega}_o\left[I^i\right]\left\{\omega_o\right\} + \tilde{\omega}_o\left[I^i\right]\tilde{\theta}^i\left\{\omega_o\right\} - \cancel{\tilde{\theta}^i\tilde{\omega}_o\left[I^i\right]\tilde{\theta}^i\left\{\omega_o\right\}} \\
& + \left[\widetilde{\tilde{\theta}^i\left\{\omega_o\right\}}\right]\left[I^i\right]\left\{\omega_o\right\} - \cancel{\tilde{\theta}^i\left[\widetilde{\tilde{\theta}^i\left\{\omega_o\right\}}\right]\left[I^i\right]\left\{\omega_o\right\}}
\end{aligned}
\qquad (4.5)
$$

Using the following identity

$$\tilde{u}\ \{v\} = -\ \tilde{v}\ \{u\}$$

and defining

$$\{h_i\} = [I^i]\ \{\omega_o\}$$

Therefore

$$\tilde{h}_i = \left[\widetilde{[I^i]\ \{\omega_o\}}\right]$$

$$\left[\widetilde{\tilde{\theta}^i\ \{\tilde{\omega}_o\}}\right]\left[I^i\right]\{\omega_o\} = -\ \tilde{h}_i\ \tilde{\theta}^i\ \{\omega_o\} = \tilde{h}_i\ \tilde{\omega}_o\ \{\theta^i\}$$

Substitution of these identities into Equation 4.5 yields the rotational equation of motion for the i^{th} rigid body of the space station.

$$\{T_i\} = \left[I^i\right]\{\dot{\omega}_{bi}\} + \left[I^i\right]\tilde{\omega}_o\ \{\omega_{bi}\} + \left[I^i\right]\{\dot{\omega}_o\}$$

$$\dot{\tilde{h}}^i\ \{\tilde{\theta}i\} - \left[I^i\right]\dot{\tilde{\omega}}_o\ \{\theta^i\} - \tilde{h}^i\ \{\omega_{bi}\} + \tilde{\omega}_o\ \left[I^i\right]\{\omega_{bi}\} + \tilde{\omega}_o\ \{h^i\} \qquad (4.6)$$

$$+ \left[\tilde{\omega}_o\widetilde{[Ii]\{\omega_2\}}\right]\{\theta i\} - \tilde{\omega}_o\ \left[I^i\right]\tilde{\omega}_o\ \{\theta^i\} + \tilde{h}_i\ \tilde{\omega}_o\ \{\theta^i\}$$

Combining Equations 4.1 and 4.6 for all n rigid bodies into one large matrix equation of column dimension 6 n yields

$$\left[m\right]\{\ddot{q}\} + \left[K\right]\{q\} = -\left[G\right]\{\dot{q}\} - \left[B\right]\{q\} + \left[R\right]\{RB\} \qquad (4.7)$$

$$+ \{F^1\} + \{L\}$$

$\{F^1\}$ - discretely applied forces and torques on those elastically connected rigid bodies which define the space station to which either

(a) fixed appendange is attached

(b) rotating array is hinged

(c) external force is applied $(\vec{F}_R)$

(d) external torque is applied $(\vec{T}_R - \tilde{\ell}_R \ F_R)$

The applied forces and torques include those resulting from appendage base constraints.

$$[B] = \begin{bmatrix} \bar{m}_1 (\dot{\tilde{\omega}}_o + \tilde{\omega}_o \tilde{\omega}_o) & 0 & \\ & -\bar{I}^1 \dot{\tilde{\omega}}_o - \tilde{\omega}_o \bar{I}^1 \tilde{\omega}_o + \tilde{h}_1 \tilde{\omega}_o + \tilde{\dot{h}}_i + \left[\widetilde{\omega_o I' \omega_o}\right] & \\ & & \ddots \\ 0 & & \end{bmatrix}$$

6n x 6n

$$\{L\} = \begin{bmatrix} -\bar{m}_1\left[+ \tilde{\omega}_o \tilde{\omega}_o (R_o + q_1) + 2 \tilde{\omega}_o \dot{R}_o\right. \\ \hline - \tilde{\omega}_o \bar{I}^1 \{\omega_o\} \\ \hline -\bar{m}_2 [\tilde{\omega}_o \tilde{\omega}_o (R_o + q_2) + 2 \tilde{\omega}_o \dot{R}_o] \\ \hline - \tilde{\omega}_o \bar{I}^2 \{\omega_o\} \\ \hline \vdots \end{bmatrix}$$

6n x 1

where

$$q = \left[x_{11}, x_{12}, x_{13}, \theta_{13}, \ldots, \theta_{n2}, \theta_{n3} \right]^T$$

$$[m] = \underset{6n \times 6n}{\begin{bmatrix} \bar{m}_1 & 0 & & & & & 0 \\ 0 & \bar{I}^1 & & & & & \\ & & \bar{m}_2 & 0 & & & \\ & & 0 & \bar{I}^2 & & & \\ & & & & \ddots & & \\ & 0 & & & & \bar{m}_n & 0 \\ & & & & & 0 & \bar{I}^n \end{bmatrix}}$$

$$\bar{m}_i = \underset{3 \times 3}{\begin{bmatrix} m_i & 0 & 0 \\ 0 & m_i & 0 \\ 0 & 0 & m_i \end{bmatrix}} \qquad \bar{I}^i = \underset{3 \times 3}{\begin{bmatrix} I_1^i & 0 & 0 \\ 0 & I_2^i & 0 \\ 0 & 0 & I_3^i \end{bmatrix}}$$

$$[G] = \begin{bmatrix} 2\bar{m}_1 \tilde{\omega}_o & & & & 0 \\ & +\bar{I}^1 \tilde{\omega}_o - \tilde{h}^1 + \tilde{\omega}_o \bar{I}^1 & & & \\ & & 2\bar{m}_2 \tilde{\omega}_o & & \\ & 0 & & \ddots & \end{bmatrix}$$

$$
\left\{ RB \right\} = \begin{bmatrix} \ddot{R}_o \\ \dot{\omega}_o \end{bmatrix}_{6 \times 1}
$$

$$
R = \left[\begin{array}{c|c}
-\bar{m}_1 & \bar{m}_1 \; (\widetilde{R_o + q_1}) \\
\hline
0 & -\bar{I}^1 \\
\hline
-\bar{m}_2 & \bar{m}_2 \; (\widetilde{R_o + q_2}) \\
\hline
0 & -\bar{I}^2 \\
\hline
\vdots & \vdots \\
6n \times 3 & 6n \times 3
\end{array} \right]
$$

4.2.1.3 Modal Analysis

Subjecting Equation 4.7 to the orthogonal transformation

$$\{q\} = [\gamma] \{n_s\}$$

and premultiplying by $[\gamma]^T$ yields, if $[\gamma]$ is a matrix whose columns are eigenvectors of the system, $[\gamma]^T [m] [\gamma] = I$,

$$\ddot{n}_s + \left[2 \xi_s \omega_s\right] \dot{n}_s + \left[\omega_s^2\right] n_s = -[\gamma]^T [G] [\gamma] \dot{n}_s$$

$$+ [\gamma]^T \{L\} - [\gamma]^T [B] [\gamma] n_s \tag{4.8}$$

$$+ [\gamma]^T [R] \{RB\} + [\gamma]^T \{F^1\}$$

Note that modal damping has been added in the classical manner of structural analysis.

For this simulation, space station "rigid body" motion is considered to be small. Thus, Equation 4.8 may be linearized to the following form

$$\ddot{n}_s + \left[2 \xi_s \omega_s\right] \dot{n}_s + \left[\omega_s^2\right] n_s = [\gamma]^T \{F^1\} + [\gamma]^T [R] \{RB\} \tag{4.9}$$

Derivations in Section 4.2.5.1 also show that $[\gamma]^T [R] \{RB\} = 0$. Thus Equation 4.9 becomes

$$\left\langle \ddot{n}_s + \left[2 \xi_s \omega_s\right] \dot{n}_s + \left[\omega_s^2\right] n_s = [\gamma]^T \{F^1\} \right\rangle$$

The above equation in diamond brackets is the equation modeled in the simulation. The diamond bracket will hence forth be utilized solely for indicating equations to be programmed.

In summary, the above equation was derived assuming:

(a) linearization of equations because of

1. small flexible motions of system
2. small space station angular velocity, and translation with respect to osculating orbit position

(b) free-free modes of space station are available for generation of $[\gamma]$ modal matrix

(c) moments of inertia for each of the n discrete rigid bodies are initially defined along axes parallel to the X_s coordinate basis

(d) external forces and torques acting on the space station to be expressed in the space station axes system

4.2.2 RIGIDLY ATTACHED APPENDAGES

Appendages, as in previous derivations, are modeled as elastically connected masses. Cantilevered mode shapes are used to represent the fixed appendage flexibility. The base of a fixed appendage must be rigidly attached to one of those rigid bodies which comprise the space station. Therefore base motion of the appendage includes translational and rotational motion of that rigid body to which it is attached plus translational and rotational motion of the entire space station with respect to inertial space.

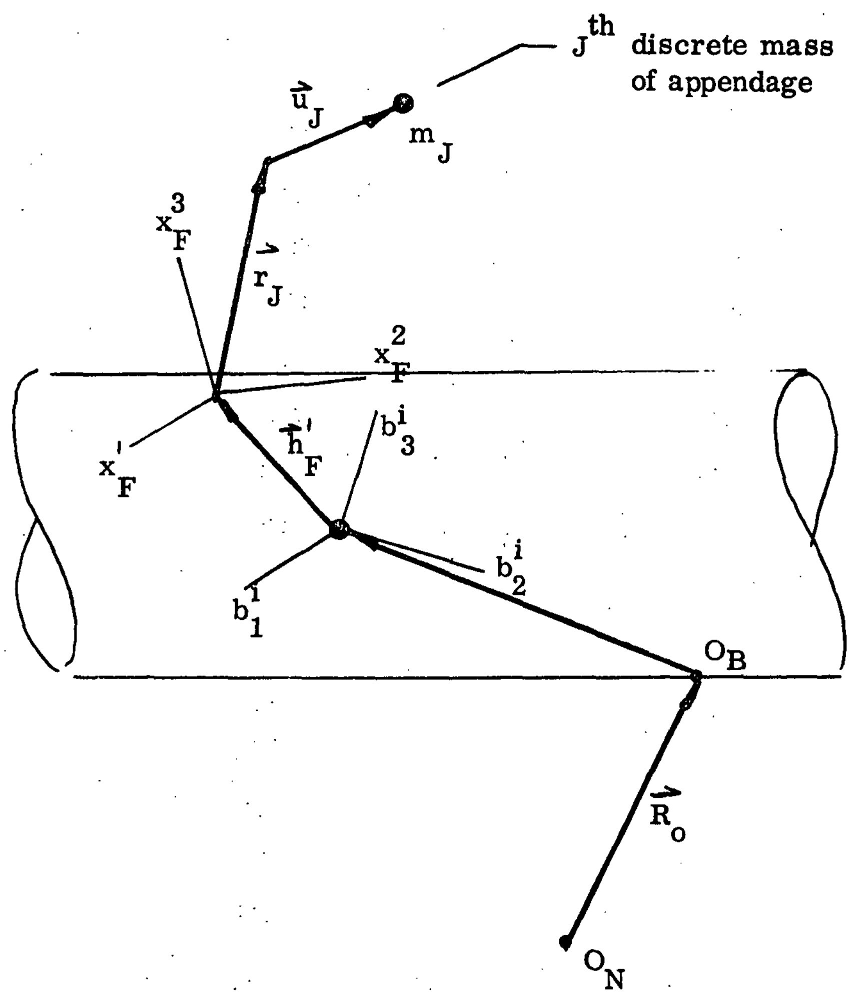

FIGURE 4-10 FIXED APPENDAGE COORDINATE SYSTEM

4.2.2.1 Coordinate Frames and Relationships

$\left[X_s\right]$ - previously defined S/S "rigid body" basis

$\left[I\right]$ - previously defined inertial basis

$\left[B_i\right]$ - previously defined basis fixed to i^{th} rigid body of space station

$\left[X_F\right]$ - coordinate basis defined with origin at attachment point of appendage and axes directed along principal axes of the appendage

$\left[C_F\right]$ - direction cosine matrix relating coordinate frames $\left[B_i\right]$ and $\left[X_F\right]$

$$\left[B_i\right] = \left[C_F\right] \left[X_F\right]$$

4.2.2.2 Equation Derivation

The total force acting on the j^{th} mass particle m_J of the appendage is, by D'Alembert's principle

$$F_J = m_J \frac{d^2}{dt^2} \left[\vec{R}_o + \vec{q}_i + \vec{x}_i + \vec{h}'_F + \vec{r}_J + \vec{u}_J \right]_I$$

where

$\vec{h}'_F$ - location of attachment point of appendage with respect to the center of mass of the i^{th} rigid body of the space station to which the appendage is rigidly attached.

$\vec{r}_J$ - undeformed location of j^{th} particle m_J of appendage.

$\vec{u}_J$ - location of m_J with respect to undeformed position.

Representative calculations, assuming $\vec{h}'_F$ is defined in the $\left[B_i\right]$ basis and $\vec{r}_J$ and $\vec{u}_J$ are defined in the $\left[X_F\right]$ basis, and noting that $\dot{C}_F = 0$ are

$$\frac{d}{dt}\vec{u}_J = \frac{d}{dt}\left[I^T C_o C_{bi} C_F u_J\right] =$$

$$I^T\left[C_o \tilde{\omega}_o C_{bi} C_F u_J + C_o C_{bi} \tilde{\omega}_{bi} C_F u_J + C_o C_{bi} C_F \dot{u}_J\right]$$

$$\frac{d^2}{dt^2}\left[u_J\right]_I = I^T\left[C_o \tilde{\omega}_o \tilde{\omega}_o C_{bi} C_F u_J + C_o \dot{\tilde{\omega}}_o C_{bi} C_F u_J\right.$$

$$+ C_o \tilde{\omega}_o C_{bi} \tilde{\omega}_{bi} C_F u_J + C_o \tilde{\omega}_o C_{bi} \dot{u}_J + C_o \tilde{\omega}_o C_{bi} \tilde{\omega}_{bi} C_G u_J$$

$$+ C_o C_{bi} \tilde{\omega}_{bi} \tilde{\omega}_{bi} C_F u_J + C_o C_{bi} \tilde{\omega}_{bi} C_F u_J + C_o C_{bi} \tilde{\omega}_{bi} C_F \dot{u}_J$$

$$\left.+ C_o \tilde{\omega}_o C_{bi} C_F \dot{u}_J + C_o C_{bi} \tilde{\omega}_{bi} C_F \dot{u}_J + C_o C_{bi} C_F \ddot{u}_J\right]$$

$$= X^T\left[\tilde{\omega}_o \tilde{\omega}_o C_{bi} C_F u_J + \dot{\tilde{\omega}}_o C_{bi} C_F u_J + 2 \tilde{\omega}_o C_{bi} \tilde{\omega}_{bi} C_F u_J\right.$$

$$+ 2 \tilde{\omega}_o C_{bi} C_F \dot{u}_J + C_{bi} \tilde{\omega}_{bi} \tilde{\omega}_{bi} C_F u_J + C_{bi} \tilde{\omega}_{bi} C_F u_J + 2 C_{bi} \omega_{bi} C_F \dot{u}_J$$

$$\left.+ C_{bi} C_F \ddot{u}_J\right]$$

$\vec{q}_i$, $\vec{h}'_F$, $\vec{r}_J$ do not vary with time in their respective frames.

$$\left\{F_J\right\} = m_J X_F^T \Big[(\tilde{\omega}_o \tilde{\omega}_o (R_o + q_i + x_i) + 2 \tilde{\omega}_o (\dot{R}_o + \dot{x}_i)$$

$$+ \dot{\tilde{\omega}}_o (R_o + q_i + x_i) + \ddot{R}_o + \ddot{x}_i) + (\tilde{\omega}_o \tilde{\omega}_o C_{bi} + 2 \tilde{\omega}_o C_{bi} \tilde{\omega}_{bi}$$

$$+ \dot{\tilde{\omega}}_o C_{bi} + C_{bi} \tilde{\omega}_{bi} \tilde{\omega}_{bi} + C_{bi} \dot{\tilde{\omega}}_{bi}) h'_F + (\tilde{\omega}_o \tilde{\omega}_o C_{bi} C_F$$

$$+ \dot{\tilde{\omega}}_o C_{bi} C_F + 2 \tilde{\omega}_o C_{bi} \tilde{\omega}_{bi} C_F + C_{bi} \tilde{\omega}_{bi} \tilde{\omega}_{bi} C_F + C_{bi} \dot{\tilde{\omega}}_{bi} C_F)^*$$

$$(r_J + u_J) + (2 \tilde{\omega}_o C_{bi} C_F + C_{bi} \tilde{\omega}_{bi} C_F) \dot{u}_J + C_{bi} C_F \ddot{u}_J \Big]$$

$$= m_J X_F^T \Big[\left\{ C_F^T \; C_{bi}^T \right\} (\tilde{\omega}_o \tilde{\omega}_o (R_o + q_i + x_i) + 2 \tilde{\omega}_o (\dot{R}_o + \dot{x}_i)$$

$$+ \dot{\tilde{\omega}}_o (R_o + q_i + x_i) + \ddot{R}_o + \ddot{x}_i) + (\tilde{\omega}_o \tilde{\omega}_o C_{bi} + 2 \tilde{\omega}_o C_{bi} \tilde{\omega}_{bi} + \dot{\tilde{\omega}}_o C_{bi}$$

$$+ C_{bi} \tilde{\omega}_{bi} \tilde{\omega}_{bi} + C_{bi} \dot{\tilde{\omega}}_{bi}) h'_F + (\tilde{\omega}_o \tilde{\omega}_o C_{bi} C_F + \dot{\tilde{\omega}}_o C_{bi} C_F$$

$$+ 2 \tilde{\omega}_o C_{bi} \tilde{\omega}_{bi} C_F + C_{bi} \tilde{\omega}_{bi} \tilde{\omega}_{bi} C_F + C_{bi} \dot{\tilde{\omega}}_{bi} C_F) (r_J + u_J)$$

$$+ (2 \tilde{\omega}_o C_{bi} C_F + C_{bi} \tilde{\omega}_{bi} C_F) \dot{u}_J + \ddot{u}_J \Big]$$

For small translational and rotational motion of the rigid body to which the appendage is attached $C_{bi}^T \cong E + \tilde{\theta}^i$

$$\therefore \quad \left\{F_J\right\} = m_J X_F^T \Bigg[\left\{C_F^T\right\} \cdot \Big\{ (\tilde{\omega}_o \tilde{\omega}_o (R_o + q_i + x_i) + 2\,\tilde{\omega}_o (\dot{R}_o + \dot{x}_i)$$

$$+ \dot{\tilde{\omega}}_o (R_o + q_i + x_i) + \ddot{R}_o + \ddot{x}_i) + \tilde{\theta}_i \; (\tilde{\omega}_o \tilde{\omega}_o (R_o + q_i) + 2\,\tilde{\omega}_o \dot{R}_o$$

$$+ \dot{\tilde{\omega}}_o (R_o + q_i) + \ddot{R}_o) + (\tilde{\omega}_o \tilde{\omega}_o + \theta_i (\tilde{\omega}_o \tilde{\omega}_o + \dot{\tilde{\omega}}_o) - (\tilde{\omega}_o \tilde{\omega}_o + \dot{\tilde{\omega}}_o) \tilde{\theta}^i$$

$$+ \dot{\tilde{\omega}}_o + 2\,\tilde{\omega}_o \tilde{\omega}_{bi} + \cancel{\tilde{\omega}_{bi} \tilde{\omega}_{bi}} + \dot{\tilde{\omega}}_{bi}) h'_F + (\tilde{\omega}_o \tilde{\omega}_o + \tilde{\theta}^i (\tilde{\omega}_o \tilde{\omega}_o + \dot{\tilde{\omega}}_o)$$

$$- (\tilde{\omega}_o \tilde{\omega}_o + \dot{\tilde{\omega}}_o) \tilde{\theta}^i + \dot{\tilde{\omega}}_o + 2\,\tilde{\omega}_o \tilde{\omega}_{bi} + \cancel{\tilde{\omega}_{bi} \tilde{\omega}_{bi}} + \dot{\tilde{\omega}}_{bi}) C_F (r_J + u_J)$$

$$+ (2\,\tilde{\omega}_o + 2\,\tilde{\theta}^i \tilde{\omega}_o - 2\,\tilde{\omega}_o \tilde{\theta}^i + \dot{\tilde{\omega}}_{bi}) C_F \dot{u}_J \Big\} + \ddot{u}_J \Bigg]$$

The space station motion is assumed to be small, thus, the above equation reduces to

$$\{F_J\} = m_J X_F^T \Big[C_F^T \; (\dot{\tilde{\omega}}_o q_i + \ddot{R}_o + \ddot{x}_i + (\dot{\tilde{\omega}}_o + \dot{\tilde{\omega}}_{bi}) h'_F \qquad (4.10)$$

$$+ (\dot{\tilde{\omega}}_o + \dot{\tilde{\omega}}_{bi})(C_F r_J) + \ddot{u}_J \Big]$$

Combining the above equation for all n particles of the appendage into one large matrix equation of column size 3 n yields

$$[m]\{\ddot{q}\} + [K]\{q\} = -[G]\{\dot{q}\} - [B]\{q\} \qquad (4.11)$$

$$+ [R]\{RB\} + [s_2]\{\ddot{s}\} + \{L\}$$

where

$$q = \left[u_{11}, u_{12}, \text{--} \quad u_{n1}, u_{n2}, u_{n3} \right]^T$$

$$\left[m\right] = \begin{bmatrix} \bar{m}_1 & & & & 0 \\ & \bar{m}_2 & & & \\ & & \cdot & & \\ & & & \cdot & \\ 0 & & & & \bar{m}_n \end{bmatrix}_{3n \times 3n} \qquad \bar{m}_i = \begin{bmatrix} m_i & 0 & 0 \\ 0 & m_i & 0 \\ 0 & 0 & m_i \end{bmatrix}_{3 \times 3}$$

$$\left[G\right] = \left[B\right] = 0$$

$$\left\{RB\right\} = \begin{bmatrix} \ddot{R}_o \\ \dot{\omega}_o \end{bmatrix}_{6 \times 1}$$ – used to define coupling of the rigid body modes of space station with cantilever modes of fixed appendages.

$$\left[R\right] = \left[\begin{array}{c|c} -\bar{m}_1 \; C_F^T & \bar{m}_1 \; C_F^T \left((\widetilde{q_i + h'_F}) + (\widetilde{C_F \, r_1}) \right) \\ \hline -\bar{m}_2 \; C_F^T & \bar{m}_2 \; C_F^T \left((\widetilde{q_i + h'_F}) + (\widetilde{C_F \, r_2}) \right) \\ \hline \cdot & \cdot \\ \cdot & \cdot \\ \cdot & \cdot \\ \hline -\bar{m}_n \; C_F^T & \bar{m}_n \; C_F^T \left((\widetilde{q_i + h'_F}) + (\widetilde{C_F \, r_n}) \right) \end{array}\right]_{3n \times 6}$$

$$\left\{ \ddot{s} \right\} = \begin{bmatrix} \ddot{x}_i \\ \dot{\omega}_{bi} \end{bmatrix}_{6 \times 1}$$ - used to define coupling of the space station flexible modes with the cantilever modes of the fixed appendage.

$$\left[s_2 \right] = \left[\begin{array}{c|c} -\bar{m}_1 \; C_F^T & \bar{m}_1 \; C_F^T \; (\tilde{h}'_F + (C_F \tilde{r}_1)) \\ \hline \vdots & \vdots \\ \hline -\bar{m}_n \; C_F^T & \bar{m}_n \; C_F^T \; (\tilde{h}'_F + (C_F \tilde{r}_n \;) \end{array} \right]_{3n \times 6}$$

$\left\{ L \right\} = 0$ (no external forces are applied to appendages)

4.2.2.3 Modal Analysis

$$q = \left[\tau \right] n$$

where $\left[\tau \right]$ - modal matrix of dimension $3n \times N_{Fi}$

n - normal modes of which there are N_{Fi}

N_{Fi} - number of normal cantilever modes used to simulate fixed appendage #i.

Assuming $\left[\tau^{T}\right] \left[m\right] \left[\tau\right] = I$, equation (2) becomes

$$\left\langle \begin{array}{l} - \tau^{T} \left[R\right] \left\{\ddot{RB}\right\} - \tau^{T} \left[s_2\right] \left[\gamma_F\right] \left\{\ddot{n}_s\right\} \\ + \left\{\ddot{n}_F\right\} + \left[2 \xi_F \omega_F\right] \left\{\dot{n}_F\right\} + \left[\omega_F^2\right] \left\{n_F\right\} = 0 \end{array} \right\rangle \tag{4.12}$$

where $\left\{\ddot{s}\right\} = \begin{pmatrix} \ddot{x}_i \\ \dot{\omega}_{bi} \end{pmatrix} = \underset{6 \times N_s}{\left[\gamma_F\right]} \underset{N_s \times 1}{\left\{\ddot{n}_s\right\}}$ is

the relationship between the translational and rotational motion of the rigid body to which the appendage is attached and the normal mode accelerations of the space station.

In summary, Equation 4.12 above is generated via the following assumptions:

(a) base motion of the fixed appendage must include translations and rotations due to both rigid body motion of the space station and flexible modes of the space station,

(b) the fixed appendage is modeled by discrete masses; cantilever modes are used to define its modal motion,

(c) the above equations are derived in the coordinate frame of the fixed appendage

(d) moments of inertia of the fixed appendage are defined with respect to principal axes with origin at base of appendage

(e) linearization of equations has resulted because of

(1) small flexible motions of space station

(2) small flexible motions of fixed array

(3) small rigid body motion of space station

4.2.3 ROTATING ARRAYS

Rotating arrays are modeled exactly as fixed appendages, except that the base of the rotating array may have rotational motion with respect to the rigid body of the space station to which it is attached.

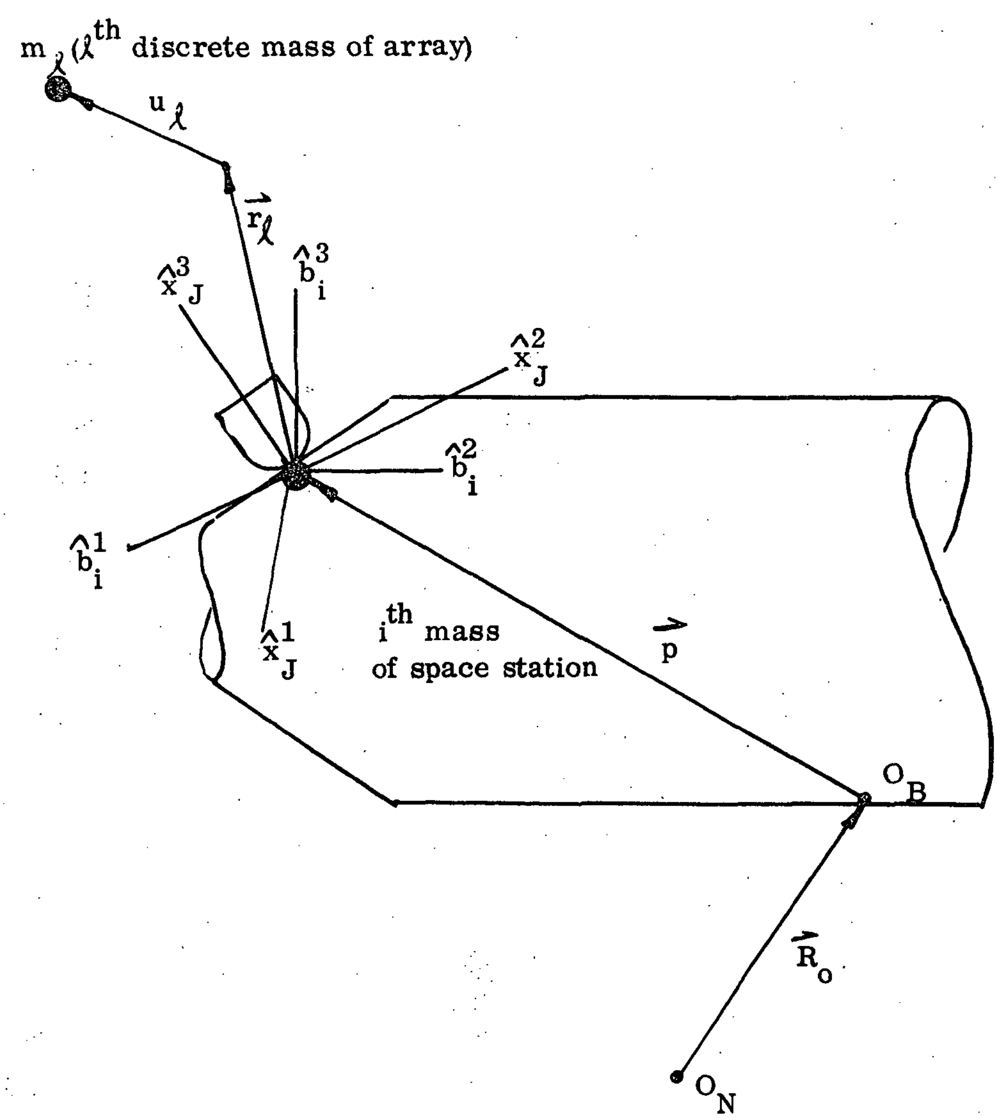

FIGURE 4-11 FLEXIBLE APPENDAGE COORDINATE SYSTEM

4.2.3.1 <u>Coordinate Frames and Relationships</u>

$[I]$ - previously defined

$[X_s]$ - previously defined

$[B_i]$ - previously defined

$[X_J]$ - coordinate basis which rotates with angular velocity $\vec{\omega}_J$ with respect to the rigid body of the space station to which it is attached with origin at the attachment point of the rotating array.

The relationship between $[X_J]$ and $[B_i]$ is defined by the direction cosine relationship

$$[B_i] = [C_J]\,[X_J]$$

Likewise, as shown in Reference 4.1

$$[\dot{C}_J] = [C_J]\,\tilde{\omega}_J$$

4.2.3.2 <u>Equation Derivations</u>

Again using D'Alembert's principle, the total force acting on the ℓ^{th} mass particle of the rotating array equals

$$F_\ell = m_\ell \frac{d^2}{dt^2}\left[\vec{R}_o + \vec{q}_i + \vec{x}_i + \vec{h}'_J + \vec{r}_\ell + \vec{u}_\ell\right]_I$$

where

$\vec{h}'_J$ - location of attachment point of appendage with respect to the center of mass of the i^{th} rigid body of the space station to which the appendage is attached

$\vec{r}_\ell$ - undeformed location of m_ℓ of array

$\vec{u}_\ell$ - time dependent location of m_ℓ with respect to undeformed location

Representative calculations, assuming $\vec{h}'_J$ is defined in the $[B_i]$ basis and $\vec{r}_\ell$ and $\vec{u}_\ell$ are defined in the $[X_J]$ basis, are

$$\frac{d}{dt}\left[\vec{u}_\ell\right]_J = \frac{d}{dt}\left[I^T \; C_o C_{bi} C_J \; u_\ell \right]$$

$$= I^T \Big[C_o \tilde{\omega}_o C_{bi} C_J u_\ell + C_o C_{bi} \tilde{\omega}_{bi} C_J u_\ell + C_o C_{bi} C_J \tilde{\omega}_J u_\ell$$

$$+ C_o C_{bi} C_J \dot{u}_\ell \Big]$$

$$\frac{d^2}{dt^2}\left[\vec{u}_\ell\right]_I = I^T \; C_o \Big[\tilde{\omega}_o \tilde{\omega}_o C_{bi} C_J u_\ell + \dot{\tilde{\omega}}_o C_{bi} C_J u_\ell + 2\tilde{\omega}_o C_{bi} \tilde{\omega}_{bi} C_J u_\ell$$

$$+ 2\tilde{\omega}_o C_{bi} C_J \tilde{\omega}_J u_\ell + 2\tilde{\omega}_o C_{bi} C_J \dot{u}_\ell + C_{bi} \tilde{\omega}_{bi} \tilde{\omega}_{bi} C_J u_\ell$$

$$+ 2 C_{bi} \tilde{\omega}_{bi} C_J \dot{u}_\ell + C_{bi} \dot{\tilde{\omega}}_{bi} C_J u_\ell + 2 C_{bi} \tilde{\omega}_{bi} C_J \tilde{\omega}_J u_\ell$$

$$+ C_{bi} C_J \tilde{\omega}_J \tilde{\omega}_J u_\ell + 2 C_{bi} C_J \tilde{\omega}_J \dot{u}_\ell + C_{bi} C_J \dot{\tilde{\omega}}_J u_\ell + C_{bi} C_J \ddot{u}_\ell \Big]$$

$$\therefore \quad \left\{F_\ell\right\} = m_\ell \, x_J^T \Big[(C_J^T \; C_{bi}^T) \big(\{ \tilde{\omega}_o \tilde{\omega}_o (R_o + q_i + x_i) + 2\tilde{\omega}_o (\dot{R}_o + \dot{x}_i)$$

$$+ \dot{\tilde{\omega}}_o (R_o + q_i + x_i) + \ddot{R}_o + \ddot{x}_i \} + \{ \tilde{\omega}_o \tilde{\omega}_o C_{bi} + \dot{\tilde{\omega}}_o C_{bi} + 2\tilde{\omega}_o C_{bi} \tilde{\omega}_{bi}$$

$$+ \cancel{C_{bi} \tilde{\omega}_{bi}} \tilde{\omega}_{bi} + C_{bi} \dot{\tilde{\omega}}_{bi} \} h'_J + \{ \tilde{\omega}_o \tilde{\omega}_o C_{bi} C_J + \dot{\tilde{\omega}}_o C_{bi} C_J$$

$$+ 2\tilde{\omega}_o C_{bi} \tilde{\omega}_{bi} C_J + 2\tilde{\omega}_o C_{bi} C_J \tilde{\omega}_J + \cancel{C_{bi} \tilde{\omega}_{bi}} \tilde{\omega}_{bi} C_J + C_{bi} \dot{\tilde{\omega}}_{bi} C_J$$

$$+ 2 C_{bi} \tilde{\omega}_{bi} C_J \tilde{\omega}_J + C_{bi} C_J \tilde{\omega}_J \tilde{\omega}_J + C_{bi} C_J \dot{\tilde{\omega}}_J \} (r_\ell + u_\ell)$$

$$+ \{ 2\tilde{\omega}_o C_{bi} C_J + 2 \cancel{C_{bi} \tilde{\omega}_{bi}} C_J \} \dot{u}_\ell \big) + 2\tilde{\omega}_J \dot{u}_\ell + \ddot{u}_\ell \Big]$$

Again, ignoring products of small variables and recalling that

$$C_{bi} \cong E - \tilde{\theta}^i$$

$$\therefore \left\{F_\ell\right\} = m_\ell \; x_J^T \Big[(C_J^T)(E + \tilde{\theta}^i)(\{\tilde{\omega}_o \tilde{\omega}_o (R_o + q_i + x_i)$$

$$+ 2\tilde{\omega}_o (\dot{R}_o + \dot{x}_i) + \dot{\tilde{\omega}}_o (R_o + q_i + x_i) + \ddot{R}_o + \ddot{x}_i\} + \{\tilde{\omega}_o \tilde{\omega}_o$$

$$- \tilde{\omega}_o \tilde{\omega}_o \tilde{\theta}^i + \dot{\tilde{\omega}}_o - \dot{\tilde{\omega}}_o \tilde{\theta}^i + 2\tilde{\omega}_o \tilde{\omega}_{bi} + \dot{\tilde{\omega}}_{bi}\} \; h'_J$$

$$+ \{\tilde{\omega}_o \tilde{\omega}_o C_J (r_\ell + u_\ell) - \tilde{\omega}_o \tilde{\omega}_o \tilde{\theta}^i C_J r_\ell + \dot{\tilde{\omega}}_o C_J (r_\ell + u_\ell) - \tilde{\omega}_o \tilde{\theta}^i C_J r_\ell$$

$$+ 2\tilde{\omega}_o \tilde{\omega}_{bi} C_J r_\ell + 2\tilde{\omega}_o C_J \tilde{\omega}_J (r_\ell + u_\ell) - 2\tilde{\omega}_o \tilde{\theta}^i C_J \tilde{\omega}_J r_\ell$$

$$+ \tilde{\omega}_{bi} C_J r_\ell + 2\omega_{bi} C_J \omega_J r_\ell + C_J \tilde{\omega}_J \tilde{\omega}_J (r_\ell + u_\ell)$$

$$- \tilde{\theta}^i C_J \tilde{\omega}_J \tilde{\omega}_J r_\ell + C_J \dot{\tilde{\omega}}_J (r_\ell + u_\ell) - \tilde{\theta}^i C_J \dot{\tilde{\omega}}_J r_\ell + 2\tilde{\omega}_o C_J \dot{u}_\ell\}$$

$$+ 2\tilde{\omega}_J \dot{u}_\ell + \ddot{u}_\ell \Big]$$

$$= m_\ell \; x_J^T \Big[(C_J^T)(\{\tilde{\omega}_o \tilde{\omega}_o (R_o + q_i + x_i) + 2\tilde{\omega}_o (\dot{R}_o + \dot{x}_i) + \dot{\tilde{\omega}}_o (R_o + q_i + x_i)$$

$$+ \ddot{R}_o + \ddot{x}_i\} + \{\tilde{\omega}_o \tilde{\omega}_o - \tilde{\omega}_o \tilde{\omega}_o \tilde{\theta}^i + \dot{\tilde{\omega}}_o - \dot{\tilde{\omega}}_o \tilde{\theta}^i + 2\tilde{\omega}_o \tilde{\omega}_{bi} + \dot{\tilde{\omega}}_{bi}\} \; h'_J$$

$$+ \tilde{\omega}_o \tilde{\omega}_o C_J (r_\ell + u_\ell) - \tilde{\omega}_o \tilde{\omega}_o \tilde{\theta}^i C_J r_\ell + \dot{\tilde{\omega}}_o C_J (r_\ell + u_\ell) - \dot{\tilde{\omega}}_o \tilde{\theta}^i C_J r_\ell$$

$$+ 2\tilde{\omega}_o \tilde{\omega}_{bi} C_J r_\ell + 2\tilde{\omega}_o C_J \tilde{\omega}_J (r_\ell + u_\ell) - 2\tilde{\omega}_o \tilde{\theta}^i C_J \omega_J r_\ell + \dot{\tilde{\omega}}_{bi} C_J r_\ell$$

$$+ 2\tilde{\omega}_{bi} C_J \omega_J r_\ell + C_J \tilde{\omega}_J \tilde{\omega}_J (r_\ell + u_\ell) - \cancel{\tilde{\theta}^i C_J \tilde{\omega}_J \tilde{\omega}_J r_\ell} + C_J \dot{\tilde{\omega}}_J (r_\ell + u_\ell)$$

$$- \cancel{\tilde{\theta}^i C_J \dot{\tilde{\omega}}_J r_\ell} + 2\tilde{\omega}_o C_J \dot{u}_\ell + \tilde{\theta}^i \tilde{\omega}_o \tilde{\omega}_o (R_o + q_i + x_i) + 2\tilde{\theta}^i \omega_o (\dot{R}_o + \dot{x}_i)$$

$$+\tilde{\theta}^i \dot{\tilde{\omega}}_o (R_o + q_i + x_i) + \tilde{\theta}^i \ddot{R}_o + \tilde{\theta}^i \ddot{x}_i + \theta^i \tilde{\omega}_o \tilde{\omega}_o h'_J + \tilde{\theta}^i \dot{\tilde{\omega}}_o h'_J$$

$$+\tilde{\theta}^i \tilde{\omega}_o \tilde{\omega}_o C_J r_\ell + \tilde{\theta}^i \dot{\tilde{\omega}}_o C_J r_\ell + 2\tilde{\theta}^i \tilde{\omega}_o C_J \omega_J r_\ell + \cancel{\tilde{\theta}^i C_J \tilde{\omega}_J \tilde{\omega}_J} r_\ell$$

$$\cancel{+\tilde{\theta}^i C_J \dot{\tilde{\omega}}_J r_\ell}) + 2\tilde{\omega}_J \dot{u}_\ell + \ddot{u}_\ell \Big]$$

Small space station motion may be assumed and therefore

$$\left\{F_\ell\right\} = m_\ell X_J^T \Big[(C_J^T)\Big(\dot{\tilde{\omega}}_o q_i + \ddot{R}_o + \ddot{x}_i + \tilde{\omega}_o h'_J + \dot{\tilde{\omega}}_{bi} h'_J$$

$$+\dot{\tilde{\omega}}_o C_J r_\ell + 2\tilde{\omega}_o C_J \tilde{\omega}_J r_\ell + \dot{\tilde{\omega}}_{bi} C_J r_\ell + 2\tilde{\omega}_{bi} C_J \tilde{\omega}_J r_\ell \qquad (4.13)$$

$$+ C_J \tilde{\omega}_J \tilde{\omega}_J (r_\ell + u_\ell) + C_J \dot{\tilde{\omega}}_J (r_\ell + u_\ell)\Big) + 2\tilde{\omega}_J \dot{u}_\ell + \ddot{u}_\ell \Big]$$

Letting $q = \left[u_{11}, u_{12}, u_{13}, \ldots, u_{n1}, u_{n2}, u_{n3}\right]^T$

$$\left[m\right]\ddot{q} + \left[K\right] q = -\left[G\right]\dot{q} - \left[B\right] q + \left[R\right]\left\{RB\right\} \qquad (4.14)$$
$$+ \left\{L\right\} + \left[s_2\right]\left\{\ddot{s}\right\}$$

where

$$\underset{3n \times 3n}{\left[G\right]} = \text{Diag}\ (2\,\overline{m}_1 \tilde{\omega}_J, 2\,\overline{m}_2 \tilde{\omega}_J, \ldots, 2\,m_n \hat{\omega}_J)$$

$$\underset{3n \times 3n}{\left[B\right]} = \text{Diag}\ (\overline{m}_1 (\dot{\tilde{\omega}}_J + \tilde{\omega}_J \tilde{\omega}_J), \ldots, \overline{m}_n (\dot{\tilde{\omega}}_J + \tilde{\omega}_J \tilde{\omega}_J))$$

$$\left\{RB\right\} = \begin{bmatrix} \ddot{R}_o \\ \dot{\omega}_o \\ \dot{\omega}_{A1} \\ \dot{\omega}_{A2} \end{bmatrix}_{10 \times 1}$$

$$\underset{3 \times 1}{\left\{\omega_J\right\}} = \underset{3 \times 2}{\left[C_J^{\,*}\right]^T} \begin{bmatrix} KG & 0 \\ 0 & 1 \end{bmatrix} \underset{2 \times 1}{\left\{\omega_{AJ}\right\}}$$

NOTE: Motion of rotating arrays is exactly as defined in Section 4.1 with only two rotation degrees of freedom allowed.

$$\left\{\ddot{s}\right\} = \begin{pmatrix} \ddot{x}_i \\ \dot{\omega}_{bi} \end{pmatrix}_{6 \times 1}$$

$$\underset{3n \times 6}{\left[s_2\right]} = \left[\begin{array}{c|c} -\bar{m}_1 \, C_J^T & \bar{m}_1 \, C_J^T \left[\widetilde{h'_J + C_J \, r_1}\right] \\ \hline \cdot & \\ \cdot & \\ \cdot & \\ \hline -\bar{m}_n \, C_J^T & \bar{m}_n \, C_J^T \left[\widetilde{h'_J + C_J \, r_n}\right] \end{array}\right]$$

$$\underset{3n \times 10}{\left[R_1\right]} = \left[\begin{array}{c|c|c|c} -\bar{m}_1 \, C_J^T & \bar{m}_1 \, C_J^T \left[q_i + \widetilde{h'_J + C_1 \, r_1}\right] & \bar{m}_1 \, \tilde{r}_1 \, C_1^{*T} \begin{bmatrix} KG & 0 \\ 0 & 1 \end{bmatrix} & 0 \\ \hline \cdot & \cdot & \cdot & \\ \cdot & \cdot & \cdot & 0 \\ \cdot & \cdot & \cdot & \\ \hline -\bar{m}_n \, C_J^T & \bar{m}_n \, C_J^T \left[q_i + \widetilde{h'_J + C_1 \, r_n}\right] & \bar{m}_n \tilde{r}_n \, C_1^{*T} \begin{bmatrix} KG & 0 \\ 0 & 1 \end{bmatrix} & 0 \end{array}\right]$$

$$\underset{3n \times 1}{\left\{ L \right\}} = - \left[m \right] . \text{Diag} \quad \left(C_J^T \left(2\, \tilde{\omega}_o C_J \tilde{\omega}_J + C_J \tilde{\omega}_J \tilde{\omega}_J \right), \; . \; . \; . \quad \right) \bar{r}$$

$$\underset{3n \times 1}{\bar{r}} = \left[r_{11}, r_{12}, r_{13}, \; . \quad . \quad r_{n1}, r_{n2}, r_{n3} \right]^T$$

4.2.3.3 <u>Modal Analysis</u>

$$q = \Phi \eta$$

$$\Phi^T \left[m \right] \Phi = I$$

$$\left\langle \begin{array}{l} -\Phi^T \left[R \right] \left\{ RB \right\} - \Phi^T \left[S_2 \right] \left[\gamma_R \right] \left\{ \ddot{\eta}_S \right\} \\ \quad + \left\{ \ddot{\eta}_R \right\} + \left[2 \zeta \omega_s \right] \left\{ \dot{\eta}_R \right\} + \left[\omega_s^2 \right] \left\{ \eta_R \right\} \\ \quad = -\Phi^T \left[G \right] \Phi \left\{ \dot{\eta}_R \right\} - \Phi^T \left[B \right] \Phi \left\{ \eta_R \right\} + \Phi^T \left\{ L \right\} \end{array} \right\rangle \quad (4.$$

In summary, the above equation was derived assuming

(a) base motion of the rotating array includes translations and rotations due to both space station rigid body motion and space station flexible motion

(b) the rotating array is modeled by discrete masses; cantilever modes are used to define its modal motion

(c) rotational motions of the array may be constrained as previously derived in Section 4.1.

(d) the above equations are derived in the coordinate frame of the rotating array

(e) small motion of the rotating arrays is not assumed to further linearize the above equation

4.2.4 TOTAL SYSTEM EQUATION

The above derived equations, along with the rigid body equations of Reference 4.1 can be combined into one large matrix ordinary differential equation of the form

$$\left\langle [M]\ \ddot{x} + [C]\ \dot{x} + [K]\ x = P \right\rangle \tag{4.16}$$

where

$$\ddot{x} = \begin{bmatrix} \ddot{R} \\ \ddot{n}_s \\ \ddot{n}_R \\ \ddot{n}_F \end{bmatrix}$$

The column dimensional size of Equation 4.16 is equal to $N_{TT} = 10 + N_s + N_R + N_F \leq 70.$

N_s - total number of simulated flexible space station modes

N_R - total number of flexible cantilever modes associated with 0, 1, or 2 rotating arrays ($= N_{R1} + N_{R2}$)

N_F - total number of flexible cantilever modes associated with 0, 1, 2, 3, or 4 fixed appendages ($= N_{F1} + N_{F2} + N_{F3} + N_{F4}$)

Before preceding with the make up of the [M] , [C] , [K] , [X], & [P] matrices it should again be made very clear that rotational motion of the two rotating arrays is exactly as defined in Section 4.1. Only two rotational degrees of freedom are allowed. Likewise, either axis of both drivers may be locked. No attempt has been made here to recount these equation derivations, or those involving array driver gear trains, etc.

The only departure from the equations derived in Sections 4.2, 4.3 and 4.4 has been to assume that the distances from the attachment points of rotating arrays ($\bar{h}'_J$) and fixed appendages ($\bar{h}'_F$) to the center of mass is negligible. This assumption has been made since the space station will be modeled as a collection of particle masses, with moments of inertia possible for each. This places the base of each array and appendage at a mass grid pt. of the space station. Therefore:

$$\vec{q}_{F_J} = \vec{h}_{F_J}$$

$$\vec{q}_{R_J} = \vec{h}_J$$

Submatrices of $\{\ddot{x}\}$

$$\underset{10 \times 1}{\{\ddot{R}\}} = \begin{bmatrix} \ddot{R}_o \\ \ddot{\omega}_o \\ \dot{\omega}_{A1} \\ \dot{\omega}_{A2} \end{bmatrix}$$ - rigid modes of space and two rotating arrays.

$$\underset{N_R \times 1}{\left\{\ddot{n}_R\right\}} = \begin{bmatrix} \ddot{n}_{R1} \\ \\ \ddot{n}_{R2} \end{bmatrix} \begin{matrix} N_{R1} \times 1 \\ \\ N_{R2} \times 1 \end{matrix}$$

$$\underset{N_F \times 1}{\left\{\ddot{n}_F\right\}} = \begin{bmatrix} \ddot{n}_{F1} \\ \ddot{n}_{F2} \\ \ddot{n}_{F3} \\ \ddot{n}_{F4} \end{bmatrix} \begin{matrix} N_{F1} \times 1 \\ N_{F2} \times 1 \\ N_{F3} \times 1 \\ N_{F4} \times 1 \end{matrix}$$

$$\underset{N_s \times 1}{\left\{\ddot{n}_s\right\}} = \begin{bmatrix} \ddot{n}_s \end{bmatrix} \quad N_s \times 1$$

$$\begin{bmatrix} M \end{bmatrix} = \left[\begin{array}{c|c|c|c} M_{11} & M_{12} & M_{13} & M_{14} \\ \hline M_{21} & M_{22} & M_{23} & M_{24} \\ \hline M_{31} & M_{32} & I & 0 \\ \hline M_{41} & M_{42} & 0 & I \end{array}\right]$$

$$
C = \begin{bmatrix} 0 & 0 & 0 & 0 \\ 0 & 2\zeta_s \omega_s & 0 & 0 \\ 0 & 0 & 2\zeta_r \omega_r & 0 \\ 0 & 0 & 0 & 2\zeta_F \omega_F \end{bmatrix} + \begin{bmatrix} 0 & 0 & 0 & 0 \\ 0 & 0 & 0 & 0 \\ 0 & 0 & \begin{matrix} \Phi_{R1}^T G_1 \Phi_{R1} & 0 \\ 0 & \Phi_{R2}^T G_2 \Phi_{R2} \end{matrix} & 0 \\ 0 & 0 & 0 & 0 \end{bmatrix}
$$

$$
P = \begin{bmatrix} P_1 & 10 \times 1 \\ P_2 & N_s \times 1 \\ P_3 & N_R \times 1 \\ P_4 & N_F \times 1 \end{bmatrix}
$$

$$
K = \left[\begin{array}{c|c|c|c}
0 & 0 & 0 & 0 \\ \hline
0 & \omega_s^2 & 0 & 0 \\ \hline
0 & 0 & \omega_R^2 & 0 \\ \hline
0 & 0 & 0 & \omega_F^2
\end{array}\right]
+
\left[\begin{array}{c|c|cc|c}
0 & 0 & 0 & & 0 \\ \hline
0 & 0 & 0 & & 0 \\ \hline
0 & 0 & \Phi_1^T B_1 \Phi_1 & 0 & 0 \\
 & & 0 & \Phi_2^T B_2 \Phi_2 & \\ \hline
0 & 0 & 0 & & 0
\end{array}\right]
$$

As the above partitioning implies, Equation 4.16 is generated via four coupled matrix equations:

$$
\left[M_{11}\right] \ddot{R} + \left[M_{12}\right] \ddot{n}_s + \left[M_{13}\right] \ddot{n}_R + \left[M_{14}\right] \ddot{n}_F = P_1 \tag{4.17}
$$

$$
\begin{aligned}
\left[M_{21}\right] \ddot{R} + \left[M_{22}\right] \ddot{n}_s + \left[M_{23}\right] \ddot{n}_R + \left[M_{24}\right] \ddot{n}_F \\
+ \left[2 \zeta_s \omega_s\right] \dot{n}_s + \left[\omega_s^2\right] n_s = P_2
\end{aligned} \tag{4.18}
$$

$$
\begin{aligned}
\left[M_{31}\right] \ddot{R} + \left[M_{32}\right] \ddot{n}_s + [I] \ddot{n}_R + 0 \\
+ \left[2 \zeta_R \omega_R\right] \dot{n}_R + \left[\omega_R^2\right] n_R = P_3
\end{aligned} \tag{4.19}
$$

$$
\begin{aligned}
\left[M_{41}\right] \ddot{R} + \left[M_{42}\right] \ddot{n}_s + 0 + [I] \ddot{n}_F \\
+ \left[2 \zeta_F \omega_F\right] \dot{n}_F + \left[\omega_F^2\right] n_F = P_4
\end{aligned} \tag{4.20}
$$

Discussing each equation in detail:

Equation 4.17 is the basic rigid body system equation of Section 4.1 with only slight modification

(1) Forces and Torques on the system induced by the flexible appendage transient response are, in their own basis

$$\left.\begin{aligned} \hat{F}_J &= -\sum_E^T M_{RJ} \Phi_{RJ} \ddot{n}_{RJ} \\ \hat{T}_J &= -\sum_E^T \tilde{\tilde{r}}_{RJ} M_{RJ} \Phi_{RJ} \ddot{n}_{RJ} \end{aligned}\right\} \begin{array}{l} \text{rotating} \\ \text{appendages} \\ J = 1,2 \end{array}$$

$$\left.\begin{aligned} \hat{\dot{F}}_{FJ} &= -\sum_E^T M_{FJ} \Phi_{FJ} \ddot{n}_{FJ} \\ \hat{T}_{FJ} &= -\sum_E^T \tilde{\tilde{r}}_{FJ} M_{FJ} \Phi_{FJ} \ddot{n}_{FJ} \end{aligned}\right\} \begin{array}{l} \text{fixed} \\ \text{appendages} \\ J = 1,2,3,4 \end{array}$$

(2) Addition of applied external torque $\bar{T}_R$ if desired

(3) Mass and moment of inertia of space station includes that do to any fixed appendages.

(4) Inclusion of terms dependent upon modal acceleration of space station at attachment points of appendages, (see 4.6.3).

Partitioning equation 4.17 into four equations:

$$\begin{aligned} & A_1 \ddot{R}_o + A_5 \dot{\omega}_o + A_9 \dot{\omega}_{A1} + A_{13} \dot{\omega}_{A2} \\ & - \sum_J^2 C_J \hat{F}_J - \sum_J^4 C_{FJ} \hat{F}_{FJ} \\ & - \sum_J^2 F_J' - \sum_J^4 F_{F_J}' = F_1 \end{aligned} \tag{4-21}$$

$$A_2 \ddot{R}_o + A_6 \dot{\omega}_o + A_{10} \dot{\omega}_{A1} + A_{13} \dot{\omega}_{A2}$$

$$- \sum_J^2 C_J \hat{T}_J + \sum_J^2 \tilde{r}'_J C_J \hat{F}_J - \sum_J^4 C_{FJ} \hat{T}_{FJ} + \sum_J^4 \tilde{r}'_{FJ} C_{FJ} \hat{F}_{FJ} \qquad (4.22)$$

$$- \sum_J^2 T'_J - \sum_J^4 T'_{F_J} = T_R + F_2 .$$

$$A_3 \ddot{R}_o + A_7 \dot{\omega}_o + A_{11} \dot{\omega}_{A1} + A_{15} \dot{\omega}_{A2} - T''_1 = F_3 \qquad (4.23)$$

$$A_4 \ddot{R}_o + A_8 \dot{\omega}_o + A_{12} \dot{\omega}_{A1} + A_{16} \dot{\omega}_{A2} - T''_2 = F_4 \qquad (4.24)$$

$$\therefore \underset{10 \times 10}{\left[M_{11}\right]} = \begin{bmatrix} A_1 & A_5 & A_9 & A_{13} \\ A_2 & A_6 & A_{10} & A_{14} \\ A_3 & A_7 & A_{11} & A_{15} \\ A_4 & A_8 & A_{12} & A_{16} \end{bmatrix}$$

previously defined rigid body matrix A of Section 4.1.

4

$$
\begin{bmatrix} M_{12} \end{bmatrix} = -\sum_{J}^{4} \left[\begin{array}{c:c} -\overline{m}_{F_i} & \overline{m}_{F_i}\left(C_{F_i}\widetilde{r_{F_i}}\right) \\ \hline -\overline{m}_{F_i}\left(C_{F_i}\widetilde{r}_{F_i}\right) + \widetilde{r}'_{F_i}\ -\overline{m}_{F_i} & \overline{m}_{F_i}\left(C_{F_i}\widetilde{r}_{F_i}\right)^2 - C_{F_i} I_{F_i} C_{F_i} - \widetilde{r}_{F_i}\overline{m}_{F_i}\left(C_{F_i}\widetilde{r}_{F_i}\right) \end{array} \right] \begin{bmatrix} G'^{T}_{F_i} \\ G''^{T}_{F_i} \end{bmatrix}
$$

$$
- \sum_{J}^{2} \left[\begin{array}{c|c} -\overline{m}_J & \overline{m}_J\left(C_J r_J\right) \\ \hline -\overline{m}_J\left(C_J\widetilde{r}_J\right) + \widetilde{r}'_J\ \overline{m}_J & \overline{m}_J\left(C_J\widetilde{r}_J\right)^2 - C_J I_J C_J^{T} - \widetilde{r}'_J\ \overline{m}_J\left(C_J\widetilde{r}_J\right) \\ \hline 0 & 0 \end{array} \right] \begin{bmatrix} G'^{T}_{R_J} \\ \hline G''^{T}_{R_J} \end{bmatrix}
$$

$$(10 \times 6) \qquad\qquad 6 \times N_S$$

$$
\begin{array}{cc}
\underset{10 \times N_R}{\left[M_{13} \right]} \quad = & \left[\begin{array}{c|c}
\underset{3 \times N_{R1}}{+ C_1 D_{R1}} & \underset{3 \times N_{R2}}{+ C_2 D_{R2}} \\
\hline
\underset{3 \times N_{R1}}{+ C_1 R_{R1} - \tilde{r}'_1 C_1 D_{R1}} & \underset{3 \times N_{R2}}{+ C_2 R_{R2} - \tilde{r}'_2 C_2 D_{R2}} \\
\hline
\underset{4 \times N_{R1}}{0} & \underset{4 \times N_{R2}}{0}
\end{array}\right] \\
 & \begin{array}{cc} 10 \times N_{R1} \qquad\qquad & \qquad\qquad 10 \times N_{R1} \end{array}
\end{array}
$$

where

$$
\underset{3 \times N_{RJ}}{\left[D_{RJ} \right]} = \sum_{E}^{T} M_{RJ} \; \Phi_{RJ} \qquad J = 1,2
$$

$$
\underset{3 \times N_{RJ}}{\left[R_{RJ} \right]} = \sum_{E}^{T} \tilde{\tilde{r}}_{RJ} \; M_{RJ} \; \Phi_{RJ} \qquad J = 1,2
$$

$$
\underset{10 \times N_F}{\left[M_{14} \right]} = \left[\begin{array}{c|c|c|c}
\underset{3 \times N_{F1}}{+C_{F1} D_{F1}} & \underset{3 \times N_{F2}}{+C_{F2} D_{F2}} & \underset{3 \times N_{F3}}{+C_{F3} D_{F3}} & \underset{3 \times N_{F4}}{+C_{F4} D_{F4}} \\
\hline
\underset{3 \times N_{F1}}{+C_{F1} R_{F1} - \tilde{r}'_{F1} C_{F1} D_{F1}} & \underset{3 \times N_{F2}}{+C_{F2} R_{F2} - \tilde{r}'_{F2} C_{F2} D_{F2}} & \underset{3 \times N_{F3}}{+C_{F3} R_{F3} - \tilde{r}'_{F3} C_{F3} D_{F3}} & \underset{3 \times N_{F4}}{+C_{F4} R_{F4} - \tilde{r}'_{F4} C_{F4} D_{F4}} \\
\hline
\underset{4 \times N_{F1}}{0} & \underset{4 \times N_{F2}}{0} & \underset{4 \times N_{F3}}{0} & \underset{4 \times N_{F4}}{0}
\end{array} \right]
$$

where

$$
\underset{3 \times N_{FJ}}{\left[D_{FJ} \right]} = \sum_{E}^{T} M_{FJ} \; \Phi_{FJ}
$$

$$
\underset{3 \times N_{FJ}}{\left[R_{FJ} \right]} = \sum_{E}^{T} \tilde{\underline{r}}_{FJ} \; M_{FJ} \; \Phi_{FJ}
$$

$$\underset{10 \times 1}{\left[P_1 \right]} = \begin{bmatrix} F_1 \\ T_R + F_2 \\ F_3 \\ F_4 \end{bmatrix}$$

as previously defined in Section 4.1
except for addition of external torque T_R

Equation 4.18 is the flexible modal equation for the space station. These flexible modes are excited by external forces and torques on the space station, including those which act at the attachment points of the rotating and fixed arrays.

Equations for the various hinge forces and torques are shown in Section 4.2.5.3.The above excluded linear terms in $\ddot{R}_o$, $\dot{\omega}_o$, $\dot{\omega}_{A1}$, $\dot{\omega}_{A2}$ are regrouped on the left-hand side of Equation 4.16 for proper coupling with the rigid body modes (forming M_{21}). Linear terms in $\ddot{n}_s$ are regrouped on the left-hand side of Equation 4.16 for proper coupling with the space station modes (M_{22}). Likewise, linear terms in $\ddot{n}_R$, and $\ddot{n}_F$ form M_{23} and M_{24}, respectively.

$$\left[M_{21}\right] = -\sum_{i=1}^{4} \left[G_{F_i}{}' \;\vdots\; G_{F_i}{}''\right] \left[\begin{array}{c|c|c} -\bar{m}_{F_i} & \bar{m}_{F_i}\,(\widetilde{h_{F_i}+C_{F_i}r_{F_i}}) & \\ \hline -\bar{m}_{F_i}(\widetilde{C_{F_i}r_{F_i}}) & -C_{F_i}I_{F_i}C_{F_i}{}^{T} + \bar{m}_{F_i}(\widetilde{C_{F_i}r_{F_i}})\,(\widetilde{h_{F_i}+C_{F_i}r_{F_i}}) & \end{array}\;0\right]$$

$$-\sum_{j=1}^{2} \left[G_{RJ} \;\vdots\; G_{RJ}\right] \left[\begin{array}{c|c} I & 0 \\ \hline 0 & C_J{}^{**} \end{array}\right] \left[\begin{array}{c|c|c|c} -\bar{m}_J & \bar{m}_J(\widetilde{h_J + C_J r_J}) & a_1 & a_3 \\ \hline -\bar{m}_J\tilde{r}_J C_J{}^{T} & -I_J C_J{}^{T} + \bar{m}_J\tilde{r}_J C_J{}^{T}(\widetilde{h_J + C_J r_J}) & a_2 & a_4 \end{array}\right] \qquad (1)$$

(1) if $J=1$ $a_3 = a_4 = 0$

$$a_1 = \bar{m}_1 C_1 \tilde{r}_1 C_1^{*T} \begin{bmatrix} 1/KG & 0 \\ 0 & 1 \end{bmatrix}$$

$$a_2 = -(I_1 - m_1\tilde{r}_1\tilde{r}_1)\, C_1^{*T} \begin{bmatrix} 1/KG & 0 \\ 0 & 1 \end{bmatrix}$$

if $J=2$ $a_1 = a_2 = 0$

$$a_3 = \bar{m}_2 C_2 \tilde{r}_2 C_2^{*T} \begin{bmatrix} 1/KG & 0 \\ 0 & 1 \end{bmatrix}$$

$$a_4 = -(I_2 - m_2\tilde{r}_2\tilde{r}_2)\, C_2^{*T} \begin{bmatrix} 1/KG & 0 \\ 0 & 1 \end{bmatrix}$$

$$
\underset{N_s \times N_s}{\begin{bmatrix} M_{22} \end{bmatrix}} = \underset{N_s \times N_s}{\begin{bmatrix} 1 & & 0 \\ & 1 & \\ & & \ddots \\ 0 & & 1 \end{bmatrix}} - \sum_J^4 \underset{N_s \times 10}{\left[G'_{F_i} \;\vdots\; G''_{F_i} \;\vdots\; 0 \right]} \underset{10 \times 6}{\left[\begin{array}{c:c} -\bar{M}_{F_i} & \bar{M}_{F_i} (C_{F_i} \tilde{r}_{F_i}) \\ \hdashline -\bar{M}_{F_i} (C_{F_i} \tilde{r}_{F_i}) & \bar{M}_{F_i} (C_{F_i} \tilde{r}_{F_i})^2 - C_{F_i} J_{F_i} C_{F_i}^T \\ \hdashline \multicolumn{2}{c}{0} \end{array} \right]} \underset{6 \times N_s}{\begin{bmatrix} G_{F_i}^{T\prime} \\ \hdashline G_{F_i}^{T\prime\prime} \end{bmatrix}}
$$

$$
- \sum_J^2 \underset{N_s \times 10}{\left[G'_{R_J} \;\vdots\; G''_{R_J} \;\vdots\; 0 \right]} \underset{10 \times 6}{\left[\begin{array}{c:c} -\bar{M}_J & \bar{M}_J (C_J \tilde{r}_J) \\ \hdashline -M_J (C_J \tilde{r}_J) & \bar{M}_J (C_J \tilde{r}_J)^2 - C_J J_J C_J^T \\ \hdashline \multicolumn{2}{c}{0} \end{array} \right]} \underset{6 \times N_s}{\begin{bmatrix} G_{R_J}^{\prime T} \\ \hdashline G_{R_J}^{\prime\prime T} \end{bmatrix}} ,
$$

$$\left[M_{23}\right] = \left[\begin{array}{c|c} +\gamma_{R1}' C_1 \sum_E^T M_{R1} \Phi_{R1} & +\gamma_{R2}' C_2 \sum_E^T M_{R2} \Phi_{R2} \\ +\gamma_{R_1}'' C_1 \sum_E^T \tilde{\tilde{r}}_{R1} M_{R1} \Phi_{R1} & +\gamma_{R2}'' C_2 \sum_E^T \tilde{\tilde{r}}_{R2} M_{R2} \Phi_{R2} \end{array}\right]$$

$$= \left[\begin{array}{c|c} +G_{R1}' C_1 D_{R1} + G_{R1}'' C_1 R_{R1} & +G_{R2}' C_2 D_{R2} + G_{R2}'' C_2 R_{R2} \\ (N_s \times N_{R1}) & (N_s \times N_{R2}) \end{array}\right]$$

$$(N_s \times N_R)$$

$$\underset{N_s \times N_F}{\left[M_{24}\right]} = \left[\begin{array}{c|c|c|c} +G_{F1}' C_{F1} D_{F1} + G_{F1}'' C_{F1} R_{F1} & +G_{F2}' C_{F2} D_{F2} + G_{F2}'' C_{F2} R_{F2} & +G_{F3}' C_{F3} D_{F3} + G_{F3}'' C_{F3} R_{F3} & +G_{F4}' C_{F4} D_{F4} + G_{F4}'' C_{F4} R_{F4} \\ N_s \times N_{F1} & N_s \times N_{F2} & N_s \times N_{F3} & N_s \times N_{F4} \end{array}\right]$$

where

$\left[G_{RJ}'\right]$ $(N_s \times 3)$ - the transpose of those rows of the modal space station matrix which define the total flexural 3-dimensional displacement of the rigid body of the space station to which the j^{th} rotating appendage is attached.

$\left[G_{RJ}''\right]$ $(N_s \times 3)$ - the transpose of those rows of the modal space station matrix which define the total flexural 3-dimensional rotation of the rigid body of the space station to which the j^{th} rotating appendage is attached.

Like definitions are also true for submatrices G_{F_i}' and G_{F_i}'' at the attachment points of each fixed appendage.

$$\underset{N_s \times 1}{\left[P_2\right]} = \sum_{i=1}^{2} \left[G_{E_i}\right] F_{R_i} + \sum_{i=1}^{2} \left[G''_{E_i}\right] T_{R_i} + \sum_{i=1}^{2} \left[G'_{R_i}\right] (-F'_{H_i})$$

$$+ \sum_{i=1}^{2} \left[G''_{R_i}\right] (-T_i + T'_{AC_i}) \qquad + \left[G''_{CMG}\right] T_{CMG}$$

$$+ \sum_{i=1}^{4} \left[G'_{F_i}\right] (-F'_{H_{F_i}}) + \sum_{i=1}^{4} \left[G''_{F_i}\right] (-T'_{H_{F_i}})$$

where

F'_{HJ} - hinge force on the j^{th} rotating array due to rigid body motion of the array, excluding linear terms in $\dot{R}_o$, $\dot{\omega}_o$, $\dot{\omega}_{A1}$, $\dot{\omega}_{A2}$, $\ddot{n}_s$

T'_{AC_J} - constraint torque exerted on spacecraft by rigid driver along constrained axis, excluding linear terms, (contains hinge torque).

T_J - hinge torque on j^{th} driver produced by control system.

$F'_{H_{F_i}}$ - hinge force on i^{th} fixed appendage excluding linear terms.

$T'_{H_{F_i}}$ - hinge torque on i^{th} fixed appendage excluding linear terms.

G'_x - modal columns (eigenvectors) associated with modal displacements at grid point to which "x" array is attached or external force or torque acts.

G''_x - modal columns associated with modal rotations at grid point to which "x" array is attached or external force or torque acts.

Equation 4.19 is the rotating appendage modal equation in which

$$
\underset{N_R \times 10}{\begin{bmatrix} M_{31} \end{bmatrix}} = \begin{bmatrix} -\Phi_{R1}^T & \begin{bmatrix} R_1 \end{bmatrix} \\ \hline -\Phi_{R2}^T & \begin{bmatrix} R_2 \end{bmatrix} \end{bmatrix}
$$

$$
= \left[\begin{array}{l} -\Phi_{R1}^T \begin{bmatrix} m_{R1} \end{bmatrix} \left[\begin{array}{c|c|c|c} -\Sigma_E C_1^T & \Sigma_E C_1^T \tilde{q}_{R1} + \tilde{\tilde{r}}_{R1} \Sigma_E C_1^T & \tilde{\tilde{r}}_{R1} \Sigma_E C_1^{*T} \begin{bmatrix} 1/KG & 0 \\ 0 & 1 \end{bmatrix} & 0 \end{array}\right] \\ \hline -\Phi_{R2}^T \begin{bmatrix} m_{R2} \end{bmatrix} \left[\begin{array}{c|c|c|c} -\Sigma_E C_2^T & \Sigma_E C_2^T \tilde{q}_{R2} + \tilde{\tilde{r}}_{R2} \Sigma_E C_2^T & 0 & \tilde{\tilde{r}}_{R2} \Sigma_E C_2^{*T} \begin{bmatrix} 1/KG & 0 \\ 0 & 1 \end{bmatrix} \end{array}\right] \end{array}\right]
$$

$$
= \begin{array}{c} \left[\begin{array}{c|c|c|c} D_{R1}^T C_1^T & -D_{R1}^T C_1^T \tilde{q}_{R1} + R_{R1}^T C_1^T & R_{R1}^T C_1^{*T} \begin{bmatrix} 1/KG & 0 \\ 0 & 1 \end{bmatrix} & 0 \\ \hline D_{R2}^T C_2^T & -D_{R2}^T C_2^T \tilde{q}_{R2} + R_{R2}^T C_2^T & 0 & R_{R2}^T C_2^{*T} \begin{bmatrix} 1/KG & 0 \\ 0 & 1 \end{bmatrix} \end{array}\right] \\ \begin{array}{cccc} N_R \times 3 & \qquad N_R \times 3 & \qquad N_R \times 2 & \qquad N_R \times 2 \end{array} \end{array}
$$

$$
\left[M_{32}\right] = \left[\begin{array}{ccc}
-\Phi^{T}_{R1} & S^{1}_{2} & \gamma^{1}_{R} \\
\hline
-\Phi^{T}_{R2} & S^{2}_{2} & \gamma^{2}_{R}
\end{array}\right]
$$

$$
= \left[\begin{array}{ccc}
-\Phi^{T}_{R1}\left[m_{R1}\right] & \left[-\Sigma_{E}\, C^{T}_{1} \;\middle|\; \approx{r}_{R1}\, \Sigma_{E}\, C^{T}_{1}\right] & \left[\gamma^{1}_{R}\right] \\
\hline
-\Phi^{T}_{R2}\left[m_{R2}\right] & \left[-\Sigma_{E}\, C^{T}_{2} \;\middle|\; \approx{r}_{R2}\, \Sigma_{E}\, C^{T}_{2}\right] & \left[\gamma^{2}_{R}\right]
\end{array}\right]
$$

$$
= \left[\begin{array}{c}
D^{T}_{R1}\, C^{T}_{1}\, G'^{T}_{R1} + R^{T}_{R1}\, C^{T}_{1}\, G''^{T}_{R1} \\
(N_{R1} \times N_{s}) \\
\hline
D^{T}_{R2}\, C^{T}_{2}\, G^{T}_{R2} + R^{T}_{R2}\, C^{T}_{2}\, G''^{T}_{R2} \\
(N_{R2} \times N_{s})
\end{array}\right]
$$

$$N_{R} \times N_{s}$$

N. B. $\left[M_{32}\right] = + \left[M_{23}\right]^{T}$

$$
\underset{N_R \times 1}{\left[P_3 \right]} = \left[\begin{array}{c} \Phi_{R_1}^T \quad L_1 \\ \quad\quad\quad N_{R_1} \times 1 \\ \hline \Phi_{R_2}^T \quad L_2 \\ \quad\quad\quad N_{R_2} \times 1 \end{array} \right]
$$

Equation 4.20 is the modal equation for the fixed appendages

$$
\underset{N_F \times 10}{\begin{bmatrix} M_{41} \end{bmatrix}} = \begin{bmatrix} -\Phi^T_{F1} \begin{bmatrix} R_{F1} \end{bmatrix} \\ \hline -\Phi^T_{F2} \begin{bmatrix} R_{F2} \end{bmatrix} \\ \hline -\Phi^T_{F3} \begin{bmatrix} R_{F3} \end{bmatrix} \\ \hline -\Phi^T_{F4} \begin{bmatrix} R_{F4} \end{bmatrix} \end{bmatrix}
$$

$$
= \underset{N_F \times 10}{\left[\begin{array}{c|c|c} D^T_{F1} C^T_{F1} & -D^T_{F1} C^T_{F1} \tilde{q}_{F1} + R^T_{F1} C^T_{F1} & 0 \\ \hline D^T_{F2} C^T_{F2} & -D^T_{F2} C^T_{F2} \tilde{q}_{F2} + R^T_{F2} C^T_{F2} & 0 \\ \hline D^T_{F3} C^T_{F3} & -D^T_{F3} C^T_{F3} \tilde{q}_{F3} + R^T_{F3} C^T_{F3} & 0 \\ \hline D^T_{F4} C^T_{F4} & -D^T_{F4} C^T_{F4} \tilde{q}_{F4} + R^T_{F4} C^T_{F4} & 0 \end{array}\right]}
$$

$$
\begin{bmatrix} M_{42} \end{bmatrix} = \begin{bmatrix} -\Phi^T_{F1} \begin{bmatrix} S^{F1}_2 \end{bmatrix} \begin{bmatrix} \gamma_{F1} \end{bmatrix} \\ \hdashline -\Phi^T_{F2} \begin{bmatrix} S^{F2}_2 \end{bmatrix} \begin{bmatrix} \gamma_{F2} \end{bmatrix} \\ \hdashline -\Phi^T_{F3} \begin{bmatrix} S^{F3}_2 \end{bmatrix} \begin{bmatrix} \gamma_{F3} \end{bmatrix} \\ \hdashline -\Phi^T_{F4} \begin{bmatrix} S^{F4}_2 \end{bmatrix} \begin{bmatrix} \gamma_{F4} \end{bmatrix} \end{bmatrix}
$$

$$
= \begin{bmatrix} D^T_{F1}\, C^T_{F1}\, G'^T_{F1} + R^T_{F1}\, C^T_{F1}\, G''^T_{F1} \\ (N_{F1} \times N_s) \\ \hline D^T_{F2}\, C^T_{F2}\, G'^T_{F2} + R^T_{F2}\, C^T_{F2}\, G''^T_{F2} \\ (N_{F2} \times N_s) \\ \hline D^T_{F3}\, C^T_{F3}\, G'^T_{F3} + R^T_{F3}\, C^T_{F3}\, G''^T_{F3} \\ (N_{F3} \times N_s) \\ \hline D^T_{F4}\, C^T_{F4}\, G'^T_{F4} + R^T_{F4}\, C^T_{F4}\, G''^T_{F4} \\ (N_{F4} \times N_s) \end{bmatrix}
$$

$$N_F \times N_s$$

$$
\underset{N_F \times 1}{\begin{bmatrix} P_4 \end{bmatrix}} = 0
$$

N. B. $\begin{bmatrix} M_{42} \end{bmatrix} = + \begin{bmatrix} M_{24} \end{bmatrix}^T$

4.2.5 AUXILIARY EQUATIONS

4.2.5.1 When free-free modes are utilized in the definition of spacecraft flexibility it can be shown that

$$
\left[\gamma^{T}\right]_{N_s \times 6n} \cdot \left[\begin{array}{c|c} -\bar{m}_1 & \bar{m}_1\,(\widetilde{R_o + q_1}) \\ \hline 0 & -\bar{I}^{1} \\ \hline -\bar{m}_2 & \bar{m}_2\,(\widetilde{R_o + q_2}) \\ \hline \cdot & \cdot \\ \cdot & \cdot \\ \cdot & \cdot \end{array}\right]_{6n \times 6} = 0
$$

Considering the first term of the product,

$$
\left[\gamma^{T}\right] \left[\begin{array}{c} \bar{m}_1 \\ 0 \\ \bar{m}_2 \\ 0 \\ \cdot \\ \cdot \end{array}\right]_{6n \times 3} = 0
$$

Since for the free-free case, the spacecraft structure is in dynamic equilibrium with respect to all forces such that

$$\ddot{n}_i \quad \sum_J \gamma_{iJ} \quad m_J = 0 \qquad \text{(Force)}$$

This equilibrium condition also applies to torques.

$$\therefore \quad \gamma^T \begin{bmatrix} 0 \\ \bar{I}^1 \\ \hdashline 0 \\ \bar{I}^2 \\ \hdashline \cdot \\ \cdot \\ \cdot \end{bmatrix}_{6n \times 3} = 0$$

Rearranging the remaining terms $m_i (R_o \tilde{+} q_i)$ by letting

$$R_o^1 = R_o + \bar{q}$$

$$q_i^1 = q_i - \bar{q}$$

where $\bar{q}$ is the constant vector from point O_B to the center of gravity of the undeformed system.

$$\therefore \quad \gamma^T \begin{bmatrix} \bar{m}_1 (R_o^1 + q_1^1) \\ \hdashline 0 \\ \hdashline \bar{m}_2 (R_o^1 + q_2^1) \\ \hdashline 0 \\ \cdot \\ \cdot \end{bmatrix} = \begin{bmatrix} \bar{m}_1 \\ 0 \\ \bar{m}_2 \\ 0 \\ \cdot \\ \cdot \\ \cdot \end{bmatrix} \left(\sum_E R_o^1 \right) + \gamma^T \begin{bmatrix} \bar{m}_1 q_1^1 \\ 0 \\ \bar{m}_2 q_2^1 \\ 0 \\ \cdot \\ \cdot \\ \cdot \end{bmatrix} = 0$$

The first term is zero as shown previously. The second term is also zero since

$$\sum_J \gamma_{iJ} \; m_J \; q_J^1$$

represents the moment about the center of mass which equals zero in the free-free case.

4.2.5.2 **Nastran Algorithm**

The integration of the system equation developed in Section 4.2.4 will be accomplished by use of the Nastran algorithm.

$$\left[\frac{M}{\Delta t^2} + \frac{C}{2\Delta t} + \frac{K}{3}\right]\left\{X_{\eta+2}\right\} = \frac{1}{3}\left[P_{\eta+2} + P_{\eta+1} + P_{\eta}\right]$$

$$+\left[\frac{2M}{\Delta t^2} - \frac{K}{3}\right]\left\{X_{\eta+1}\right\} + \left[-\frac{M}{\Delta t^2} + \frac{C}{2\Delta t} - \frac{K}{3}\right]\left\{X_{\eta}\right\}$$

$$\left\{\dot{X}_{\eta}\right\} = \frac{1}{2\Delta t}\left[\left\{X_{\eta+1}\right\} - \left\{X_{\eta-1}\right\}\right]$$

$$\left\{\ddot{X}_{\eta}\right\} = \frac{1}{\Delta t^2}\left[\left\{X_{\eta+1}\right\} - 2\left\{X_{\eta}\right\} - \left\{X_{\eta-1}\right\}\right]$$

* See Reference 4.7

4.2.5.3 Interaction Forces and Torques

The interaction forces (torques) which exist at the attachment points of the various arrays are calculated by summing the hinge force (torque) due to rigid body motion of the system at the attachment point and the flexible appendage transient response.

Hinge force for rotating array*:

$$F_{H_i} = m_i \left[\ddot{R}_o + 2\,\tilde{\omega}_o \dot{R}_o + (\dot{\tilde{\omega}}_o + \tilde{\omega}_o\ \tilde{\omega}_o)(R_o + h_i + C_i r_i)\right.$$

$$\left. + 2\,\tilde{\omega}_o C_i \tilde{\omega}_i\ r_i\ + C_i(\tilde{\omega}_i \tilde{\omega}_i + \dot{\tilde{\omega}}_i) r_i\right] + F_i'$$

Hinge torque for rotating array*:

$$T_{H_i} = C_i \left[((C_i^T \omega_o)^{\sim} + \tilde{\omega}_i) \left[I_i\right] (\omega_i + C_i^T\ \omega_o)\right.$$

$$\left. + \left[I_i\right](\dot{\omega}_i + C_i^T\ \dot{\omega}_o) + \left[I_i\right](C_i^T\ \tilde{\omega}_o C_i\ \omega_i)\right]$$

$$+ C_i \tilde{r}_i C_i^T F_{H_i} + T_i'$$

Force induced by flexible appendage transient response

$$\hat{F}_i = -\left(\sum_E^T\ M_i\ \phi_i\right)\ddot{n}_i$$

Torque induced by flexible appendage transient response

$$\hat{T}_i = -\sum_E^T \tilde{\tilde{r}}_i\ M_i\ \phi_i\ \ddot{n}_i$$

* Equations for hinge forces and torques for fixed appendages are identical except that ω_i=0 (the negative of these hinge forces and torques acts on the space station). Admittedly, for the rotating case, some products have been neglected which couple ω_i with modal variables and ω_o, basically assuming that ω_i will also be small.

Hinge force for rotating array due to space station modal accelerations of attachment point:

$$F_i' = \underset{3 \times 6}{\left[\bar{m}_i \;\vdots\; -\bar{m}_i \;\; (C_i \tilde{r}_i) \right]} \underset{6 \times N_s}{\begin{bmatrix} G_i'^T \\ \hdashline G_i''^T \end{bmatrix}} \ddot{n}_s$$

Hinge torque for rotating array due to space station modal accelerations of attachment point:

$$T_i' = \underset{3 \times 6}{\left[\bar{m}_i (C_i \tilde{r}_i) \;\vdots\; C_i I_i C_i^T - \bar{m}_i (C_i \tilde{r}_i)^2 \right]} \underset{6 \times N_s}{\begin{bmatrix} G_i'^T \\ \hdashline G_i''^T \end{bmatrix}} \ddot{n}_s$$

The total interaction force at the attachment point of an array is

$$F_{iNT_i} = - F_{H_i} + \hat{F}_i$$

Likewise, the total interaction torque acting on the space station due to the attachment of a flexible array is

$$T_{iNT_i} = -T_{H_i} + \hat{T}_i$$

4.3 FLEXIBLE SPINNING SPACE STATION

4.3.1 MODAL EQUATIONS

(1) $$[m]\left[\ddot{q}\right] + [K]\{q\} = -[G]\{\dot{q}\} - [B]\{q\} + [R]\{RB\} + \{F'\} + \{L\}$$

where $[R]$ and $\{L\}$ are rigid body terms. If we choose $u = R_o + q_i + x_i$ we can form the following set of equations of motion

(2) $$[m]\{\ddot{u}\} + [G]\{\dot{u}\} + [K']\{u\} \doteq \{F'\}$$

where $[m]$ is mass matrix of the space station,

$[G]$ is skew symmetric matrix of coriolis acceleration terms

and $[K'] = [K_e] + [K_c] + [B]$

$[K_e] =$ elastic stiffness matrix

$[K_c] =$ symmetric matrix of centrifugal acceleration terms

$[B] =$ geometric stiffness matrix

The second-order matrix equation (2) can be reduced to a first order state equation (3) by introducing the following matrices

$$U = \begin{bmatrix} \dot{u} \\ u \end{bmatrix} \quad \text{and} \quad \dot{U} = \begin{bmatrix} \ddot{u} \\ \dot{u} \end{bmatrix}$$

(3) $$[D]\{\dot{U}\} + [E]\{U\} = \{F\}$$

where $$[D] = \left[\begin{array}{c|c} [0] & -[m] \\ \hline [m] & [G] \end{array}\right], \quad [E] = \left[\begin{array}{c|c} [m] & [0] \\ \hline [0] & [K'] \end{array}\right]$$

and $$\{F\} = \begin{bmatrix} \{0\} \\ \{F'\} \end{bmatrix}$$

The reduced equation of motion (3) can be uncoupled by the transformation

(4) $\{U\} = [\Phi]\{Y\}$, where $[\Phi] = \begin{bmatrix} [\lambda_n][\phi^{(n)}] \\ [\phi^{(n)}] \end{bmatrix}$

and the transformation matrix $[\Phi]$ consists of complex eigenvectors and their conjugates pairs.

$$[\phi^{(n)}] = \left[\{\phi^1\}\{\phi^2\} --- \{\phi^N\} \mid \{\phi^{1*}\}\{\phi^{2*}\} --- \{\phi^{N*}\}\right], \quad [\lambda_n] = \text{DIAG}(-jw_1, --, -jw_n)$$

$\{\phi^*\}$ = complex conjugate of $\{\phi\}$,

$$Y \equiv \left[Y_1 Y_2 --- Y_N \mid Y_1^* Y_2^* --- Y_N^*\right]^T$$

where w_i are eigenvalues and ϕ^i are eignevectors.
In terms of the new coordinates Y, Equation (3) becomes

(5) $[D][\Phi]\{\dot{Y}\} + [E][\Phi]\{Y\} = \{F\}$

Premultiplication of Equation (5) by $[\Phi^*]^T$

(6) $[\Phi^*]^T [D] \Phi \{\dot{Y}\} + [\Phi^*][E][\Phi]\{Y\} = [\Phi^*]^T\{F\}$

Since $[E]$ is symmetric and $[D]$ skew symmetric, $[\Phi^*]^T [\Phi]$ = diagonal matrix.(2)
Writing equation (6) in simplier form

(7) $[D']\{\dot{Y}\} + [E']\{Y\} = [\Phi^*]^T\{F\}$

where

$[D'] = [\Phi^*]^T [D][\Phi]$ = diagonal matrix

$[E'] = [\Phi^*]^T [E][\Phi]$ = diagonal matrix

If $[\Lambda]$ is the matrix of the complex eigenvalues of the operator in Equation (7), then upon premultiplication by $[D']^{-1}$ we obtain

(8) $\{\dot{Y}\} = -[\Lambda]\{Y\} + \{\bar{F}\}$

where $\{\bar{F}\} = [D']^{-1}[\Phi^*]^T\{F\}$

$$
[\Lambda] \equiv \begin{bmatrix} \Lambda_1 & & & & & & 0 \\ & \Lambda_2 & & & & & \\ & & \ddots & & & & \\ & & & \Lambda_N & & & \\ & & & & \Lambda_1^* & & \\ & & & & & \ddots & \\ 0 & & & & & & \Lambda_N^* \end{bmatrix}
$$

$(2N \times 2N)$

N is the number of modes of the space station to be preserved in the simulation.

Equation (8) can be written as:

$$
(9) \quad \begin{bmatrix} \dot{\bar{Y}} \\ \dot{\bar{Y}}^* \end{bmatrix} = - \begin{bmatrix} \bar{\Lambda} & 0 \\ 0 & \bar{\Lambda}^* \end{bmatrix} \begin{bmatrix} \bar{Y} \\ \bar{Y}^* \end{bmatrix} + \{\bar{F}\}
$$

where $\bar{Y} \equiv \begin{bmatrix} Y_1 & Y_2 & --- & Y_N \end{bmatrix}^T$

$\bar{Y}^* \equiv \begin{bmatrix} Y_1^* & Y_2^* & --- & Y_N^* \end{bmatrix}^T$

$$
\bar{\Lambda} \equiv \begin{bmatrix} \Lambda_1 & & & 0 \\ & \Lambda_2 & & \\ & & \ddots & \\ 0 & & & \Lambda_N \end{bmatrix}
$$

$$
\bar{\Lambda}^* \equiv \begin{bmatrix} \Lambda_1^* & & & 0 \\ & \Lambda_2^* & & \\ & & \ddots & \\ 0 & & & \Lambda_N^* \end{bmatrix}
$$

Multiply both sides of Equation (9) by

$$
1/2 \left[\begin{array}{c|c} I & I \\ \hline J & -J \end{array} \right]
$$

I = unity matrix

J = $\sqrt{-1}\ I$

and let

$$Z_i^{(1)} = (1/2)(Y_i + Y_i^*)$$

$$Z_i^{(2)} = (1/2) J\ (Y_i - Y_i^*)$$

$$(10)\quad \begin{bmatrix} \dot{\bar{Z}}^{(1)} \\ \dot{\bar{Z}}^{(2)} \end{bmatrix} = \begin{bmatrix} 0 & \lceil\Lambda\rfloor \\ -\lceil\Lambda\rfloor & 0 \end{bmatrix} \begin{bmatrix} \bar{Z}^{(1)} \\ \bar{Z}^{(2)} \end{bmatrix} + \begin{bmatrix} V \end{bmatrix} \begin{bmatrix} F' \end{bmatrix}$$

where

$$\begin{bmatrix} V \end{bmatrix} = 1/2 \left[\begin{array}{c|c} I & I \\ \hline J & -J \end{array}\right] \begin{bmatrix} D' \end{bmatrix}^{-1} \begin{bmatrix} \Phi^* \end{bmatrix}^T \ **$$

when N modes are retained

$$\bar{Z}^{(1)} \equiv \begin{bmatrix} Z_1^{(1)} \\ \vdots \\ Z_N^{(1)} \end{bmatrix}$$

$$\bar{Z}^{(2)} \equiv \begin{bmatrix} Z_1^{(2)} \\ \vdots \\ Z_N^{(2)} \end{bmatrix}$$

Modal damping may be introduced in Equation (1) by the matrix $-2\xi\lceil\Lambda\rfloor$

$$(11)\quad \begin{bmatrix} \dot{\bar{Z}}^{(1)} \\ \dot{\bar{Z}}^{(2)} \end{bmatrix} + \begin{bmatrix} 0 & -\lfloor\Lambda\rfloor \\ \lfloor\Lambda\rfloor & 2\xi\lfloor\bar{\Lambda}\rfloor \end{bmatrix} \begin{bmatrix} \bar{Z}^{(1)} \\ \bar{Z}^{(2)} \end{bmatrix} = \begin{bmatrix} V \end{bmatrix} \begin{bmatrix} F' \end{bmatrix}$$

where ξ = arbitrary chosen damping factor.

** See Section 4.3.6.

In terms of the new coordinates $\overline{Z}$, Equation (4) may be written as

(12) $$\{U\} = [\Phi]\{Y\} = [\Phi]\left[\begin{array}{c|c} I & -J \\ \hline I & J \end{array}\right]\begin{bmatrix} \overline{Z}^{(1)} \\ \overline{Z}^{(2)} \end{bmatrix}$$

or

(13) $$\{U\} = [W][\overline{Z}]$$

where

$$[W] \equiv [\Phi]\left[\begin{array}{c|c} I & -J \\ \hline I & J \end{array}\right]$$

$$[\overline{Z}] \equiv \begin{bmatrix} \overline{Z}^{(1)} \\ \overline{Z}^{(2)} \end{bmatrix}$$

Equations (11) and (13) are to be implemented in the simulation.

N. B. If desired, the variation of ω_o about the nominal can be accommodated by setting

(14) $$G' = \frac{\partial [G]}{\partial \omega}$$

(15) $$B' = \frac{\partial [B]}{\partial \omega}$$

(16) $$\Delta\omega = (\omega_o - \omega_{nom})$$

For this case (10) is modified to give

(10a) $$\begin{bmatrix} \dot{\overline{Z}}^{(1)} \\ \dot{\overline{Z}}^{(2)} \end{bmatrix} + \begin{bmatrix} 0 & -\lfloor\overline{\Lambda}\rfloor \\ \lfloor\overline{\Lambda}\rfloor & 0 \end{bmatrix}\begin{bmatrix} \overline{Z}^{(1)} \\ \overline{Z}^{(2)} \end{bmatrix} = [V]\,[F] - [V]\left([G'] + [B']\right)\Delta\omega$$

4.3.2 RIGID BODY EQUATIONS

The equations developed in Section 4.3.1 will be used to simulate N complex flexible modes for the space station. The rigid body modes will not be used. Instead, the rigid body motion will be given by the Newton-Euler equations for the rotating space station taken as a rigid body.

The rigid body system given in Figure 4-12 describes the force and torque relationships which exist for two rigid appendages and a rigid body space station.

Newton's and Euler's vector equations of motion for the space station can be written as

Total system force equation

(17) $$M_T \left. \frac{d^2}{dt^2} \right|_I (\bar{R}_o + \bar{C}) = \bar{F}_E$$

Space station moment equation

(18) $$\left. \frac{d}{dt} \right|_I (\bar{\bar{I}}_T \cdot \bar{\omega}_o) = \bar{T}_E$$

where M_T = total system mass.

$\bar{C}$ = vector from space station reference to system rigid body CG.

$\bar{R}_o$ = location of space station reference point with respect to inertial space

$\bar{\bar{I}}_T$ = inertia dyadics of the space station about its center of mass.

$\bar{\omega}_o$ = angular velocity vector of the space station, with respect to inertial space

$\bar{h}_{F_J}$ = location of attachment point of appendage with respect to space station reference point

$\bar{r}_{F_J}$ = location of rigid body center of mass of appendage with respect to attachment point

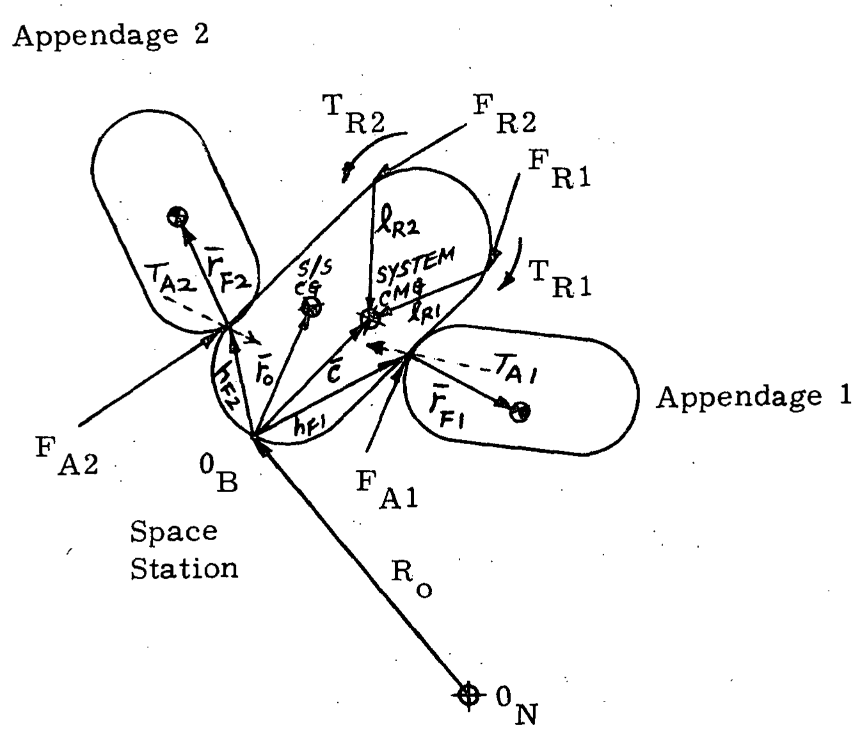

FIGURE 4-12. RIGID BODY SYSTEM CONFIGURATION

$\bar{F}_{Ext}$ = external forces applied to space station

$\bar{T}_{Ext}$ = external torques applied to space station

Defining $\bar{R}_o$ and $\bar{C}$ in the X_S frame (coordinate basis fixed to and moving with the space station taken as rigid body) and carrying out the differentiation w.r.t.time we obtain (see Section 4.2 for the following derivation conventions)

(19) $$\vec{R}_o = I^T C_o R_o \, , \quad \vec{C} = I^T C_o C$$

(20) $$\left.\frac{d}{dt}\right|_I (\vec{R}_o + \vec{C}) = I^T \left[C_o \tilde{\omega}_o R_o + C_o \dot{R}_o + C_o \tilde{\omega}_o C \right]$$

(21) $$\left.\frac{d^2}{dt^2}\right|_I (\vec{R}_o + \vec{C}) = I^T \Big[C_o \tilde{\omega}_o \tilde{\omega}_o R_o + C_o \dot{\tilde{\omega}}_o R_o + 2\, C_o \tilde{\omega}_o \dot{R}_o + C_o \ddot{R}_o + C_o \tilde{\omega}_o \tilde{\omega}_o C + C_o \dot{\tilde{\omega}}_o C \Big]$$
$$= X_S^T \left[\left(\tilde{\omega}_o \tilde{\omega}_o + \dot{\tilde{\omega}}_o \right) \left(R_o + C \right) + 2\, \tilde{\omega}_o \dot{R}_o + \ddot{R}_o \right]$$

(22) $$\left.\frac{d}{dt}\right|_I \left(\bar{\bar{I}}_T \cdot \bar{\omega}_o \right) = I_T \dot{\omega}_o + \tilde{\omega}_o I_T \omega_o$$

Substituting equation (21) and (22) in equation (17) and (18), we obtain rigid body equations of motion for the space station

(23) $$M_T \left(\ddot{R}_o + (\dot{\tilde{\omega}}_o + \tilde{\omega}_o \tilde{\omega}_o) \, (R_o + C) + 2\, \tilde{\omega}_o \dot{R}_o \right) = F_E$$

(24) $$I_T \dot{\omega}_o + \tilde{\omega}_o I_T \omega_o = T_E$$

where $$M_T = M_o + \sum_{i=1}^{4} m_{Fi}$$

$$\bar{C} = \frac{M_o \bar{r}_o + \sum_{i=1}^{4} m_{Fi} \left(\bar{h}_{Fi} + C_{Fi} \bar{r}_{Fi}\right)}{M_T}$$

$$I_T = I_o - M_o \left(\widetilde{\bar{r}_o - \bar{C}}\right)^2 + \sum_{i=1}^{4} C_{Fi} \left[I'_{Fi}\right] C_{Fi}^T$$

$$I'_{Fi} = I_{Fi} - m_{Fi} \left(\widetilde{C_{Fi}^T \bar{h}_{Fi} + \bar{r}_{Fi} - C_{Fi}^T \bar{C}}\right)^2$$

F_E = external forces (F_{R_J})

+ force due to flexible appendage motion (F_{A_J})

+ force due to flexible motion of base point of appendage $\left(F_{A'_J}\right)$

$$= F_{R1} + F_{R2} + \sum_{J=1}^{4} C_{F_J} \left(F_{A_J} + F_{A'_J}\right)$$

$$F_{A_J} = - \Sigma_E^T M_{F_J} W_{F_J} \dot{Z}_{F_J}$$

$$F_{A'_J} = m_{F_i} W_{S_i} Z_S$$ } see section 2.5.1

T_E = external torques

+ torque due to flexible appendage motion

+ torque due to flexible motion of base point of appendage

$$T_E = T_{R1} + T_{R2} - (\tilde{l}_{R1}) F_1 - (\tilde{l}_{R2}) F_2$$

$$- \sum_{i=1}^{4} C_{F_i} T_{A_i} + \sum_{i=1}^{4} r_{F'_i} C_{F_i} \left(F_{A_i} + F_{A'_i}\right)$$

$$- \sum_{i=1}^{4} C_{F_i} I_{F_i} C_{F_i}^T W_{S_{b_i}} \dot{Z}_S$$

$$T_{A_i} = \sum_{E}^{T} \tilde{\tilde{R}}_{F_i} M_{F_i} W_{F_i} \dot{z}_{F_i}$$

T_{R_J} = externally applied torque (J = 1, 2)

F_{R_J} = externally applied forces (J = 1, 2)

M_{F_i} = mass of i^{th} appendage

M_o = mass of space station

l_{R_i} = location of application point of i^{th} external force with respect to system center of mass (negative of)

I_{F_i} = inertia matrix of i^{th} appendage

I_o = inertia matrix of space station

R_o = location of space station center of mass with respect to space station reference point

$r_{F'_i}$ = $(r_o - h_{F_i})$

Equation (23) and (24) may be expressed in matrix form

(25) $$\left[\begin{array}{c|c} M_T & -M_T\bar{C} \\ \hline 0 & I_T \end{array}\right] \left[\begin{array}{c} \ddot{\bar{R}}_o \\ \hline \dot{\omega}_o \end{array}\right] + \left[0\right] \left[\begin{array}{c} \dot{\bar{R}}_o \\ \hline \omega_o \end{array}\right] + \left[0\right] \left[\begin{array}{c} \bar{R}_o \\ \hline \theta_o \end{array}\right]$$

$$= \left[\begin{array}{c} F_E - M_T \left(\dot{\tilde{\omega}}_o + \tilde{\omega}_o \tilde{\omega}_o\right) R_o + \tilde{\omega}_o \tilde{\omega}_o \bar{C} + 2 \tilde{\omega}_o \dot{R}_o \\ \hline T_E - \tilde{\omega}_o I_T \omega_o \end{array}\right]$$

4.3.3 EQUATIONS OF FLEXIBLE APPENDAGES ATTACHED TO THE SPINNING SPACE STATION

The motion of a fixed flexible appendage is modeled as in previous derivations . Cantilevered mode shapes are used to represent the flexible appendage, whose fixed base is excited by the translational and rotational motion of the rigid body of the spinning space station, and the modal motions of the flexible space station at that point.

4.3.3.1 COORDINATE FRAMES AND RELATIONSHIPS

$[I]$ = inertially fixed coordinates

$[X_S]$ = coordinate basis fixed and moving with the space station taken as rigid body, origin at reference point O_B. (See Figure 4-13).

$[X_F]$ = coordinate basis defined with origin at attachment point of appendage and axes directed along principal axes of the appendage.

The relationship between $[I]$ and $[X_F]$ is defined by the direction cosine relationship

$$[I] = C_o C_F [X_F]$$

4.3.3.2 EQUATION DERIVATIONS

Using D'Alembert's principle, the total force acting on the j^{th} particle of the i^{th} appendage equals

$$(26) \quad \{F_j\} = m_j \frac{d^2}{dt^2}\left[\vec{a}_i + \vec{r}_j + \vec{u}_j\right]_I$$

where $\bar{a}_i$ is the position vector of the hinge point of i^{th} fixed appendage w.r.t. inertial space

$$\vec{a}_i = I^T a_i$$

$$\vec{r}_j = I^T C_o C_F r_j$$

$$\vec{u}_j = I^T C_o C_F u_j$$

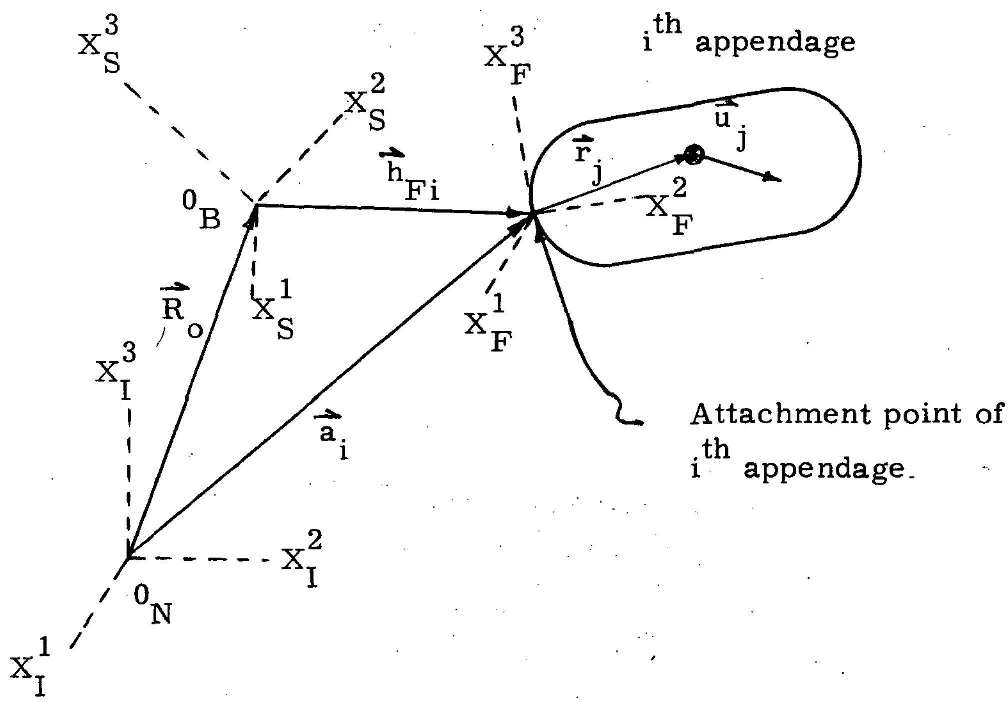

Figure 4-13 Flexible Appendage Coordinate System

$$\frac{d}{dt}\vec{r}_j = \frac{d}{dt}\left[I^T C_o C_F r_j \right] = I^T \left[C_o \omega_o C_F r_j \right]$$

$$\frac{d^2}{dt^2}\vec{r}_j = \frac{d}{dt}\left[I^T C_o \tilde{\omega}_o C_F r_j \right]$$

$$= I^T C_o \tilde{\omega}_o \tilde{\omega}_o C_F r_j + I^T C_o \dot{\tilde{\omega}}_o C_F r_j$$

$$\frac{d}{dt}\vec{u}_j = \frac{d}{dt}\left[I^T C_o C_F u_j \right] = I^T C_o \tilde{\omega}_o C_F u_j + I^T C_o C_F \dot{u}_j$$

$$\frac{d^2}{dt^2}\vec{u}_j = \frac{d}{dt}\left[I^T C_o \tilde{\omega}_o C_F u_j + I^T C_o C_F \dot{u}_j \right]$$

$$= I^T \left[C_o \tilde{\omega}_o \tilde{\omega}_o C_F u_j + C_o \dot{\tilde{\omega}}_o C_F u_j + 2\, C_o \tilde{\omega}_o C_F \dot{u}_j + C_o C_F \ddot{u}_j \right]$$

Substituting the above equations in equation (26), we obtain

$$(27) \quad \left\{ F_j \right\} = m_j I^T \left\{ \ddot{a}_i + C_o \left[(\tilde{\omega}_o \tilde{\omega}_o + \dot{\tilde{\omega}}_o)\, C_F r_j \right.\right.$$
$$\left.\left. + (\tilde{\omega}_o \tilde{\omega}_o + \dot{\tilde{\omega}}_o)\, C_F u_j + 2\,\tilde{\omega}_o C_F \dot{u}_j + C_F \ddot{u}_j \right] \right\}$$
$$= m_j I^T C_o C_F \left\{ C_F{}^T C_o{}^T \ddot{a}_i + C_F{}^T \left[(\tilde{\omega}_o \tilde{\omega}_o + \dot{\tilde{\omega}}_o)\, C_F r_j \right.\right.$$
$$\left.\left. + (\tilde{\omega}_o \tilde{\omega}_o + \dot{\tilde{\omega}}_o)\, C_F u_j + 2\,\tilde{\omega}_o C_F \dot{u}_j \right] + \ddot{u}_j \right\}$$

where $C_o{}^T \ddot{a}_i$ is sum of rigid body and space station modal accelerations at the attached point of i^{th} appendage

$$(28) \quad C_o{}^T \ddot{a}_i = (\ddot{R}_i)' + U_{S_i}$$

$(\ddot{R}_i)'$ ~ rigid body acceleration of the i^{th} appendage attachment point

$(\ddot{U}_{S_i})$ ~ space station modal acceleration of the i^{th} appendage attachment point

$$(29)\quad {}_I{}^TC_o(\ddot{R})' = \frac{d^2}{dt^2}\left[\vec{R}_o + \vec{h}_{F_i}\right]_I = \frac{d^2}{dt^2}\left[{}_I{}^TC_o(R_o + h_{F_i})\right]$$

$$= {}_I{}^TC_o\left[\tilde{\omega}_o\tilde{\omega}_o(R_o+h_{F_i}) + \dot{\tilde{\omega}}_o(R_o+h_{F_i}) + 2\tilde{\omega}_o\dot{R}_o + \ddot{R}_o\right]$$

Combining the above equations for all n particles of the appendage yields in matrix form

$$(30)\quad \underset{3n\times 3n}{[m]}\underset{3n\times 1}{\{\ddot{q}\}} + [K]\{q\} = -[G]\{\dot{q}\} - [B]\{q\} + [R]\{RB\} + \{L\} + [S_2]\{\ddot{S}\}$$

where

$$[G] = \underset{(3n\times 3n)}{\begin{bmatrix} 2\bar{m}_1 C_F{}^T\tilde{\omega}_o C_F & & 0 \\ & 2\bar{m}_2 C_F{}^T\tilde{\omega}_o C_F & \\ & & \ddots & \\ 0 & & & 2\bar{m}_n C_F{}^T\tilde{\omega}_o C_F \end{bmatrix}}$$

$$[B] = \underset{(3n\times 3n)}{\begin{bmatrix} \bar{m}_1 C_F{}^T(\tilde{\omega}_o\tilde{\omega}_o + \dot{\tilde{\omega}}_o)C_F & & \\ & \ddots & \\ & & \bar{m}_n C_F{}^T(\tilde{\omega}_o\tilde{\omega}_o + \dot{\tilde{\omega}}_o)C_F \end{bmatrix}}$$

$$\{RB\} = \underset{(6\times 1)}{\begin{bmatrix} \ddot{R}_o \\ \dot{\omega}_o \end{bmatrix}}$$

$$[R] = \underset{(3n\times 6)}{\left[\begin{array}{c|c} -\bar{m}_1 C_F{}^T & \bar{m}_1 C_F{}^T(h_{F_i} + C_F r_1) \\ \hline \vdots & \vdots \\ \hline -\bar{m}_n C_F{}^T & \bar{m}_n C_F{}^T(h_{F_i} + C_F r_n) \end{array}\right]}$$

$$[L] = \begin{bmatrix} -\bar{m}_1 C_F^T \left[\tilde{\omega}_o \tilde{\omega}_o \left(R_o + h_{F_i} + C_F r_1 \right) + \dot{\tilde{\omega}}_o R_o + 2 \tilde{\omega}_o \dot{R}_o \right] \\ \hdashline \cdot \\ \cdot \\ \cdot \\ \hdashline -\bar{m}_n C_F^T \left[\tilde{\omega}_o \tilde{\omega}_o \left(R_o + h_{F_i} + C_F r_n \right) + \dot{\tilde{\omega}}_o R_o + 2 \tilde{\omega}_o \dot{R}_o \right] \end{bmatrix}$$

$$S = \begin{bmatrix} -\bar{m}_1 C_F^T \\ \hdashline \cdot \\ \cdot \\ \cdot \\ \cdot \\ \hdashline -\bar{m}_n C_F^T \end{bmatrix}$$

$3n \times 6$

Choosing $Q = \begin{bmatrix} \dot{q} \\ q \end{bmatrix}$, we reformulate equation (30) as follows

$$(31) \qquad [D_F]\{\dot{Q}\} + [E_F]\{Q\} = [R]\{RB\} + [S_2]\{\ddot{S}\} + \{L\}$$

where

$$[D_F] = \left[\begin{array}{c|c} [0] & [m] \\ \hline [m] & [G] \end{array}\right] \qquad E_F = \left[\begin{array}{c|c} [m] & [0] \\ \hline [0] & [K] \end{array}\right]$$

By the same reasoning as in Section 2.1.

$$(32) \qquad \begin{bmatrix} \dot{\bar{Z}}^{(1)} \\ \dot{\bar{Z}}^{(2)} \end{bmatrix}_F + \begin{bmatrix} 0 & -|\Lambda| \\ |\Lambda| & 2\xi|\Lambda| \end{bmatrix} \begin{bmatrix} \bar{Z}^{(1)} \\ \bar{Z}^{(2)} \end{bmatrix}_F$$

$$= [V_F]\,[R]\,\{RB\} + [V_F]\,[S]\,\{\ddot{S}\} + [V_F]\,\{L\}$$

We can express $\{Q\}$ and $\{\ddot{S}\}$ in terms of the new coordinates $\bar{Z}$

$$(33) \qquad \{Q\} = \begin{bmatrix} \dot{q} \\ q \end{bmatrix} = [W_F]\,[\bar{Z}]_F$$

$$(34) \qquad \{\ddot{S}\} = [W_S]\,[\ddot{Z}]_S$$

4.3.4 INTERACTION FORCES AND TORQUES

4.3.4.1 INTERACTION FORCES OF RIGID APPENDAGE

Using D'Alembert's principle in Figure 14 the interaction force of i^{th} appendage is

(35) $$\vec{F}_{H_i} = -m_{F_i} \frac{d^2}{dt^2} \left[\vec{a}_i + \vec{r}_i\right]_I$$

where

$\vec{a}_i = I^T a_i$ = total displacement of attachment point of i^{th} appendage with respect to inertial space (See Fig. 14)

$\vec{r}_i \equiv$ location of C. M. of rigid appendage w. r. t. attachment point

$$\vec{r}_i = I^T C_o C_{F_i} r_i$$

(36) $$F_{H_i} = -m_{F_i} I^T C_o \left[C_o^T \ddot{a}_i + \left(\tilde{\omega}_o \tilde{\omega}_o + \dot{\tilde{\omega}}_o\right) C_F r_{F_i}\right]$$

but $C_o^T \ddot{a}_i = \ddot{R}_i' + \ddot{u}_{S_i}$

where $\ddot{R}_i' \equiv$ space station rigid body acceleration at attachment point i.

$$\ddot{R}_i' = \left[\tilde{\omega}_o \tilde{\omega}_o \left(R_o + h_{F_i}\right) + \dot{\tilde{\omega}}_o \left(R_o + h_{F_i}\right) + 2 \tilde{\omega}_o \dot{R}_o + \ddot{R}_o\right]$$

$\ddot{u}_i \equiv$ space station modal acceleration at point i (measured relative to rigid body space station motion).

$$\ddot{u}_{S_i} = \underset{(3 \times 2N_S)}{\left[W_{S_i}\right]} \dot{Z}_S{}^*$$

*Approximation

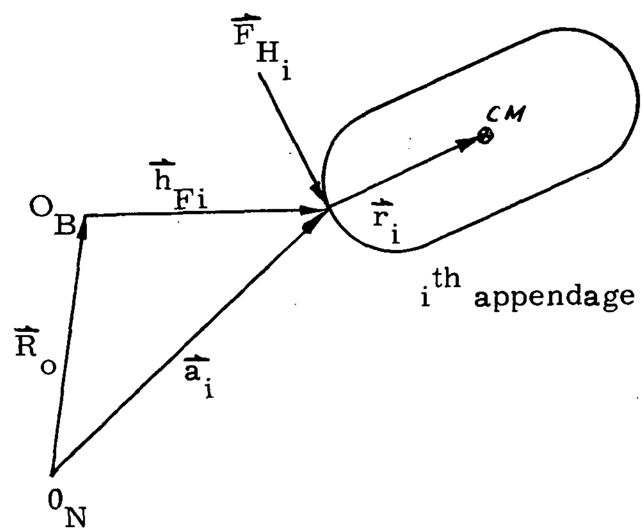

Figure 4-14 Interaction Force of Rigid Appendage to S/S

Therefore, the interaction force of a rigid appendage on the space station can be written as

$$(37) \qquad F_{H_i} = \left[F'_{H_i} - m_{F_i}\left(\ddot{R}_o - \left(\widetilde{h_{F_i} + C_F r_{F_i}}\right) \dot{\omega}_o\right)\right] + F_{A'_i}$$

where

$$F'_{H_i} = -m_{F_i}\left[\tilde{\omega}_o\tilde{\omega}_o\left(R_o + h_{F_i} + C_F r_{F_i}\right) + \dot{\tilde{\omega}}_o R_o + 2\tilde{\omega}_o \dot{R}_o\right]$$

$$F_{A'_i} = -m_{F_i} W_{j_i} \dot{z}_s$$

4.3.4.2 INTERACTION TORQUES OF RIGID APPENDAGE

(38) $$\frac{d}{dt} L_i = -\tilde{r}_i F_{H_i} - T_{H_i}$$

where
$$L_i = (X_i)^T I_i (X_i) \left[(X_i)^T \left(\omega_o + \omega_{b_i}\right)\right]$$

$$= \left[\left(I^T C_o\right) C_i I_i C_i^T \left(C_o^T I\right)\right]\left[\left(I^T C_o\right)\left(\omega_o + \omega_{b_i}\right)\right]$$

$$= I^T C_o C_i I_i C_i^T \left(\omega_o + \omega_{b_i}\right)$$

$$\frac{d\mathbf{L}_i}{dt} = I^T \left[C_o \tilde{\omega}_o C_i I_i C_i^T \left(\omega_o + \omega_{b_i}\right) + C_o \left(C_i I_i C_i^T\right)\left(\dot{\omega}_o + \dot{\omega}_{b_i}\right)\right]$$

$$= X^T \left[\tilde{\omega}_o C_i I_i C_i^T \left(\omega_o + \omega_{b_i}\right) + C_i I_i C_i^T \left(\dot{\omega}_o + \dot{\omega}_{b_i}\right)\right]$$

where I_i = inertia matrix of i^{th} appendage

$\dot{\omega}_{b_i} \equiv$ modal angular acceleration at attachment point of i^{th} appendage

$$\dot{\omega}_{b_i} = \underset{(3 \times N_i)}{\left[W_{S_{bi}}\right]} \dot{Z}_S^*$$

Therefore, the interaction torque of i^{th} appendage of rigid motion on space station is

(39) $$T_{H_i} = -\left(\widetilde{C_{F_i} r_{F_i}}\right) F_{H_i} - C_i I_i C_i^T W_{S_{b_i}} \ddot{Z}_S - C_i I_i C_i^T \dot{\omega}_o - \left(\tilde{\omega}_o C_i I_i C_i^T\right)\left(\omega_o + W_{S_{b_i}} Z_S\right)$$

*Approximation

or

$$T_{H_i} = -\left(\widetilde{C_{F_i} r_{F_i}}\right) F_{H_i} - (E + \omega_o)\,(C_i I_i C_i^T)\, W_{S_{b_i}}\, \dot{Z}_S$$

$$-\left(C_i I_i C_i^T\right)\dot{\omega}_o - \tilde{\omega}_o \left(C_i I_i C_i^T\right) \omega_o$$

where E is the identity matrix.

4.3.4.3 INTERACTION FORCES AND TORQUES OF FLEXIBLE APPENDAGE

(40) $$F_{A_i} = -C_{F_i} \Sigma_E^T M_{F_i} W_{F_i} \dot{Z}_{F_i}$$

(41) $$T_{A_i} = -C_{F_i} \Sigma_E^T \tilde{\tilde{R}}_{F_i} M_{F_i} W_{F_i} \dot{Z}_{F_i}$$

See Section 4.3.7 for computational considerations

4.3.4.4 TOTAL INTERACTION FORCES AND TORQUES

The total interaction forces and torques at the attachment point of the appendages can be obtained by summing the interaction forces (torques) of the rigid and the flexible appendages at the attachment point.

(42) $$F_{t_i} = F_{H_i} + F_{A_i}$$

(43) $$F_{t_i} = -\left[F_{H_i}' + m_{F_i}\left(\ddot{R}_o - \left(\widetilde{h_{F_i} + C_F r_{F_i}}\right)\dot{\omega}_o\right) + m_{F_i} W_{S_i} \dot{Z}_S\right]$$

$$-C_{F_i} \Sigma_E^T M_{F_i} W_{F_i} \dot{Z}_{F_i}$$

(44)
$$
\begin{aligned}
T_{t_i} &= T_{H_i} + T_{A_i} \\
&= -\Big[\big(\widetilde{C_{F_i} r_{F_i}}\big) F_{H_i} + \big(E + \widetilde{\omega}_o\big)\big(C_i I_i C_i{}^T\big) W_{S_{b_i}} \dot{Z}_S \\
&\quad + \big(C_i I_i C_i{}^T\big)\dot{\omega}_o + \widetilde{\omega}_o \big(C_i I_i C_i{}^T \omega_o\big)\Big] \\
&\quad - C_{F_i} \Sigma_E^T \tilde{\tilde{\bar{R}}}_{F_i} M_{F_i} W_{F_i} \dot{Z}_{F_i}
\end{aligned}
$$

4.3.5 TOTAL SYSTEM EQUATION

The above derived equations of motion of spinning space station with the attached appendages can be written in matrix notation as

$$[M]\left\{\ddot{X}\right\} + [C]\left\{\dot{X}\right\} + [K]\left\{X\right\} = \left\{P\right\} \tag{45}$$

where

$$M = \begin{array}{cl} \left[\begin{array}{c|c|c} M_{11} & M_{12} & M_{13} \\ \hline M_{21} & M_{22} & M_{23} \\ \hline M_{31} & M_{32} & M_{33} \end{array}\right] & \begin{array}{l} \leftarrow \text{Rigid Body} \\ \leftarrow \text{Space Station} \\ \leftarrow \text{Appendages} \end{array} \end{array}$$

$$C = \left[\begin{array}{c|c|c} C_{11} & C_{12} & C_{13} \\ \hline C_{21} & C_{22} & C_{23} \\ \hline C_{31} & C_{32} & C_{33} \end{array}\right]$$

$$K = \left[\begin{array}{c|c|c} K_{11} & K_{12} & K_{13} \\ \hline K_{21} & K_{22} & K_{23} \\ \hline K_{31} & K_{32} & K_{33} \end{array}\right]$$

$$\ddot{X} = \left\{\begin{array}{c} \dddot{R}_o \\ \dot{\omega}_o \\ \hline \ddot{Z}_S \\ \hline \ddot{Z}_F \end{array}\right\} \qquad X = \left\{\begin{array}{c} \dot{R}_o \\ \omega_o \\ \hline Z_s \\ \hline Z_F \end{array}\right\} \qquad P = \left\{\begin{array}{c} P_1 \\ \hline P_2 \\ \hline P_3 \end{array}\right\}$$

For the previously derived state equations, we find that M = O.

Thus, the rigid body equations (25) lead to the first equation of the total system, which is

$$\text{(46)} \quad \left[C_{11}\right]\begin{Bmatrix}\ddot{R}_o \\ \dot{\omega}_o\end{Bmatrix} + \left[C_{12}\right]\left\{\dot{Z}_S\right\} + \left[C_{13}\right]\left\{\dot{Z}_F\right\} = \left\{P_1\right\}$$

$$(6x6)\ (6x1) \qquad (6x2N_S) \qquad (6x2N_F) \qquad (6x1)$$

where

$$\left[C_{11}\right] = \left[\begin{array}{c|c} M_T & -M_T C \\ \hline 0 & I_T \end{array}\right]$$

$$\left[C_{12}\right] = -\sum_{i=1}^{4} \left[\begin{array}{c|c} -m_{F_i} & 0 \\ \hline -m_{F_i}(C_{F_i}\tilde{r}_{F_i}) & -C_i I_i C_i^T \end{array}\right] \left[\begin{array}{c} W_{S_i}^T \\ \hline W_{S_{b_i}}^T \end{array}\right]$$

$$\left[C_{13}\right] = \left[\begin{array}{c|c|c} \begin{array}{c} C_{F1}\Sigma_E^T M_{F1} W_{F1} \\ (3x2N_{F1}) \end{array} & \cdots & \begin{array}{c} C_{F4}\Sigma_E^T M_{F4} W_{F4} \\ (3x2N_{F4}) \end{array} \\ \hline \begin{array}{c} C_{F1}\Sigma_E^T \tilde{\tilde{R}}_{F1} M_{F1} W_{F1} \ -\tilde{r}'_{F1}\Sigma_E^T M_{F1} W_{F1} \\ (3x2N_{F1}) \end{array} & \cdots & \begin{array}{c} C_{F4}\Sigma_E^T \tilde{\tilde{R}}_{F4} M_{F4} W_{F4} \\ -\tilde{r}'_{F4} C_{F4}\Sigma_E^T M_{F4} W_{F4} \\ (3x2N_{F4}) \end{array} \end{array}\right]$$

$$(6x2\,N_F)$$

$$P_1 = \left(\begin{array}{c} F_{R1} + F_{R2} - M_T\left[(\tilde{\dot{\omega}}_o + \tilde{\omega}_o\tilde{\omega}_o)R_o + \tilde{\omega}_o\tilde{\omega}_o C + 2\,\tilde{\omega}_o\dot{R}_o\right] \\ \hline T_{R1} + T_{R2} - \tilde{l}_{R1}F_{R1} - \tilde{l}_{R2}F_{R2} - \tilde{\omega}_o I_T \omega_o \end{array}\right)$$

$$\left[K_{11}\right] = \left[K_{12}\right] = \left[K_{13}\right] = 0$$

The flexible spinning space station equation (11) leads to the second equation of the total system which is

$$(47)\qquad [C_{21}]\begin{Bmatrix}\ddot{R}_o\\ \dot{\omega}_o\end{Bmatrix} + [C_{22}]\{\dot{Z}_S\} + [C_{23}]\{\dot{Z}_F\} + [K_{22}]\{Z_S\} = \{P_2\}$$

where

$$[C_{21}] = -\sum_{i=1}^{4}\left[V_F\right]\left[\begin{array}{c|c} -m_{F_i} & m_{F_i}\left(\widetilde{h_{F_i} + C_{F_i} r_{F_i}}\right) \\ \hline -\left(\widetilde{C_{F_i} r_{F_i}}\right) m_{F_i} & -C_{F_i} I_{F_i} C_{F_i}^T + \left(\widetilde{C_{F_i} r_{F_i}}\right) m_{F_i}\left(\widetilde{h_{F_i} + C_{F_i} r_{F_i}}\right) \end{array}\right]$$

$$= -\sum_{i=1}^{4}\left[V'_{Fi} \,\middle|\, V''_{Fi}\right]\left[\begin{array}{c|c} -m_{Fi} & m_{Fi}\left(\widetilde{h_{Fi} + C_{Fi} r_{Fi}}\right) \\ \hline -\left(\widetilde{C_{Fi} r_{Fi}}\right) m_{Fi} & -C_{Fi} I_{Fi} C_{Fi}^T + \left(\widetilde{C_{Fi} r_{Fi}}\right) M_{Fi}\left(\widetilde{h_{Fi} + C_{Fi} r_{Fi}}\right) \end{array}\right]$$

$$\qquad (N_S \times 6) \qquad\qquad\qquad (6 \times 6)$$

$$\left[\ {}_{22}\right] = -\sum_{i=1}^{4}\left[V'_{Fi} \,\middle|\, V''_{Fi}\right]\left[\begin{array}{c|c} -m_{Fi} & 0 \\ \hline -m_{Fi}\left(\widetilde{C_{Fi} r_{Fi}}\right) & -C_i I_i C_i^T \end{array}\right]\left[\begin{array}{c} W_{si}^T \\ \hline W_{s_{b_i}}^T \end{array}\right] + \begin{bmatrix}1 & & 0\\ & 1 & \\ 0 & & \ddots\end{bmatrix}$$

$$\qquad (N_S \times 6) \qquad\qquad\qquad (6 \times 6)$$

$$\underset{2N_S \times 2N_F}{\left[C_{23}\right]} = \left[\begin{array}{c|c|c} V'_{F1}\left(C_{F1} \Sigma_E^T M_{F1} W_{F1}\right) & \cdots & V'_{F4}\left(C_{F4} \Sigma_E^T M_{F4} W_{F4}\right) \\ \hline V''_{F1}\left(C_{F1} \Sigma_E^T \tilde{\tilde{R}}_{F1} M_{F1} W_{F1}\right) & \cdots & V''_{F4}\left(C_{F4} \Sigma_E^T \tilde{\tilde{R}}_{F4} M_{F4} W_{F4}\right) \end{array}\right]$$

Forces and torques acting on space station and exciting flexible motion include:

1. 2 external forces
2. 2 external torques
3. up to 4 hinge forces and torques due to 4 attached rigid appendages
4. up to 4 forces and torques due to flexible motion of 4 fixed appendages
5. wobble damper control torque

$$\left[P_2\right] = \sum_{i=1}^{4} V'_{Fi} \left[m_{Fi}(2\omega_o \dot{R}_o + \tilde{\omega}_o \tilde{\omega}_o (R_o + h_{Fi} + C_{Fi} r_{Fi}) + \dot{\omega}_o R_o)\right]$$

$$+ \sum_{i=1}^{4} V''_{Fi} \left\{ C_{Fi} \, (C^T_{Fi} \, \omega_o) \, I_{Fi} C^T_{Fi} \, \omega_o + (\widetilde{C_{Fi} \, r_{Fi}})(m_{Fi}) \left[2\omega_o \dot{R}_o + \right.\right.$$

$$\left.\left. \tilde{\dot{\omega}}_o R_o + \tilde{\omega}_o \tilde{\omega}_o (R_o + h_{Fi} + C_{Fi} \, r_{Fi}) \right] \right\}$$

$$+ \sum_{i=1}^{2} V'_{Ri} F_{Ri} + \sum_{i=1}^{2} V''_{Ri} T_{Ri} + V''_{WOB} T_{WOB}$$

$$\left[K_{22}\right] = \left[\begin{array}{c|c} 0 & -\left|\bar{\Lambda}\right| \\ \hline \left|\bar{\Lambda}\right| & 2\xi_S \left|\bar{\Lambda}\right| \end{array}\right]$$

$$\left[K_{21}\right] = \left[K_{23}\right] = 0$$

The flexible appendage equations (22) lead to the third equation of the total system, which is

(48)

$$[C_{31}]\begin{Bmatrix}\ddot{R}_o\\ \dot{\omega}_o\end{Bmatrix} + [C_{32}]\{\ddot{Z}_S\} + \cancel{[C_{33}]\{\dot{Z}_F\}}^{\,0} + [K_{33}]\{Z_F\} = \{P_3\}$$

where

$$[M_{31}] = \begin{bmatrix} V''_{F1}R_{F1} \\ \hdashline V''_{F2}R_{F2} \\ \hdashline V''_{F3}R_{F3} \\ \hdashline V''_{F4}R_{F4} \end{bmatrix} \qquad M_{32} = \begin{bmatrix} V''_{F1}S_1 \\ \hdashline V''_{F2}S_2 \\ \hdashline V''_{F3}S_3 \\ \hdashline V''_{F4}S_4 \end{bmatrix}$$

$$[K_{33}] = \begin{bmatrix} 0 & -\lfloor\bar{\Lambda}\rfloor_F \\ \lfloor\Lambda\rfloor_F & 2\,\xi_F\lfloor\bar{\Lambda}\rfloor_F \end{bmatrix} \quad \text{(for each appendage)}$$

$$[K_{31}] = [K_{32}] = O$$

$$P_3 = \begin{bmatrix} V''_{F1}\,L_1 \\ \hdashline \vdots \\ \hdashline V''_{F4}\,L_4 \end{bmatrix}$$

In order to evaluate the coefficient matrices in equation (48) the transformation matrix $[V_F]$ derived in Section 4.3.6 may be used.

For computational speed and storage considerations, the elements of $\left[C_{31}\right]$ may be obtained as follows:

(49)

$$\left[V_F\right]\begin{Bmatrix} 0 \\ \hline R \end{Bmatrix} = \left[\begin{array}{c|c} 0 & d' \\ \hline -d' & 0 \end{array}\right] \left[\begin{array}{c|c} R_E\,(\Phi_B^T) & R_E\,(\Phi_B^T) \\ \hline I_m\,(\Phi_T^T) & I_m\,(\Phi_B^T) \end{array}\right] \begin{Bmatrix} 0 \\ \hline R \end{Bmatrix}$$

$$= \left[\begin{array}{c} d'\, I_m(\Phi_B^T) \\ \hline -d'\, R_E(\Phi_B^T) \end{array}\right] [R]$$

$$= \left[\begin{array}{c} d'\, I_m(\Phi_B^T) \\ \hline -d'R_E(\Phi_B^T) \end{array}\right] [m] \left[\begin{array}{c|c} -\Sigma_E C_F^T & \Sigma_E C_F^T \tilde{h}_F + \tilde{\tilde{r}}\Sigma_E C_F^T \end{array}\right]$$

$$(2N_F \times 3n) \qquad (3n \times 3n) \qquad (3n \times 3) \qquad\qquad (3n \times 3)$$

Define:

$$d_{RE} = \Sigma_E^T\,[m]\,R_E\,(\Phi_B)$$

$$d_{Im} = \Sigma_E^T\,[m]\,I_m\,(\Phi_B)$$

thus,

$$d_{RE}^T = R_E(\Phi_B^T)\,[m]\Sigma_E$$

$$d_{Im}^T = I_m(\Phi_B^T)\,[m]\Sigma_E$$

Also define:

$$r_{RE} = \Sigma_E^T\,\tilde{\tilde{r}}\,[m]\,R_E(\Phi_B)$$

$$r_{Im} = \Sigma_E^T\,\tilde{\tilde{r}}\,[m]\,I_m\,(\Phi_B)$$

then

$$r_{RE}^T = -R_E(\Phi_B^T)\,[m]\,\tilde{\tilde{r}}\,\Sigma_E$$

$$r_{Im}^T = -I_m(\Phi_B^T)\,[m]\,\tilde{\tilde{r}}\,\Sigma_E$$

In terms of the above definitions equation (49) can be written as

$$(50)\quad \left[V_F\right]\begin{Bmatrix} 0 \\ R \end{Bmatrix} = \left[\begin{array}{c|c} d'd_{I_m}^T\; C_F^T & -d'd_{I_m}^T\; C_F^T\,\tilde{h}_F + d'r_{I_m}^T\; C_F^T \\ \hline -d'd_{R_E}^T\; C_F^T & -d'd_{R_E}^T\; C_F^T\,\tilde{h}_F + d'r_{R_E}^T\; C_F^T \end{array}\right]$$

Similarly, we have the elements of the matrix $\left[M_{32}\right]$ as

$$(51)\quad \left[V_F\right]\begin{Bmatrix} 0 \\ S \end{Bmatrix} = \left[V_F''\right][S] = \left[V_F''\right]\underset{(3n \times 6)}{\left[\begin{array}{c|c} -m_1 C_F^T & 0 \\ \hline \vdots & \vdots \\ \hline -m_n C_F^T & 0 \end{array}\right]}\underset{(b \times N_s)}{\left[\begin{array}{c} W_{si} \\ \hline W_{sbi} \end{array}\right]}$$

$$= -\underset{(2N_F \times 3\,n)}{\left[V_F''\right]}\underset{(3n \times N_s)}{[m]\Sigma_E\, C_F^T\, W_{si}}$$

Finally, we can write equation (51) as

$$(52)\quad -\left[V_F''\right][S]\underset{(2N_F \times 3n)}{\left[\begin{array}{c} d'_{Im}\;(\Phi_B^T) \\ \hline -d'_{R_E}\;(\Phi_B^T) \end{array}\right]}\underset{(3n \times N_s)}{[m]\Sigma_E C_F^T W_{si}}$$

$$
= \left[\begin{array}{c} d'd_{I_m}^T \; C_F^T \, W_{si} \\ \hdashline -d'd_{R_E}^T \, C_F^T \; W_{si} \end{array}\right]
$$

$$
(2N_F \times N_s)
$$

The matrix $[P_3]$ is equation (48) can similarly be evaluated as

$$
(53) \quad \left[V_F\right] \begin{Bmatrix} 0 \\ \hdashline L \end{Bmatrix} = \left[V_F''\right][L]
$$

$$
= \left[V_F''\right] \left[\begin{array}{c} -m_1 C_F^T \left[\tilde{\omega}_o \; \tilde{\omega}_o \; (R_o + h_{Fi} + C_F r_1) + \dot{\tilde{\omega}}_o R_o + 2\tilde{\omega}_o \dot{R}_o\right] \\ \hdashline \vdots \\ \hdashline -m_n C_F^T \left[\tilde{\omega}_o \; \tilde{\omega}_o \; (R_o + h_{Fi} + C_F r_n) + \dot{\tilde{\omega}}_o R_o + 2\tilde{\omega}_o \dot{R}_o\right] \end{array}\right]
$$

$$
= \left[\begin{array}{c} d'd_{IM}^T C_F T \left[\tilde{\omega}_o \tilde{\omega}_o \left(R_o + h_{Fi}\right) + \dot{\tilde{\omega}}_o R_o + 2\, \omega_o \dot{R}_o\right] \\ \hdashline -d'd_{RE}^T \, C_F T \left[\tilde{\omega}_o \tilde{\omega}_o \left(R_o + h_{F_i}\right) + \dot{\tilde{\omega}}_o R_o + 2\,\tilde{\omega}_o \dot{R}_o\right] \end{array}\right]
$$

$$
-V_F'' \;\; [m] \;\; \mathrm{DIAG}\,(C_F^T \, \tilde{\omega}_o \, \tilde{\omega}_o \, C_F \, r_1, \, \ldots\ldots, \, C_F^T \tilde{\omega}_o \tilde{\omega}_o \, C_F \, r_n)
$$

4.3.6 Transformation Matrix [V]

By Definition

$$(54)\qquad V = 1/2 \left[\begin{array}{c|c} I & I \\ \hline J & -J \end{array}\right] \left[\Phi^{*^T} D\Phi\right]^{-1} \Phi^{*^T}$$

where D is a skew symmetric matrix defined in equation (3)

$$(55)\qquad D \equiv \left[\begin{array}{c|c} [0] & -[m] \\ \hline [m] & [G] \end{array}\right]$$

$$(56)\text{ and } \Phi \equiv \left[\begin{array}{c|c} \bar{\lambda}\Phi_B & \bar{\lambda}\Phi_B^* \\ \hline \Phi_B & \Phi_B^* \end{array}\right] \equiv \left[\begin{array}{c|c} \Phi_T & \Phi_T^* \\ \hline \Phi_B & \Phi_B^* \end{array}\right]$$

where
$$\bar{\lambda} = \begin{bmatrix} \lambda_1 j & & 0 \\ & \lambda_2 j & \\ & & \ddots \\ 0 & & & \lambda_N j \end{bmatrix}$$

$$\Phi_T = \Phi_B\bar{\lambda} \qquad\qquad \Phi_B = \left[\{\phi^{(1)}\}\ \{\phi^{(2)}\}\ \ldots\ \{\phi^{(N)}\}\right]$$

$$\Phi_B^* = \left[\{\phi^{(1)*}\}\ \{\phi^{(2)*}\}\ \ldots\ \{\phi^{(N)*}\}\right]$$

$\{\phi^*\}$ is complex conjugate of $\{\phi\}$

Using the above defined matrices, we may formulate the following equation

$$(57)\qquad \Phi^{*^T} D\,\Phi = \left[\begin{array}{c|c} \Phi_T^{*^T} & \Phi_B^{*^T} \\ \hline \Phi_T^T & \Phi_B^T \end{array}\right] \begin{bmatrix} [0] & -[m] \\ [m] & [G] \end{bmatrix} \left[\begin{array}{c|c} \Phi_T & \Phi_T^* \\ \hline \Phi_B & \Phi_B^* \end{array}\right]$$

$$= \left[\begin{array}{c|c} \Phi_B^{*^T}[m] & -\Phi_T^{*^T}[m] + \Phi_B^{*^T}[G] \\ \hline \Phi_B^T[m] & -\Phi_T^T[m] + \Phi_B^T[G] \end{array}\right] \left[\begin{array}{c|c} \Phi_T & \Phi_T^* \\ \hline \Phi_B & \Phi_B^* \end{array}\right]$$

$$= \left[\begin{array}{c|c} \Phi_B^{*T}[m]\Phi_T - \Phi_T^{*T}[m]\Phi_B + \Phi_B^{*T}[G]\Phi_B & \Phi_B^{*T}[m]\Phi_T^* - \Phi_T^{*T}[m]\Phi_B^* + \Phi_B^{*T}[G]\Phi_B^* \\ \hline \Phi_B^T[m]\Phi_T - \Phi_T^T[m]\Phi_B + \Phi_B^T[G]\Phi_B & \Phi_B^T[m]\Phi_T^* - \Phi_T^T[m]\Phi_B^* + \Phi_B^T[G]\Phi_B^* \end{array}\right]$$

(Note that the cross terms are the complex conjugate of each other)

In order to evaluate the matrices in equation (57) we introduce the following method.

(58.) Let $\psi \equiv (1/2)\Phi\left[\begin{array}{c|c} I & -J \\ \hline I & J \end{array}\right]$

$$= (1/2)\left[\begin{array}{c|c} \Phi_T & \Phi_T^* \\ \hline \Phi_B & \Phi_B^* \end{array}\right]\left[\begin{array}{c|c} I & -J \\ \hline I & J \end{array}\right] = (1/2)\left[\begin{array}{c|c} \Phi_T + \Phi_T^* & J(\Phi_T^* - \Phi_T) \\ \hline \Phi_B + \Phi_B^* & J(\Phi_B^* - \Phi_B) \end{array}\right]$$

$$= \left[\begin{array}{c|c} R_E(\Phi_T) & I_m(\Phi_T) \\ \hline R_E(\Phi_B) & I_m(\Phi_B) \end{array}\right]$$

The transpose of ψ may be written as

(59) $\psi^T = 1/2 \left[\begin{array}{c|c} I & I \\ \hline -J & J \end{array}\right]\Phi^T$

$$= 1/2\left[\begin{array}{c|c} I & I \\ \hline -J & J \end{array}\right]\left[\begin{array}{c|c} \Phi_T^T & \Phi_B^T \\ \hline \Phi_T^{*T} & \Phi_B^{*T} \end{array}\right]$$

and the conjugate transpose of ψ as

(60) $\psi^{*T} = (1/2)\left[\begin{array}{c|c} I & I \\ \hline J & -J \end{array}\right]\left[\begin{array}{c|c} \Phi_T^{*T} & \Phi_B^{*T} \\ \hline \Phi_T^T & \Phi_B^T \end{array}\right]$

$$= (1/2)\left[\begin{array}{c|c} \Phi_T^{*T} + \Phi_T^T & \Phi_B^{*T} + \Phi_B^T \\ \hline J(\Phi_T^{*T} - \Phi_T^T) & J(\Phi_B^{*T} - \Phi_B^T) \end{array}\right]$$

$$= \left[\begin{array}{c|c} R_E(\Phi_T^T) & R_E(\Phi_B^T) \\ \hline I_m(\Phi_T^T) & I_m(\Phi_B^T) \end{array}\right]$$

Defining Φ in terms of ψ

$$(61) \qquad \Phi = \psi \left[\begin{array}{c|c} I & I \\ \hline J & -J \end{array}\right] (1/2)$$

$$= \left[\begin{array}{c|c} R_E(\Phi_T) & I_m(\Phi_T) \\ \hline R_E(\Phi_B) & I_m(\Phi_B) \end{array}\right] \left[\begin{array}{c|c} I & I \\ \hline J & -J \end{array}\right]$$

and the conjugate transpose of Φ as

$$(62) \quad \Phi^{*^T} = \left[\begin{array}{c|c} I & -J \\ \hline I & J \end{array}\right] \left[\begin{array}{c|c} R_E(\Phi_T{}^T) & R_E(\Phi_B{}^T) \\ \hline I_m(\Phi_T{}^T) & I_m(\Phi_B{}^T) \end{array}\right]$$

Combining equation (2), (3), and (8), we can formulate equation (63)

$$(63) \qquad \Phi^{*^T} D\, \Phi = \left[\begin{array}{c|c} I & -J \\ \hline I & J \end{array}\right] \left[\begin{array}{c|c} R_E(\Phi_T{}^T) & R_E(\Phi_B{}^T) \\ \hline I_m(\Phi_T{}^T) & I_m(\Phi_B{}^T) \end{array}\right] \left[\begin{array}{c|c} [0] & [m] \\ \hline [m] & [G] \end{array}\right] \left[\begin{array}{c|c} R_E(\Phi_T) & I_m(\Phi_T) \\ \hline R_E(\Phi_B) & I_m(\Phi_B) \end{array}\right] \left[\begin{array}{c|c} I & I \\ \hline J & -J \end{array}\right]$$

$$= \left[\begin{array}{c|c} I & -J \\ \hline I & J \end{array}\right] \left[\begin{array}{c|c} R_E(\Phi_T{}^T) & R_E(\Phi_B{}^T) \\ \hline I_m(\Phi_T{}^T) & I_m(\Phi_B{}^T) \end{array}\right] \left[\begin{array}{c|c} -[m]\, R_E(\Phi_B) & -[m]\, I_m(\Phi_B) \\ \hline [m]\, R_E(\Phi_T) + [G]\, R_E(\Phi_B) & [m]\, I_m(\Phi_T) + [G]\, I_m(\Phi_B) \end{array}\right]$$

$$\left[\begin{array}{c|c} I & I \\ \hline J & -J \end{array}\right]$$

$$= \left[\begin{array}{c|c} I & -J \\ \hline I & J \end{array}\right] \left[\begin{array}{c|c} -R_E(\Phi_T{}^T)\,[m]\, R_E(\Phi_B) + R_E(\Phi_B{}^T)\left([m]\, R_E(\Phi_T) + [G] R_E(\Phi_B)\right) & -R_E(\Phi_T{}^T)\,[m]\, I_m(\Phi_B) + R_E(\Phi_B{}^T)\left([m]\, I_m(\Phi_T) + [G]\, I_m(\Phi_B)\right) \\ \hline -I_m(\Phi_T{}^T)\,[m]\, R_E(\Phi_B) + I_m(\Phi_B{}^T)\left([m]\, R_E(\Phi_T) + [G]\, R_E(\Phi_B)\right) & -I_m(\Phi_T{}^T)\,[m]\, I_m(\Phi_B) + I_m(\Phi_B{}^T)\left([m]\, I_m(\Phi_T) + [G]\, I_m(\Phi_B)\right) \end{array}\right] \left[\begin{array}{c|c} I & I \\ \hline J & -J \end{array}\right]$$

Substituting the following relations in equation (62)

$$\Phi_T = \Phi_B \bar{\lambda} = \phi_B \lambda(-j)$$

and $\quad R_E(\Phi_T) = +I_m(\Phi_B)\lambda, \quad R_E(\Phi_T^T) = +\lambda I_m(\Phi_B^T)$

$\quad I_m(\Phi_T) = -R_E(\Phi_B)\lambda, \quad I_m(\Phi_T^T) = -\lambda R_E(\Phi_B^T)$

we obtain

$$\Phi^{*T} D \Phi = \left[\begin{array}{c|c} I & -J \\ \hline I & J \end{array}\right] \left[\begin{array}{c|c} a & c \\ \hline b & d \end{array}\right] \left[\begin{array}{c|c} I & J \\ \hline J & -J \end{array}\right] \tag{64}$$

where

$$a = -\lambda I_m(\Phi_B^T)[m] R_E(\Phi_B) + R_R(\Phi_B^T)\left(+[m] I_m(\Phi_B)\lambda + [G] R_E(\Phi_B)\right)$$

$$b = +\lambda R_E(\Phi_B^T)[m] R_E(\Phi_B) + I_m(\Phi_B^T)\left(+[m] I_m(\Phi_B)\lambda + [G] R_E(\Phi_B)\right)$$

$$c = -\lambda I_m(\Phi_B^T)[m] I_m(\Phi_B) + R_E(\Phi_B^T)\left(-[m] R_E(\Phi_B)\lambda + [G] I_m(\Phi_B)\right)$$

$$d = +\lambda R_E(\Phi_B^T)[m] I_m(\Phi_B) + I_m(\Phi_B^T)\left(-[m] R_E(\Phi_B)\lambda + [G] I_m(\Phi_B)\right)$$

Let

$$\Phi^{*T} D \Phi = \left[\begin{array}{c|c} e & g \\ \hline f & h \end{array}\right] \tag{65}$$

where

$$\left.\begin{array}{lcl} e & = & (a+d) - (b+c)J \\ f & = & (a-d) + (b+c)J \\ g & = & (a-d) - (b+c)J \\ h & = & (a+d) + (b-c)J \end{array}\right\} \tag{66}$$

From the orthogonality relation of eigenvectors, $\Phi^{*T} D \Phi$ should be diagonal matrix,[3] hence,

$f = g = 0$, e and h are diagonal matrices.

Applying the above conditions in equation (66) , we have the following set of equations

$$(67)\quad \begin{cases} e = 2\,(a-bj) \\ h = 2\,(a+bj) \\ c = -b \\ \text{and } a = d \end{cases}$$

Then equation (64) becomes

$$(68)\qquad \Phi^{*^T} D\,\Phi = 2\left[\begin{array}{c|c} a-bj & 0 \\ \hline 0 & a+bj \end{array}\right]$$

It can be shown that the diagonal terms of equation (57) are purely imaginary; therefore, a in equation (68) must vanish, and hence

$$(69)\qquad \Phi^{*^T} D\,\Phi = \left[\begin{array}{c|c} -2bj & 0 \\ \hline 0 & +2bj \end{array}\right]$$

where

$$2bj = =2j\left[\lambda R_E(\Phi_B^{\ T})\,[m]\,R_E(\Phi_B) + I_M(\Phi_B^{\ T})\left(+[m]\,I_m(\Phi_B) \quad +[G]R_E(\Phi_B)\right)\right]$$

$$= \Phi_B^{*^T}\,[m]\,\Phi_T - \Phi_T^{*^T}\,[m]\,\Phi_B + \Phi_B^{*^T}\,[G]\,\Phi_B$$

Substituting equation (69) in equation (54), we obtain

$$V = 1/2\left[\begin{array}{c|c} I & I \\ \hline J & -J \end{array}\right]\left[\begin{array}{c|c} -2bj & 0 \\ \hline 0 & +2bj \end{array}\right]^{-1}\Phi^{*^T}$$

$$(70)\qquad = 1/2\left[\begin{array}{c|c} I & I \\ \hline J & -J \end{array}\right]\left[\begin{array}{c|c} d'j & 0 \\ \hline 0 & -d'j \end{array}\right]\Phi^{*^T}$$

$$= 1/2\left[\begin{array}{c|c} d'J & -d'J \\ \hline d' & -d' \end{array}\right]\Phi^{*^T}$$

$$= \quad 1/2 \left[\begin{array}{c|c} 0 & d' \\ \hline -d' & 0 \end{array}\right] \left[\begin{array}{c|c} I & -I \\ \hline J & -J \end{array}\right] \Phi^{*^T}$$

$$= 1/2 \left[\begin{array}{c|c} 0 & d' \\ \hline -d' & 0 \end{array}\right] \left[\begin{array}{c|c} I & I \\ \hline J & -J \end{array}\right] \left[\begin{array}{c|c} \Phi_T{}^{*T} & \Phi_B{}^{*T} \\ \hline \Phi_T{}^T & \Phi_B{}^T \end{array}\right]$$

$$= \quad \left[\begin{array}{c|c} 0 & d' \\ \hline -d' & 0 \end{array}\right] \left[\begin{array}{c|c} R_E(\Phi_T{}^T) & R_E(\Phi_B{}^T) \\ \hline I_m(\Phi_T{}^T & I_m(\Phi_B{}^T) \end{array}\right]$$

where $\left[\begin{array}{c|c} -2bj & 0 \\ \hline 0 & 2bj \end{array}\right]^{-1} = \left[\begin{array}{c|c} d'j & 0 \\ \hline 0 & -d'j \end{array}\right]$ is used.

4.3.7 Computational Considerations

$$F_{A_i} = \sum_E^T M_{F_i} W_{F_i} \dot{z}_{F_i}$$

$$= [EE.....E] \left[\begin{array}{c|c} m & o \\ \hline o & o \end{array}\right] \left[\begin{array}{c|c} \phi_T & \phi_T^* \\ \hline \phi_B & \phi_B^* \end{array}\right] \left[\begin{array}{c|c} I & -J \\ \hline I & J \end{array}\right] \dot{z}_{F_i}$$

$$= [E.......E] \left[\begin{array}{c|c} m & o \\ \hline o & o \end{array}\right] \left[\begin{array}{c|c} 2R_E(\phi_T) & 2I_m(\phi_T) \\ \hdashline 2R_E(\phi_B) & 2I_m(\phi_B) \end{array}\right] \dot{z}_{F_i}$$

$$= [E........E] \left[\begin{array}{c|c} 2mR_E(\phi_T) & 2mI_m(\phi_T) \\ \hline O & O \end{array}\right] \dot{z}_{F_i}$$

$$= \left[\begin{array}{c:c} \sum_{j=1}^{n} 2m_j R_E(\phi^1_{Bjx}) \ldots & \sum_{j=1}^{n} 2m_j I_m(\phi^1_{Bjx}) \ldots \\ \hdashline \sum_{j=1}^{n} 2m_j R_E(\phi^1_{Bjy}) \ldots & \sum_{j=1}^{n} 2m_j I_m(\phi^1_{Bjy}) \ldots \\ \hdashline \sum_{j=1}^{n} 2m_j R_E(\phi^1_{Bjz}) \ldots & \sum_{j=1}^{n} 2m_j I_m(\phi^1_{Bjz}) \ldots \\ & \end{array}\right] \dot{z}_{F_i}$$

$(3 \times 2N)$

Likewise -

$$T_{A_i} = \sum_E^T \tilde{\tilde{R}}_{F_i} M_{F_i} W_{F_i} \dot{Z}_{F_i}$$

$$= [E.......E]\left[\begin{array}{c|c} \tilde{\tilde{R}}_{F_i} & O \\ \hline O & O \end{array}\right]\left[\begin{array}{c|c} m & O \\ \hline O & O \end{array}\right]\left[\begin{array}{c|c} \Phi_T & \Phi_T^* \\ \hline \Phi_B & \Phi_B^* \end{array}\right]\left[\begin{array}{c|c} I & -J \\ \hline I & J \end{array}\right] \dot{Z}_{F_i}$$

$$= [E.......E]\left[\begin{array}{c|c} 2\tilde{\tilde{R}}_{F_i} mR_E(\phi_T) & 2\tilde{\tilde{R}}_{F_i} mI_m(\phi_T) \\ \hline O & O \end{array}\right] \dot{Z}_{F_i}$$

$$= 2\begin{bmatrix} \bar{m}_1\tilde{F}_1 & & O \\ & \ddots & \\ O & & \bar{m}_n\tilde{F}_n \end{bmatrix} \left[\begin{array}{c|c} R_E(\phi_T) & I_m(\phi_T) \end{array}\right] \dot{Z}_{F_i}$$

4.4 REFERENCES

Ref. 4.1 "Dynamics and Control of Flexible Space Vehicles", P. W. Likens, NASA CR 105592.

Ref. 4.2 "Small Eccentricities or Inclinations in the Brouwer Theory of the Artificial Satellite", R. H. Lyddane, Astronomical Journal, Volume 68, No. 8, October 1963, P. 555.

Ref. 4.3 Space Station Study (Phase B), Selected Control Moment Gyro Configuration Report 505, General Electric Company Avionic Controls Department, Binghamton, New York.

Ref. 4.4 Space Station Study (Phase B), Control Moment Gyro Assembly Candidate CMG Assemblies Report 504, General Electric Company Avionic Controls Department, Binghamton, New York.

Ref. 4.5 Space Station Study (Phase B), Control Moment Gyro Assembly Report EL 506-D, "Preliminary Synthesis and Simulation of Selected CMG Attitude Control System," General Electric Co. Avionic Controls Department, Binghamton, New York.

Ref. 4.6 Likens, P. W., "Modal Method for Analysis of Free Rotations of Spacecraft," AIAA Journal, Vol. 5, #7, July 1967.

Ref. 4.7 MacNeal, R. H., "The NASTRAN Theoretical Manual," SP-221, pg. 11.3-1 to 11.3-13, Office of Technology Utilization, NASA, Washington, D. C.

5. SOLAR ARRAY AND SPACE STATION STRUCTURAL DYNAMIC ANALYSES AND DATA

Structural dynamic analyses were performed on various solar array and space station configurations to compliment the formulation of the dynamic interactions methodology. The results of these analyses in terms of modal property definitions are required as basic input to the simulation program. Described in this report section are the performed structural analyses for two phases of the interactions study. The first study phase considered only the derivation of solar array modal properties since the space station was considered to be a rigid body. The second study phase considered the influence of space station flexibility in the dynamic interactions methodology and therefore structural mode analyses are also presented for a space station conceptual design.

5.1 PHASE I STUDY ANALYSES

The structural analyses described in this report section were performed to obtain the necessary solar array vibration mode data for use as input to the dynamic interaction analysis simulation. By direction from NASA/LRC, two solar array configurations were considered in the structural analyses; these being a rollup flexible array, configured by the Lockheed Missile and Space Corporation, and a fold out panel array, configured from a Boeing Aircraft Corporation design concept. Both arrays meet the 100 KW power requirement for the North American Rockwell Space Station. In addition, the stowage configuration of both arrays for the launch phase of flight are compatible with the present geometrical constraints imposed by the space station shroud. It is noted, however, that the design criteria for the rollup array includes the loading environment associated with an artificial "G" environment while the fold out panel array is configured for the zero "G" mode of operation only.

5

A discrete structural element and mass representation of the solar arrays was utilized in the analysis method of deriving the required modal data. This technical approach required the generation of large-order stiffness and mass matrices for subsequent use in a matrix displacement method of modal analysis (Reference 5.1). Details of the modal analyses and analytical results are given in the following report subsections for both the rollup and foldout panel arrays.

5.1.1 FLEXIBLE ROLLUP ARRAY

The stiffness and mass characteristics used to model the flexible array for the determination of vibration modes are based upon information received from LMSC for the North American space station flexible array concept. The array wing section (Figure 5-1) consists of a central extendible boom with inner and outer array support members attached perpendicular to the boom (Reference 5.2). Ten kapton membrane strips are tensioned between the inner and outer support members to which the solar cells are attached. Primary structural member sizes are dictated by the loading associated with the artificial "G" mode of operation which presents the most severe design condition. If the array were designed only for the zero "G" environment, a lighter weight structure would result.

The total array area (2 wing sections) is approximately 10,000 sq. ft. and the electrical power output is rated as 10 watts per sq. ft. A six inch spacing is assumed to exist between the membrane strips and each strip carries a preset tension force of 2 pounds per foot of width. The main boom and support member are specified as frames. However, they are modeled for the discrete element method of analysis as equivalent stiffness beams. The stiffness properties of the structural members are given below.

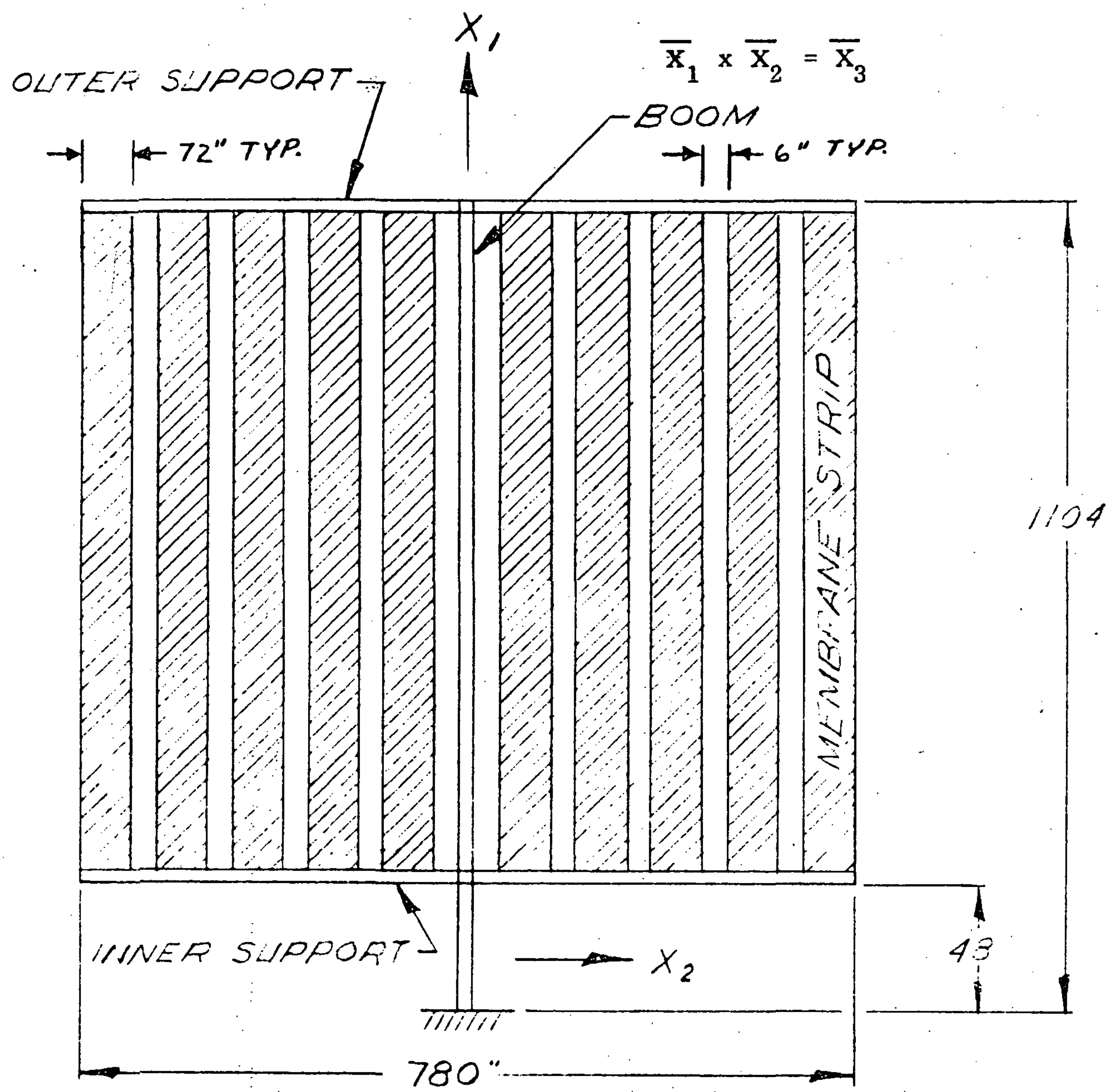

Figure 5-1. Flexible Array Wing Section Dimensions

Member	AE (lbs.)	$EIxi_1$ * ($lb.-in.^2$)	$EIxi_2$ * ($lb.-in.^2$)	$EIxi_3$ * ($lb.-in.^2$)	JG ($lb.-in.^2$)
Boom	11.45×10^6		1489×10^6	1585×10^6	23.1×10^6
Inner and Outer Support	23.4×10^6	160×10^6		840×10^6	

*EIxi refers to moments about the Xi axis where the axis designation is shown on Figure 5-1.

The weight distribution used for each of the structural elements are as follows:

	Running Weight
Boom	0.133 lb/in
Inner Support	0.958 lb/in
Outer Support	0.565 lb/in
Membrane Strips	2.45 (10^{-3}) lbs/in^2

5.1.1.1 Out of Plane Motion - Array Vibration Model

In solving for the out of plane array vibration modes, advantage was taken of the structural and mass symmetry of the rollup array wing section. This enables utilizing a structural model of only one half of the wing section. By suitable adjustment of the boundary conditions along the boom centerline, the symmetric and antisymmetric modes about the boom axes were obtained. Figure 5-2 is a sketch of the finite element model similar to that used for the mathematical representation of the continuous structure.

The out of plane motion degree of freedom given the membrane nodes was an X_3 translation. The support member nodes

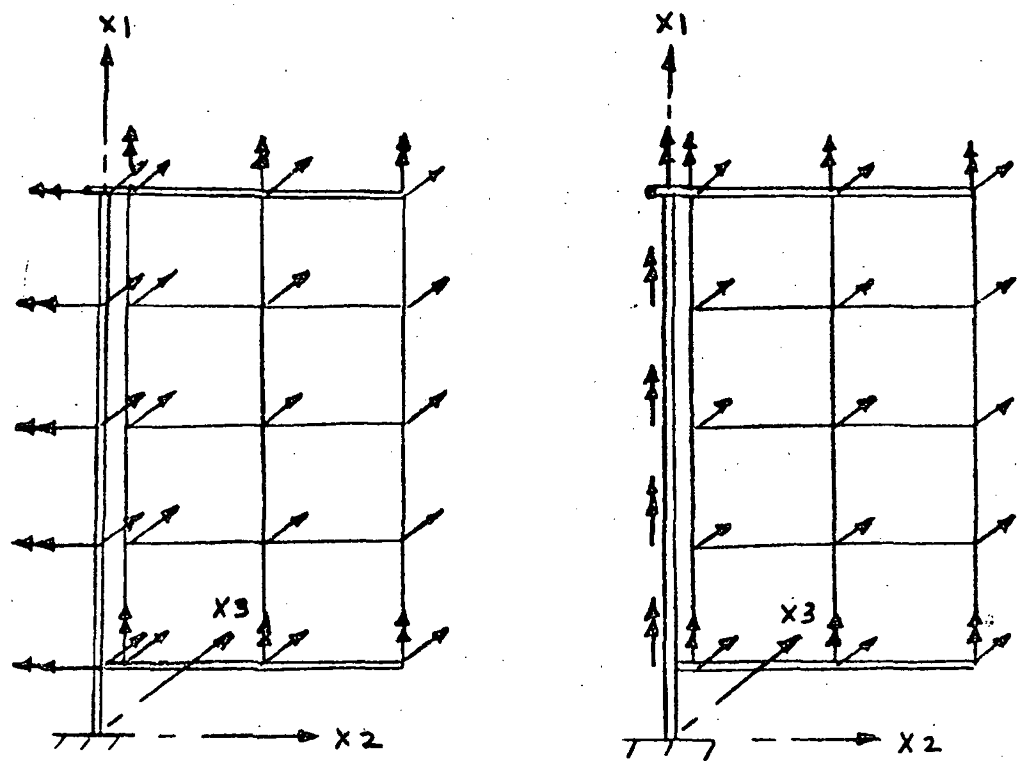

a) Symmetric Model

b) Antisymmetric Model

Figure 5-2 Finite Element Model Rollup Array were allowed degrees of freedom in X_3 translation and X_1 rotation. The boom nodes were allowed to translate in the X_3 direction and rotate about the X_2 axis for the symmetrical condition, and rotate about the X_1 axis only for the antisymmetrical condition.

The discrete element model used for computing the out of plane modes is shown in Figure 5-3. A one-hundred node model was used with the boom rigidly constrained at node 100 as shown. The discrete weights derived for each of the various nodes are tabulated in Table 5-1. The weight associated with this model does not include equipment weight located on the space station tunnel.

TABLE 5-1. NODAL WEIGHTS ASSOCIATED WITH ROLLUP ARRAY DYNAMIC MODEL

Node	Weight (lbs.)
1	26.22
2-8, 11-17, 20-26, 29-35, 28-44, 47-53	11.63
56-62, 65-71, 74-80, 83-89	11.63
10, 19, 28, 37, 46, 55, 64, 73, 82	27.92
9	40.32
18, 27, 36, 45, 54, 63, 72, 81, 90	43.22
91	10.5
92, 93, 94, 95, 96, 97, 98	17.6
99	14.87
100	3.2

Ross' rectangular membrane finite element representation (Reference 5.3) was used to model the membrane strips. A pictorial sketch of this element with the forces and degrees of freedom associated with the element nodes is shown in Figure 5-4a together with the corresponding formulation of the stiffness matrix.

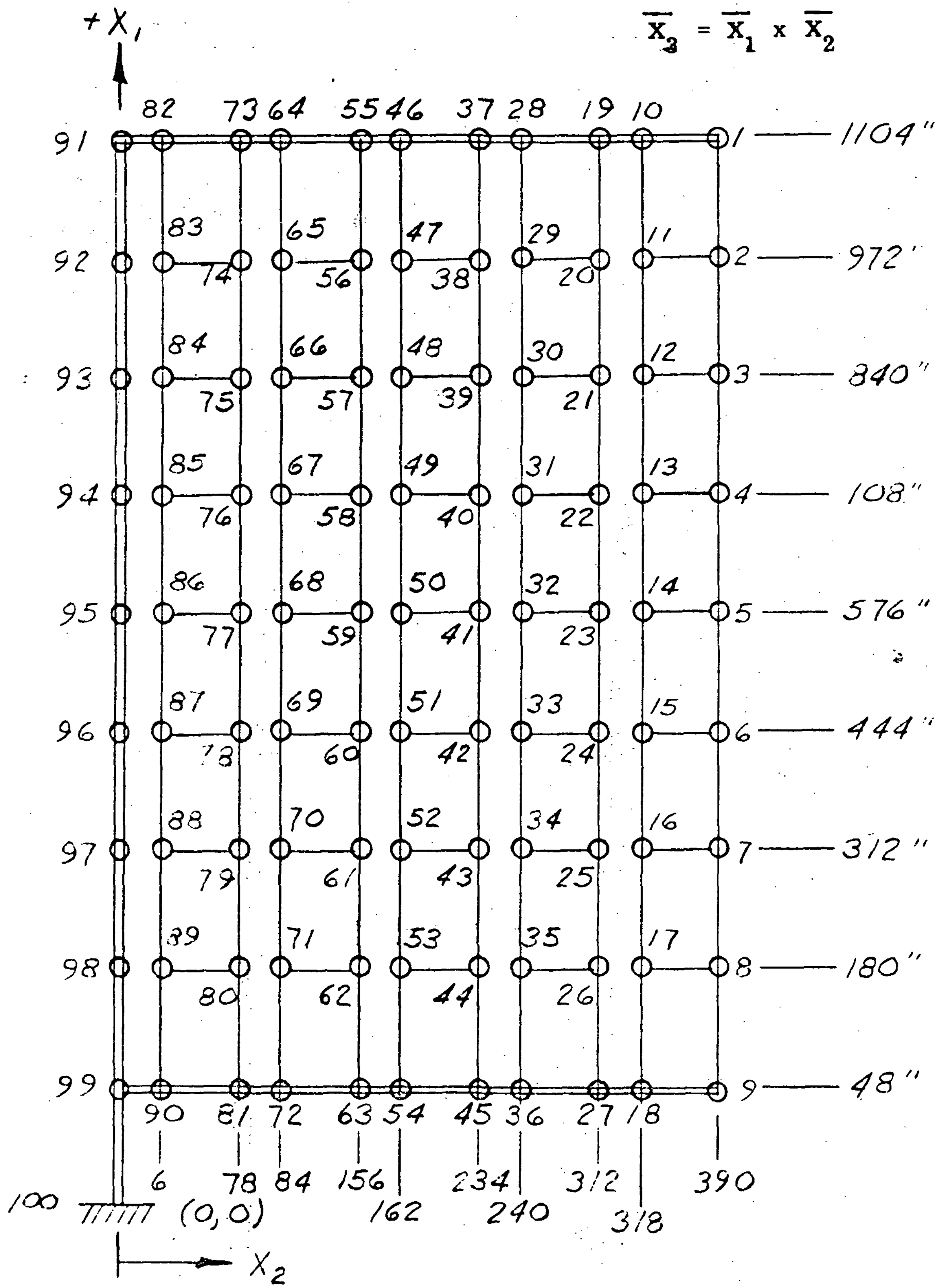

Figure 5 — 3 Dynamic Model, Rollup Array, Out of Plane Modes

$$
K = \frac{T}{6\,l_1}
\begin{array}{c}
\begin{array}{cccc} \mu_1 & \mu_2 & \mu_3 & \mu_4 \end{array} \\
\begin{bmatrix}
2 & & \text{Sym.} & \\
-2 & 2 & & \\
-1 & 1 & 2 & \\
1 & -1 & -2 & 2
\end{bmatrix}
\end{array}
$$

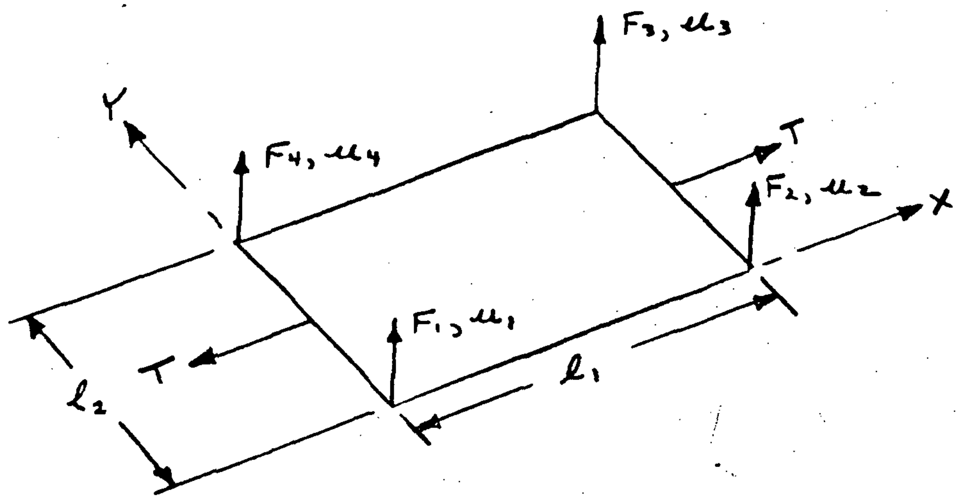

Figure 5—4a Rectangular Membrane Finite Element

$$
K = \frac{2\,EI}{l^3}
\begin{array}{c}
\begin{array}{cccc} \mu_1 & \theta_1 & \mu_2 & \theta_2 \end{array} \\
\begin{bmatrix}
6 & & & \text{Sym.} \\
3\,l & 2\,l^2 & & \\
-6 & -3\,l & 6 & \\
3\,l & l^2 & -3\,l & 2\,l^2
\end{bmatrix}
\end{array}
+ P/5
\begin{array}{c}
\begin{array}{cccc} \mu_1 & \theta_1 & \mu_2 & \theta_2 \end{array} \\
\begin{bmatrix}
6/l & & & \text{Sym.} \\
1/2 & 2l/3 & & \\
-6/l & -1/2 & 6/l & \\
1/2 & -1/6 & -1/2 & 2l/3
\end{bmatrix}
\end{array}
$$

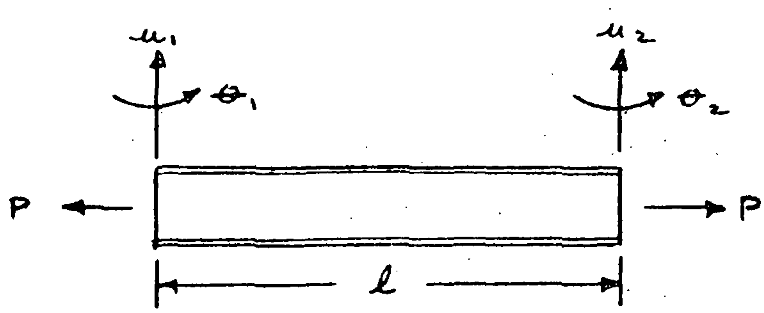

Figure 5 -4b Beam Column Finite Element

Figure 5-4. Stiffness Matrices

An axial compression load due to the tensioning of the membrane strips causes a decrease in the lateral stiffness of the boom. This beam column effect was accounted for in the stiffness matrix representing the boom, although for the values of bending and torsional stiffnesses used, the effect is small. The beam columning effect on the stiffness matrix (References 5.3 and 5.4) is shown in Figure 5-4b.

5.1.1.2 In-Plane Motion - Array Vibration Model

The in-plane rollup array model had the same nodes, mass properties and geometry as the out of plane model. Only one half of the wing section was modeled since the wing section is symmetric about the boom axis. Adjustments in the boundary conditions of the boom were made to obtain both the symmetrical and antisymmetrical modes. The model is shown in Figure 5-5. The membrane finite element representation utilized triangular plate elements which are described in Reference 5.1. These elements resist in-plane forces only. The effect of membrane tension upon the elemental in-plane stiffness representation was found to be negligible by use of the stiffness derivation method given in Reference 5.5. All nodes were allowed in-plane motion degrees of freedom only. The symmetrical modes were produced by allowing the boom to deflect only in the X_1 direction, and the antisymmetrical modes were produced by allowing the boom modes to deflect only in the X_2 direction and rotate about the X_3 axis. The symmetric modes induce axial forces into the boom while the antisymmetric modes produce in-plane shear forces and bending moments. The physical characteristics of the Kapton membrane substrate that were utilized for the analysis were:

thickness = 0.004 inch
Youngs Modulus = 450,000 psi
Poisson's ratio = 0.5

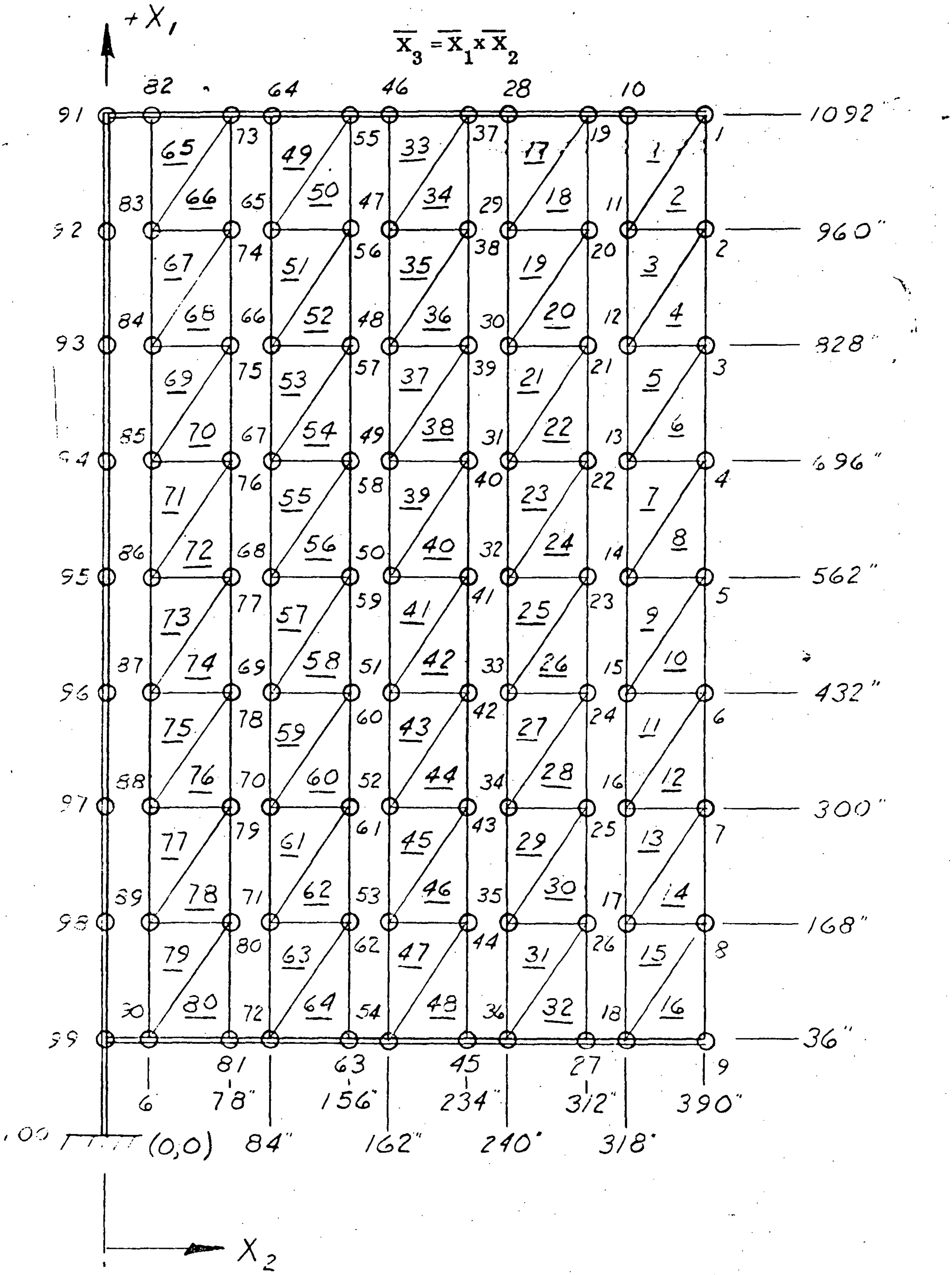

Figure 5 — 5 In-Plane Rollup Array Model

5.1.1.3 Rollup Array Vibration Modes

From the rollup array out of plane modal analysis, 60 symmetric and 99 antisymmetric eigenvalues were obtained with the corresponding sets of eigenvectors. It was necessary to obtain a large number of modes in order to determine those of importance to the interactions study. Many of the modes are local torsion or bending of the individual membrane strips and do not contribute significantly as external loadings upon the space station.

The first forty-one frequencies for the out of plane modes are tabulated in Tables 5-2 and 5-3 with a description of the modes. Pictorial presentations of each of the lower symmetric and antisymmetric modes along with other higher modes which are considered to be important for inclusion in the interactions study are shown in Figures 5-6 to 5-22. In determining which modes to be used for interaction computer program runs (a total of 12 modes can presently be used for both in- plane and out of plane motion), use was made to modal participation factors. For the symmetric modes, the percent participation is based on the shear at the point of structural constraint due to a base translational acceleration when the value is equal to:

$$\% \text{ participation} = \frac{(\Sigma m_i \phi_{in})^2}{R_n M} \times 100$$

For the antisymmetric modes, the participation is based on the moment at the point of structural constraint due to a base rotational acceleration. The percent participation is equal to:

$$\% \text{ participation} = \frac{(\Sigma m_i \phi_{in} r_i)^2}{R_n I_{x1}} \times 100$$

TABLE 5 - 2 LIST OF OUT OF PLANE SYMMETRIC MODE FREQUENCIES FOR ROLLUP ARRAY

Mode	Frequency (Hz)	Description
1	.0441	First torsion modes of membrane strips
2	.0441	
3	.0441	
4	.0441	
5	.0441	
6	.0734	First bending modes of membrane strips
7	.0762	
8	.0763	
9	.0763	
10	.0763	
11	.0864	Second torsion modes of membrane strips.
12	.0864	
13	.0864	
14	.0864	
15	.0864	
16	.1255	Third torsion modes of membrane strips.
17	.1255	
18	.1255	
19	.1255	
20	.1255	
21	.1429	Second bending modes of membrane strips
22	.1495	
23	.1497	
24	.1497	
25	.1497	
26	.1597	Fourth torsion modes of membrane strips.
27	.1597	
28	.1597	
29	.1597	
30	.1597	
31	.1878	Fifth torsion modes of membrane strips
32	.1878	
33	.1878	
34	.1878	
35	.1878	
36	.2026	First boom bending mode
37	.2086	Sixth torsion modes of membrane strips
38	.2086	
39	.2086	
40	.2086	
41	.2086	

TABLE 5 - 3 LIST OF OUT OF PLANE ANTISYMMETRIC MODE FREQUENCIES FOR ROLLUP ARRAY

Mode	Frequency (Hz)	Description
1	.0439	First torsion modes of membrane strips
2	.0441	
3	.0441	
4	.0441	
5	.0441	
6	.0557 -	First torsion mode of boom
7	.0763	First bending modes of membrane strips
8	.0763	
9	.0763	
10	.0763	
11	.0863	Second torsion modes of membrane strips
12	.0864	
13	.0864	
14	.0864	
15	.0864	
16	.1082 -	First bending mode of outer support
17	.1255	Third torsion modes of membrane strips
18	.1255	
19	.1255	
20	.1255	
21	.1256	
22	.1497	Second bending modes of membrane strips
23	.1497	
24	.1497	
25	.1497	
26	.1595	Fourth torsion modes of membrane strips
27	.1597	
28	.1597	
29	.1597	
30	.1597	
31	.1620 -	Second torsion mode of boom
32	.1878	Fifth torsion modes of membrane strips
33	.1878	
34	.1878	
35	.1878	
36	.1878	
37	.2086	Sixth torsion modes of membrane strips
38	.2086	
39	.2086	
40	.2086	
41	.2086	

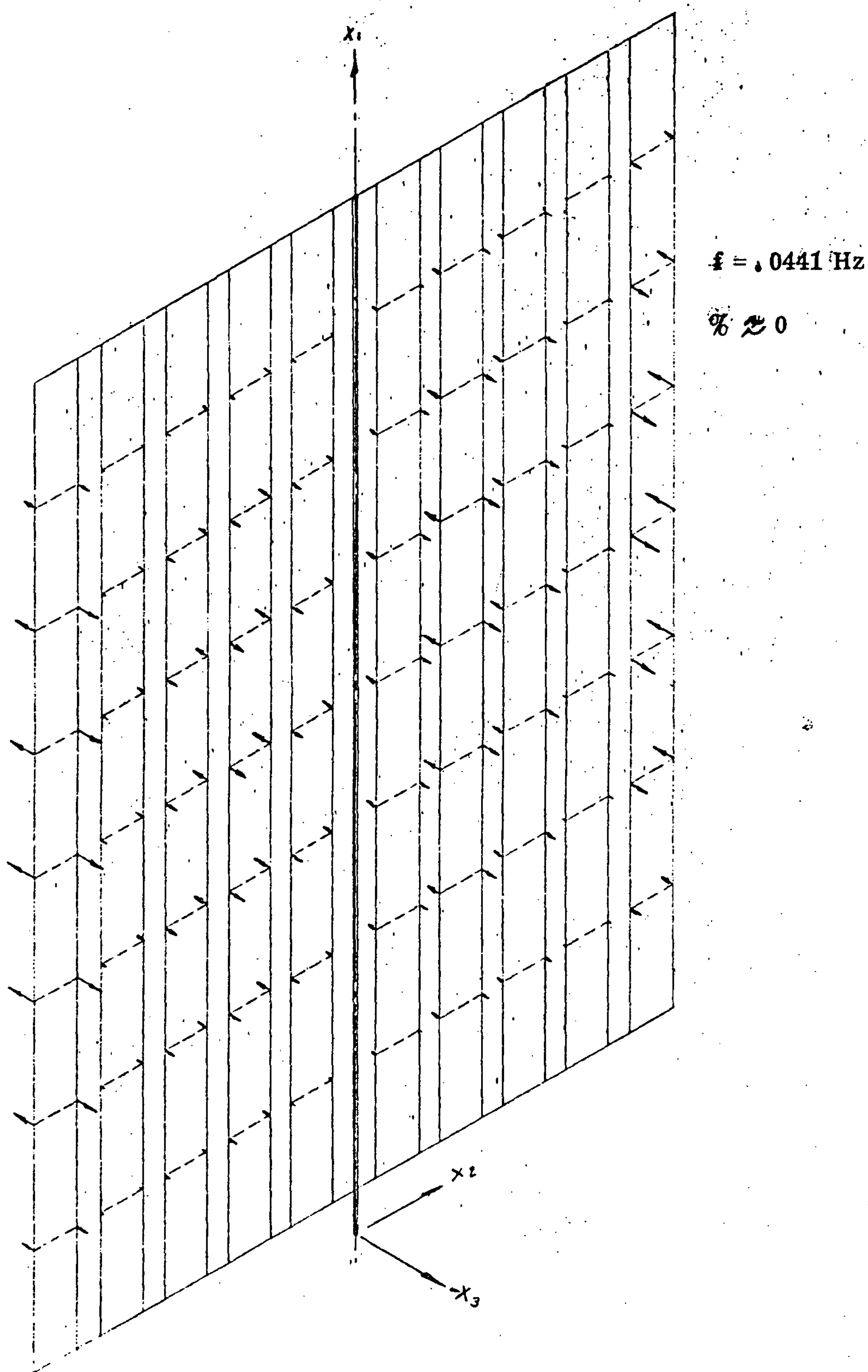

Figure 5-6. Mode 1, Rollup Array, Out of Plane, Symmetric

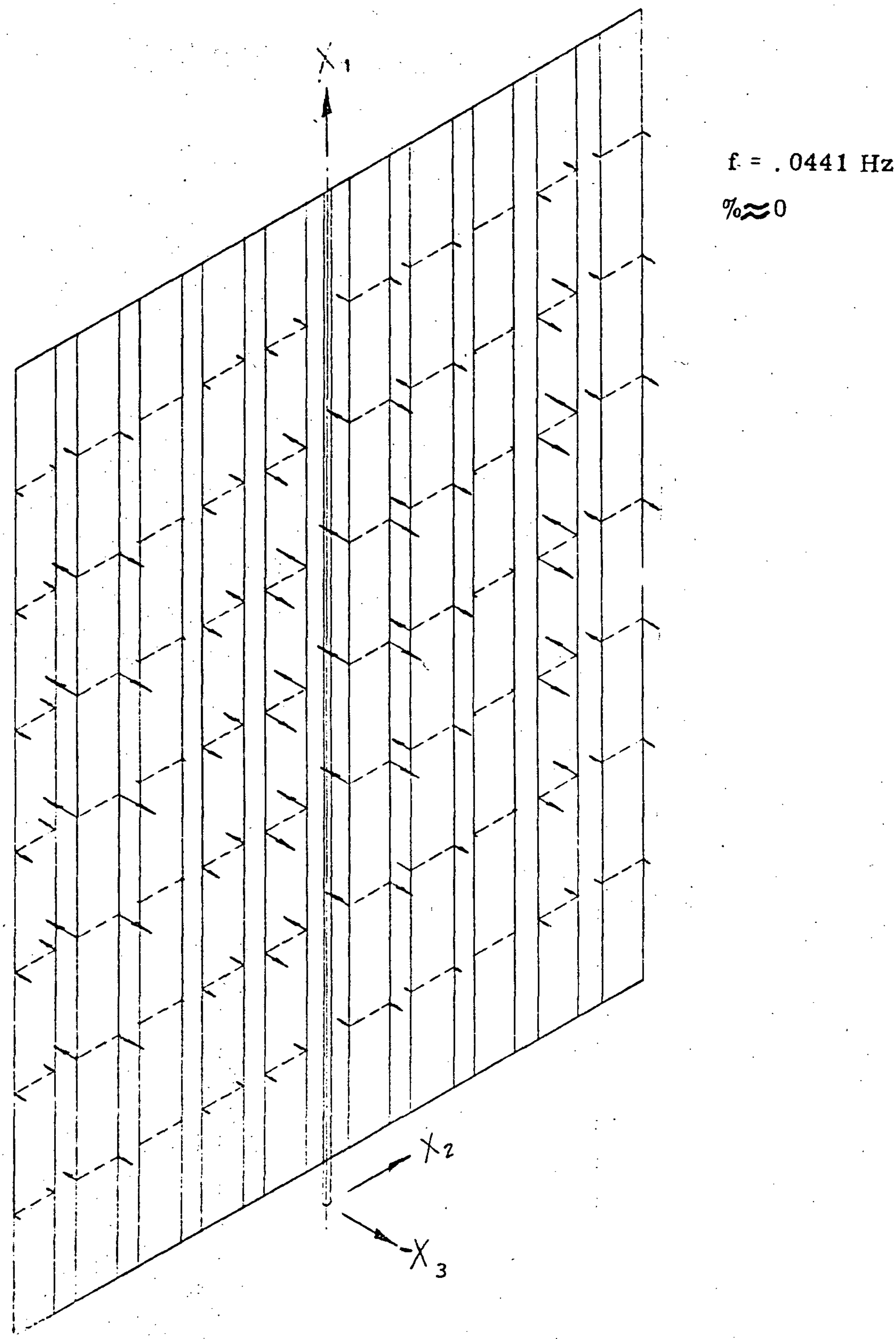

Figure 5-7 Mode 2, Rollup Array, Out of Plane, Symmetric

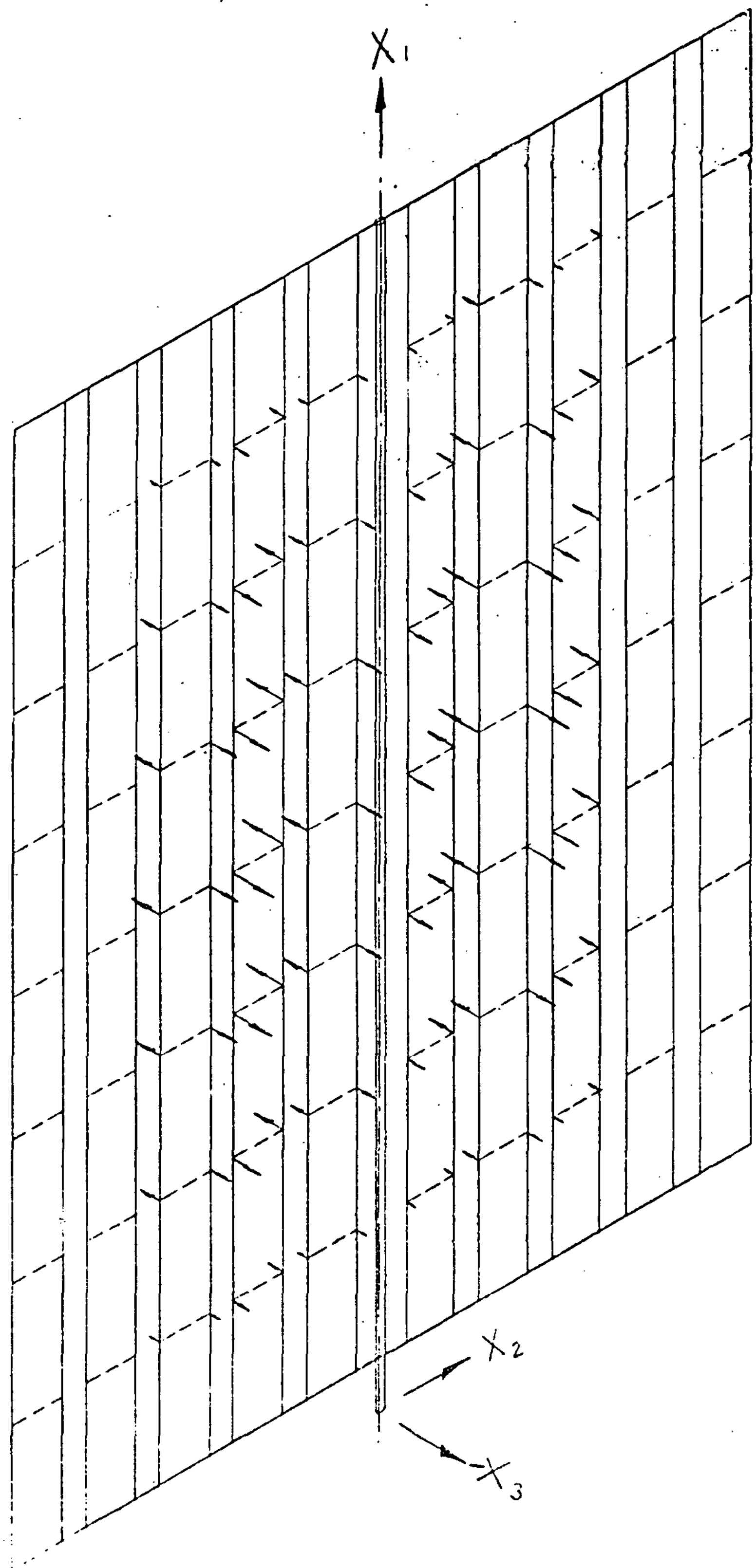

f = .0441 Hz

% ≈ 0

Figure 5-8. Mode 3, Rollup Array, Out of Plane, Symmetric

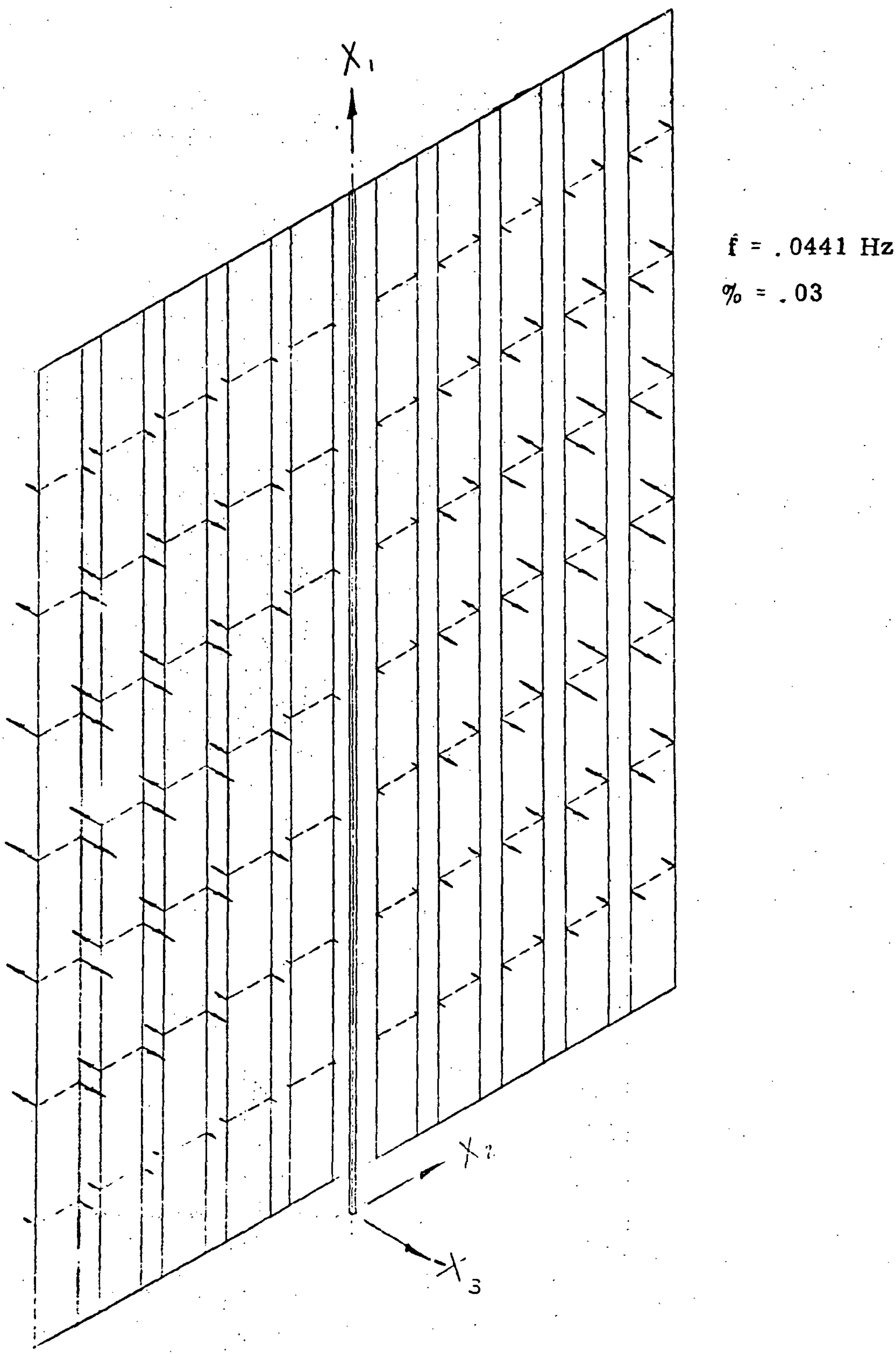

Figure 5-9. Mode 4, Rollup Array, Out of Plane, Symmetric

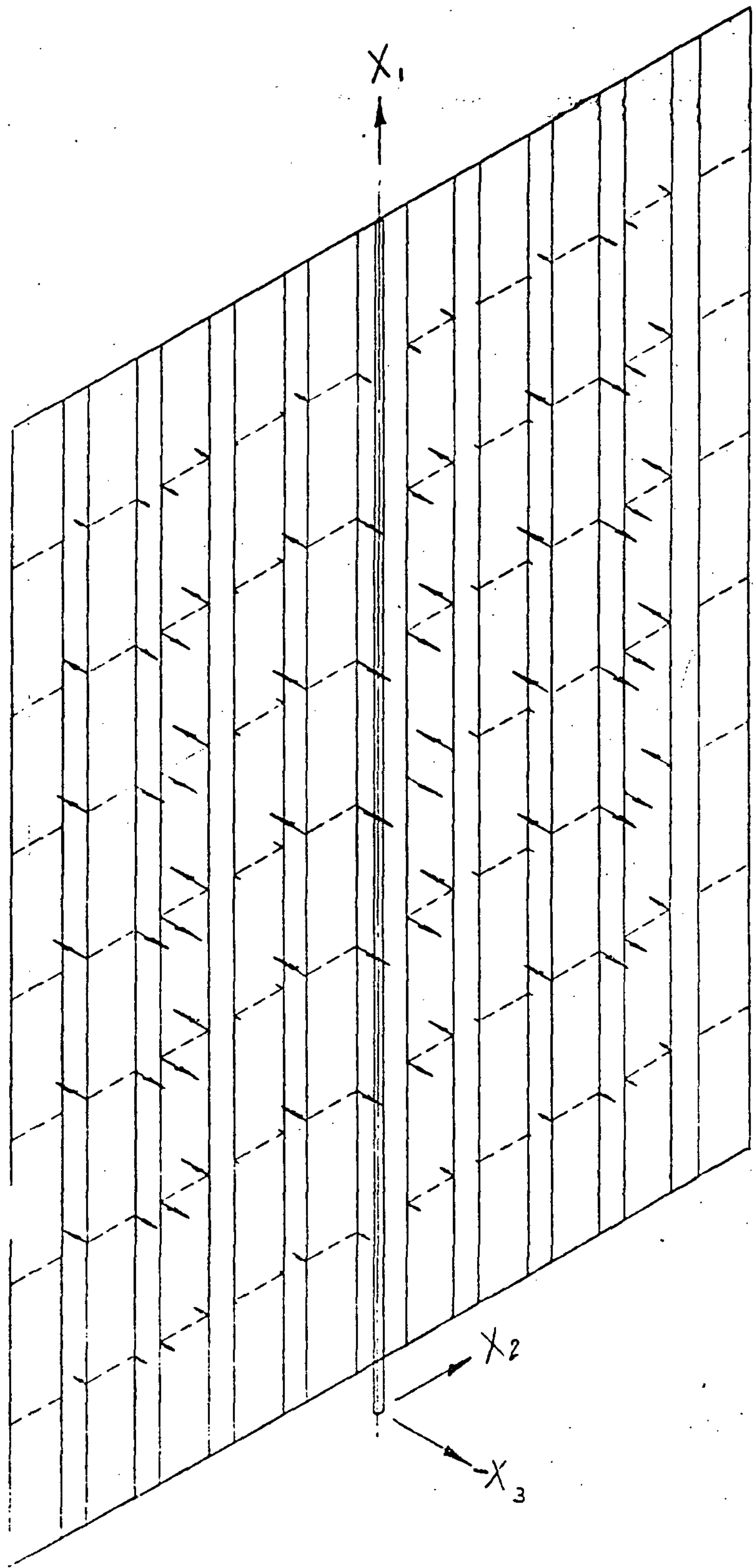

f = .0441 Hz

% $\gtrsim$ 0

Figure 5-10 Mode 5, Rollup Array, Out of Plane, Symmetric

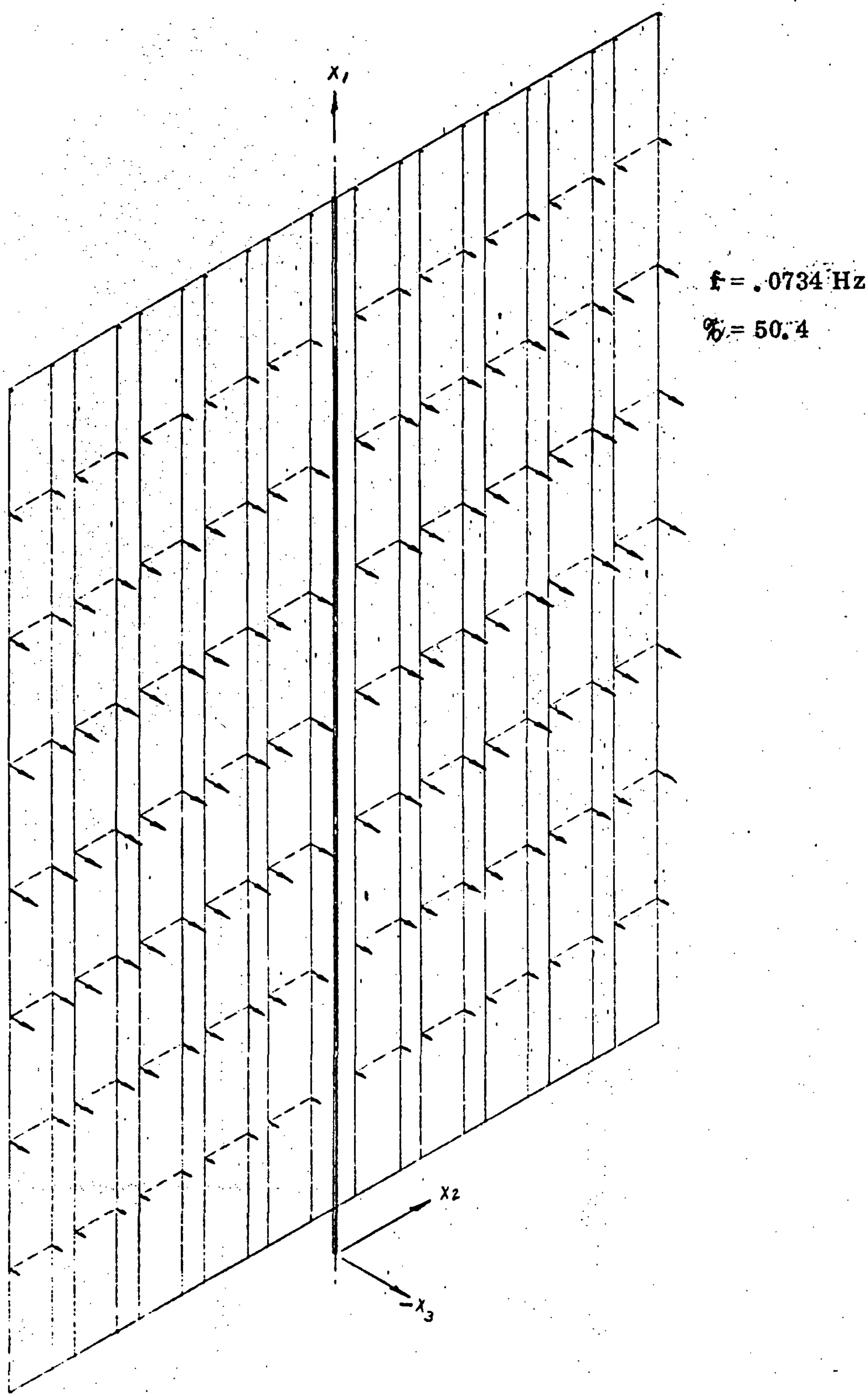

Figure 5-11 Mode 6, Rollup Array, Out of Plane, Symmetric

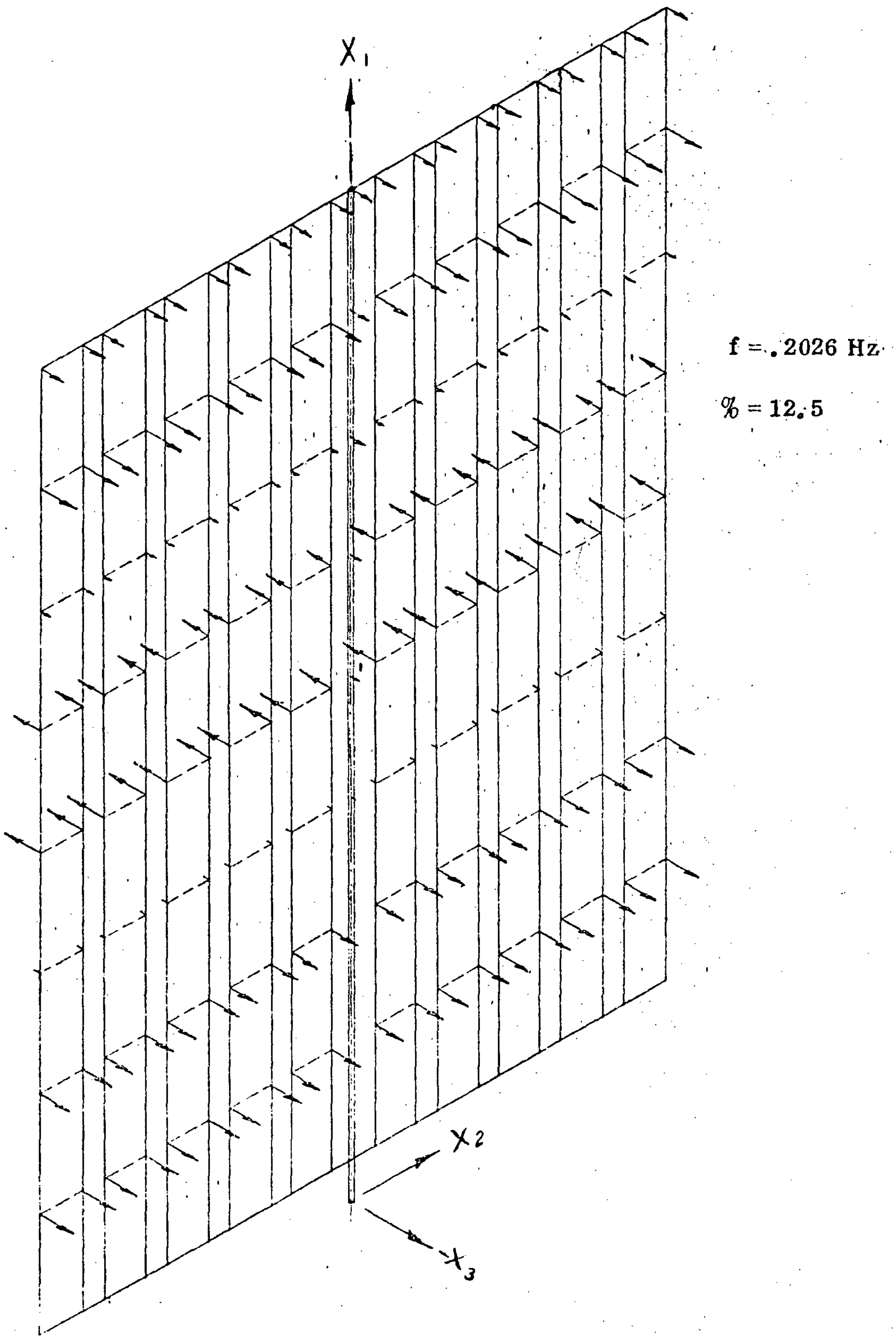

Figure 5-12 Mode 36, Rollup Array, Out of Plane, Symmetric

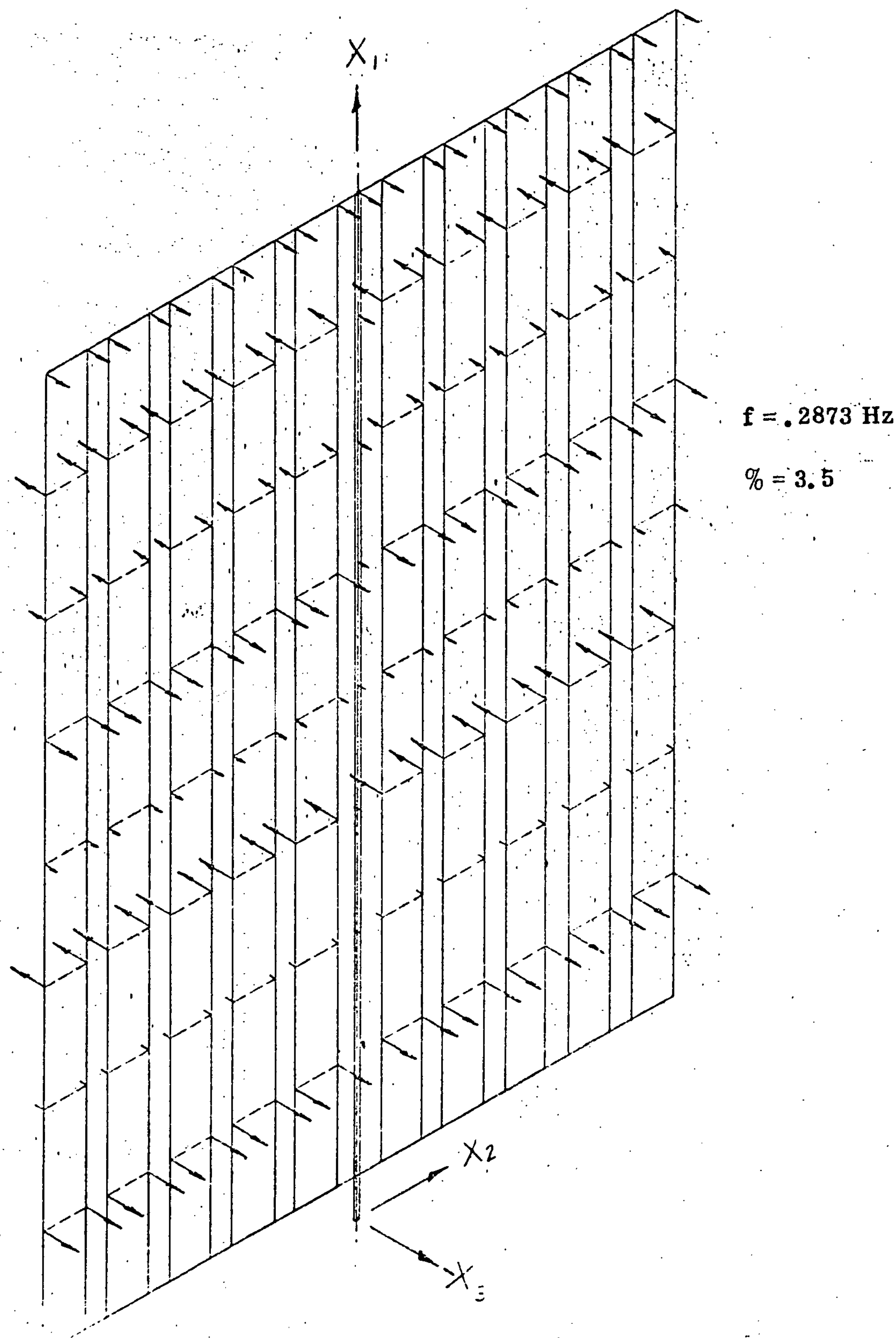

Figure 5-13 Mode 56, Rollup Array, Out of Plane, Symmetric

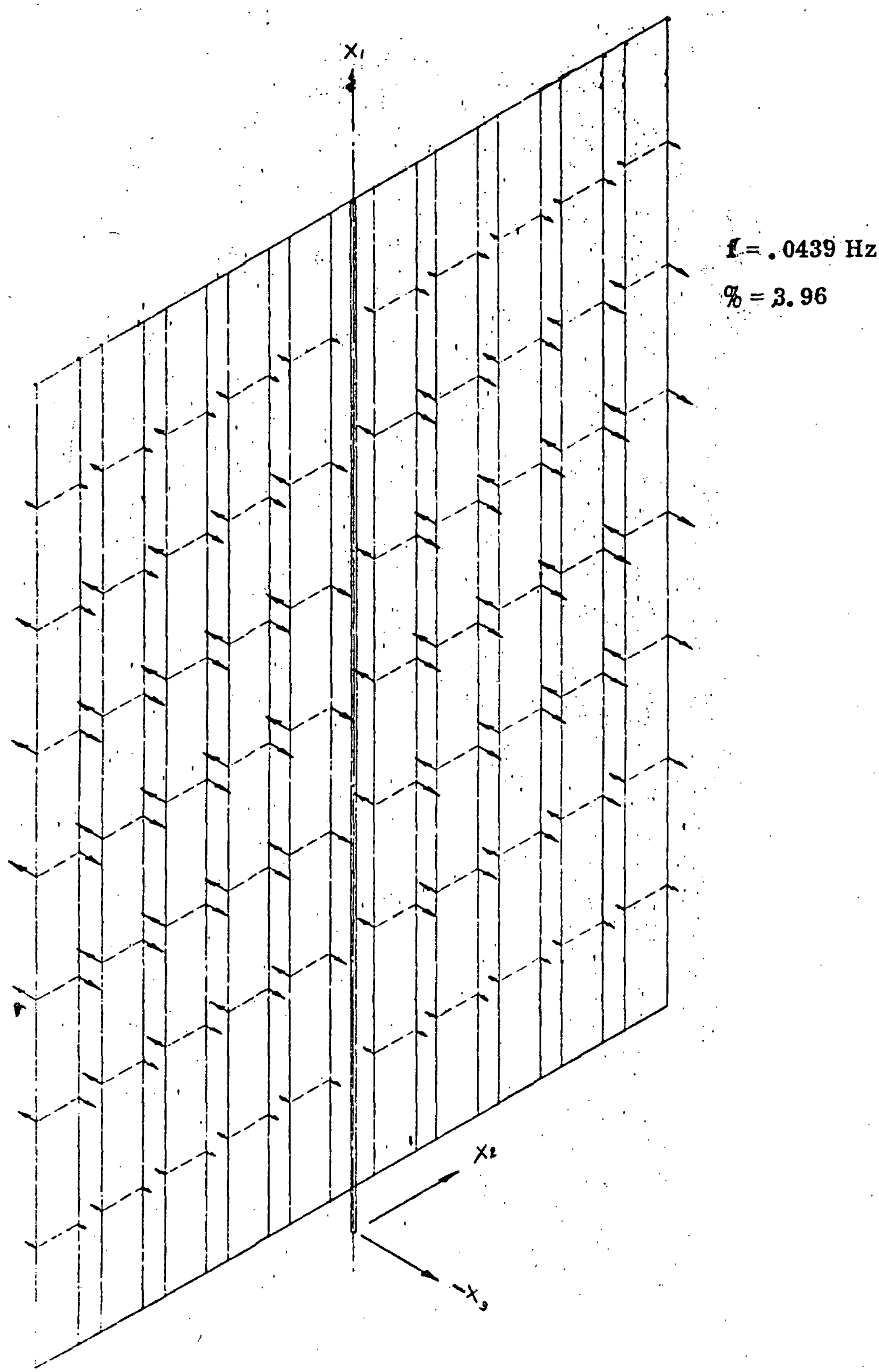

Figure 5-14 Mode 1, Rollup Array, Out of Plane, Antisymmetric

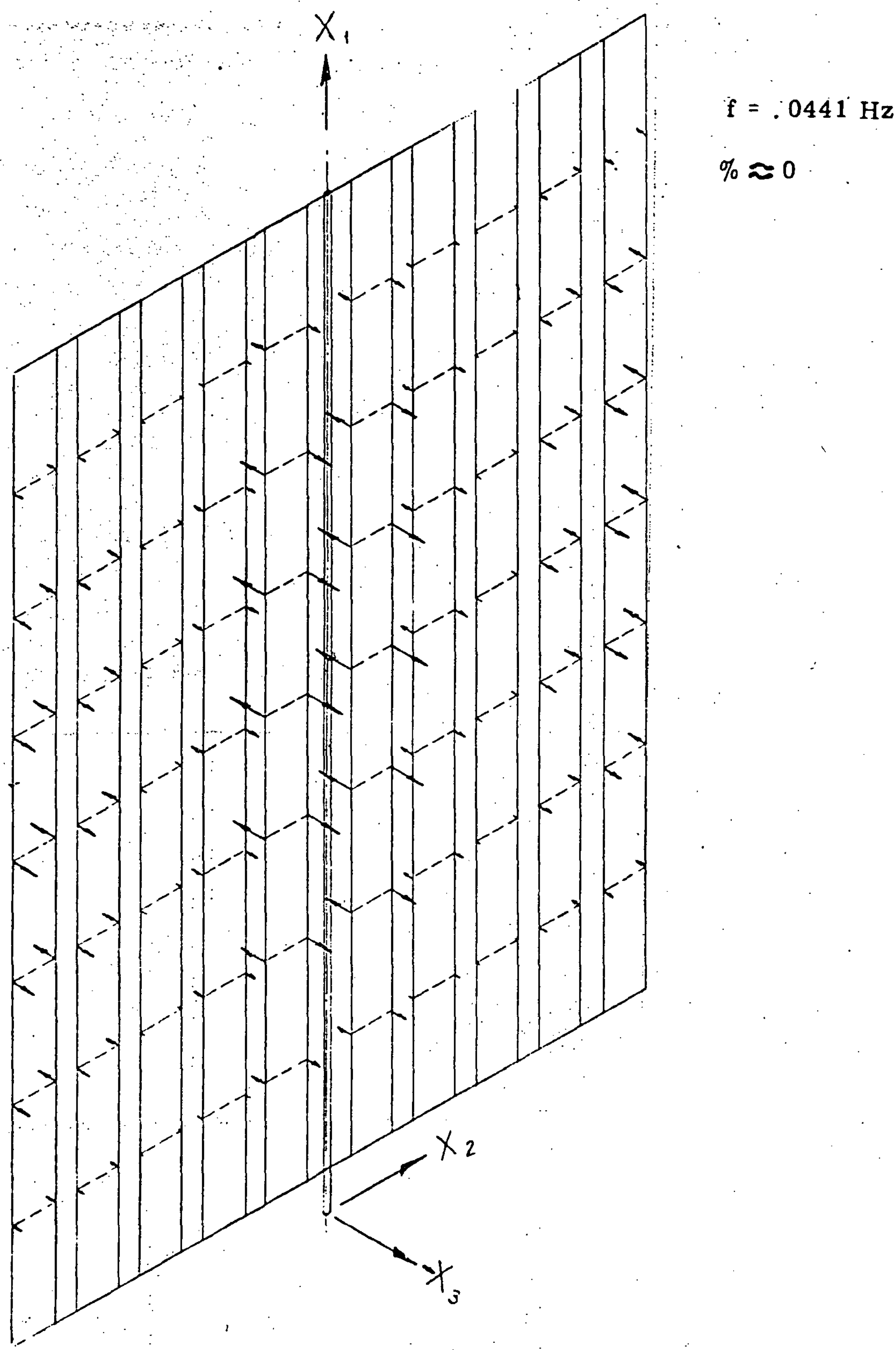

Figure 5-15 Mode 2, Rollup Array, Out of Plane, Antisymmetric

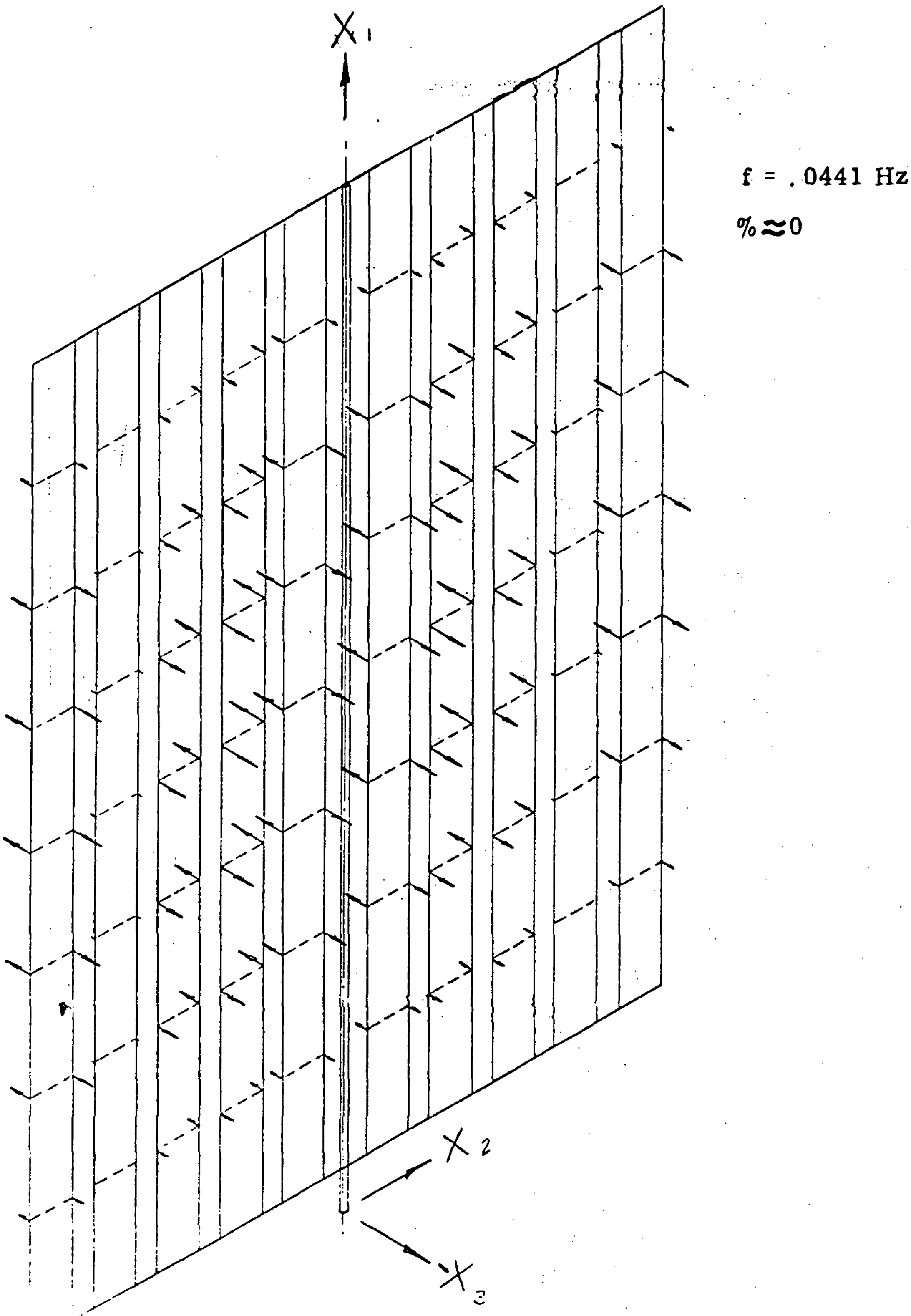

Figure 5-16 Mode 3, Rollup Array, Out of Plane, Antisymmetric

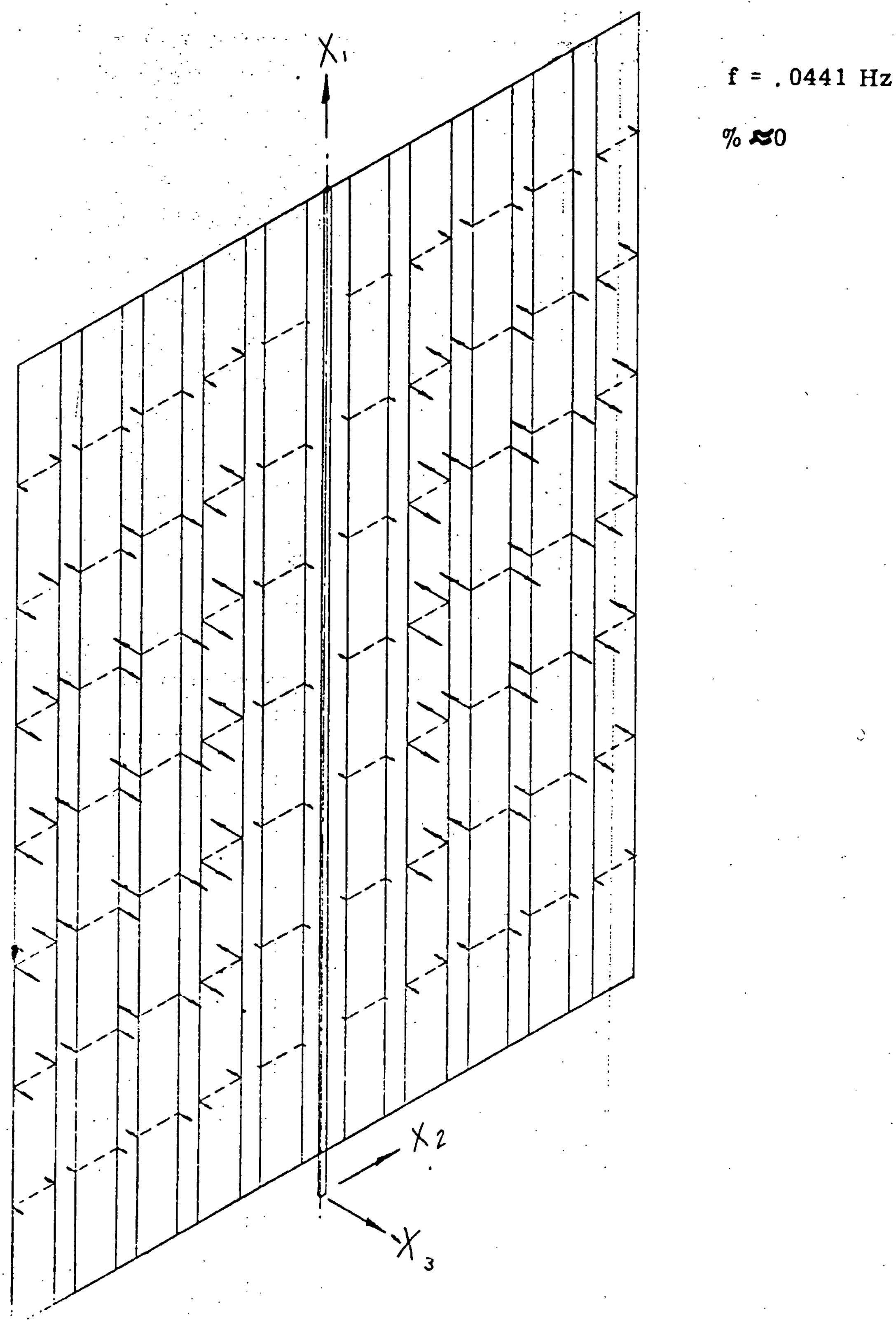

Figure 5-17 Mode 4, Rollup Array, Out of Plane, Antisymmetric

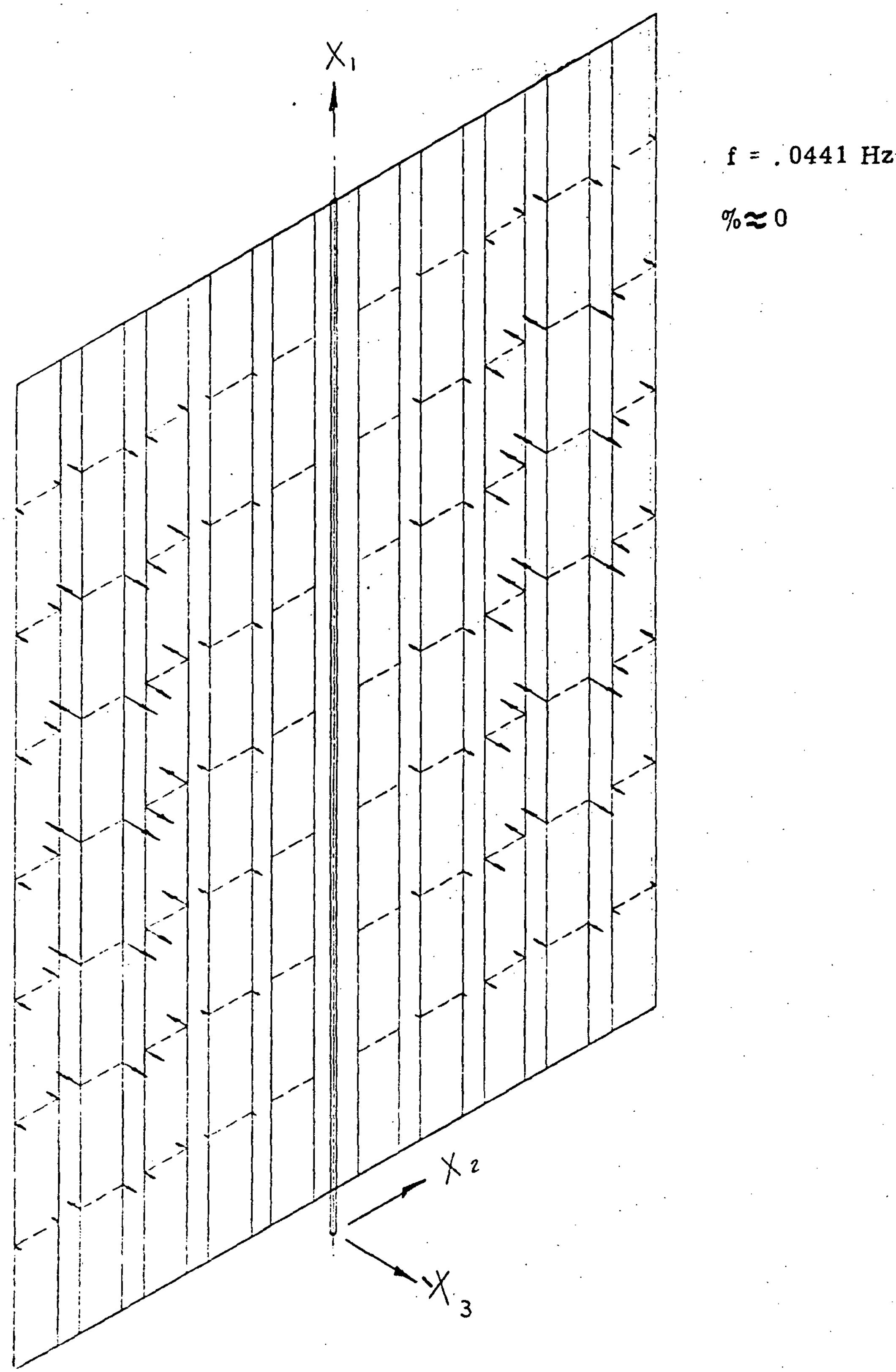

Figure 5-18. Mode 5, Rollup Array, Out of Plane, Antisymmetric

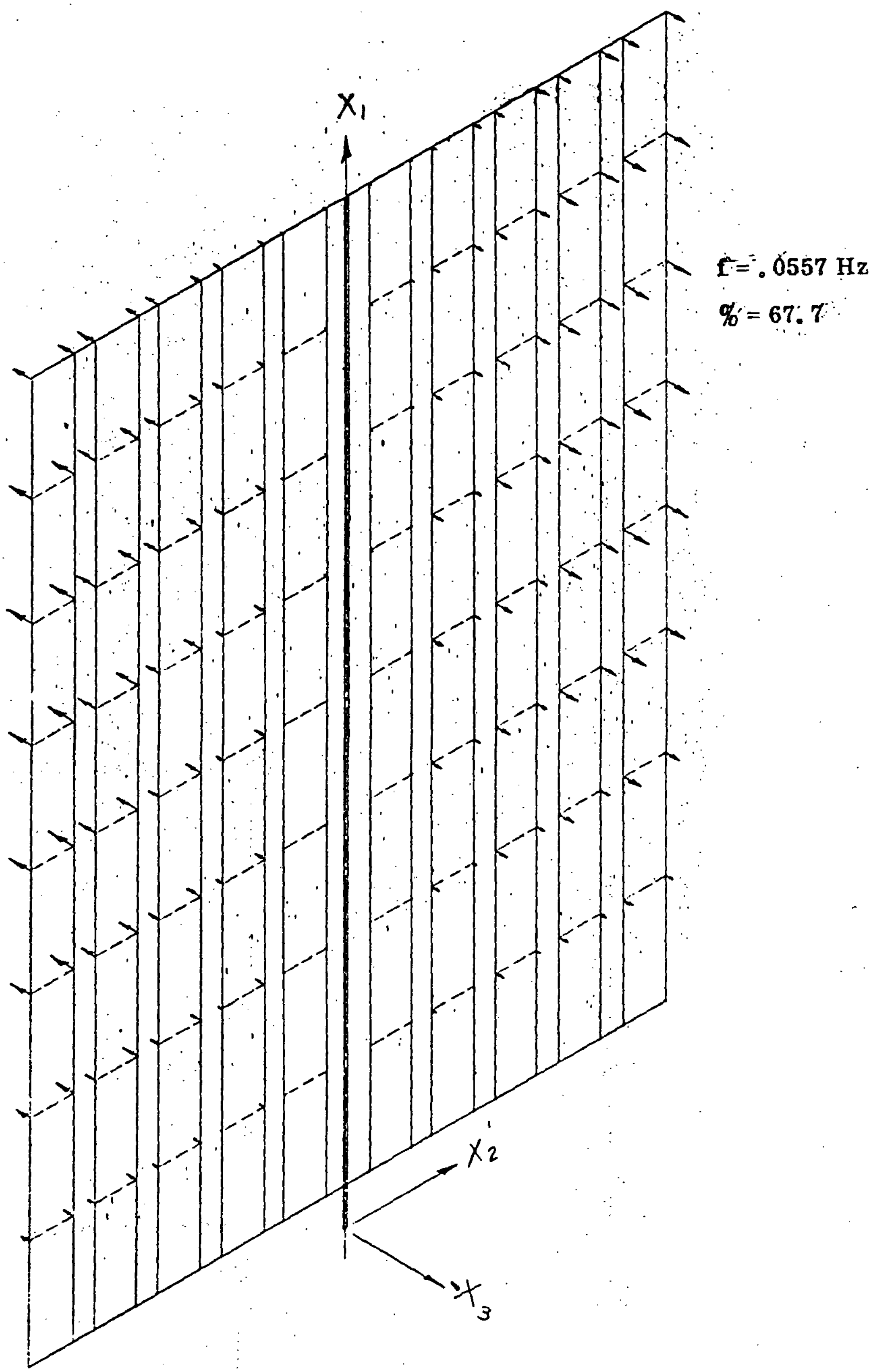

Figure 5-19 Mode 6, Rollup Array, Out of Plane, Antisymmetric

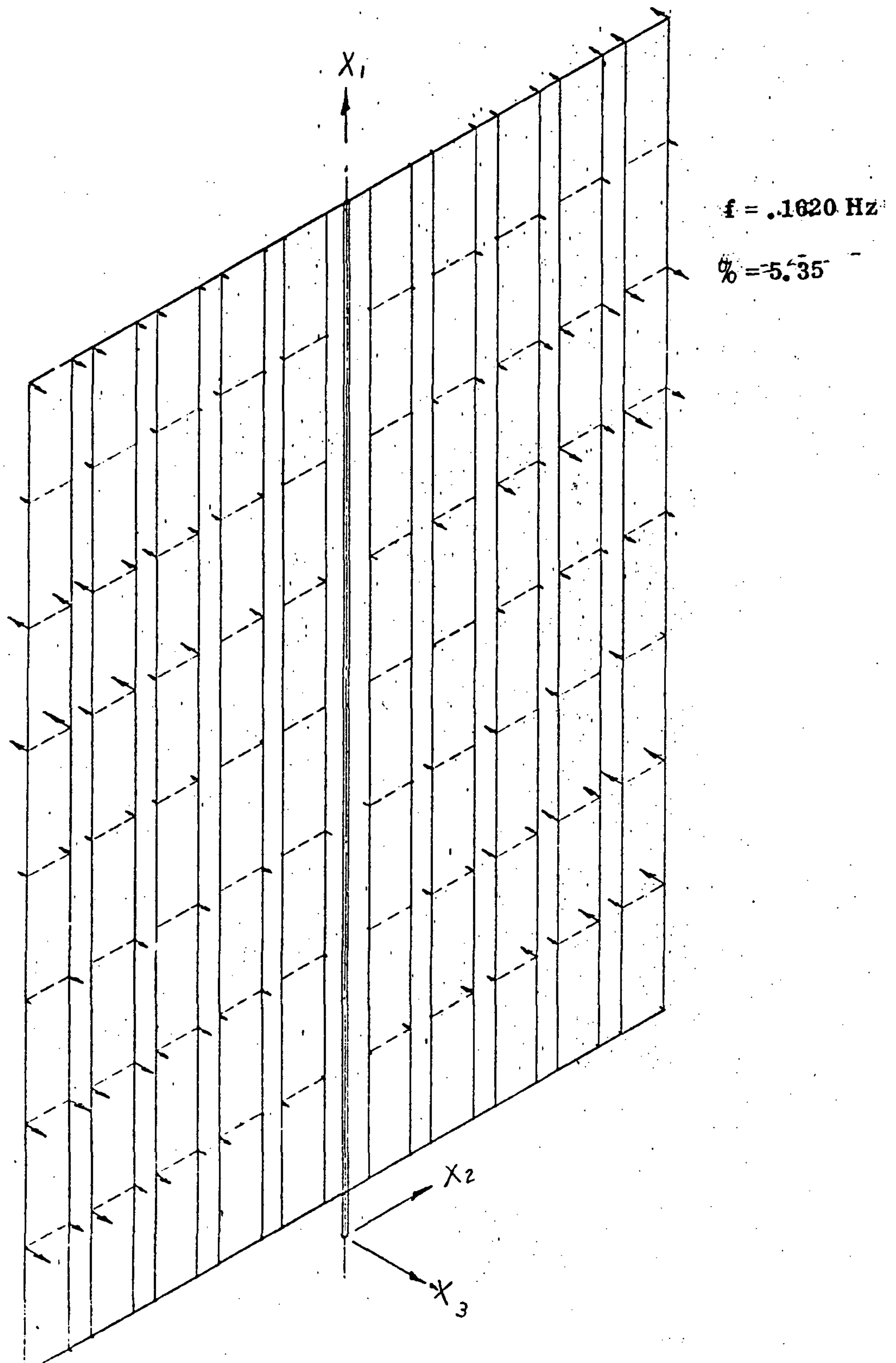

Figure 5-20 Mode 31, Rollup Array, Out of Plane, Antisymmetric

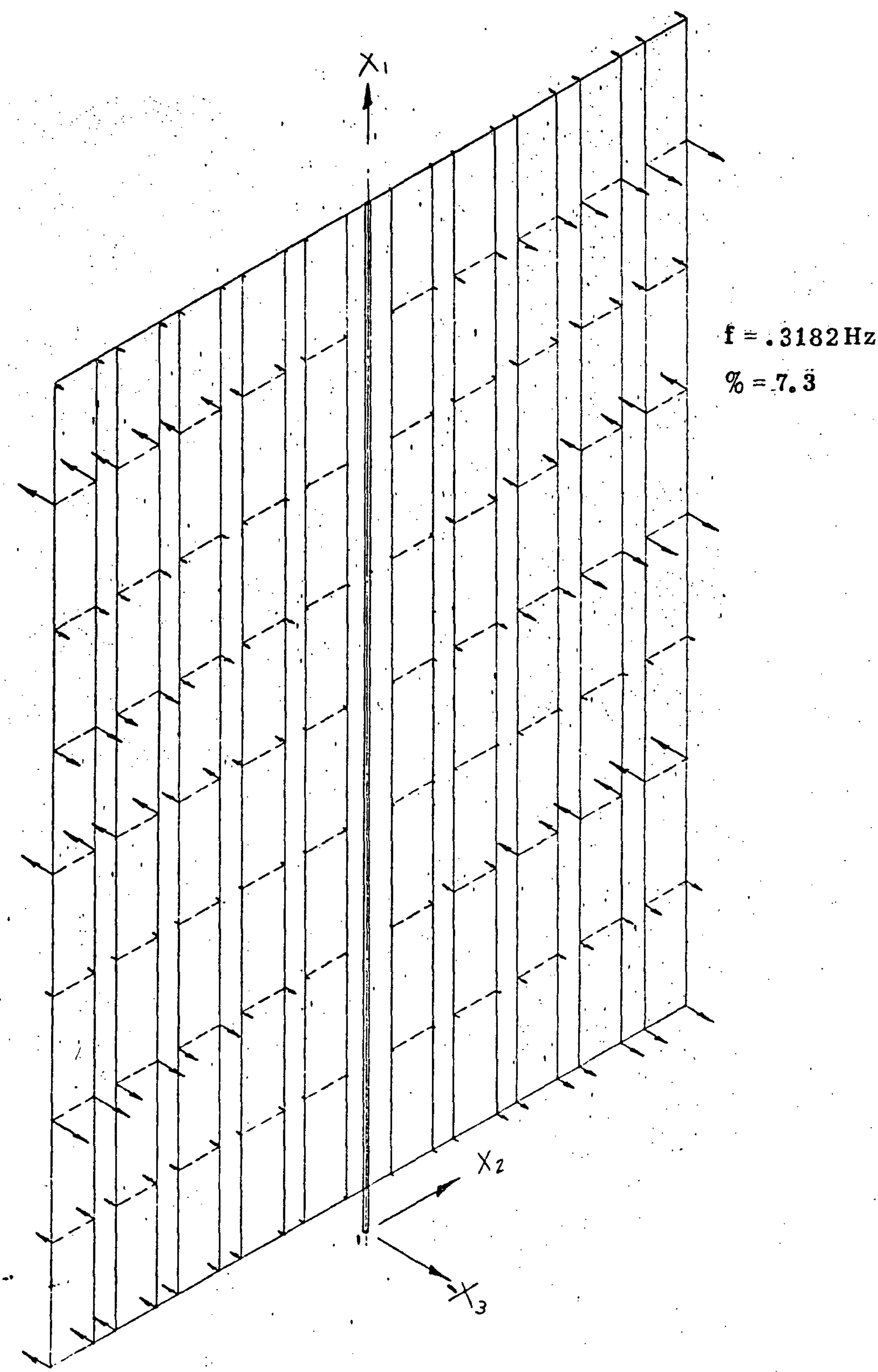

Figure 5-21 Mode 57, Rollup Array, Out of Plane, Antisymmetric

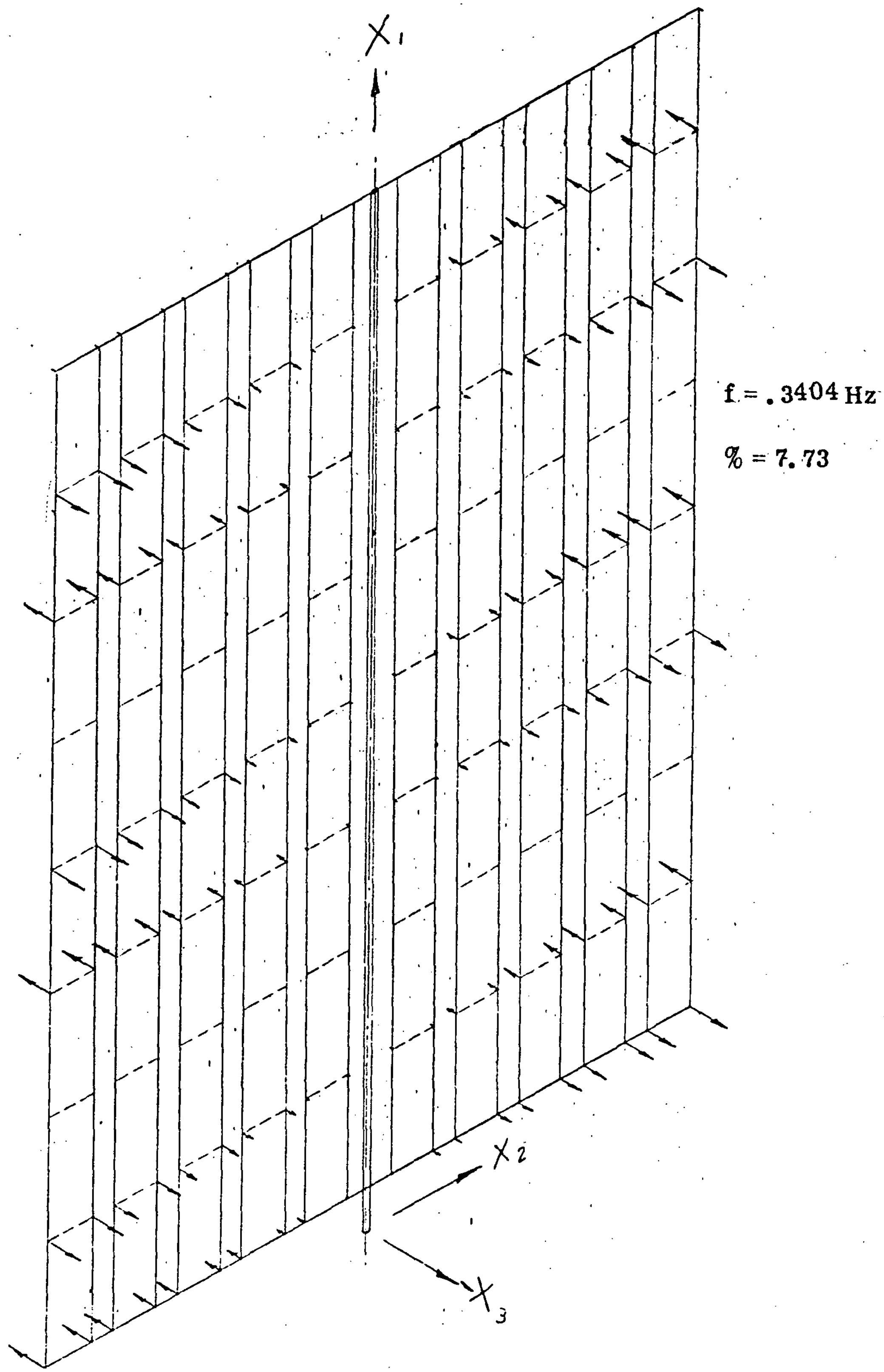

Figure 5-22. Mode 62, Rollup Array, Out of Plane, Antisymmetric

where

m_i - mass of discrete node i (lb.-sec.^{2}/in.)

$\emptyset_{in}$ - deflection of node i for mode n

R_n - generalized inertia of mode n (lb.-sec.^{2}/in.)

M - mass of dynamic model (lb.-sec.^{2}/in.)

r_i - distance along X_2 axis of mass i. (in.) (Ref. Fig. 5.1-3)

I_{x1} - moment of inertia of dynamic model about the X_1 axis (lb.-in.-sec.^{2})

The participation factors for the full wing section are shown on the mode shape plots along with the frequencies. The modes which were chosen to be important for subsequent interaction analyses were antisymmetric modes 6, 31, 57 and 62 and symmetric modes 6, 36, and 56.

From the rollup array in-plane modal analysis, eigenvalues and corresponding eigenvectors were computed up to 5 Hz. Frequencies within this range should be sufficient to determine the effects of the array flexibility on the spacecraft control system. Six symmetric and eight antisymmetric modes were obtained for these cases. The frequencies for these modes are listed in Table 5-4.

TABLE 5 - 4 FREQUENCIES OF IN-PLANE MODES FOR ROLLUP ARRAY

Mode	Frequency (Hz)	
	Symmetric	Antisymmetric
1	2.1199	.2911
2	2.2604	1.939
3	2.3825	2.177
4	2.4486	2.4139
5	2.4895	2.4757
6	2.5038	2.4999
7	------	2.7056
8	------	4.1198

The modal participation factors for these cases are based on axial load due to a base translational acceleration for the symmetric modes and shear load due to a base translational acceleration for the antisymmetric case. The mode shapes for the full wing section and percent modal participations are shown in Figures 5-23 to 5-29. On these figures, the solid lines are the deflected shapes while the dashed lines are the the undeflected outline of the wing section. The modes which were chosen to be important for interaction analyses are symmetric mode 2 and antisymmetric modes 1, 2, 7 and 8. The complete list of frequencies and modal participation factors for the modes selected for use in the interaction program for the rollup array are listed in Table 5-5.

TABLE 5 —5 FREQUENCIES AND MODAL PARTICIPATION FACTORS OF ROLLUP ARRAY MODES USED IN INTERACTION ANALYSIS

Out of Plane					
Symmetric			Antisymmetric		
Mode	Frequency (Hz)	Percent Participation	Mode	Frequency (Hz)	Percent Participation
6	.0734	50.4	6	.0557	67.7
36	.2026	12.5	31	.1620	5.35
56	.2873	3.5	57	.3182	7.3
			62	.3404	7.73
In-Plane					
Symmetric			Antisymmetric		
Mode	Frequency (Hz)	Percent Participation	Mode	Frequency (Hz)	Percent Participation
2	2.2604	57	1	.2911	55
			2	1.939	3.1
			7	2.7056	6.5
			8	4.1198	2.7

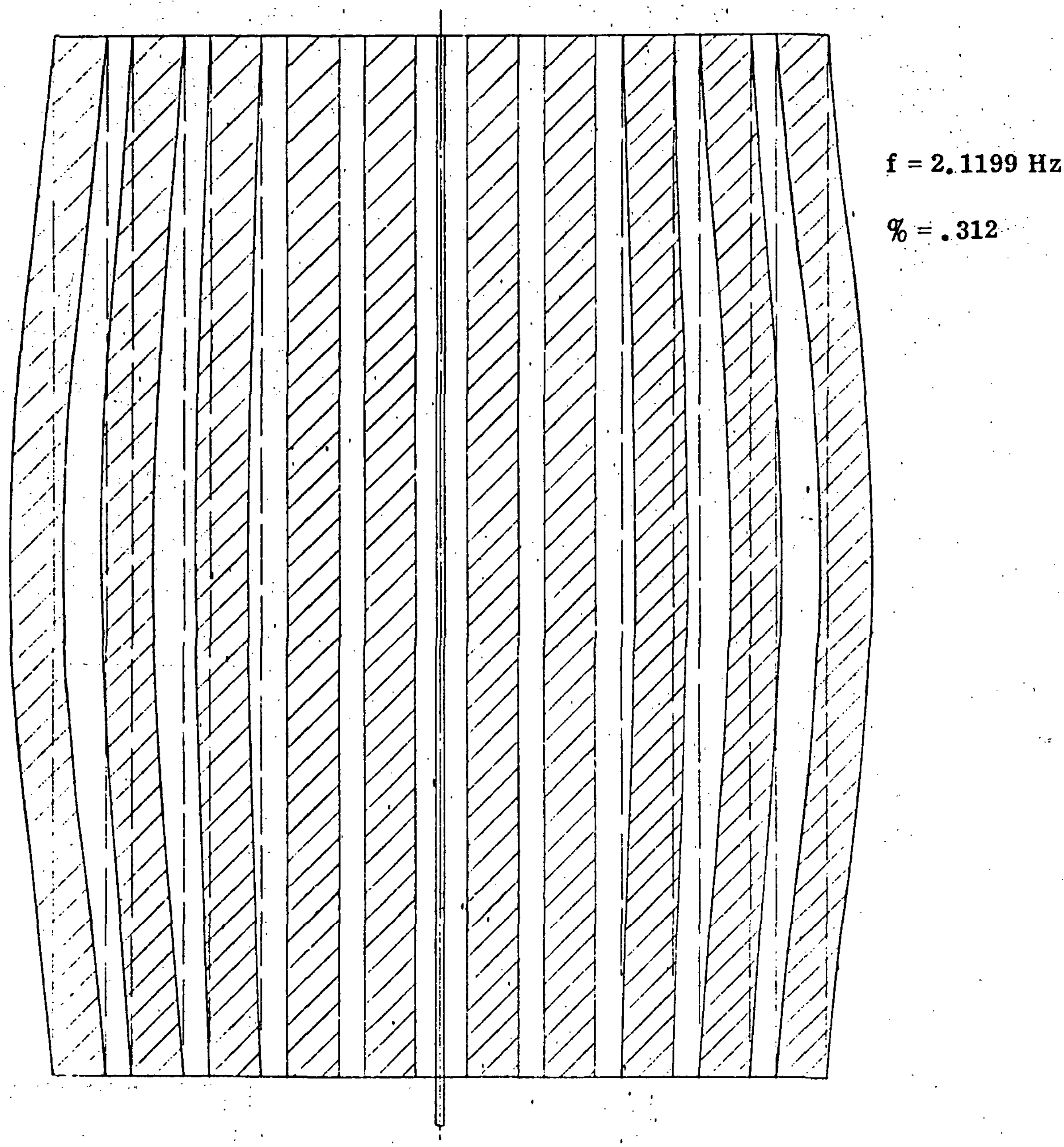

Figure 5-23. Mode 1, Rollup Array, Inplane, Symmetric

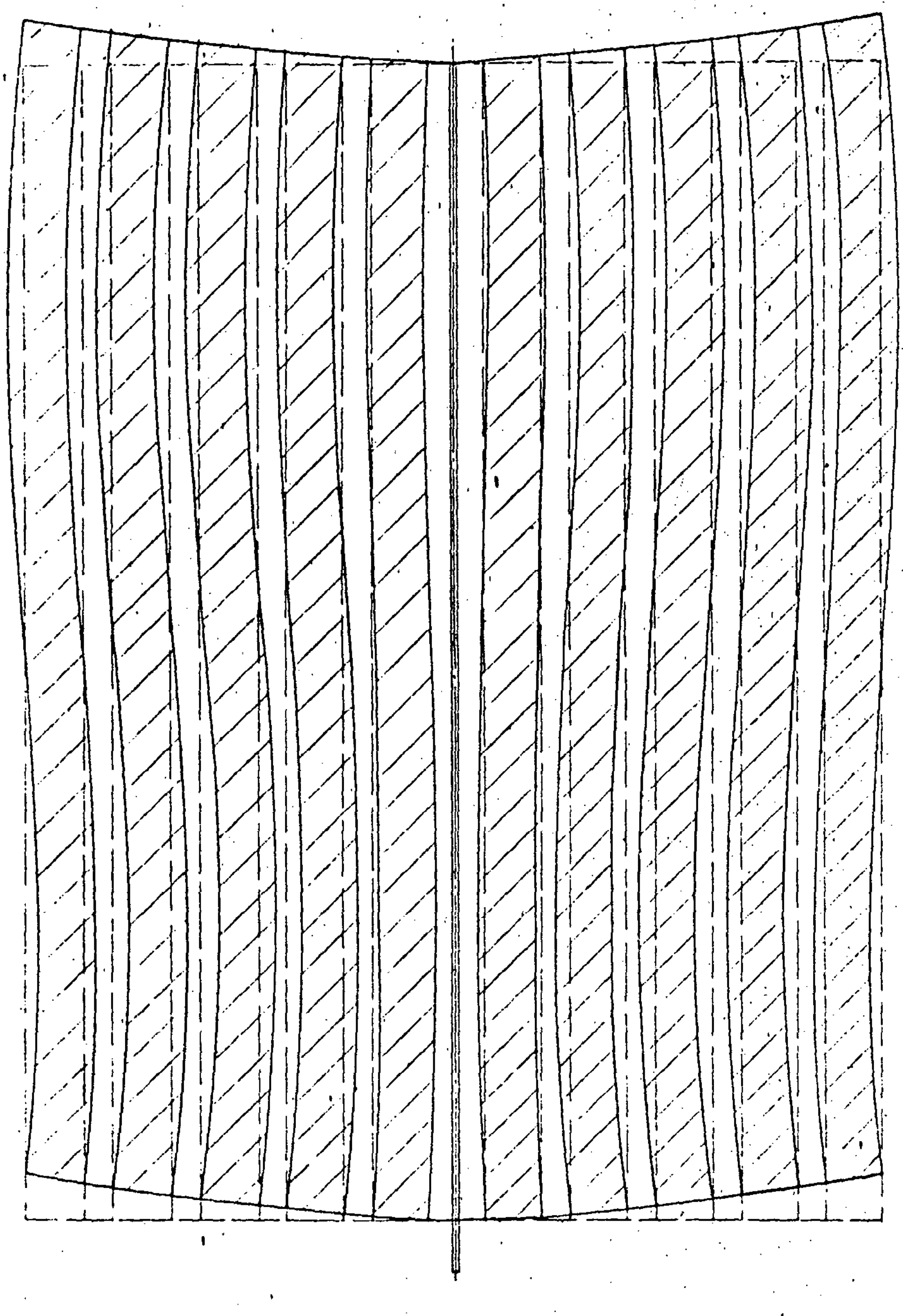

Figure 5-24. Mode 2, Rollup Array, Inplane, Symmetric

f = 2.3825 Hz

% = .358

Figure 5-25. Mode 3, Rollup Array, Inplane, Symmetric

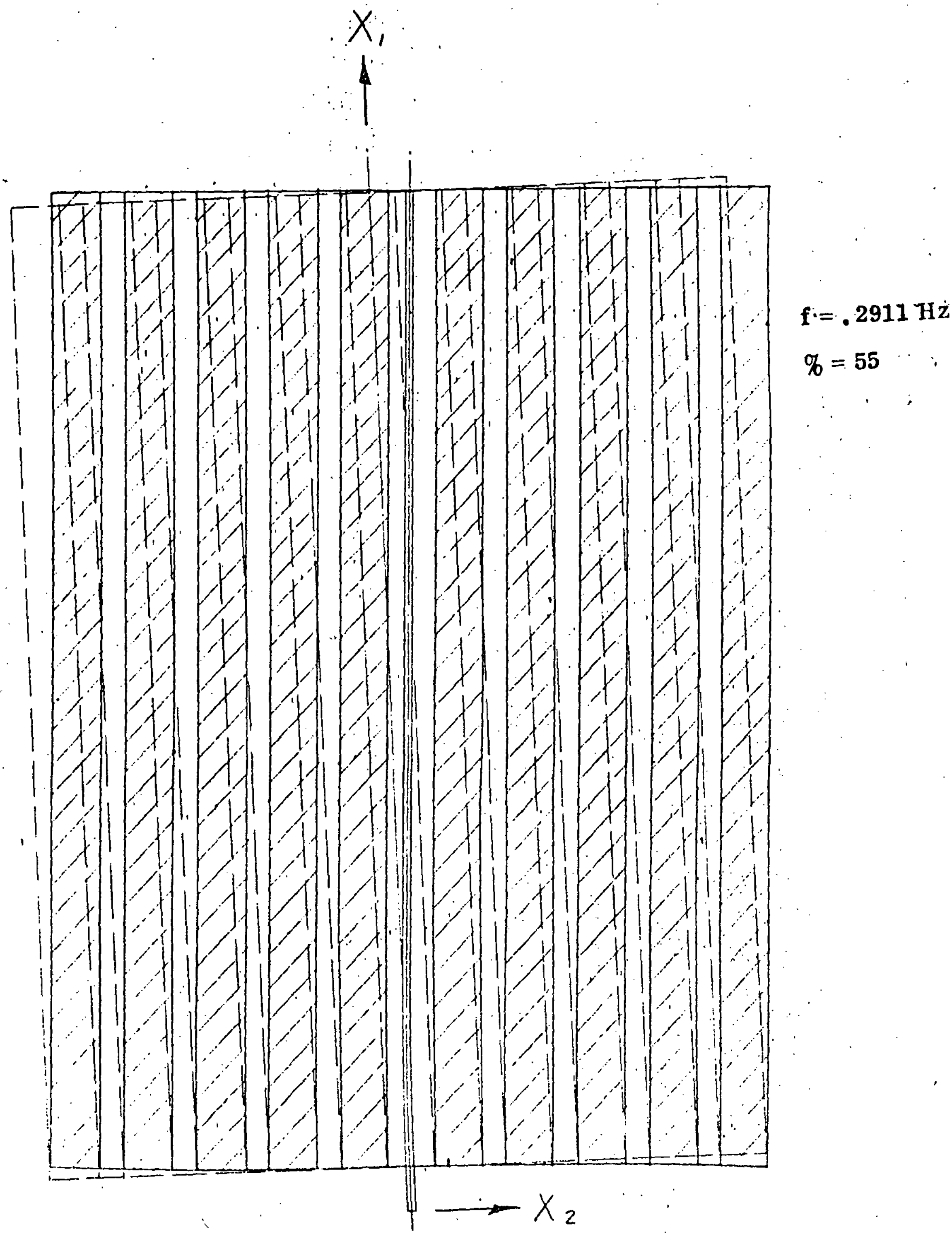

Figure 5-26. Mode 1, Rollup Array, Inplane, Antisymmetric

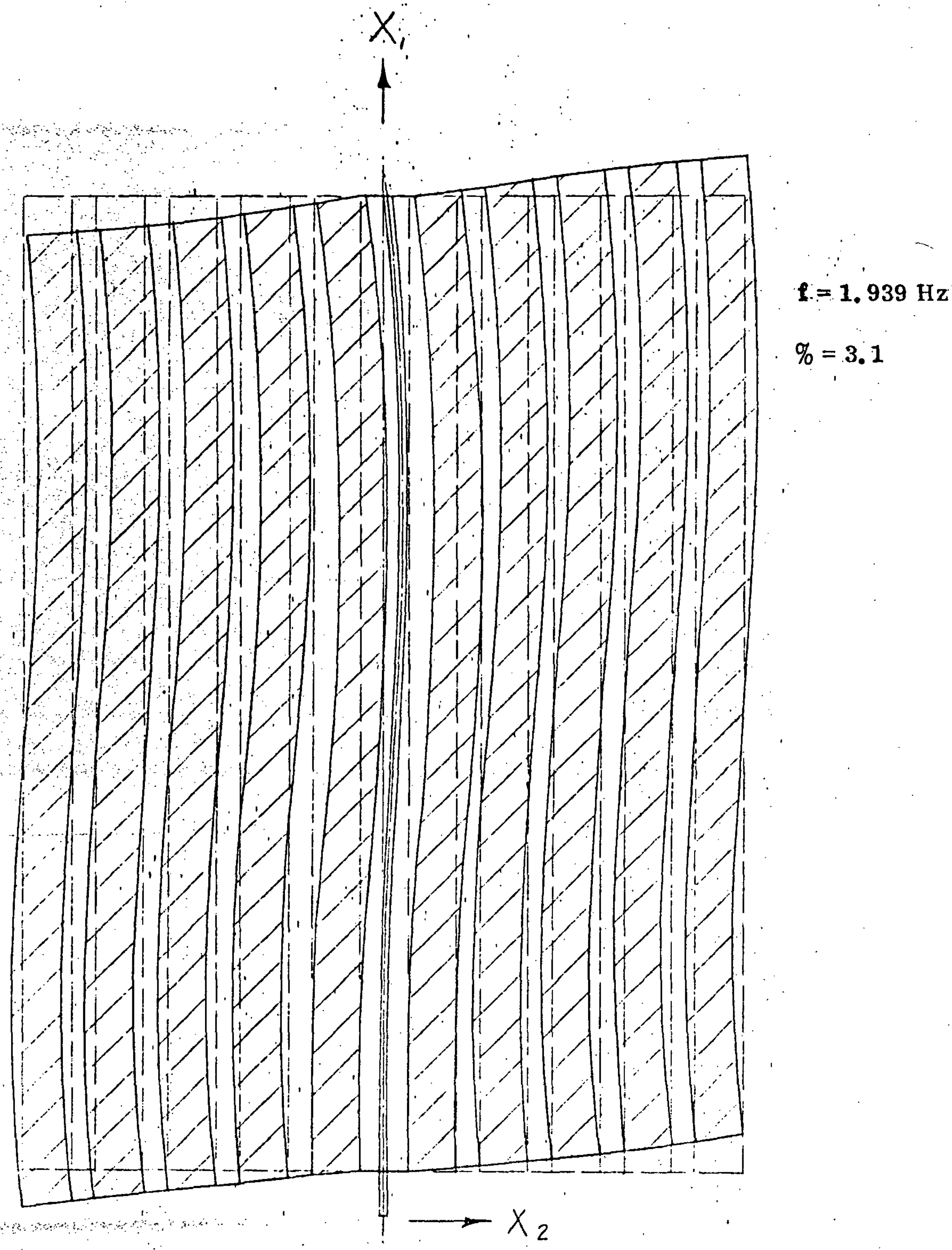

Figure 5-27 Mode 2, Rollup Array, Inplane, Antisymmetric

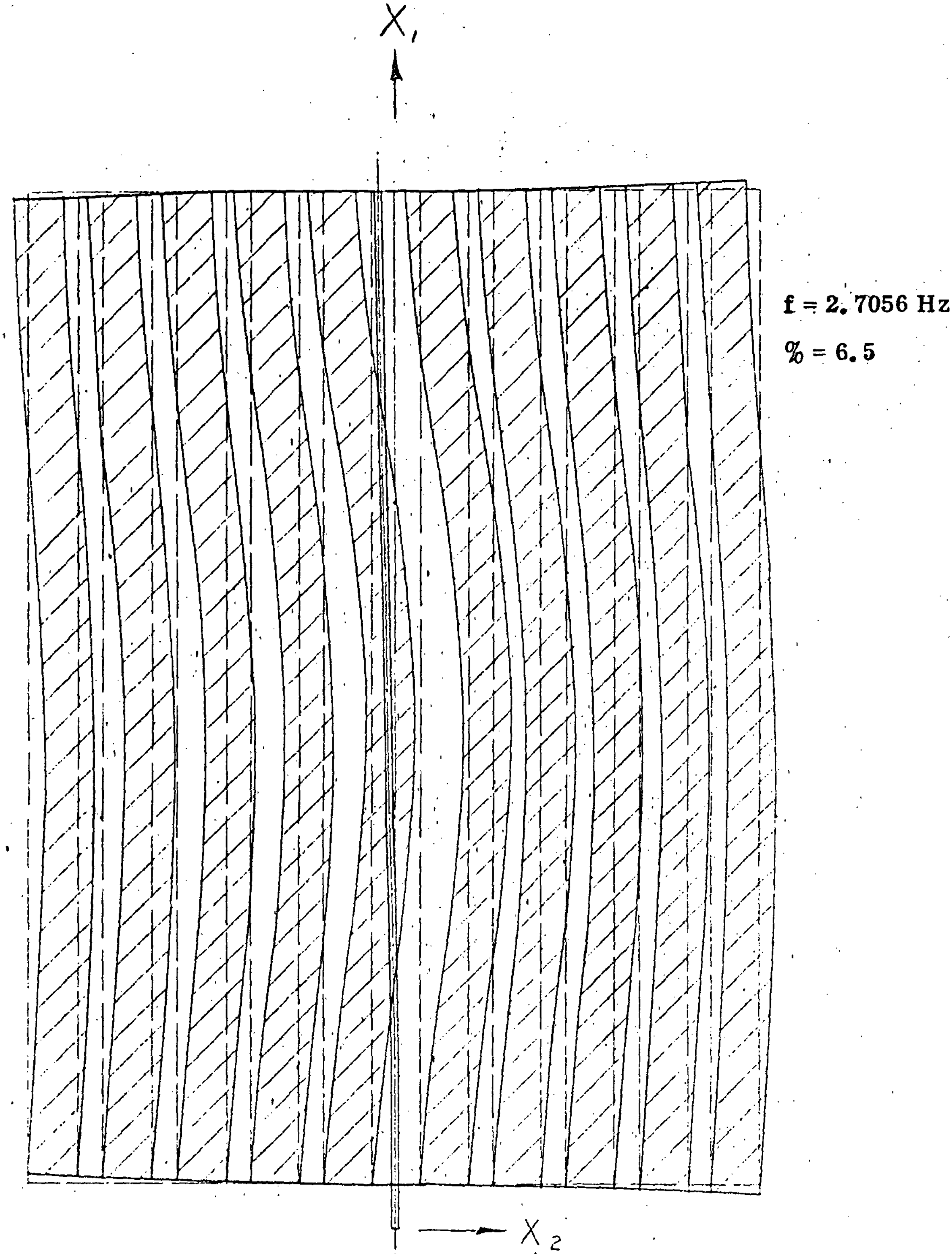

Figure 5-28. Mode 7, Rollup Array, Inplane, Antisymmetric

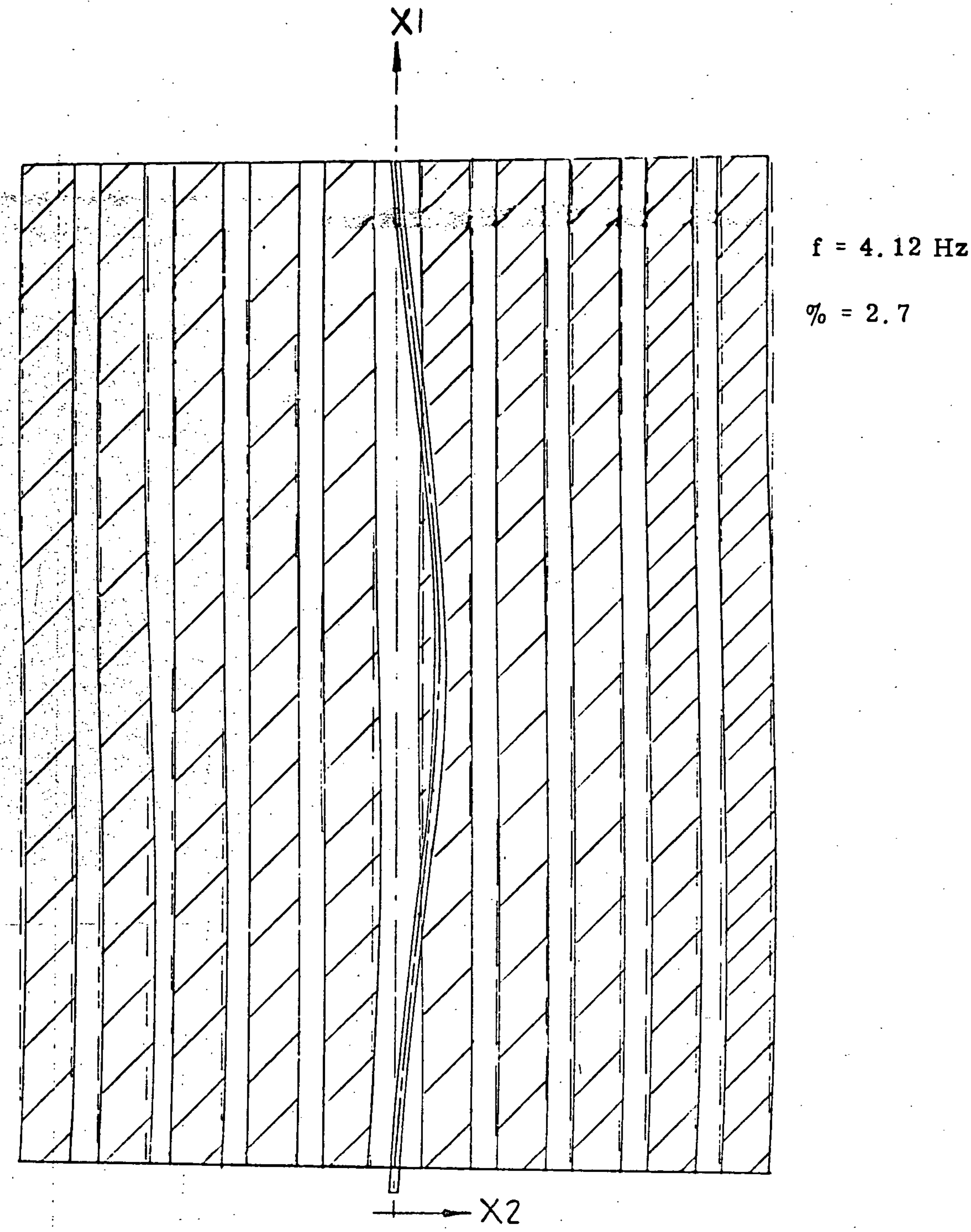

Figure 5-29. Mode 8, Rollup Array, Inplane, Antisymmetric

5.1.2 FOLDOUT PANEL ARRAY

The foldout panel array is a multipanel array consisting of a beryllium framework with a tape substrate. The array is based on a Boeing concept (Reference 5.6) for a lightweight rigid array designed for an unmanned Mars mission. The overall dimensions of one wing section of the array as modified for the space station are shown in Figure 5-30. The wing section consists of thirty panels which were required in varying lengths so as to meet the internal shroud geometry constraints for stowage during the flight launch phase. Panels 1 through 6 are hinged together and are the main load carrying members of the array. Attached to each main panel are four subpanels (such as 1A, 1B, 1C and 1D) hinged at the long side only. The entire wing section is attached to the spacecraft tunnel through members attached to main panel 1.

Each panel consists of a beryllium rectangular x-braced frame with lateral and longitudinal stiffeners as shown in Figure 5-31. Corresponding section properties are given in Figure 5-32. The overall dimensions shown are for panels 1 through 1D. The stiffeners and outer frame members are split in a horizontal plane to hold a tape membrane substrate to which the solar cells are bonded. Details of this frame construction are discussed in Reference 5.6.

Ten mill cells with six mill coverglas were used in determining the solar stack weight. The remaining weight of the array was formulated by ratioing the weight breakdown listed in Reference 5.6 by the respective areas of the 100 and 50 KW arrays. The weight breakdown and total weight of the foldout panel array used for the structural analysis is tabulated in Table 5-6.

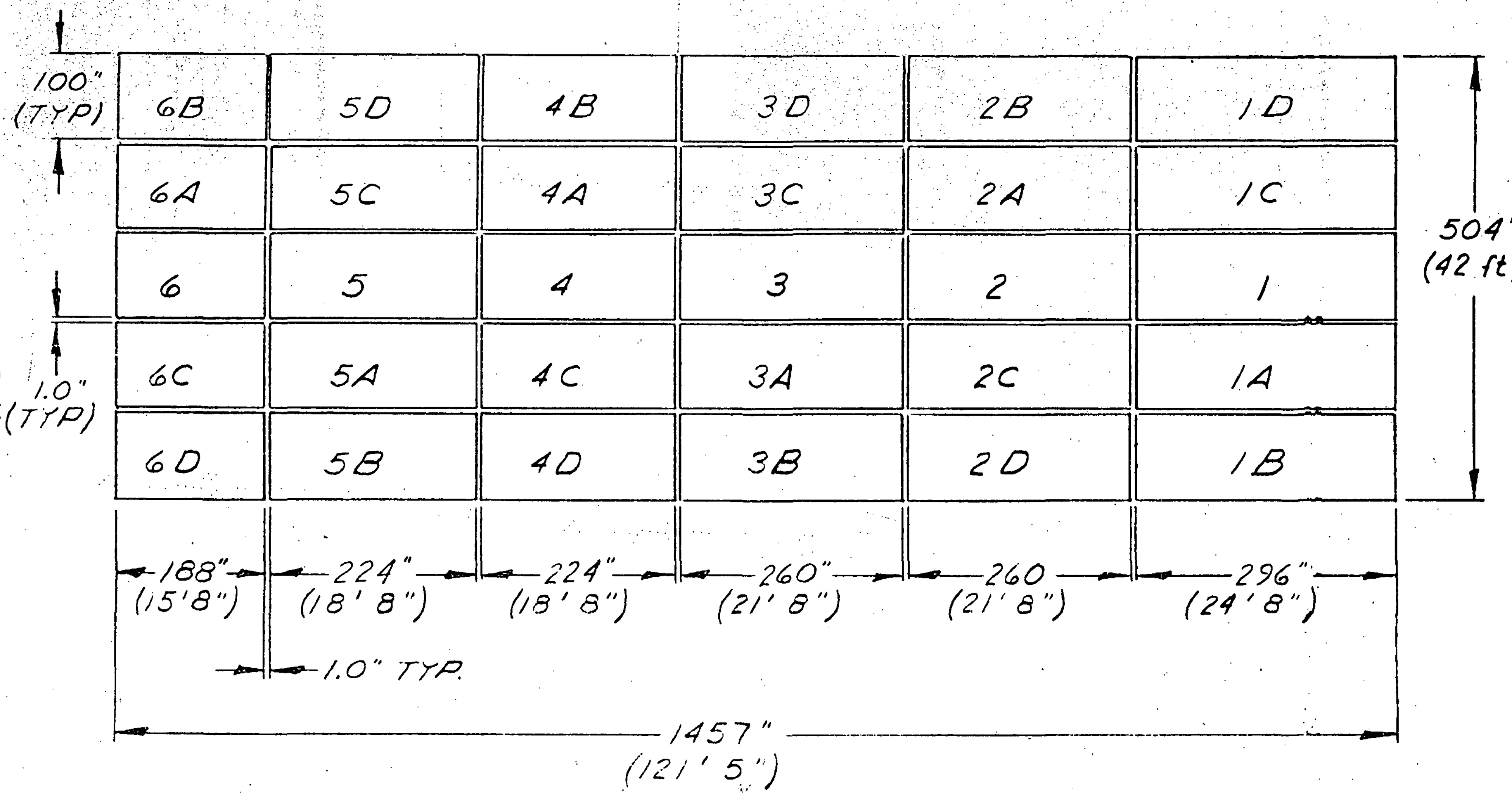

Figure 5-30. Dimensions of Wing Section of Foldout Panel Array

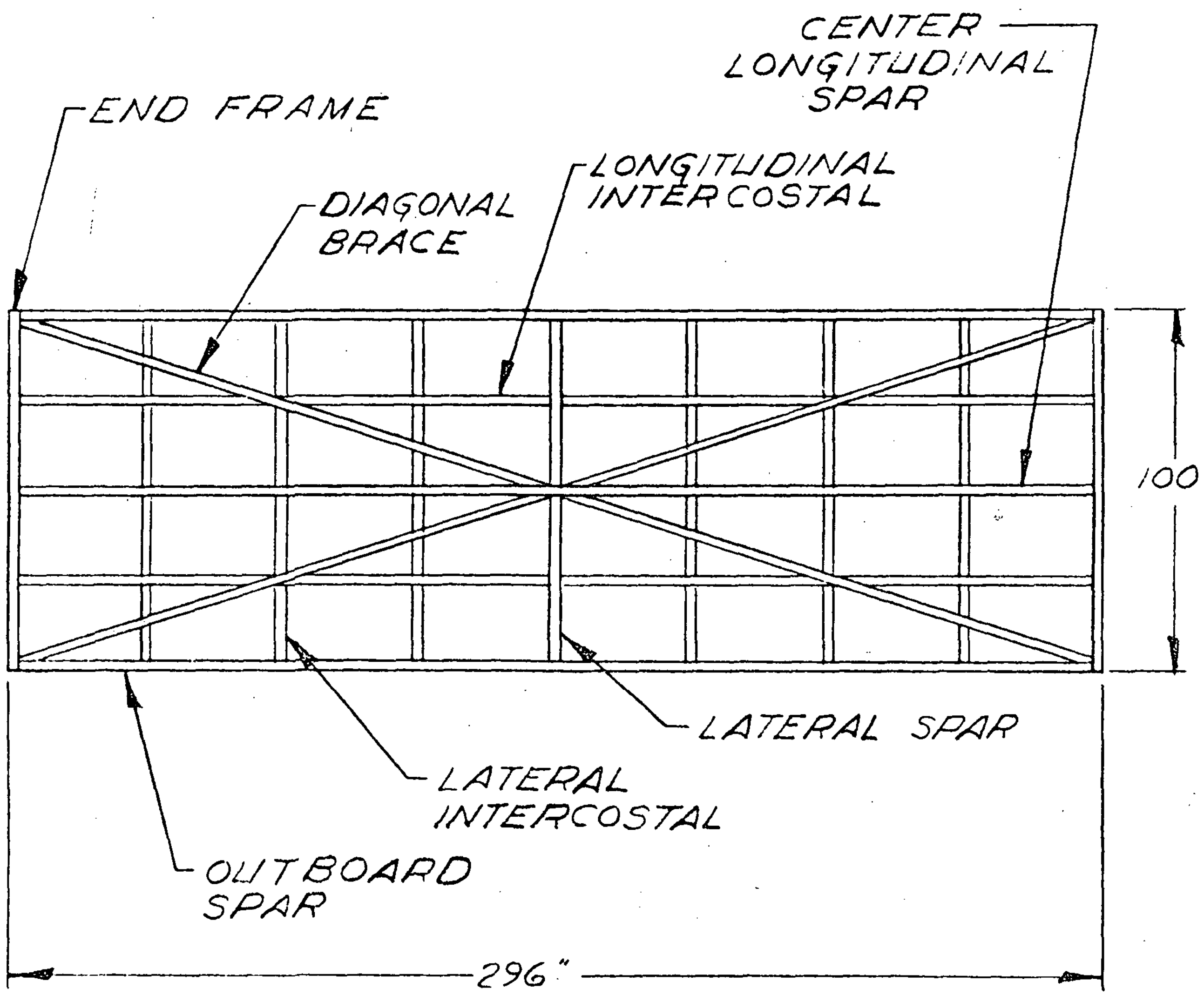

Figure 5-31. Foldout Panel Construction

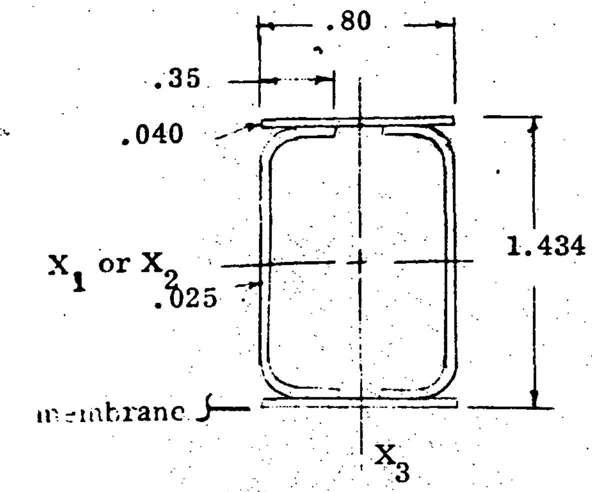

(a) Intercostals

$A = .1642 \text{ in}^2$

$I_{x1} = I_{x2} = .0558 \text{ in}^4$

$I_{x3} = .054 \text{ in}^4$

$J = .0336 \text{ in}^4$

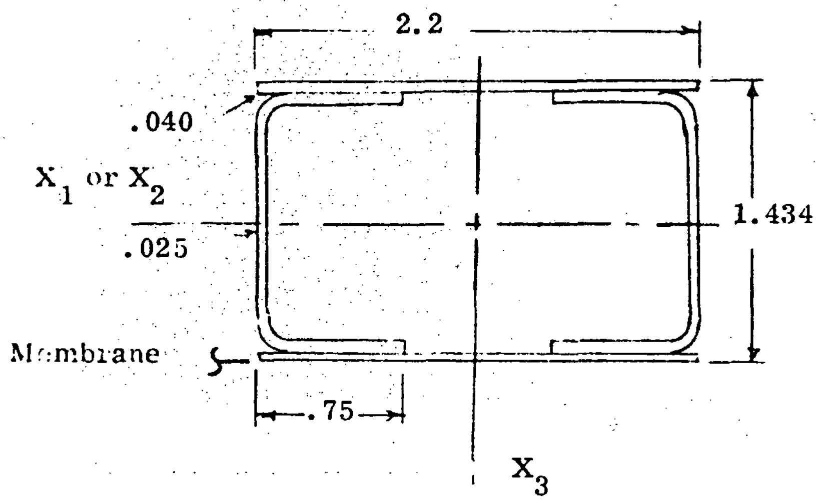

(b) Diagonals

$A = .3162 \text{ in}^2$

$I_{x1} = I_{x2} = .1278 \text{ in}^4$

$I_{x3} = .1911 \text{ in}^4$

$J = .1924 \text{ in}^4$

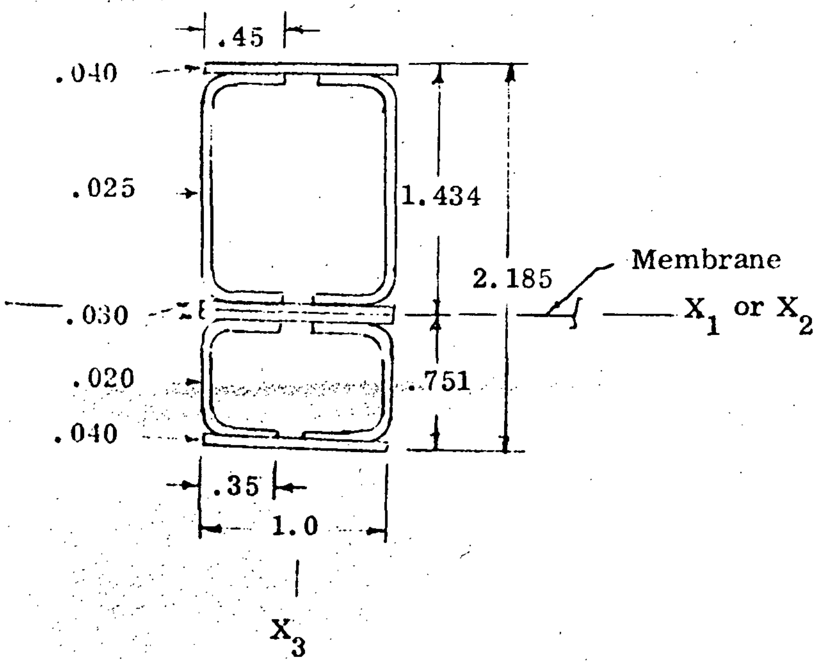

(c) Spars and End Frames

$A = .3043 \text{ in}^2$

$I_{x1} = I_{x2} = .175 \text{ in}^2$

$I_{x3} = .0407 \text{ in}^4$

$J = .0986 \text{ in}^4$

Material: Beryllium

$E = 42.5 \times 10^6 \text{ lbs/in}^2$

$G = 20 \times 10^6 \text{ lbs/in}^2$

Figure 5-32. Member Properties

TABLE 5-6 WEIGHT BREAKDOWN FOR FOLDOUT PANEL ARRAY

Cell Stack, Substrate and Thermal Coating		Weight (lbs)	
Cover Glass		674	
Cover Glass Adhesive		38	
Cells		938	
Connectors		116	
Solder		8	
Substrate Adhesive		130	
Substrate		156	
Thermal Coating		190	
	Total		2250
Mechanisms			
Main Hinges and Latches		60	
Auxiliary Hinges, Latches and Dampers		72	
Quadrants and Sequencers		56	
Strut Assemblies		30	
Solar Curtains		28	
Boost Tie-down System		144	
Cable, Drive and Miscellaneous		84	
	Total		474
Electrical Connectors			
Busses and Diodes		194	
Pigtails and Connectors		26	
Squib Wiring		8	
Terminals and Crossover Busses		52	
	Total		280
Structure			
Shear Clips		12	
Gusset Plates		34	
Diagonal Tension Ties		156	
Shear Ties		206	
Internal Fittings		38	
Main Members		2642	
	Total		3088
	TOTAL		6092

5.1.2.1 Array Vibration Model

To derive a dynamic model of the total array and simulate all of the structural members for each foldout panel results in an unusually large problem and would be unnecessary for an adequate analytical simulation. Therefore, each panel was idealized into a simpler model. Also, since the array is symmetric, it was possible to model only one-half the array and adjust the boundary conditions of the center longitudinal spar nodes (Figure 5-31) of the main panel members in the same manner as was done for the rollup array. The dynamic model derived is shown in Figure 5-33. The construction of one panel, such as the panel bounded by nodes 1, 3, 15 and 13, can be considered as an X-braced rectangular frame with a lateral and longitudinal spar. To account for the stiffness of the remaining lateral and longitudinal intercostals of the frame (Figure 5-31), the stiffnesses of these members were distributed and added to the stiffnesses of the end frames and lateral and longitudinal intercostals. Adjacent panels of the structure are hinged and the two adjacent beams on which the hinges are located were considered as a single beam. These beams are shown as the heavy lines on Figure 5-33. The wing section is attached by struts to the space station tunnel at nodes 97 and 98 and in determining the frequencies of the model, the array was considered as rigidly constrained at nodes 97 and 98.

Mass loading for the idealized panel consists of a center mass point and a mass point at each corner. One quarter of the panel weight was allocated to the center point and the balance was divided equally between the four corners. The weight associated with the nodes of Figure 5-33 are listed in Table 5-7.

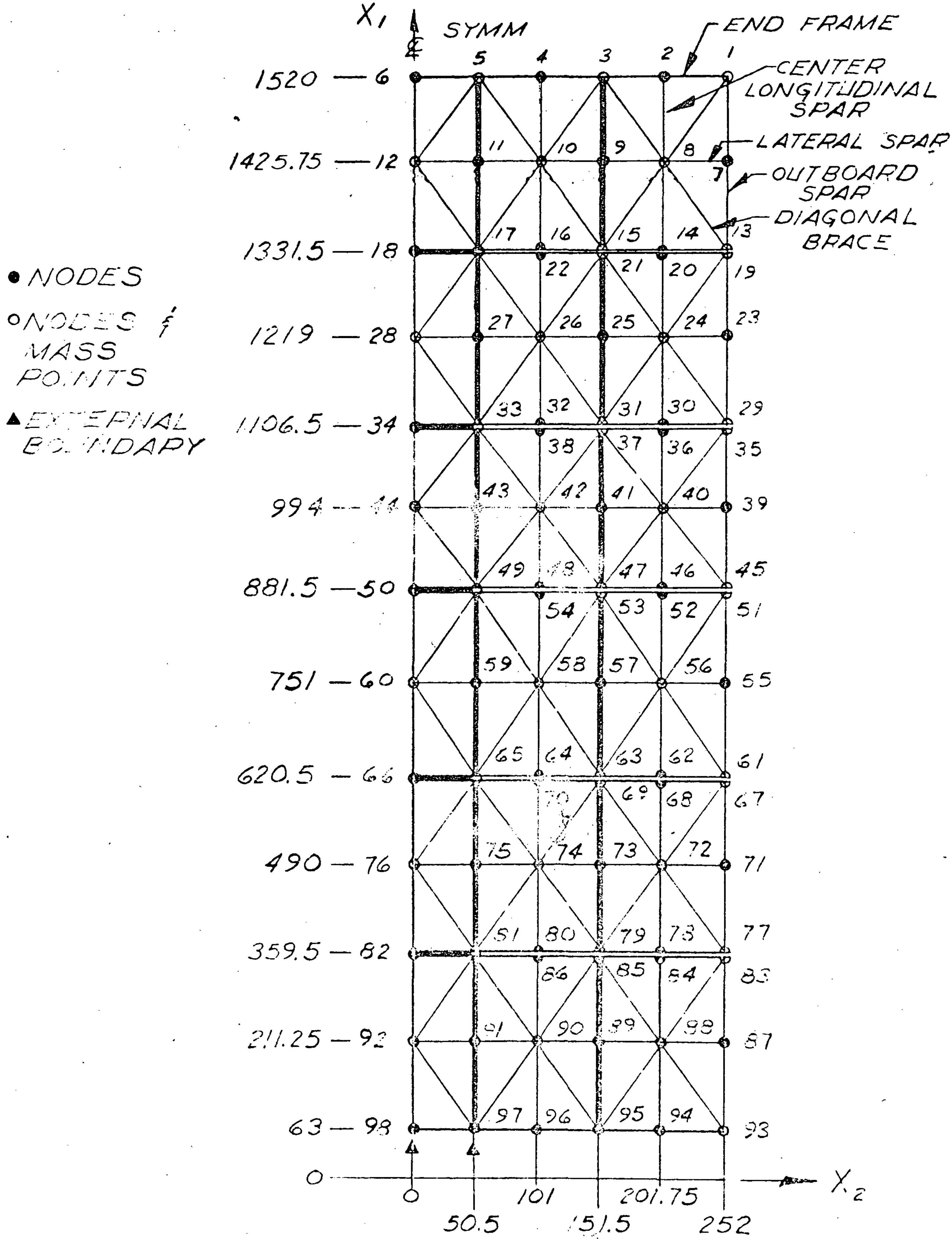

Figure 5-33. Idealized Dynamic Model for Foldout Panel Array

TABLE 5-7 NODAL WEIGHTS, FOLDOUT PANEL ARRAY MODEL

Nodes	Weight (lbs)
1,13	15.4
3,5,15	30.8
8,10	20.52
12	10.26
17	66.42
19,29,35,45	17.81
21,31,37,47	35.62
24,26,40,42	23.75
28,44	11.87
33	71.24
49	76.12
51,61,67,77	20.25
53,63,69,79	40.5
56,58,72,74	27.0
60,76	13.5
65	81.0
81	85.88
83,93	22.69
85,95,97	45.38
88,90	30.25
92	15.13

5.1.2.2 Foldout Panel Array Modes

Foldout panel array frequencies and corresponding modal deflections were computed up to 25 Hz. For the out of plane motions, 48 symmetric and 42 antisymmetric vibration modes were obtained. For the in-plane motions, one symmetric and five antisymmetric modes were obtained. The antisymmetric, out of plane modes represent the torsional deflections of the array while the symmetric modes represent out of plane bending deflections. For the in-plane modes, the symmetric modes represent axial deflections and the antisymmetric modes represent in-plane bending deflections. Resulting modal frequencies for the various cases are listed in Tables 5-8, 5-9, and 5-10.

Graphical presentations of selected modes and corresponding modal participation factors are given in Figures 5-34 to Figure 5-45. The participation factors are based on the same quantities as described for the rollup array modes. The displacement vectors for the out of plane modes (Figures 5-34 through 5-41) are only plotted at nodes with associated mass points. In Figure 5-42 the undeflected array is shown in dashed lines while the deflected shape is shown in solid lines. In Figures 5-43 through 5-45, only the deflected mode shapes are shown. All the modes shown are to be inputs to subsequent dynamic interaction analyses using the generated computer program. The frequencies and modal participation factors for these modes are listed in Table 5-11.

5.1.2.3 Panel Breathing Mode

As a verification of the dynamic model used, a more detailed model of one panel (Figure 5-31) was derived to analytically evaluate the fundamental panel breathing mode. It is required to maintain

TABLE 5-8. FREQUENCIES OF FOLDOUT PANEL ARRAY, OUT OF PLANE, SYMMETRIC

Mode	Frequency (Hz)	Mode	Frequency (Hz)
1	.0344	25	6.9385
2	.2072	26	7.0980
3	.5293	27	7.1827
4	.8861	28	7.5044
5	1.1429	29	7.6312
6	1.2950	30	7.7656
7	1.4353	31	7.8235
8	1.4971	32	7.9082
9	1.5291	33	8.3442
10	1.6078	34	8.5362
11	1.6344	35	9.4665
12	1.7653	36	10.0173
13	1.9877	37	10.0992
14	2.2596	38	11.1912
15	2.5279	39	11.9995
16	2.8494	40	12.6855
17	3.3752	41	13.3285
18	4.2284	42	13.8218
19	5.6543	43	14.0497
20	6.3315	44	14.6318
21	6.4331	45	15.6202
22	6.5716	46	16.1680
23	6.7198	47	17.5238
24	6.8655	48	18.8390

TABLE 5-9. FREQUENCIES OF FOLDOUT PANEL ARRAY, OUT OF PLANE, ANTISYMMETRIC

Mode	Frequency (Hz)
1	.1184
2	.3606
3	.6075
4	.8607
5	1.0980
6	1.2871
7	1.5609
8	1.7386
9	1.8536
10	1.9813
11	2.1327
12	2.3362
13	3.7286
14	3.9908
15	4.2144
16	4.4811
17	4.9012
18	5.6379
19	5.7335
20	6.4064
21	6.6507
22	6.8024
23	7.0102
24	7.4163
25	7.8218
26	7.8506
27	7.9083
28	9.2626
29	9.6278
30	9.9170
31	9.9937
32	10.1300
33	10.3267
34	10.6231
35	11.2053
36	11.4311
37	11.5634
38	12.4228
39	13.2525
40	13.7070
41	14.9116
42	17.2326

TABLE 5-10. FREQUENCIES OF FOLDOUT PANEL ARRAY, IN-PLANE

Mode	Description	Frequency (Hz)
1	Symmetric	24.76
1	Antisymmetric	1.669
2	Antisymmetric	6.934
3	Antisymmetric	13.765
4	Antisymmetric	19.771
5	Antisymmetric	23.5

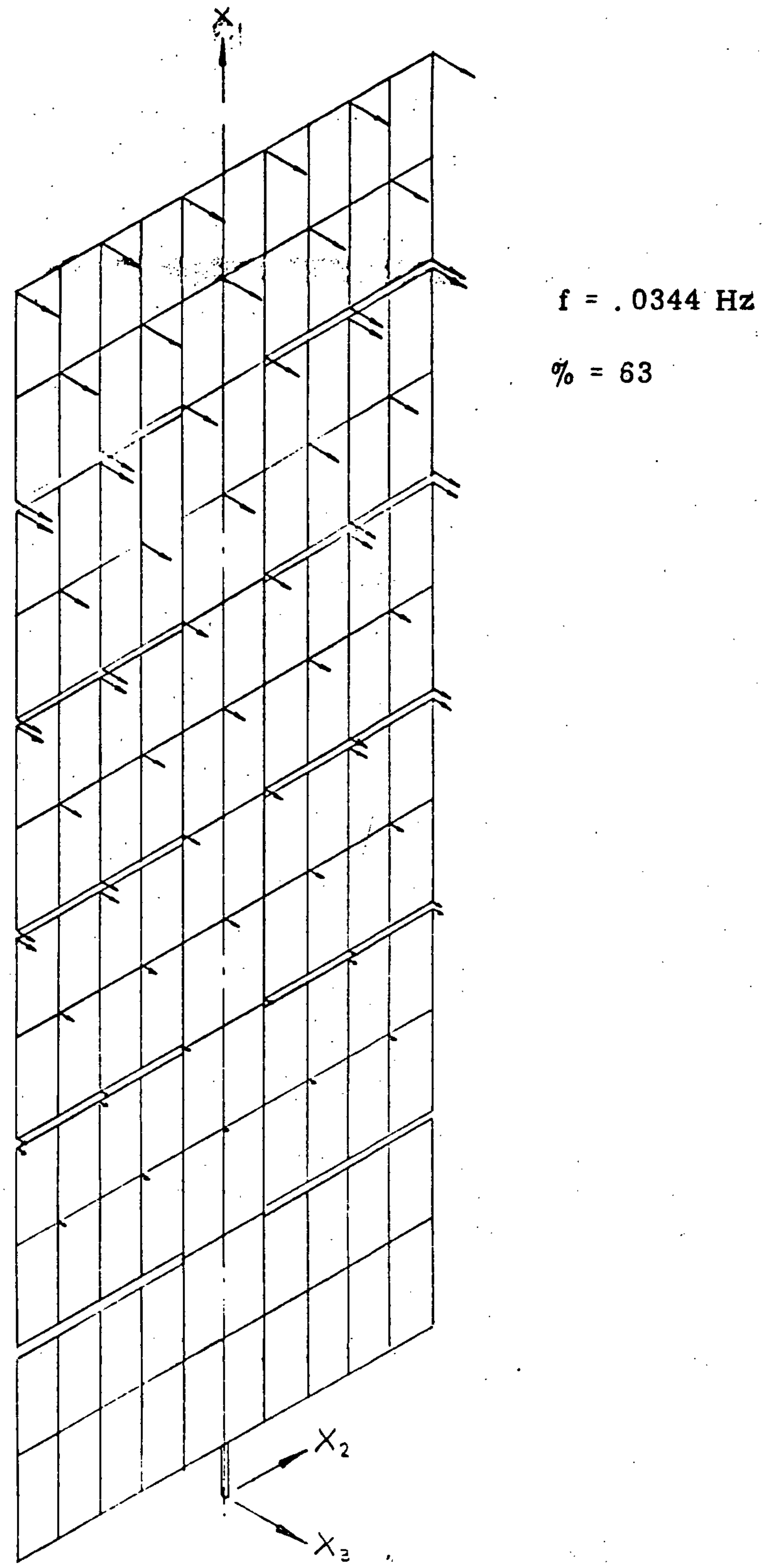

Figure 5-34. Mode 1, Foldout Panel Array, Out of Plane, Symmetric

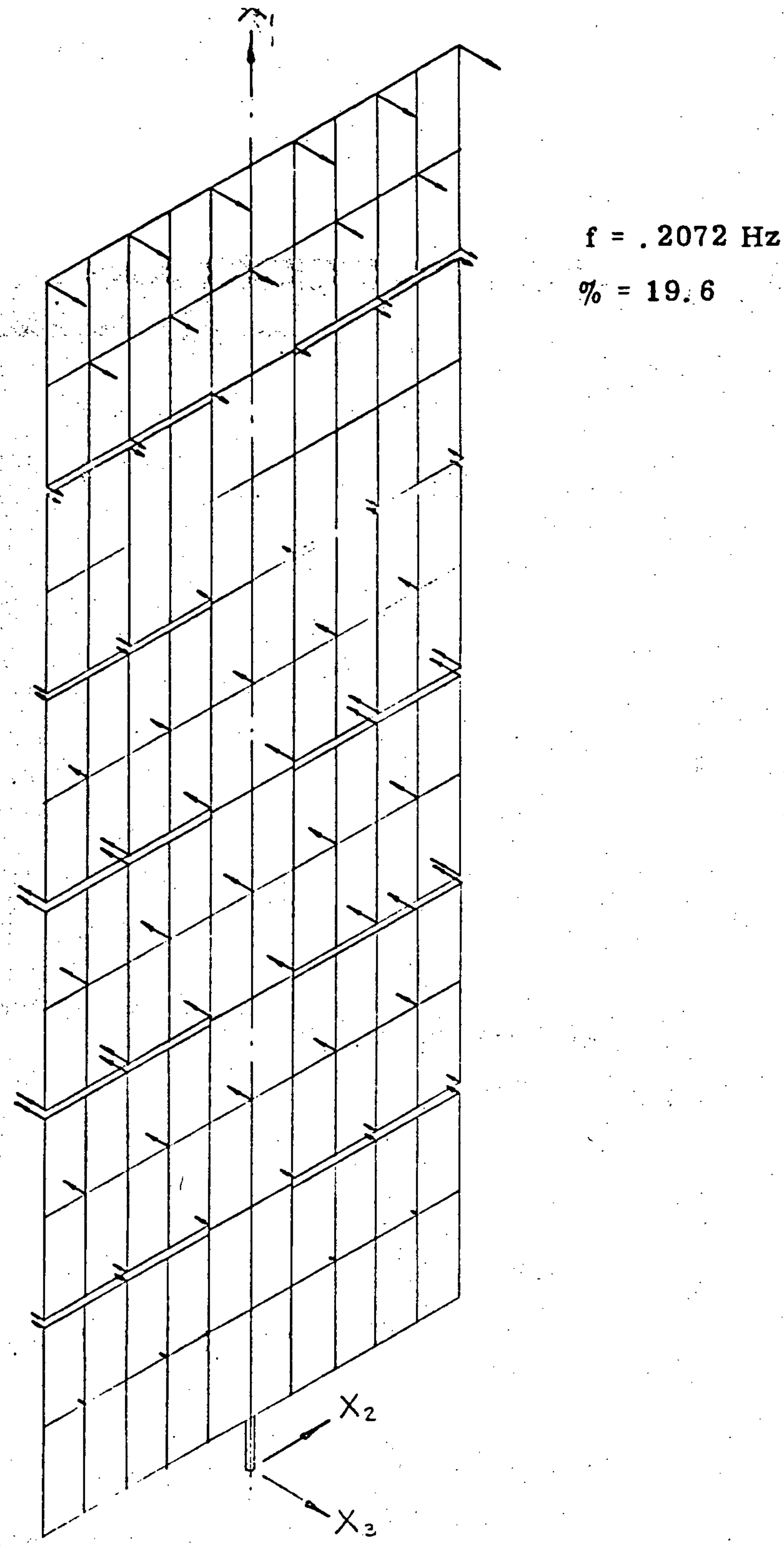

Figure 5-35. Mode 2, Foldout Panel Array, Out of Plane, Symmetric

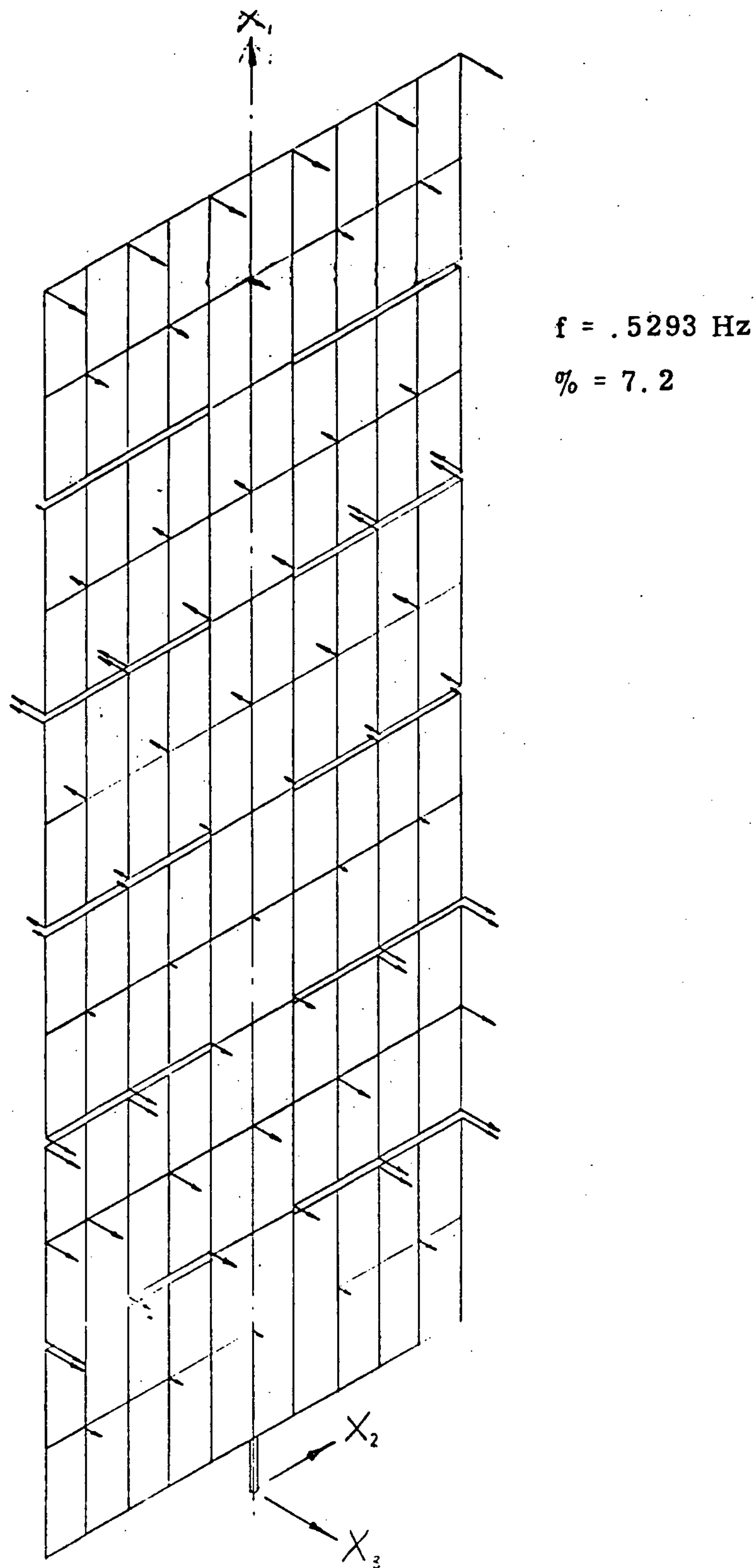

Figure 5-36 Mode 3, Foldout Panel Array, Out of Plane, Symmetric

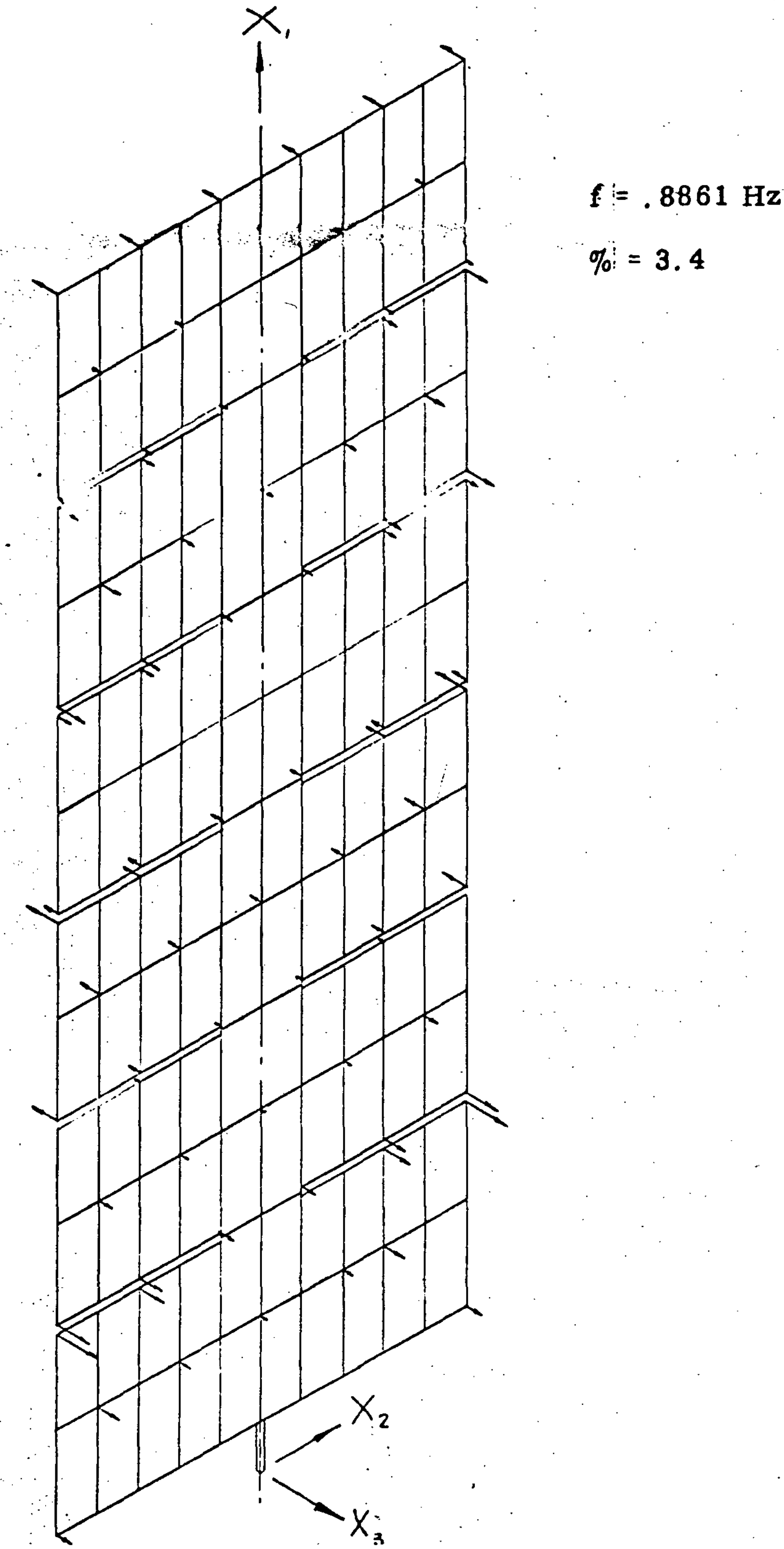

Figure 5-37 Mode 4, Foldout Panel Array, Out of Plane, Symmetric

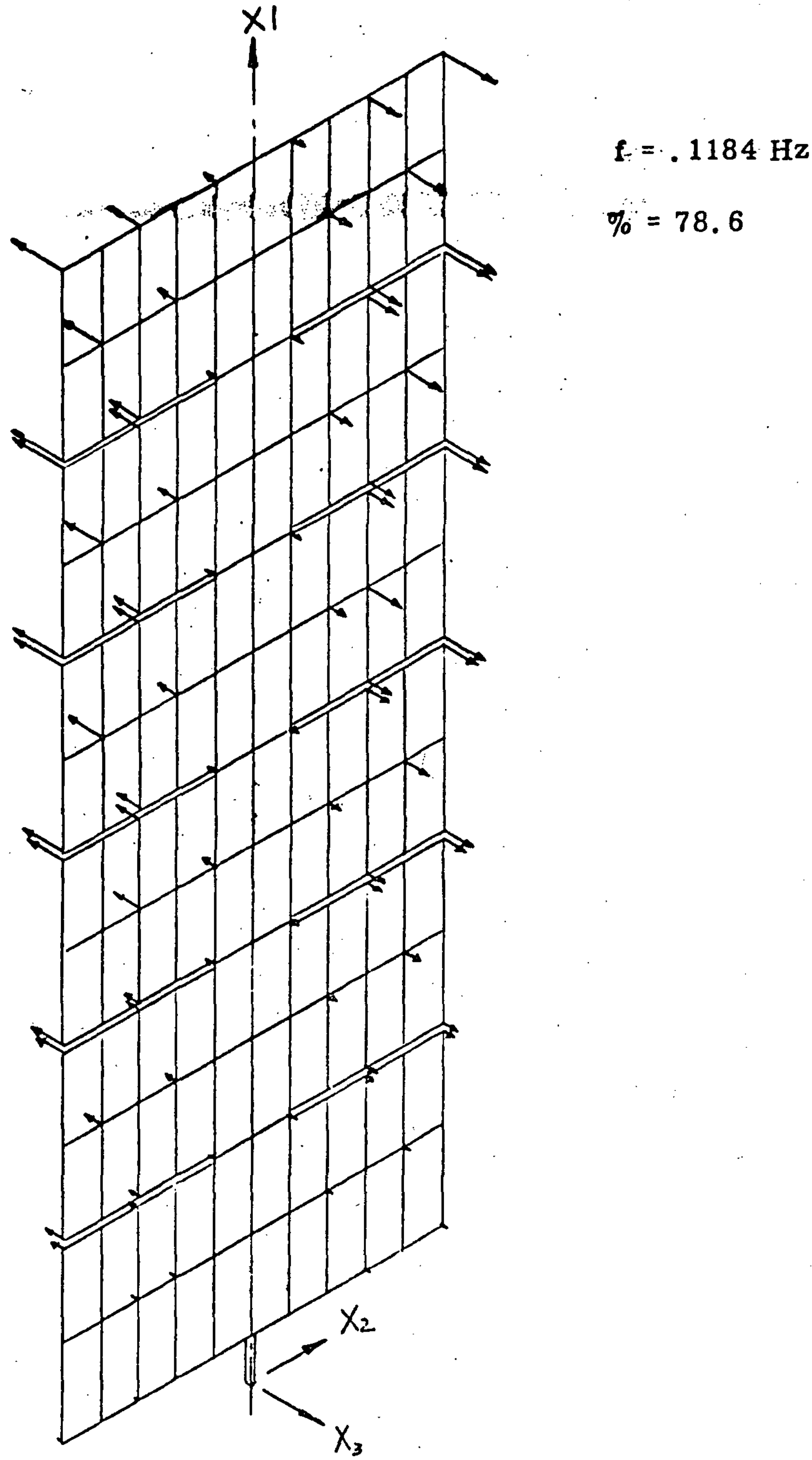

Figure 5-38 Mode 1, Foldout Panel Array, Out of Plane, Antisymmetric

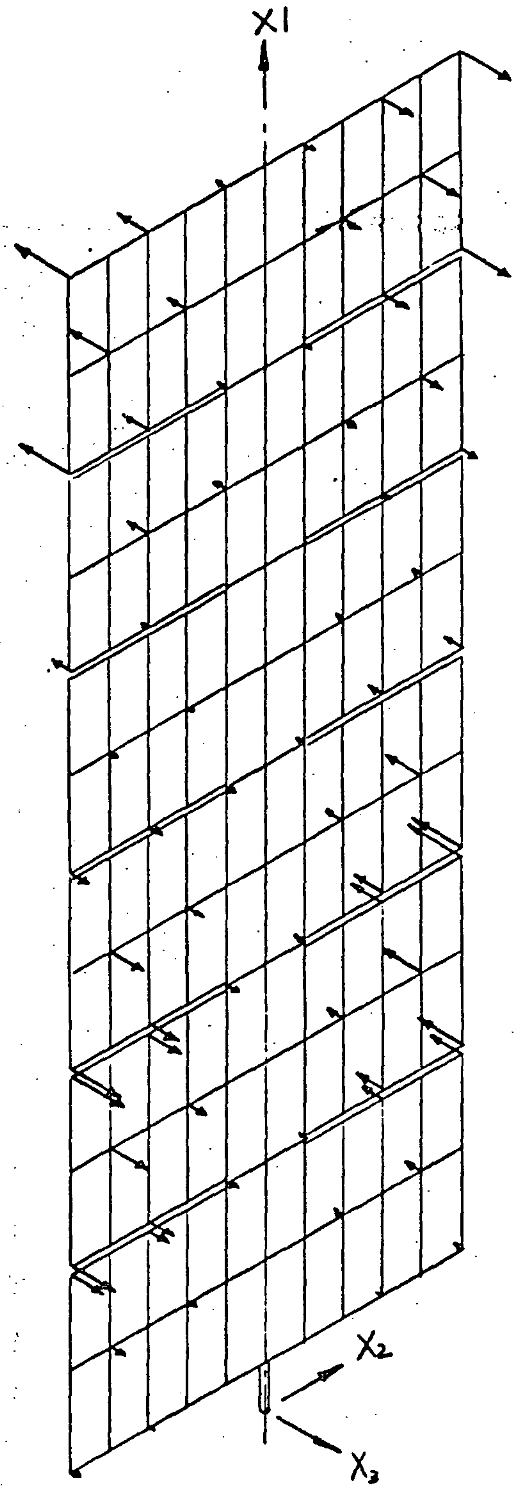

f = .3606 Hz

% = 9.4

Figure 5-39. Mode 2, Foldout Panel Array, Out of Plane, Antisymmetric

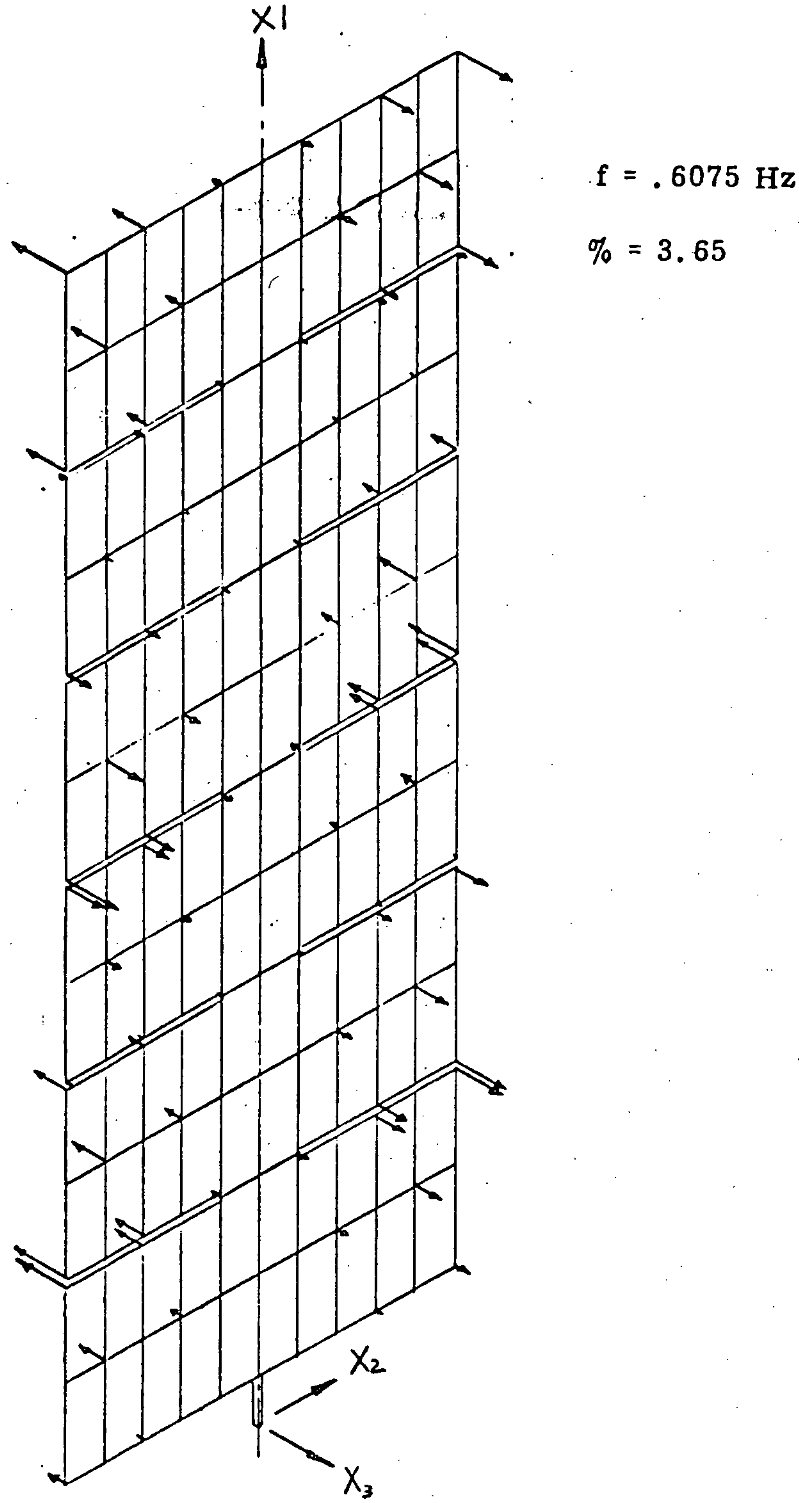

Figure 5-40 Mode 3, Foldout Panel Array, Out of Plane, Antisymmetric

6

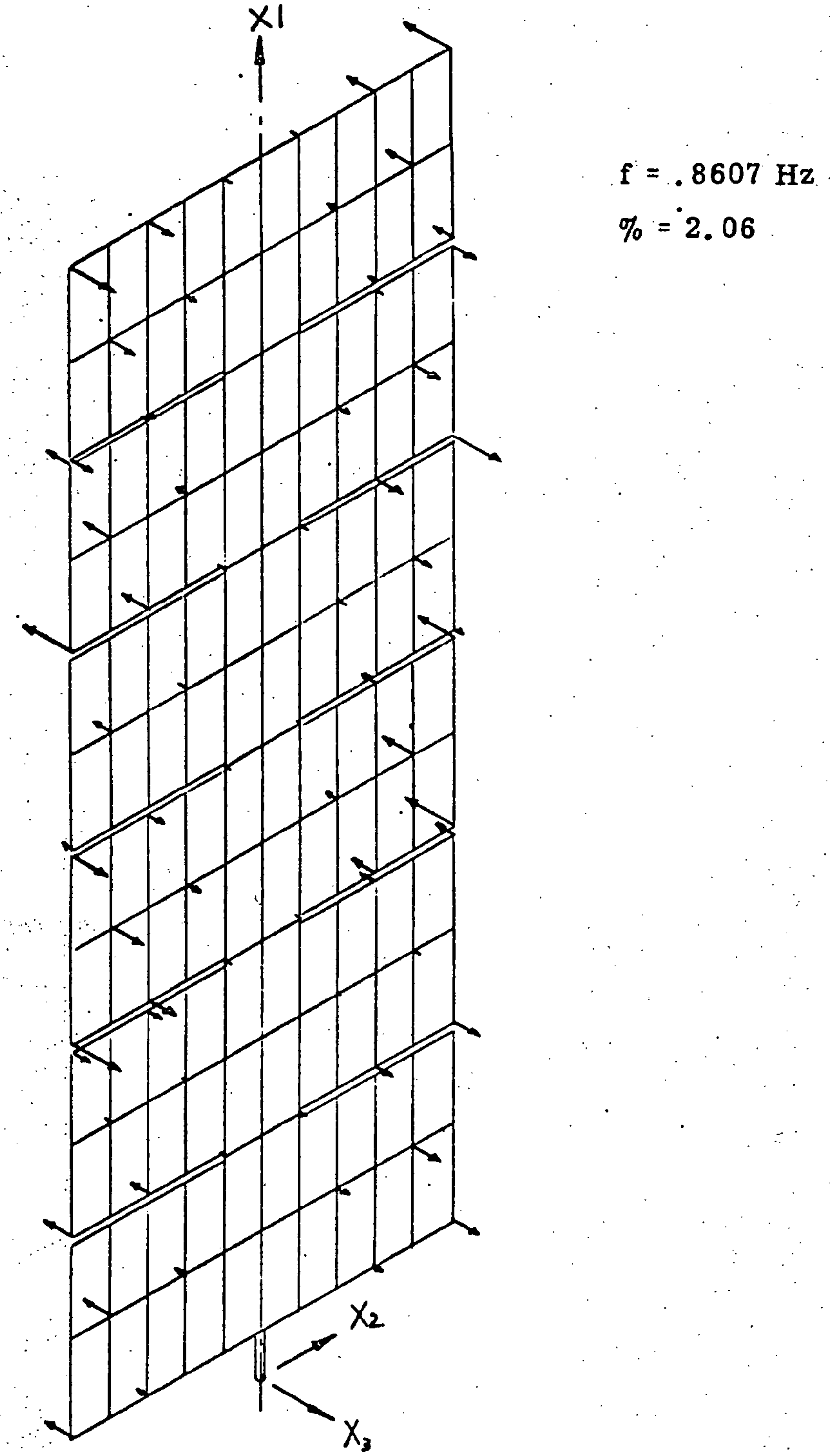

Figure 5-41 Mode 4, Foldout Panel Array, Out of Plane, Antisymmetric

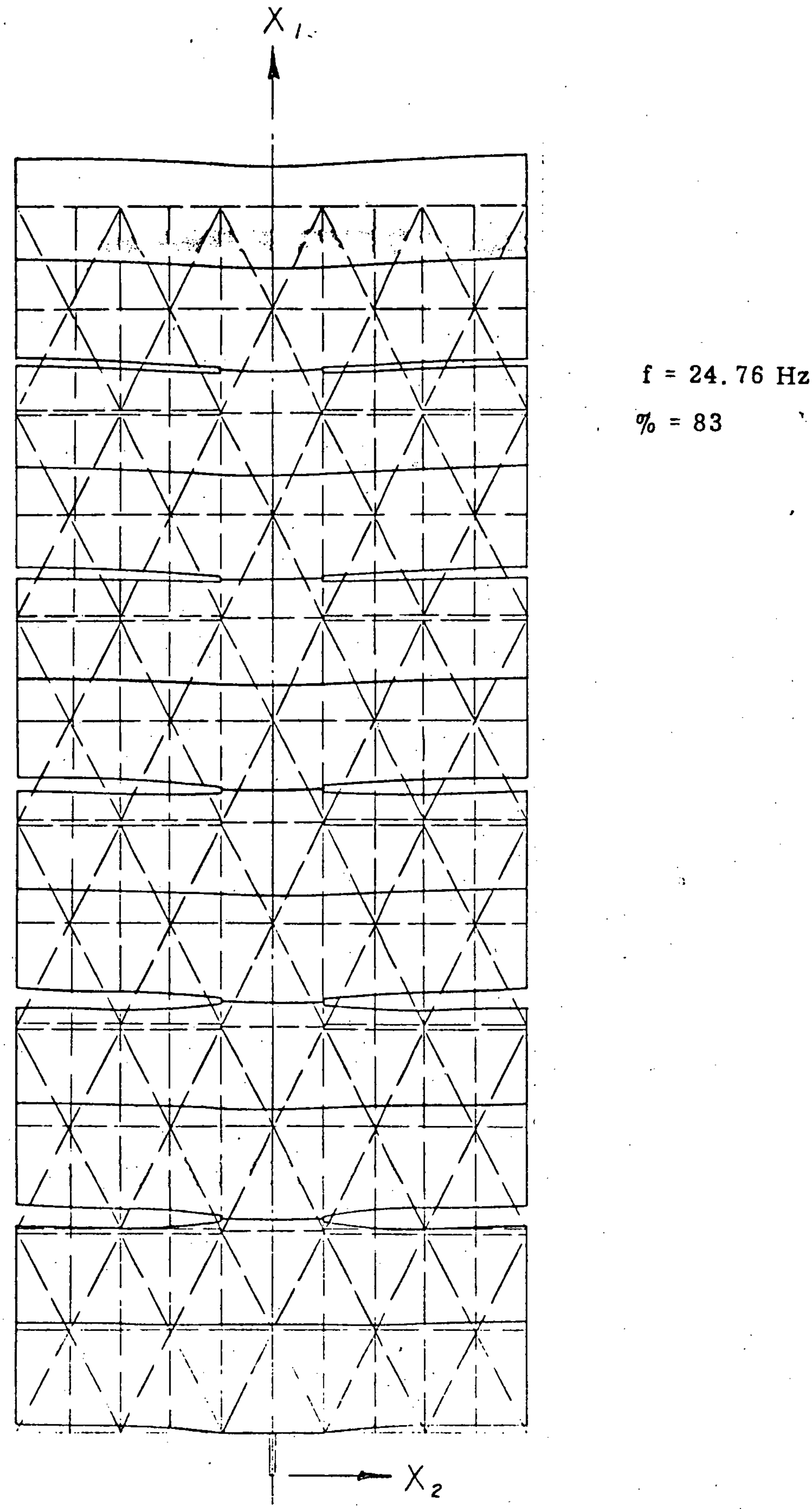

Figure 5-42 Mode 1, Foldout Panel Array, Inplane, Symmetric

6

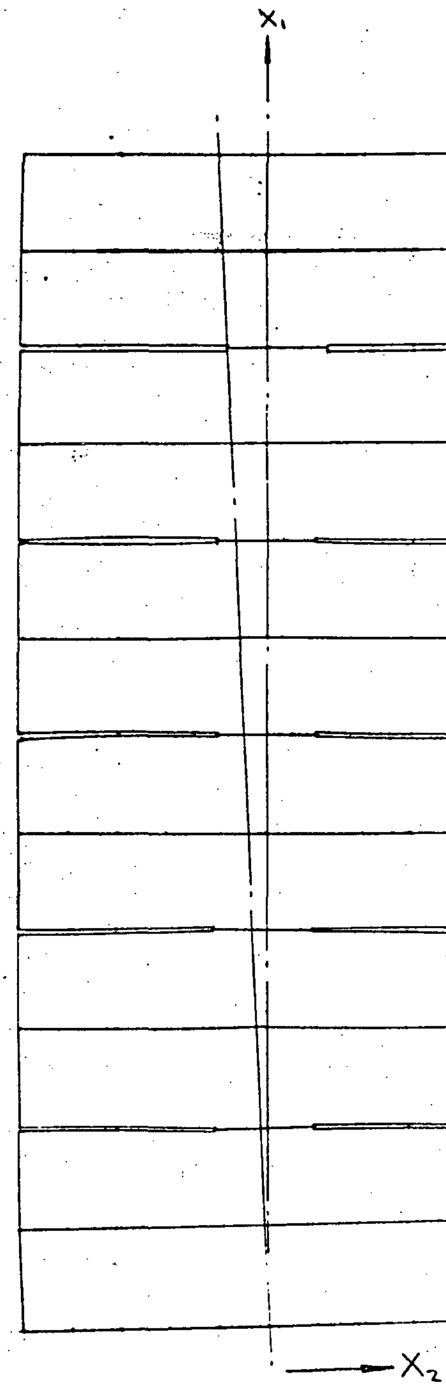

f = 1.669 Hz

% = 64.5

Figure 5-43. Mode 1, Foldout Panel Array, Inplane, Antisymmetric

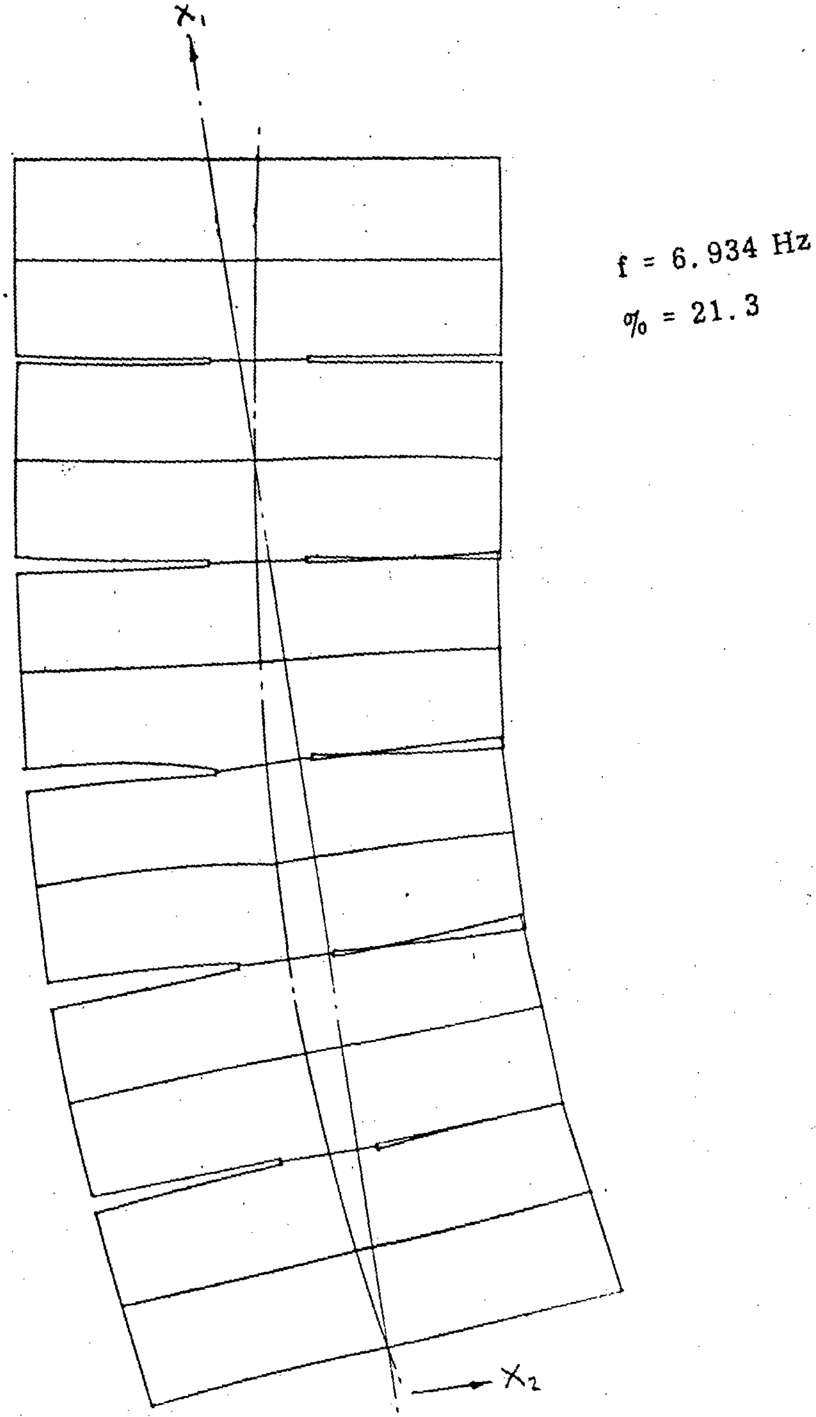

Figure 5-44. Mode 2, Foldout Panel Array, Inplane, Antisymmetric

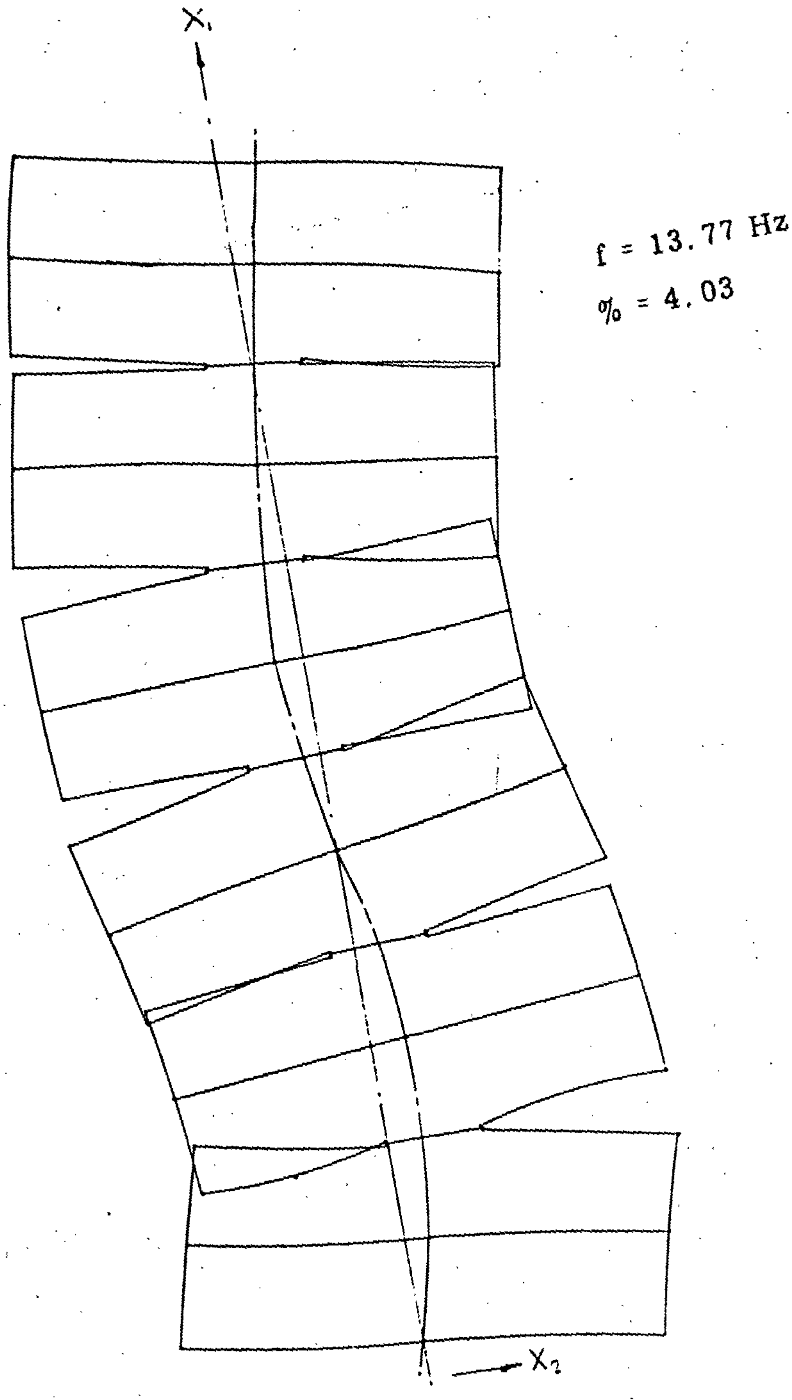

Figure 5-45 Mode 3, Foldout Panel Array, Inplane, Antisymmetric

TABLE 5-11. FOLDOUT PANEL ARRAY, MODAL PARTICIPATION FACTORS

Out of Plane					
Symmetric			Antisymmetric		
Mode	Frequency (Hz)	Percent Participation	Mode	Frequency (Hz)	Percent Participation
1	.0344	63	1	.1184	78.6
2	.2072	19.6	2	.3606	9.4
3	.5293	7.2	3	.6075	3.65
4	.8861	3.4	4	.8607	2.06
In-Plane					
Symmetric			Antisymmetric		
Mode	Frequency (Hz)	Percent Participation	Mode	Frequency (Hz)	Percent Participation
1	24.76	83	1	1.669	64.5
2	---	---	2	6.934	21.3
3	---	---	3	13.765	4.03

an adequate frequency separation between the breathing mode and the array's out of plane modal frequencies since the model used in the array analysis did not include sufficient degrees of freedom for the description of breathing modes. The nodal numbering and dimensions of the panel model analyzed is shown on Figure 5-46. There are 53 nodes in the model and nodes 44 through 53 were rigidly constrained for the dynamic analysis. The first mode of this model was 7.634 Hz which is sufficiently separated from the array out of plane mode frequencies. The nodal weights are tabulated in Table 5-12 and the mode shape of the breathing mode is shown on Figure 5-47.

5.2 PHASE II STUDY ANALYSES

The structural analyses described were performed to obtain modal data to compliment the formulated digital simulations. The analyses were conducted on the solar array and space station configurations described in Section 2.0, which correspond to both the zero "G" and artificial "G" conditions. A requirement of the dynamic interaction analysis digital simulation is that cantilever modal data for the solar arrays and free-free modal data for the space station be initially determined and used as input. Each of the structural models and corresponding modal data is described in the following.

5.2.1 ZERO "G" SPACE STATION CONFIGURATION

The stiffness and mass properties used to represent the space station structural arrangement were those resulting from preliminary configuration studies performed by North American Rockwell (Reference 5.7). These properties were obtained from NAR and are given in Table 5-13 and Figure 5-48, comprising the total structural arrangement.

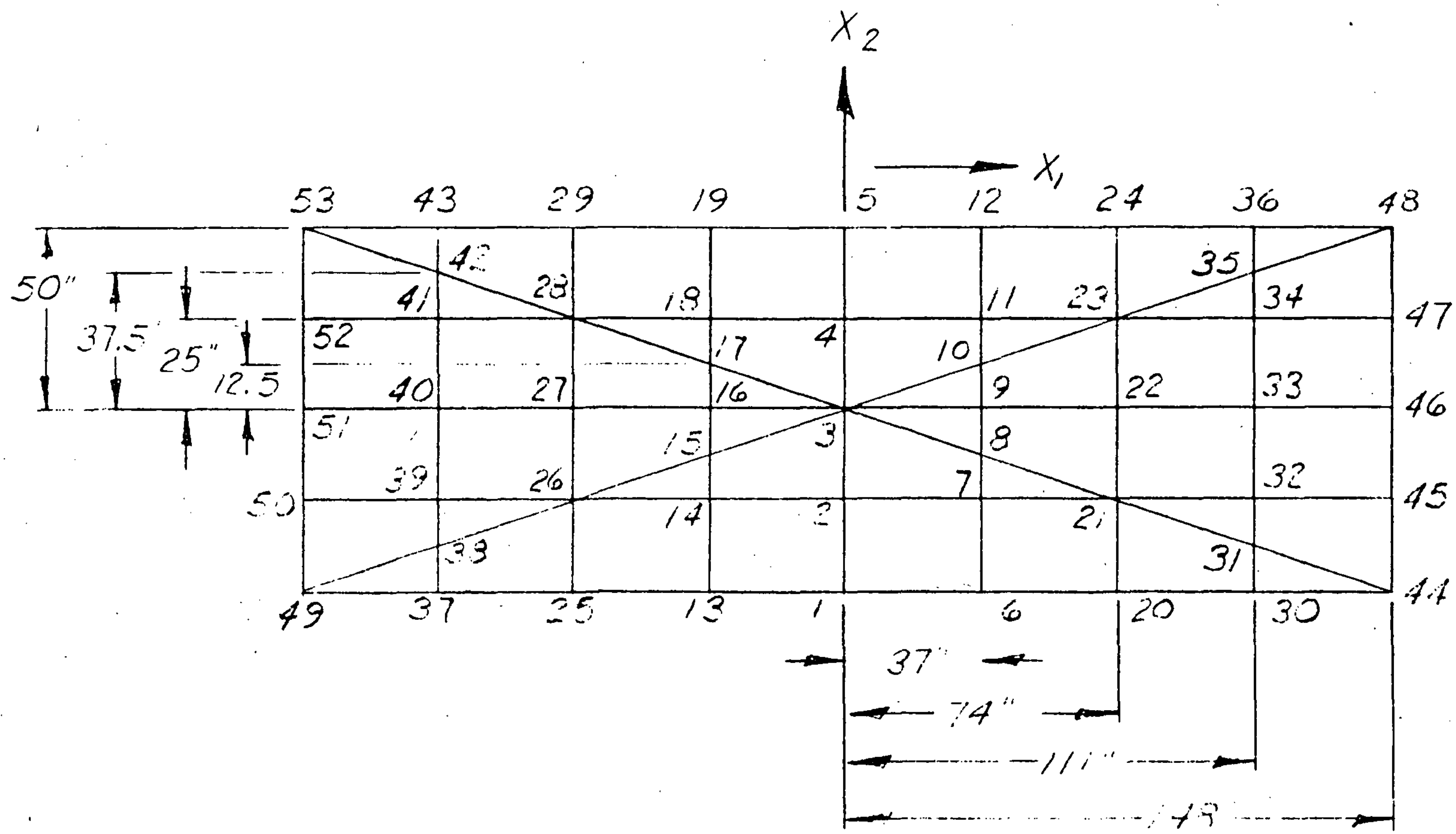

Figure 5-46 Breathing Mode Model

TABLE 5-12. NODAL WEIGHTS FOR BREATHING MODE MODEL

Node	Weight (lbs)
1,5	2.059
2,4	3.401
3	4.578
6,9,12,13,16,19,20,24,25,29	1.955
7,11,14,18	2.261
8,10,15,17	2.066
21,23,26,28	3.708
22,27,33,40	3.191
30,36,37,43	1.336
31,35,38,42	2.064
32,34,39,41	2.284

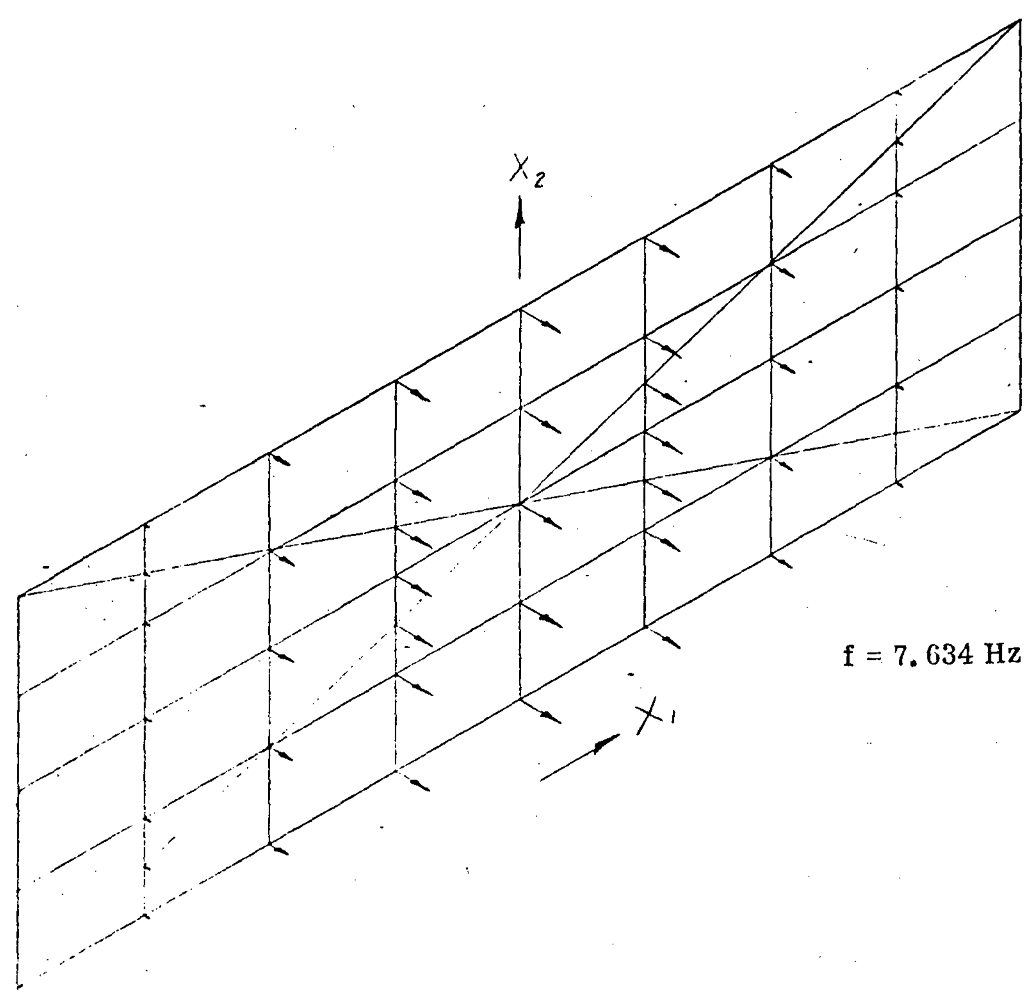

Figure 5-47 Mode 1, Foldout Panel Array, Breathing Mode

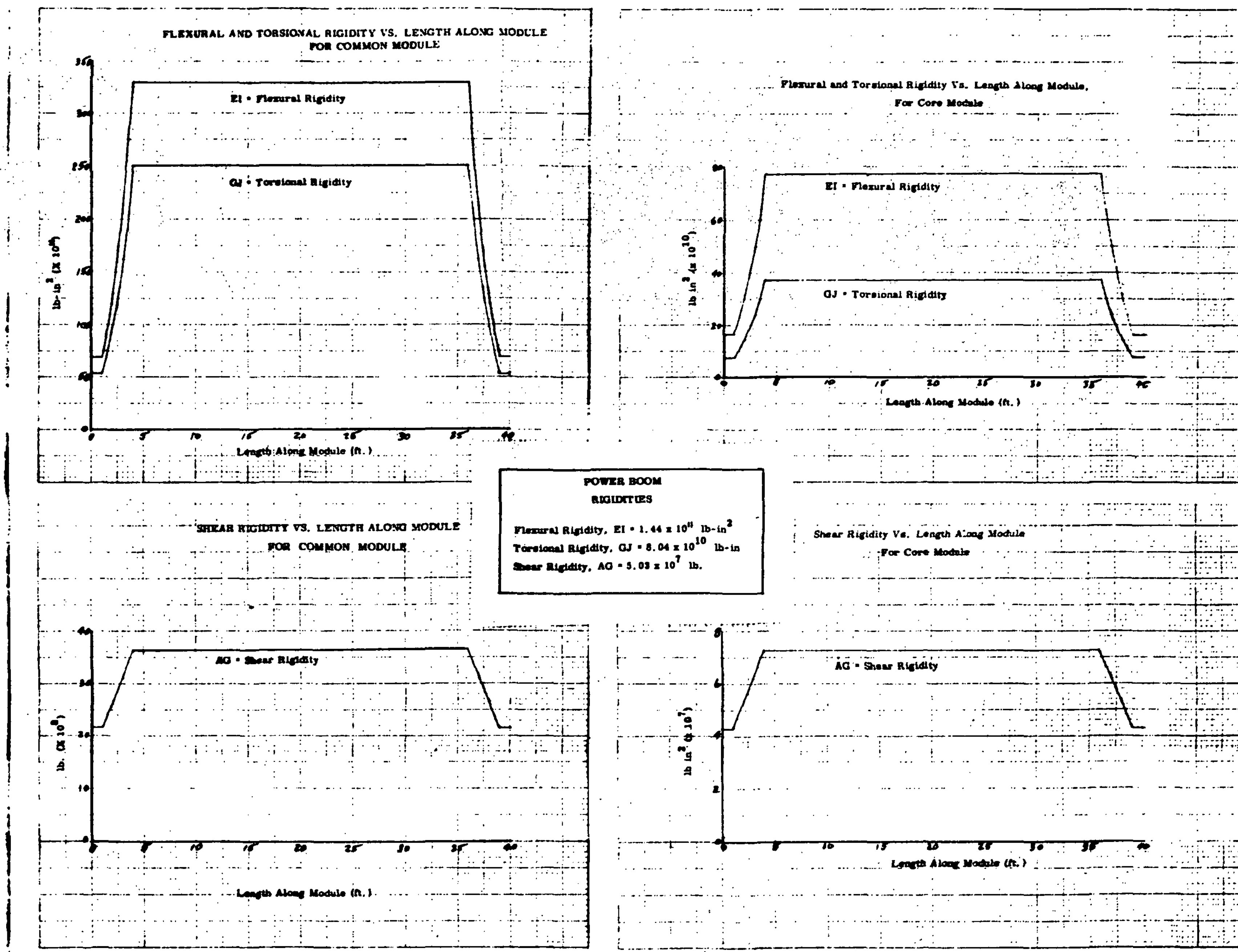

Figure 5 -48 Space Station Stiffness Properties

TABLE 5-13

Mass Properties of Zero "G" Space Station Configuration

COMPONENT	WEIGHT (LBS.)
Core Module	25,000
Common Module (8 in configuration)	25,000/module
Power Boom	17,500

A finite element model representing this configuration was derived, using a limited number of nodal points, and it is depicted in Figure 5-49. The corresponding descrete masses of the model and grid point geometry is given in Table 5-14. Each of the discrete points was allowed three translational degrees-of-freedom and one rotational degree-of-freedom, corresponding to torsion of each module. Shear flexibility was considered for appropriate degrees-of-freedom because of the relatively small length to diameter ratio of each module. The model geometry, inertial properties and stiffness properties were input to the NASTRAN program (Reference 5.12) for the determination of modal properties, i.e., frequencies, mode shapes, and modal masses. A partial list of these quantities are listed in Table 5-15. A comprehensive listing of the zero "G" modal properties, together with a graphical presentation of lower modes of vibration, are given in Appendix A to this report.

5.2.2 ARTIFICIAL "G" SPACE STATION CONFIGURATION

The artificial "G" space station configuration was discretized into the finite element model presented in Figure 5-50. Stiffness and inertial properties are similar to those presented for corresponding modules in Table 5-13 and Figure 5-48 except for the power boom and extended boom; the mass

Structural Model Of Space Station

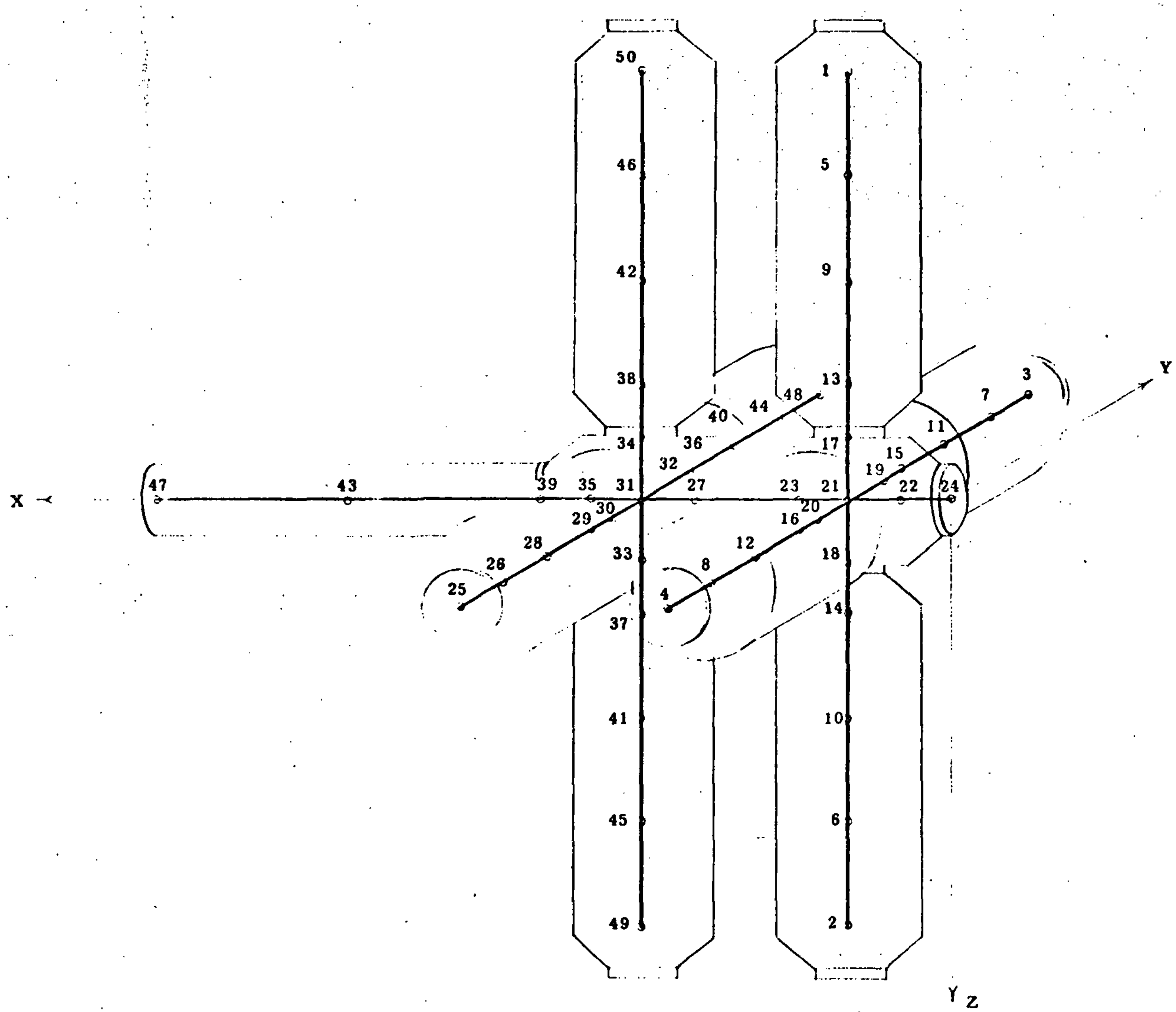

Figure 5-49

TABLE 5 -14

Mass - Geometry Data

Of Zero G Space Station

NODE NO.	MASS $\left(\frac{\text{lb.-sec}^2}{\text{in.}}\right)$	X	Y	Z
1	16.189	120.	0.	-492.
2	16.189	120.	0.	492.
3	16.189	120.	492.	0.
4	16.189	120.	-492.	0.
5	16.189	120.	0.	-372.
6	16.189	120.	0.	372.
7	16.189	120.	372.	0.
8	16.189	120.	-372.	0.
9	16.189	120.	0.	-252.
10	16.189	120.	0.	252.
11	16.189	120.	252.	0.
12	16.189	120.	-252.	0.
13	16.189	120.	0.	-132.
14	16.189	120.	0.	132.
15	16.189	120.	132.	0.
16	16.189	120.	-132.	0.
17	0.	120.	0.	-72.
18	0.	120.	0.	72.
19	0.	120.	72.	0.
20	0.	120.	-72.	0.
21	8.1	120.	0.	0.
22	8.1	60.	0.	0.
23	0.	180.	0.	0.
24	4.05	0.	0.	0.
25	16.189	360.	-492.	0.
26	16.189	360.	-372.	0.
27	12.15	300.	0.	0.
28	16.189	360.	-252.	0.
29	16.189	360.	-132.	0.
30	0.	360.	-72.	0.
31	8.1	360.	0.	0.
32	12.15	360.	72.	0.
33	0.	360.	0.	72.
34	0.	360.	0.	-72.
35	8.1	420.	0.	0.
36	16.189	360.	132.	0.
37	16.189	360.	0.	132.
38	16.189	360.	0.	-132.
39	12.7919	480.	0.	0.
40	16.189	360.	252.	0.
41	16.189	360.	0.	252.
42	16.189	360.	0.	-252.
43	17.4839	700.5	0.	0.
44	16.189	360.	372.	0.
45	16.189	360.	0.	372.
46	16.189	360.	0.	-372.
47	19.086	921.	0.	0.
48	16.189	360.	492.	0.
49	16.189	360.	0.	492.
50	16.189	360.	0.	-492.

Table 5-15. Modal Data, Space Station

(Zero G Configuration)

Mode	Frequency (Hz)		Generalized Mass (lb.-sec.²/in.)
1	0.0	Rigid Body Modes	6.281594E 02
2	0.0		6.281594E 02
3	0.0		6.281594E 02
4	0.0		2.477312E 02
5	0.0		1.244991E 02
6	0.0		1.244991E 02
7	1.557577E 00		2.297717E 02
8	2.277407E 00		3.636589E 01
9	2.278777E 00		3.660057E 01
10	3.147397E 00		8.373244E 01
11	3.246078E 00		1.085563E 02
12	4.391578E 00		1.511882E 02
13	4.483892E 00		3.124590E 02
14	5.702700E 00		7.439223E 01
15	6.035457E 00		7.142155E 01
16	6.477657E 00		8.401511E 01
17	6.875389E 00		1.111700E 02
18	6.875395E 00		1.111700E 02
19	7.765384E 00		5.186711E 01
20	8.263874E 00		1.006247E 02
21	8.860953E 00		
22	8.935523E 00		
23	1.013241E 01		
24	1.130443E 01		
25	1.131781E 01		
26	1.475548E 01		
27	1.534728E 01		
28	1.958418E 01		
29	1.988515E 01		
30	2.277832E 01		
31	2.319455E 01		
32	2.339781E 01		
33	2.342052E 01		
34	2.490974E 01		
35	2.574709E 01		
36	2.658902E 01		
37	2.698964E 01		
38	2.752139E 01		
39	2.941002E 01		
40	2.942180E 01		
41	2.967250E 01		
42	2.967250E 01		
43	2.977396E 01		
44	2.984723E 01		
45	2.984726E 01		
46	2.992293E 01		
47	3.003922E 01		
48	3.005589E 01		
49	3.005730E 01		
50	3.027989E 01		

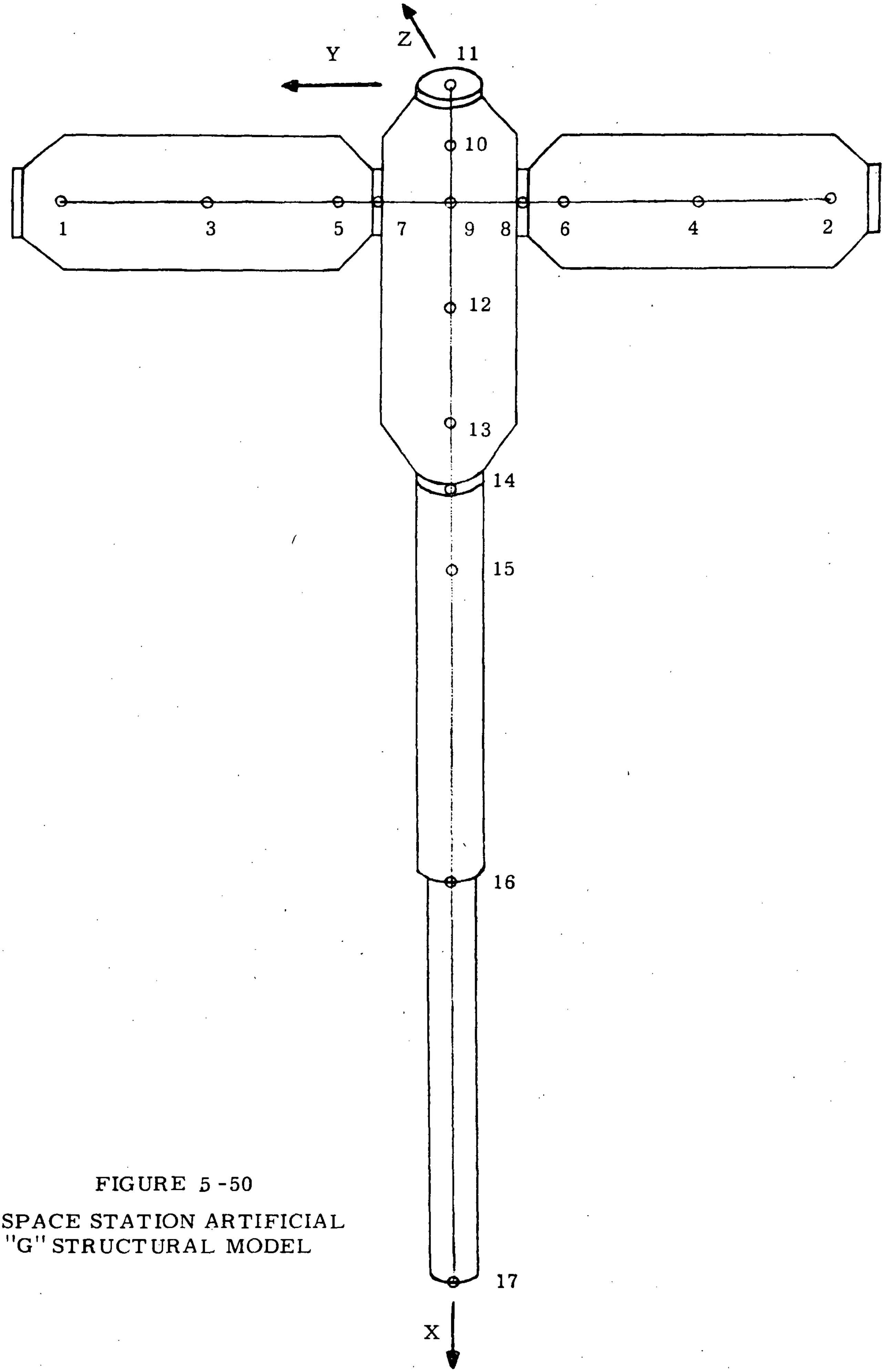

FIGURE 5-50

SPACE STATION ARTIFICIAL
"G" STRUCTURAL MODEL

and geometry properties for this modal are listed in Table 5-16. It was originally intended to utilize the stated capability of the NASTRAN program in the performance of the modal analysis of the spinning structure; however, initial attempts with NASTRAN failed (Version 12). An eigenvalue-eigenvector program obtained from the Jet Propulsion Laboratory (JPL) in Pasadena, California, and formulated by Dr. K. K. Gupta (Reference 5.8 and 5.9) was used. As is required for modal analysis of spinning structures, a coriolis force matrix and centrifugal force matrix were derived for the total description of the equations of equilibrium of the discretized system. A comprehensive description of typical terms in these matrices can be found in Reference 5.10. The centrifugal force matrix is a function of the motion variables while the coroilis force matrix is dependent upon the first derivatives of the motion variables. Orthogonalization of this system of equations results in complex conjugate pairs of eigenvalues (zero real part) and corresponding complex conjugate pairs of eigenvectors. The digital simulation, for the artificial "G" condition, is programmed to accept this modal data format.

For the structural configuration shown, the artificial "G" condition was attained by spinning the space station at 4 RPM about a point 44 feet outboard of the space station-solar array attachment as depicted in Figure 5-51. The coriolis force and centrifugal force matrices were computed by hand and the stiffness matrix was generated with the NASTRAN computer program. It was also determined that the influence of static spin loads upon the station's structural stiffness (beam column effect) was negligible and therefore neglected. The matrices together with the mass matrix were input into the JPL program for determination of complex eigenvalues and eigenvectors for a range of steady state spin rates. Resulting frequencies are presented in Table 5-17 for spin rates of 0, 4, 8, and 12 RPM together with

TABLE 5-16

ARTIFICIAL "G" SPACE STATION

FINITE ELEMENT MODEL DATA

NODE	MASS LB SEC^2/IN	INERTIA LB SEC^2 IN			NO. OF STRUCTURAL D.O.F.	D.O.F. SEQUENCE NO.
		x Axis	y Axis	z Axis		
1	21.578	--	66641	--	6	1-6
2	21.578	--	66641	--	6	7-12
3	21.578	--	66641	--	6	13-18
4	21.578	--	66641	--	6	19-24
5	21.578	--	66641	--	6	25-30
6	21.578	--	66641	--	6	31-36
7	--	--	--	--	6	37-42
8	--	--	--	--	6	43-48
9	15.382	41621	--	--	6	49-54
10	8.094	21886	--	--	6	55-60
11	4.047	10956	--	--	6	61-66
12	17.814	49417	--	--	6	67-72
13	15.379	41595	--	--	6	73-78
14	12.795	18700	--	--	6	79-84
15	10.632	9350			6	85-90
16	25.952	20642			6	91-96
17	.01295	10.282			6	97-102

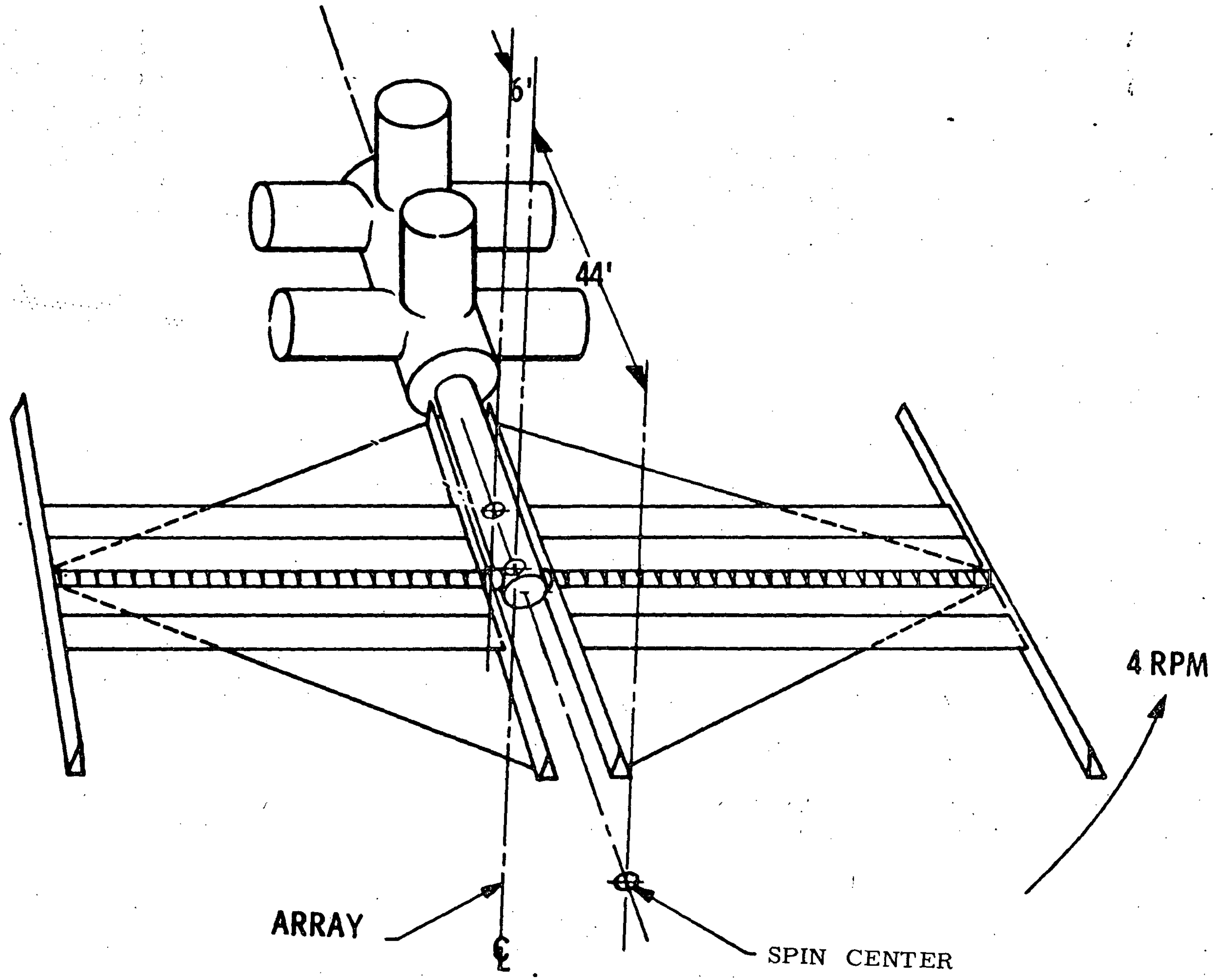

Figure 5 -51. Space Station-Solar Array Artificial "G" Configuration

TABLE 5-17

Artificial "G" Space Station Configuration

List of Eigen Values in Hertz

Elastic Mode No.	NASTRAN Results	"GUPTA" Program Results			
	$\Omega = 0$	$\Omega = 0$	Ω = 4RPM	Ω = 8RPM	Ω = 12 RPM
1	2.2967	2.2948	2.2929	2.2890	2.2851
2	4.2003	4.2027	4.2027	4.2026	4.2027
3	8.4202	8.4224	8.4147	8.4068	8.3914
4	8.6787	8.6711	8.6789	8.6867	8.6944

the modal frequencies obtained by NASTRAN for the same model in a zero-spin condition. It is seen that the frequency correlation between NASTRAN and Gupta's program is excellent and that the frequency change with spin rate is minimal. A comprehensive list of modal data in terms of modal deflection and graphical description of the lower frequency modes in terms of absolute deflection coefficients, are given in Appendix A to this report. Also presented are the structural degrees of freedom considered in the analysis. Examination of the shape for the second mode shows this mode is represented by out-of-the-spin-plane bending only and would not be influenced by centrifugal or coriolis forces. This explains the constant frequency results with spin rate for the second mode which is shown in Table 5-17. The general conclusion indicated by the performed modal analyses is that the spin rate does not significantly alter the zero spin modal frequencies if the zero spin modal frequencies are sufficiently separated from the spin frequency.

5.2.3 ZERO "G" SOLAR ARRAY CONFIGURATION

The rollup solar array was analyzed in a similar manner as is described for past study analyses in Section 5.1. Updates in configuration data, however, were obtained from the Lockheed Space and Missiles Company and these were incorporated into the description of the derived vibration analysis model.

The total array area (two wing sections) is approximately 10,000 square feet and the electrical power output is rated as 10 watts per square foot. The rollup array dimensions and structural components are depicted in Figure 5-52. It is comprised of 10 membrane substrates

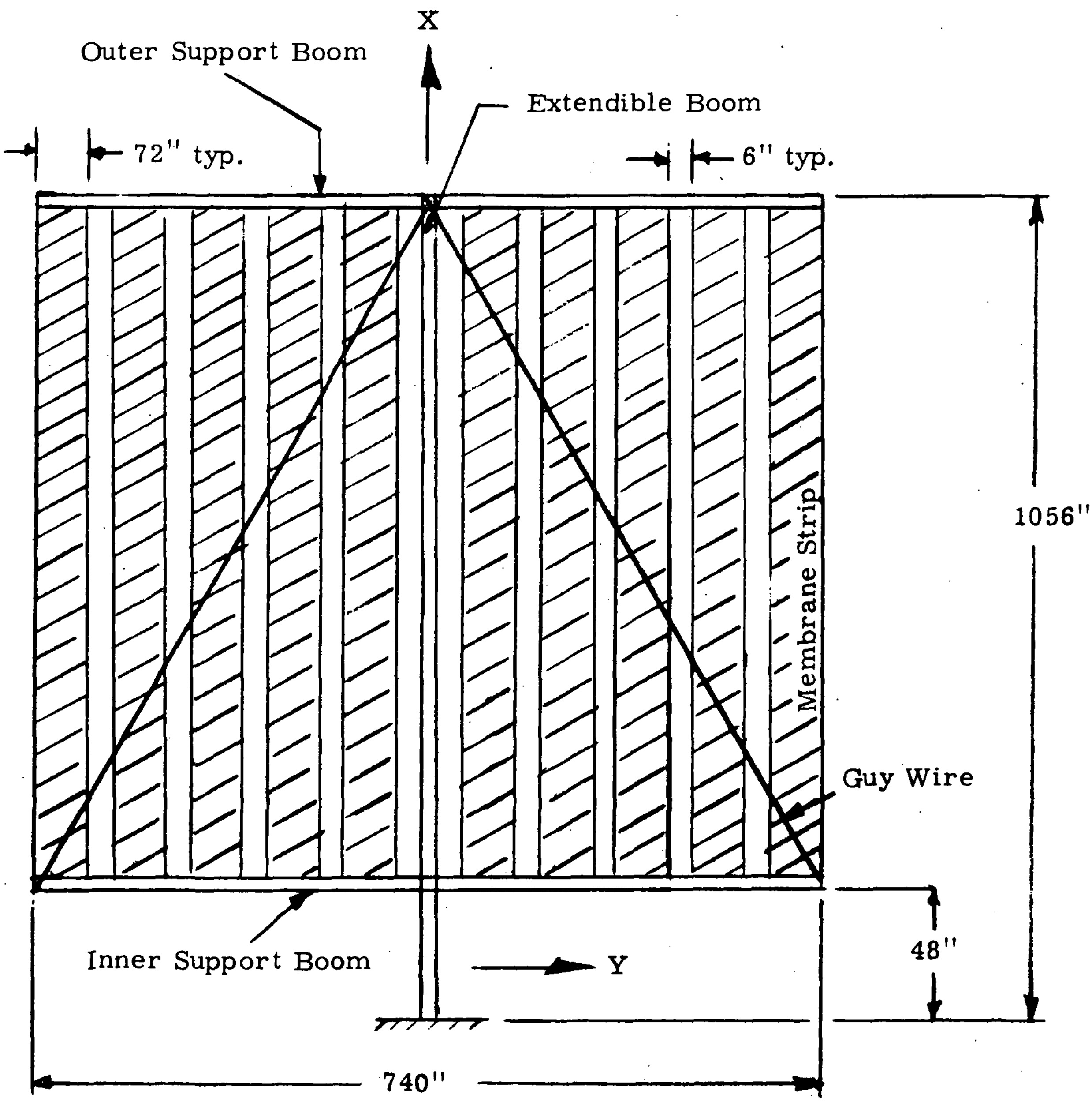

Figure 5 -52 Zero "G" Solar Array Configuration per wing section, tensioned between an inner and outer boom by an extendible boom. Two guide wires are provided for each membrane strip and each is tensioned to 5.1 pounds. Each strip is attached to the inner boom assembly by a linear spring and tensioned to 12 pounds. A guy wire is also provided between the outboard end of the extendible boom and the extremity of the inner boom and acts as a tension load carrying member only. Pertinent stiffness and mass properties data for the array structural components are given in Table 5-18.

As was considered in Section 5.1, the symmetry properties of the solar array were utilized in the performance of its modal analysis. Only one-half of the wing section was discretized into a finite element model and it is presented in Figure 5-53. Four separate vibration conditions were established for the complete evaluation of modal properties and correspond to out-of-plane symmetric bending, out-of-plane antisymmetric bending (about the extendible boom), in-plane symmetric bending and in-plane antisymmetric bending. The NASTRAN finite element program (Reference 5.11) was utilized to obtain the modes; the four vibration conditions were obtained by constraining appropriate structural degrees-of-freedom. The nodal weights associated with the rollup array dynamic model and nodal geometry are given in Table 5-19. An assumption was made in the analyses for treating the stiffness provided by the guy wire; it was considered as a tension-compression member with only one-half of its actual tension stiffness properties. In addition, the lateral stiffness of the membrane strips was assumed to be described in terms of the tension force only. These stiffness terms were entered in the NASTRAN program by means of the "CELAS" stiffness elements.

A complete list of modal results and graphical presentation of modes for the four vibration conditions are given in Appendix A of this report. Modal participation factors, for each normal mode of the solar

TABLE 5 -18

STIFFNESS AND MASS PROPERTIES DATA FOR ROLLUP SOLAR ARRAY

MEMBER	AE (lbs.)	EI_X^* (lb-in.^{2})	EI_Y^* (lb.-in.^{2})	EI_Z^* (lb.-in.^{2})	GJ (lb-in.^{2})	RUNNING WEIGHT (lbs/in.)
Extendible Boom (Full)	22.4×10^6		2.8×10^8	2.8×10^8		.212
Outer Support	10.4×10^6 (Y=0 to 72) 5.9×10^6 (Y=72 to 369)	9.3×10^8		3.32×10^8 (Y=0 to72) 1.87×10^8 (Y=72 to 369)	26.8×10^6	.130
Inner Support	5.9×10^6	9.3×10^8		1.87×10^8	26.8×10^6	.115
Membrane Strip	3.33 lb/in.					.2
Guy Wire	$.203 \times 10^6$					

* - For axis system refer to Figure 5-52.

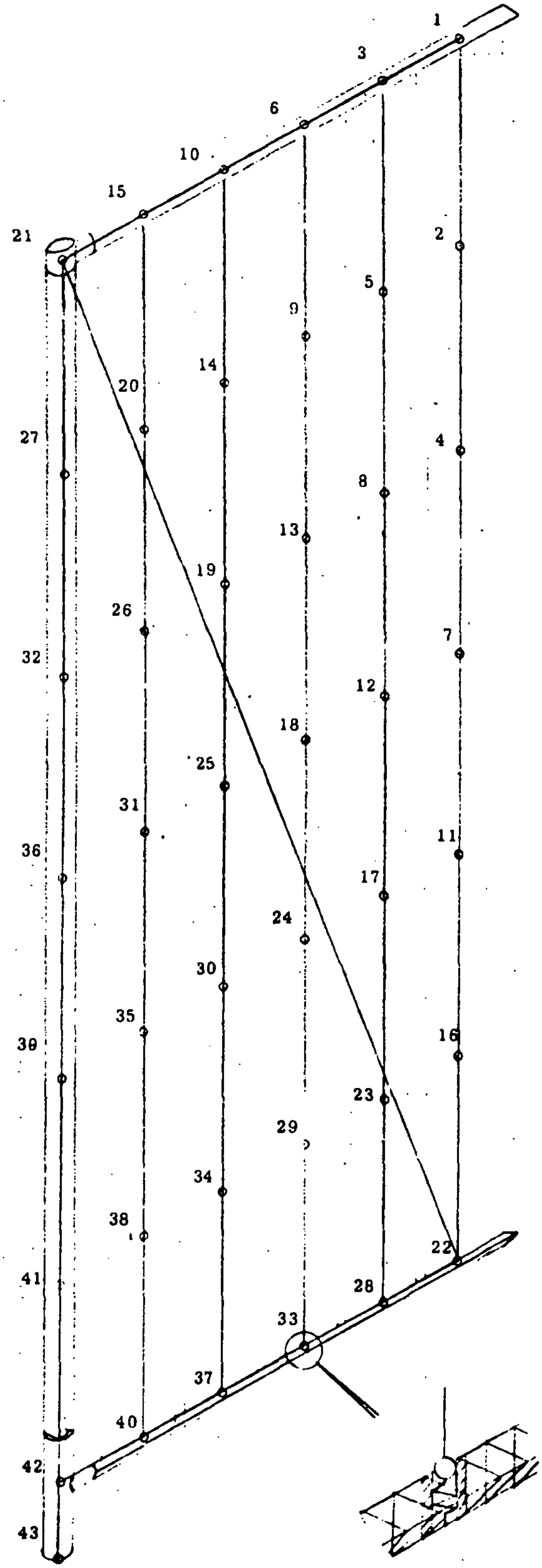

Figure 5-53
Structural Model for Roll-up Solar Array Zero "G" Configuration

TABLE 5-19

Mass - Geometry Data

Of Zero G Solar Array

NODE NO.	WEIGHT(lbs.)	X	Y	Z
1	21.48	1056.	347.	0.
2	32.3	888.	347.	0.
3	26.06	1056.	275.	0.
4	32.3	720.	347.	0.
5	32.3	888.	275.	0.
6	26.06	1056.	203.	0.
7	32.3	552.	347.	0.
8	32.3	720.	275.	0.
9	32.3	888.	203.	0.
10	26.06	1056.	131.	0.
11	32.3	384.	347.	0.
12	32.3	552.	275.	0.
13	32.3	720.	203.	0.
14	32.3	888.	131.	0.
15	25.32	1056.	59.	0.
16	32.3	216.	347.	0.
~~17~~	~~32.3~~	~~384.~~	~~275.~~	~~0.~~
18	32.3	552.	203.	0.
19	32.3	720.	131.	0.
~~20~~	~~32.3~~	~~888.~~	~~59.~~	~~0.~~
21	12.74	1056.	0.	0.
22	20.84	48.	347.	0.
23	32.3	216.	275.	0.
24	32.3	384.	203.	0.
25	32.3	552.	131.	0.
26	32.3	720.	59.	0.
27	17.81	888.	0.	0.
28	24.98	48.	275.	0.
29	32.3	216.	203.	0.
30	32.3	384.	131.	0.
31	32.3	552.	59.	0.
32	17.81	720.	0.	0.
33	24.98	48.	203.	0.
34	32.3	216.	131.	0.
35	32.3	384.	59.	0.
36	17.81	552.	0.	0.
37	24.98	48.	131.	0.
38	32.3	216.	59.	0.
39	17.81	384.	0.	0.
40	24.23	48.	59.	0.
41	17.31	216.	0.	0.
42	12.30	48.	0.	0.
43	0.	0.	0.	0.

NOTE: Weights along the boom (Y = 0.) are one half the actual weight.

array, using root constraint loads were also computed in order to determine those modes of importance for describing interaction loads. The properties of those modes having relatively large load participation factors are listed in Table 5-20.

5.2.4 ARTIFICIAL "G" SOLAR ARRAY CONFIGURATION

The rollup solar array for the artificial "G" condition consists of the same structural geometry as that of the zero "G" configuration, however, only four membrane strips are utilized-- the two on each side of and adjacent to the extendible boom. The derived finite model of the artificial "G" array is presented in Figure 5-54. Average tension in each strip during spin is increased to 340 pounds and the strips lateral deflection stiffness values are based upon this tension. The stiffness matrix for each finite element of the extendible boom was computed by hand so as to include the beam columning effect and input into the NASTRAN program by the "direct matrix input" method. Additional structural restraints are provided at the extremities of the inner boom for this spin condition and were included in the dynamic model. The stiffness matrix for the entire model was formulated by NASTRAN and the coriolis force coefficient and centrifugal force coefficient matrices were generated by hand computations. The configuration was taken to spin in a plane containing the solar arrays. These matrices, together with the mass matrix were input in the JPL program (References 5.8 and 5.9). A list of all resulting modal data for spin rates of 0, 4, 8, and 12 RPM are presented in Appendix A of this report. A list of data for those modes which were identified to have large load participation (zero spin) are presented in Table 5-21. The modal constraint forces used in the calculation of participation factor were those resulting at each point of array restraint. Table 5-22 lists the frequencies of these modes with large participation factors for each

TABLE 5-20 ROLLUP SOLAR ARRAY MODAL DATA, ZERO "G" CONFIGURATION

Direction	Type	Mode No.	Frequency (Hz)	Generalized Mass (lb. -sec. ^{2}/ in.)	Modal Participation Factor		
					Force	Bending Moment	Torque
Out of Plane	Symmetric	1	.0925	1.36	.681	.415	
		6	.187	1.30	.003	.044	
		22	.835	.158	.119	.001	
	Anti-Symmetric	1	.0640	.609			.779
		6	.167	.547			.074
		11	.241	.689			.078
In Plane	Symmetric	26	1.35	.705	.520		
		27	3.28	.770	.165		
		28	3.49	.607	.058		
		31	6.07	.104	.062		
	Anti-Symmetric	1	.0974	1.35	.712	.514	
		6	.189	1.41	.001	.137	
		11	.265	1.46	.077	.105	
		16	.324	1.83	.055	.084	

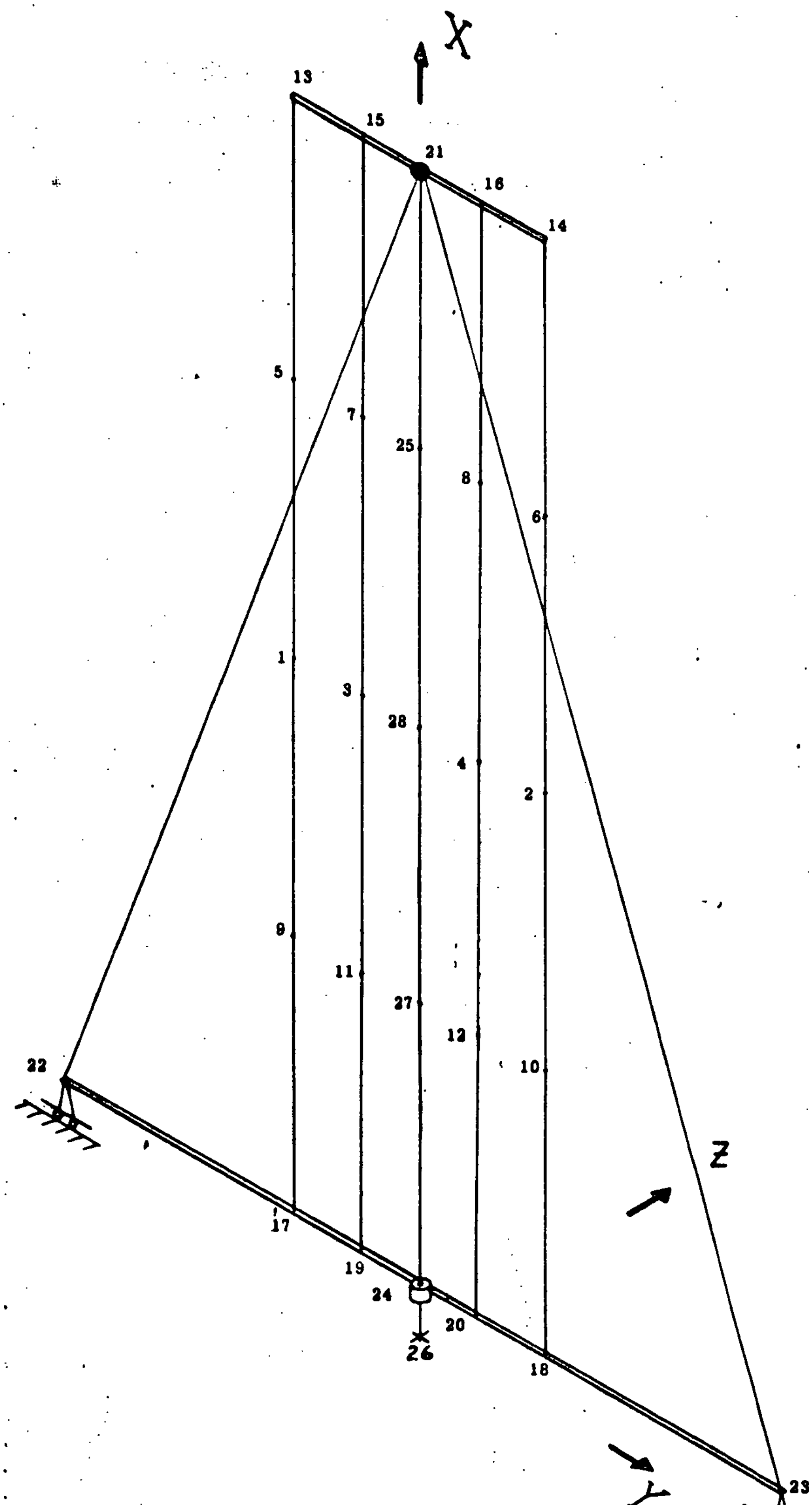

Figure 5-54
SOLAR ARRAY ARTIFICIAL "G" STRUCTURAL MODEL

Table 5-21 Artificial "G" Solar Array,

Modal Participation Factors

Zero Spin

Out of Plane

Symmetric				Antisymmetric		
Mode	Frequency (Hz.)	% Participation Shear	% Participation Moment	Mode	Frequency (Hz.)	% Participation Moment
2	0.203	41.9	15.2	1	0.199	12.5
9	0.504	1.7	0	10	0.521	1.4
17	0.778	2.1	0	18	0.794	2.0
				19	0.905	78.6

In Plane

Symmetric			Antisymmetric			
Mode	Frequency (Hz.)	% Participation Shear	Mode	Frequency (Hz.)	% Participation Shear	% Participation Moment
32	3.84	76.5	3	0.378	33.2	30.0
			11	0.704	0.5	9.6
			20	0.935	4.7	7.0
			28	1.065	7.6	17.7

TABLE 5-22

ART "G" SOLAR ARRAY CONFIGURATION

LIST OF EIGENVALUES IN HERTZ

ELASTIC MODE NO.	NASTRAN RESULTS $\Omega=0$	"GUPTA" PROGRAM RESULTS			
		$\Omega=0$	$\Omega=4$ RPM	$\Omega=8$ RPM	$\Omega=12$ RPM
1	0.1989	0.1786	0.1786	0.1787	0.1787
2	0.2032	0.1977	0.1977	0.1977	0.1977
3	0.3784	0.3768	0.3710	0.3524	0.3185
9	0.5037	0.5031	0.5025	0.5025	0.5025
10	0.5215	0.5142	0.5151	0.5151	0.5151
11	0.7045	0.7010	0.6969	0.6881	0.6716
17	0.7782	0.7774	0.7777	0.7777	0.7777
18	0.7941	0.7912	0.7911	0.7911	0.7911
19	0.9051	0.9047	0.9049	0.9049	0.9049
20	0.9349	0.9315	0.9291	0.9224	0.9090
28	1.0654	1.0544	1.0506	1.0454	1.0331
32	3.8422	3.8402	3.8413	3.8441	3.8462

Modes 1, 2, 9, 10, 17, 18, 19 are out-of-plane modes.

Modes 3, 11, 20, 28, 32 are in-plane modes.

of the considered spin rates. It is noted that out-of-plane modal frequencies are invariant with spin rate; this is due to the coriolis forces and centrifugal forces not coupling these associated motions. The in-plane modal frequencies are seen to be significantly influenced by spin rate. The zero spin frequency of mode No. 3, whose zero spin natural frequency is nearest to the highest spin frequency considered, is reduced considerably (15%) at $\Omega = 12$ RPM. It is to be emphasized that the membrane (strip) tension was considered invariant for all spin rates considered and corresponded to the LMSC average tension specified for 4 RPM. Higher spin rates would decrease this average tension, thereby further reducing frequency.

It is noted that the fundamental mode frequency obtained by the NASTRAN program is significantly different than obtained by the JPL program and cannot be explained at this time. Dr. K. K. Gupta of JPL (private communications) relates the numerical accuracies afforded by digital computers are not sufficient to accurately obtain this modal frequency by the "Givens" eigenvalue-eigenvector extraction method, contained in the NASTRAN program.

5.3 REFERENCES

Ref. 5.1 Rosen, Richard, "STARDYNE User's Manual", Mechanics Research, Inc. Document, Los Angeles, California, January, 1970.

Ref. 5.2 "Proposal for Large Space Station Solar Array Technology Evaluation Program - Vol. I.", LMSC A96774, Lockheed Missile and Space Company Report.

Ref. 5.3 Coyner, J. V. and Ross, R. G., "Analysis of Performance Characteristics and Weight Variations of Large Area Roll-Up Solar Arrays", 69-WA/Ener-11, paper presented at the ASME Winter Annual Meeting, Nov. 16-20, 1969, Los Angeles, California.

Ref. 5.4 Martin, H. C., "On the Derivation of Stiffness Matrices for the Analysis of Large Deflection and Stability Problems," Proceedings on Conference, Matrix Methods in Structural Mechanics, AFFDL-TR-66-80, October, 1965.

Ref. 5.5 "Quarterly Report No. 3, Rollup Subsolar Array", General Electric Company Report No. GE-SSO-69SD4373, December 15, 1969.

Ref. 5.6 "Third Quarterly Report - Large Area Solar Array", The Boeing Company Report No. D2-113355-3, July 1967.

Ref. 5.7 "Modular Space Station-Phase B Extension, First Quarterly Review", North American Rockwell, Space Division, PDS-71-2, May 1971.

Ref. 5.8 K. K. Gupta, "Eigenvalues of (B - A*) Y=O with Positive Definite Band Symmetric B and Band Hermitian A* and its Application to Natural Frequency Analysis of Flexible Space Vehicles," Space Program Summary 37-60, Volume 3, Jet Propulsion Lab, Pasadena, California, December 1969.

Ref. 5.9 K. K. Gupta, "Free Vibration Analysis of Spinning Structural Systems," International Journal for Numerical Methods in Engineering, to be published.

Ref. 5.10 Patel, J. A., and Seltzer, S. M., "Complex Eigenvalue Solution to a Spinning Skylab Problem," NASTRAN: USERS EXPERIENCES, NASA TMX-2378, September 1971.

Ref. 5.11 "The NASTRAN Users Manual," NASA SP-222, Section 3-4, 1970, Office of Technology Utilization, NASA, Washington, D. C.

6. SIMULATION VERIFICATION ANALYSIS

Various simplified analyses were performed to verify the formulated interactions computer program and contained methodology. These analyses were divided into two parts--one part to verify the structural dynamics methodology used (Reference 6-1) and to gain some insight into the accuracy of this methodology, and the other part to verify the various subroutines or subprograms contained within the simulation.

6.1 STRUCTURAL DYNAMICS VERIFICATION

6.1.1 SIMULATION OF FLEXIBLE APPENDAGES & RIGID SPACE STATION

A planar problem considering a structural arrangement of two uniform beams representing flexible appendages and connected to a rigid space station mass (taken to be zero) was formulated and analyzed for interaction (interface) forces caused by an applied step force. The closed form solution to this problem is presented in Reference 6-2 when using a finite number of orthogonal cantilever modes as flexible appendage degrees-of-freedom. As represented in the simulation program, this structural arrangement of two cantilevers simulates a free-free beam (Figure 6-1).

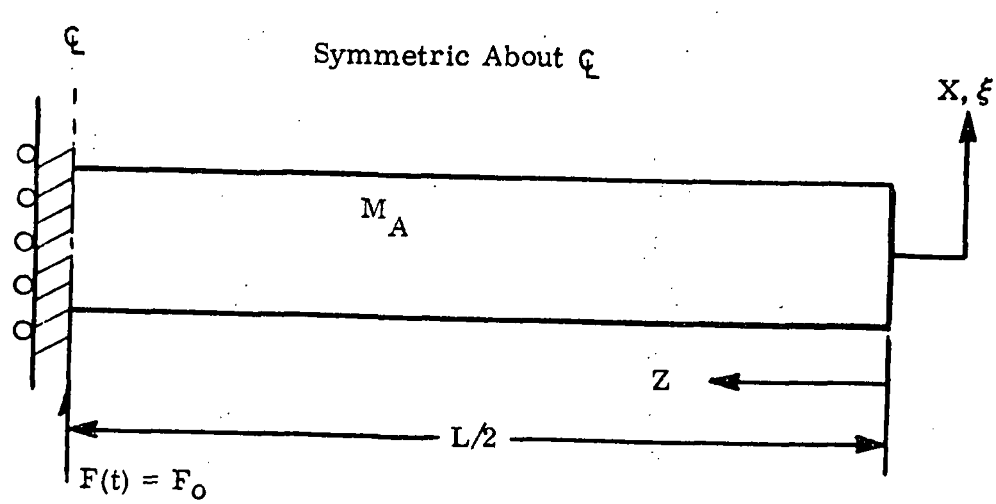

Figure 6-1. Cantilever Beam Simulation of a Free-Free Beam

An orthogonalization of the coupled motion equations of the two cantilever beams (appendages), which are formulated within the simulation from the input data, produces the comparisons shown in Figure 6-2 and Table 6-1. Figure 6-2 presents the comparison of the resulting orthogonal deflection shapes using three cantilever mode degrees-of-freedom for each beam appendage and theoretical free-free beam shapes obtained from Reference 6.3.

TABLE 6-1

Frequency Comparison of (Uniform Beam) Cantilever + Rigid Body Mode Representation of a Free-Free Uniform Beam

Frequency Ratios: f_n/f_1 free-free

Reference Frequency Ratios			Calculated Coupled Mode Frequency Ratios				
Symmetric Mode No., n	Free-Free Beam	Uncoupled Cantilever Beam	1 Mode Cantilever Beam + Rigid Body	2 Mode Cantilever Beam + Rigid Body	3 Mode Cantilever Beam + Rigid Body	4 Mode Cantilever Beam + Rigid Body	5 Mode Cantilever Beam + Rigid Body
1	1.000	0.632	1.0101	1.0006	1.0003	1.0000	1.0000
2	5.404	3.958	---	5.548	5.420	5.408	5.405
3	13.344	11.074	---	---	13.749	13.410	13.367
4	24.814	21.652	---	---	---	25.584	24.965
5	39.812	35.861	---	---	---	---	41.030

Table 6-1 presents the comparison of resulting frequencies using a varied number of cantilever mode degrees of freedom for each beam appendage with theoretical free-free beam frequencies.

These comparisons show the adequacy of the structural dynamics methodology that has been used in the interactions simulation; the degree of accuracy in the approximation is seen to be dependent upon the number of cantilever modes used. Transient load responses were obtained for this structural system using the formulated computer program with all control systems inactive. Each of the cantilever beam modes was input into the program by modal descriptions of 25 discrete mass points representing 50 inertial degrees of freedom. A step force was applied at the zero-mass space station C.G. The shear force at the 1/4 span of the free-free arrangement, as obtained by the simulation, is compared with results obtained by Reference 6.4 in Figure 6.-3. The entire free-free structural configuration (2 connected cantilevers) was modeled by 40 discrete mass points for input into the "direct transient method" of Reference 6.4. Comparisons are seen to be good, and as expected, higher frequency transients result in the force history obtained by Reference 6.4 since all system modes of vibration are represented. Another comparison is provided for the simulation results in Reference 6.2 and reproduced in Figure 6-4. A variable order Adams numerical integration method and the first five symmetric free-free beam modes were used to obtain the 1/4 span shear force resulting from a step input. Again, the comparison shows the simulation results to be very comparable.

6.1.2 SIMULATION OF RIGID APPENDAGES AND RIGID SPACE STATION

A simple planar problem was formulated to show verification of the rigid body dynamics solutions given by the simulation. This formulation consisted of two simulated rigid appendages connected to a simulated rigid space station and perturbed by a step force. The resulting appendage interaction forces and moments given by the simulation are compared to the exact result in Figure 6-5.

6.1.3 SIMULATION OF FLEXIBLE APPENDAGES AND FLEXIBLE SPACE STATION

A planar problem was formulated for verification purposes and consisted of three uniform beams forming a "T" arrangement (Figure 6-6). This arrangement is representative of a flexible center body (space station) and two flexible appendages (solar arrays). Stiffness and mass properties of each beam were chosen so that the center beam had an uncoupled fundamental free-free axial deflection mode frequency of 1 Hz and that the appendage beams had an uncoupled fundamental cantilever bending frequency of 1 Hz. Initially, results were obtained from the simulation and by hand calculations using the same simulated methodology (Reference 6.2) considering one cantilever mode of each flexible appendage and a rigid center body. Corresponding shear and moment interaction histories are presented in Figure 6-7. It is seen that the solutions are coincident at time zero but are slightly different in amplitude and phase. This is attributable to integration interval used (Δt = 0.05 sec.) together with the NASTRAN numerical integration algorithm (Reference 6.4) which is coded in the simulation computer program. Although not directly applicable to the above formulated problem, the variation of amplitude, frequency and phase errors with integration sample rate per cycle of the highest system frequency resulting from use of this algorithm, were determined for a five cantilever mode representation of the flexible appendages and are presented in Figure 6-8. A higher degree of required simulation solution accuracy than that shown in Figure 6-7 therefore requires the use of a smaller integration interval.

Several methods of obtaining interaction moment solutions of the formulated problem, with the flexibility of the center body included, were used and compared with the simulation results to show the adequacy of the methodology. These solutions, together with that obtained from the simulation program are presented in Figure 6-9. Modal solutions of the structural arrangement considered as a system were obtained by the transient response solution method provided in Reference 6.5 and an independent method utilizing a variable order Adams integration method. The results shown using system modes utilize one rigid body translational degree of freedom and the first four orthogonal elastic modes. Both the modal displacement and modal acceleration methods of load calculation were considered. A solution of interaction moment produced by a coupled system response, as given by the direct transient response method of NASTRAN, is also presented. The finite element model of the "T" beam for input for the above solutions is represented by a total of 79 discrete mass points and complete description of this model and system mode results are given in Reference 6.6. The interaction moment of the "T" beam given by the simulation reflects the use of the first 10 free-free axial deflection modes of the center body and the first two cantilever modes of the flexible appendages. The results obtained by all of the methods compare very well and show the adequacy of the methodology contained in the simulation.

6.1.4 VERIFICATION OF COMPLEX EIGENVALUE-EIGENVECTOR ROUTINE (REFERENCES 6.7 AND 6.8)

As part of the study program effort, a computer program received from the Jet Propulsion Laboratory (References 6.7 and 6.8) and formulated by Dr. K. K. Gupta, was converted for operation on the CDC 6000 Series Computer. This program has the capability of solving for the orthogonal properties of a set of coupled second order equations having non-zero coefficients of the first derivatives of the time dependent variables, which are representative of a finite element structural model in a spinning environment. A simple uniform beam problem was formulated to verify the correctness of program conversion. The finite element model and results from both the converted program and the NASTRAN program, for a zero-spin condition, are shown in Table 6-2. The comparisons show both a comparable method of orthogonalization with the similar techniques of NASTRAN and the verification of the converted program.

6.2 SUBPROGRAM VERIFICATION

The various subprograms comprising the complete digital simulation of the space station and solar arrays were verified for correctness of formulations by a number of program executions with simple structural arrangements and initializations. Each of the program executions was performed with the derived simulation of the first study phase which is described in References 6.9 and 6.10. This simulation considers the flexible dynamics of appendages and only the rigid body dynamics of the space station. The simulation resulting from the second study phase and described in Report Section 4 utilizes many of the same subprograms; and therefore, the performed subprogram verification is taken to be a partial verification of the Phase II digital simulation.

The total subprogram verification is represented by the following outline. Verification of each of the given program output quantities is made by comparison with hand computed results.

SYSTEM RIGID BODY MOTION

- Space Station Rigid Body Motion

  X-, Y-, and Z- translations: due to a force input to space station

  θ_X-, θ_Y-, and θ_Z- rotations: due to a force input to space station

  Disturbance force input variations for check of interpolation procedure

  Location variation of disturbance force, {LR}

- Solar Array Rigid Body Motion

  Sun Vector Misalignment, {Sun}

  Initial Attitude Error {EULER (7)}, {EULER (8)}

  Solar Array Drive Selection {RBC (1)}, {RBC (2)}

  θ_X- and θ_Z- rotations: due to a force input to space station.

SPACE STATION CONTROL DYNAMICS

- Response to Reaction Jet Control Torques

  Threshold not exceeded, i.e., $\theta_\epsilon < 1/2^\circ$ {EULER (1-6)}

  Threshold exceeded, i.e., $\theta_\epsilon > 1/2^\circ$

  Variable SS guidance commands, {SSGTIME}, {DELTSSG}

- Response to CMG Control Torques

  Threshold not exceeded, i.e., $T_{CMG_{REG'D}} < T_{CMG_{LIMIT}}$
  {EULER (1-6)}

  Threshold exceeded, i.e., $T_{CMG_{REG'D}} > T_{CMG_{LIMIT}}$
  {EULER (1-6)}

  Variable SS guidance commands, {SSGTIME}, {DELTSSG}

SOLAR ARRAY CONTROL DYNAMICS

- <u>Linear OCS Response</u>

  Solar Array Drive Gear-train variation, {GEARKON}
  Sun Vector Misalignment, {Sun}
  Initial Attitude Error, {EULER (7)} , {EULER (8)}
  Variable SA guidance commands, {SAGTIME} , {DELTSAG}

- <u>Non-Linear OCS Response</u>

  Solar Array Drive Gear-train variation, {GEARKON}
  Threshold not exceeded, i.e., $\theta_\epsilon < 5^o$ } {EULER (7-8)}
  Threshold exceeded, i.e., $\theta_\epsilon > 5^o$ }
  Variable SA guidance commands, {SAGTIME} , {DELTSAG}

SYSTEM ELASTIC BODY MOTION

- <u>Solar Array Modal Response, DEBUG (20) = .F.</u>

  Cantilever Dynamics, {RBC (1) = .T.} , {RBC (2) = .T.}
  Pinned-joint Dynamics, {RBC (1) = .F.} , {RBC (2) = .F.}
  Initial SA attitude error, {EULER (7)}, {EULER (8)}
  Variable SA guidance commands, {SAGTIME} , {DELTSAG}

- <u>Orbital Mechanics</u>

  Semi-major axis variation, {A}
  Orbit Eccentricity variation, {E}
  Orbit Inclination variation, {INC}
  Orbit Initialization point, {M}, {P}, {N}

  } No SS or SA Control

The above bracketed quantities are variable names used in the various subprograms and are defined in Reference 6.9.

6.3 REFERENCES

6.1 "Dynamics and Control of Flexible Space Vehicles," P. W. Likens, NASA CR 105592.

6.2 "Integrated Dynamic Analysis of a Space Station, with Controllable Solar Arrays," J. A. Heinrichs, et al, paper presented at the 42nd Shock and Vibration Symposium.

6.3 D. Young and R. P. Felgar, Jr., "Tables of Characteristic Functions Representing Normal Modes of Vibration of A Beam," University of Texas Publication No. 4913, 1 July 1949.

6.4 "The NASTRAN Theoretical Manual," NASA-SP-221, Section 11.3, 1970., Office of Technology Utilization, NASA, Washington, D. C.

6.5 "The NASTRAN Users Manual," NASA SP-222, Sections 3.10 and 3.13, 1970., Office of Technology Utilization, NASA, Washington, D. C.

6.6 "The Study of Dynamic Interactions of Solar Cell Arrays with Space Stations and the Development of Solar Array Structural Requirements," Fairchild Industries/FSED Monthly Progress Report for October 1971, NASA/LRC Contract NAS5-10155.

6.7 K. K. Gupta, "Eigenvalues of $(B-\lambda A^*)$ Y=0 with Positive Definite Band Symmetric B and Band Hermitian A^* and its Application to Natural Frequency Analysis of Flexible Space Vehicles," Space Programs Summary 37-60, Volume 3, Jet Propulsion Lab, Pasadena, California, December 1969.

6.8 K. K. Gupta, "Free Vibration Analysis of Spinning Structural Systems," International Journal for Numerical Methods in Engineering, to be published.

6.9 "Solar Array-Space Station Dynamic Interaction Analysis, Digital Simulation Documentation Users Manual," prepared by Fairchild Hiller Corporation, SESD, February 26, 1971, under NASA/LRC Contract NAS5-10155.

6.10 "Interim Report, The Study of Dynamic Interactions of Solar Arrays with Space Stations and Development of Array Structural Requirements," Fairchild Industries Report 858-IR-1, February 1971, Fairchild Industries, Germantown, Maryland.

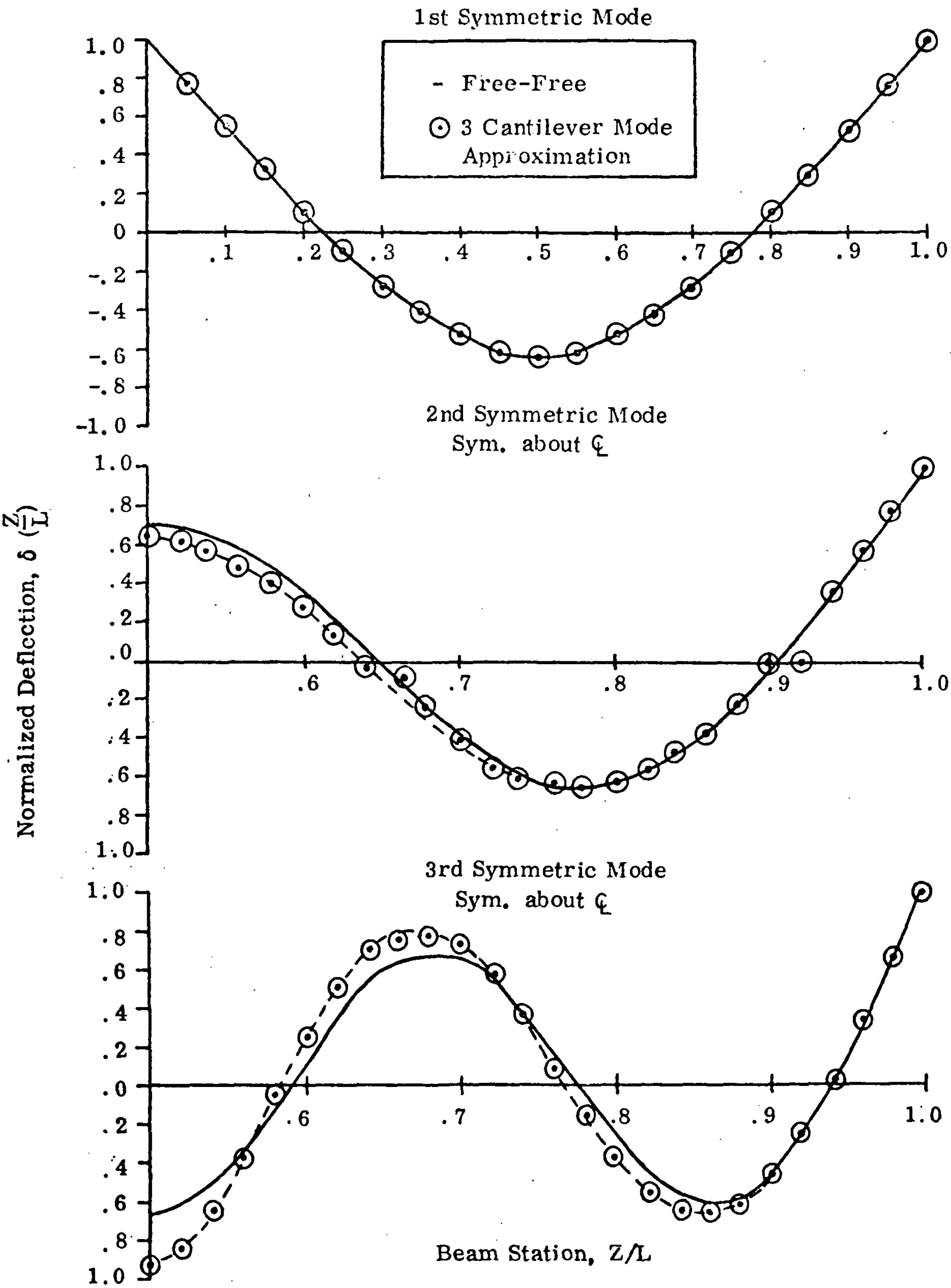

Figure 6-2. Comparison of Mode Shapes for a Free-Free Uniform Beam and a 3 Cantilever Mode Approximation

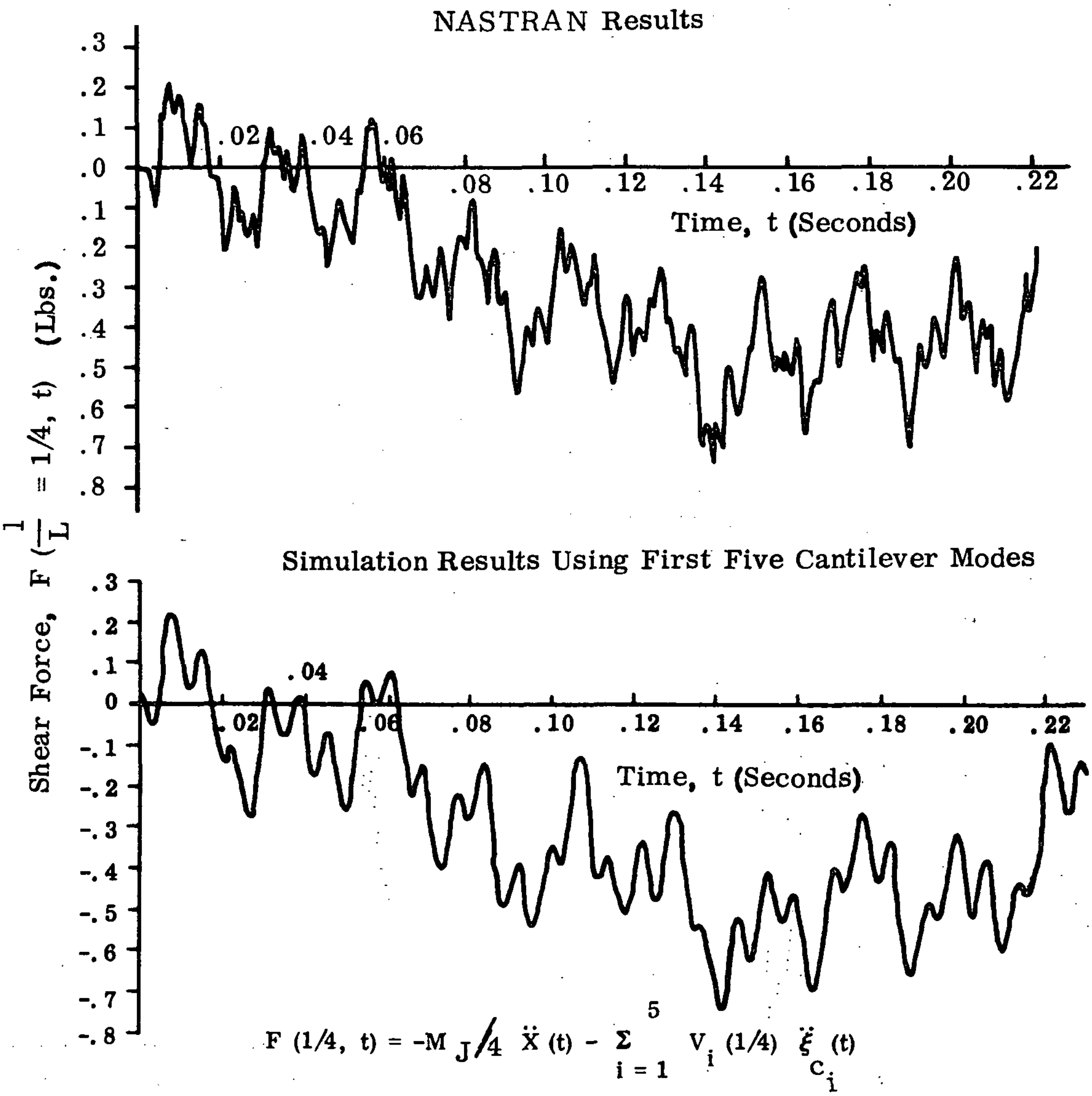

Figure 6.3 Uniform Beam Comparisons of Shear History at 1/4 Span for a Unit Step Force Applied at Mid-Span

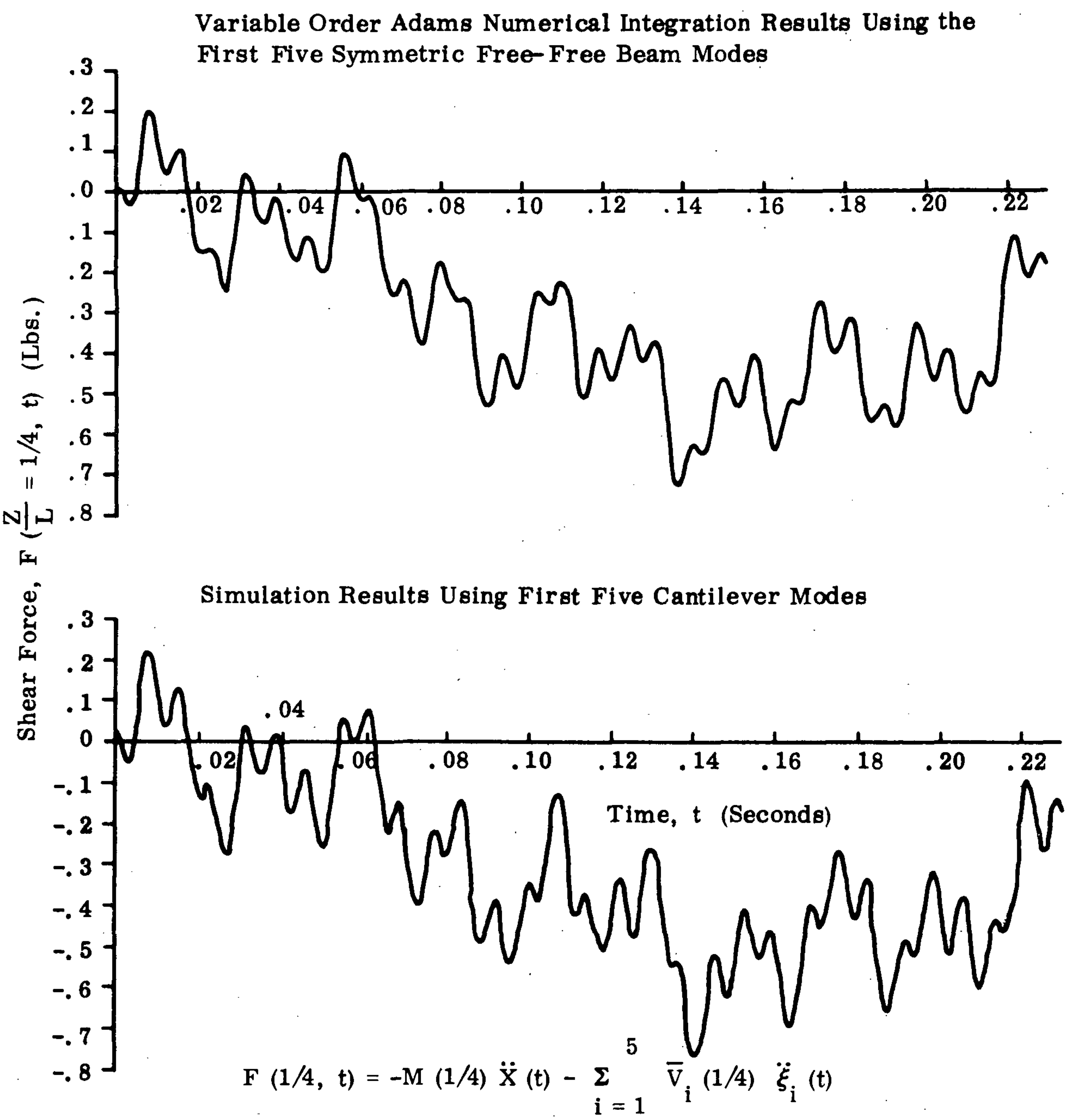

Figure 6-4. Uniform Beam Comparisons of Shear Histories @1/4 Span for a Unit Step Force Applied at Mid-Span

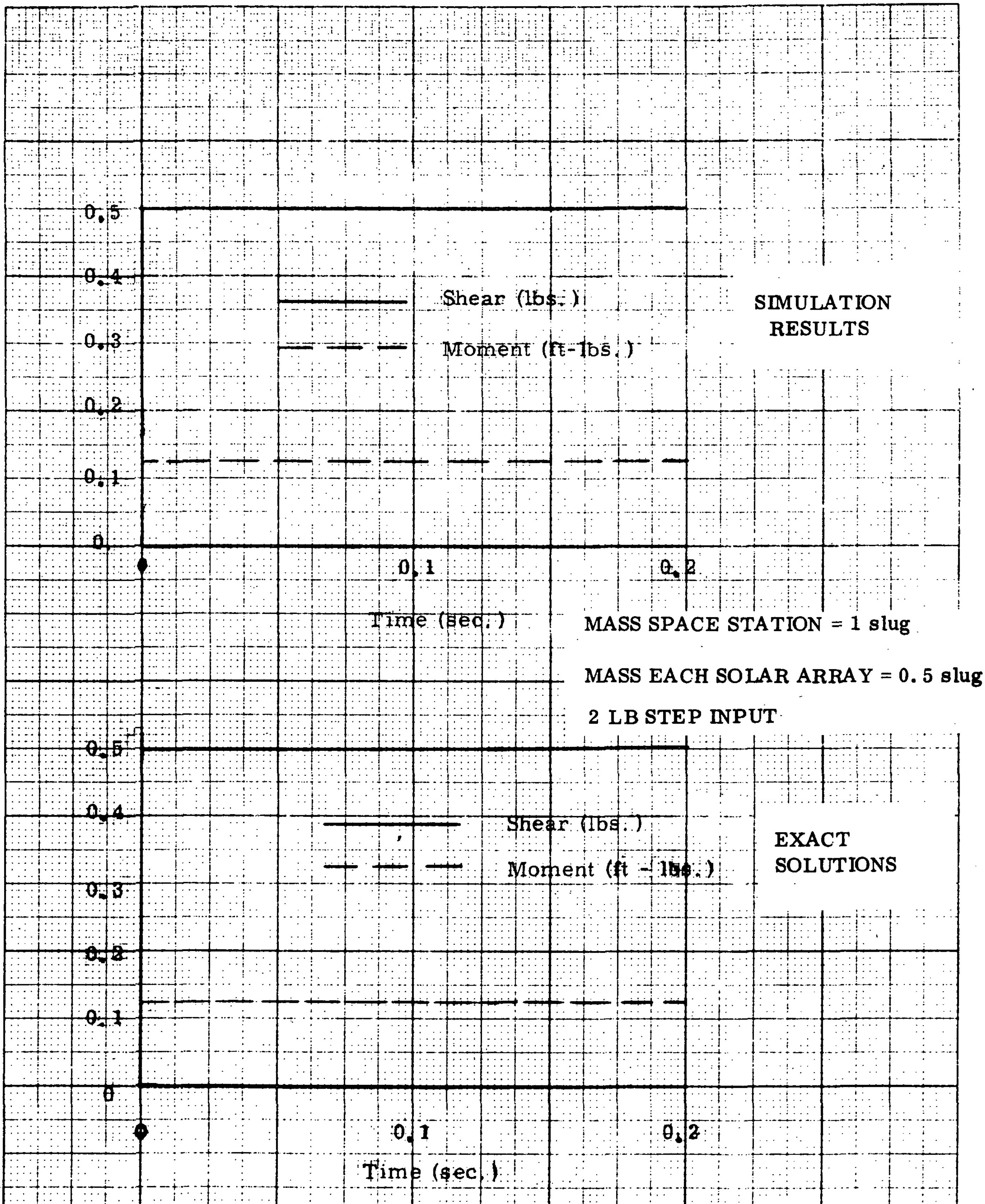

FIGURE 6-5. Interaction Shear and Moment

Beam	length (in)	No. of Nodes	EA (lbs.)	EI ($lb\text{-}in^2$)	Mass ($lb\text{-}sec^2/in$)	Mass/Node * ($lb\text{-}sec^2/in$)
I	12	27	2.	---	0.0416	.0016
II	6	26	-	28.4	0.0416	.0016

* nodes 1, 27, 53 have no mass

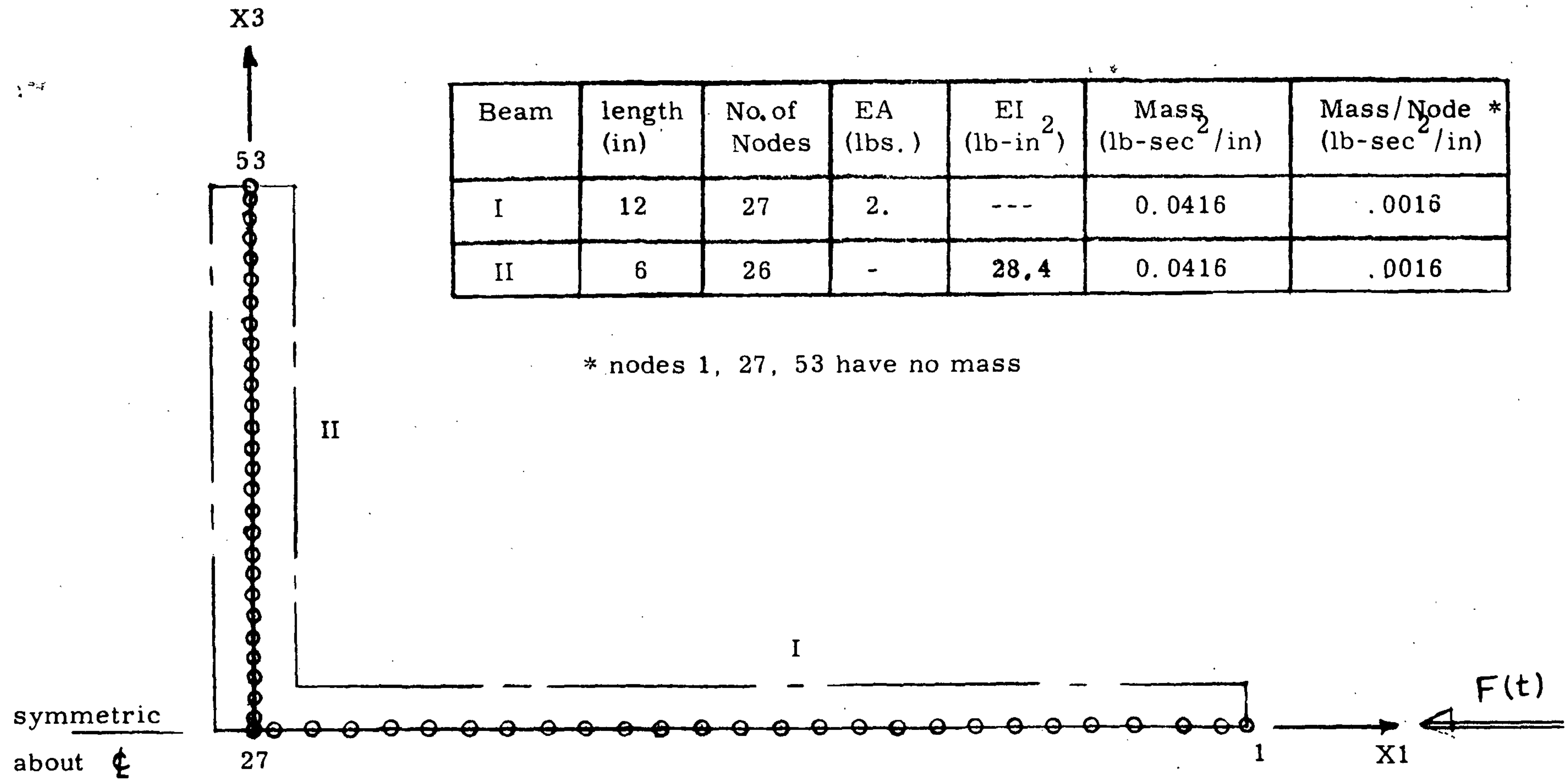

Figure 6-6. T-Beam Structural Model

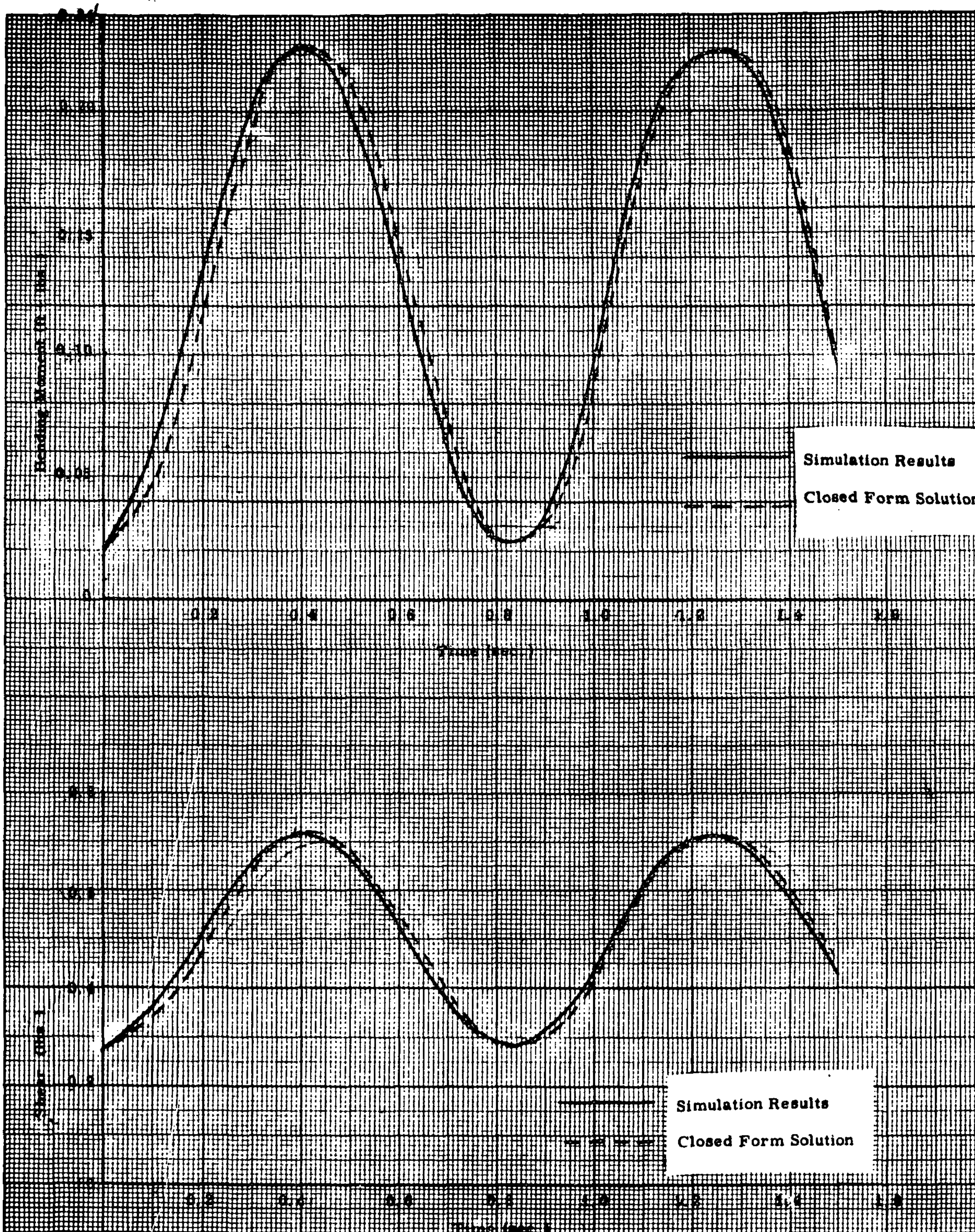

RIGID CENTER BODY AND ONE MODE REPRESENTATION OF FIXED APPENDAGES PERTURBED BY A STEP FORCE HISTORY

Figure 6-7 Interaction Forces vs. Time

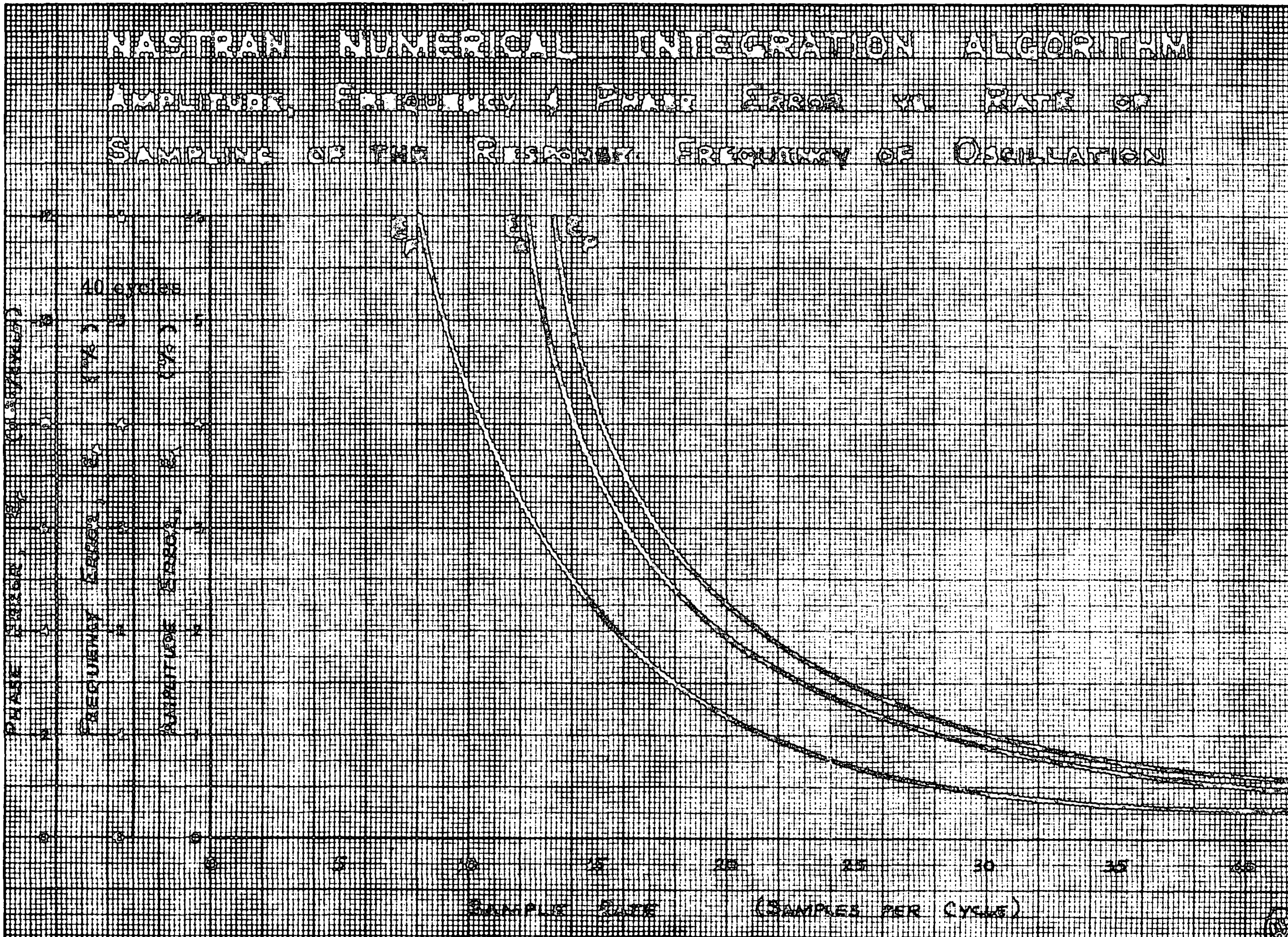

NASTRAN NUMERICAL INTEGRATION ALGORITHM
40 cycles
SAMPLE RATE (SAMPLES PER CYCLE)

Figure 6-8

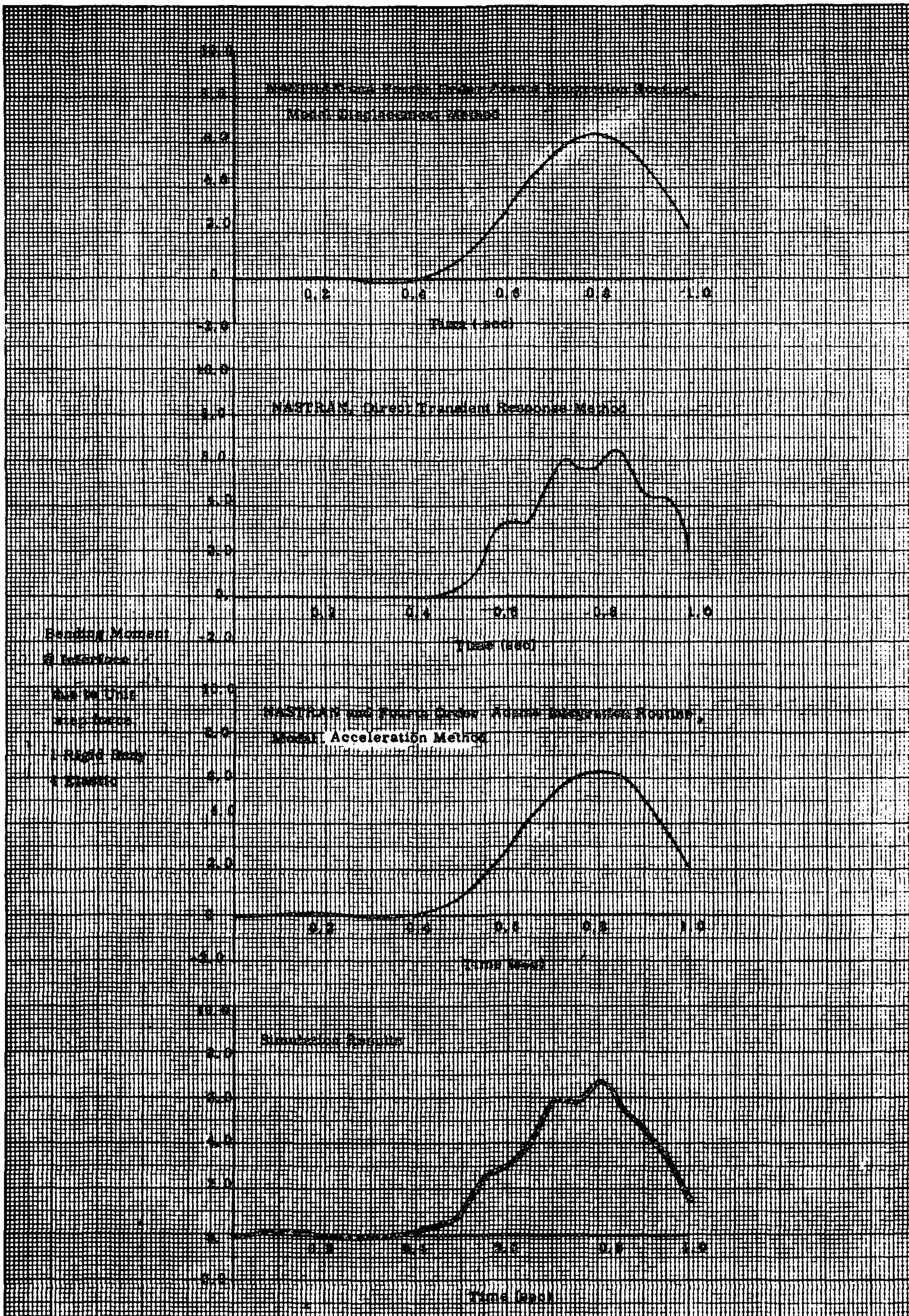

Fig. 6-9. "T" Beam Transient Analysis

TABLE 6-2

COMPARISON OF NASTRAN AND GUPTA EIGENVALUE SOLUTIONS FOR CANTILEVER BEAM

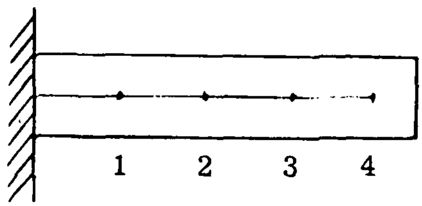

$$MASS/IN. = 0.01 \frac{LB.\ SEC.^2}{IN.^2}$$

$$EI = 1 \times 10^7 \ LB.IN.^2$$

FREQUENCY COMPARISON (RAD./SEC.)

MODE	GUPTA	NASTRAN
1	55.5344	55.5349
2	357.7820	357.8042
3	1009.7656	1010.5280

MODE SHAPE COMPARISON

POINT #	MODE 1		MODE 2		MODE 3	
	GUPTA	NASTRAN	GUPTA	NASTRAN	GUPTA	NASTRAN
1	0.0925	0.0925	-0.5052	0.5052	1.0000	1.0000
2	0.3281	0.3281	-1.0000	1.0000	0.3358	0.3389
3	0.6470	0.6470	-0.5438	0.5438	-0.9656	-0.9724
4	1.0000	1.0000	0.7265	-0.7266	0.4162	0.4270

APPENDIX A

This Appendix presents detailed vibration mode data which were derived for the space station and solar array structural configurations considered in Phase 2. Analytical data are presented for the structural configurations in both Zero "G" and Artifical "G" environments. Explanations of the presented data can be found in Report Section 5. The data are presented in the following appendix sections:

A. 1 VIBRATION MODE DATA
ZERO "G" SPACE STATION CONFIGURATION

CONTENTS

NOTE: Mode shapes shown are elastic mode shapes. Mode 1 in Figure A-2 is the first elastic mode, which corresponds to Mode 7 in Table A-1.

Table A-1, Modal Data, Space Station

(Zero G Configuration)

Mode	Frequency (Hz)		Generalized Mass (lb.-sec.²/in.)
1	0.0	Rigid Body Modes	6.281594E 02
2	0.0		6.281594E 02
3	0.0		6.281594E 02
4	0.0		2.477312E 02
5	0.0		1.244991E 02
6	0.0		1.244991E 02
7	1.557577E 00		2.297717E 02
8	2.277407E 00		3.636589E 01
9	2.278777E 00		3.660057E 01
10	3.147397E 00		8.373244E 01
11	3.245078E 00		1.085563E 02
12	4.391578E 00		1.511882E 02
13	4.483892E 00		3.124590E 02
14	5.702710E 00		7.439223E 01
15	5.035457E 00		7.142155E 01
16	6.477557E 00		8.431511E 01
17	6.875389E 00		1.111700E 02
18	6.875395E 00		1.111700E 02
19	7.765364E 00		5.185711E 01
20	8.263874E 00		1.006247E 02
21	8.850953E 00		
22	8.935523E 00		
23	1.013241E 01		
24	1.130443E 01		
25	1.131781E 01		
26	1.475546E 01		
27	1.534728E 01		
28	1.958418E 01		
29	1.988515E 01		
30	2.277832E 01		
31	2.319455E 01		
32	2.339781E 01		
33	2.342052E 01		
34	2.490974E 01		
35	2.574709E 01		
36	2.658902E 01		
37	2.698954E 01		
38	2.752139E 01		
39	2.941002E 01		
40	2.942180E 01		
41	2.967250E 01		
42	2.967250E 01		
43	2.977396E 01		
44	2.984723E 01		
45	2.984726E 01		
46	2.992293E 01		
47	3.003922E 01		
48	3.005589E 01		
49	3.005730E 01		
50	3.027969E 01		

Structural Model Of Space Station

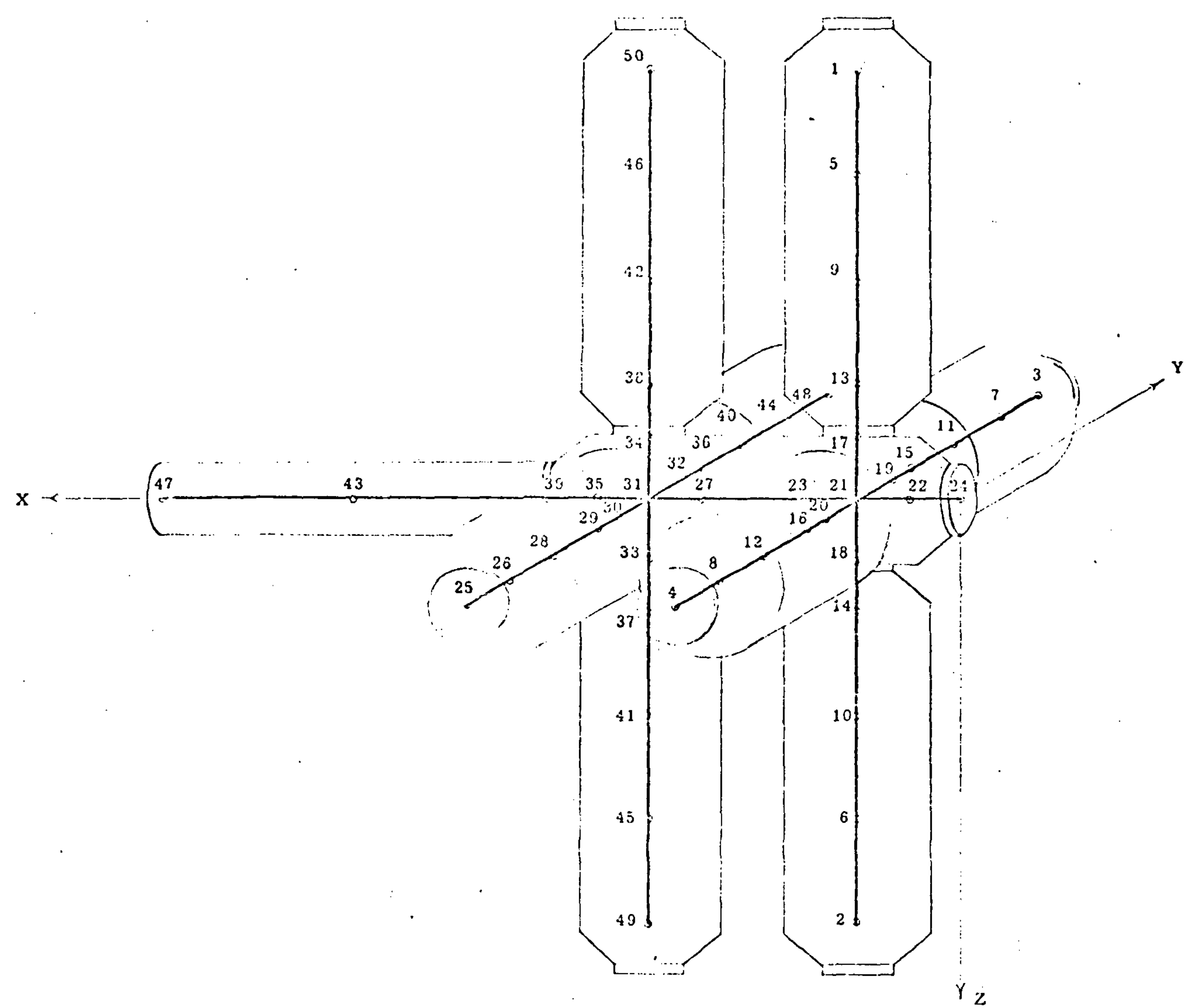

Figure A-1

TABLE A - 2
Listing of Mass - Geometry Data
Of Zero G Space Station

NODE NO.	MASS *	X	Y	Z
1	16.189	120.	0.	-492.
2	16.189	120.	0.	492.
3	16.189	120.	492.	0.
4	16.189	120.	-492.	0.
5	16.189	120.	0.	-372.
6	16.189	120.	0.	372.
7	16.189	120.	372.	0.
8	16.189	120.	-372.	0.
9	16.189	120.	0.	-252.
10	16.189	120.	0.	252.
11	16.189	120.	252.	0.
12	16.189	120.	-252.	0.
13	16.189	120.	0.	-132.
14	16.189	120.	0.	132.
15	16.189	120.	132.	0.
16	16.189	120.	-132.	0.
17	0.	120.	0.	-72.
18	0.	120.	0.	72.
19	0.	120.	72.	0.
20	0.	120.	-72.	0.
21	8.1	120.	0.	0.
22	8.1	60.	0.	0.
23	0.	180.	0.	0.
24	4.05	0.	0.	0.
25	16.189	360.	-492.	0.
26	16.189	360.	-372.	0.
27	12.15	300.	0.	0.
28	16.189	360.	-252.	0.
29	16.189	360.	-132.	0.
30	0.	360.	-72.	0.
31	8.1	360.	0.	0.
32	12.15	360.	72.	0.
33	0.	360.	0.	72.
34	0.	360.	0.	-72.
35	8.1	420.	0.	0.
36	16.189	360.	132.	0.
37	16.189	360.	0.	132.
38	16.189	360.	0.	-132.
39	12.7919	480.	0.	0.
40	16.189	360.	252.	0.
41	16.189	360.	0.	252.
42	16.189	360.	0.	-252.
43	17.4839	700.5	0.	0.
44	16.189	360.	372.	0.
45	16.189	360.	0.	372.
46	16.189	360.	0.	-372.
47	19.086	921.	0.	0.
48	16.189	360.	492.	0.
49	16.189	360.	0.	492.
50	16.189	360.	0.	-492.

* - Mass units are lb-sec^2/in.

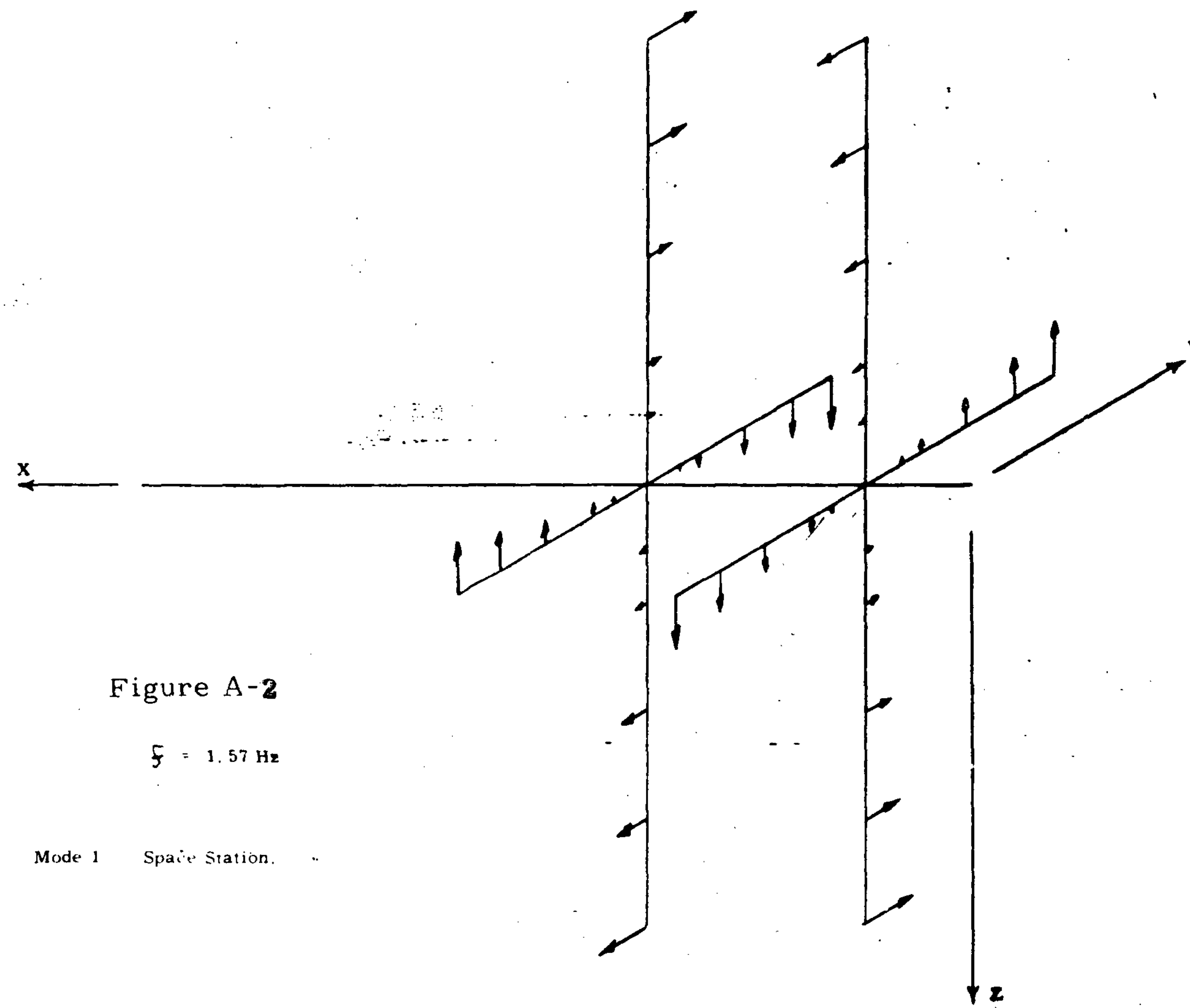

Figure A-2

f = 1.57 Hz

Mode 1 Space Station.

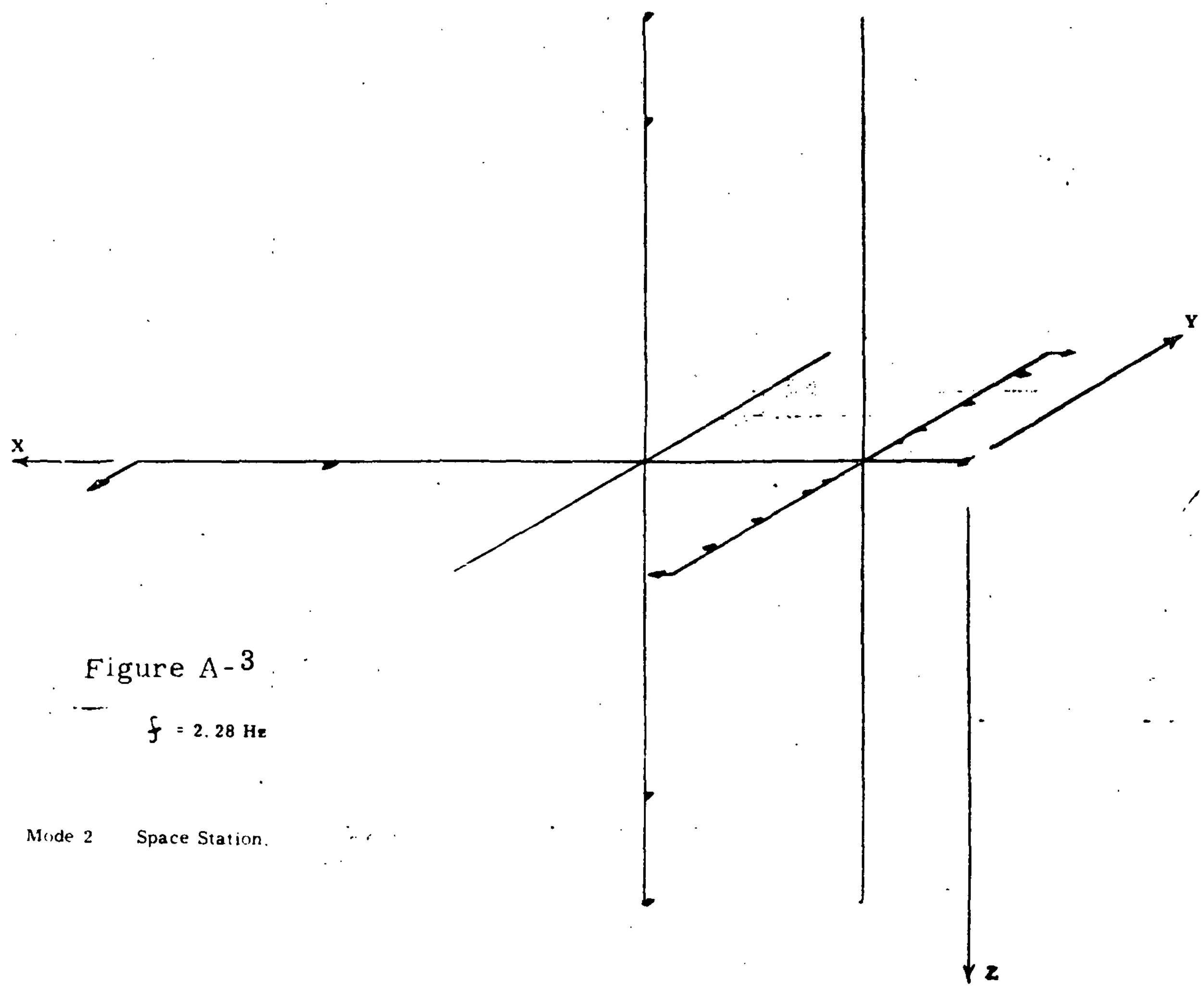

Figure A-3

f = 2.28 Hz

Mode 2 Space Station.

7

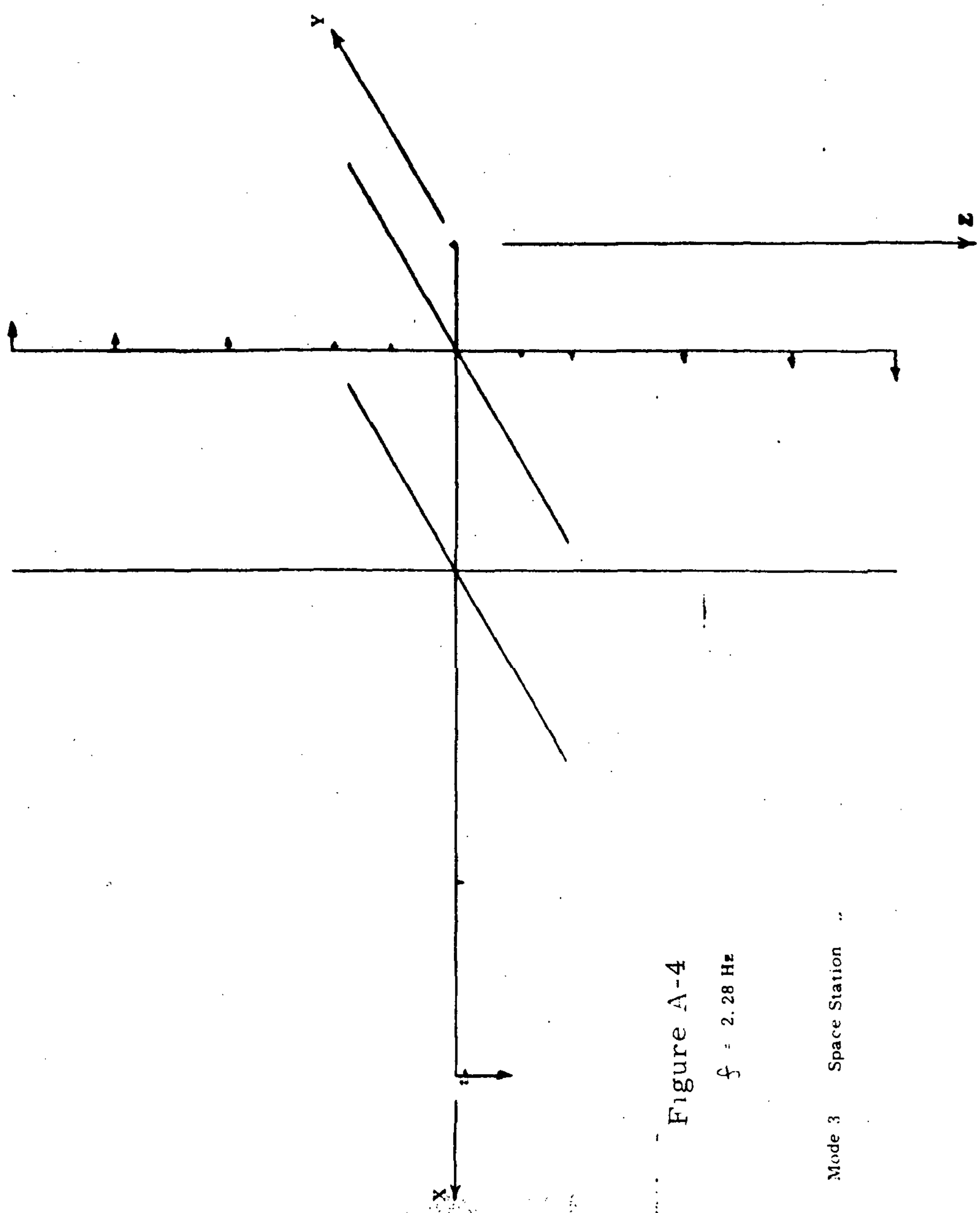

Figure A-4

f = 2.28 Hz

Mode 3 Space Station

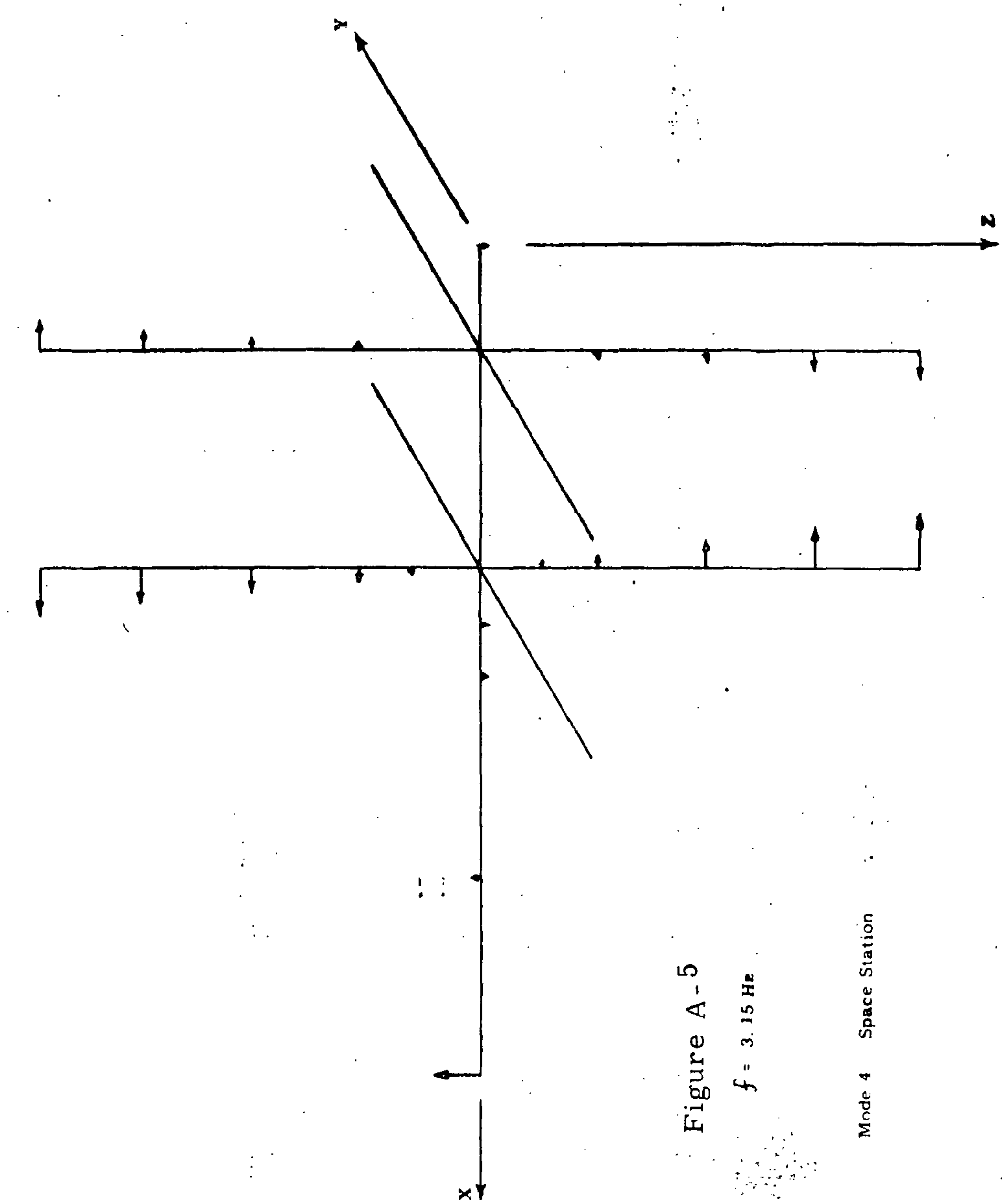

Figure A-5

f = 3.15 Hz

Mode 4 Space Station

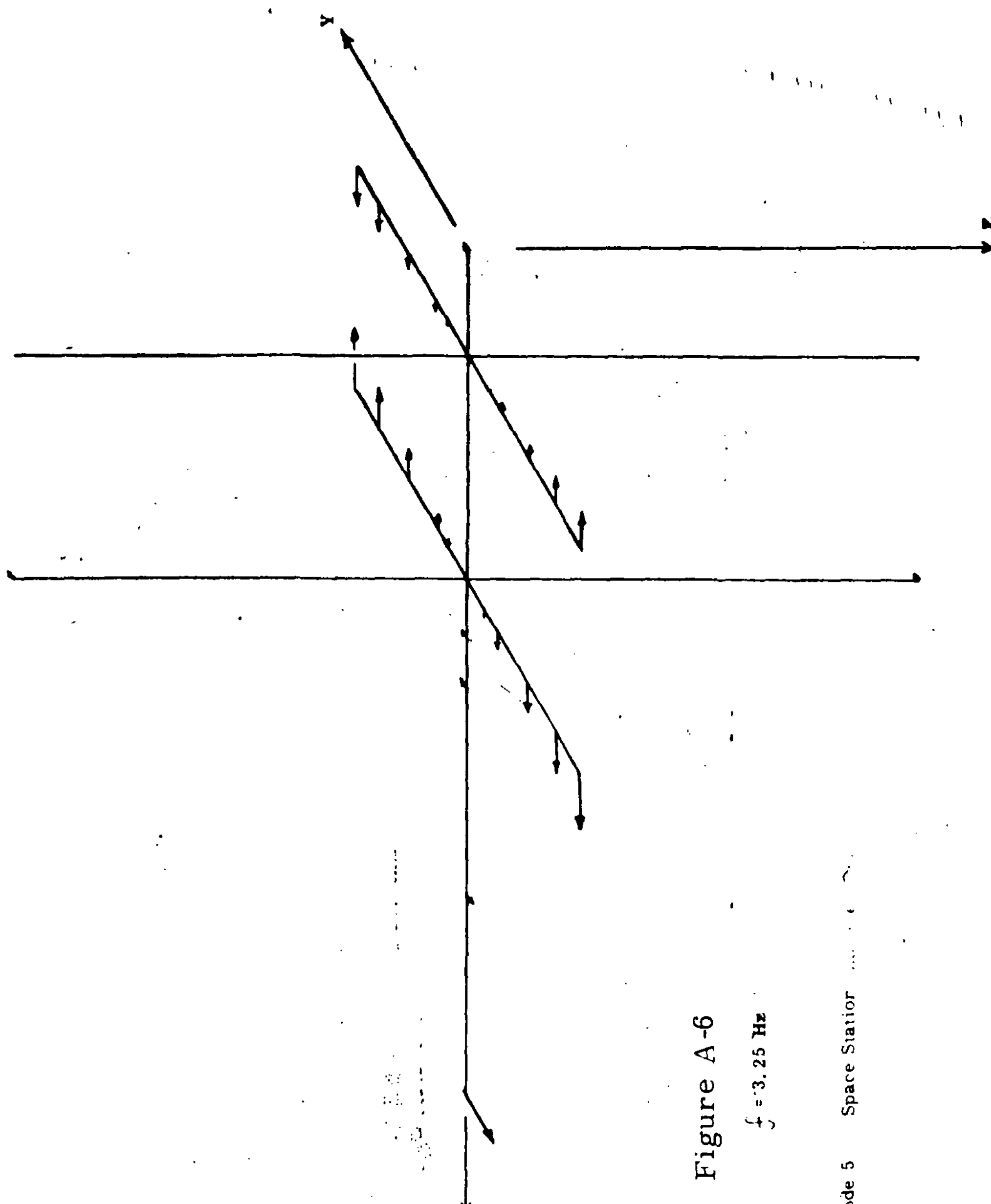

Figure A-6

$f = 3.25$ Hz

Mode 5 Space Station

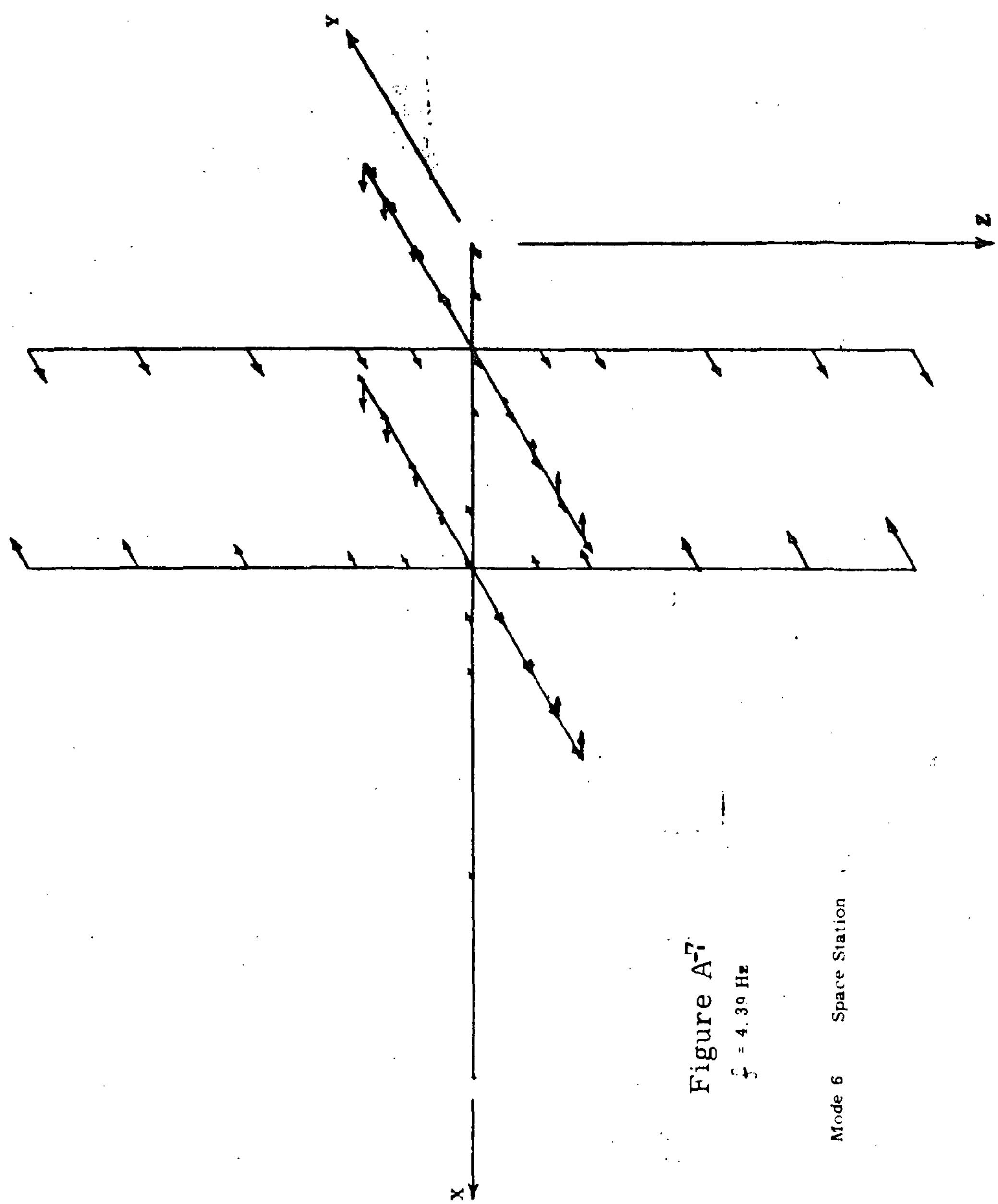

Figure A-7
$f = 4.39$ Hz

Mode 6 Space Station

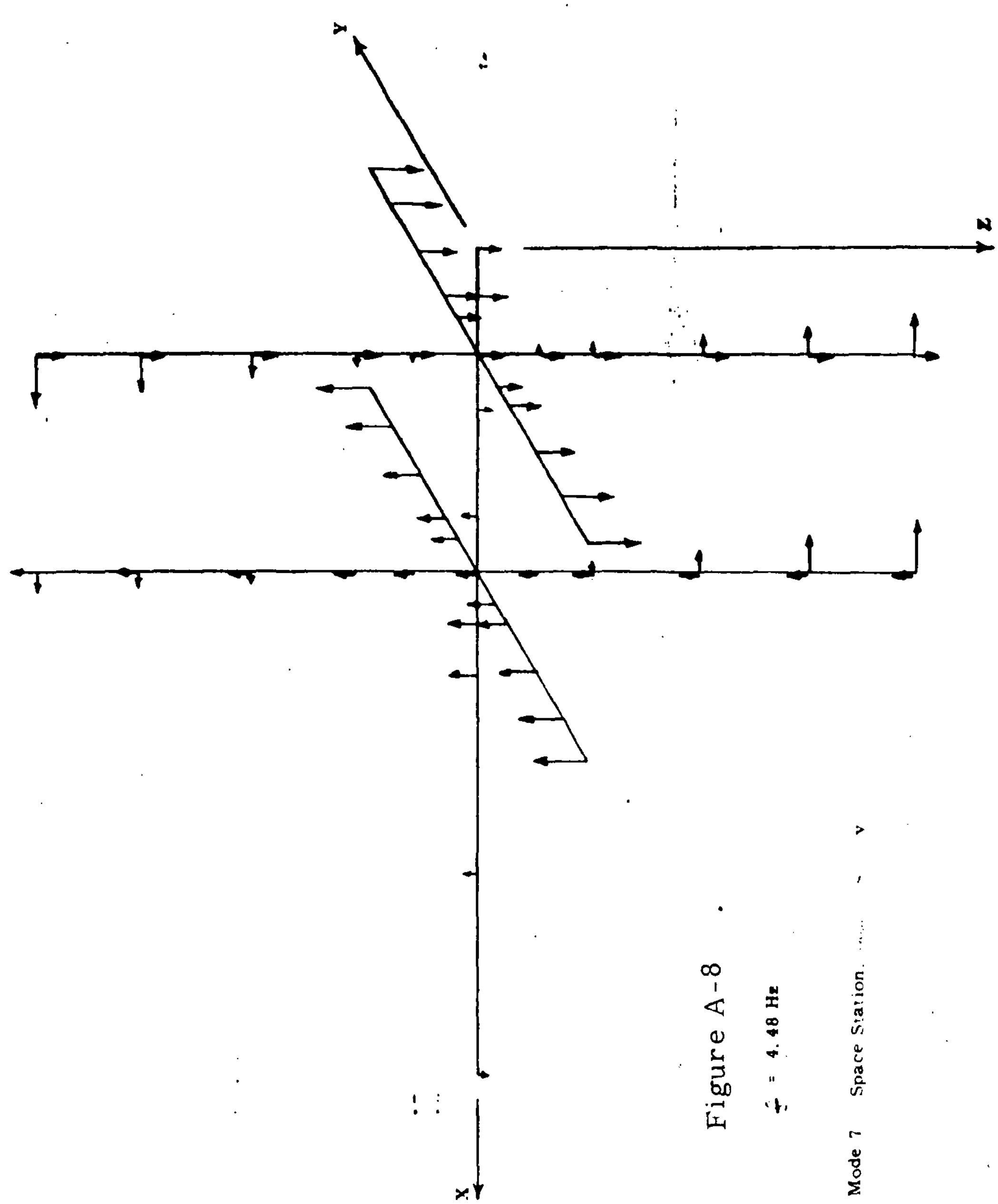

Figure A-8

Mode 7 Space Station. f = 4.48 Hz

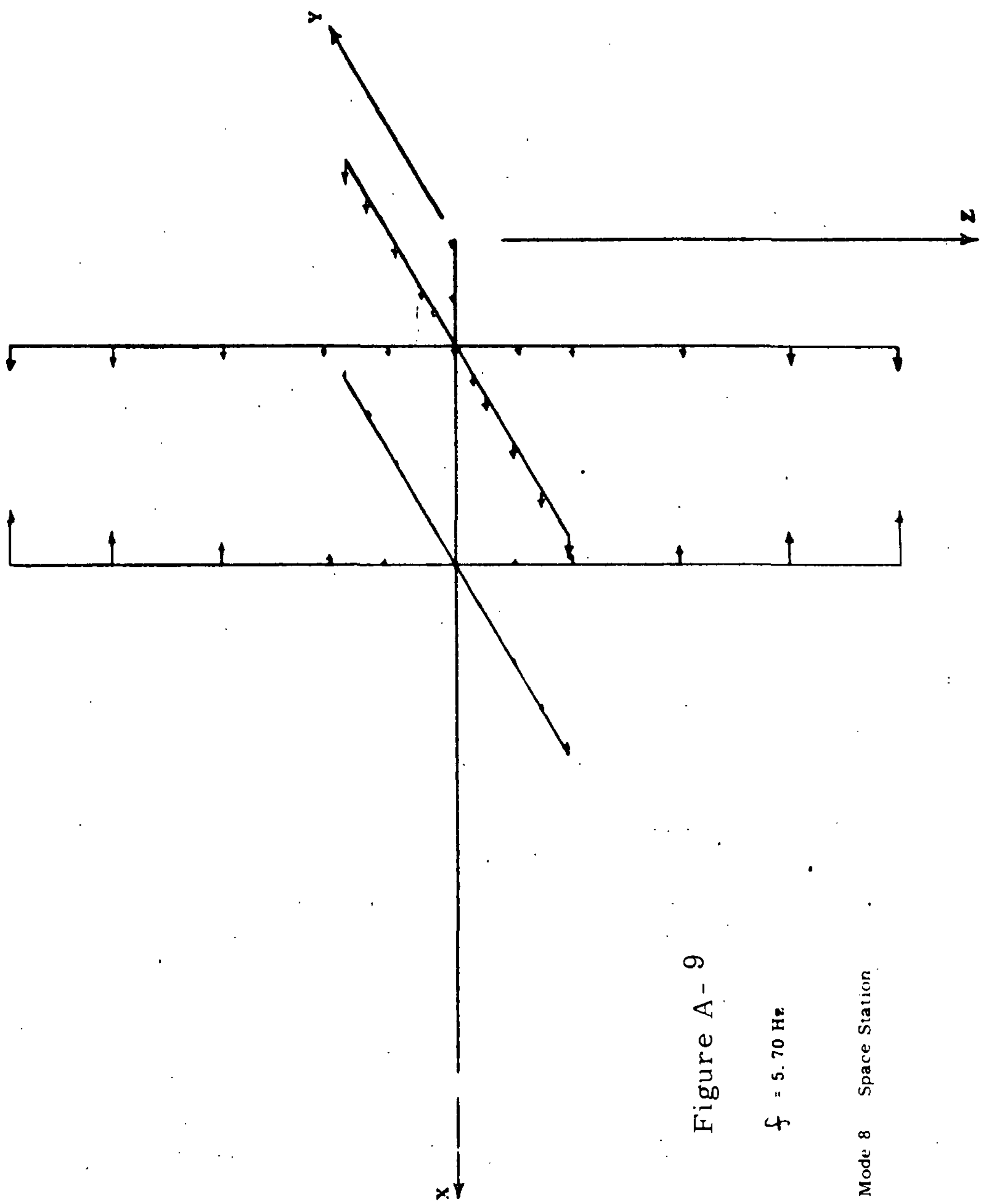

Figure A- 9

f = 5.70 Hz

Mode 8 Space Station

A.2 VIBRATION MODE DATA
ZERO "G" ROLLUP SOLAR ARRAY CONFIGURATION

CONTENTS

Table A-3 , Modal Data, Solar Array, Inplane, Antisymmetric, Zero G

Mode	Frequency (Hz)	Generalized Mass (lb.-sec.^{2}/in.)
1	9.737372E-02	1.350713E 00
2	1.035253E-01	6.274160E-01
3	1.035253E-01	4.967223E-01
4	1.035253E-01	6.000971E-01
5	1.035253E-01	6.934807E-01
6	1.687441E-01	1.409378E 00
7	1.999952E-01	9.246593E-01
8	1.999956E-01	8.365394E-01
9	1.999955E-01	9.231566E-01
10	1.999955E-01	8.366065E-01
11	2.654166E-01	1.456272E 00
12	2.828362E-01	6.936469E-01
13	2.828363E-01	6.273965E-01
14	2.828363E-01	6.923639E-01
15	2.828363E-01	6.274614E-01
16	3.237091E-01	1.832071E 00
17	3.464023E-01	9.248542E-01
18	3.464025E-01	8.365350E-01
19	3.464025E-01	9.231666E-01
20	3.464025E-01	8.366050E-01
21	3.612237E-01	1.765825E 00
22	3.863518E-01	6.936590E-01
23	3.863516E-01	4.845103E-01
24	3.863518E-01	5.731879E-01
25	3.863516E-01	5.045668E-01
26	3.891559E-01	1.503639E 00
27	5.941957E-01	8.893200E-01
28	2.523427E 00	1.298081E-01
29	3.197628E 00	8.005888E-01
30	3.495915E 00	7.669923E-01
31	3.523190E 00	6.305750E-01
32	3.528254E 00	6.607162E-01
33	4.358931E 00	1.495981E-01
34	6.507502E 00	4.571142E-01
35	6.931433E 00	2.305118E-01
36	9.297757E 00	8.740416E-01
37	1.008611E 01	7.663497E-01
38	1.013479E 01	6.293153E-01
39	1.015728E 01	6.567687E-01
40	1.240681E 01	2.131746E-01
41	1.286052E 01	4.911602E-01
42	1.496896E 01	7.352544E-01
43	1.592579E 01	7.507545E-01
44	1.630150E 01	6.193690E-01
45	1.671517E 01	6.539617E-01
46	1.772331E 01	1.098866E 00
47	1.834437E 01	4.004465E-01
48	1.965033E 01	7.068785E-01
49	2.051942E 01	7.531123E-01
50	2.056432E 01	6.381914E-01

Table A-4, Modal Data, Solar Array, Inplane, Symmetric, Zero G

Mode	Frequency (Hz)	Generalized Mass (lb.-sec.^{2}/in.)
1	1.035250E-01	6.471123E-01
2	1.035251E-01	6.662618E-01
3	1.035252E-01	7.732370E-01
4	1.035253E-01	3.702315E-01
5	1.035319E-01	5.658236E-01
6	1.999946E-01	8.627804E-01
7	1.999952E-01	8.883575E-01
8	1.999952E-01	6.197678E-01
9	1.999952E-01	8.961747E-01
10	1.999955E-01	6.240916E-01
11	2.828338E-01	6.471033E-01
12	2.828356E-01	4.734812E-01
13	2.828363E-01	6.536539E-01
14	2.828363E-01	6.072990E-01
15	2.828363E-01	6.702858E-01
16	3.464020E-01	8.628003E-01
17	3.464025E-01	1.045781E 00
18	3.464025E-01	7.491596E-01
19	3.464026E-01	6.347124E-01
20	3.464026E-01	8.882823E-01
21	3.863617E-01	6.470776E-01
22	3.863618E-01	7.813119E-01
23	3.863618E-01	5.618995E-01
24	3.863618E-01	4.768397E-01
25	3.863618E-01	6.663127E-01
26	1.354412E 00	7.051653E-01
27	3.278625E 00	7.702565E-01
28	3.490318E 00	6.074610E-01
29	3.519975E 00	5.617070E-01
30	3.527668E 00	6.061066E-01
31	6.072317E 00	1.035868E-01
32	6.882595E 00	4.122061E-01
33	9.511100E 00	8.556120E-01
34	1.007151E 01	6.032084E-01
35	1.014669E 01	5.632485E-01
36	1.016592E 01	6.006349E-01
37	1.280494E 01	4.343082E-01
38	1.518822E 01	7.910441E-01
39	1.590481E 01	5.698990E-01
40	1.599190E 01	5.694355E-01
41	1.601352E 01	5.922735E-01
42	1.783336E 01	5.283089E-01
43	1.987668E 01	8.288176E-01
44	2.049608E 01	5.615127E-01
45	2.055783E 01	5.868033E-01
46	2.057259E 01	5.877689E-01
47	2.154462E 01	4.647811E-01
48	2.300127E 01	1.731334E-01
49	2.315868E 01	6.691886E-01
50	2.344269E 01	5.389919E-01

Table A-5 , Modal Data, Solar Array, Out of Plane, Symmetric, Zero G

Mode	Frequency (Hz)	Generalized Mass (lb.-sec.^{2}/in.)
1	9.244967E-02	1.363355E 00
2	1.225055E-01	4.851304E-01
3	1.227098E-01	5.956523E-01
4	1.227105E-01	5.221769E-01
5	1.227164E-01	5.439427E-01
6	1.866132E-01	1.301536E 00
7	2.335492E-01	4.738768E-01
8	2.338332E-01	6.763698E-01
9	2.338462E-01	5.873230E-01
10	2.338475E-01	5.149174E-01
11	2.723567E-01	1.215317E 00
12	3.224205E-01	4.755982E-01
13	3.226471E-01	6.820915E-01
14	3.226523E-01	5.924900E-01
15	3.226532E-01	5.194927E-01
16	3.411543E-01	1.341820E 00
17	3.800172E-01	4.683110E-01
18	3.800961E-01	6.776543E-01
19	3.800981E-01	5.888550E-01
20	3.800984E-01	5.163653E-01
21	3.848683E-01	1.156975E 00
22	8.345175E-01	1.581258E-01
23	1.016372E 00	2.447064E-01
24	1.021062E 00	2.410409E-01
25	1.021616E 00	1.859574E-01
26	1.021757E 00	2.290614E-01
27	1.619896E 00	1.406597E-01
28	2.273774E 00	1.105896E-01
29	3.660591E 00	1.346217E-01
30	5.304781E 00	1.555309E-01
31	1.037197E 01	1.700534E-01
32	1.150986E 01	2.381182E-01
33	1.742712E 01	1.640180E-01
34	2.036168E 01	2.053636E-01
35	2.451262E 01	1.479549E-01
36	3.032007E 01	2.375647E-01
37	5.002257E 01	1.682047E-01
38	5.146941E 01	1.800458E-01
39	7.553278E 01	1.761178E-01
40	9.195334E 01	1.597598E-01
41	1.138354E 02	6.968695E-02
42	1.408619E 02	9.482276E-02

Table A-6, Modal Data, Solar Array, Out of Plane, Antisymmetric, Zero G

Mode	Frequency (Hz)	Generalized Mass (lb. -sec. ^{2}/in.)
1	6.399534E-02	6.094149E-01
2	1.225912E-01	6.959703E-01
3	1.227031E-01	7.329165E-01
4	1.227102E-01	6.202382E-01
5	1.227106E-01	6.423883E-01
6	1.667802E-01	5.472140E-01
7	2.338042E-01	6.814334E-01
8	2.338445E-01	7.183616E-01
9	2.338476E-01	6.182398E-01
10	2.338432E-01	6.334028E-01
11	2.413185E-01	5.890857E-01
12	3.084885E-01	7.381489E-01
13	3.225234E-01	6.943066E-01
14	3.226912E-01	7.346921E-01
15	3.226535E-01	6.107412E-01
16	3.226538E-01	6.392808E-01
17	3.531117E-01	5.835944E-01
18	3.800878E-01	6.890357E-01
19	3.800975E-01	7.275511E-01
20	3.800982E-01	6.101235E-01
21	3.800984E-01	6.354181E-01
22	3.890288E-01	5.942361E-01
23	1.011542E 00	2.524251E-01
24	1.020890E 00	2.669843E-01
25	1.021528E 00	2.242702E-01
26	1.021753E 00	2.333972E-01
27	1.584146E 00	2.103242E-01
28	8.225140E 00	1.584330E-01
29	1.054482E 01	1.610069E-01
30	2.514871E 01	2.037958E-01
31	3.402454E 01	2.118104E-01
32	5.335814E 01	1.683161E-01
33	6.955161E 01	1.759176E-01
34	8.298788E 01	1.814231E-01
35	1.082325E 02	1.893509E-01

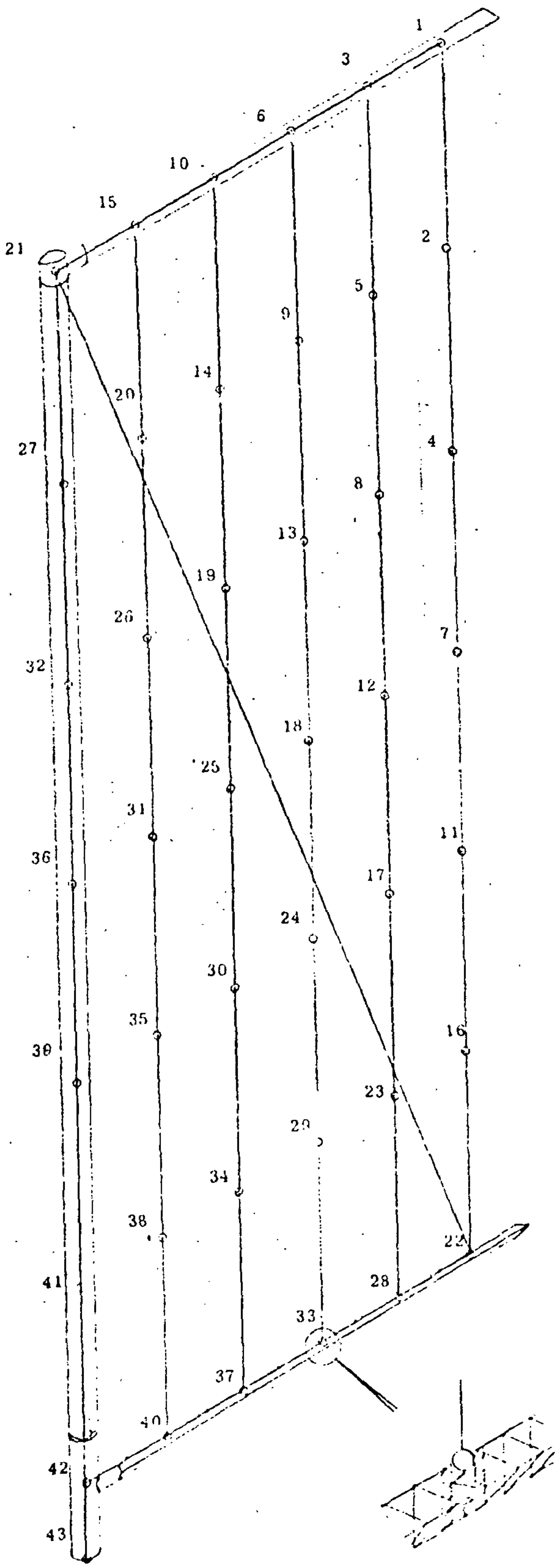

Figure A-10 Structural Model for Rollup Solar Array
Zero "G" Configuration

TABLE A-7

Mass - Geometry Data

Of Zero G Solar Array

NODE NO.	WEIGHT(lbs.)	X	Y	Z
1	21.48	1056.	347.	0.
2	32.3	888.	347.	0.
3	26.06	1056.	275.	0.
4	32.3	720.	347.	0.
5	32.3	888.	275.	0.
6	26.06	1056.	203.	0.
7	32.3	552.	347.	0.
8	32.3	720.	275.	0.
9	32.3	888.	203.	0.
10	26.06	1056.	131.	0.
11	32.3	384.	347.	0.
12	32.3	552.	275.	0.
13	32.3	720.	203.	0.
14	32.3	888.	131.	0.
15	25.32	1056.	59.	0.
16	32.3	216.	347.	0.
17	32.3	384.	275.	0.
18	32.3	552.	203.	0.
19	32.3	720.	131.	0.
20	32.3	888.	59.	0.
21	12.74	1056.	0.	0.
22	20.84	48.	347.	0.
23	32.3	216.	275.	0.
24	32.3	384.	203.	0.
25	32.3	552.	131.	0.
26	32.3	720.	59.	0.
27	17.81	888.	0.	0.
28	24.98	48.	275.	0.
29	32.3	216.	203.	0.
30	32.3	384.	131.	0.
31	32.3	552.	59.	0.
32	17.81	720.	0.	0.
33	24.98	48.	203.	0.
34	32.3	216.	131.	0.
35	32.3	384.	59.	0.
36	17.81	552.	0.	0.
37	24.98	48.	131.	0.
38	32.3	216.	59.	0.
39	17.81	384.	0.	0.
40	24.23	48.	59.	0.
41	17.31	216.	0.	0.
42	12.30	48.	0.	0.
43	0.	0.	0.	0.

NOTE: Weights along the boom (Y = 0.) are one half the actual weight.

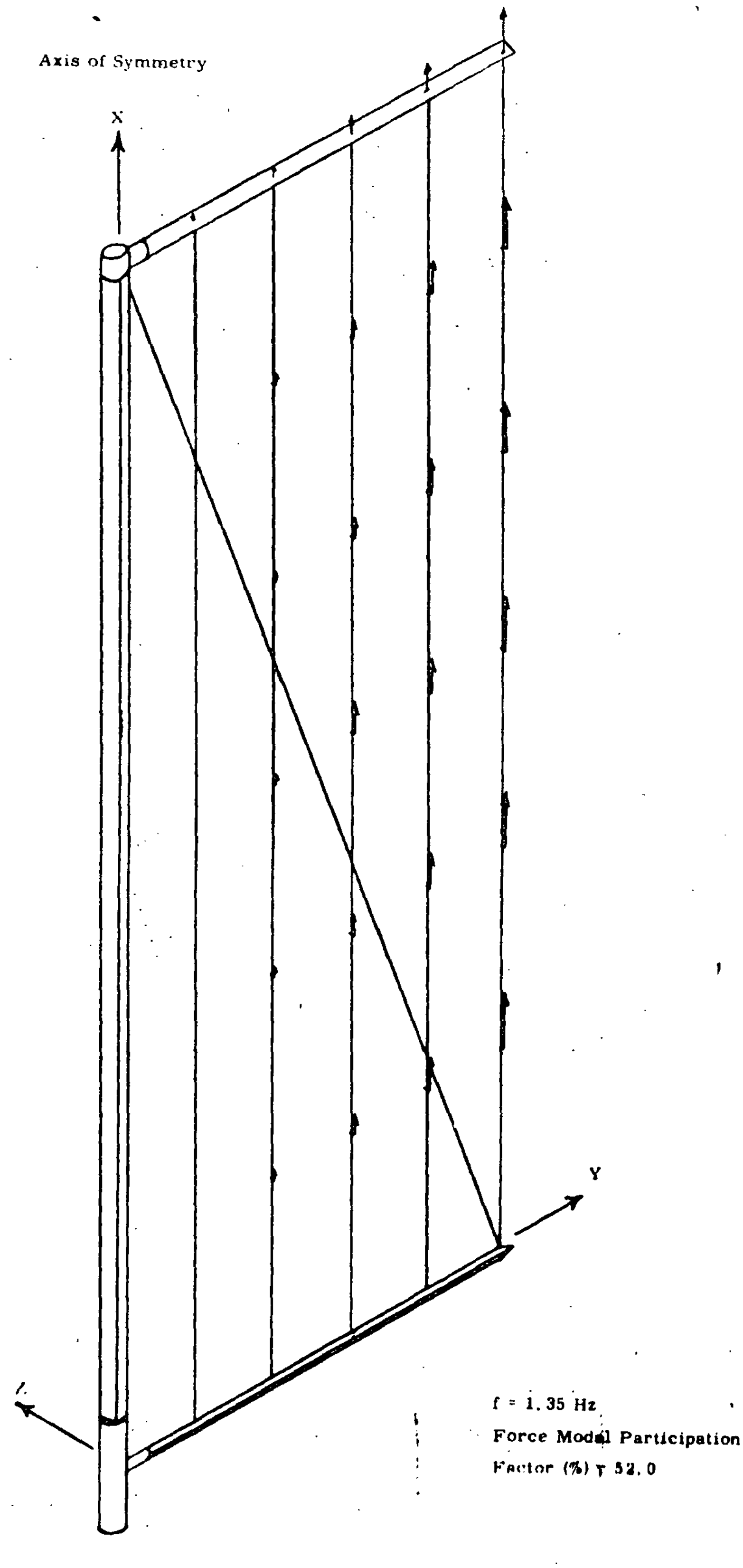

Figure A-11 Mode 26 String Solar Array, In Plane Symmetric

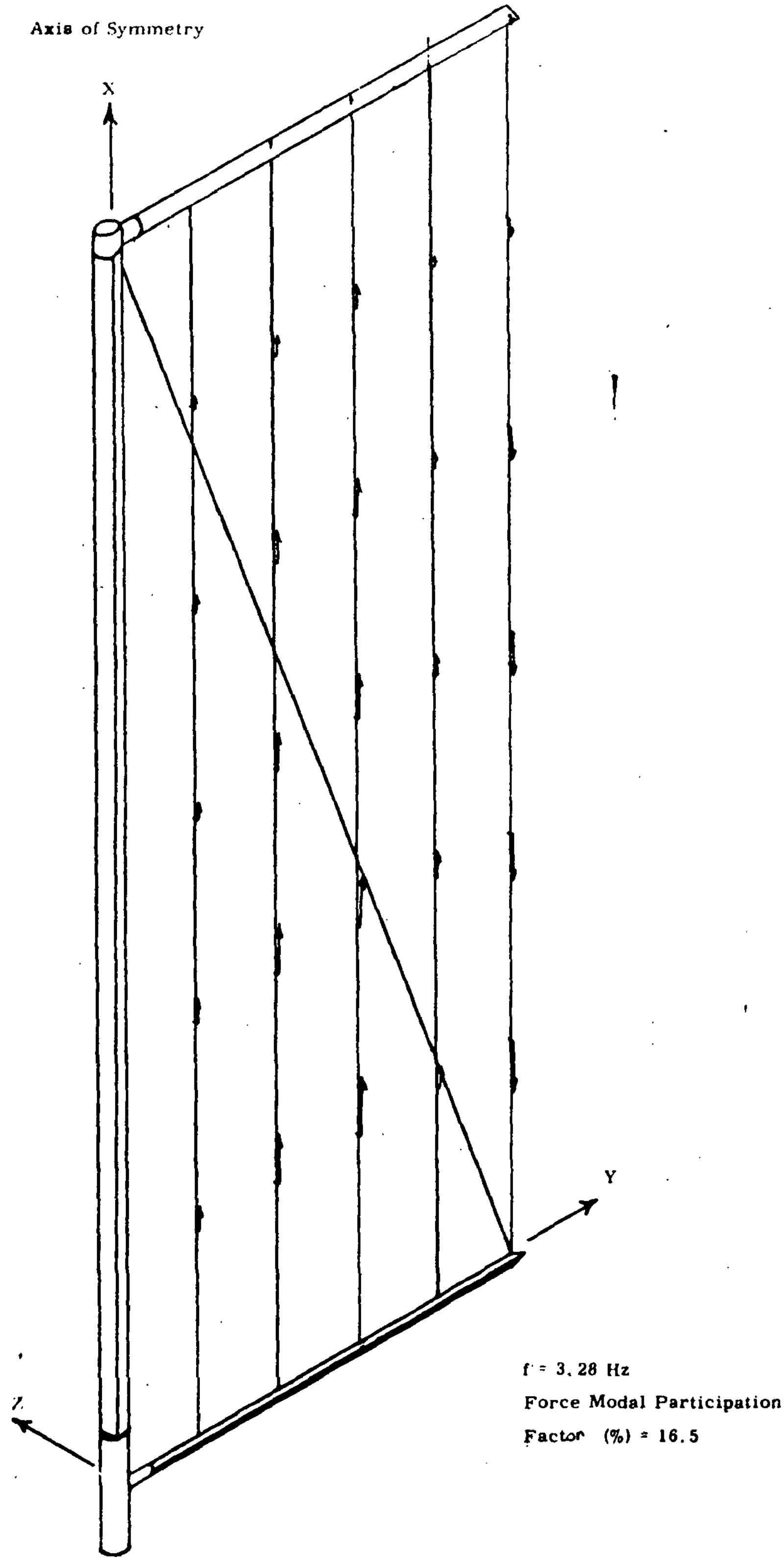

Figure A-12 Mode 27 String Solar Array, In Plane Symmetric

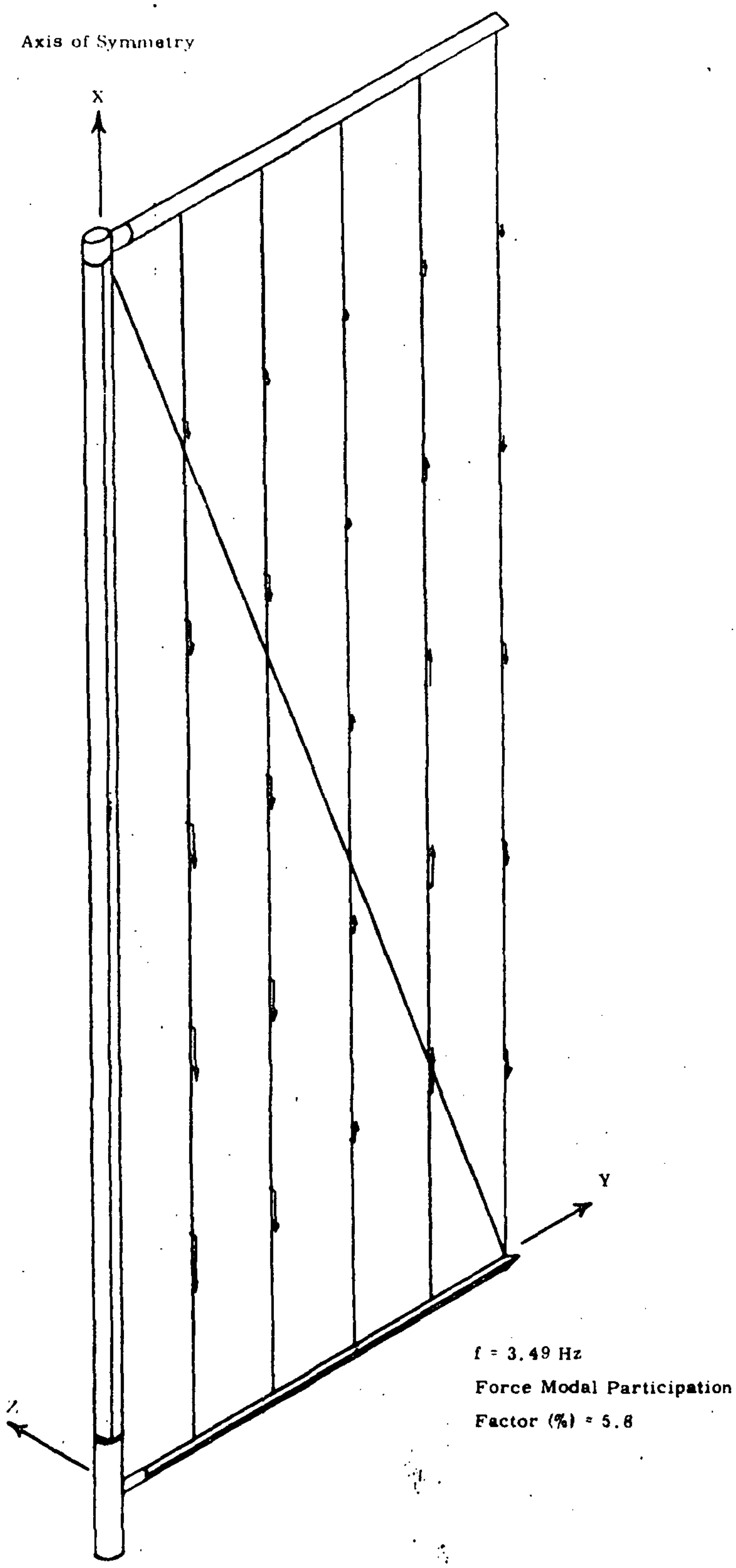

Figure A-13 Mode 28 String Solar Array, In-Plane Symmetric

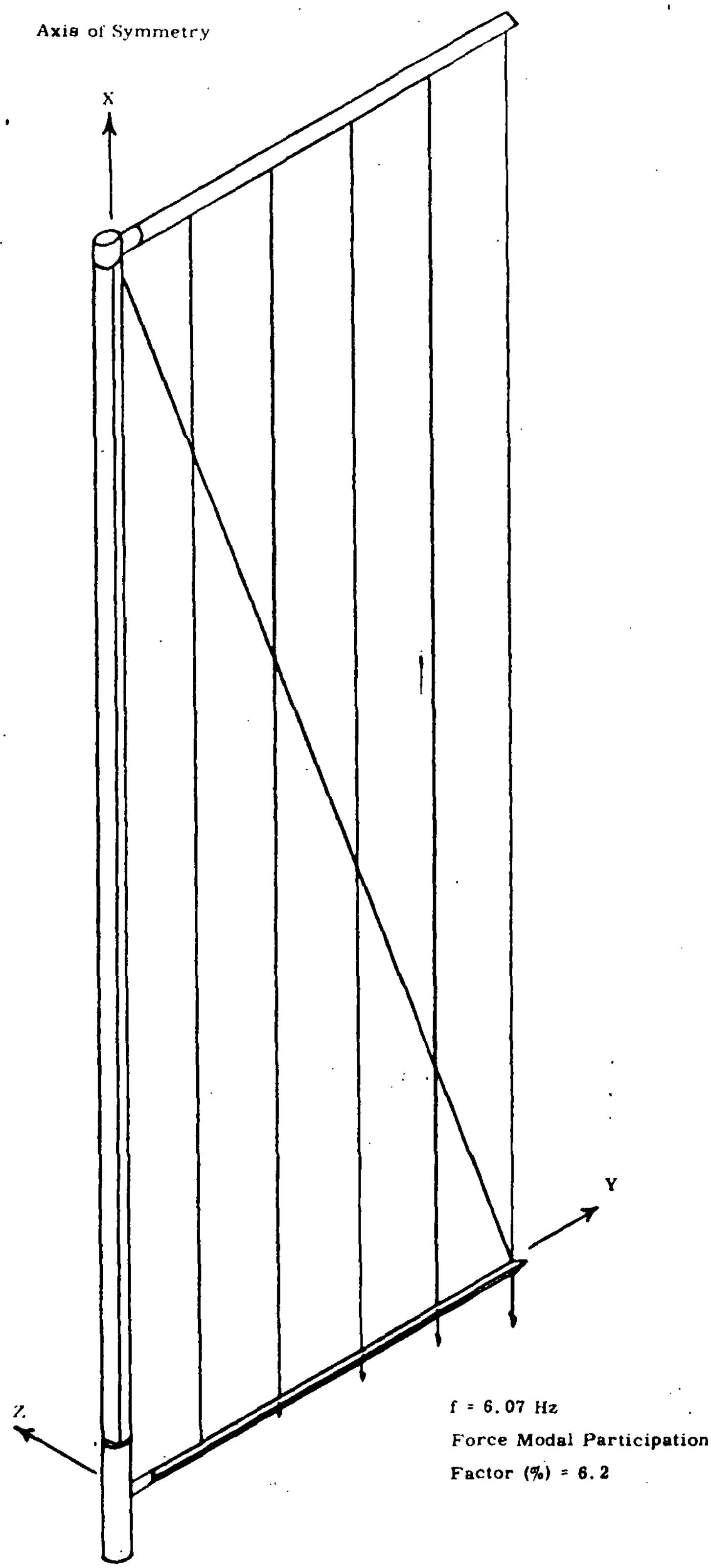

Figure A-14 Mode 31 Solar Array, In Plane Symmetric

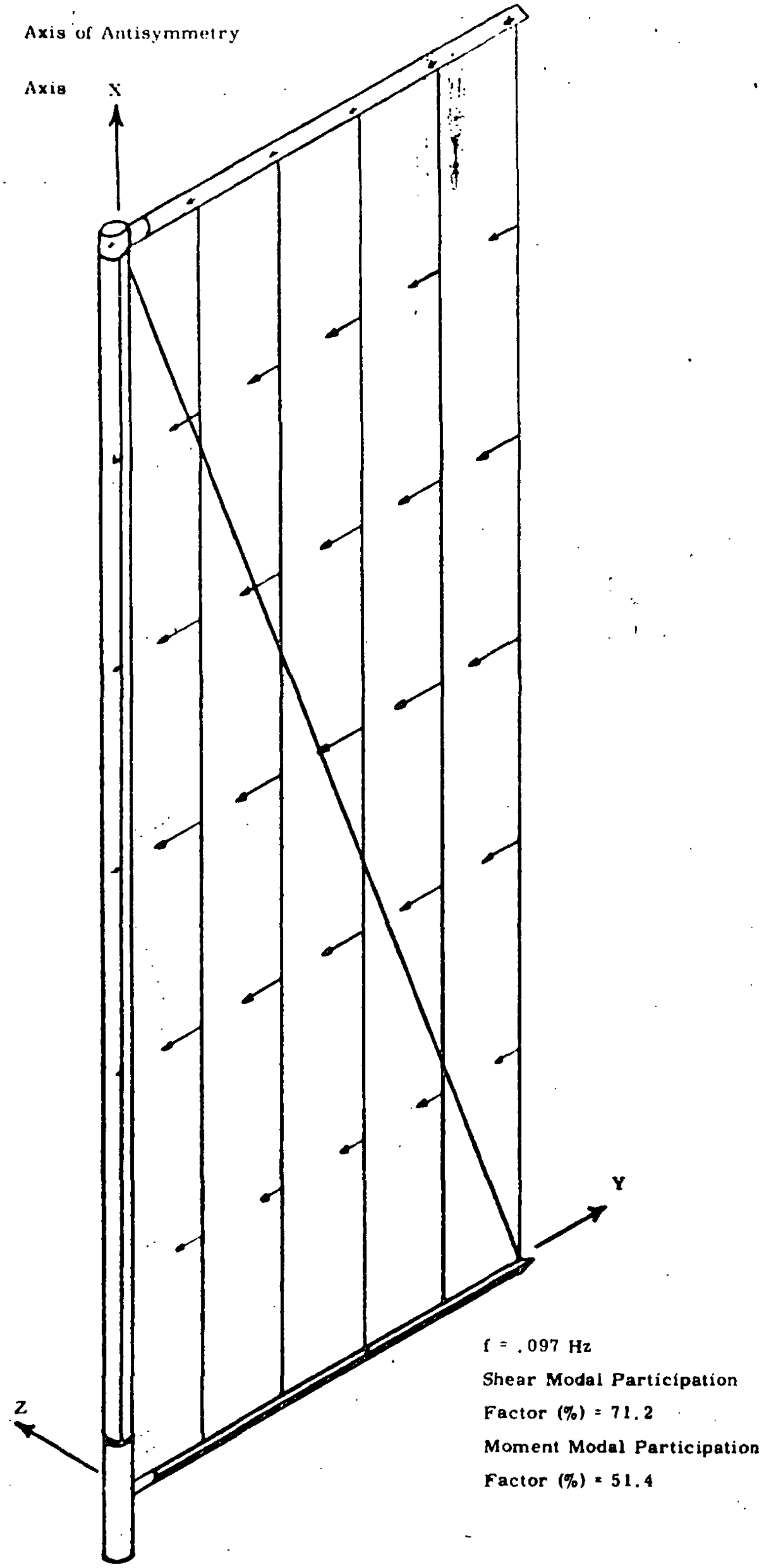

Figure A-15 Mode 1 String Solar Array, In Plane Antisymmetric

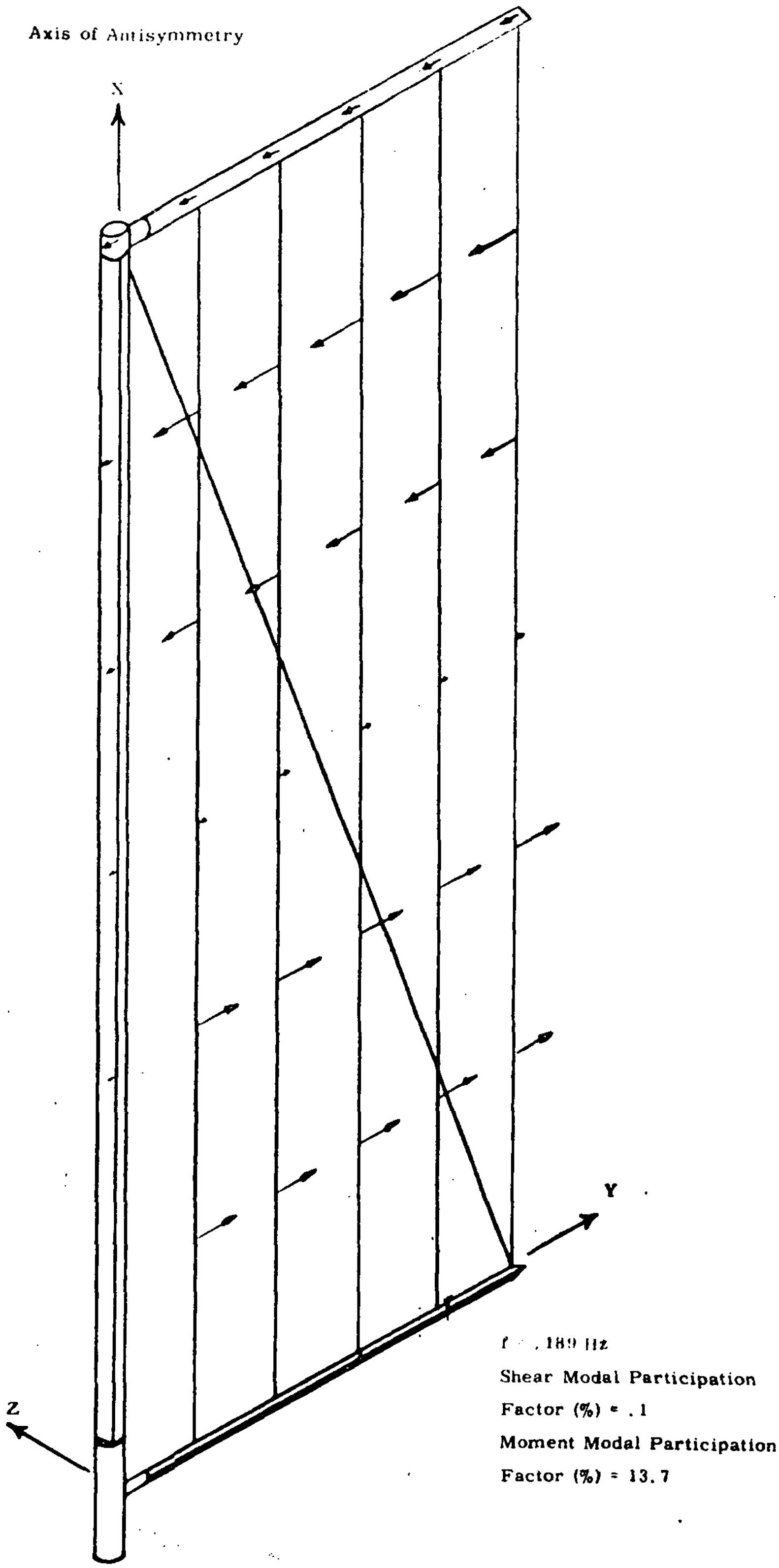

Figure A-16 Mode 6 String Solar Array, In Plane Antisymmetric

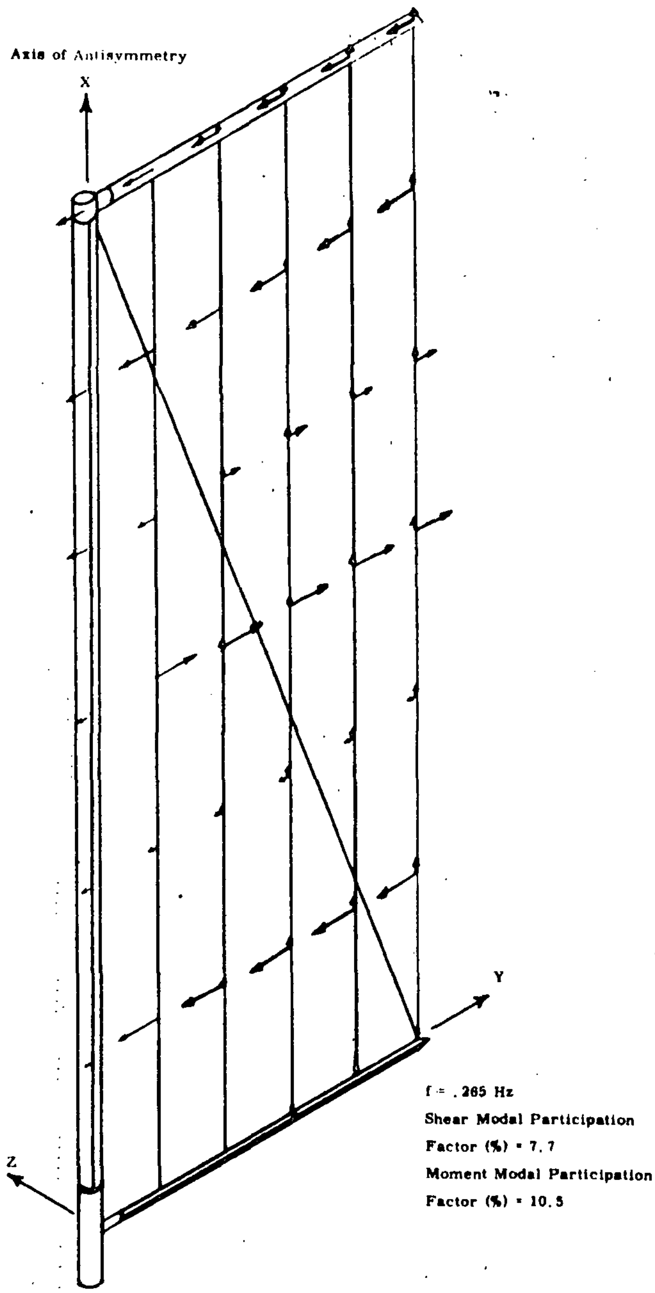

Mode 11 String Solar Array, In Plane Antisymmetric

Figure A-17

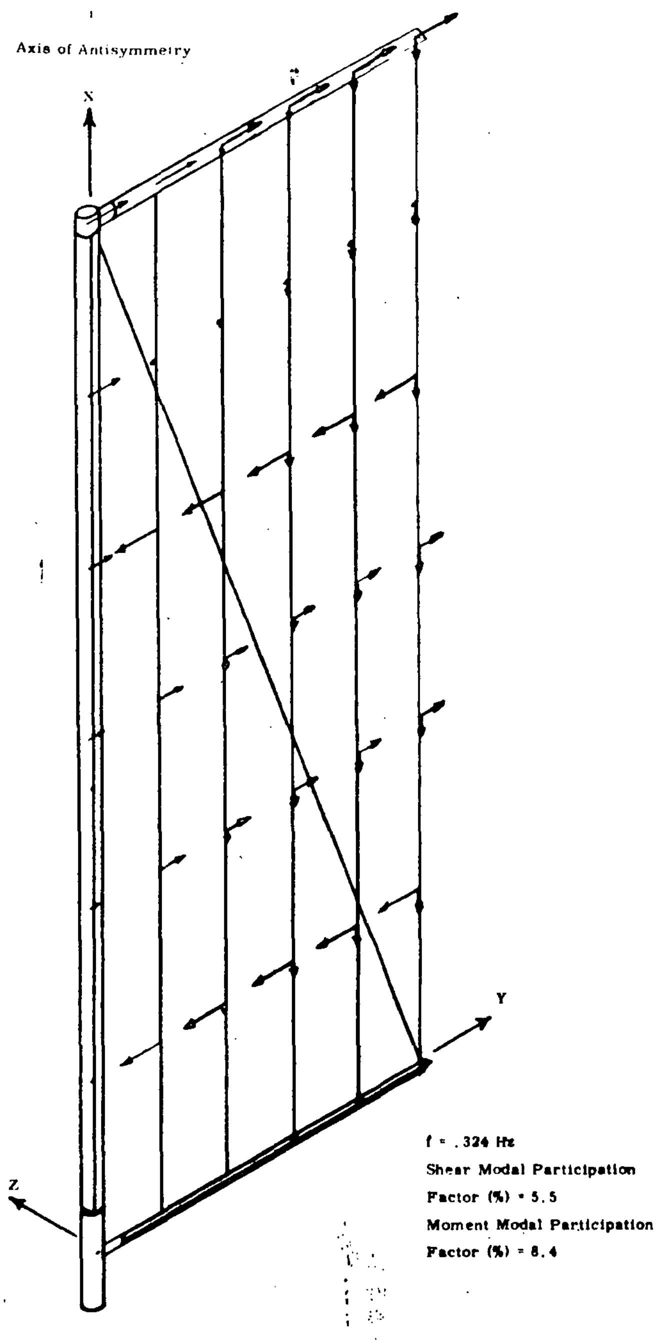

Figure A-18 Mode 16 String Solar Array, In-Plane Antisymmetric

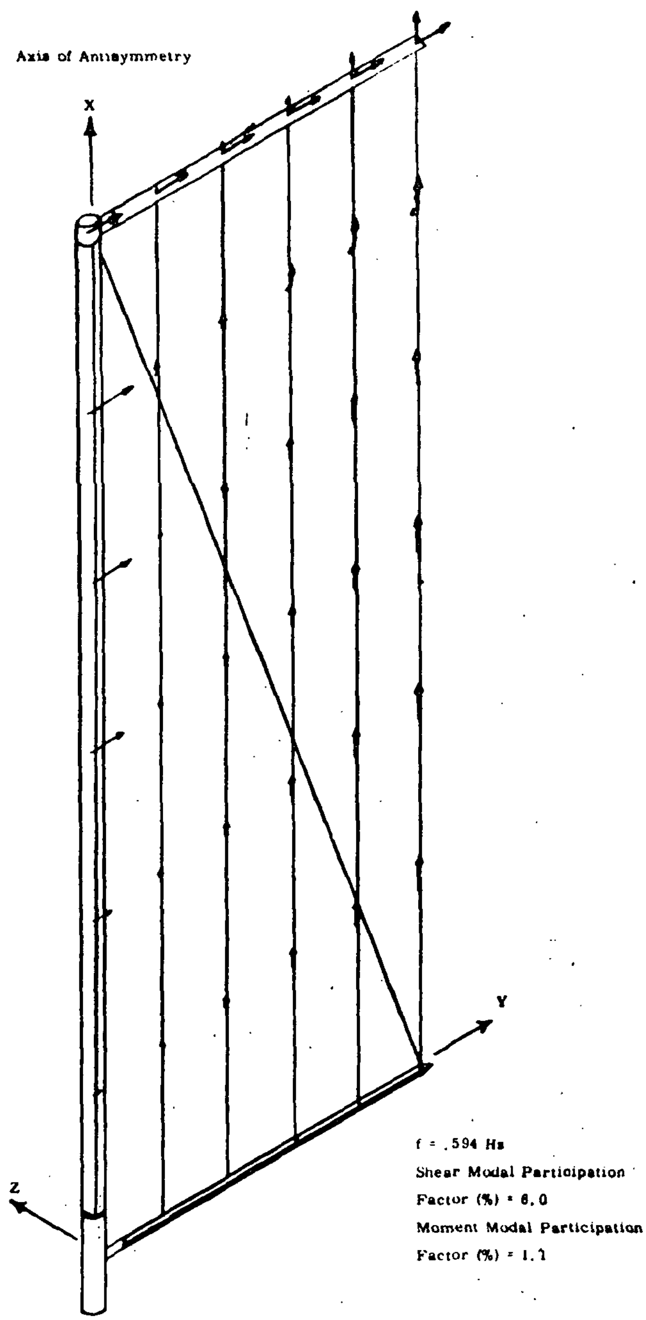

Figure A-19 Mode 27 String Solar Array, In Plane Antisymmetric

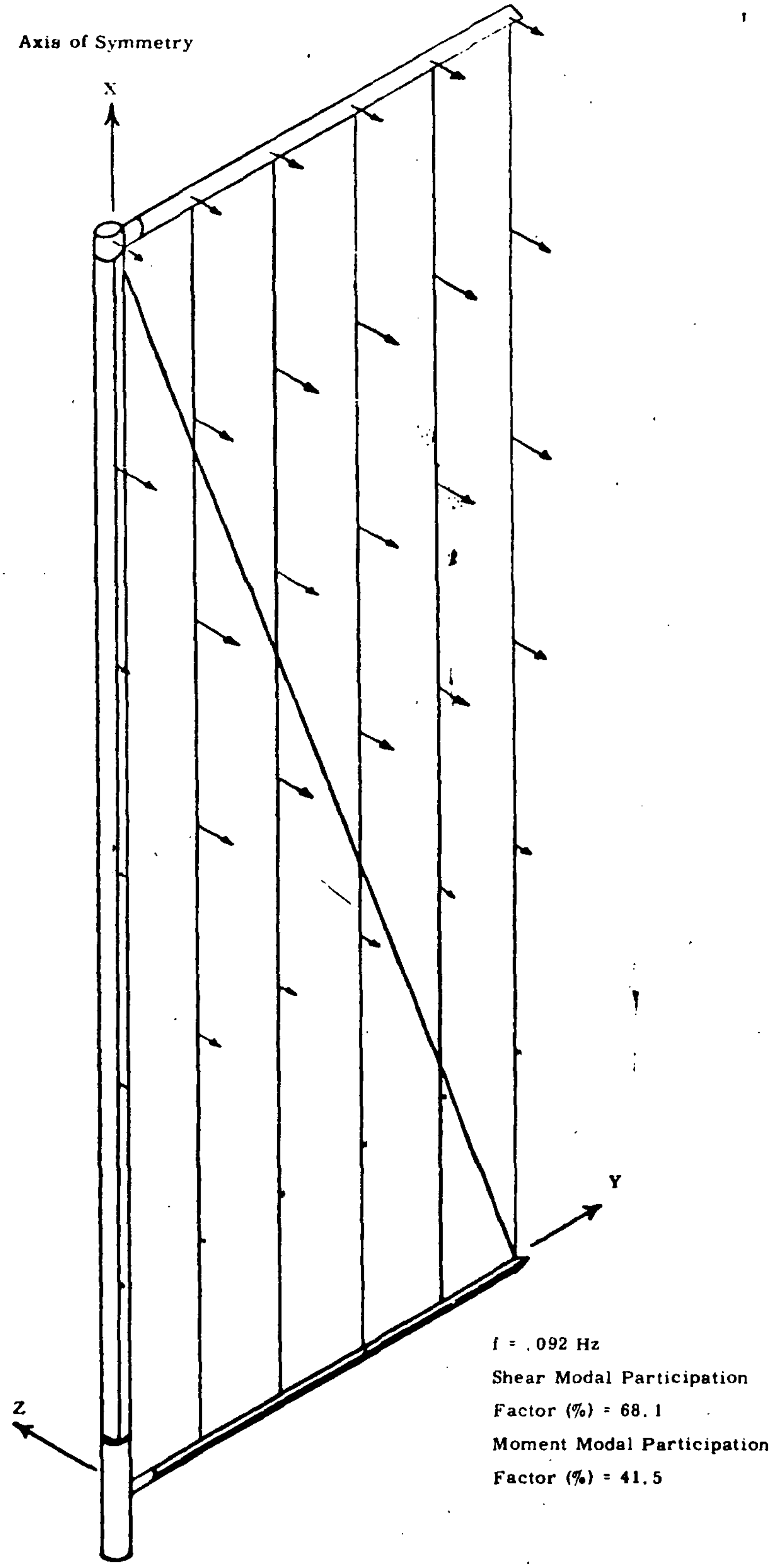

Mode 1 String Solar Array, Out of Plane Symmetric

Figure A-20

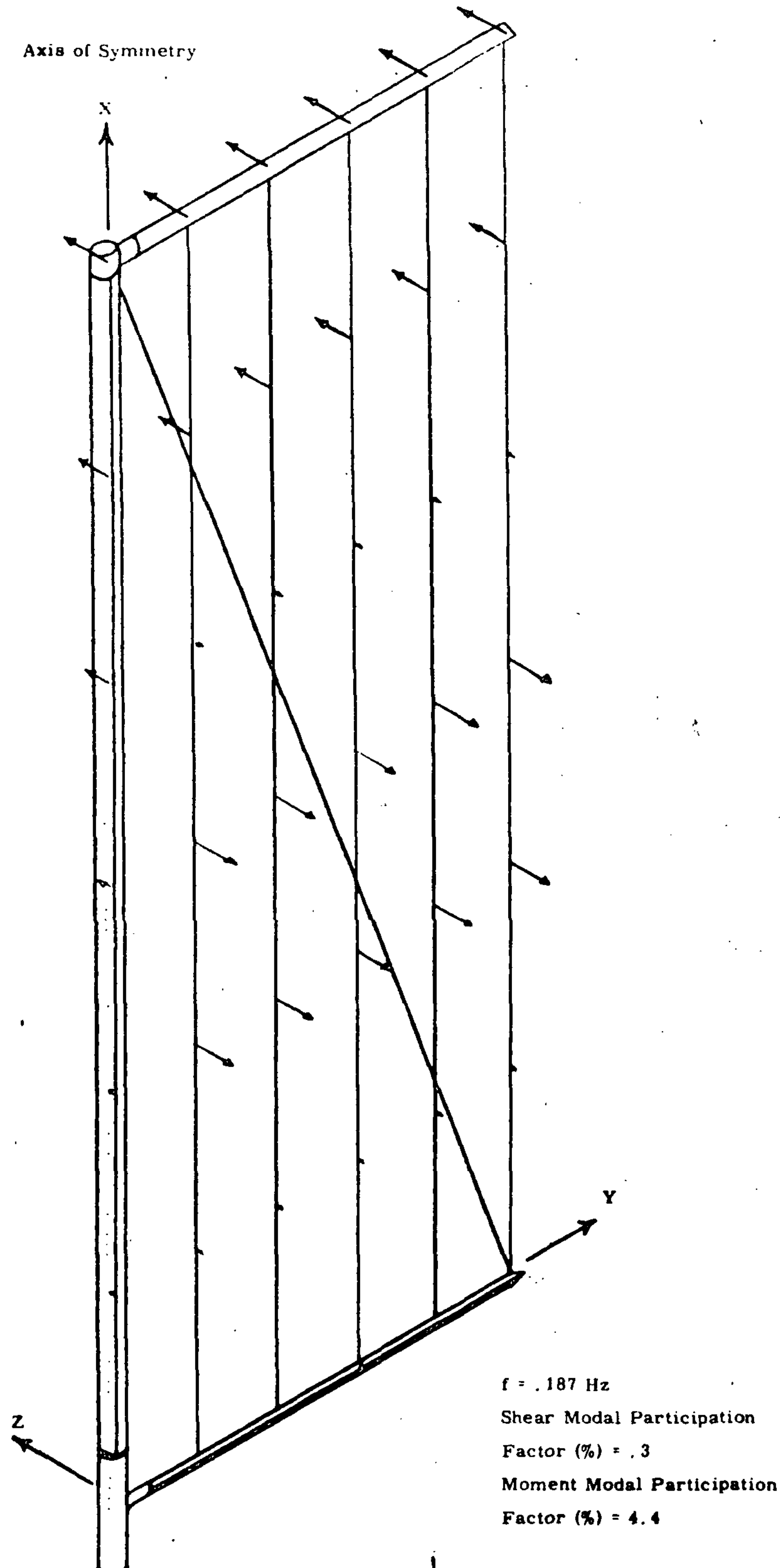

Figure A-21 Mode 6 String Solar Array, Out of Plane Symmetric

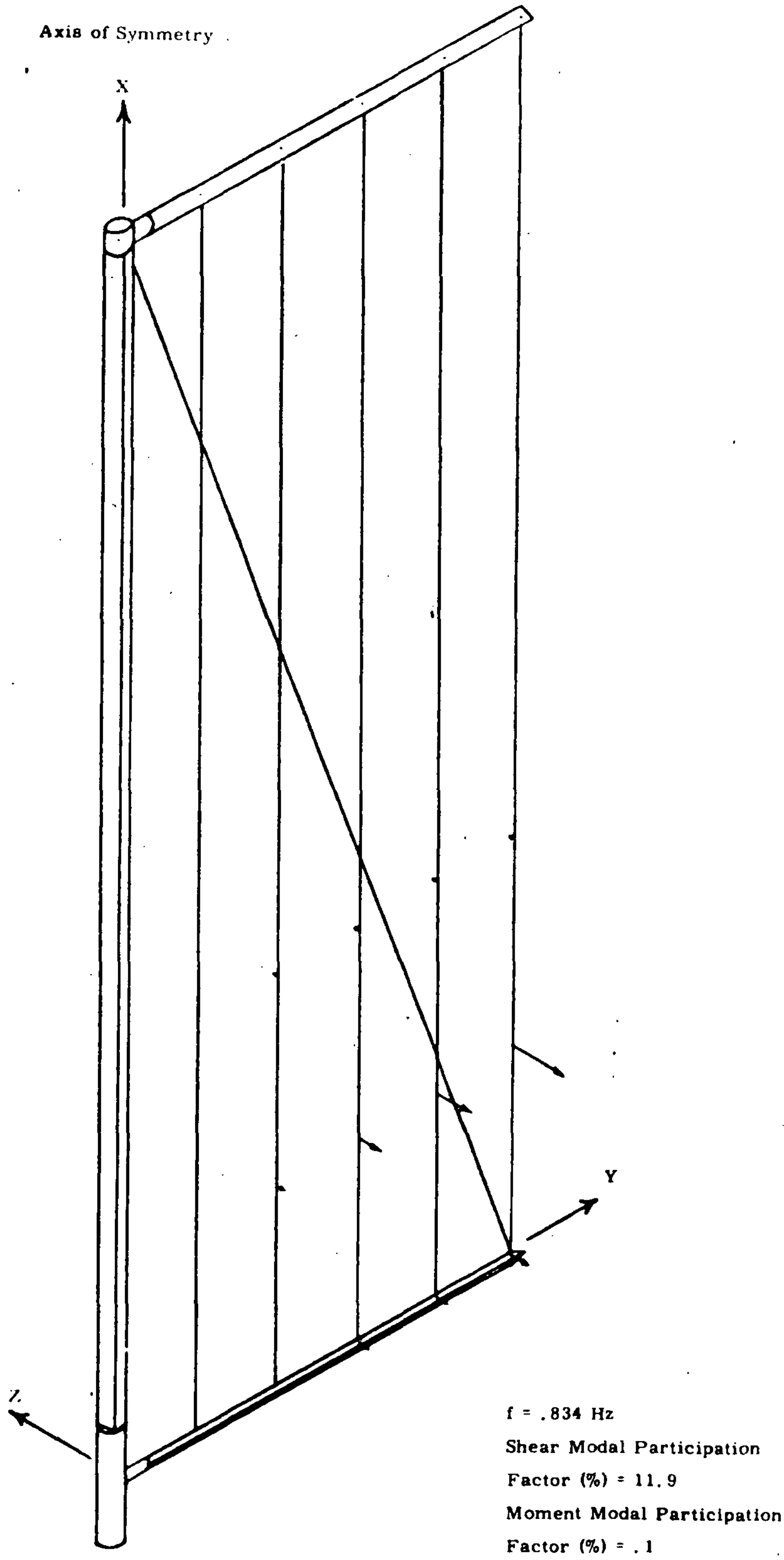

Figure A-22 Mode 22 String Solar Array, Out of Plane, Symmetric

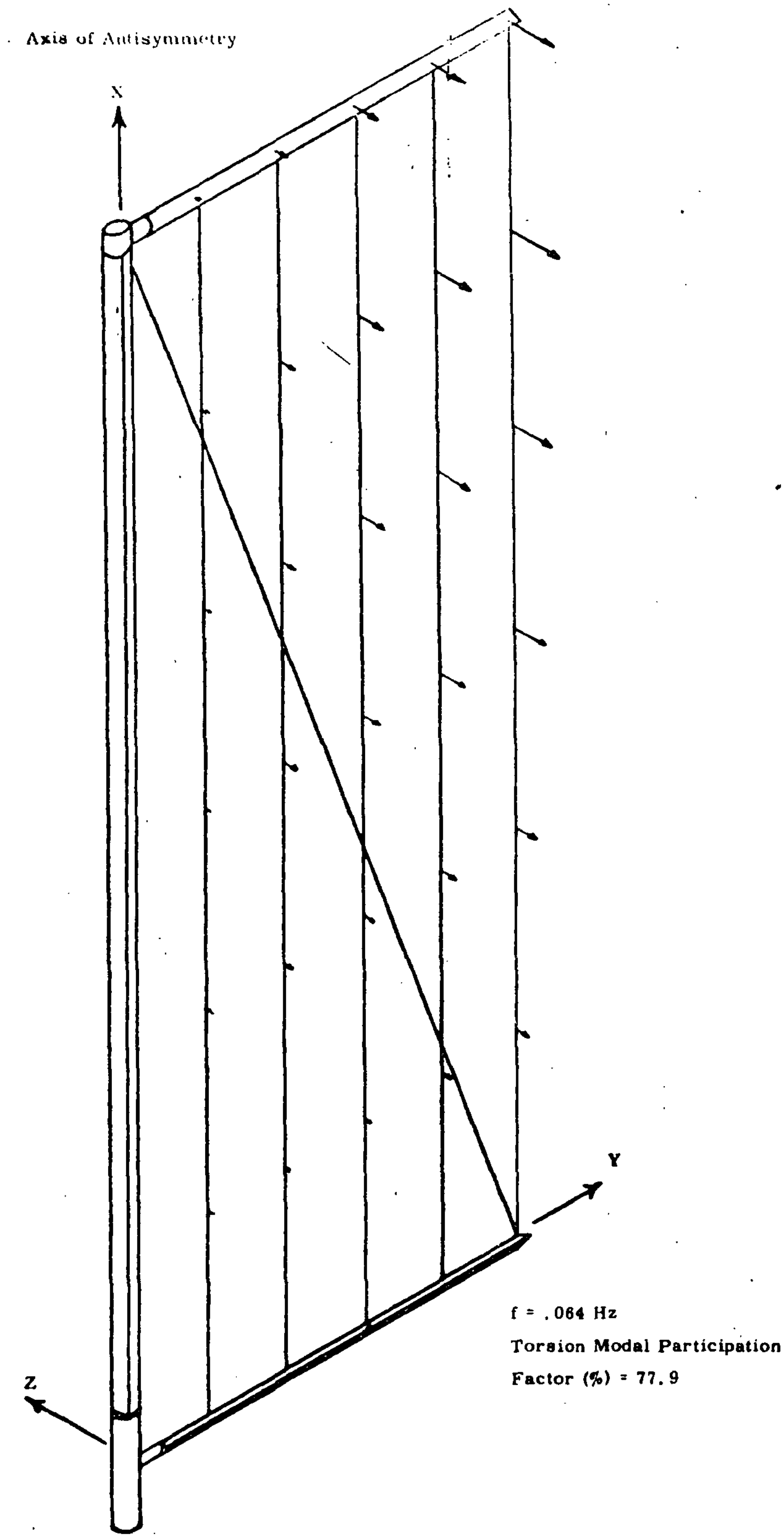

Figure A-23 Mode 1 Solar Array, Out of Plane, Antisymmetric

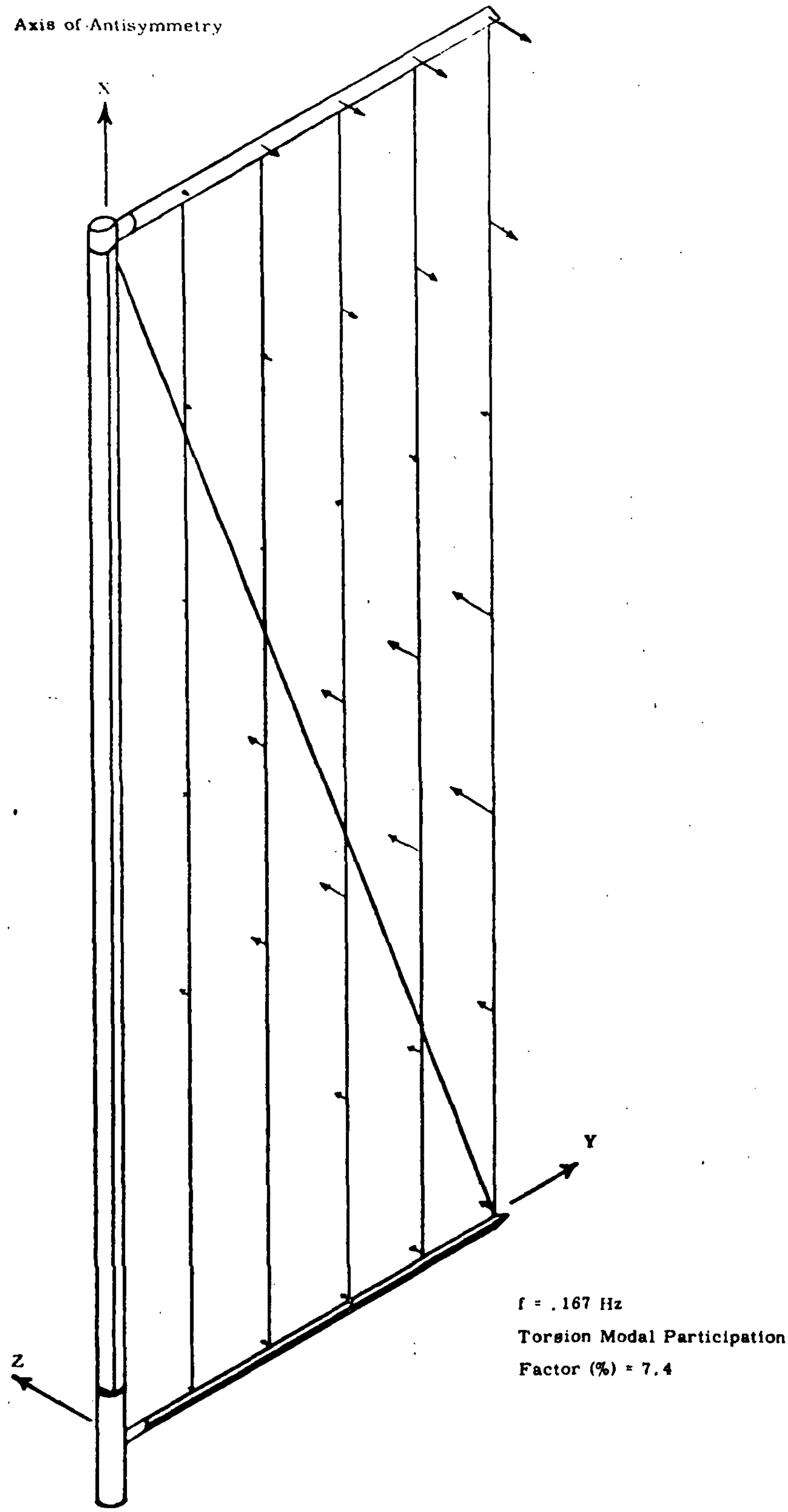

Figure A-24 Mode 6 String Solar Array, Out of Plane, Antisymmetric

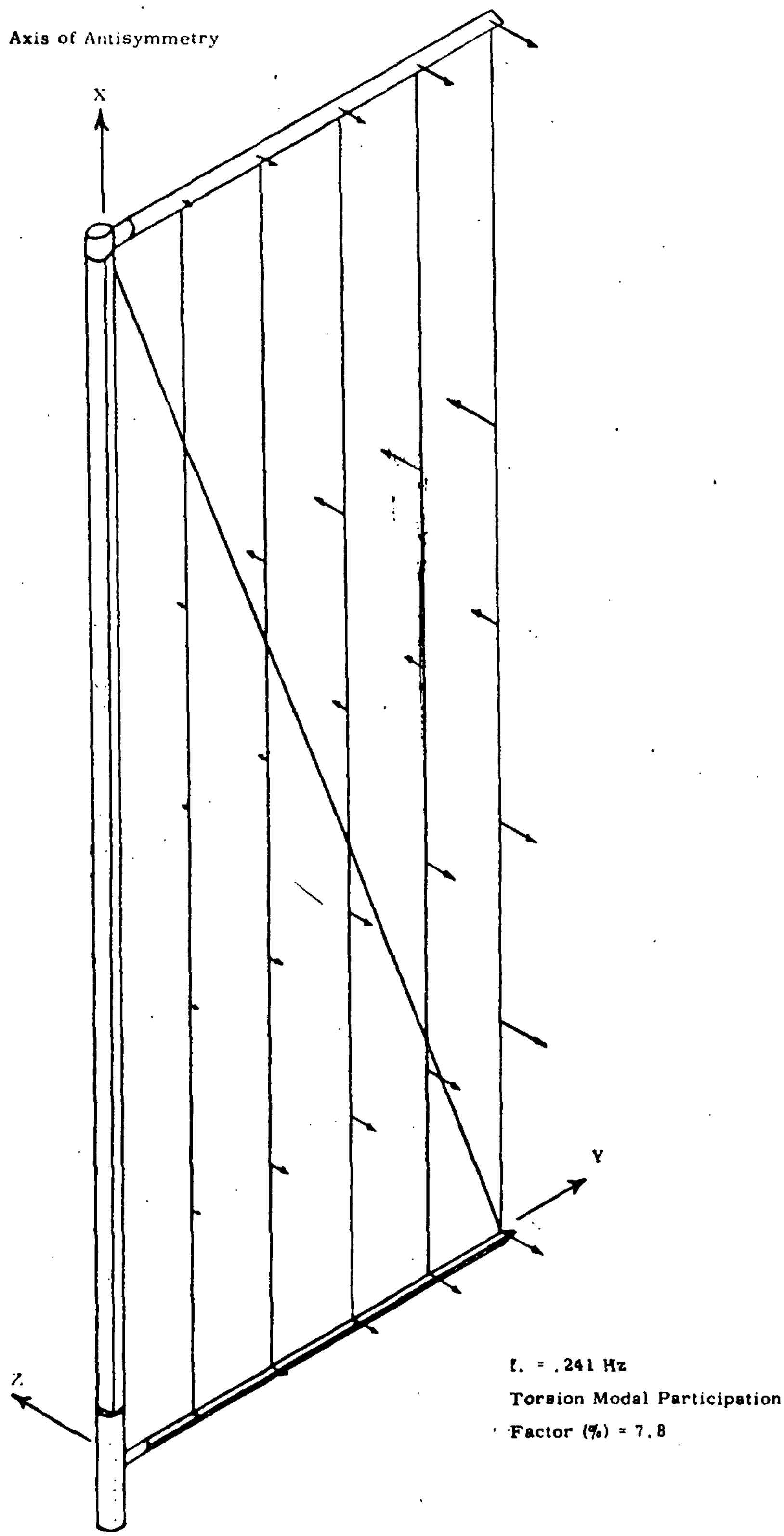

Figure A-25 Mode 11 String Solar Array, Out of Plane, Antisymmetric

A.3 VIBRATION MODE DATA
ARTIFICIAL "G" SPACE STATION CONFIGURATION

CONTENTS

NOTE: Mode 1 shown in Figure A-27 isthe first elastic mode and corresponds to Mode 7 of Table A-8.

TABLE A-8 MODAL DATA ARTIFICIAL "G" SPACE STATION CONFIGURATION ZERO SPIN, NASTRAN RESULTS

MODE	FREQUENCY (HZ)		GENERALIZED MASS ($LBS\text{-}SEC^2/IN$)
1	4.221[illegible]2E-03	Rigid Body Modes	2.874500E 02
2	4.13[illegible]2E-[illegible]		6.274835E 01
3	6.192792E-0[illegible]		1.266219E 02
4	6.868873E-0[illegible]		1.162889E 02
5	7.158235E-06		1.794931E 02
6	8.5[illegible]3952E-06		1.572773E 01
7	2.296729E 00		8.672661E 00
8	4.2[illegible]339E [illegible]		5.868550E 00
9	8.4[illegible]2[illegible]E 00		7.261933E 00
10	8.578683E 00		7.816177E 01
11	1.[illegible]479[illegible]7E 01		7.559761E 01
12	1.25[illegible]378E 01		7.482590E 03
13	1.5325[illegible]E 01		4.555014E 01
14	1.733186E 01		1.018629E 01
15	2.156968E 01		2.924060E 03
16	2.799[illegible]1E 01		5.702884E 01
17	3.[illegible]31332E 01		2.432465E 05
18	3.281332E 01		6.314181E 00
19	3.3[illegible]37[illegible]E 01		7.612518E 01
20	3.[illegible]2[illegible]E 01		1.149187E 02
21	3.922133E 01		1.977763E 00
22	4.253[illegible]65[illegible]E 01		1.850132E 00
23	5.[illegible]7[illegible]E 01		3.670874E 03
24	5.518927E 01		3.518304E 01
25	5.629476E 01		3.503325E 00
26	[illegible].711367E 01		3.315749E 00
27	6.[illegible]72267E 01		8.260[illegible]58E 02
28	6.331728E 01		1.964404E 01
29	6.389556E 01		1.996732E 04
30	6.77[illegible]826E 01		5.345604E-01
31	7.[illegible]739E 01		
32	7.5[illegible]8[illegible]27E 01		
33	8.357213E 01		
34	8.[illegible]53325E 01		
35	8.52[illegible]222E 01		
36	9.11389[illegible]E 01		
37	9.125[illegible]27E 01		
38	9.35[illegible]2E 01		
39	9.73[illegible]0E 01		
40	1.[illegible]2553[illegible]E 02		
41	1.[illegible]3715[illegible]E 02		
42	1.[illegible]E 02		
43	1.1[illegible]9E 02		
44	1.1[illegible]593[illegible]E 02		
45	1.19[illegible]E 02		
46	1.2[illegible]E 02		
47	1.21731[illegible]E 02		
48	1.283153[illegible]E 02		
49	1.247[illegible]9[illegible]E 02		
50	1.5[illegible]3121[illegible]E 02		

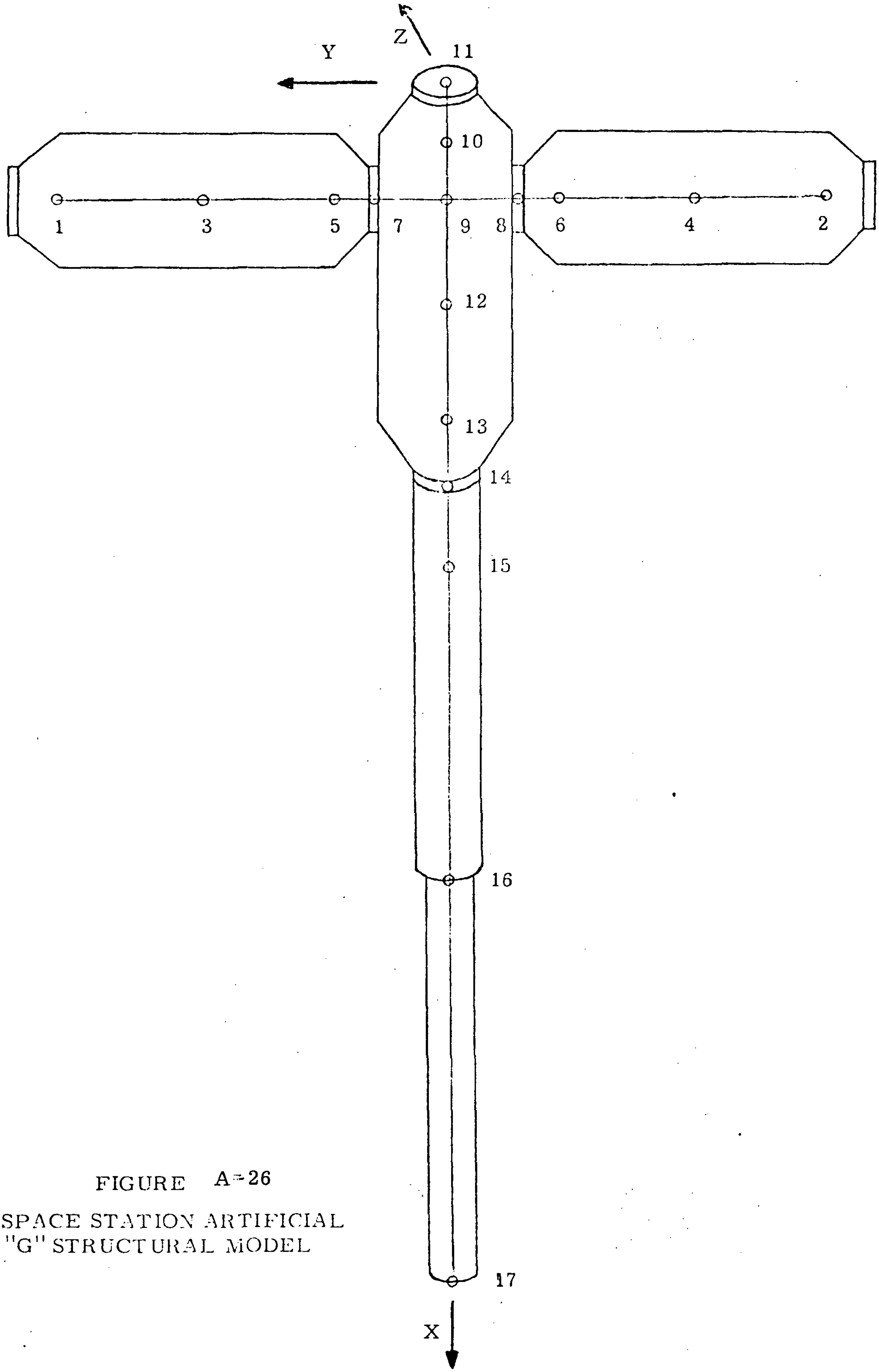

FIGURE A-26

SPACE STATION ARTIFICIAL "G" STRUCTURAL MODEL

TABLE A-9

MASS - GEOMETRY DATA

FOR ARTIFICIAL "G" SPACE STATION

Node	Mass *	X	Y	Z
1	21.578	120.	492.	.0
2	21.578	120.	-492.	.0
3	21.578	120.	312.	.0
4	21.578	120.	-312.	.0
5	21.578	120.	132.	.0
6	21.578	120.	-132.	.0
7	0.	120.	72.	.0
8	0.	120.	-72.	.0
9	15.382	120.	.0	.0
10	8.094	60.	.0	.0
11	4.047	.0	.0	.0
12	17.814	270.	.0	.0
13	15.379	420.	.0	.0
14	12.795	480.	.0	.0
15	10.632	552.	.0	.0
16	25.952	921.0	.0	.0
17	.01295	1290.	.0	.0

* - Mass units are lb-sec^2/in.

FIGURE A-27
ARTIFICIAL "G" SPACE STATION
MODE 1 FREQ. = 2.30 Hz
ZERO SPIN

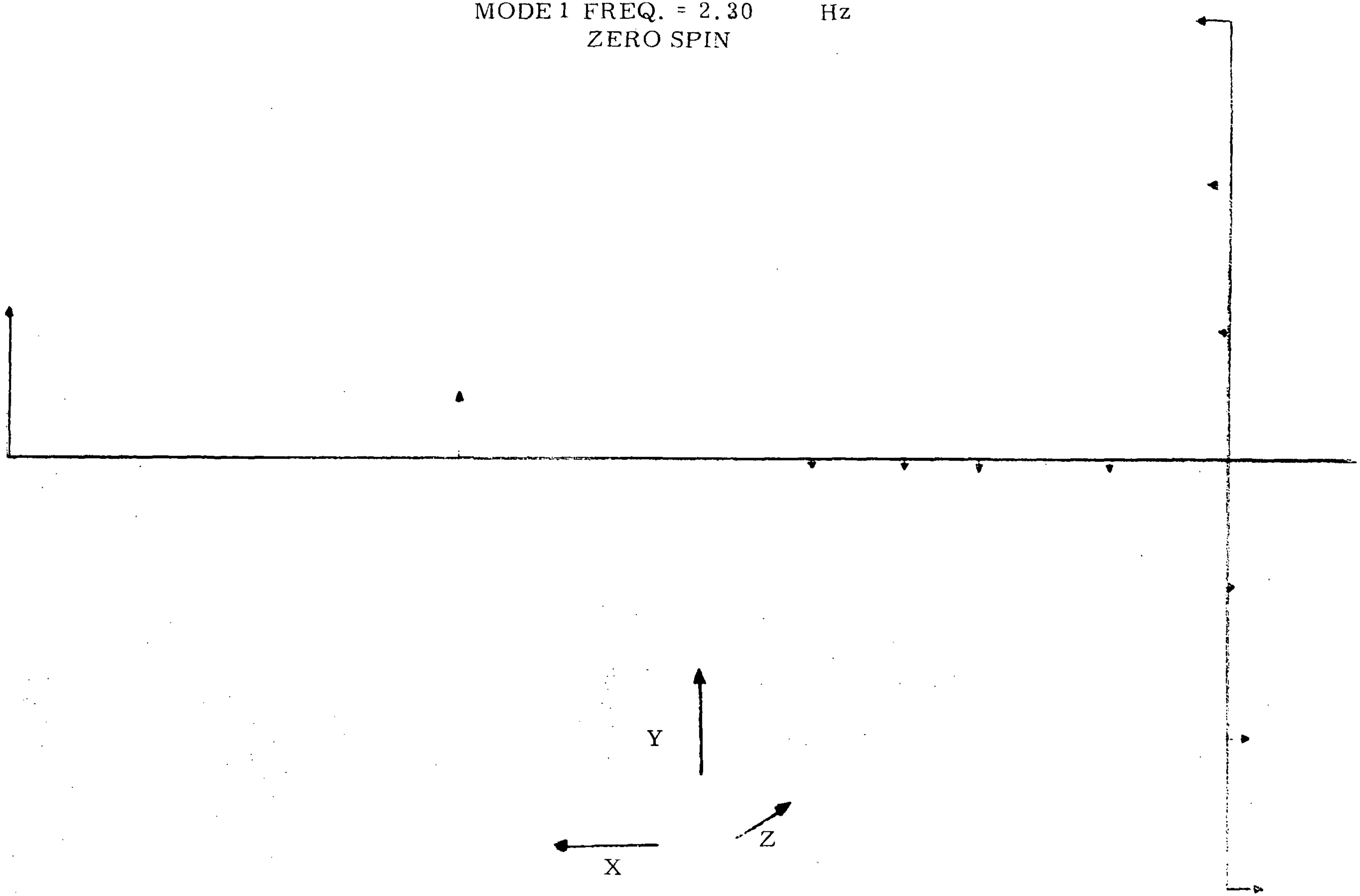

FIGURE A-28
ARTIFICIAL "G" SPACE STATION
MODE 2 FREQ. = 4.20 Hz
ZERO SPIN

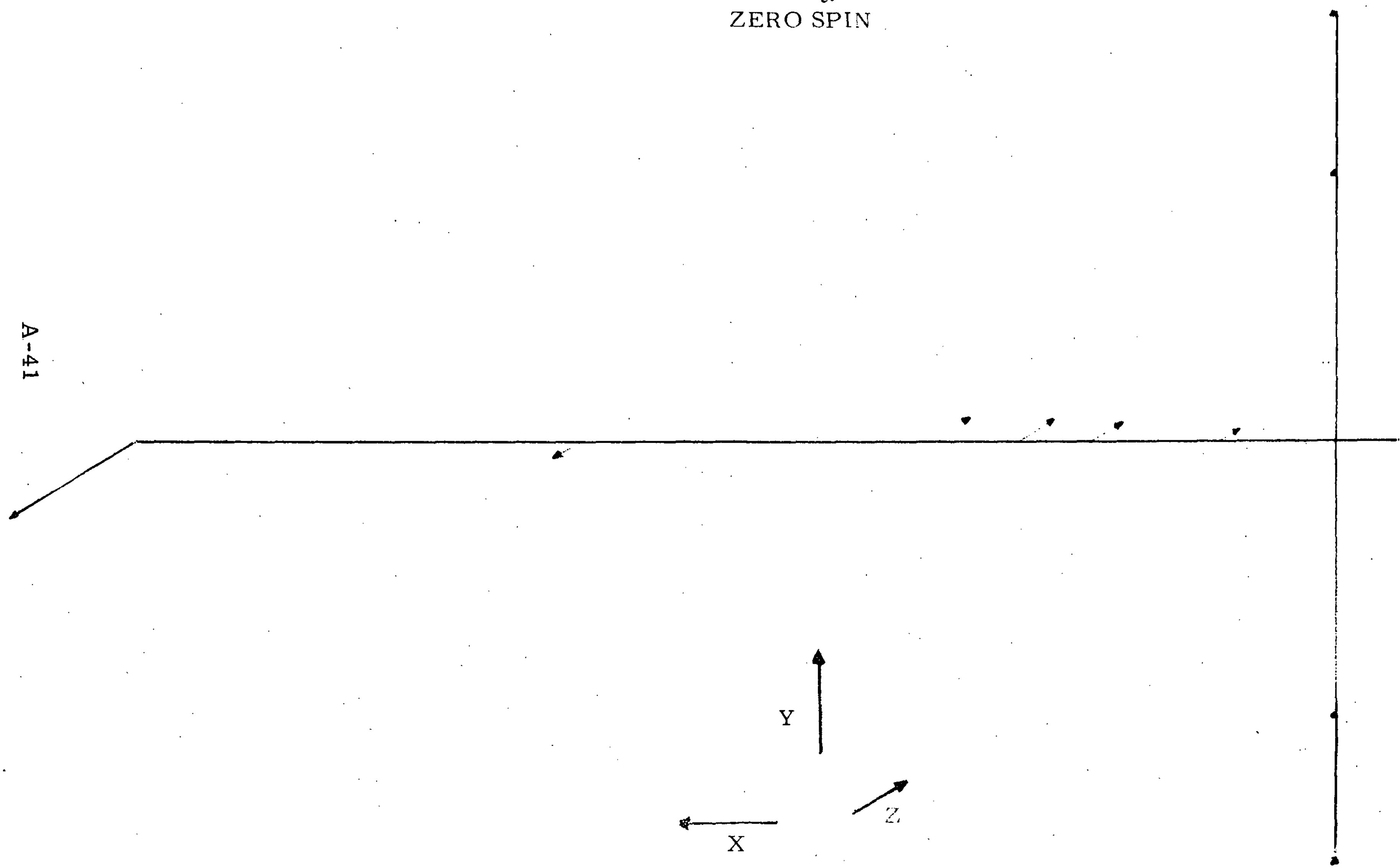

FIGURE A-29
ARTIFICIAL "G" SPACE STATION
MODE 3 FREQ. = 8.42 Hz
ZERO SPIN

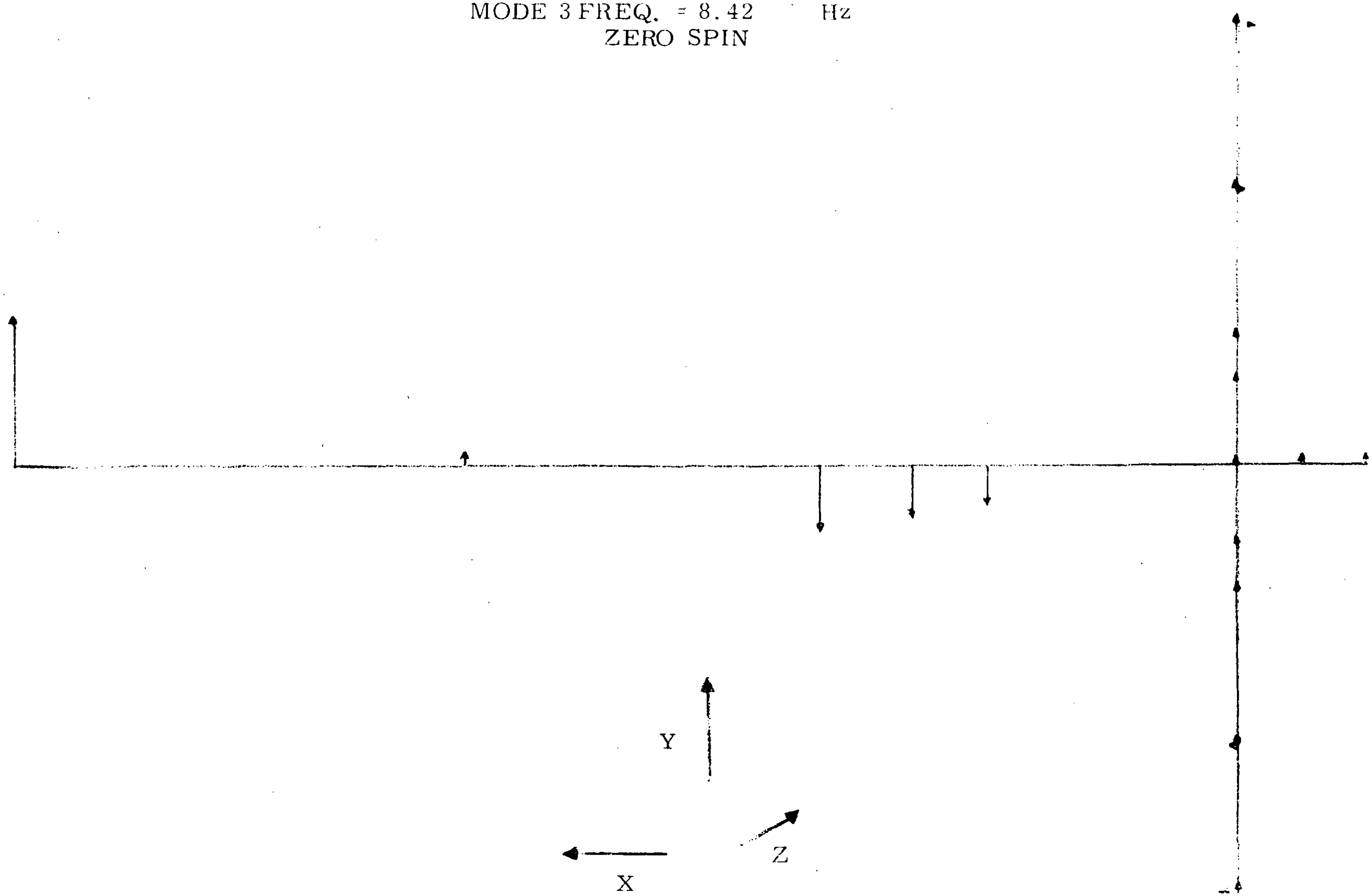

FIGURE A-30
ARTIFICIAL "G" SPACE STATION
MODE 4 FREQ. = 8.68 Hz
ZERO SPIN

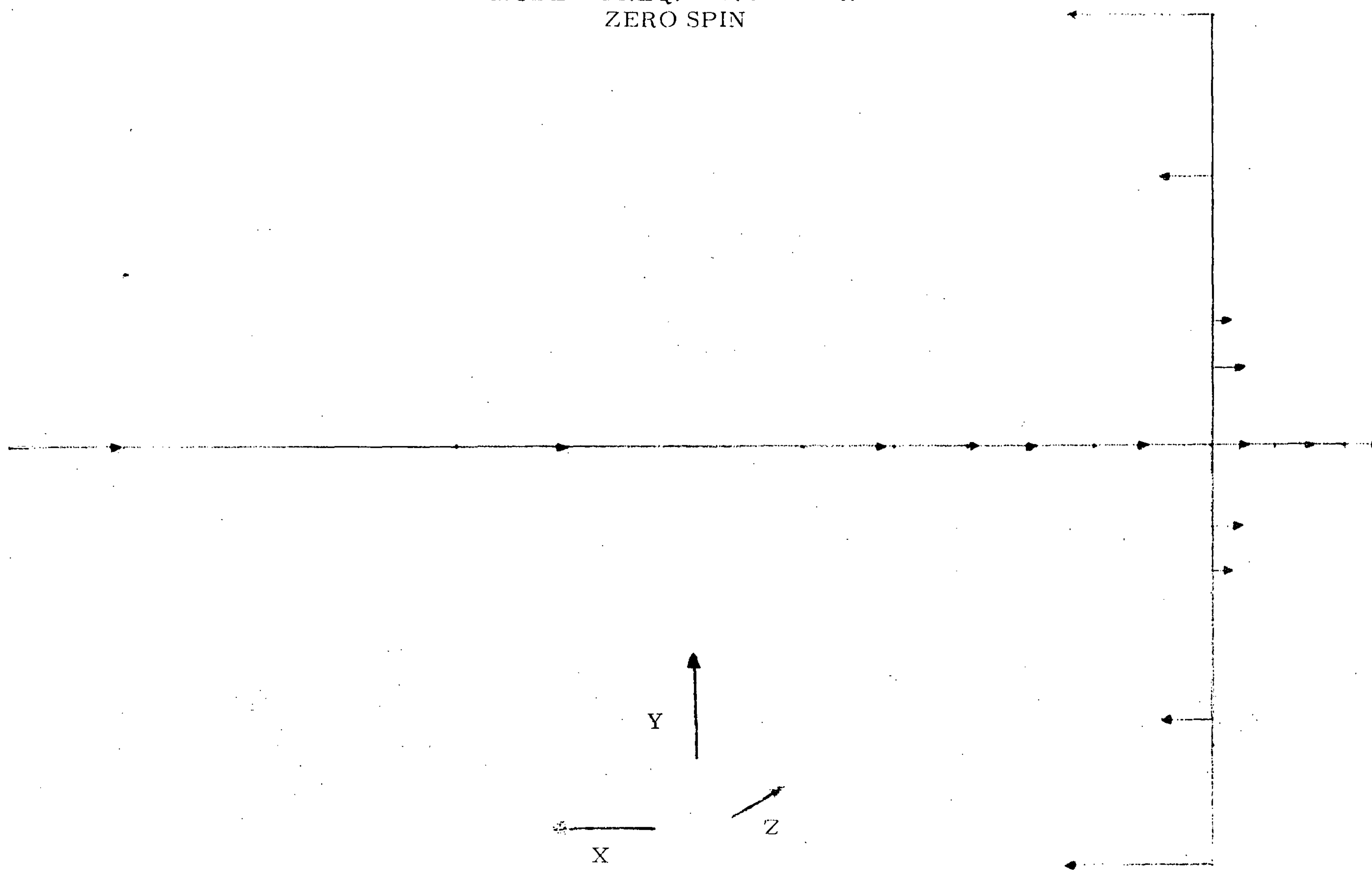

FIGURE A-31
ARTIFICIAL "G" SPACE STATION
MODE 5 FREQ. = 10.5 Hz
ZERO SPIN

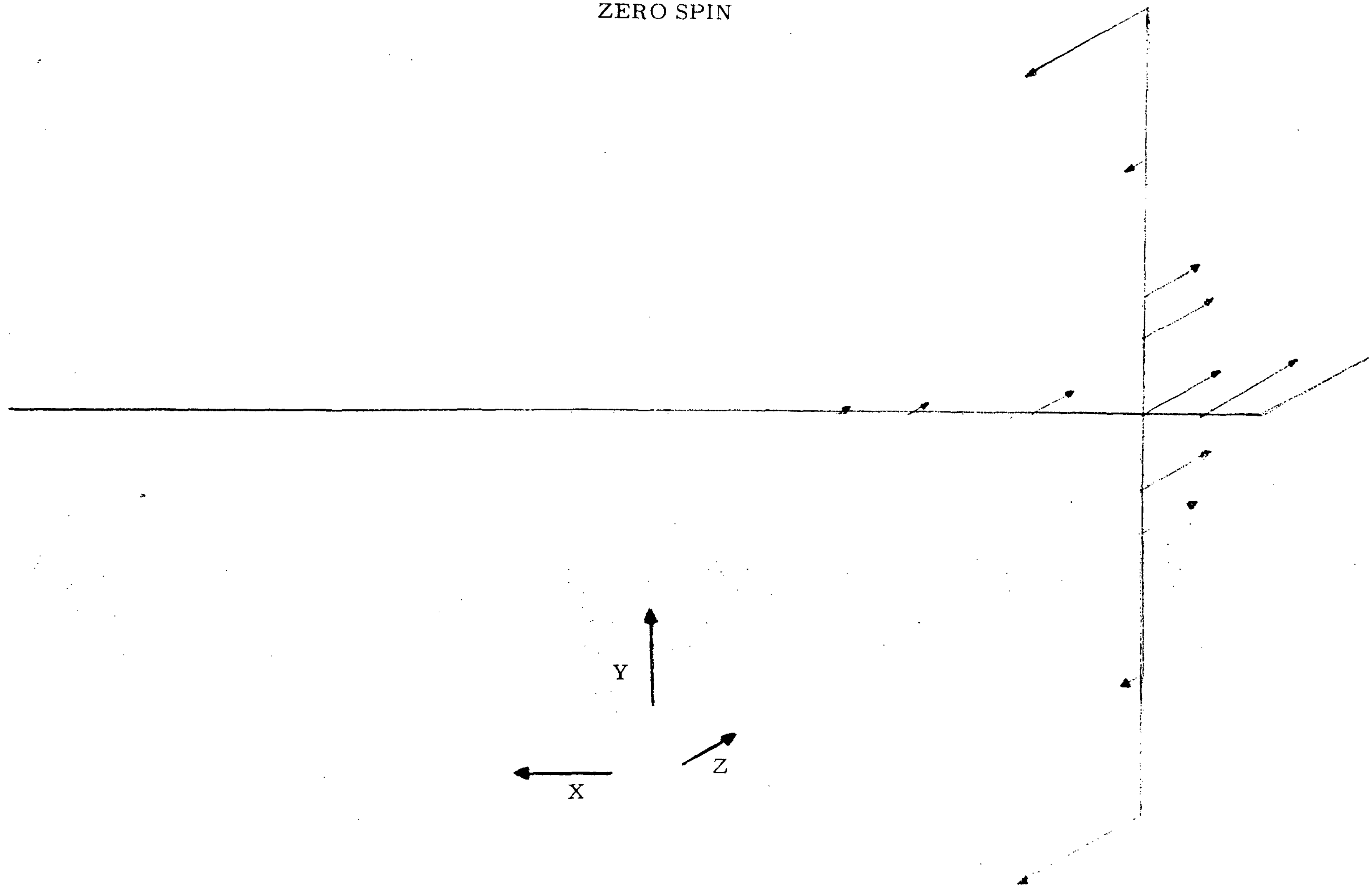

FIGURE A-32
ARTIFICIAL "G" SPACE STATION
MODE 6 FREQ. = 12.6 Hz
ZERO SPIN

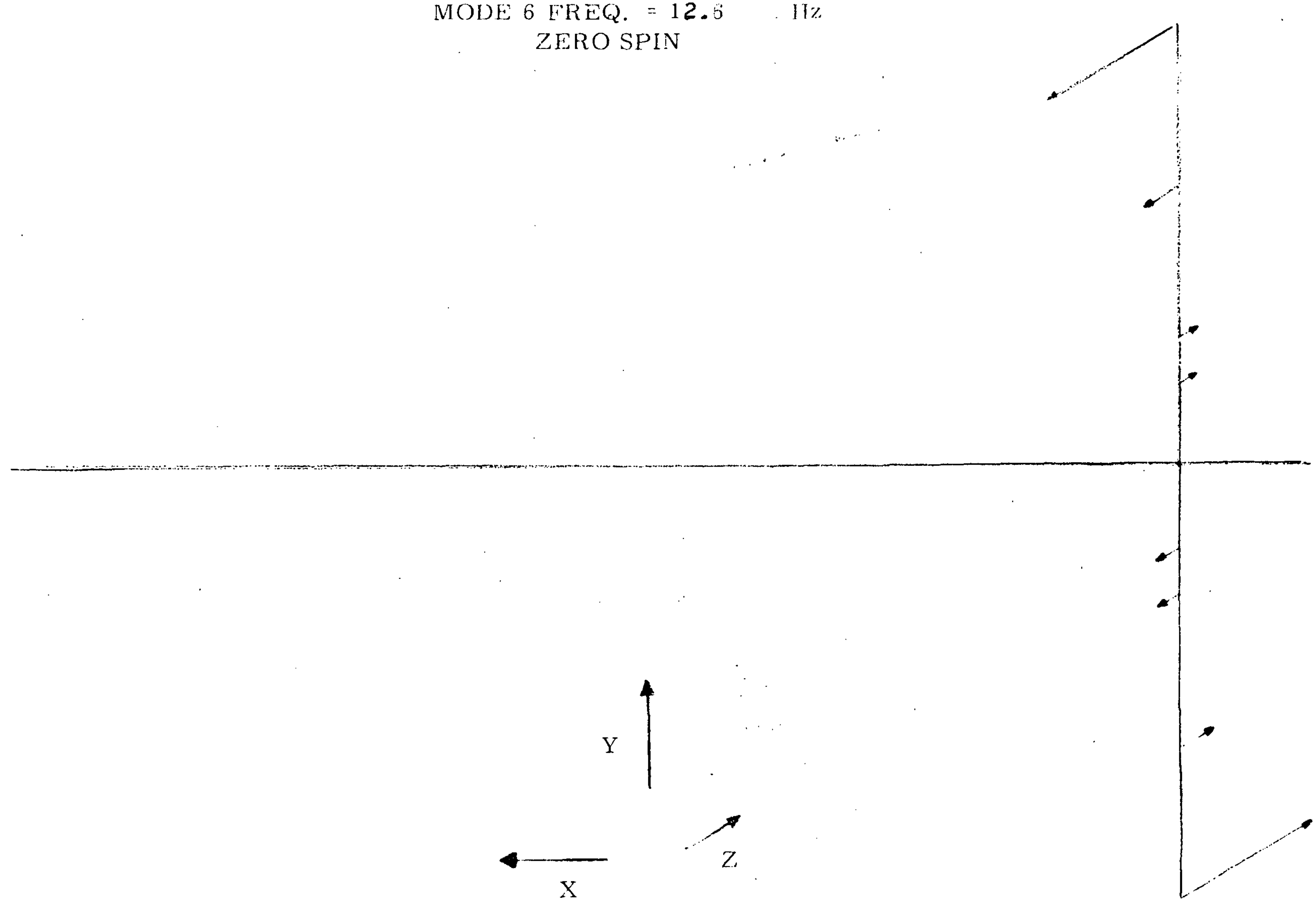

TABLE A-10

ARTIFICIAL "G" SPACE STATION

FINITE ELEMENT MODEL DATA

NODE	MASS LB SEC²/IN	INERTIA LB SEC² IN x Axis	y Axis	z Axis	NO. OF STRUCTURAL D.O.F.	D.O.F. SEQUENCE NO.
1	21.578	--	66641	--	6	1-6
2	21.578	--	66641	--	6	7-12
3	21.578	--	66641	--	6	13-18
4	21.578	--	66641	--	6	19-24
5	21.578	--	66641	--	6	25-30
6	21.578	--	66641	--	6	31-36
7	--	--	--	--	6	37-42
8	--	--	--	--	6	43-48
9	15.382	41621	--	--	6	49-54
10	8.094	21886	--	--	6	55-60
11	4.047	10956	--	--	6	61-66
12	17.814	49417	--	--	6	67-72
13	15.379	41595	--	--	6	73-78
14	12.795	18700	--	--	6	79-84
15	10.632	9350			6	85-90
16	25.952	20642			6	91-96
17	.01295	10.282			6	97-102

TABLE A-11

CORIOLIS FORCE MATRIX

(NORMALIZED TO Ω)

D. O. F.* Sequence No.			
1 - 3	-43.15581	0.	0.
4 - 6	0.	0.	0.
etc.	-43.15581	0.	0.
	0.	0.	0.
	-43.15581	0.	0.
	0.	0.	0.
	-43.15581	0.	0.
	0.	0.	0.
	-43.15581	0.	0.
	0.	0.	0.
	-43.15581	0.	0.
	0.	0.	0.
	0.	0.	0.
	0.	0.	0.
	0.	0.	0.
	0.	0.	0.
	-30.76417	0.	0.
	-41621.02691	0.	0.
	-16.18755	0.	0.
	-21885.53002	0.	0.
	-8.09377	0.	0.
	-10955.20496	0.	0.
	-35.62841	0.	0.
	-49417.88198	0.	0.
	-30.75889	0.	0.
	-41595.14699	0.	0.
	-25.49926	0.	0.
	-18699.30020	0.	0.
	-21.26381	0.	0.
	-9349.65010	0.	0.
	-51.90365	0.	0.
	-20642.29399	0.	0.
	-0.02588	0.	0.
100 - 102	-10.28432	0.	0.

* - Refer to Table A-10 for corresponding node number.

TABLE A-12

CENTRIFUGAL FORCE MATRIX
(NORMALIZED TO Ω^2)

D. O. F.* Sequence No.			
1 - 3	-21.57791	-21.57791	0.
4 - 6	0.	0.	0.
	-21.57791	-21.57791	0.
etc.	0.	0.	0.
	-21.57791	-21.57791	0.
	0.	0.	0.
	-21.57791	-21.57791	0.
	0.	0.	0.
	-21.57791	-21.57791	0.
	0.	0.	0.
	-21.57791	-21.57791	0.
	0.	0.	0.
	0.	0.	0.
	0.	0.	0.
	0.	0.	0.
	0.	0.	0.
	-15.38208	-15.38208	0.
	0.	0.	0.
	-8.09375	-8.09375	0.
	0.	0.	0.
	-4.04687	-4.04687	0.
	0.	0.	0.
	-17.81401	-17.81401	0.
	0.	0.	0.
	-15.37949	-15.37949	0.
	0.	0.	0.
	-12.79468	-12.79468	0.
	0.	0.	0.
	-10.63191	-10.63191	0.
	0.	0.	0.
	-25.95188	-25.95188	0.
	0.	0.	0.
	-0.01294	-0.01294	0.
100 - 102	0.	0.	0.

* - Refer to Table A-10 for corresponding node number.

EIGENVECTOR FOR ROOT NO.= 1

Mode 1, Frequency = 2.2948 Hz, Ω = 0 RPM

EIGENVALUE= 0.14419945E 02 (rad/sec.)

REAL PART								
1 TO 7	0.2895E 00	-0.3381E-01	-0.7647E-05	-0.3272E-08	-0.2953E-07	-0.6066E-03	-0.2895E 00
8 TO 14	-0.3385E-01	-0.7649E-05	0.3249E-08	-0.2953E-07	-0.6066E-03	0.1806E 00	-0.3380E-01
15 TO 21	-0.7075E-05	-0.2986E-08	-0.2949E-07	-0.6012E-03	-0.1806E 00	-0.3382E-01	-0.7080E-05
22 TO 28	0.2973E-08	-0.2949E-07	-0.6012E-03	0.7399E-01	-0.3374E-01	-0.6619E-05	-0.1912E-08
29 TO 35	-0.2943E-07	-0.5801E-03	-0.7399E-01	-0.3375E-01	-0.6624E-05	0.1931E-08	-0.2943E-07
36 TO 42	-0.5801E-03	0.3974E-01	-0.3370E-01	-0.6533E-05	-0.8932E-09	-0.2937E-07	-0.5605E-03
43 TO 49	-0.3975E-01	-0.3371E-01	-0.6537E-05	0.9372E-09	-0.2937E-07	-0.5605E-03	-0.4130E-05
50 TO 56	-0.3366E-01	-0.6501E-05	0.2631E-10	-0.2933E-07	-0.5428E-03	-0.4145E-05	-0.1091E-02
57 TO 63	-0.8236E-05	0.2637E-10	-0.2864E-07	-0.5429E-03	-0.4163E-05	0.3149E-01	-0.9945E-05
64 TO 70	0.2642E-10	-0.2841E-07	-0.5430E-03	-0.4232E-05	-0.9412E-01	-0.2119E-05	0.2681E-10
71 TO 77	-0.2879E-07	-0.2682E-03	-0.4317E-05	-0.1158E 00	0.2222E-05	0.2717E-10	-0.2598E-07
78 TO 84	-0.2790E-04	-0.4351E-05	-0.1133E 00	0.3476E-05	0.2732E-10	-0.2240E-07	0.1116E-03
85 TO 91	-0.4391E-05	-0.9932E-01	0.4283E-05	0.2767E-10	-0.1732E-09	0.5425E-03	-0.4533E-05
92 TO 98	0.3722E 00	-0.8961E-05	0.2892E-10	0.5220E-07	0.1546E-02	-0.4559E-05	0.1000E 01
99 TO 102	-0.2738E-04	0.2926E-10	0.4876E-07	0.1729E-02			
IMAGINARY PART							
1 TO 7	0.0	0.0	0.0	0.0	0.0	0.0	0.0
8 TO 14	0.0	0.0	0.0	0.0	0.0	0.0	0.0
15 TO 21	0.0	0.0	0.0	0.0	0.0	0.0	0.0
22 TO 28	0.0	0.0	0.0	0.0	0.0	0.0	0.0
29 TO 35	0.0	0.0	0.0	0.0	0.0	0.0	0.0
36 TO 42	0.0	0.0	0.0	0.0	0.0	0.0	0.0
43 TO 49	0.0	0.0	0.0	0.0	0.0	0.0	0.0
50 TO 56	0.0	0.0	0.0	0.0	0.0	0.0	0.0
57 TO 63	0.0	0.0	0.0	0.0	0.0	0.0	0.0
64 TO 70	0.0	0.0	0.0	0.0	0.0	0.0	0.0
71 TO 77	0.0	0.0	0.0	0.0	0.0	0.0	0.0
78 TO 84	0.0	0.0	0.0	0.0	0.0	0.0	0.0
85 TO 91	0.0	0.0	0.0	0.0	0.0	0.0	0.0
92 TO 98	0.0	0.0	0.0	0.0	0.0	0.0	0.0
99 TO 102	0.0	0.0	0.0	0.0			

EIGENVECTOR FOR ROOT NO.= 2

Mode 2, Frequency 4.2027 Hz, Ω = 0 RPM

EIGENVALUE= 0.2640625E 02 (rad/sec.)

REAL PART

1 TO 7	-0.4023E-05	0.1255E-05	-0.4898E-01	-0.5198E-04	-0.1153E-02	0.9347E-08	0.4023E-05
8 TO 14	0.1254E-05	-0.4894E-01	0.5191E-04	-0.1169E-02	0.9351E-08	-0.2360E-05	0.1250E-05
15 TO 21	-0.3988E-01	-0.4754E-04	-0.1164E-02	0.9067E-08	0.2353E-05	0.1250E-05	-0.3986E-01
22 TO 28	0.4744E-04	-0.1164E-02	0.8970E-08	-0.8497E-06	0.1241E-05	-0.3262E-01	-0.3061E-04
29 TO 35	-0.1155E-02	0.7621E-08	0.8520E-06	0.1241E-05	-0.3261E-01	0.3051E-04	-0.1155E-02
36 TO 42	0.7623E-08	-0.4265E-06	0.1235E-05	-0.3124E-01	-0.1475E-04	-0.1148E-02	0.6448E-08
43 TO 49	0.4237E-06	0.1235E-05	-0.3123E-01	0.1464E-04	-0.1143E-02	0.6449E-08	0.1108E-08
50 TO 56	0.1230E-05	-0.3068E-01	-0.5914E-07	-0.1142E-02	0.5394E-08	0.1174E-08	0.9062E-06
57 TO 63	-0.3337E-01	-0.5836E-07	-0.1147E-02	0.5401E-08	0.1295E-08	0.5816E-06	-0.1683E 00
64 TO 70	-0.5848E-07	-0.1149E-02	0.5416E-08	0.8202E-09	0.9021E-06	0.1309E 00	-0.6062E-07
71 TO 77	-0.3277E-03	-0.8962E-08	0.5750E-09	-0.1216E-05	0.2594E 00	-0.6226E-07	-0.7097E-03
78 TO 84	-0.1847E-07	0.4911E-09	-0.2427E-05	0.2955E 00	-0.6235E-07	-0.4901E-03	-0.2171E-07
85 TO 91	0.3745E-09	-0.3739E-05	0.3036E 00	-0.6412E-07	0.2521E-03	-0.1447E-07	0.4863E-10
92 TO 98	-0.4402E-05	-0.2367E 00	-0.5868E-07	0.2070E-02	0.3027E-08	-0.7443E-10	-0.4029E-05
99 TO 102	-0.1000E 01	-0.6868E-07	0.2068E-02	0.9962E-12			

IMAGINARY PART

1 TO 7	0.0	0.0	0.0	0.0	0.0	0.0	0.0
8 TO 14	0.0	0.0	0.0	0.0	0.0	0.0	0.0
15 TO 21	0.0	0.0	0.0	0.0	0.0	0.0	0.0
22 TO 28	0.0	0.0	0.0	0.0	0.0	0.0	0.0
29 TO 35	0.0	0.0	0.0	0.0	0.0	0.0	0.0
36 TO 42	0.0	0.0	0.0	0.0	0.0	0.0	0.0
43 TO 49	0.0	0.0	0.0	0.0	0.0	0.0	0.0
50 TO 56	0.0	0.0	0.0	0.0	0.0	0.0	0.0
57 TO 63	0.0	0.0	0.0	0.0	0.0	0.0	0.0
64 TO 70	0.0	0.0	0.0	0.0	0.0	0.0	0.0
71 TO 77	0.0	0.0	0.0	0.0	0.0	0.0	0.0
78 TO 84	0.0	0.0	0.0	0.0	0.0	0.0	0.0
85 TO 91	0.0	0.0	0.0	0.0	0.0	0.0	0.0
92 TO 98	0.0	0.0	0.0	0.0	0.0	0.0	0.0
99 TO 102	0.0	0.0	0.0	0.0			

EIGENVECTOR FOR ROOT NO.= 3

Mode 3, Frequency = 8.4224 Hz, Ω = 0 RPM

EIGENVALUE= [illegible] (rad/sec.)

REAL PART

1	TO	7	-0.1213E 00	[illegible]	[illegible]	[illegible]-08	0.2999E-07	0.3795E-03	0.1213E 00
8	TO	14	0.7999E-01	[illegible]	[illegible]	0.2999E-07	0.3795E-03	-0.5559E-01	0.7876E-01
15	TO	21	0.4681E-06	[illegible]	[illegible]-07	0.3357E-03	0.5559E-01	0.7874E-01	0.4681E-06
22	TO	28	-0.5356E-08	[illegible]	[illegible]-03	-0.6983E-02	0.7649E-01	-0.3370E-06	0.3317E-08
29	TO	35	0.2859E-07	[illegible]	[illegible]-02	0.7649E-01	-0.3370E-06	-0.3317E-08	0.2859E-07
36	TO	42	0.1840E-03	0.2312E-02	[illegible]	-0.4813E-06	0.1447E-08	0.2782E-07	0.5233E-04
43	TO	49	-0.2310E-[illegible]	0.7507E-[illegible]	-0.4012E-[illegible]	-0.1443E-08	0.27[illegible]-07	0.5233E-04	0.1215E-[illegible]
50	TO	56	[illegible]	[illegible]	0.6284E-[illegible]	[illegible]-07	-0.62[illegible]	0.1219E-03	0.7785E-[illegible]
57	TO	63	0.1114E [illegible]	[illegible]	0.2761E-07	[illegible]	0.12[illegible]E-06	0.8240E-01	0.2777E-[illegible]
64	TO	70	0.6469E-13	[illegible]-07	-0.7693E-04	0.1464E-06	-0.4[illegible]	-0.3106E-05	0.8183E-13
71	TO	77	0.8207E-[illegible]	-0.134[illegible]	0.1691E-06	-0.2910E 00	-0.30[illegible]	0.9694E-13	-0.8815E-08
78	TO	84	-0.1660E-02	[illegible]	-0.3767E 00	[illegible]-05	0.1[illegible]-12	-0.[illegible]15E-07	0.1478E-02
85	TO	91	0.1832E-05	[illegible]	-0.9757E-06	[illegible]-12	-0.17[illegible]	-0.4665E-03	0.2329E-[illegible]
92	TO	98	0.2032E-[illegible]	[illegible]	0.1790E-[illegible]	[illegible]-08	[illegible]	0.2257E-[illegible]	0.1000E 01
99	TO	102	[illegible]	[illegible]	[illegible]	[illegible]			

IMAGINARY PART

1	TO	7	0.0	0.0	0.0	0.0	0.0	0.0	0.0
8	TO	14	0.0	0.0	0.0	0.0	0.0	0.0	0.0
15	TO	21	0.0	0.0	0.0	0.0	0.0	0.0	0.0
22	TO	28	0.0	0.0	0.0	0.0	0.0	0.0	0.0
29	TO	35	0.0	0.0	0.0	0.0	0.0	0.0	0.0
36	TO	42	0.0	0.0	0.0	0.0	0.0	0.0	0.0
43	TO	49	0.0	0.0	0.0	0.0	0.0	0.0	0.0
50	TO	56	0.0	0.0	0.0	0.0	0.0	0.0	0.0
57	TO	63	0.0	0.0	0.0	0.0	0.0	0.0	0.0
64	TO	70	0.0	0.0	0.0	0.0	0.0	0.0	0.0
71	TO	77	0.0	0.0	0.0	0.0	0.0	0.0	0.0
78	TO	84	0.0	0.0	0.0	0.0	0.0	0.0	0.0
85	TO	91	0.0	0.0	0.0	0.0	0.0	0.0	0.0
92	TO	98	0.0	0.0	0.0	0.0	0.0	0.0	0.0
99	TO	102	0.0	0.0	0.0	0.0			

EIGENVECTOR FOR ROOT NO.= 4

Mode 4. Frequency = 8.6711 Hz, Ω = [illegible] RPM

EIGENVALUE= 0.54482422E 02 (rad/sec.)

REAL PART

1 TO 7	-0.1000E 01	0.1405E-02	0.4022E-05	0.2172E-08	-0.24[illegible]E-06	0.3715E-02	-0.9962E 00
8 TO 14	0.1400E-02	-0.1238E-05	0.1203E-07	-0.2476E-06	-0.3[illegible]E-02	-0.3546E 00	0.1377E-02
15 TO 21	0.3585E-05	0.2844E-08	-0.2435E-06	0.3327E-02	-0.3[illegible]E 00	0.1374E-02	0.8537E-06
22 TO 28	0.1070E-07	-0.2435E-06	-0.2316E-02	0.1429E 00	0.1[illegible]E-02	0.3010E-05	0.3207E-08
29 TO 35	-0.2354E-06	0.2026E-02	0.1431E 00	0.1330E-02	0.2[illegible]E-05	0.6681E-08	-0.2354E-06
36 TO 42	-0.2021E-02	0.2325E 00	0.1304E-02	0.2874E-05	0.1[illegible]	-0.2286E-06	0.9289E-03
43 TO 49	0.2324E 00	0.1304E-02	0.2732E-05	0.2382E-08	-0.2[illegible]	-0.9279E-03	0.2668E 00
50 TO 56	0.1280E-02	0.2923E-05	0.1278E-09	-0.2238E-06	-0.1[illegible]E-05	0.2698E 00	0.1366E-02
57 TO 63	-0.1078E-04	0.1306E-09	-0.2279E-06	-0.1456E-05	0.2[illegible]E 00	0.1453E-02	-0.2442E-04
64 TO 70	0.1324E-09	-0.2272E-06	-0.1448E-05	0.3741E 00	-0.5[illegible]E-03	0.2928E-04	0.1797E-09
71 TO 77	-0.1208E-05	-0.2183E-04	0.4659E 00	-0.4428E-02	0.3[illegible]E-04	0.2201E-09	0.1268E-07
78 TO 84	-0.2546E-04	0.5046E 00	-0.5838E-02	0.3412E-04	0.[illegible]E-09	0.9953E-07	-0.2106E-04
85 TO 91	0.5547E 00	-0.6612E-02	0.1742E-04	0.2873E-09	0.3[illegible]E-06	-0.2213E-06	0.7520E 00
92 TO 98	0.3511E-02	-0.2014E-02	0.4826E-09	0.4918E-06	0.2[illegible]E-04	0.7509E 00	0.6990E-02
99 TO 102	-0.2730E-03	0.5209E-09	0.3970E-07	0.3079E-06			

IMAGINARY PART

1 TO 7	0.0	0.0	0.0	0.0	0.0	0.0	0.0
8 TO 14	0.0	0.0	0.0	0.0	0.0	0.0	0.0
15 TO 21	0.0	0.0	0.0	0.0	0.0	0.0	0.0
22 TO 28	0.0	0.0	0.0	0.0	0.0	0.0	0.0
29 TO 35	0.0	0.0	0.0	0.0	0.0	0.0	0.0
36 TO 42	0.0	0.0	0.0	0.0	0.0	0.0	0.0
43 TO 49	0.0	0.0	0.0	0.0	0.0	0.0	0.0
50 TO 56	0.0	0.0	0.0	0.0	0.0	0.0	0.0
57 TO 63	0.0	0.0	0.0	0.0	0.0	0.0	0.0
64 TO 70	0.0	0.0	0.0	0.0	0.0	0.0	0.0
71 TO 77	0.0	0.0	0.0	0.0	0.0	0.0	0.0
78 TO 84	0.0	0.0	0.0	0.0	0.0	0.0	0.0
85 TO 91	0.0	0.0	0.0	0.0	0.0	0.0	0.0
92 TO 98	0.0	0.0	0.0	0.0	0.0	0.0	0.0
99 TO 102	0.0	0.0	0.0	0.0			

EIGENVECTOR FOR ROOT NO.= 1

Mode 1, Frequency = 2.2729 Hz, Ω = 4RPM

EIGENVALUE= 0.14406738E 02 (rad/sec.)

REAL PART							
1 TO 7	0.3613E 00	-0.2108E-01	-0.1556E-04	-0.5927E-08	-0.5178E-08	-0.7497E-03	-0.3613E 00
8 TO 14	-0.2116E-01	-0.1553E-04	0.5730E-08	-0.5178E-08	-0.7496E-03	0.2266E 00	-0.2110E-01
15 TO 21	-0.1452E-04	-0.5423E-08	-0.5170E-08	-0.7457E-03	-0.2266E 00	-0.2116E-01	-0.1452E-04
22 TO 28	0.5283E-08	-0.5170E-08	-0.7457E-03	0.9370E-01	-0.2110E-01	-0.1369E-04	-0.3471E-08
29 TO 35	-0.6156E-08	-0.7278E-03	-0.9370E-01	-0.2112E-01	-0.1371E-04	0.3495E-08	-0.6156E-08
36 TO 42	-0.7278E-03	0.5054E-01	-0.2108E-01	-0.1353E-04	-0.1613E-08	-0.6144E-08	-0.7099E-03
43 TO 49	-0.5055E-01	-0.2109E-01	-0.1355E-04	0.1765E-08	-0.6144E-08	-0.7100E-03	-0.2343E-05
50 TO 56	-0.2106E-01	-0.1348E-04	0.1011E-09	-0.6135E-08	-0.6933E-03	-0.2336E-05	0.2055E-01
57 TO 63	-0.1378E-04	0.1014E-09	-0.4401E-08	-0.6937E-03	-0.2325E-05	0.6218E-01	-0.1402E-04
64 TO 70	0.1016E-09	-0.3741E-08	-0.6929E-03	-0.2576E-05	-0.1049E 00	-0.1224E-04	0.1033E-09
71 TO 77	-0.9988E-08	-0.4276E-03	-0.2785E-05	-0.1504E 00	-0.1066E-04	0.1048E-09	-0.1036E-07
78 TO 84	-0.1838E-03	-0.2969E-05	-0.1570E 00	-0.1011E-04	0.1055E-09	-0.7761E-08	-0.3693E-04
85 TO 91	-0.2974E-05	-0.1426E 00	-0.1033E-04	0.1071E-09	0.1416E-07	0.4262E-03	-0.3342E-05
92 TO 98	0.3121E 00	-0.2892E-04	0.1128E-09	0.6418E-07	0.1733E-02	-0.3456E-05	0.1000E 01
99 TO 102	-0.5052E-04	0.1146E-09	0.5561E-07	0.1930E-02			
IMAGINARY PART							
1 TO 7	0.4649E-03	0.1005E-03	0.5932E-08	0.8129E-11	0.5998E-11	-0.4900E-06	0.5464E-03
8 TO 14	-0.9165E-04	-0.2005E-08	0.8939E-11	0.6002E-11	0.6602E-05	0.3795E-03	0.7718E-04
15 TO 21	0.4456E-08	0.8352E-11	0.5993E-11	-0.4438E-06	0.4304E-03	-0.6836E-04	-0.1300E-08
22 TO 28	0.8932E-11	0.5995E-11	0.5126E-06	0.3133E-03	0.3991E-04	0.2901E-08	0.8982E-11
29 TO 35	0.5980E-11	-0.2620E-06	0.3342E-03	-0.3110E-04	0.3421E-09	0.9304E-11	0.5981E-11
36 TO 42	0.4254E-06	0.3026E-03	0.2163E-04	0.2342E-08	0.9678E-11	0.5969E-11	-0.8764E-07
43 TO 49	0.3138E-03	-0.1283E-04	0.9152E-09	0.9821E-11	0.5970E-11	0.2459E-06	0.3019E-03
50 TO 56	0.4393E-05	0.1631E-08	0.1008E-10	0.5961E-11	0.7674E-07	0.2874E-03	-0.2120E-06
57 TO 63	0.1982E-08	0.1022E-10	0.5737E-11	0.7677E-07	0.2688E-03	-0.4819E-05	0.2319E-08
64 TO 70	0.1029E-10	0.5559E-11	0.7679E-07	0.2988E-03	0.1307E-04	0.7250E-09	0.9126E-11
71 TO 77	0.6086E-11	0.3951E-07	0.2768E-03	0.1650E-04	-0.1723E-09	0.6929E-11	0.5769E-11
78 TO 84	0.6875E-08	0.2535E-03	0.1633E-04	-0.5018E-09	0.4776E-11	0.5195E-11	-0.1223E-07
85 TO 91	0.1992E-03	0.1326E-04	-0.7476E-09	-0.3301E-11	0.1614E-11	-0.7142E-07	-0.1432E-03
92 TO 98	-0.4926E-04	0.8981E-09	-0.4098E-10	-0.7183E-11	-0.2250E-06	-0.1461E-03	-0.1355E-03
99 TO 102	0.3409E-08	-0.4100E-10	-0.5654E-11	-0.2381E-06			

EIGENVECTOR FOR ROOT NO.= 2 Mode 2, Frequency = 4.2027 Hz, Ω = 4 RPM

EIGENVALUE= 0.26406250E 02 (rad/sec.)

REAL PART

1 TO 7	-0.3823E-05	0.1226E-05	-0.4896E-01	-0.5194E-04	-0.1169E-02	0.8939E-08	0.3825E-05
8 TO 14	0.1226E-05	-0.4992E-01	0.5196E-04	-0.1169E-02	0.8941E-08	-0.2237E-05	0.1222E-05
15 TO 21	-0.3988E-01	-0.4750E-04	-0.1164E-02	0.8558E-08	0.2239E-05	0.1222E-05	-0.3985E-01
22 TO 28	0.4742E-04	-0.1164E-02	0.8560E-08	-0.7992E-06	0.1213E-05	-0.3261E-01	-0.3058E-04
29 TO 35	-0.1155E-02	0.7222E-09	0.8011E-06	0.1213E-05	-0.3262E-01	0.3048E-04	-0.1155E-02
36 TO 42	0.7223E-09	-0.3994E-06	0.1208E-05	-0.3123E-01	-0.1474E-04	-0.1148E-02	0.6063E-08
43 TO 49	0.4014E-06	0.1209E-05	-0.3122E-01	0.1463E-04	-0.1143E-02	0.6064E-08	0.9486E-09
50 TO 56	0.1202E-05	-0.3068E-01	-0.5799E-07	-0.1142E-02	0.5024E-08	0.1013E-08	0.9008E-06
57 TO 63	-0.9937E-01	-0.5833E-07	-0.1147E-02	0.5030E-08	0.1132E-08	0.5984E-06	-0.1682E 00
64 TO 70	-0.5852E-07	-0.1149E-02	0.5044E-08	0.6806E-09	0.8359E-06	0.1309E 00	-0.6079E-07
71 TO 77	-0.9876E-03	-0.9105E-08	0.4536E-09	-0.1291E-05	0.2594E 00	-0.6234E-07	-0.7097E-03
78 TO 84	-0.1848E-07	0.3670E-09	-0.2501E-05	0.2955E 00	-0.6271E-07	-0.4901E-03	-0.2167E-07
85 TO 91	0.2692E-09	-0.3808E-05	0.3036E 00	-0.6307E-07	0.2527E-03	-0.1442E-07	-0.2841E-10
92 TO 98	-0.4490E-05	-0.2367E 00	-0.6324E-07	0.2070E-02	0.2965E-08	-0.1267E-09	-0.4126E-05
99 TO 102	-0.1000E 01	-0.6324E-07	0.2068E-02	0.9807E-12			

IMAGINARY PART

1 TO 7	-0.2571E-07	0.3250E-09	-0.1508E-03	-0.2368E-06	-0.2166E-05	0.7608E-10	-0.1254E-07
8 TO 14	0.3825E-08	-0.2987E-04	-0.4615E-07	-0.2166E-05	-0.4513E-10	-0.1236E-07	0.7639E-09
15 TO 21	-0.1091E-03	-0.2226E-06	-0.2157E-05	0.7023E-10	-0.4633E-08	0.3410E-08	-0.3831E-04
22 TO 28	-0.4829E-07	-0.2157E-05	-0.4066E-10	-0.1402E-08	0.1444E-08	-0.7296E-04	-0.1704E-06
29 TO 35	-0.2140E-05	0.4808E-10	0.1321E-08	0.2725E-08	-0.4772E-04	-0.5818E-07	-0.2140E-05
36 TO 42	-0.2330E-10	0.9911E-09	0.1769E-08	-0.6412E-04	-0.1224E-06	-0.2126E-05	0.2749E-10
43 TO 49	0.2247E-08	0.7389E-08	-0.5151E-04	-0.6858E-07	-0.2126E-05	-0.6854E-11	0.2212E-08
50 TO 56	0.2071E-08	-0.5680E-04	-0.7902E-07	-0.2116E-05	0.8459E-11	0.2056E-08	0.1564E-08
57 TO 63	-0.1841E-03	-0.1146E-07	-0.2125E-05	0.8450E-11	0.1915E-08	0.1056E-08	-0.3117E-03
64 TO 70	0.2566E-07	-0.2128E-05	0.8460E-11	0.6352E-08	0.1342E-08	0.2426E-03	0.9382E-07
71 TO 77	-0.1830E-05	-0.1679E-10	0.1069E-07	-0.2543E-08	0.4837E-03	0.4660E-07	-0.1315E-05
78 TO 84	-0.3359E-10	0.1271E-07	-0.4739E-08	0.5475E-03	-0.7174E-07	-0.9089E-06	-0.3934E-10
85 TO 91	0.1543E-07	-0.7102E-08	0.5628E-03	-0.5618E-06	0.4641E-06	-0.2596E-10	0.2591E-07
92 TO 98	-0.8291E-08	-0.4365E-03	-0.2937E-05	0.3831E-05	0.5437E-11	0.2592E-07	-0.7622E-08
99 TO 102	-0.1851E-02	-0.2938E-05	0.3833E-05	-0.3248E-19			

EIGENVECTOR FOR ROOT NO.= 3   Mode 3, Frequency = 8.4147 Hz, Ω = 4 RPM

EIGENVALUE= 0.52871094E 02 (rad/sec.)

REAL PART

1 TO 7	-0.2553E-01	-0.1612E-01	-0.2562E-04	-0.1312E-06	-0.4720E-06	0.6430E-04	0.2380E-01
8 TO 14	-0.1604E-01	-0.2447E-04	0.1269E-06	-0.4717E-06	0.5456E-04	-0.1411E-01	-0.1532E-01
15 TO 21	-0.2965E-05	-0.1156E-06	-0.4646E-06	0.6167E-04	0.1402E-01	-0.1528E-01	-0.2479E-05
22 TO 28	0.1121E-06	-0.4644E-06	0.5334E-04	-0.3949E-02	-0.1461E-01	0.1404E-04	-0.6797E-07
29 TO 35	-0.4499E-06	0.4962E-04	0.5087E-02	-0.1459E-01	0.1407E-04	0.6631E-07	-0.4498E-06
36 TO 42	0.4375E-04	-0.1412E-02	-0.1434E-01	0.1701E-04	-0.3023E-07	-0.4377E-06	0.3541E-04
43 TO 49	0.2762E-02	-0.1433E-01	0.1698E-04	0.3023E-07	-0.4277E-06	0.3323E-04	0.7153E-03
50 TO 56	-0.1420E-01	0.1811E-04	0.2944E-09	-0.4290E-06	0.2312E-04	0.7143E-03	-0.1501E-01
57 TO 63	-0.7750E-05	0.3005E-09	-0.4318E-06	0.5691E-05	0.7120E-03	-0.1495E-01	-0.3362E-04
64 TO 70	0.3048E-09	-0.4308E-06	-0.4394E-05	0.7919E-03	-0.2027E-01	0.7038E-04	0.4032E-09
71 TO 77	-0.2457E-06	-0.1048E-03	0.8621E-03	-0.4711E-01	0.8761E-04	0.4875E-09	0.2198E-07
78 TO 84	-0.2625E-03	0.8893E-03	-0.6687E-01	0.8067E-04	0.5265E-09	0.2087E-06	-0.4010E-03
85 TO 91	0.9231E-03	-0.1114E 00	0.4409E-04	0.6268E-09	0.7905E-06	-0.7847E-03	0.1060E-02
92 TO 98	-0.2043E 00	-0.4540E-03	0.1029E-08	0.1095E-05	0.1405E-02	0.9917E-03	0.1000E 01
99 TO 102	-0.6019E-03	0.1111E-08	0.7877E-07	0.4194E-02			

IMAGINARY PART

1 TO 7	0.1152E-01	-0.7237E-05	0.1020E-05	0.1624E-08	0.4234E-10	-0.6784E-04	0.1164E-01
8 TO 14	0.1369E-02	-0.1016E-05	0.1624E-08	0.4315E-10	0.6221E-04	-0.1947E-03	0.2340E-04
15 TO 21	0.7131E-06	0.1868E-08	0.4227E-10	-0.5958E-04	-0.1357E-03	0.1556E-03	-0.7086E-06
22 TO 28	0.1968E-05	0.4248E-10	0.5991E-04	-0.8334E-02	0.5710E-04	0.3353E-06	0.2320E-08
29 TO 35	0.4104E-10	-0.3477E-04	-0.8928E-02	0.1184E-03	-0.3310E-06	0.2319E-08	0.4114E-10
36 TO 42	0.3495E-04	-0.1046E-01	0.7149E-04	0.1890E-06	0.2545E-08	0.3999E-10	-0.1549E-04
43 TO 49	-0.1045E-01	0.1013E-03	-0.1847E-06	0.2546E-08	0.4003E-10	0.1556E-04	-0.1102E-01
50 TO 56	0.8506E-04	0.2162E-08	0.2633E-08	0.3924E-10	-0.6350E-07	-0.1106E-01	0.8977E-04
57 TO 63	0.4538E-06	0.2724E-08	0.4011E-10	-0.8921E-07	-0.1117E-01	0.9557E-04	0.6994E-08
64 TO 70	0.2775E-08	0.4136E-10	-0.1004E-06	-0.1191E-01	-0.5347E-04	-0.1982E-08	0.2769E-08
71 TO 77	0.1578E-10	-0.1599E-05	-0.1255E-01	-0.3410E-03	-0.2613E-08	0.2641E-08	-0.6826E-11
78 TO 84	-0.2062E-05	-0.1274E-01	-0.4620E-03	-0.1843E-08	0.2450E-08	-0.1799E-10	-0.1943E-05
85 TO 91	-0.1291E-01	-0.5716E-03	-0.3485E-09	0.1899E-08	-0.1962E-10	-0.1033E-05	-0.1345E-01
92 TO 98	-0.3712E-04	0.4246E-09	-0.5563E-09	-0.1315E-10	0.3556E-05	-0.1232E-01	0.1703E-02
99 TO 102	0.9531E-08	-0.5559E-09	-0.8887E-11	0.5295E-05			

EIGENVECTOR FOR ROOT NO.= 4 Mode 4. Frequency = 8.6789 Hz, Ω = 4 RPM

EIGENVALUE= 0.54531252E 02 (rad/sec.)

REAL PART

1 TO 7	0.6187E 00	0.5157E-02	-0.8899E-06	-0.7218E-08	-0.1372E-06	-0.2237E-02	0.6237E 00
8 TO 14	0.5277E-02	0.2133E-05	-0.1046E-08	-0.1372E-06	0.2254E-02	0.2299E 00	0.5304E-02
15 TO 21	0.3615E-06	-0.6436E-08	-0.1350E-06	-0.2007E-02	0.2318E 00	0.5380E-02	0.1924E-05
22 TO 28	-0.1432E-03	-0.1350E-06	0.2022E-02	-0.7030E-01	0.5434E-02	0.1329E-05	-0.4045E-08
29 TO 35	-0.1305E-06	-0.1228E-02	-0.7089E-01	0.5468E-02	0.1628E-05	-0.1696E-08	-0.1305E-06
36 TO 42	0.1235E-02	-0.1252E 00	0.5443E-02	0.1493E-05	-0.1382E-09	-0.1267E-06	-0.5666E-03
43 TO 49	-0.1254E 00	0.5460E-02	0.1559E-05	-0.5108E-09	-0.1267E-06	0.5657E-03	-0.1463E 00
50 TO 56	0.5453E-02	0.1541E-05	0.7212E-10	-0.1240E-06	-0.3478E-05	-0.1482E 00	0.5679E-02
57 TO 63	-0.5991E-05	0.7411E-10	-0.1262E-06	-0.3949E-05	-0.1491E 00	0.5917E-02	-0.1354E-04
64 TO 70	0.7541E-10	-0.1257E-06	-0.3963E-05	-0.2141E 00	0.2096E-02	0.1624E-04	0.1009E-09
71 TO 77	-0.6740E-07	-0.3849E-04	-0.2723E 00	-0.4991E-02	0.2090E-04	0.1227E-09	0.6432E-08
78 TO 84	-0.5150E-04	-0.2970E 00	-0.7997E-02	0.1994E-04	0.1328E-09	0.5458E-07	-0.4749E-04
85 TO 91	-0.3291E 00	-0.1042E-01	0.9832E-05	0.1594E-09	0.1955E-06	-0.1938E-04	-0.4556E 00
92 TO 98	-0.3160E-02	-0.1105E-03	0.2678E-09	0.2716E-06	0.2226E-04	-0.4590E 00	-0.3289E-02
99 TO 102	-0.1505E-03	0.2890E-09	0.2179E-07	-0.1166E-04			

IMAGINARY PART

1 TO 7	0.7615E 00	0.5322E-02	-0.1609E-05	-0.4433E-08	0.3821E-08	-0.2815E-02	0.7817E 00
8 TO 14	0.5570E-02	0.1870E-05	-0.5597E-09	0.3823E-08	0.2881E-02	0.2722E 00	0.5125E-02
15 TO 21	-0.3266E-06	-0.4169E-08	0.3758E-08	-0.2523E-02	0.2812E 00	0.5288E-02	0.8861E-06
22 TO 28	-0.5209E-08	0.3760E-08	0.2580E-02	-0.1054E 00	0.4807E-02	-0.1703E-06	-0.2863E-08
29 TO 35	0.3633E-08	-0.1541E-02	-0.1046E 00	0.4891E-02	0.7466E-07	-0.3497E-08	0.3634E-08
36 TO 42	0.1571E-02	-0.1737E 00	0.4652E-02	-0.6568E-07	-0.5494E-09	0.3529E-08	-0.7111E-03
43 TO 49	-0.1739E 00	0.4687E-02	-0.5738E-07	-0.8224E-09	0.3529E-08	0.7172E-03	-0.2002E 00
50 TO 56	0.4508E-02	-0.6655E-07	0.6155E-09	0.3455E-08	-0.7210E-05	-0.2026E 00	0.4949E-02
57 TO 63	0.1435E-06	0.6410E-09	0.3537E-08	-0.7418E-05	-0.2036E 00	0.5395E-02	0.3574E-06
64 TO 70	0.6549E-09	0.3580E-08	-0.7449E-05	-0.2835E 00	-0.6190E-02	-0.4189E-06	0.6452E-09
71 TO 77	0.1235E-08	-0.1181E-03	-0.3547E 00	-0.2607E-01	-0.4488E-06	0.6056E-09	-0.7521E-09
78 TO 84	-0.1320E-03	-0.3848E 00	-0.3324E-01	-0.3747E-06	0.5612E-09	-0.1671E-08	-0.1048E-03
85 TO 91	-0.4238E 00	-0.3645E-01	-0.2593E-06	0.4043E-09	-0.1563E-08	0.1598E-04	-0.5775E 00
92 TO 98	0.2695E-01	-0.1759E-07	-0.2592E-09	-0.4495E-10	0.1656E-03	-0.5778E 00	0.4745E-01
99 TO 102	-0.4883E-07	-0.2591E-09	0.6306E-11	-0.3843E-08			

EIGENVECTOR FOR ROOT NO.= 1 Mode 1, Frequency = 2.4421 Hz Ω = 8 RPM

EIGENVALUE= 0.14322324E 02 (rad/sec.)

REAL PART

1 TO 7	0.7267E 00	0.4391E-01	-0.3981E-04	-0.5256E-08	0.4358E-05	-0.1477E-02	-0.7267E 00
8 TO 14	0.4359E-01	-0.3963E-04	0.4366E-08	0.4358E-06	-0.1477E-02	0.4606E 00	0.4368E-01
15 TO 21	-0.3870E-04	-0.5957E-08	0.4353E-06	-0.1481E-02	-0.4505E 00	0.4347E-01	-0.3882E-04
22 TO 28	0.4669E-08	0.4354E-06	-0.1481E-02	0.1940E 00	0.4343E-01	-0.3777E-04	-0.3817E-08
29 TO 35	0.4344E-06	-0.1479E-02	-0.1940E 00	0.4334E-01	-0.3799E-04	0.4256E-08	0.4344E-06
36 TO 42	-0.1479E-02	0.1055E 00	0.4333E-01	-0.3761E-04	-0.1358E-08	0.4335E-06	-0.1470E-02
43 TO 49	-0.1055E 00	0.4328E-01	-0.3777E-04	0.3144E-08	0.4335E-06	-0.1470E-02	0.1247E-04
50 TO 56	0.4324E-01	-0.3760E-04	0.1154E-08	0.4329E-06	-0.1459E-02	0.1312E-04	0.1309E 00
57 TO 63	-0.1137E-04	0.1157E-08	0.4405E-06	-0.1461E-02	0.1398E-04	0.2185E 00	0.1521E-04
64 TO 70	0.1159E-08	0.4442E-06	-0.1462E-02	0.1075E-04	-0.1598E 00	-0.9978E-04	0.1177E-08
71 TO 77	0.3940E-06	-0.1240E-02	0.9204E-05	-0.3267E 00	-0.1556E-03	0.1194E-08	0.3520E-06
78 TO 84	-0.9793E-03	0.8599E-05	-0.3799E 00	-0.1761E-03	0.1202E-08	0.3290E-06	-0.7955E-03
85 TO 91	0.7902E-05	-0.4144E 00	-0.1978E-03	0.1219E-08	0.2782E-06	-0.1687E-03	0.5733E-05
92 TO 98	0.4818E-02	-0.2704E-03	0.1280E-08	0.1368E-06	0.2173E-02	0.4687E-05	0.1000E 01
99 TO 102	-0.3119E-03	0.1299E-08	0.9898E-07	0.2958E-02			

IMAGINARY PART

1 TO 7	0.2085E-02	0.3993E-03	0.2340E-06	0.4842E-09	-0.3962E-10	0.7506E-06	0.1834E-02
8 TO 14	-0.3984E-03	-0.2591E-06	0.5381E-09	-0.3956E-10	-0.1257E-05	0.2216E-02	0.3018E-03
15 TO 21	0.1468E-06	0.4848E-09	-0.3955E-10	0.6697E-06	0.2058E-02	-0.3008E-03	-0.1625E-06
22 TO 28	0.5326E-09	-0.3952E-10	-0.1185E-05	0.2312E-02	0.1476E-03	0.5966E-07	0.4824E-09
29 TO 35	-0.3945E-10	0.3490E-06	0.2246E-02	-0.1465E-03	-0.6827E-07	0.5114E-09	-0.3943E-10
36 TO 42	-0.8576E-06	0.2324E-02	0.7189E-04	0.3034E-07	0.4778E-09	-0.3936E-10	0.4252E-07
43 TO 49	0.2289E-02	-0.7079E-04	-0.3816E-07	0.4914E-09	-0.3935E-10	-0.5426E-06	0.2318E-02
50 TO 56	0.5603E-06	-0.3407E-08	0.4732E-09	-0.3930E-10	-0.2464E-06	0.2200E-02	0.1534E-04
57 TO 63	-0.5755E-08	0.4454E-09	-0.3970E-10	-0.2463E-06	0.2055E-02	0.3012E-04	-0.8222E-08
64 TO 70	0.4300E-09	-0.4184E-10	-0.2461E-06	0.2578E-02	-0.3179E-04	0.2576E-08	0.2516E-09
71 TO 77	-0.3936E-10	-0.1848E-06	0.2976E-02	-0.5487E-04	0.8184E-08	0.1239E-09	-0.3502E-10
78 TO 84	-0.1230E-06	0.3076E-02	-0.5105E-04	0.1017E-07	0.8673E-10	-0.3113E-10	-0.8322E-07
85 TO 91	0.3155E-02	-0.6228E-04	0.1182E-07	0.2747E-10	-0.1496E-10	0.4696E-07	0.3177E-02
92 TO 98	0.4630E-04	0.8047E-08	-0.1320E-09	0.2074E-10	0.4704E-06	0.3157E-02	0.2457E-03
99 TO 102	0.1529E-08	-0.1320E-09	0.1612E-10	0.5754E-06			

EIGENVECTOR FOR ROOT NO.= 2

Mode 2, Frequency = 4.2026 Hz, Ω = 8 RPM

EIGENVALUE= 0.26406250E 02 (rad/sec.)

REAL PART

1	TO	7	-0.3738E-05	0.1209E-05	-0.4893E-01	-0.5189E-04	-0.1169E-02	0.8758E-08	0.3741E-05
8	TO	14	0.1209E-05	-0.4889E-01	0.5180E-04	-0.1169E-02	0.8761E-08	-0.2184E-05	0.1225E-05
15	TO	21	-0.3986E-01	-0.4745E-04	-0.1164E-02	0.8279E-08	0.2196E-05	0.1204E-05	-0.3983E-01
22	TO	28	0.4737E-04	-0.1164E-02	0.8382E-08	-0.7732E-06	0.1196E-05	-0.3260E-01	-0.3055E-04
29	TO	35	-0.1155E-02	0.7052E-08	0.7800E-06	0.1196E-05	-0.3259E-01	0.3045E-04	-0.1155E-02
36	TO	42	0.7054E-08	-0.3884E-06	0.1190E-05	-0.3122E-01	-0.1472E-04	-0.1148E-02	0.5934E-08
43	TO	49	0.3901E-06	0.1190E-05	-0.3121E-01	0.1461E-04	-0.1143E-02	0.5905E-08	0.9381E-09
50	TO	56	0.1185E-05	-0.3067E-01	-0.5762E-07	-0.1142E-02	0.4874E-08	0.9014E-09	0.9927E-06
57	TO	63	-0.9936E-01	-0.5834E-07	-0.1147E-02	0.4880E-08	0.1018E-08	0.5993E-06	-0.1682E 00
64	TO	70	-0.5875E-07	-0.1149E-02	0.4894E-08	0.5509E-09	0.8080E-06	0.1309E 00	-0.6142E-07
71	TO	77	-0.9877E-03	-0.9119E-08	0.3025E-09	-0.1315E-05	0.2595E 00	-0.6270E-07	-0.7097E-03
78	TO	84	-0.1841E-07	0.2056E-09	-0.2520E-05	0.2955E 00	-0.6239E-07	-0.4901E-03	-0.2157E-07
85	TO	91	0.9311E-10	-0.3820E-05	0.3037E 00	-0.5995E-07	0.2520E-03	-0.1431E-07	-0.2634E-09
92	TO	98	-0.4476E-05	-0.2367E 00	-0.4651E-07	0.2270E-02	0.2991E-08	-0.3608E-09	-0.4108E-05
99	TO	102	-0.1000E 01	-0.4650E-07	0.2068E-02	0.9248E-12			

IMAGINARY PART

1	TO	7	-0.5151E-07	0.9878E-09	-0.3065E-03	-0.4798E-06	-0.4434E-05	0.1518E-09	-0.2375E-07
8	TO	14	0.7759E-08	-0.6423E-04	-0.8679E-07	-0.4434E-05	-0.8573E-10	-0.2487E-07	0.1817E-08
15	TO	21	-0.2719E-03	-0.4510E-06	-0.4417E-05	0.1403E-09	-0.9659E-09	0.6942E-08	-0.9014E-04
22	TO	28	-0.9161E-07	-0.4417E-05	-0.7800E-10	-0.2954E-08	0.3124E-08	-0.1488E-03	-0.3445E-06
29	TO	35	-0.4383E-05	0.9641E-10	0.2813E-08	0.5502E-08	-0.9923E-04	-0.1134E-06	-0.4383E-05
36	TO	42	-0.4410E-10	0.1659E-08	0.3746E-08	-0.1309E-03	-0.2472E-06	-0.4354E-05	0.5556E-10
43	TO	49	0.4537E-08	0.4948E-08	-0.1057E-03	-0.1360E-06	-0.4354E-05	-0.1195E-10	0.4364E-08
50	TO	56	0.4329E-08	-0.1162E-03	-0.1584E-06	-0.4333E-05	0.1722E-10	0.3994E-08	0.3250E-08
57	TO	63	-0.3769E-03	-0.2332E-07	-0.4351E-05	0.1797E-10	0.3641E-08	0.2171E-08	-0.6382E-03
64	TO	70	0.5091E-07	-0.4358E-05	0.1799E-10	0.1269E-07	0.2830E-08	0.4968E-03	0.1373E-06
71	TO	77	-0.3747E-05	-0.3435E-10	0.2137E-07	-0.5097E-08	0.9846E-03	0.9283E-07	-0.2694E-05
78	TO	84	-0.6911E-10	0.2541E-07	-0.9618E-08	0.1121E-02	-0.1430E-06	-0.1861E-05	-0.8099E-10
85	TO	91	0.3084E-07	-0.1449E-07	0.1153E-02	-0.1124E-05	0.9503E-06	-0.5354E-10	0.5174E-07
92	TO	98	-0.1692E-07	-0.8839E-03	-0.5873E-05	0.7846E-05	0.1126E-10	0.5176E-07	-0.1554E-07
99	TO	102	-0.3790E-02	-0.5976E-05	0.7851E-05	0.2713E-19			

EIGENVECTOR FOR ROOT NO.= 3   Mode 3, Frequency = 8.4068 Hz, Ω = 8 RPM

EIGENVALUE= 0.5282226E 02 (rad/sec.)

REAL PART

1 TO 7	[illegible]	0.1109E-01	-0.1487E-04	-0.7760E-07	[illegible]	0.1524E-03	0.5104E-01
8 TO 14	[illegible]	-0.1419E-04	0.7508E-07	-0.2650E-06	[illegible]	-0.2571E-01	0.1140E-01
15 TO 21	[illegible]	-0.6829E-07	-0.2610E-06	0.1382E-03	[illegible]	0.1162E-01	-0.1189E-05
22 TO 28	[illegible]	-0.2609E-06	0.1327E-03	-0.4816E-02	[illegible]	0.8563E-05	-0.4007E-07
29 TO 35	[illegible]	0.2611E-04	0.5457E-02	0.1143E-01	[illegible]	0.3909E-07	-0.2527E-06
36 TO 42	[illegible]	-0.9998E-03	0.1115E-01	0.1031E-04	[illegible]	-0.2459E-06	0.3955E-04
43 TO 49	[illegible]	0.1120E-01	0.1030E-04	0.1782E-07	[illegible]	0.3808E-04	0.4188E-03
50 TO 56	[illegible]	0.1096E-04	0.1700E-09	-0.2411E-06	[illegible]	0.4185E-03	0.1151E-01
57 TO 63	[illegible]	0.1735E-09	-0.2425E-06	-0.1713E-04	0.4173E-03	0.1287E-01	-0.1809E-04
64 TO 70	[illegible]	-0.2419E-06	-0.2541E-04	0.4804E-03	[illegible]	0.4052E-04	0.2330E-09
71 TO 77	[illegible]	-0.4556E-03	0.5364E-03	-0.1131E 00	[illegible]	0.2819E-09	0.1074E-07
78 TO 84	[illegible]	0.5597E-02	-0.1541E 00	0.4666E-04	[illegible]	0.1171E-06	-0.7051E-03
85 TO 91	[illegible]	-0.2062E 00	0.2568E-04	0.3676E-09	[illegible]	-0.6945E-03	0.6917E-03
92 TO 98	[illegible]	-0.2651E-03	0.5959E-09	0.6363E-06	[illegible]	0.6565E-03	0.1000E 01
99 TO 102	[illegible]	0.6439E-09	0.4366E-07	0.3708E-02			

IMAGINARY PART

1 TO 7	[illegible]	-0.4191E-03	0.1161E-05	0.1893E-08	[illegible]	-0.3379E-04	-0.1527E-02
8 TO 14	[illegible]	-0.1155E-05	0.1846E-08	-0.1237E-09	[illegible]	-0.6187E-02	-0.3573E-03
15 TO 21	[illegible]	0.2162E-09	-0.1218E-09	-0.2849E-04	[illegible]	-0.8601E-04	-0.8062E-06
22 TO 28	[illegible]	-0.1218E-09	0.2548E-04	-0.1019E-01	[illegible]	0.3695E-06	0.2644E-08
29 TO 35	[illegible]	-0.1498E-04	-0.1026E-01	-0.1519E-03	[illegible]	0.2623E-08	-0.1180E-09
36 TO 42	[illegible]	-0.1082E-01	-0.2411E-03	0.2041E-06	[illegible]	-0.1148E-09	-0.6041E-05
43 TO 49	[illegible]	-0.1709E-03	-0.2133E-06	0.2848E-08	[illegible]	0.5481E-05	-0.1103E-01
50 TO 56	[illegible]	-0.4702E-08	0.2930E-08	-0.1125E-09	[illegible]	-0.1105E-01	-0.2177E-03
57 TO 63	[illegible]	0.3033E-08	-0.1140E-09	0.2125E-06	[illegible]	-0.2314E-03	-0.1835E-07
64 TO 70	[illegible]	-0.1136E-09	0.2366E-06	-0.1026E-01	[illegible]	0.6878E-08	0.3059E-08
71 TO 77	[illegible]	0.4440E-05	-0.9419E-02	0.9714E-03	[illegible]	0.2893E-09	0.1904E-10
78 TO 84	[illegible]	-0.3977E-02	0.1300E-02	0.6413E-08	[illegible]	0.4903E-10	0.5232E-05
85 TO 91	[illegible]	0.1534E-02	0.2485E-08	0.2006E-08	[illegible]	0.2491E-05	-0.6136E-02
92 TO 98	[illegible]	0.3552E-09	-0.9161E-09	0.2541E-10	[illegible]	-0.4554E-02	-0.4574E-02
99 TO 102	[illegible]	-0.9157E-09	0.2369E-10	-0.1355E-04			

EIGENVECTOR FOR ROOT NO.= 4 Mode 4. Frequency = 8.6867 Hz, Ω = 8 RPM

EIGENVALUE= 0.54580078E 02 (rad/sec.)

REAL PART

1 TO 7	0.8512E 00	0.5309E-02	-0.1269E-05	-0.9741E-08	-0.1785E-06	-0.3073E-02	0.8534E 00
8 TO 14	0.5362E-02	0.2944E-05	-0.1483E-08	-0.1795E-06	0.3083E-02	0.3169E 00	0.5502E-02
15 TO 21	0.4201E-06	-0.9707E-09	-0.1755E-06	-0.2757E-02	0.3175E 00	0.5530E-02	0.2550E-05
22 TO 28	-0.1998E-08	-0.1756E-06	0.2765E-02	-0.9623E-01	0.5590E-02	0.1732E-05	-0.5502E-08
29 TO 35	-0.1697E-06	-0.1697E-02	-0.3661E-01	0.5702E-02	0.2140E-05	-0.2328E-08	-0.1697E-06
36 TO 42	0.1689E-02	-0.1710E 00	0.5720E-02	0.1956E-05	-0.1884E-08	-0.1648E-06	-0.7777E-03
43 TO 49	-0.1713E 00	0.5726E-02	0.2046E-05	-0.7002E-09	-0.1648E-06	0.7751E-03	-0.1999E 00
50 TO 56	0.5749E-02	0.2021E-05	0.9953E-10	-0.1613E-06	-0.3090E-05	-0.2025E 00	0.5951E-02
57 TO 63	-0.7775E-05	0.1040E-09	-0.1641E-06	-0.3496E-05	-0.2037E 00	0.6157E-02	-0.1760E-04
64 TO 70	0.1068E-09	-0.1635E-06	-0.3412E-05	-0.2931E 00	0.3606E-02	0.2113E-04	0.1369E-09
71 TO 77	-0.8744E-07	-0.2497E-04	-0.2730E 00	-0.1179E-02	0.2714E-04	0.1623E-09	0.8652E-08
78 TO 84	-0.3595E-04	-0.4069E 00	-0.3312E-02	0.2471E-04	0.1742E-09	0.7123E-07	-0.3400E-04
85 TO 91	-0.4510E 00	-0.5096E-02	0.1273E-04	0.2070E-09	0.2539E-06	-0.1564E-04	-0.6242E 00
92 TO 98	-0.5225E-02	-0.1433E-03	0.3453E-09	0.3520E-06	-0.1618E-04	-0.6288E 00	-0.2275E-01
99 TO 102	-0.1952E-03	0.3728E-09	0.2934E-07	-0.6316E-04			

IMAGINARY PART

1 TO 7	0.4685E 00	0.1361E-01	-0.2232E-06	-0.7257E-09	0.1025E-07	-0.1740E-02	0.5213E 00
8 TO 14	0.1440E-01	0.9954E-06	-0.3921E-08	0.1026E-07	0.1910E-02	0.1660E 00	0.1311E-01
15 TO 21	-0.1067E-06	-0.5898E-09	0.1009E-07	-0.1561E-02	0.1895E 00	0.1362E-01	0.2961E-06
22 TO 28	-0.3505E-08	0.1009E-07	0.1710E-02	-0.6902E-01	0.1229E-01	-0.4366E-07	-0.1092E-10
29 TO 35	0.9751E-09	-0.9585E-03	-0.6591E-01	0.1252E-01	-0.2028E-06	-0.1792E-08	0.9754E-08
36 TO 42	0.1036E-02	-0.1107E 00	0.1139E-01	-0.7634E-07	0.1150E-08	0.9472E-08	-0.4500E-03
43 TO 49	-0.1114E 00	0.1200E-01	-0.2469E-06	0.3731E-09	0.9473E-08	0.4657E-03	-0.1280E 00
50 TO 56	0.1152E-01	-0.1761E-06	0.1522E-08	0.9273E-08	-0.1904E-04	-0.1295E 00	0.1268E-01
57 TO 63	0.3870E-06	0.1589E-08	0.9473E-08	-0.1959E-04	-0.1301E 00	0.1386E-01	0.9596E-06
64 TO 70	0.1726E-08	0.9576E-08	-0.1969E-04	-0.1514E 00	-0.1650E-01	-0.1130E-05	0.1706E-08
71 TO 77	0.3404E-03	-0.3090E-03	-0.2271E 00	-0.6346E-01	-0.1224E-05	0.1608E-09	-0.1925E-08
78 TO 84	-0.3445E-03	-0.2464E 00	-0.8716E-01	-0.1230E-05	0.1494E-08	-0.4426E-08	-0.2730E-03
85 TO 91	-0.2714E 00	-0.9550E-01	-0.7014E-06	0.1091E-08	-0.4296E-08	0.4371E-04	-0.3700E 00
92 TO 98	0.7130E-01	-0.7735E-09	-0.6145E-09	-0.4571E-09	0.4373E-03	-0.3702E 00	0.1252E 00
99 TO 102	0.3333E-07	-0.6142E-09	0.2817E-11	0.2218E-06			

MODE VECTOR FOR ROOT NO.= 1 Mode 1, frequency = 2.2851 Hz, Ω = 12 RPM

EIGENVALUE= 0.14357910E 02 (rad/sec)

REAL PART							
1 TO 7	0.2232E 00	-0.4531E-01	0.1344E-05	0.5414E-09	-0.1746E-07	-0.4746E-03	-0.2232E 00
8 TO 14	-0.4531E-01	0.1344E-05	-0.5444E-09	-0.1746E-07	-0.4746E-03	0.1392E 00	-0.4526E-01
15 TO 21	0.1250E-05	0.4891E-09	-0.1744E-07	-0.4678E-03	-0.1392E 00	-0.4527E-01	0.1249E-05
22 TO 28	-0.4907E-09	-0.1744E-07	-0.4678E-03	0.5590E-01	-0.4517E-01	0.1176E-05	0.3016E-09
29 TO 35	-0.1740E-07	-0.4439E-03	-0.5590E-01	-0.4517E-01	0.1176E-05	-0.2994E-09	-0.1740E-07
36 TO 42	-0.4439E-03	0.2978E-01	-0.4511E-01	0.1162E-05	0.1585E-09	-0.1737E-07	-0.4227E-03
43 TO 49	-0.2977E-01	-0.4511E-01	0.1162E-05	-0.1531E-09	-0.1737E-07	-0.4227E-03	0.4074E-05
50 TO 56	-0.4506E-01	0.1156E-05	0.3360E-11	-0.1734E-07	-0.4038E-03	0.4058E-05	-0.2083E-01
57 TO 63	0.1073E-06	0.3360E-11	-0.1758E-07	-0.4038E-03	0.4042E-05	0.3398E-02	-0.9505E-06
64 TO 70	0.3362E-11	-0.1766E-07	-0.4038E-03	0.4860E-05	-0.8392E-01	0.3514E-06	0.3400E-11
71 TO 77	-0.1407E-07	-0.1211E-03	0.5798E-05	-0.8367E-01	0.5788E-05	0.3444E-11	-0.1100E-07
78 TO 84	0.1160E-03	0.6332E-05	-0.7265E-01	0.5977E-05	0.3473E-11	-0.8686E-08	0.2488E-03
85 TO 91	0.7297E-05	-0.3987E-01	0.6044E-05	0.3567E-11	0.4326E-08	0.6500E-03	0.1234E-04
92 TO 98	0.4279E 00	-0.4055E-05	0.3973E-11	0.4207E-07	0.1565E-02	0.1235E-04	0.1000E 01
99 TO 100	-0.2073E-04	0.4006E-11	0.4311E-07	0.1543E-02			
IMAGINARY PART							
1 TO 7	0.1952E-02	0.1302E-04	-0.3753E-08	-0.1146E-10	-0.7340E-10	-0.4680E-05	0.2132E-03
8 TO 14	-0.3269E-03	0.5474E-08	-0.1162E-10	-0.7340E-10	0.1203E-05	0.1025E-02	-0.2753E-04
15 TO 21	-0.1724E-08	-0.1090E-10	-0.7332E-10	-0.4417E-05	0.3670E-05	-0.2860E-03	0.3418E-08
22 TO 28	-0.1102E-10	-0.7332E-10	0.9866E-06	0.3077E-03	-0.9339E-04	0.7506E-10	-0.8742E-11
29 TO 35	-0.7315E-10	-0.3390E-05	-0.1034E-03	-0.2195E-03	0.1606E-08	-0.8749E-11	-0.7315E-10
36 TO 42	0.1256E-06	0.1324E-03	-0.1256E-03	0.5067E-09	-0.5502E-11	-0.7300E-10	-0.2410E-05
43 TO 49	-0.8721E-04	-0.1868E-03	0.1171E-08	-0.5592E-11	-0.7300E-10	-0.7039E-06	-0.9436E-05
50 TO 56	-0.1560E-03	0.8373E-09	-0.3604E-11	-0.7290E-10	-0.1490E-05	-0.3048E-05	-0.6663E-04
57 TO 63	-0.3555E-08	-0.1916E-11	-0.7340E-10	-0.1490E-05	0.2317E-05	0.2278E-04	-0.7966E-08
64 TO 70	-0.9858E-12	-0.7359E-10	-0.1490E-05	-0.2263E-03	-0.3078E-03	0.1098E-07	-0.9843E-12
71 TO 77	-0.6711E-10	-0.4895E-06	-0.4857E-03	-0.3108E-03	0.1944E-07	-0.3444E-11	-0.5077E-10
78 TO 84	0.3540E-06	-0.6384E-03	-0.2750E-03	0.2221E-07	-0.7252E-11	-0.4162E-10	0.8284E-06
85 TO 91	-0.9073E-03	-0.1622E-03	0.2307E-07	-0.2272E-10	0.1608E-10	0.2265E-05	-0.2331E-02
92 TO 98	0.1497E-02	-0.1637E-07	-0.9699E-10	0.1532E-09	0.5593E-05	-0.2333E-02	0.3552E-02
99 TO 100	-0.7339E-07	-0.9693E-10	0.1551E-09	0.5556E-05			

EIGENVECTOR FOR ROOT NO.= 2 Mode 2, frequency = 4.2027 Hz, Ω = 12 RPM

EIGENVALUE= 0.26406250E 02 (rad/sec)

REAL PART

1 TO 7	-0.3641E-05	0.1142E-05	-0.4962E-01	-0.5351E-04	-0.1144E-02	0.8770E-08	0.4101E-05
8 TO 14	0.1157E-05	-0.4961E-01	0.5353E-04	-0.1143E-02	0.9133E-08	-0.2082E-05	0.1151E-05
15 TO 21	-0.4027E-01	-0.4990E-04	-0.1139E-02	0.8436E-08	0.2473E-05	0.1168E-05	-0.4075E-01
22 TO 28	0.4891E-04	-0.1139E-02	0.8774E-08	-0.6548E-06	0.1154E-05	-0.3279E-01	-0.3144E-04
29 TO 35	-0.1130E-02	0.7245E-08	0.9988E-06	0.1162E-05	-0.3279E-01	0.3130E-04	-0.1130E-02
36 TO 42	0.7468E-08	-0.2502E-06	0.1153E-05	-0.3137E-01	-0.1513E-04	-0.1123E-02	0.6212E-08
43 TO 49	0.5840E-06	0.1157E-05	-0.3136E-01	0.1504E-04	-0.1123E-02	0.6321E-08	0.1649E-06
50 TO 56	0.1150E-05	-0.3092E-01	-0.5609E-07	-0.1117E-02	0.5283E-08	0.1748E-06	0.8315E-06
57 TO 63	-0.9800E-01	-0.5639E-07	-0.1122E-02	0.5348E-08	0.1932E-06	0.5082E-06	-0.1654E 00
64 TO 70	-0.5655E-07	-0.1124E-02	0.5406E-08	0.1263E-06	0.8662E-06	0.1272E 00	-0.5871E-07
71 TO 77	-0.9647E-03	-0.8347E-05	0.9374E-07	-0.1127E-05	0.2524E 00	-0.6023E-07	-0.6877E-03
78 TO 84	-0.1747E-07	0.8141E-07	-0.2273E-05	0.2871E 00	-0.6064E-07	-0.4679E-03	-0.2056E-07
85 TO 91	0.6760E-07	-0.3496E-05	0.2925E 00	-0.6122E-07	0.2733E-03	-0.1287E-07	0.2631E-07
92 TO 98	-0.3434E-05	-0.2553E 00	-0.6252E-07	0.2060E-02	0.4506E-08	0.1102E-07	-0.2833E-05
99 TO 102	-0.1000E 01	-0.6252E-07	0.1998E-02	0.1471E-09			

IMAGINARY PART

1 TO 7	-0.2840E-07	-0.4627E-07	-0.6529E-04	-0.1758E-06	-0.5068E-06	0.1142E-09	-0.8928E-07
8 TO 14	-0.2810E-07	0.2222E-04	-0.1298E-06	-0.5068E-06	-0.2451E-08	-0.8690E-08	-0.4032E-07
15 TO 21	-0.3516E-04	-0.1505E-06	-0.5048E-06	0.9974E-10	-0.4412E-07	-0.2731E-07	0.1149E-06
22 TO 28	-0.1084E-06	-0.5043E-06	-0.2289E-09	0.5118E-08	-0.3443E-07	-0.1433E-04	-0.7137E-07
29 TO 35	-0.5009E-06	0.4512E-10	-0.9672E-08	-0.2837E-07	-0.1427E-04	-0.4431E-07	-0.5009E-06
36 TO 42	-0.1658E-09	0.6371E-08	-0.3228E-07	-0.1195E-04	-0.6247E-08	-0.4976E-06	-0.5533E-11
43 TO 49	-0.1429E-08	-0.2923E-07	-0.1544E-04	0.5764E-08	-0.4976E-06	-0.1064E-09	0.4353E-08
50 TO 56	-0.3060E-07	-0.1745E-04	0.4953E-07	-0.4952E-06	-0.5229E-10	0.4457E-08	-0.2714E-07
57 TO 63	-0.4323E-04	0.2489E-06	-0.4972E-06	-0.6301E-10	0.4974E-08	-0.2300E-07	-0.7310E-04
64 TO 70	0.3584E-06	-0.4981E-06	-0.7182E-10	0.1513E-07	-0.3237E-07	0.5659E-04	0.5446E-06
71 TO 77	-0.4279E-06	0.2994E-10	0.2662E-07	-0.2273E-07	0.1122E-03	0.3911E-06	-0.3063E-06
78 TO 84	0.8990E-10	0.3701E-07	-0.1683E-07	0.1277E-03	0.3444E-07	-0.2101E-06	0.1045E-09
85 TO 91	0.3926E-07	-0.9036E-08	0.1309E-03	-0.1432E-05	0.1151E-06	0.1004E-09	0.6670E-07
92 TO 98	0.3247E-08	-0.1075E-03	-0.8504E-05	0.9045E-06	0.4412E-12	0.6907E-07	0.3326E-08
99 TO 102	-0.4380E-03	-0.8507E-05	0.9915E-06	-0.1789E-16			

EIGENVECTOR FOR ROOT NO.= 3

Mode 3, frequency = 8.3914 Hz, Ω= 12 RPM

EIGENVALUE= 0.52724609E 02 (rad/sec)

REAL PART

1 TO 7	0.1028E 00	-0.1429E 00	-0.8659E-04	[illegible]	-0.1735E-05	-0.3541E-03	-0.1075E 00
8 TO 14	-0.1405E 00	-0.8247E-04	0.4155E-06	[illegible]	-0.3215E-03	0.4219E-01	-0.1399E 00
15 TO 21	-0.1217E-04	-0.3800E-06	-0.1708E-05	[illegible]	-0.4214E-01	-0.1374E 00	-0.1041E-04
22 TO 28	0.3676E-06	-0.1708E-05	-0.3257E-03	[illegible]	-0.1337E 00	0.4382E-04	-0.2242E-06
29 TO 35	-0.1655E-05	-0.1330E-03	0.2603E-02	-0.1331E 00	0.4392E-04	0.2182E-06	-0.1655E-05
36 TO 42	-0.1470E-03	-0.2827E-02	-0.1309E 00	0.5342E-04	-0.1000E-06	-0.1610E-05	0.1022E-04
43 TO 49	0.7023E-02	-0.1306E 00	0.5353E-04	0.9376E-07	-0.1610E-05	0.3974E-05	0.2212E-02
50 TO 56	-0.1286E 00	0.5726E-04	0.1039E-08	-0.1575E-05	0.1333E-03	0.2207E-02	-0.1357E 00
57 TO 63	-0.3793E-04	0.1060E-08	-0.1599E-05	0.1057E-03	0.2198E-02	-0.1413E 00	-0.1332E-03
64 TO 70	0.1075E-08	-0.1587E-05	0.8656E-04	0.2416E-02	0.1391E-01	0.2489E-03	0.1420E-08
71 TO 77	-0.8999E-06	0.1541E-02	0.2607E-02	0.2655E 00	0.3125E-03	0.1715E-08	0.7389E-07
78 TO 84	0.1583E-02	0.2681E-02	0.3448E 00	0.2977E-03	0.1951E-08	0.7472E-06	0.1015E-02
85 TO 91	0.2771E-02	0.3345E 00	0.1577E-03	[illegible]	0.2798E-05	-0.1231E-02	0.3140E-02
92 TO 98	-0.5042E 00	-0.1592E-02	0.3607E-08	0.3773E-05	0.2269E-04	0.2922E-02	0.1000E 01
99 TO 102	-0.2126E-02	0.3897E-08	0.2892E-06	[illegible]			

IMAGINARY PART

1 TO 7	0.1675E 00	-0.9886E-04	0.1148E-04	0.1561E-07	-0.3466E-11	-0.7800E-03	0.1665E 00
8 TO 14	0.3546E-03	-0.1142E-04	0.1841E-07	-0.1542E-11	0.7770E-03	0.3238E-01	0.8488E-05
15 TO 21	0.7972E-05	0.2120E-07	-0.2812E-11	-0.6917E-03	0.3188E-01	0.2669E-03	-0.7946E-05
22 TO 28	0.2103E-07	-0.1521E-11	0.6889E-03	[illegible]	0.5009E-04	0.3715E-05	0.2599E-07
29 TO 35	-0.2113E-11	-0.4126E-03	-0.7017E-01	[illegible]	-0.2713E-05	0.2590E-07	-0.1475E-11
36 TO 42	0.4110E-03	-0.3820E-01	0.1107E-03	[illegible]	0.2938E-07	-0.1700E-11	-0.1866E-03
43 TO 49	-0.8823E-01	0.1692E-03	-0.2082E-05	0.2535E-07	-0.1435E-11	0.1860E-03	-0.9508E-01
50 TO 56	0.1400E-03	-0.1134E-09	0.2933E-07	-0.1417E-11	-0.1206E-06	-0.9557E-01	0.1485E-03
57 TO 63	-0.1250E-09	0.3034E-07	0.9035E-12	-0.1555E-06	-0.3548E-01	0.1583E-03	-0.7805E-09
64 TO 70	0.3090E-07	0.1114E-10	-0.1675E-06	-0.1115E 00	0.5215E-04	-0.1382E-08	0.3113E-07
71 TO 77	0.3354E-12	-0.9866E-06	-0.1255E 00	-0.1294E-03	-0.5306E-09	0.3001E-07	-0.1161E-10
78 TO 84	-0.1321E-05	-0.1306E 00	-0.2067E-03	0.3924E-09	0.3840E-07	-0.1897E-10	-0.1228E-05
85 TO 91	-0.1362E 00	-0.2729E-03	0.2157E-08	[illegible]	-0.3039E-10	-0.6174E-06	-0.1546E 00
92 TO 98	-0.9585E-04	0.1932E-07	-0.2642E-08	-0.2552E-10	0.1167E-05	-0.1474E 00	0.4027E-03
99 TO 102	0.1818E-07	-0.2637E-09	-0.2494E-11	0.1444E-05			

EIGENVECTOR FOR ROOT NO.= 4 Mode 4, frequency = 8.6944 Hz, Ω = 12 RPM

EIGENVALUE= 0.54629906E 02 (rad/sec)

REAL PART

1 TO 7	0.9012E 00	0.8418E-02	0.3569E-05	-0.2611E-07	-0.9892E-[illegible]	-0.3245E-02	0.9108E 00
8 TO 14	0.8210E-02	0.7909E-05	0.1361E-07	-0.9893E-06	0.3279E-[illegible]	0.3370E 00	0.8546E-02
15 TO 21	0.7982E-05	-0.2160E-07	-0.9728E-06	-0.2913E-02	0.3409E [illegible]	0.8393E-02	0.1016E-04
22 TO 28	0.9966E-08	-0.5728E-06	0.2941E-02	-0.9964E-01	0.8627E-[illegible]	0.1096E-04	-0.1100E-07
29 TO 35	-0.9402E-06	-0.1784E-02	-0.2968E-01	0.8556E-02	0.1132E-[illegible]	0.2973E-08	-0.9402E-06
36 TO 42	0.1797E-02	-0.1787E 00	0.8592E-02	0.1139E-04	-0.3421E-[illegible]	-0.9130E-06	-0.8239E-03
43 TO 49	-0.1791E 00	0.8558E-02	0.1143E-04	0.1373E-08	-0.9130E-[illegible]	0.9234E-03	-0.2093E 00
50 TO 56	0.8559E-02	0.1149E-04	0.5300E-09	-0.8937E-06	-0.5796E-[illegible]	-0.2121E 00	0.8936E-02
57 TO 63	-0.4282E-04	0.5471E-09	-0.2100E-06	-0.6532E-05	-0.2134E [illegible]	0.9328E-02	-0.9730E-04
64 TO 70	0.5581E-09	-0.9073E-06	-0.6530E-05	-0.3088E 00	0.2502E-[illegible]	0.1170E-03	0.7382E-09
71 TO 77	-0.4908E-06	-0.6896E-04	-0.3940E 00	-0.9989E-02	0.1497E-[illegible]	0.8917E-09	0.5302E-07
78 TO 84	-0.8932E-04	-0.4301E 00	-0.1514E-01	0.1359E-03	0.9631E-[illegible]	0.3997E-06	-0.8026E-04
85 TO 91	-0.4770E 00	-0.1895E-01	0.6914E-04	0.1153E-08	0.1416E-[illegible]	-0.2489E-04	-0.6606E 00
92 TO 98	-0.1259E-02	-0.8025E-03	0.1935E-08	0.1959E-05	0.4577E-[illegible]	-0.6659E 00	-0.3378E-02
99 TO 102	-0.1088E-02	0.2088E-08	0.1587E-06	-0.3153E-04			

IMAGINARY PART

1 TO 7	0.3241E 00	0.2228E-01	0.6021E-05	0.1072E-07	0.1588E-[illegible]	-0.1210E-02	0.4129E 00
8 TO 14	0.2491E-01	-0.4789E-05	0.5321E-08	0.1689E-07	0.1496E-[illegible]	0.1137E 00	0.2253E-01
15 TO 21	0.4021E-05	0.1189E-07	0.1660E-07	-0.1087E-02	0.1531E [illegible]	0.2359E-01	-0.3726E-05
22 TO 28	0.7090E-08	0.1661E-07	0.1338E-02	-0.4987E-01	0.2123E-[illegible]	0.1685E-05	0.1396E-07
29 TO 35	0.1605E-07	-0.6746E-03	-0.4633E-01	0.2172E-01	-0.2109E-[illegible]	0.1103E-07	0.1605E-07
36 TO 42	0.8051E-03	-0.8017E-01	0.2060E-01	0.8099E-06	0.1520E-[illegible]	0.1559E-07	-0.3266E-03
43 TO 49	-0.8144E-01	0.2083E-01	-0.1359E-05	0.1394E-07	0.1559E-[illegible]	0.3529E-03	-0.9337E-01
50 TO 56	0.2001E-01	-0.2983E-06	0.1551E-07	0.1526E-07	-0.3210E-[illegible]	-0.9450E-01	0.2198E-01
57 TO 63	0.6286E-06	0.1610E-07	0.1550E-07	-0.3323E-04	-0.9439E-[illegible]	0.2398E-01	0.1572E-05
64 TO 70	0.1642E-07	0.1577E-07	-0.3347E-04	-0.1332E 00	-0.7710E-[illegible]	-0.1859E-05	0.1670E-07
71 TO 77	0.5503E-08	-0.5199E-03	-0.1673E 00	-0.1146E 00	-0.1997E-[illegible]	0.1623E-07	-0.3305E-08
78 TO 84	-0.5810E-03	-0.1817E 00	-0.1462E 00	-0.1669E-05	0.1542E-[illegible]	-0.7414E-08	-0.4615E-03
85 TO 91	-0.2004E 00	-0.1605E 00	-0.1125E-05	0.1239E-07	-0.7033E-[illegible]	0.6905E-04	-0.2742E 00
92 TO 98	0.1177E 00	-0.2463E-07	-0.5693E-09	-0.5401E-09	0.7311E-[illegible]	-0.2747E 00	0.2076E 00
99 TO 102	-0.4090E-07	-0.5662E-08	0.1370E-10	-0.4308E-07			

A.4 VIBRATION MODE DATA
ARTIFICIAL "G" ROLLUP SOLAR ARRAY CONFIGURATION

CONTENTS

TABLE A-13 MODAL DATA, ARTIFICIAL "G" SOLAR ARRAY CONFIGURATION

ZERO SPIN, NASTRAN RESULTS

MODE	FREQUENCY (HZ)	GENERALIZED MASS ($LBS-SEC^2/IN$)
1	1.988690E-01	7.167556E-01
2	2.031515E-01	1.292258E 00
3	3.784189E-01	1.063949E 00
4	3.979775E-01	1.001644E 00
5	3.980261E-01	6.105757E-01
6	3.980299E-01	9.539251E-01
7	3.980302E-01	6.210912E-01
8	3.980324E-01	6.018445E-01
9	5.036502E-01	1.465514E 00
10	5.214531E-01	9.017361E-01
11	7.044816E-01	1.066769E 00
12	7.353594E-01	9.928919E-01
13	7.354488E-01	5.991474E-01
14	7.354546E-01	6.097919E-01
15	7.354608E-01	3.408555E-01
16	7.354647E-01	4.338064E-01
17	7.731657E-01	1.038958E 00
18	7.941298E-01	6.538786E-01
19	9.051450E-01	8.818694E-01
20	9.348565E-01	1.096124E 00
21	9.609272E-01	5.915505E-01
22	9.609300E-01	6.108234E-01
23	9.609315E-01	9.547644E-01
24	9.609319E-01	6.211893E-01
25	9.609702E-01	9.569576E-01
26	9.713216E-01	1.036751E 00
27	9.772314E-01	6.586445E-01
28	1.065360E 00	1.054537E 00
29	1.652814E 00	2.813135E-01
30	2.106756E 00	4.305415E-01
31	2.825887E 00	
32	3.842224E 00	
33	4.707289E 00	
34	5.006941E 00	
35	5.713924E 00	
36	5.790833E 00	
37	6.093275E 00	
38	6.099439E 00	
39	6.462175E 00	
40	8.135055E 00	
41	8.676979E 00	
42	9.569734E 00	
43	1.006908E 01	
44	1.067541E 01	
45	1.136669E 01	
46	1.143346E 01	
47	1.267509E 01	
48	1.302590E 01	
49	1.485096E 01	
50	1.497922E 01	

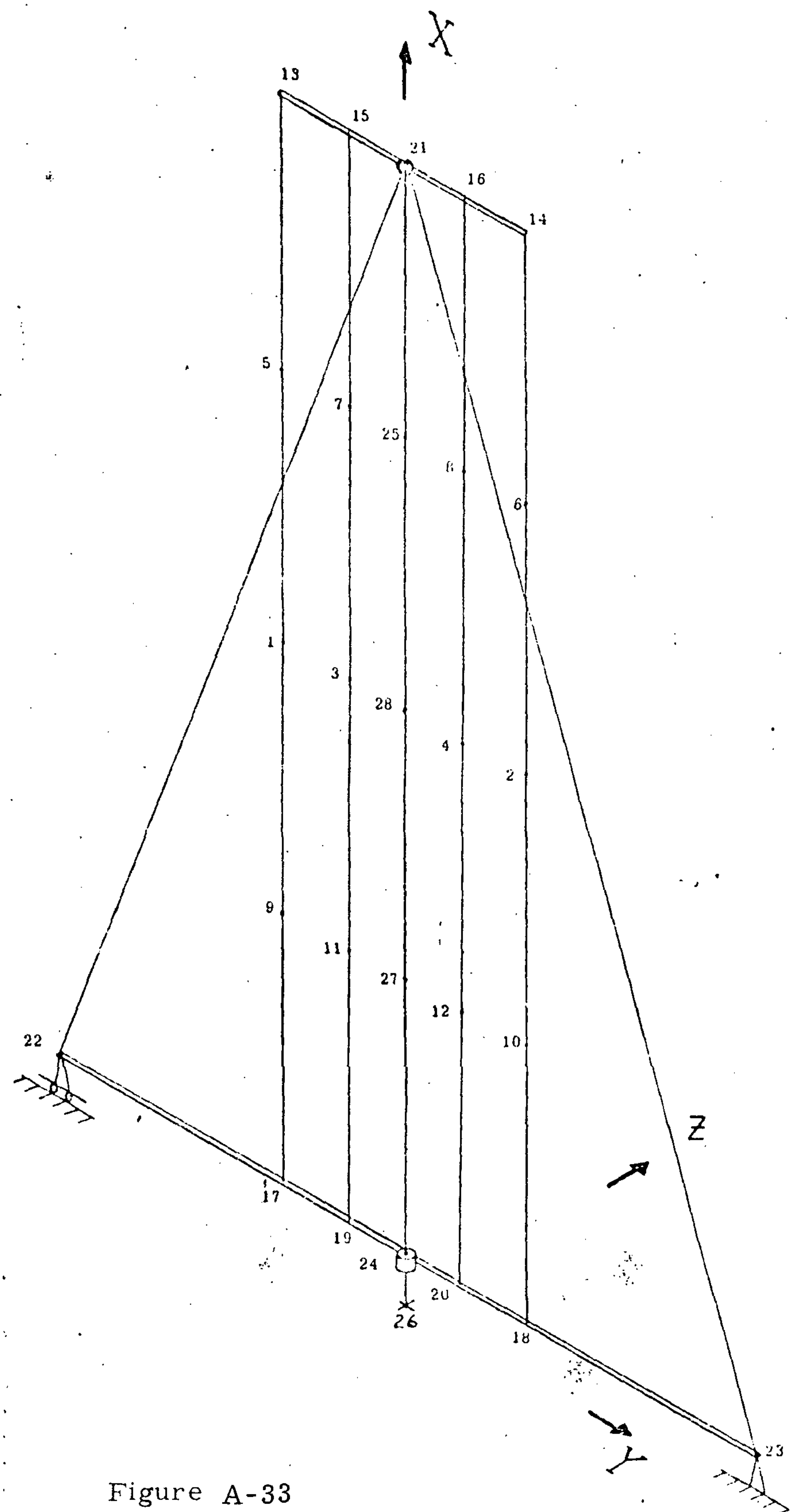

Figure A-33
SOLAR ARRAY ARTIFICIAL "G" STRUCTURAL MODEL

TABLE A-14

MASS-GEOMETRY DATA

FOR ARTIFICIAL "$\bar{G}$" SOLAR ARRAY

Node	Mass*	X	Y	Z
1	.1252	552.	-130.5	.0
2	.1252	552.	130.5	.0
3	.1252	552.	-58.5	.0
4	.1252	552.	58.5	.0
5	.1252	804.	-130.5	.0
6	.1252	804.	130.5	.0
7	.1252	804.	-58.5	.0
8	.1252	804.	58.5	.0
9	.1252	300.	-130.5	.0
10	.1252	300.	130.5	.0
11	.1252	300.	-58.5	.0
12	.1252	300.	58.5	.0
13	.1394	1056.	-130.5	.0
14	.1394	1056.	130.5	.0
15	.0897	1056.	-58.5	.0
16	.0897	1056.	58.5	.0
17	.8609	48.	-130.5	.0
18	.8609	48.	130.5	.0
19	.0822	48.	-58.5	.0
20	.0822	48.	58.5	.0
21	.1418	1056.	.0	.0
22	.7873	48.	-369.0	.0
23	0.	48.	369.0	.0
24	.0996	48.	.0	.0
25	.1383	804.	.0	.0
26	0.	.0	.0	.0
27	.1383	300.	.0	.0
28	.1383	552.	.0	.0

* - Mass units are $lb\text{-}sec^2/in.$

8

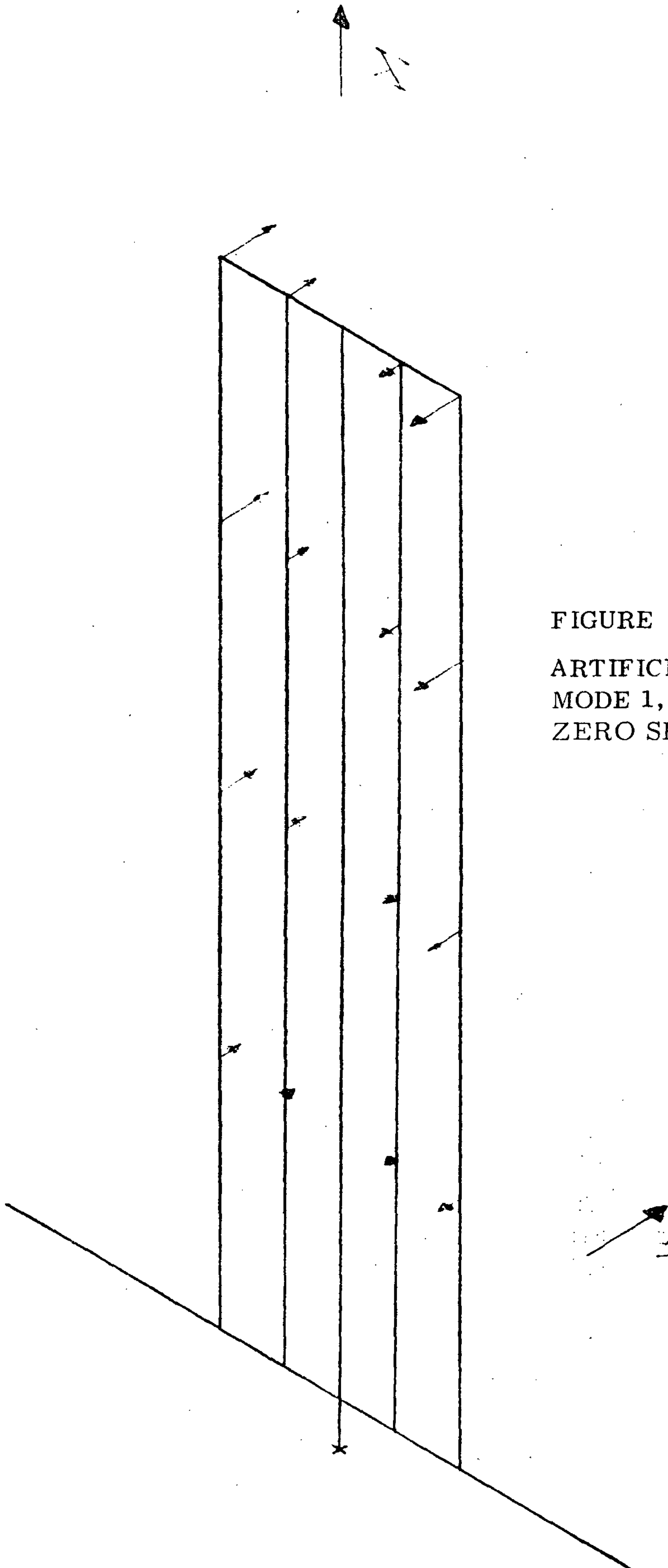

FIGURE A-34

ARTIFICIAL "G" SOLAR ARRAY
MODE 1, FREQUENCY = 0.199 Hz
ZERO SPIN

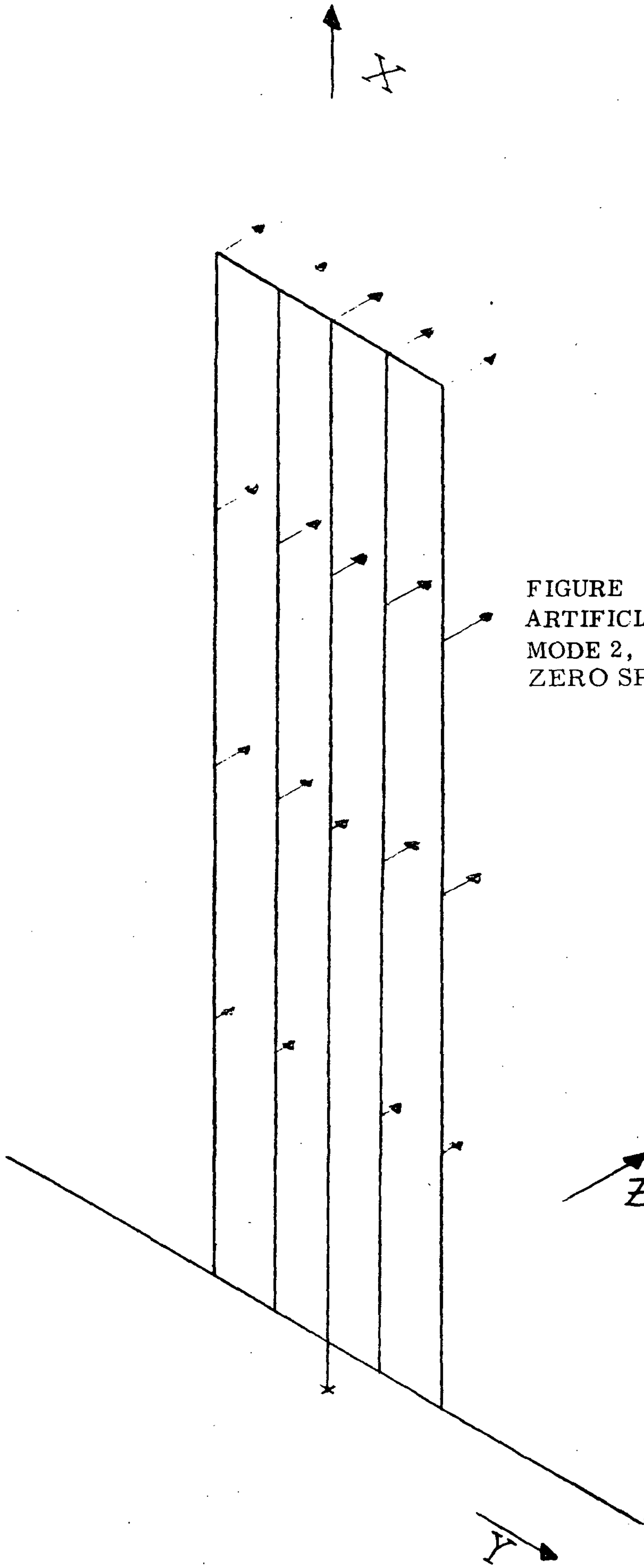

FIGURE A-35
ARTIFICIAL "G" SOLAR ARRAY
MODE 2, FREQUENCY = 0.203 Hz
ZERO SPIN

Figure A-36
Artificial "G" Solar Array
Mode 3

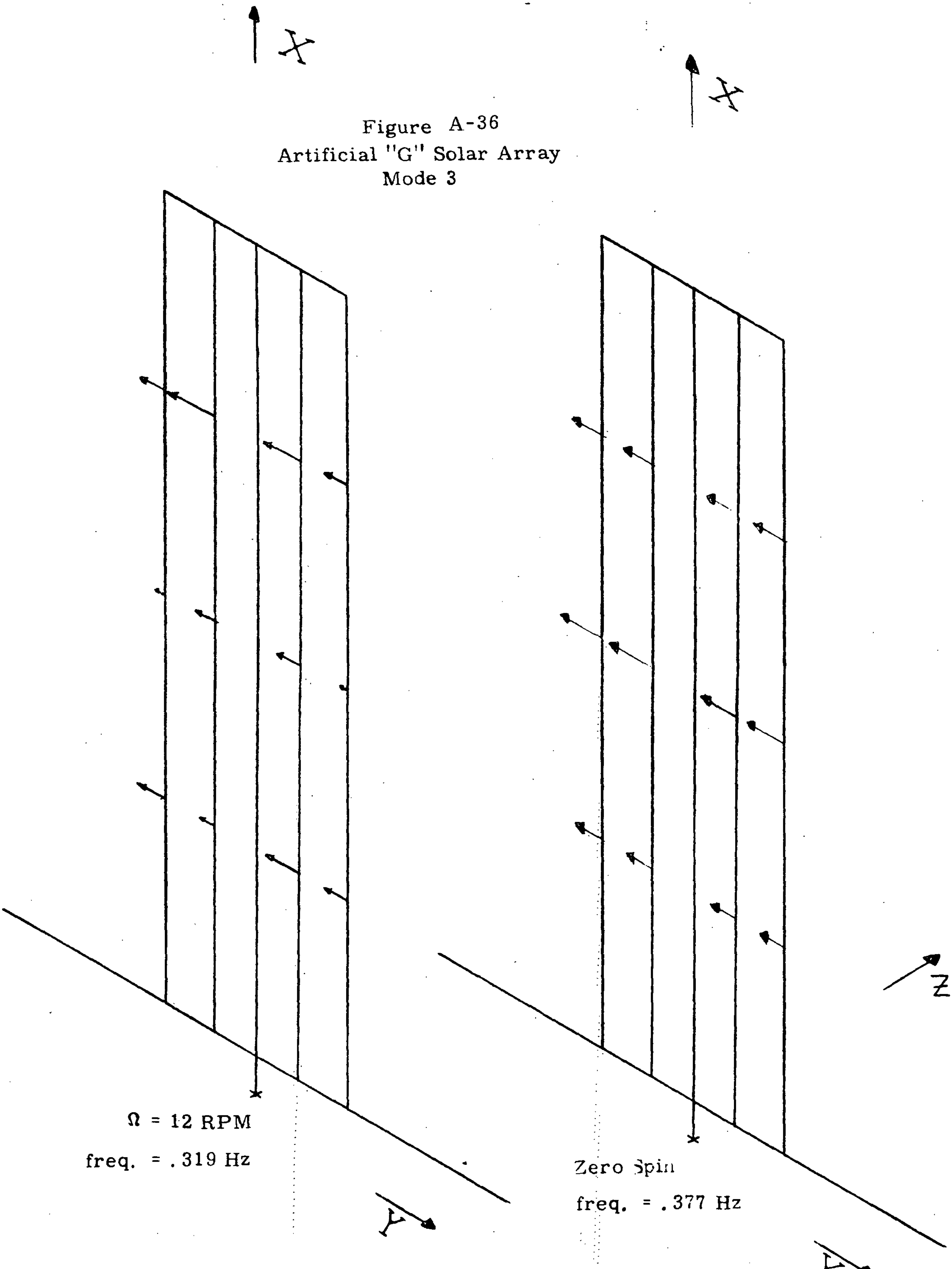

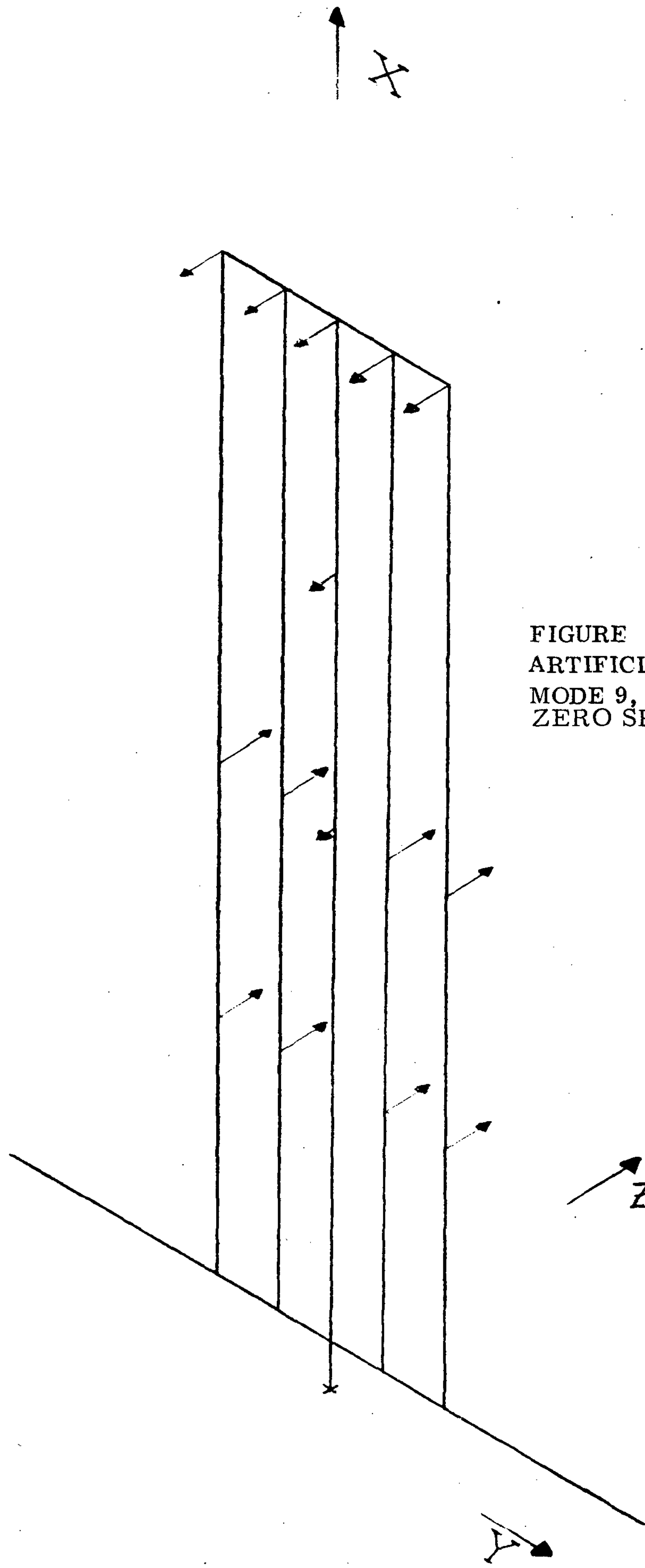

FIGURE A-37
ARTIFICIAL "G" SOLAR ARRAY
MODE 9, FREQUENCY = 0.504 Hz
ZERO SPIN

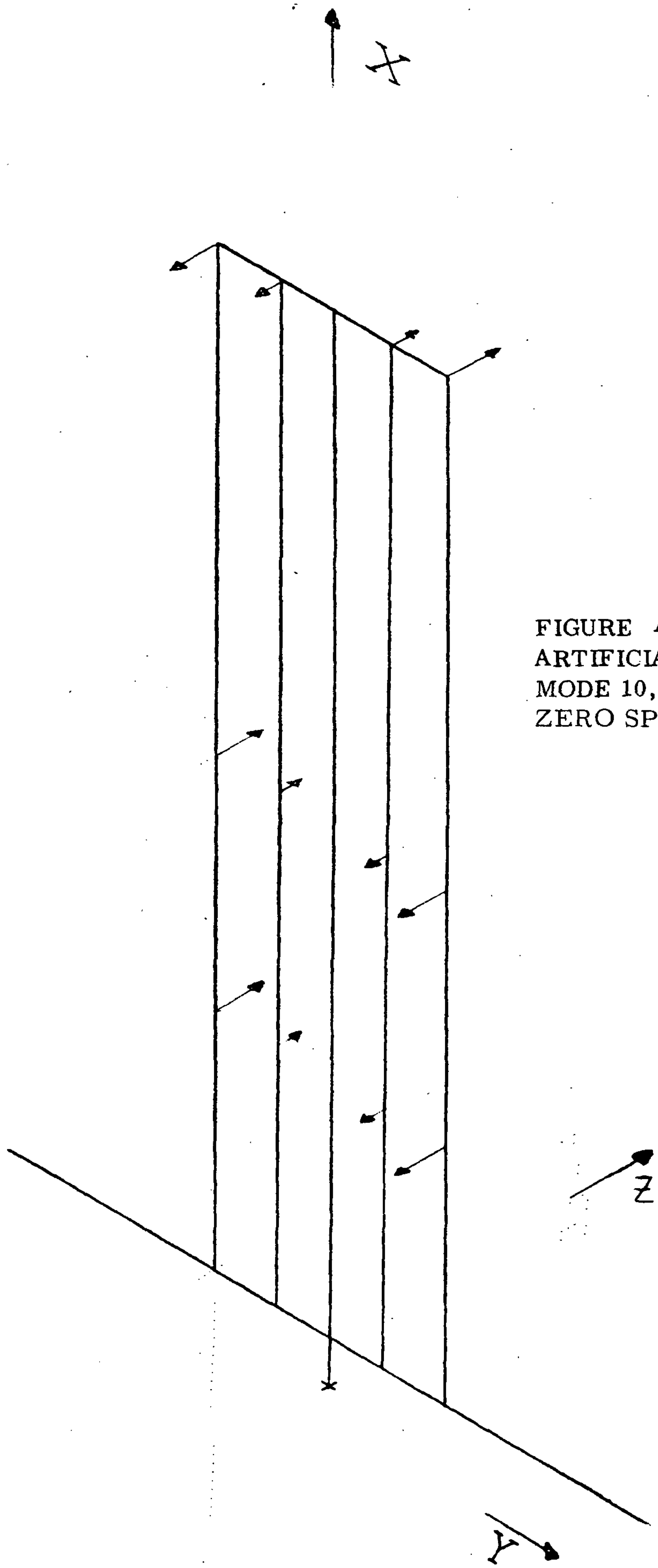

FIGURE A-38
ARTIFICIAL "G" SOLAR ARRAY
MODE 10, FREQUENCY = 0.521 Hz
ZERO SPIN

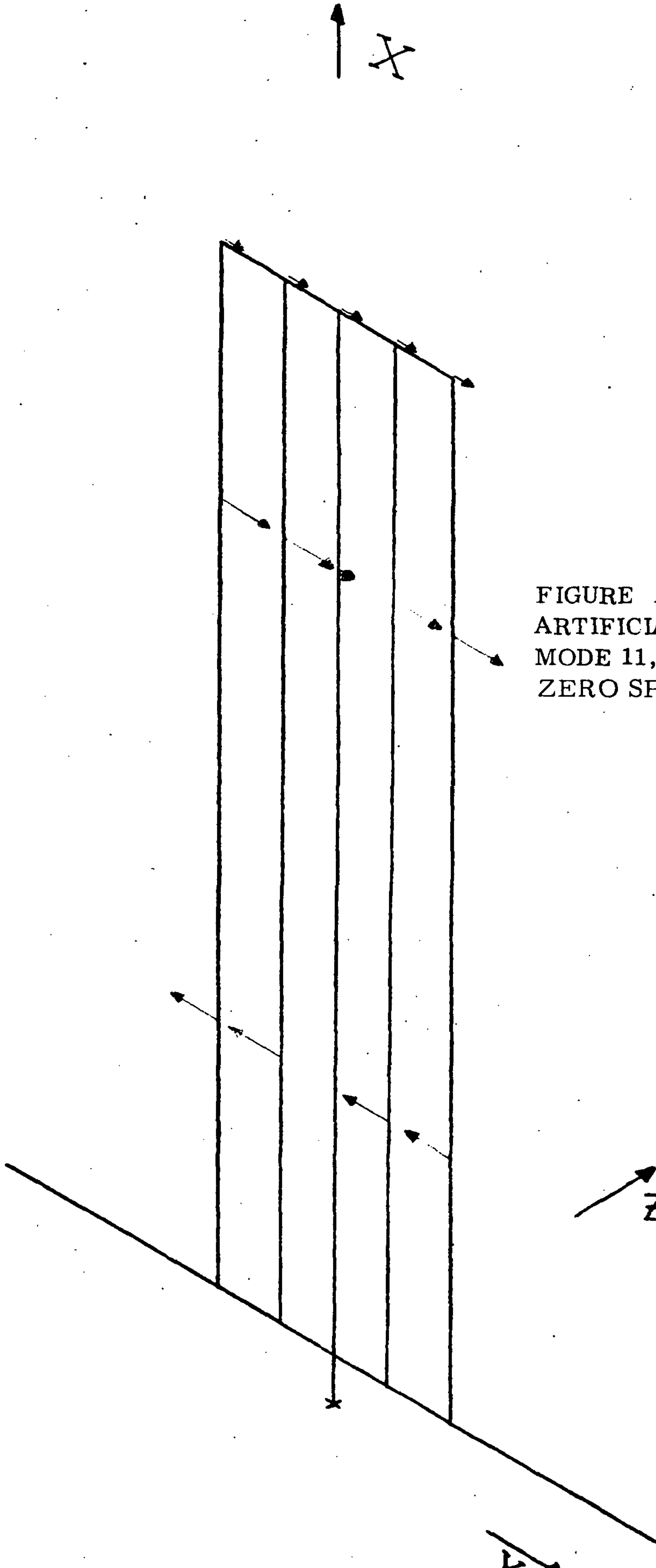

FIGURE A-39
ARTIFICIAL "G" SOLAR ARRAY
MODE 11, FREQUENCY = 0.704 Hz
ZERO SPIN

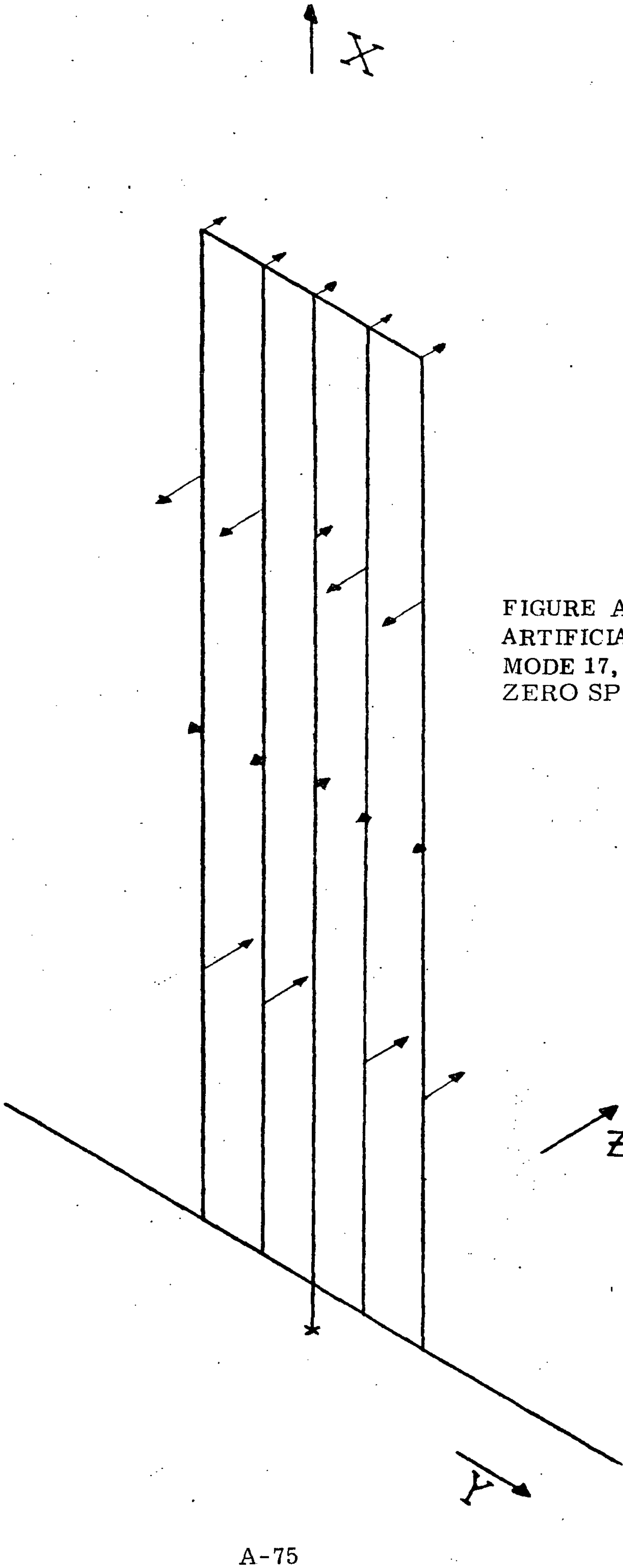

FIGURE A-40
ARTIFICIAL "G" SOLAR ARRAY
MODE 17, FREQUENCY = 0.778 Hz
ZERO SPIN

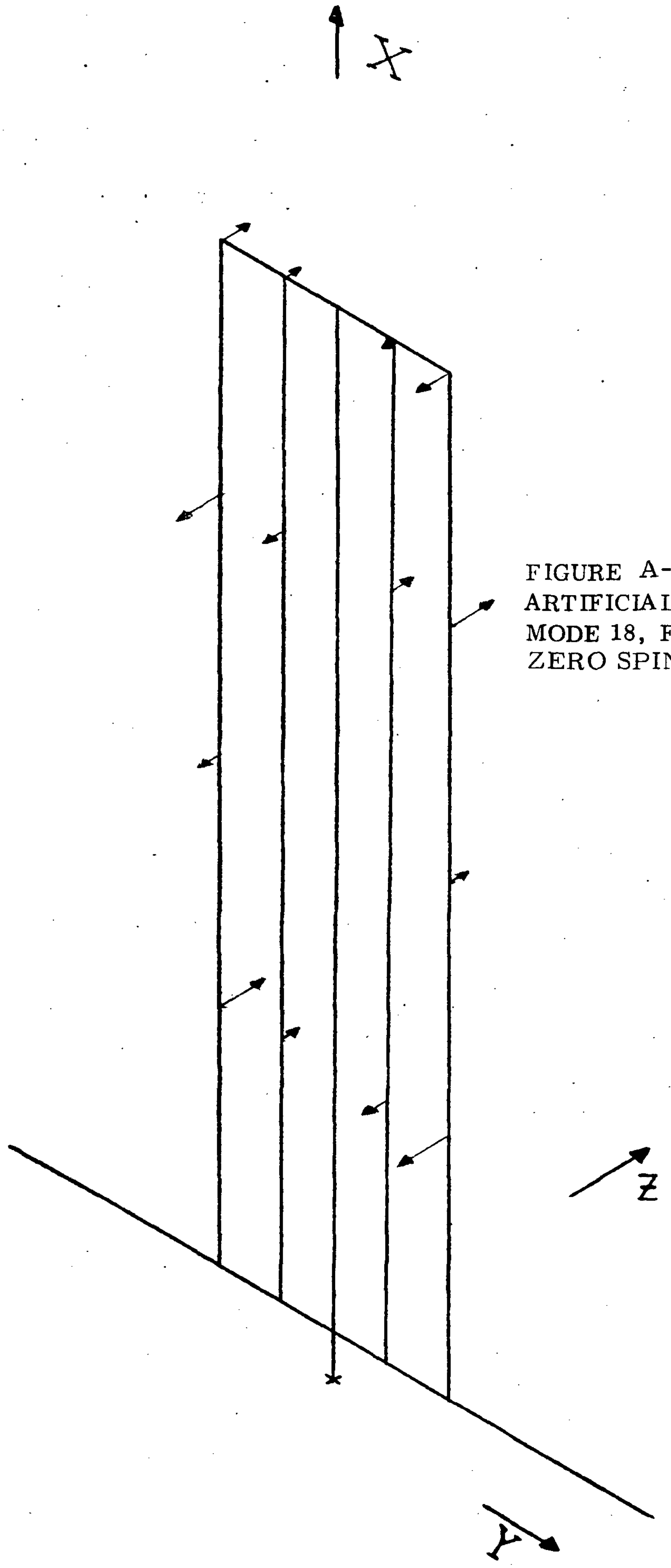

FIGURE A-41
ARTIFICIAL "G" SOLAR ARRAY
MODE 18, FREQUENCY = 0.794 Hz
ZERO SPIN

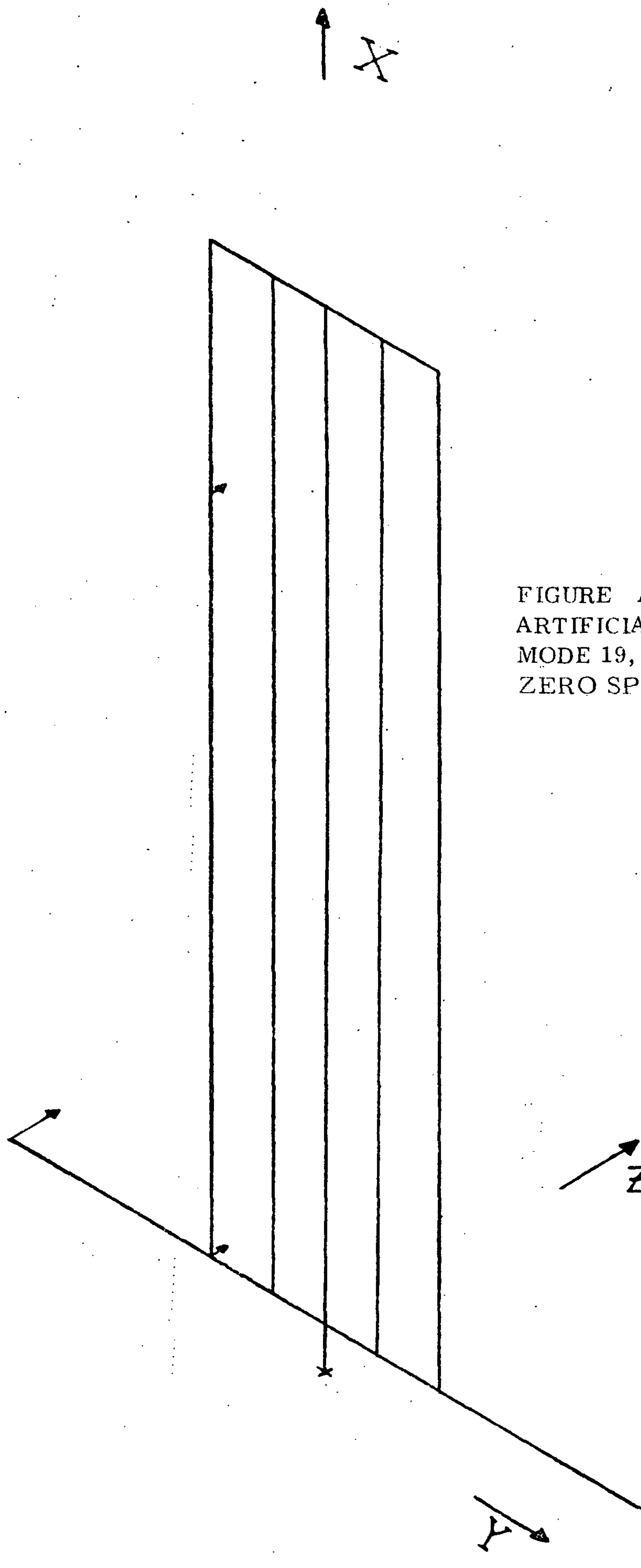

FIGURE A-42
ARTIFICIAL "G" SOLAR ARRAY
MODE 19, FREQUENCY = 0.905 Hz
ZERO SPIN

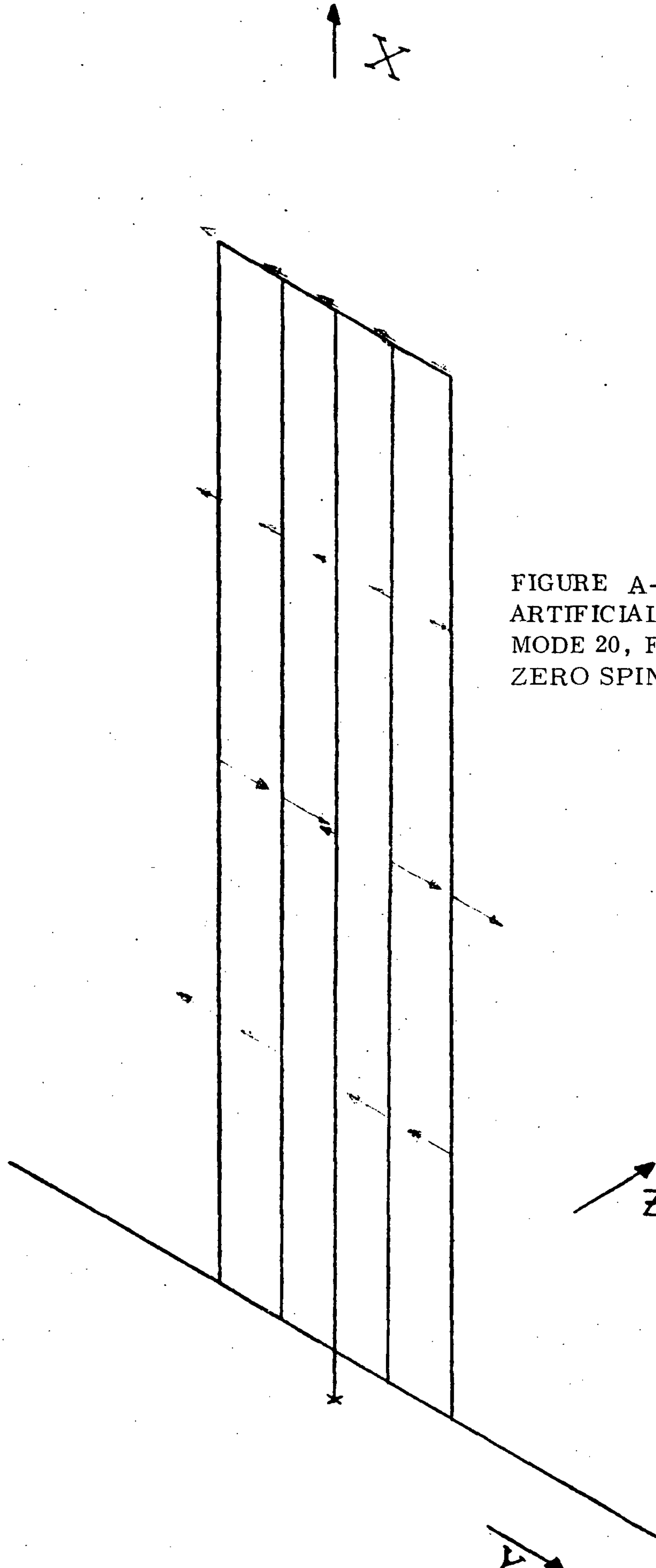

FIGURE A-43
ARTIFICIAL "G" SOLAR ARRAY
MODE 20, FREQUENCY = 0.935 Hz
ZERO SPIN

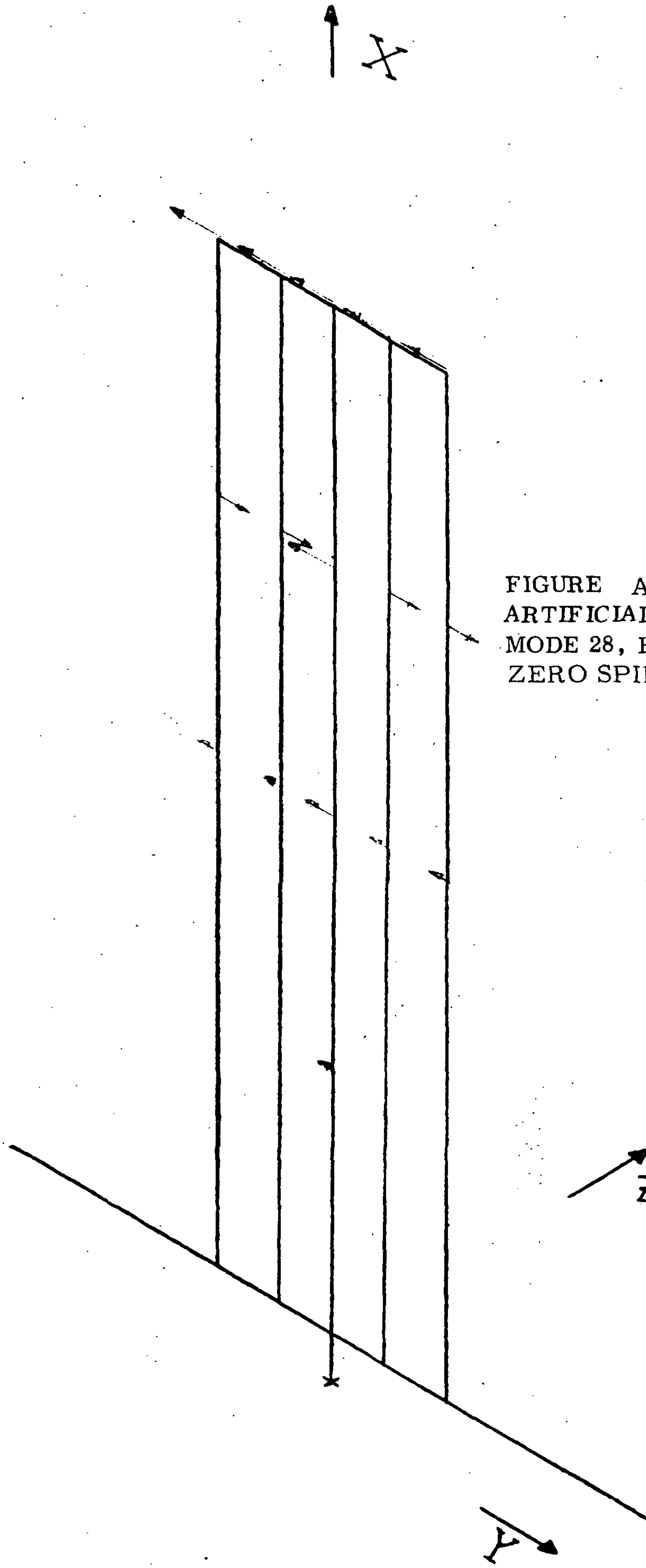

FIGURE A-44
ARTIFICIAL "G" SOLAR ARRAY
MODE 28, FREQUENCY = 1.07 Hz
ZERO SPIN

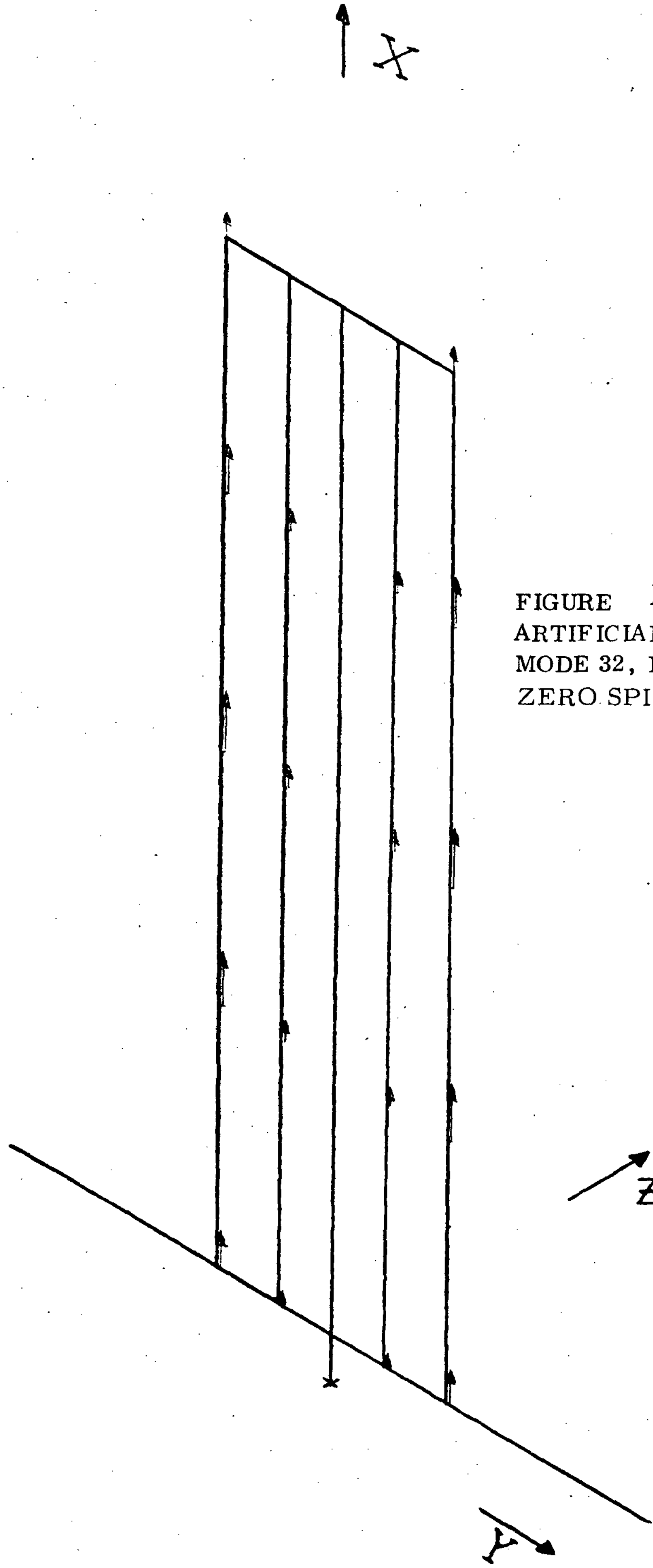

FIGURE A-45
ARTIFICIAL "G" SOLAR ARRAY
MODE 32, FREQUENCY = 3.84 Hz
ZERO SPIN

TABLE A-15

Artificial "G" Solar Array

Finite Element Model Data

Node	Mass $lb\text{-}sec^2/in$	No. of Structural D.O.F.	D.O.F. Sequence No.
1	0.1252	3	1 - 3
2	0.1252	3	4 - 6
3	0.1252	3	7 - 9
4	0.1252	3	10 - 12
5	0.1252	3	13 - 15
6	0.1252	3	16 - 18
7	0.1252	3	19 - 21
8	0.1252	3	22 - 24
9	0.1252	3	25 - 27
10	0.1252	3	28 - 30
11	0.1252	3	31 - 33
12	0.1252	3	34 - 36
13	0.1394	5	37 - 41
14	0.1394	5	42 - 46
15	0.0897	5	47 - 51
16	0.0897	5	52 - 56
17	0.8609	5	57 - 61
18	0.8609	5	62 - 66
19	0.0822	5	67 - 71
20	0.0822	5	72 - 76
21	0.1418	6	77 - 82
22	0.7873	5	83 - 87
23	0.0	3	88 - 90
24	0.0996	6	91 - 96

(TABLE A-15- CONTINUED)
Artificial "G" Solar Array

Finite Element Model Data

Node	Mass $lb\text{-}sec^2/in$	No. of Structural D.O.F.	D.O.F. Sequence No.
25	0.1383	6	97 - 102
26	0.0	0	-------
27	0.1383	6	103 - 108
28	0.1383	6	109 - 114

TABLE A-16

CORIOLIS FORCE MATRIX

(NORMALIZED TO Ω)

D. O. F.* Sequence No.			
1 - 3	-0.25043	0.	0.
4 - 6	-0.25043	0.	0.
	-0.25043	0.	0.
e t c.	-0.25043	0.	0.
	-0.25043	0.	0.
	-0.25043	0.	0.
	-0.25043	0.	0.
	-0.25043	0.	0.
	-0.25043	0.	0.
	-0.25043	0.	0.
	-0.25043	0.	0.
	-0.25043	0.	0.
	-0.27878	0.	0.
	0.	0.	-0.27878
	0.	0.	0.
	0.	-0.17940	0.
	0.	0.	0.
	-0.17940	0.	0.
	0.	0.	-1.72184
	0.	0.	0.
	0.	-1.72184	0.
	0.	0.	0.
	-0.16439	0.	0.
	0.	0.	-0.16439
	0.	0.	0.
	0.	-0.28364	0.
	0.	0.	0.
	0.	0.	0.
	0.	0.	0.
	0.	0.	0.
	-0.19928	0.	0.
	0.	0.	0.
	-0.27652	0.	0.
	0.	0.	0.
	-0.27652	0.	0.
	0.	0.	0.
	-0.27652	0.	0.
112 - 114	0.	0.	0.

* - Refer to Table A-15for corresponding node number.

TABLE A-17

CENTRIFUGAL FORCE MATRIX

(NORMALIZED TO Ω^2)

D.. O. F.* Sequence No.			
1 - 3	-0.12527	-0.12527	0.
4 - 6	-0.12527	-0.12527	0.
etc.	-0.12527	-0.12527	0.
	-0.12527	-0.12527	0.
	-0.12527	-0.12527	0.
	-0.12527	-0.12527	0.
	-0.12527	-0.12527	0.
	-0.12527	-0.12527	0.
	-0.12527	-0.12527	0.
	-0.12527	-0.12527	0.
	-0.12527	-0.12527	0.
	-0.12527	-0.12527	0.
	-0.13939	-0.13939	0.
	0.	0.	-0.13939
	-0.13939	0.	0.
	0.	-0.08970	-0.08970
	0.	0.	0.
	-0.08970	-0.08970	0.
	0.	0.	-0.86092
	-0.86092	0.	0.
	0.	-0.86092	-0.86092
	0.	0.	0.
	-0.08219	-0.08219	0.
	0.	0.	-0.08219
	-0.08219	0.	0.
	0.	-0.14192	-0.14192
	0.	0.	0.
	0.	-0.78787	0.
	0.	0.	0.
	0.	0.	0.
	-0.09964	-0.09964	0.
	0.	0.	0.
	-0.13836	-0.13836	0.
	0.	0.	0.
	-0.13836	-0.13836	0.
	0.	0.	0.
	-0.13836	-0.13836	0.
112 - 114	0.	0.	0.

* - Refer to Table A-15 for corresponding node number.

EIGENVECTOR FOR ROOT NO.= 1 Mode 1, frequency = 0.1786 Hz, Ω = 0 RPM

EIGENVALUE= 0.11224365E 01 (rad/sec)

REAL PART

1 TO 7	0.1039E-06	0.2416E-02	-0.9595E 00	-0.7518E-08	0.2416E-02	0.9600E 00	0.5677E-07
8 TO 14	0.2416E-02	-0.4295E 00	0.1730E-08	0.2416E-02	0.4311E 00	0.9106E-07	0.1473E-02
15 TO 21	-0.1000E 01	-0.2323E-07	0.1473E-02	0.9997E 00	0.5032E-07	0.1473E-02	-0.4481E 00
22 TO 28	-0.7054E-03	0.1473E-02	0.4494E 00	0.6355E-07	0.1007E-02	-0.3953E 00	-0.2181E-07
29 TO 35	0.1007E-02	0.3948E 00	0.4535E-07	0.1007E-02	-0.1769E 00	-0.1651E-07	0.1007E-02
36 TO 42	0.1775E 00	0.5435E-07	0.1216E-05	-0.5859E 00	0.4488E-02	0.4648E-09	-0.4402E-07
43 TO 49	0.1219E-05	0.5955E 00	0.4488E-02	0.3265E-09	0.2231E-07	0.1218E-05	-0.2628E 00
50 TO 56	0.4488E-02	0.4074E-09	-0.2017E-07	0.1219E-05	0.2623E 00	0.4488E-02	0.3407E-09
57 TO 63	0.3211E-07	0.1388E-07	-0.1754E-02	0.1416E-04	-0.6963E-10	-0.3301E-07	0.8839E-03
64 TO 70	0.8499E-03	0.2105E-05	-0.8155E-10	0.2907E-07	0.1376E-07	-0.7559E-03	0.1331E-04
71 TO 77	0.2374E-09	-0.3021E-07	0.1150E-07	0.5130E-03	0.7259E-05	0.2540E-09	0.1322E-09
78 TO 84	0.1219E-05	-0.2511E-03	0.4488E-02	0.4543E-06	0.3525E-09	0.1425E-07	-0.5149E-02
85 TO 91	0.1427E-04	0.1824E-12	-0.1671E-09	-0.6399E-05	0.1824E-12	-0.1669E-09	0.5770E-11
92 TO 98	0.1365E-07	-0.3048E-04	0.1125E-04	0.8855E-06	0.7900E-09	0.9511E-10	0.1451E-05
99 TO 105	-0.1536E-03	0.3369E-02	0.2507E-06	-0.3360E-08	0.3905E-10	0.1175E-05	-0.1260E-03
106 TO 112	0.1131E-02	0.6977E-07	0.6670E-08	0.6355E-10	0.2371E-05	-0.1285E-03	0.2250E-02
113 TO 114	0.1868E-08	0.3245E-11					

IMAGINARY PART

1 TO 7	0.0	0.0	0.0	0.0	0.0	0.0	0.0
8 TO 14	0.0	0.0	0.0	0.0	0.0	0.0	0.0
15 TO 21	0.0	0.0	0.0	0.0	0.0	0.0	0.0
22 TO 28	0.0	0.0	0.0	0.0	0.0	0.0	0.0
29 TO 35	0.0	0.0	0.0	0.0	0.0	0.0	0.0
36 TO 42	0.0	0.0	0.0	0.0	0.0	0.0	0.0
43 TO 49	0.0	0.0	0.0	0.0	0.0	0.0	0.0
50 TO 56	0.0	0.0	0.0	0.0	0.0	0.0	0.0
57 TO 63	0.0	0.0	0.0	0.0	0.0	0.0	0.0
64 TO 70	0.0	0.0	0.0	0.0	0.0	0.0	0.0
71 TO 77	0.0	0.0	0.0	0.0	0.0	0.0	0.0
78 TO 84	0.0	0.0	0.0	0.0	0.0	0.0	0.0
85 TO 91	0.0	0.0	0.0	0.0	0.0	0.0	0.0
92 TO 98	0.0	0.0	0.0	0.0	0.0	0.0	0.0
99 TO 105	0.0	0.0	0.0	0.0	0.0	0.0	0.0
106 TO 112	0.0	0.0	0.0	0.0	0.0	0.0	0.0
113 TO 114	0.0	0.0					

EIGENVECTOR FOR ROOT NO.= 2 Mode 2, frequency = 0.1977 Hz, Ω = 0 RPM

EIGENVALUE= 0.12421875E 01 (rad/sec)

REAL PART

1 TO 7	0.1393E-09	0.3345E-05	-0.5144E 00	-0.1597E-10	0.3345E-05	-0.6533E 00	0.8857E-10
8 TO 14	0.3345E-05	-0.5524E 00	-0.1070E-11	0.3345E-05	-0.6147E 00	0.1247E-09	0.2049E-05
15 TO 21	-0.6905E 00	-0.3773E-10	0.2048E-05	-0.9792E 00	0.6834E-10	0.2049E-05	-0.7423E 00
22 TO 28	-0.1304E-10	0.2049E-05	-0.8269E 00	0.8506E-10	0.1399E-05	-0.2863E 00	-0.3171E-10
29 TO 35	0.1399E-05	-0.3613E 00	0.5997E-10	0.1399E-05	-0.3067E 00	-0.2324E-10	0.1399E-05
36 TO 42	-0.3404E 00	0.7877E-10	0.1616E-08	-0.7841E 00	-0.8259E-03	0.6602E-12	-0.6522E-10
43 TO 49	0.1621E-08	-0.1000E 01	-0.8297E-03	0.4781E-12	0.3293E-10	0.1619E-08	-0.8436E 00
50 TO 56	-0.8262E-03	0.5920E-12	-0.3015E-10	0.1621E-08	-0.9403E 00	-0.8282E-03	0.5047E-12
57 TO 63	0.4251E-10	0.1815E-10	-0.4916E-02	0.1593E-04	-0.8615E-13	-0.4379E-10	0.1156E-10
64 TO 70	-0.1973E-02	0.7387E-05	-0.1031E-12	0.3811E-10	0.1799E-10	-0.3805E-02	0.1457E-04
71 TO 77	0.3149E-12	-0.3975E-10	0.1503E-10	-0.2507E-02	0.7865E-05	0.3385E-12	0.1713E-12
78 TO 84	0.1620E-08	-0.8919E 00	-0.8270E-03	0.1239E-02	0.5318E-12	0.1865E-10	-0.8775E-02
85 TO 91	0.1630E-04	0.2332E-15	-0.2242E-12	0.8714E-05	0.2332E-15	-0.2240E-12	0.8770E-14
92 TO 98	0.1794E-10	-0.3042E-02	0.1100E-04	0.1233E-03	0.1032E-11	0.1234E-12	0.1896E-08
99 TO 105	-0.5849E 00	-0.6176E-03	0.1178E-02	-0.4293E-11	0.5062E-13	0.1530E-08	-0.1020E 00
106 TO 112	-0.1996E-03	0.6347E-03	0.8690E-11	0.8251E-13	0.3022E-08	-0.3093E 00	-0.4081E-03
113 TO 114	0.9838E-03	0.4244E-14					

IMAGINARY PART

1 TO 7	0.0	0.0	0.0	0.0	0.0	0.0	0.0
8 TO 14	0.0	0.0	0.0	0.0	0.0	0.0	0.0
15 TO 21	0.0	0.0	0.0	0.0	0.0	0.0	0.0
22 TO 28	0.0	0.0	0.0	0.0	0.0	0.0	0.0
29 TO 35	0.0	0.0	0.0	0.0	0.0	0.0	0.0
36 TO 42	0.0	0.0	0.0	0.0	0.0	0.0	0.0
43 TO 49	0.0	0.0	0.0	0.0	0.0	0.0	0.0
50 TO 56	0.0	0.0	0.0	0.0	0.0	0.0	0.0
57 TO 63	0.0	0.0	0.0	0.0	0.0	0.0	0.0
64 TO 70	0.0	0.0	0.0	0.0	0.0	0.0	0.0
71 TO 77	0.0	0.0	0.0	0.0	0.0	0.0	0.0
78 TO 84	0.0	0.0	0.0	0.0	0.0	0.0	0.0
85 TO 91	0.0	0.0	0.0	0.0	0.0	0.0	0.0
92 TO 98	0.0	0.0	0.0	0.0	0.0	0.0	0.0
99 TO 105	0.0	0.0	0.0	0.0	0.0	0.0	0.0
106 TO 112	0.0	0.0	0.0	0.0	0.0	0.0	0.0
113 TO 114	0.0	0.0					

EIGENVECTOR FOR ROOT NO.= 3 Mode 3, frequency = 0.3768 Hz, Ω = 0 RPM

EIGENVALUE= 0.23671875E 01 (rad/sec)

REAL PART

1 TO 7	0.4418E-04	-0.5151E 00	-0.1950E-01	-0.4098E-04	-0.2105E 00	-0.1205E-01	0.2782E-04
8 TO 14	-0.1674E 00	0.4492E-01	-0.2873E-04	-0.1146E 00	0.1424E-01	0.2220E-04	-0.1000E 01
15 TO 21	-0.5845E-01	-0.1614E-04	-0.5568E 00	-0.3353E-01	0.1139E-04	-0.4613E 00	0.8745E-01
22 TO 28	-0.1102E-04	-0.4579E 00	0.2831E-01	0.4782E-04	-0.5332E 00	-0.3773E-01	-0.4777E-04
29 TO 35	-0.5097E 00	-0.3391E-01	0.3508E-04	-0.5212E 00	0.1067E 00	-0.3751E-04	-0.5120E 00
36 TO 42	0.3364E-01	-0.1364E-04	0.4944E-02	-0.4473E-05	0.2600E-07	0.1743E-07	0.2245E-04
43 TO 49	0.4954E-02	0.2547E-05	0.3070E-07	-0.1091E-06	-0.1167E-04	0.4950E-02	-0.2613E-05
50 TO 56	0.2535E-07	-0.1154E-06	0.1326E-04	0.4953E-02	0.4019E-06	0.2802E-07	-0.1663E-06
57 TO 63	0.5470E-04	0.2335E-04	0.1894E-06	-0.1053E-08	-0.1005E-07	-0.5777E-04	0.1497E-04
64 TO 70	0.2306E-06	0.1145E-08	-0.4976E-07	0.4362E-04	0.2247E-04	0.1878E-06	0.1700E-09
71 TO 77	0.3831E-06	-0.4751E-04	0.1915E-04	0.1439E-06	0.3679E-09	0.4395E-06	0.1849E-06
78 TO 84	0.4952E-02	-0.1141E-05	0.2530E-07	0.3034E-07	-0.3079E-06	0.2564E-04	0.1426E-05
85 TO 91	-0.7251E-08	0.6148E-12	-0.3390E-06	-0.2024E-08	0.6149E-12	-0.3389E-06	0.9868E-08
92 TO 98	0.2226E-04	0.1706E-06	-0.6954E-09	-0.7841E-08	0.1231E-05	0.1520E-06	0.5071E-02
99 TO 105	0.5890E-05	0.2041E-07	0.2262E-07	0.4023E-06	0.5971E-07	0.1856E-02	0.5758E-05
106 TO 112	0.7126E-08	-0.2447E-07	0.1065E-04	0.1094E-06	0.4276E-02	0.9045E-05	0.1426E-07
113 TO 114	0.5375E-10	0.6921E-05					

IMAGINARY PART

1 TO 7	0.0	0.0	0.0	0.0	0.0	0.0	0.0
8 TO 14	0.0	0.0	0.0	0.0	0.0	0.0	0.0
15 TO 21	0.0	0.0	0.0	0.0	0.0	0.0	0.0
22 TO 28	0.0	0.0	0.0	0.0	0.0	0.0	0.0
29 TO 35	0.0	0.0	0.0	0.0	0.0	0.0	0.0
36 TO 42	0.0	0.0	0.0	0.0	0.0	0.0	0.0
43 TO 49	0.0	0.0	0.0	0.0	0.0	0.0	0.0
50 TO 56	0.0	0.0	0.0	0.0	0.0	0.0	0.0
57 TO 63	0.0	0.0	0.0	0.0	0.0	0.0	0.0
64 TO 70	0.0	0.0	0.0	0.0	0.0	0.0	0.0
71 TO 77	0.0	0.0	0.0	0.0	0.0	0.0	0.0
78 TO 84	0.0	0.0	0.0	0.0	0.0	0.0	0.0
85 TO 91	0.0	0.0	0.0	0.0	0.0	0.0	0.0
92 TO 98	0.0	0.0	0.0	0.0	0.0	0.0	0.0
99 TO 105	0.0	0.0	0.0	0.0	0.0	0.0	0.0
106 TO 112	0.0	0.0	0.0	0.0	0.0	0.0	0.0
113 TO 114	0.0	0.0					

EIGENVECTOR FOR ROOT NO.= 9

Mode 9, frequency = 0.5031 Hz, Ω = 0 RPM

EIGENVALUE= 0.31611328E 01 (rad/sec)

REAL PART							
1 TO 7	0.1954E-06	0.3770E-02	0.6135E 00	0.6648E-07	0.3771E-02	-0.1279E 00	0.14[illegible]
8 TO 14	0.3656E-02	-0.9345E 00	0.4677E-07	0.3424E-02	0.7609E 00	0.1791E-06	0.5[illegible]
15 TO 21	0.4929E 00	0.9426E-08	0.6994E-02	-0.2642E 00	0.1013E-06	0.5146E-02	-0.1[illegible]
22 TO 28	0.1824E-07	0.3395E-02	0.7120E 00	0.1544E-06	0.7076E-02	-0.4820E 00	-0.33[illegible]
29 TO 35	0.7077E-02	-0.4423E 00	0.1167E-06	0.4256E-02	-0.4587E 00	-0.3771E-07	0.425[illegible]
36 TO 42	-0.4495E 00	0.1830E-06	0.3749E-05	-0.8483E-01	0.1970E-04	0.1634E-08	-0.141[illegible]
43 TO 49	0.3747E-05	-0.7905E-01	0.2298E-04	0.1150E-08	0.7185E-07	0.3749E-05	-0.234[illegible]
50 TO 56	0.2096E-04	0.1359E-08	-0.6133E-07	0.3747E-05	-0.8072E-01	0.2367E-04	0.1[illegible]
57 TO 63	0.9439E-07	0.4143E-07	-0.1106E-02	0.5731E-05	-0.1950E-09	-0.9899E-07	0.2[illegible]
64 TO 70	-0.1013E-03	0.1961E-05	-0.2549E-09	0.8533E-07	0.4114E-07	-0.7400E-03	0.44[illegible]
71 TO 77	0.6779E-09	-0.9120E-07	0.3438E-07	-0.2896E-03	0.3229E-05	0.7629E-09	0.37[illegible]
78 TO 84	0.3747E-05	-0.8212E-01	0.2354E-04	0.5854E-04	0.1091E-08	0.4267E-07	-0.2[illegible]
85 TO 91	0.8023E-05	0.4809E-12	-0.4958E-09	-0.3433E-06	0.4909E-12	-0.4951E-09	0.1[illegible]
92 TO 98	0.4096E-07	-0.4996E-03	0.3848E-05	0.2087E-04	0.2384E-08	0.2725E-09	0.44[illegible]
99 TO 105	-0.6616E-01	0.1761E-04	0.7256E-04	-0.1006E-07	0.1111E-09	0.3579E-05	-0.15[illegible]
106 TO 112	0.5717E-05	0.9857E-04	0.2027E-07	0.1825E-09	0.7036E-05	-0.4409E-01	0.115[illegible]
113 TO 114	0.1037E-03	0.8980E-11					
IMAGINARY PART							
1 TO 7	0.0	0.0	0.0	0.0	0.0	0.0	0.0
8 TO 14	0.0	0.0	0.0	0.0	0.0	0.0	0.0
15 TO 21	0.0	0.0	0.0	0.0	0.0	0.0	0.0
22 TO 28	0.0	0.0	0.0	0.0	0.0	0.0	0.0
29 TO 35	0.0	0.0	0.0	0.0	0.0	0.0	0.0
36 TO 42	0.0	0.0	0.0	0.0	0.0	0.0	0.0
43 TO 49	0.0	0.0	0.0	0.0	0.0	0.0	0.0
50 TO 56	0.0	0.0	0.0	0.0	0.0	0.0	0.0
57 TO 63	0.0	0.0	0.0	0.0	0.0	0.0	0.0
64 TO 70	0.0	0.0	0.0	0.0	0.0	0.0	0.0
71 TO 77	0.0	0.0	0.0	0.0	0.0	0.0	0.0
78 TO 84	0.0	0.0	0.0	0.0	0.0	0.0	0.0
85 TO 91	0.0	0.0	0.0	0.0	0.0	0.0	0.0
92 TO 98	0.0	0.0	0.0	0.0	0.0	0.0	0.0
99 TO 105	0.0	0.0	0.0	0.0	0.0	0.0	0.0
106 TO 112	0.0	0.0	0.0	0.0	0.0	0.0	0.0
113 TO 114	0.0	0.0					

EIGENVECTOR FOR ROOT NO.= 10 Mode 10, frequency = 0.5142 Hz, Ω = 0 RPM

EIGENVALUE= 0.32309570E 01 (rad/sec)

REAL PART							
1 TO 7	0.6055E-07	0.1019E-02	0.6613E 00	0.1266E-[illegible]	0.9643E-[illegible]	-0.6553E 00	0.4205E-07
8 TO 14	0.9635E-03	0.2377E 00	0.9993E-08	0.9634E-[illegible]	-0.9457E-[illegible]	0.5781E-07	0.1462E-02
15 TO 21	0.7958E-01	-0.4927E-08	0.9466E-03	-0.8297E-[illegible]	0.3273E-[illegible]	0.1905E-02	-0.1355E-01
22 TO 28	0.1319E-08	0.1906E-02	0.1896E 00	0.4672E-[illegible]	0.1922E-[illegible]	0.1020E 01	-0.1476E-07
29 TO 35	0.1920E-02	-0.9953E 00	0.3449E-07	0.1176E-[illegible]	0.4293E [illegible]	-0.1252E-07	0.1176E-02
36 TO 42	-0.4412E 00	0.6014E-07	0.1103E-05	-0.5795E [illegible]	0.4444E-[illegible]	0.5211E-09	-0.4826E-07
43 TO 49	0.1107E-05	0.5803E 00	0.4444E-02	0.3806E-[illegible]	0.2434E-[illegible]	0.1107E-05	-0.2595E 00
50 TO 56	0.4444E-02	0.4498E-09	-0.2134E-07	0.1107E-[illegible]	0.2624E [illegible]	0.4444E-02	0.3630E-09
57 TO 63	0.2778E-07	0.1195E-07	0.5328E-02	-0.4530E-[illegible]	-0.5151E-[illegible]	-0.2921E-07	0.7507E-08
64 TO 70	-0.2350E-02	-0.6041E-05	-0.7011E-10	0.2475E-[illegible]	0.1137E-[illegible]	0.2222E-02	-0.4007E-04
71 TO 77	0.2002E-09	-0.2659E-07	0.9924E-08	-0.1399E-[illegible]	-0.7034E-[illegible]	0.2266E-09	0.1075E-09
78 TO 84	0.1107E-05	0.4205E-03	0.4443E-02	0.1648E-[illegible]	0.3928E-[illegible]	0.1230E-07	0.1679E-01
85 TO 91	-0.4944E-04	0.1341E-12	-0.1489E-09	0.1790E-[illegible]	0.1341E-12	-0.1497E-09	0.5477E-11
92 TO 98	0.1192E-07	0.1146E-03	-0.3116E-04	-0.3491E-[illegible]	0.6331E-[illegible]	0.7795E-10	0.1278E-05
99 TO 105	0.7984E-03	0.3324E-02	0.1204E-05	-0.2810E-[illegible]	0.3170E-[illegible]	0.1022E-05	0.7616E-03
106 TO 112	0.1087E-02	-0.1655E-05	0.5800E-08	0.5219E-[illegible]	0.2019E-05	0.9635E-03	0.2206E-02
113 TO 114	0.3417E-08	0.2593E-11					
IMAGINARY PART							
1 TO 7	0.0	0.0	0.0	0.0	0.0	0.0	0.0
8 TO 14	0.0	0.0	0.0	0.0	0.0	0.0	0.0
15 TO 21	0.0	0.0	0.0	0.0	0.0	0.0	0.0
22 TO 28	0.0	0.0	0.0	0.0	0.0	0.0	0.0
29 TO 35	0.0	0.0	0.0	0.0	0.0	0.0	0.0
36 TO 42	0.0	0.0	0.0	0.0	0.0	0.0	0.0
43 TO 49	0.0	0.0	0.0	0.0	0.0	0.0	0.0
50 TO 56	0.0	0.0	0.0	0.0	0.0	0.0	0.0
57 TO 63	0.0	0.0	0.0	0.0	0.0	0.0	0.0
64 TO 70	0.0	0.0	0.0	0.0	0.0	0.0	0.0
71 TO 77	0.0	0.0	0.0	0.0	0.0	0.0	0.0
78 TO 84	0.0	0.0	0.0	0.0	0.0	0.0	0.0
85 TO 91	0.0	0.0	0.0	0.0	0.0	0.0	0.0
92 TO 98	0.0	0.0	0.0	0.0	0.0	0.0	0.0
99 TO 105	0.0	0.0	0.0	0.0	0.0	0.0	0.0
106 TO 112	0.0	0.0	0.0	0.0	0.0	0.0	0.0
113 TO 114	0.0	0.0					

EIGENVECTOR FOR ROOT NO.= 11   Mode 11, frequency = 0.7010 Hz, Ω = 0 RPM

EIGENVALUE= 0.4404296 9E 01 (rad/sec)

REAL PART							
1 TO 7	0.4422E-02	0.9962E-01	0.5792E-01	-0.4349E-03	0.7599E-03	0.2923E-01	0.2104E-03
8 TO 14	0.6332E-03	-0.4944E-01	-0.2094E-03	-0.1190E-01	-0.2526E-02	0.6423E-03	0.1000E 01
15 TO 21	0.1312E 00	-0.6220E-03	0.4743E 00	0.6877E-01	0.3083E-03	0.4145E 00	-0.1502E 00
22 TO 28	-0.3053E-03	0.3545E 00	-0.2316E-01	0.2594E-03	-0.9831E 00	-0.1136E 00	-0.2546E-03
29 TO 35	-0.4747E 00	-0.5449E-01	0.1206E-03	-0.4187E 00	0.1578E 00	-0.1195E-03	-0.3608E 00
36 TO 42	0.3472E-01	0.8523E-03	0.7134E-02	-0.1504E-04	0.7180E-07	0.5974E-05	-0.8391E-03
43 TO 49	0.7122E-02	-0.3963E-05	0.2623E-07	0.5758E-05	0.4108E-03	0.7126E-02	-0.1026E-04
50 TO 56	0.5472E-07	0.6544E-05	-0.4079E-03	0.7122E-02	-0.5873E-05	0.2702E-07	0.6450E-05
57 TO 63	0.5934E-04	-0.2262E-05	0.2491E-05	-0.7205E-07	0.3503E-06	-0.6909E-04	-0.2251E-05
64 TO 70	0.3737E-04	-0.6419E-09	0.3540E-06	0.2865E-04	-0.2959E-05	0.9236E-06	-0.1568E-07
71 TO 77	0.7040E-06	-0.2833E-04	-0.2596E-05	0.3913E-06	0.3340E-09	0.6996E-06	-0.1099E-07
78 TO 84	0.7122E-02	-0.7631E-05	0.3546E-07	0.8116E-07	0.7656E-05	0.1210E-05	0.6007E-05
85 TO 91	-0.1054E-07	0.9950E-12	-0.6113E-06	-0.2066E-08	0.3950E-12	-0.6111E-06	-0.1421E-09
92 TO 98	-0.2574E-05	0.4277E-06	-0.2983E-08	-0.1783E-07	0.9593E-08	-0.1285E-07	0.3755E-02
99 TO 105	0.1132E-04	0.2390E-07	0.5985E-07	0.1645E-04	-0.9770E-08	-0.4048E-03	0.1170E-04
106 TO 112	0.5455E-02	-0.5169E-07	-0.1497E-05	-0.1608E-07	0.2195E-03	0.1928E-04	0.1406E-07
113 TO 114	0.4824E-10	0.9622E-05					
IMAGINARY PART							
1 TO 7	0.0	0.0	0.0	0.0	0.0	0.0	0.0
8 TO 14	0.0	0.0	0.0	0.0	0.0	0.0	0.0
15 TO 21	0.0	0.0	0.0	0.0	0.0	0.0	0.0
22 TO 28	0.0	0.0	0.0	0.0	0.0	0.0	0.0
29 TO 35	0.0	0.0	0.0	0.0	0.0	0.0	0.0
36 TO 42	0.0	0.0	0.0	0.0	0.0	0.0	0.0
43 TO 49	0.0	0.0	0.0	0.0	0.0	0.0	0.0
50 TO 56	0.0	0.0	0.0	0.0	0.0	0.0	0.0
57 TO 63	0.0	0.0	0.0	0.0	0.0	0.0	0.0
64 TO 70	0.0	0.0	0.0	0.0	0.0	0.0	0.0
71 TO 77	0.0	0.0	0.0	0.0	0.0	0.0	0.0
78 TO 84	0.0	0.0	0.0	0.0	0.0	0.0	0.0
85 TO 91	0.0	0.0	0.0	0.0	0.0	0.0	0.0
92 TO 98	0.0	0.0	0.0	0.0	0.0	0.0	0.0
99 TO 105	0.0	0.0	0.0	0.0	0.0	0.0	0.0
106 TO 112	0.0	0.0	0.0	0.0	0.0	0.0	0.0
113 TO 114	0.0	0.0					

EIGENVECTOR FOR ROOT NO.= 17 Mode 17, frequency = 0.7774 Hz, Ω = 0 RPM

EIGENVALUE= 0.48843094E 01 (rad/sec)

REAL PART									
1	TO	7	-0.4008E-05	0.2759E-02	0.7402E-01	0.5210E-05	0.2537E-01	0.1845E-02	-0.1577E-05
8	TO	14	-0.1759E-01	-0.1739E-01	0.2583E-05	0.2059E-01	0.6148E-01	-0.6795E-05	0.2965E-01
15	TO	21	0.9072E 00	0.7483E-05	-0.1656E-01	0.7538E 00	-0.3114E-05	0.7516E-01	0.9704E 00
22	TO	28	0.3706E-05	-0.5668E-02	0.9941E 00	-0.1743E-05	0.3296E-02	-0.9340E 00	0.2374E-05
29	TO	35	0.4695E-01	-0.7654E 00	-0.4544E-05	-0.3973E-01	-0.1000E 01	0.1029E-05	0.3673E-01
36	TO	42	-0.9117E 00	-0.9704E-05	-0.1427E-04	-0.2138E-01	0.1195E-04	-0.6677E-07	0.9502E-05
43	TO	49	-0.1418E-04	-0.1805E-01	0.1303E-04	-0.6384E-07	-0.4711E-05	-0.1422E-04	-0.2051E-01
50	TO	56	0.1230E-04	-0.7447E-07	0.4692E-05	-0.1418E-04	-0.1900E-01	0.1330E-04	-0.7317E-07
57	TO	63	0.5979E-06	0.3290E-06	0.1778E-02	-0.1526E-04	-0.4457E-08	-0.3896E-06	0.2068E-05
64	TO	70	-0.4893E-03	-0.1692E-05	-0.1851E-08	0.7091E-06	0.3326E-06	0.7856E-03	-0.1212E-04
71	TO	77	0.5172E-08	-0.4476E-06	0.2699E-06	-0.2398E-03	-0.5341E-05	0.1388E-08	0.2416E-08
78	TO	84	-0.1419E-04	-0.1977E-01	0.1305E-04	0.6647E-04	-0.8876E-07	0.3194E-06	0.6107E-02
85	TO	91	-0.1960E-04	0.2310E-11	-0.1531E-08	0.3918E-05	0.2310E-11	-0.1525E-08	0.1249E-09
92	TO	98	0.3215E-06	0.1708E-03	-0.8775E-05	-0.6483E-05	0.1747E-07	0.1761E-08	0.2409E-04
99	TO	105	-0.4130E-02	0.9351E-05	0.5354E-04	-0.1711E-06	0.7304E-09	0.2619E-04	0.3613E-02
105	TO	112	0.2040E-05	-0.1596E-04	0.1459E-06	0.1237E-08	0.5080E-04	0.4929E-07	0.5682E-05
113	TO	114	0.1370E-04	0.2742E-09					
IMAGINARY PART									
1	TO	7	0.0	0.0	0.0	0.0	0.0	0.0	0.0
8	TO	14	0.0	0.0	0.0	0.0	0.0	0.0	0.0
15	TO	21	0.0	0.0	0.0	0.0	0.0	0.0	0.0
22	TO	28	0.0	0.0	0.0	0.0	0.0	0.0	0.0
29	TO	35	0.0	0.0	0.0	0.0	0.0	0.0	0.0
36	TO	42	0.0	0.0	0.0	0.0	0.0	0.0	0.0
43	TO	49	0.0	0.0	0.0	0.0	0.0	0.0	0.0
50	TO	56	0.0	0.0	0.0	0.0	0.0	0.0	0.0
57	TO	63	0.0	0.0	0.0	0.0	0.0	0.0	0.0
64	TO	70	0.0	0.0	0.0	0.0	0.0	0.0	0.0
71	TO	77	0.0	0.0	0.0	0.0	0.0	0.0	0.0
78	TO	84	0.0	0.0	0.0	0.0	0.0	0.0	0.0
85	TO	91	0.0	0.0	0.0	0.0	0.0	0.0	0.0
92	TO	98	0.0	0.0	0.0	0.0	0.0	0.0	0.0
99	TO	105	0.0	0.0	0.0	0.0	0.0	0.0	0.0
105	TO	112	0.0	0.0	0.0	0.0	0.0	0.0	0.0
113	TO	114	0.0	0.0					

EIGENVECTOR FOR ROOT NO.= 18 Mode 18, frequency = 0.7912 Hz, Ω = 0 RPM

EIGENVALUE= 0.49714355E 01 (rad/sec)

REAL PART								
1	TO 7	-0.1375E-05	-0.8983E-02	-0.1155E 00	0.1818E-05	-0.4196E-02	0.8353E-01	-0.5428E-05
8	TO 14	0.3690E-04	0.6572E-01	0.8985E-06	0.1780E-01	-0.1244E 00	-0.2335E-05	0.2401E-01
15	TO 21	-0.7416E 00	0.2602E-05	0.1703E-01	0.8700E 00	-0.1076E-05	0.1035E-01	-0.6159E 00
22	TO 28	0.1289E-05	-0.1783E-01	0.9351E 00	-0.5833E-06	-0.1009E-01	0.8822E 00	0.7920E-06
29	TO 35	-0.3804E-02	-0.1000E 01	-0.1565E-06	0.2221E-02	0.6643E 00	0.3303E-06	0.2758E-01
36	TO 42	-0.9431E 00	-0.3309E-05	-0.2073E-05	-0.3501E-01	0.2660E-03	-0.2255E-07	0.3260E-05
43	TO 49	-0.2043E-05	0.3469E-01	0.2672E-03	-0.2181E-07	-0.1616E-05	-0.2055E-05	-0.1584E-01
50	TO 56	0.2666E-03	-0.2542E-07	0.1610E-05	-0.2043E-05	0.1544E-01	0.2676E-03	-0.2512E-07
57	TO 63	0.2150E-06	0.1272E-06	-0.1591E-02	0.1451E-04	-0.1024E-08	-0.1893E-06	0.8172E-07
64	TO 70	0.5865E-03	0.1375E-05	-0.7005E-09	0.2327E-06	0.1290E-06	-0.6315E-03	0.1180E-04
71	TO 77	0.1372E-08	-0.2000E-06	0.1064E-06	0.3575E-03	0.5053E-05	0.8981E-09	0.2826E-09
78	TO 84	-0.2046E-05	-0.2170E-03	0.2675E-03	-0.1192E-06	-0.3056E-07	0.1209E-06	-0.5498E-02
85	TO 91	0.1732E-04	0.8697E-12	-0.8400E-09	-0.4376E-05	0.8697E-12	-0.8379E-09	0.4903E-10
92	TO 98	0.1265E-06	-0.3545E-04	0.8469E-05	0.1052E-05	0.7195E-08	0.7361E-09	0.1122E-04
99	TO 105	-0.2415E-03	0.2032E-03	-0.4509E-07	-0.5931E-07	0.2921E-09	0.1127E-04	-0.1884E-03
106	TO 112	0.7337E-04	0.3076E-06	0.5870E-07	0.4969E-09	0.2046E-04	-0.2351E-03	0.1395E-03
113	TO 114	0.9399E-07	0.9130E-10					
IMAGINARY PART								
1	TO 7	0.0	0.0	0.0	0.0	0.0	0.0	0.0
8	TO 14	0.0	0.0	0.0	0.0	0.0	0.0	0.0
15	TO 21	0.0	0.0	0.0	0.0	0.0	0.0	0.0
22	TO 28	0.0	0.0	0.0	0.0	0.0	0.0	0.0
29	TO 35	0.0	0.0	0.0	0.0	0.0	0.0	0.0
36	TO 42	0.0	0.0	0.0	0.0	0.0	0.0	0.0
43	TO 49	0.0	0.0	0.0	0.0	0.0	0.0	0.0
50	TO 56	0.0	0.0	0.0	0.0	0.0	0.0	0.0
57	TO 63	0.0	0.0	0.0	0.0	0.0	0.0	0.0
64	TO 70	0.0	0.0	0.0	0.0	0.0	0.0	0.0
71	TO 77	0.0	0.0	0.0	0.0	0.0	0.0	0.0
78	TO 84	0.0	0.0	0.0	0.0	0.0	0.0	0.0
85	TO 91	0.0	0.0	0.0	0.0	0.0	0.0	0.0
92	TO 98	0.0	0.0	0.0	0.0	0.0	0.0	0.0
99	TO 105	0.0	0.0	0.0	0.0	0.0	0.0	0.0
106	TO 112	0.0	0.0	0.0	0.0	0.0	0.0	0.0
113	TO 114	0.0	0.0					

EIGENVECTOR FOR ROOT NO.= 19 **Mode 19, frequency = 0.9047 Hz, Ω = 0 RPM**

EIGENVALUE= 0.56845703E 01 (rad/sec)

REAL PART								
1 TO	7	-0.5162E-06	-0.1928E-01	0.6491E 00	0.7858E-06	-0.2187E-02	-0.5776E-01	-0.2191E-05
9 TO	14	-0.7346E-03	-0.8894E 00	0.4477E-06	-0.6982E-03	-0.6334E-01	-0.8240E-06	0.1151E-01
15 TO	21	-0.1231E 00	0.9723E-06	0.3703E-02	0.6231E-01	-0.3698E-06	0.3799E-03	-0.4893E-01
22 TO	28	0.5022E-06	0.3610E-03	0.2237E-01	-0.3957E-06	-0.7677E-03	-0.4988E 00	0.5419E-05
29 TO	35	-0.7686E-03	-0.2196E-01	-0.1918E-06	0.2118E-02	0.1000E 01	0.3288E-06	0.2112E-02
36 TO	42	0.9320E-02	-0.1218E-05	-0.1080E-04	0.2926E-02	-0.3699E-04	-0.8998E-09	0.1159E-05
43 TO	49	-0.1075E-04	-0.6716E-02	-0.3699E-04	-0.8223E-08	-0.5628E-06	-0.1077E-04	0.2632E-03
50 TO	56	-0.3697E-04	-0.9292E-08	0.5510E-06	-0.1075E-04	-0.4059E-02	-0.3691E-04	-0.8926E-03
57 TO	63	-0.2394E-06	-0.8677E-07	-0.5274E-02	0.5947E-04	-0.8097E-09	0.2961E-06	-0.5493E-07
64 TO	70	0.2067E-02	0.4469E-05	-0.8169E-10	-0.1453E-06	-0.8553E-07	-0.2429E-02	0.4593E-04
71 TO	77	-0.1439E-09	0.2180E-06	-0.7171E-07	0.1277E-02	0.1803E-04	-0.2491E-08	-0.3547E-03
78 TO	84	-0.1075E-04	-0.1899E-02	-0.3694E-04	0.2470E-05	-0.1011E-07	-0.9033E-07	-0.2295E-01
85 TO	91	0.7511E-04	0.5179E-12	0.1905E-08	-0.1523E-04	0.5179E-12	0.1902E-08	-0.1554E-10
92 TO	98	-0.9438E-07	-0.1609E-03	0.3149E-04	0.4857E-05	-0.4728E-08	-0.2891E-09	-0.8920E-05
99 TO	105	-0.1306E-02	-0.1920E-04	0.2109E-05	0.6063E-08	-0.9844E-10	-0.6607E-05	-0.9122E-03
106 TO	112	0.1621E-04	0.1035E-05	-0.3412E-07	-0.2036E-09	-0.1193E-04	-0.9491E-03	-0.1496E-05
113 TO	114	0.3851E-06	0.2159E-09					
IMAGINARY PART								
1 TO	7	0.0	0.0	0.0	0.0	0.0	0.0	0.0
8 TO	14	0.0	0.0	0.0	0.0	0.0	0.0	0.0
15 TO	21	0.0	0.0	0.0	0.0	0.0	0.0	0.0
22 TO	28	0.0	0.0	0.0	0.0	0.0	0.0	0.0
29 TO	35	0.0	0.0	0.0	0.0	0.0	0.0	0.0
36 TO	42	0.0	0.0	0.0	0.0	0.0	0.0	0.0
43 TO	49	0.0	0.0	0.0	0.0	0.0	0.0	0.0
50 TO	56	0.0	0.0	0.0	0.0	0.0	0.0	0.0
57 TO	63	0.0	0.0	0.0	0.0	0.0	0.0	0.0
64 TO	70	0.0	0.0	0.0	0.0	0.0	0.0	0.0
71 TO	77	0.0	0.0	0.0	0.0	0.0	0.0	0.0
78 TO	84	0.0	0.0	0.0	0.0	0.0	0.0	0.0
85 TO	91	0.0	0.0	0.0	0.0	0.0	0.0	0.0
92 TO	98	0.0	0.0	0.0	0.0	0.0	0.0	0.0
99 TO	105	0.0	0.0	0.0	0.0	0.0	0.0	0.0
106 TO	112	0.0	0.0	0.0	0.0	0.0	0.0	0.0
113 TO	114	0.0	0.0					

EIGENVECTOR FOR ROOT NO.= 20

Mode 20, frequency = 0.9315 Hz, Ω = 0 RPM

EIGENVALUE= 0.58530273E 01 (rad/sec)

REAL PART

1 TO	7	-0.2881E-03	0.1000E 01	0.1234E-01	0.2855E-03	0.5430E 00	-0.2575E-01	-0.1256E-03
8 TO	14	0.3401E 00	-0.9853E-01	0.1290E-03	0.3976E 00	-0.5505E-01	-0.4736E-03	-0.6788E 00
15 TO	21	0.1305E-01	0.4657E-03	-0.8795E-01	0.1853E-01	-0.2230E-03	0.5622E-01	0.2034E-02
22 TO	28	0.2236E-03	0.8139E-01	0.1799E-01	-0.1152E-03	-0.2620E 00	-0.2577E-01	0.1167E-03
29 TO	35	-0.2622E 00	0.7156E-02	-0.3502E-04	-0.1798E 00	0.7955E-01	0.4033E-04	-0.2438E 00
36 TO	42	0.1993E-01	-0.6632E-03	0.1545E-02	-0.4673E-04	-0.2219E-08	-0.4556E-05	0.6499E-03
43 TO	49	0.1559E-02	-0.4681E-04	-0.2667E-08	-0.4377E-05	-0.3223E-03	0.1554E-02	-0.4689E-04
50 TO	56	-0.1130E-08	-0.5091E-05	0.3199E-03	0.1559E-02	-0.4671E-04	0.1186E-08	-0.4996E-05
57 TO	63	0.6013E-04	0.2937E-04	-0.7899E-05	0.9942E-07	-0.1459E-06	-0.5432E-04	0.1955E-04
64 TO	70	0.4085E-06	0.2547E-08	-0.7413E-07	0.5590E-04	0.2895E-04	-0.7960E-06	0.6937E-07
71 TO	77	0.4205E-06	-0.4863E-04	0.2410E-04	0.4336E-06	-0.9274E-08	0.3152E-06	0.2052E-05
78 TO	84	0.1557E-02	-0.4687E-04	0.2227E-08	0.2925E-06	-0.6077E-05	0.3050E-04	-0.1677E-04
85 TO	91	0.6166E-08	0.2249E-11	-0.3051E-06	-0.3832E-08	0.2249E-11	-0.3051E-06	0.1125E-07
92 TO	98	0.2857E-04	0.9468E-06	0.7229E-09	-0.3890E-07	0.1604E-05	0.1652E-06	0.4091E-02
99 TO	105	0.2065E-04	0.1399E-07	0.2165E-06	-0.1055E-04	0.6797E-07	0.2573E-02	0.2730E-04
106 TO	112	0.3331E-07	-0.1383E-06	0.1446E-04	0.1245E-06	0.5320E-02	0.5066E-04	0.2444E-07
113 TO	114	0.1434E-09	0.3563E-05					

IMAGINARY PART

1 TO	7	0.0	0.0	0.0	0.0	0.0	0.0	0.0
8 TO	14	0.0	0.0	0.0	0.0	0.0	0.0	0.0
15 TO	21	0.0	0.0	0.0	0.0	0.0	0.0	0.0
22 TO	28	0.0	0.0	0.0	0.0	0.0	0.0	0.0
29 TO	35	0.0	0.0	0.0	0.0	0.0	0.0	0.0
36 TO	42	0.0	0.0	0.0	0.0	0.0	0.0	0.0
43 TO	49	0.0	0.0	0.0	0.0	0.0	0.0	0.0
50 TO	56	0.0	0.0	0.0	0.0	0.0	0.0	0.0
57 TO	63	0.0	0.0	0.0	0.0	0.0	0.0	0.0
64 TO	70	0.0	0.0	0.0	0.0	0.0	0.0	0.0
71 TO	77	0.0	0.0	0.0	0.0	0.0	0.0	0.0
78 TO	84	0.0	0.0	0.0	0.0	0.0	0.0	0.0
85 TO	91	0.0	0.0	0.0	0.0	0.0	0.0	0.0
92 TO	98	0.0	0.0	0.0	0.0	0.0	0.0	0.0
99 TO	105	0.0	0.0	0.0	0.0	0.0	0.0	0.0
106 TO	112	0.0	0.0	0.0	0.0	0.0	0.0	0.0
113 TO	114	0.0	0.0					

EIGENVECTOR FOR ROOT NO.= 28

Mode 28, Frequency = 1.0544 Hz, Ω = 0 RPM

EIGENVALUE= 0.66254983E 01 (rad/sec.)

REAL PART							
1 TO 7	0.7459E-02	-0.1000E 01	-0.1483E 00	-0.7269E-02	-0.9997E 00	-0.2443E 00	0.3396E-02
8 TO 14	-0.9999E 00	-0.1773E 00	-0.3477E-02	-0.9993E 00	-0.2204E 00	0.1094E-01	0.9575E 00
15 TO 21	0.1606E 00	-0.1056E-01	0.9569E 00	0.2458E 00	0.5122E-02	0.9573E 00	0.1854E 00
22 TO 28	-0.5111E-02	0.9571E 00	0.2735E 00	0.3717E-02	0.3779E 00	0.1380E 00	-0.3743E-02
29 TO 35	0.3769E 00	0.1726E 00	0.1538E-02	0.3778E 00	0.1497E 00	-0.1731E-02	0.3773E 00
36 TO 42	0.1652E 00	0.1416E-01	0.4235E-01	-0.1494E-02	0.6962E-06	0.1006E-03	-0.1361E-01
43 TO 49	0.4243E-01	-0.1332E-02	0.5961E-06	0.9304E-04	0.6728E-02	0.4240E-01	-0.1445E-02
50 TO 56	0.6667E-06	0.1083E-03	-0.6629E-02	0.4243E-01	-0.1374E-02	0.5759E-06	0.1047E-03
57 TO 63	-0.8807E-04	-0.1750E-03	0.2615E-03	-0.2239E-05	0.4907E-05	-0.1487E-03	-0.1167E-03
64 TO 70	-0.5025E-04	-0.2214E-06	0.1932E-05	-0.3531E-03	-0.1779E-03	0.1146E-03	-0.1718E-05
71 TO 77	-0.8210E-06	0.5550E-04	-0.1517E-03	-0.1886E-04	-0.5691E-06	0.3484E-05	-0.9650E-05
78 TO 84	0.4241E-01	-0.1408E-02	0.6071E-06	0.8709E-05	0.1743E-03	-0.1650E-03	0.8370E-03
85 TO 91	-0.2500E-05	0.5281E-10	-0.1999E-05	0.4271E-06	0.5281E-10	-0.1907E-05	-0.4901E-07
92 TO 98	-0.1802E-03	0.3295E-04	-0.1114E-05	-0.1277E-05	-0.1014E-04	-0.7555E-06	-0.2566E-02
99 TO 105	0.5992E-03	0.6035E-06	0.6425E-05	0.1572E-03	-0.2957E-06	-0.1557E-01	0.8025E-03
106 TO 112	0.4250E-06	-0.4005E-05	-0.5595E-04	-0.5448E-06	-0.2212E-01	0.1486E-02	0.5399E-06
113 TO 114	0.2986E-08	0.1636E-04					
IMAGINARY PART							
1 TO 7	0.0	0.0	0.0	0.0	0.0	0.0	0.0
8 TO 14	0.0	0.0	0.0	0.0	0.0	0.0	0.0
15 TO 21	0.0	0.0	0.0	0.0	0.0	0.0	0.0
22 TO 28	0.0	0.0	0.0	0.0	0.0	0.0	0.0
29 TO 35	0.0	0.0	0.0	0.0	0.0	0.0	0.0
36 TO 42	0.0	0.0	0.0	0.0	0.0	0.0	0.0
43 TO 49	0.0	0.0	0.0	0.0	0.0	0.0	0.0
50 TO 56	0.0	0.0	0.0	0.0	0.0	0.0	0.0
57 TO 63	0.0	0.0	0.0	0.0	0.0	0.0	0.0
64 TO 70	0.0	0.0	0.0	0.0	0.0	0.0	0.0
71 TO 77	0.0	0.0	0.0	0.0	0.0	0.0	0.0
78 TO 84	0.0	0.0	0.0	0.0	0.0	0.0	0.0
85 TO 91	0.0	0.0	0.0	0.0	0.0	0.0	0.0
92 TO 98	0.0	0.0	0.0	0.0	0.0	0.0	0.0
99 TO 105	0.0	0.0	0.0	0.0	0.0	0.0	0.0
106 TO 112	0.0	0.0	0.0	0.0	0.0	0.0	0.0
113 TO 114	0.0	0.0					

EIGENVECTOR FOR ROOT NO.= 32

Mode 32, Frequency = 3.8402 Hz, Ω = 0 RPM

EIGENVALUE= 0.24128906E 02 (rad/sec.)

REAL PART							
1 TO 7	0.9995E 00	0.8945E-02	0.8947E-02	0.1000E 01	0.8945E-02	0.8944E-02	0.3568E 00
8 TO 14	0.8945E-02	0.8946E-02	0.3559E 00	0.8945E-02	0.8944E-02	0.8446E 00	0.9611E-02
15 TO 21	0.9587E-02	0.9454E 00	0.9611E-02	0.9650E-02	0.3066E 00	0.9611E-02	0.9608E-02
22 TO 28	0.3066E 00	0.9611E-02	0.9637E-02	0.8372E 00	0.9685E-02	0.9670E-02	0.8381E 00
29 TO 35	0.9686E-02	0.9690E-02	0.2935E 00	0.9685E-02	0.9676E-02	0.2919E 00	0.9686E-02
36 TO 42	0.9685E-02	0.4783E 00	0.1191E-03	-0.3217E-03	0.7628E-06	0.4769E-02	0.4764E 00
43 TO 49	0.1063E-03	-0.2226E-03	0.2301E-06	-0.4728E-02	0.1789E 00	0.1106E-03	-0.2698E-03
50 TO 56	0.6219E-06	0.2338E-02	0.1791E 00	0.1063E-03	-0.2362E-03	0.1015E-06	-0.2929E-02
57 TO 63	0.6633E 00	0.2626E-03	0.1148E-03	-0.5499E-07	0.4432E-02	0.6604E 00	0.1297E-03
64 TO 70	0.1136E-03	-0.1184E-06	-0.4416E-02	0.2250E 00	0.2276E-03	0.1049E-03	-0.8665E-07
71 TO 77	0.6135E-02	0.2237E 00	0.1680E-03	0.1131E-03	0.9705E-07	-0.6108E-02	0.8311E-01
78 TO 84	0.1078E-03	-0.2429E-03	0.2469E-06	0.1490E-04	-0.4845E-05	0.3728E-03	0.1396E-04
85 TO 91	0.6614E-06	0.3788E-08	-0.6398E-02	-0.6552E-06	0.3798E-09	0.6363E-02	0.1034E-01
92 TO 98	0.1990E-03	0.1064E-03	0.1014E-06	-0.4630E-05	0.8538E-05	0.6537E-01	0.2538E-02
99 TO 105	0.2755E-02	0.2578E-06	0.5770E-05	-0.1153E-04	0.2890E-01	0.2636E-02	0.2656E-02
106 TO 112	0.2552E-06	-0.7408E-05	0.1027E-04	0.4727E-01	0.4376E-02	0.2971E-02	0.2080E-06
113 TO 114	0.1633E-06	0.3351E-07					
IMAGINARY PART							
1 TO 7	0.0	0.0	0.0	0.0	0.0	0.0	0.0
8 TO 14	0.0	0.0	0.0	0.0	0.0	0.0	0.0
15 TO 21	0.0	0.0	0.0	0.0	0.0	0.0	0.0
22 TO 28	0.0	0.0	0.0	0.0	0.0	0.0	0.0
29 TO 35	0.0	0.0	0.0	0.0	0.0	0.0	0.0
36 TO 42	0.0	0.0	0.0	0.0	0.0	0.0	0.0
43 TO 49	0.0	0.0	0.0	0.0	0.0	0.0	0.0
50 TO 56	0.0	0.0	0.0	0.0	0.0	0.0	0.0
57 TO 63	0.0	0.0	0.0	0.0	0.0	0.0	0.0
64 TO 70	0.0	0.0	0.0	0.0	0.0	0.0	0.0
71 TO 77	0.0	0.0	0.0	0.0	0.0	0.0	0.0
78 TO 84	0.0	0.0	0.0	0.0	0.0	0.0	0.0
85 TO 91	0.0	0.0	0.0	0.0	0.0	0.0	0.0
92 TO 98	0.0	0.0	0.0	0.0	0.0	0.0	0.0
99 TO 105	0.0	0.0	0.0	0.0	0.0	0.0	0.0
106 TO 112	0.0	0.0	0.0	0.0	0.0	0.0	0.0
113 TO 114	0.0	0.0					

EIGENVECTOR FOR ROOT NO.= 1

Mode 1, Frequency = 0.1786 Hz, Ω = 4 RPM

EIGENVALUE= 0.11227112E 01 (rad/sec.)

REAL PART								
1 TO 7	0.1100E-06	0.2545E-02	-0.9593E 00	-0.1232E-07	0.2545E-02	0.9594E 00	0.5979E-07
8 TO 14	0.2545E-02	-0.4296E 00	-0.7649E-09	0.2545E-02	0.4313E 00	0.3827E-07	0.1556E-02
15 TO 21	-0.1000E 01	-0.2940E-07	0.1556E-02	0.9997E 00	0.5379E-07	0.1556E-02	-0.4431E 00
22 TO 28	-0.1016E-07	0.1556E-02	0.4424E 00	0.5701E-07	0.1053E-02	-0.3953E 00	-0.2474E-07
29 TO 35	0.1063E-02	0.3349E 00	0.4713E-07	0.1063E-02	-0.1769E 00	-0.1819E-07	0.1063E-02
36 TO 42	0.1775E 00	0.5163E-07	0.1255E-05	-0.5851E 00	0.4481E-07	0.5145E-09	-0.5102E-07
43 TO 49	0.1259E-05	0.5946E 00	0.4431E-02	0.3740E-09	0.2576E-07	0.1257E-05	-0.2624E 00
50 TO 56	0.4481E-02	0.4632E-05	-0.2359E-07	0.1269E-05	0.2619E 00	0.4482E-02	0.3948E-09
57 TO 63	0.3327E-07	0.1421E-07	-0.1752E-07	0.1414E-04	-0.6754E-10	-0.3427E-07	0.3046E-09
64 TO 70	0.8498E-03	0.2102E-05	-0.9079E-10	0.2993E-07	0.1408E-07	-0.7549E-03	0.1329E-04
71 TO 77	0.2464E-09	-0.3111E-07	0.1176E-07	0.5123E-03	0.7249E-05	0.2649E-09	0.1342E-09
78 TO 84	0.1259E-05	-0.7511E-03	0.4431E-02	0.4556E-06	0.4150E-09	0.1460E-07	-0.5141E-02
85 TO 91	0.1425E-04	0.1329E-12	-0.1754E-09	-0.6399E-05	0.1923E-12	-0.1753E-09	0.5971E-11
92 TO 98	0.1376E-07	-0.3044E-04	0.1124E-04	0.8842E-06	0.8092E-09	0.9667E-10	0.1485E-05
99 TO 105	-0.1534E-03	0.3364E-02	0.2516E-06	-0.3362E-09	0.3966E-10	0.1109E-05	-0.1259E-03
106 TO 112	0.1123E-02	0.4922E-07	0.6797E-09	0.6463E-10	0.2366E-05	-0.1231E-03	0.2247E-02
113 TO 114	0.1884E-09	0.3377E-11					
IMAGINARY PART							
1 TO 7	-0.1042E-05	0.2151E-05	0.0	-0.1041E-05	0.3079E-06	0.0	-0.1041E-05
8 TO 14	0.9816E-06	0.0	-0.1041E-05	0.1088E-06	0.0	-0.6983E-06	0.1365E-05
15 TO 21	0.0	-0.6232E-05	0.1719E-06	0.0	-0.6977E-06	0.4735E-06	0.0
22 TO 28	-0.6277E-06	0.5421E-07	0.0	-0.4595E-06	0.9092E-05	0.0	-0.4694E-05
29 TO 35	0.4434E-07	0.0	-0.4692E-06	0.3578E-06	0.0	-0.4621E-06	-0.6173E-07
36 TO 42	0.0	-0.1087E-08	-0.3644E-11	0.0	0.0	-0.9645E-11	-0.1049E-08
43 TO 49	-0.3955E-11	0.0	0.0	0.9100E-11	-0.4745E-09	-0.3507E-11	0.0
50 TO 56	0.0	-0.6236E-11	-0.4476E-09	-0.3775E-11	0.0	0.0	0.6005E-11
57 TO 63	-0.2946E-09	0.1340E-12	0.0	0.0	-0.1365E-11	-0.2733E-09	-0.9449E-12
64 TO 70	0.0	0.0	0.1310E-11	-0.1268E-09	-0.1327E-12	0.0	0.0
71 TO 77	-0.2683E-11	-0.1216E-09	-0.7363E-12	0.0	0.0	0.2583E-11	-0.2656E-09
78 TO 84	-0.3674E-11	0.0	0.0	0.0	-0.3001E-13	-0.5453E-12	0.0
85 TO 91	0.0	0.0	0.2472E-11	0.0	0.0	-0.2376E-11	-0.1996E-10
92 TO 98	-0.4585E-12	0.0	0.0	0.0	-0.2703E-13	-0.2113E-09	-0.2536E-11
99 TO 105	0.0	0.0	0.0	0.2475E-14	-0.9835E-10	-0.2241E-11	0.0
106 TO 112	0.0	0.0	0.2272E-14	-0.1696E-09	-0.1739E-11	0.0	0.0
113 TO 114	0.0	0.6657E-20					

EIGENVECTOR FOR ROOT NO.= 2

Mode 2, Frequency = 0.1977 Hz, Ω = 4 RPM

EIGENVALUE= 0.12424211E 01 (rad/sec.)

REAL PART							
1 TO 7	0.1969E-09	0.4932E-05	-0.5096E 00	-0.2539E-10	0.4931E-05	-0.6463E 00	0.1243E-09
8 TO 14	0.4932E-05	-0.5463E 00	-0.3383E-11	0.4931E-05	-0.6091E 00	0.1777E-09	0.2969E-05
15 TO 21	-0.6855E 00	-0.5627E-10	0.2968E-05	-0.8734E 00	0.9667E-10	0.2968E-05	-0.7372E 00
22 TO 28	-0.2022E-10	0.2969E-05	-0.8214E 00	0.1129E-09	0.2026E-05	-0.2943E 00	-0.4570E-10
29 TO 35	0.2026E-05	-0.3520E 00	0.3381E-10	0.2025E-05	-0.3046E 00	-0.3321E-10	0.2026E-05
36 TO 42	-0.3381E 00	0.1135E-09	0.2254E-03	-0.7834E 00	-0.8276E-03	0.9443E-12	-0.3464E-10
43 TO 49	0.2260E-09	-0.1000E 01	-0.9205E-03	0.5311E-12	0.4773E-10	0.2258E-03	-0.9432E 00
50 TO 56	-0.8279E-03	0.9534E-12	-0.4390E-10	0.2260E-08	-0.9402E 00	-0.9300E-03	0.7323E-12
57 TO 63	0.5916E-10	0.2515E-10	-0.4918E-02	0.1598E-04	-0.1156E-12	-0.6100E-10	0.1601E-10
64 TO 70	-0.1969E-12	0.7782E-05	-0.1410E-12	0.5294E-10	0.2492E-10	-0.3303E-02	0.1460E-04
71 TO 77	0.4393E-12	-0.5519E-10	0.2032E-10	-0.2503E-02	0.7972E-05	0.4725E-12	0.2365E-12
78 TO 84	0.2259E-08	-0.9917E 00	-0.8238E-03	0.1239E-02	0.7764E-12	0.2584E-10	-0.3791E-02
85 TO 91	0.1637E-04	-0.3129E-15	-0.3136E-12	0.9591E-05	0.3198E-15	-0.3134E-12	0.1210E-13
92 TO 98	0.2471E-10	-0.3039E-02	0.1102E-04	0.1232E-03	0.1430E-11	0.1704E-12	0.2626E-08
99 TO 105	-0.5846E 00	-0.6189E-03	0.1178E-02	-0.5820E-11	0.6986E-13	0.2117E-09	-0.1019E 00
106 TO 112	-0.1991E-03	0.6343E-03	0.1200E-10	0.1140E-12	0.4178E-09	-0.3391E 00	-0.4090E-03
113 TO 114	0.9935E-03	0.5876E-14					
IMAGINARY PART							
1 TO 7	-0.2203E-08	0.4625E-08	0.0	-0.2203E-08	0.5907E-09	0.0	-0.2202E-08
8 TO 14	0.2098E-09	0.0	-0.2202E-08	0.1964E-09	0.0	-0.1482E-08	0.2941E-09
15 TO 21	0.0	-0.1482E-08	0.3291E-09	0.0	-0.1481E-08	0.1308E-09	0.0
22 TO 28	-0.1481E-09	0.9133E-10	0.0	-0.1002E-08	0.1952E-09	0.0	-0.1001E-08
29 TO 35	0.7394E-10	0.0	-0.1001E-08	0.7779E-10	0.0	-0.1001E-08	-0.1424E-09
36 TO 42	0.0	-0.2202E-11	-0.7540E-14	0.0	0.0	-0.1353E-13	-0.2125E-11
43 TO 49	-0.9231E-14	0.0	0.0	0.1949E-13	-0.9585E-12	-0.7496E-14	0.0
50 TO 56	0.0	-0.1267E-13	-0.9444E-12	-0.7352E-14	0.0	0.0	0.1220E-13
57 TO 63	-0.5882E-12	0.2457E-15	0.0	0.0	-0.2823E-14	-0.5657E-12	-0.1912E-14
64 TO 70	0.0	0.0	0.2713E-14	-0.2519E-12	-0.2820E-15	0.0	0.0
71 TO 77	-0.5569E-14	-0.2514E-12	-0.1496E-14	0.0	0.0	0.5359E-14	-0.5338E-12
78 TO 84	-0.7633E-14	0.0	0.0	0.0	-0.6155E-16	-0.1187E-14	0.0
85 TO 91	0.0	0.0	0.5111E-14	0.0	0.0	-0.4919E-14	-0.3795E-13
92 TO 98	-0.9356E-15	0.0	0.0	0.0	-0.5442E-16	-0.4249E-12	-0.5138E-14
99 TO 105	0.0	0.0	0.0	0.4557E-17	-0.1970E-12	-0.5921E-14	0.0
106 TO 112	0.0	0.0	0.6019E-17	-0.3398E-12	-0.3485E-14	0.0	0.0
113 TO 114	0.0	0.1872E-22					

EIGENVECTOR FOR ROOT NO.= 3 Mode 3, Frequency = 0.3710 Hz, Ω = 4 RPM

EIGENVALUE= 0.23303326E 01 (rad/sec.)

REAL PART

1 TO 7	-0.5957E-03	-0.4827E 00	0.7806E-02	-0.2521E-03	-0.2489E 00	0.1190E-03	0.1734E-03
8 TO 14	-0.2271E 00	0.4913E-01	0.4297E-04	-0.3862E-01	0.2319E-01	-0.6012E-03	-0.9511E 00
15 TO 21	-0.1871E-01	-0.1155E-03	-0.4798E 00	-0.9715E-02	0.4947E-04	-0.4194E 00	0.7228E-01
22 TO 28	0.3571E-04	-0.5605E 00	0.3898E-01	-0.3049E-03	-0.4977E 00	0.3614E-01	-0.2202E-03
29 TO 35	-0.4117E 00	-0.2354E-01	0.1374E-03	-0.4210E 00	0.9942E-01	-0.3313E-04	-0.6095E 00
36 TO 42	0.4747E-01	-0.3603E-03	0.9525E-03	-0.2122E-04	0.1022E-06	-0.2995E-05	0.1540E-03
43 TO 49	0.9622E-03	0.2632E-05	0.8980E-07	-0.2530E-06	-0.1516E-03	0.9585E-03	-0.1403E-04
50 TO 56	0.9496E-07	-0.2705E-05	0.1107E-03	0.9631E-03	-0.3750E-05	0.8652E-07	-0.1289E-05
57 TO 63	-0.5292E-04	0.1237E-04	-0.1599E-06	0.6279E-03	-0.7492E-06	-0.7641E-04	0.8352E-05
64 TO 70	0.2692E-06	-0.7139E-09	0.4062E-06	0.5724E-05	0.1195E-04	0.4551E-06	0.6720E-08
71 TO 77	-0.5072E-06	-0.3497E-04	0.1206E-04	0.3759E-06	-0.3202E-08	0.5992E-06	0.4321E-06
78 TO 84	0.9613E-03	-0.9756E-05	0.9635E-07	0.1159E-06	-0.2537E-05	0.1434E-04	0.1901E-05
85 TO 91	-0.1616E-07	0.2134E-11	0.7069E-06	-0.1338E-08	0.2134E-11	-0.6841E-06	0.2653E-06
92 TO 98	0.1295E-04	0.5799E-06	-0.1891E-08	-0.2586E-07	0.7418E-06	0.7633E-06	0.2096E-02
99 TO 105	0.1911E-04	0.6974E-07	0.8654E-07	-0.4995E-05	0.4125E-06	0.1278E-02	0.1861E-04
106 TO 112	0.2447E-07	-0.8175E-07	0.7255E-05	0.7195E-06	0.2669E-02	0.3020E-04	0.4881E-07
113 TO 114	0.2494E-09	0.1861E-05					

IMAGINARY PART

1 TO 7	0.7865E-03	-0.2870E 00	0.0	0.7128E-03	-0.2035E 00	0.0	0.5524E-03
8 TO 14	0.2074E 00	0.0	0.7551E-03	0.1214E 00	0.0	0.7013E-03	-0.3090E 00
15 TO 21	0.0	0.6994E-03	-0.1551E 00	0.0	0.4549E-03	0.1136E 00	0.0
22 TO 28	0.7569E-03	-0.2475E-01	0.0	0.5158E-03	-0.2320E 00	0.0	0.5474E-03
29 TO 35	-0.1619E 00	0.0	0.4824E-03	0.1364E 00	0.0	0.7311E-03	-0.2573E-01
36 TO 42	0.0	-0.2769E-03	0.5733E-04	0.0	0.0	-0.3152E-05	0.2008E-03
43 TO 49	-0.5594E-04	0.0	0.0	-0.2106E-05	-0.8101E-04	-0.5439E-04	0.0
50 TO 56	0.0	-0.1917E-05	0.6290E-04	-0.5401E-04	0.0	0.0	-0.1360E-05
57 TO 63	-0.2257E-05	0.2270E-05	0.0	0.0	-0.1637E-06	0.1812E-04	0.7490E-06
64 TO 70	0.0	0.0	-0.2975E-06	0.7211E-05	0.4399E-05	0.0	0.0
71 TO 77	0.1123E-07	-0.3408E-05	0.3541E-05	0.0	0.0	-0.1332E-06	-0.3185E-05
78 TO 84	-0.5410E-04	0.0	0.0	0.0	-0.1102E-05	0.4112E-05	0.0
85 TO 91	0.0	0.0	0.9604E-07	0.0	0.0	0.2626E-06	-0.2783E-06
92 TO 98	0.3914E-05	0.0	0.0	0.0	0.1558E-06	-0.3595E-05	0.3297E-03
99 TO 105	0.0	0.0	0.0	-0.1521E-05	-0.1915E-05	0.1589E-03	0.0
106 TO 112	0.0	0.0	0.1306E-05	-0.3139E-05	0.5031E-03	0.0	0.0
113 TO 114	0.0	0.5646E-06					

EIGENVECTOR FOR ROOT NO.= 9 Mode 9. Frequency = 0.5025 Hz, Ω = 4 RPM

EIGENVALUE= 0.31574402E 01 (rad/sec.)

REAL PART							
1 TO 7	0.2054E-06	0.3956E-02	0.6391E 00	0.8209E-07	0.3723E-02	-0.1352E 00	0.1504E-06
8 TO 14	0.3742E-02	-0.9697E 00	0.5519E-07	0.3741E-02	0.8027E 00	0.1903E-06	0.5441E-02
15 TO 21	0.4790E 00	0.1624E-07	0.1540E-02	-0.2821E 00	0.1105E-06	0.7288E-02	-0.1000E 01
22 TO 28	0.2149E-07	0.7288E-02	0.7443E 00	0.1595E-06	0.7360E-02	-0.5214E 00	-0.3184E-07
29 TO 35	0.7360E-02	-0.4642E 00	0.1229E-06	0.4457E-02	-0.4952E 00	-0.3494E-07	0.4457E-02
36 TO 42	-0.4905E 00	0.2092E-06	0.4056E-05	-0.9223E-01	0.2597E-04	0.1837E-08	-0.1653E-06
43 TO 49	0.4052E-05	-0.8450E-01	0.3040E-04	0.1321E-08	0.8354E-07	0.4053E-05	-0.9030E-01
50 TO 56	0.2835E-04	0.1559E-08	-0.7239E-07	0.4052E-05	-0.9671E-01	0.3124E-04	0.1240E-08
57 TO 63	0.1022E-06	0.4439E-07	-0.1159E-02	0.6014E-05	-0.1997E-09	-0.1072E-06	0.2816E-07
64 TO 70	-0.1154E-03	0.2086E-05	-0.2641E-09	0.9159E-07	0.4398E-07	-0.7857E-03	0.4676E-05
71 TO 77	0.7363E-09	-0.9800E-07	0.3675E-07	-0.3145E-03	0.3397E-05	0.8291E-09	0.4009E-09
78 TO 84	0.4052E-05	-0.3855E-01	0.3109E-04	0.6380E-04	0.1234E-08	0.4564E-07	-0.2986E-02
85 TO 91	0.8417E-05	0.5055E-12	-0.5430E-09	-0.3171E-06	0.5055E-12	-0.5423E-09	0.2041E-10
92 TO 98	0.4373E-07	-0.5346E-03	0.4021E-05	0.2235E-04	0.2549E-08	0.2898E-09	0.4731E-05
99 TO 105	-0.7119E-01	0.2326E-04	0.7970E-04	-0.1057E-07	0.1191E-09	0.3814E-05	-0.1815E-01
106 TO 112	0.7545E-05	0.1059E-03	0.2154E-07	0.1941E-09	0.7495E-05	-0.4733E-01	0.1541E-04
113 TO 114	0.1117E-03	0.9605E-11					
IMAGINARY PART							
1 TO 7	-0.1230E-04	0.9534E-06	0.0	-0.1126E-04	0.8367E-05	0.0	-0.1010E-04
8 TO 14	0.1749E-05	0.0	-0.1010E-04	0.5459E-05	0.0	-0.1099E-04	-0.6260E-05
15 TO 21	0.0	-0.9123E-05	0.1065E-04	0.0	-0.1061E-04	-0.9649E-06	0.0
22 TO 28	-0.1061E-04	0.4379E-05	0.0	-0.9654E-05	-0.8161E-05	0.0	-0.9654E-05
29 TO 35	0.1231E-04	0.0	-0.5847E-05	-0.2593E-05	0.0	-0.5847E-05	0.6506E-05
36 TO 42	0.0	-0.5417E-09	0.2537E-10	0.0	0.0	0.8194E-12	-0.5670E-09
43 TO 49	0.2715E-10	0.0	0.0	-0.7675E-12	-0.6149E-09	0.2577E-10	0.0
50 TO 56	0.0	0.1409E-11	-0.6320E-09	0.2574E-10	0.0	0.0	-0.1173E-11
57 TO 63	0.2065E-08	0.9252E-11	0.0	0.0	0.9778E-11	0.2099E-08	0.8839E-13
64 TO 70	0.0	0.0	-0.1005E-10	0.8763E-09	0.5422E-11	0.0	0.0
71 TO 77	0.2165E-10	0.9849E-09	0.2059E-11	0.0	0.0	-0.2196E-10	-0.6788E-09
78 TO 84	0.2626E-10	0.0	0.0	0.0	0.1553E-12	0.1180E-10	0.0
85 TO 91	0.0	0.0	-0.1739E-10	0.0	0.0	0.1823E-10	-0.2442E-10
92 TO 98	0.3389E-11	0.0	0.0	0.0	0.3185E-13	-0.6524E-09	0.5391E-11
99 TO 105	0.0	0.0	0.0	0.3364E-13	-0.3225E-09	0.3505E-11	0.0
106 TO 112	0.0	0.0	-0.1190E-13	-0.5625E-09	0.2056E-11	0.0	0.0
113 TO 114	0.0	0.5951E-21					

EIGENVECTOR FOR ROOT NO.= 10

Mode 10, Frequency = 0.5151 Hz, Ω = 4 RPM

EIGENVALUE= 0.32366943E 01 (rad/sec.)

REAL PART

1 TO 7	0.7444E-07	0.1242E-02	-0.8736E 00	0.2130E-07	0.1134E-02	0.9148E 00	0.5297E-07
8 TO 14	0.1176E-02	-0.5059E 00	0.1529E-07	0.1175E-02	0.9008E 00	0.7087E-07	0.1948E-02
15 TO 21	0.1123E 00	-0.1922E-08	0.1195E-02	-0.1017E 00	0.4026E-07	0.2360E-02	0.5083E-01
22 TO 28	0.3492E-09	0.2360E-02	0.4554E 00	0.5625E-07	0.2375E-02	0.2149E 00	-0.1443E-07
29 TO 35	0.2376E-02	-0.1615E 00	0.4275E-07	0.1465E-02	0.4020E-01	-0.1372E-07	0.1465E-02
36 TO 42	-0.5598E-01	0.7713E-07	0.1402E-05	0.9983E 00	-0.7657E-02	0.6651E-09	-0.6223E-07
43 TO 49	0.1400E-05	-0.1000E 01	-0.7657E-02	0.4986E-09	0.3135E-07	0.1401E-05	0.4470E 00
50 TO 56	-0.7657E-02	0.5759E-09	-0.2760E-07	0.1400E-05	-0.4487E 00	-0.7656E-02	0.4686E-09
57 TO 63	0.3523E-07	0.1509E-07	-0.9196E-02	0.7914E-04	-0.6373E-10	-0.3724E-07	0.9599E-09
64 TO 70	0.4953E-02	0.1040E-04	-0.8724E-10	0.3129E-07	0.1499E-07	-0.3931E-02	0.5909E-04
71 TO 77	0.2543E-09	-0.3359E-07	0.1252E-07	0.2414E-02	0.3507E-04	0.2977E-09	0.1353E-09
78 TO 84	0.1401E-05	-0.9101E-03	-0.7655E-02	-0.2199E-05	0.4959E-09	0.1552E-07	-0.2901E-01
85 TO 91	0.9558E-04	0.1678E-12	-0.1896E-09	-0.3069E-04	0.1679E-12	-0.1994E-09	0.6997E-11
92 TO 98	0.1492E-07	-0.1961E-03	0.5377E-04	0.5960E-05	0.8681E-09	0.9796E-10	0.1611E-05
99 TO 105	-0.1409E-02	-0.5729E-02	-0.1554E-05	-0.3523E-08	0.3999E-10	0.1295E-05	-0.1273E-02
106 TO 112	-0.1874E-02	0.2675E-05	0.7305E-08	0.6570E-10	0.2542E-05	-0.1624E-02	-0.3802E-02
113 TO 114	0.1237E-06	0.3264E-11					

IMAGINARY PART

1 TO 7	-0.4054E-05	0.6405E-06	0.0	-0.3682E-05	0.2919E-05	0.0	-0.3341E-05
8 TO 14	0.7344E-06	0.0	-0.3341E-05	0.1835E-05	0.0	-0.3753E-05	-0.1433E-05
15 TO 21	0.0	-0.3069E-05	0.3028E-05	0.0	-0.3575E-05	-0.1996E-06	0.0
22 TO 28	-0.3574E-05	0.1214E-05	0.0	-0.3077E-05	-0.2447E-05	0.0	-0.3077E-05
29 TO 35	0.3386E-05	0.0	-0.1898E-05	-0.7097E-06	0.0	-0.1898E-05	0.1991E-05
36 TO 42	0.0	-0.4136E-09	0.7347E-11	0.0	0.0	-0.1334E-11	-0.4241E-09
43 TO 49	0.8266E-11	0.0	0.0	0.1862E-11	-0.3061E-09	0.7923E-11	0.0
50 TO 56	0.0	-0.9439E-12	-0.3107E-09	0.8173E-11	0.0	0.0	0.9964E-12
57 TO 63	0.6372E-09	0.2694E-11	0.0	0.0	0.3017E-11	0.6506E-09	-0.1327E-12
64 TO 70	0.0	0.0	-0.3115E-11	0.2691E-09	0.1719E-11	0.0	0.0
71 TO 77	0.6733E-11	0.2729E-09	0.5421E-12	0.0	0.0	-0.6955E-11	-0.2799E-09
78 TO 84	0.8055E-11	0.0	0.0	0.0	0.4570E-13	0.3734E-11	0.0
85 TO 91	0.0	0.0	-0.5516E-11	0.0	0.0	0.5650E-11	-0.1165E-10
92 TO 98	0.1099E-11	0.0	0.0	0.0	0.4829E-14	-0.2583E-09	0.1763E-11
99 TO 105	0.0	0.0	0.0	0.1199E-13	-0.1254E-08	0.5517E-12	0.0
105 TO 112	0.0	0.0	-0.3372E-14	-0.2200E-09	0.2894E-12	0.0	0.0
113 TO 114	0.0	0.1469E-20					

EIGENVECTOR FOR ROOT NO.= 11

Mode 11, Frequency = 0.6969 Hz, Ω = 4 RPM

EIGENVALUE= 0.43796711E 01 (rad/sec.)

REAL PART							
1 TO 7	0.3049E-03	0.1204E 00	0.1903E 00	-0.3139E-03	0.2930E-01	0.2004E 00	0.1361E-03
8 TO 14	0.3029E-01	-0.1026E 00	-0.1367E-03	0.2139E-01	-0.1702E 00	0.4326E-03	0.1000E 01
15 TO 21	0.4049E 00	-0.4473E-03	0.4926E 00	0.4534E 00	0.2065E-03	0.4287E 00	-0.3195E 00
22 TO 28	-0.2097E-03	0.3830E 00	-0.4554E 00	0.1371E-03	-0.2630E 00	-0.3472E 00	-0.2015E-03
29 TO 35	-0.4740E 00	-0.3962E 00	0.7557E-04	-0.4079E 00	0.3461E 00	-0.7559E-04	-0.3653E 00
36 TO 42	0.4754E 00	0.5765E-03	0.2335E-02	-0.2425E-04	-0.3952E-09	0.3845E-05	-0.5974E-03
43 TO 49	0.2323E-02	-0.9733E-05	0.6550E-07	0.4136E-05	0.2950E-03	0.2328E-02	-0.2333E-04
50 TO 56	0.3943E-07	0.4453E-05	-0.2888E-03	0.2323E-02	-0.1477E-04	0.7840E-07	0.4587E-05
57 TO 63	0.8410E-04	-0.1280E-04	-0.2301E-05	0.4373E-07	0.3097E-06	-0.8372E-04	-0.8341E-05
64 TO 70	0.7614E-06	0.3707E-08	0.8159E-06	0.1268E-04	-0.1305E-04	0.8463E-06	0.2774E-07
71 TO 77	0.8294E-06	-0.1216E-04	-0.1074E-04	0.5617E-06	-0.6400E-08	0.8222E-06	-0.8541E-07
78 TO 84	0.2324E-02	-0.1960E-04	0.8041E-07	0.2335E-06	0.5396E-05	-0.1156E-04	-0.4287E-05
85 TO 91	-0.9374E-08	0.2846E-11	-0.9338E-06	-0.6672E-09	0.2845E-11	-0.9340E-06	-0.4514E-09
92 TO 98	-0.1259E-04	0.1271E-05	-0.7687E-08	-0.5353E-07	-0.5967E-06	-0.6987E-07	-0.8094E-05
99 TO 105	0.3404E-04	0.5345E-07	0.1720E-06	0.1036E-04	-0.2778E-07	-0.1327E-02	0.3546E-04
106 TO 112	0.1112E-07	-0.1548E-06	-0.6541E-05	-0.5100E-07	-0.2023E-02	0.5778E-04	0.3072E-07
113 TO 114	0.1440E-09	0.2824E-05					
IMAGINARY PART							
1 TO 7	-0.2449E-03	-0.1719E-02	0.0	-0.9969E-04	0.1839E-02	0.0	-0.9718E-04
8 TO 14	-0.8964E-03	0.0	-0.8111E-04	0.2356E-03	0.0	-0.8519E-03	0.1415E-02
15 TO 21	0.0	-0.4203E-03	-0.1420E-02	0.0	-0.3770E-03	0.4385E-03	0.0
22 TO 28	-0.3339E-03	-0.6096E-03	0.0	0.5315E-03	-0.3597E-02	0.0	0.2621E-03
29 TO 35	0.3647E-02	0.0	0.2254E-03	-0.1522E-02	0.0	0.2019E-03	0.1702E-02
36 TO 42	0.0	-0.5708E-05	-0.5670E-05	0.0	0.0	-0.6261E-07	-0.4303E-05
43 TO 49	-0.5699E-05	0.0	0.0	0.5499E-07	-0.1654E-05	-0.5675E-05	0.0
50 TO 56	0.0	-0.4360E-07	-0.8931E-06	-0.5593E-05	0.0	0.0	0.3243E-07
57 TO 63	0.4096E-05	-0.9479E-08	0.0	0.0	0.2727E-07	0.2709E-05	0.1642E-08
64 TO 70	0.0	0.0	-0.1519E-07	0.1399E-05	-0.7054E-08	0.0	0.0
71 TO 77	0.3768E-07	0.1071E-05	-0.1994E-09	0.0	0.0	-0.2589E-07	-0.2717E-09
78 TO 84	-0.5678E-05	0.0	0.0	0.0	-0.7445E-08	-0.1161E-07	0.0
85 TO 91	0.0	0.0	-0.3940E-07	0.0	0.0	0.2462E-07	0.8319E-07
92 TO 98	-0.4133E-09	0.0	0.0	0.0	0.1778E-10	0.3510E-06	-0.2312E-05
99 TO 105	0.0	0.0	0.0	-0.1525E-07	0.3439E-06	-0.1045E-05	0.0
106 TO 112	0.0	0.0	0.2295E-09	0.6139E-06	0.7330E-07	0.0	0.0
113 TO 114	0.0	-0.1404E-10					

EIGENVECTOR FOR ROOT NO.= 17

Mode 17, Frequency = 0.7777 Hz, Ω = 4 RPM

EIGENVALUE= 0.48864746E 01 (rad/sec.)

REAL PART

1	TO	7	-0.2457E-05	-0.7500E-03	0.7159E-01	0.3631E-05	0.2267E-01	0.1268E-21	-0.9105E-06
8	TO	14	-0.4297E-01	-0.1660E-01	0.1872E-05	0.1980E-01	0.3337E-01	-0.4156E-05	0.3019E-01
15	TO	21	0.9227E 00	0.4771E-05	-0.1805E-01	0.7425E 00	-0.1824E-05	0.1105E 00	0.9753E 00
22	TO	28	0.2413E-05	-0.1106E-01	0.2665E 00	-0.8560E-05	0.6022E-03	-0.9513E 00	0.1489E-05
29	TO	35	0.4575E-01	-0.7580E 00	-0.1733E-06	-0.7448E-01	-0.1000E 01	0.6936E-05	0.3929E-01
36	TO	42	-0.9673E 00	-0.5366E-05	-0.8707E-05	-0.2330E-01	0.1331E-04	-0.3679E-07	0.5251E-05
43	TO	49	-0.8797E-05	-0.1961E-01	0.1442E-04	-0.3469E-07	-0.2612E-05	-0.3761E-05	-0.2233E-01
50	TO	56	0.1366E-04	-0.4119E-07	0.2609E-05	-0.8787E-05	-0.2065E-01	0.1459E-04	-0.4064E-07
57	TO	63	0.4018E-06	0.1504E-06	0.1742E-02	-0.1501E-04	-0.3334E-03	-0.2134E-06	0.1029E-06
64	TO	70	-0.4896E-03	-0.1653E-05	-0.9736E-09	0.4797E-06	0.1500E-06	0.7565E-03	-0.1192E-04
71	TO	77	0.4179E-08	-0.2430E-06	0.1344E-06	-0.2426E-03	-0.5269E-05	0.7529E-09	0.1466E-08
78	TO	84	-0.8778E-05	-0.2151E-01	0.1444E-04	0.6864E-04	-0.4934E-07	0.1198E-06	0.5004E-02
85	TO	91	-0.1930E-04	0.2087E-11	-0.8580E-09	0.3900E-05	0.2087E-11	-0.8567E-09	0.9095E-10
92	TO	98	0.1602E-06	0.1670E-03	-0.8636E-05	-0.6150E-05	0.9529E-08	0.1100E-08	0.1236E-04
99	TO	105	-0.5316E-02	0.1046E-04	0.5577E-04	-0.3473E-07	0.4678E-03	0.1373E-04	0.3386E-02
106	TO	112	0.2584E-05	-0.1466E-04	0.7784E-07	0.7650E-09	0.2712E-04	0.4283E-02	0.6507E-05
113	TO	114	0.1567E-04	0.1060E-09					

IMAGINARY PART

1	TO	7	0.1639E-04	0.3785E-04	0.0	-0.9139E-05	0.4215E-04	0.0	0.6131E-04
8	TO	14	-0.6401E-05	0.0	-0.5049E-05	0.2912E-04	0.0	0.3225E-06	-0.1204E-03
15	TO	21	0.0	0.6131E-04	0.1093E-03	0.0	-0.1650E-04	0.6249E-05	0.0
22	TO	28	0.5719E-04	0.5390E-04	0.0	-0.5797E-06	0.1000E-03	0.0	-0.4422E-04
29	TO	35	-0.6862E-04	0.0	0.7196E-04	-0.1177E-04	0.0	-0.3797E-04	-0.3566E-04
36	TO	42	0.0	-0.4891E-08	-0.3594E-09	0.0	0.0	-0.1125E-10	-0.4316E-08
43	TO	49	-0.3918E-09	0.0	0.0	0.5941E-11	-0.4077E-08	-0.3710E-09	0.0
50	TO	56	0.0	-0.1105E-10	-0.3968E-08	-0.3969E-09	0.0	0.0	0.5947E-11
57	TO	63	0.7527E-09	-0.4704E-10	0.0	0.0	-0.3218E-11	0.1168E-08	0.1723E-10
64	TO	70	0.0	0.0	0.9932E-12	0.5416E-09	-0.3776E-10	0.0	0.0
71	TO	77	0.1539E-10	0.7151E-09	0.1924E-11	0.0	0.0	-0.1899E-10	-0.3617E-08
78	TO	84	-0.3791E-09	0.0	0.0	0.0	-0.1602E-11	-0.4275E-10	0.0
85	TO	91	0.0	0.0	-0.3118E-11	0.0	0.0	0.6933E-11	-0.3342E-09
92	TO	98	-0.2270E-10	0.0	0.0	0.0	-0.9993E-12	-0.3734E-09	-0.2034E-09
99	TO	105	0.0	0.0	0.0	-0.8038E-13	-0.2161E-08	-0.1723E-09	0.0
106	TO	112	0.0	0.0	-0.3436E-12	-0.3497E-08	-0.2212E-09	0.0	0.0
113	TO	114	0.0	0.9588E-14					

EIGENVECTOR FOR ROOT NO.= 18

Mode 18, Frequency = 0.7911 Hz, Ω = 4 RPM

EIGENVALUE= 0.49705811E 01 (rad/sec)

REAL PART							
1 TO 7	-0.1537E-05	-0.1048E-01	-0.4999E-01	0.2044E-05	-0.4822E-02	0.7488E-01	-0.6194E-06
8 TO 14	-0.5113E-04	-0.2211E-01	0.1011E-05	-0.1970E-01	-0.9530E-01	-0.2637E-05	0.2594E-01
15 TO 21	-0.8924E 00	0.2918E-05	0.1812E-01	0.9343E 00	-0.1205E-05	0.1097E-01	-0.2720E 00
22 TO 28	0.1445E-05	-0.1870E-01	0.7499E 00	-0.6498E-06	-0.1063E-01	0.1000E 01	0.8821E-06
29 TO 35	-0.3661E-02	-0.9491E 00	-0.1918E-06	0.2641E-02	0.3459E 00	0.3653E-06	0.2907E-01
36 TO 42	-0.7533E 00	-0.3732E-05	-0.2217E-05	-0.3355E-01	0.2558E-03	-0.2544E-07	0.3677E-05
43 TO 49	-0.2181E-05	0.3313E-01	0.2551E-03	-0.2459E-07	-0.1823E-05	-0.2195E-05	-0.1514E-01
50 TO 56	0.2556E-03	-0.2868E-07	0.1816E-05	-0.2191E-05	0.1476E-01	0.2554E-03	-0.2833E-07
57 TO 63	0.2487E-06	0.1453E-06	-0.1449E-02	0.1306E-04	-0.1140E-09	-0.2196E-06	0.9341E-07
64 TO 70	0.5654E-03	0.1272E-05	-0.7809E-09	0.2664E-06	0.1474E-06	-0.5903E-03	0.1072E-04
71 TO 77	0.1591E-08	-0.2300E-06	0.1216E-06	0.3471E-03	0.4905E-05	0.1065E-08	0.1110E-08
78 TO 84	-0.2185E-05	-0.1934E-03	0.2555E-03	-0.1483E-06	-0.3449E-07	0.1383E-06	-0.5131E-02
85 TO 91	0.1663E-04	0.9484E-12	-0.9934E-09	-0.4191E-05	0.9484E-12	-0.9911E-09	0.5635E-10
92 TO 98	0.1446E-06	-0.3381E-04	0.8113E-05	0.1095E-05	0.8221E-08	0.8330E-09	0.1281E-04
99 TO 105	-0.2254E-03	0.1241E-03	-0.7423E-07	-0.6704E-07	0.3300E-09	0.1283E-04	-0.1823E-03
106 TO 112	0.7005E-04	0.3010E-06	0.6668E-07	0.5629E-08	0.2325E-04	-0.2255E-03	0.1322E-03
113 TO 114	0.7293E-07	0.1110E-09					
IMAGINARY PART							
1 TO 7	0.1433E-04	0.1637E-04	0.0	0.8437E-05	0.1698E-04	0.0	0.3363E-05
8 TO 14	-0.2262E-05	0.0	-0.1763E-04	0.1287E-04	0.0	0.8796E-06	-0.1608E-05
15 TO 21	0.0	0.5359E-05	0.4923E-05	0.0	0.9371E-05	0.1965E-04	0.0
22 TO 28	0.2636E-04	0.1500E-05	0.0	0.1107E-04	0.5482E-05	0.0	0.3812E-05
29 TO 35	0.1605E-06	0.0	-0.2756E-05	-0.1572E-04	0.0	-0.3030E-04	0.7775E-07
36 TO 42	0.0	-0.3593E-08	-0.1634E-09	0.0	0.0	0.3025E-11	-0.3010E-09
43 TO 49	-0.1633E-09	0.0	0.0	-0.9151E-11	-0.3770E-08	-0.1696E-09	0.0
50 TO 56	0.0	0.1260E-11	-0.3576E-08	-0.1649E-09	0.0	0.0	-0.5346E-11
57 TO 63	-0.2260E-09	-0.2633E-10	0.0	0.0	-0.1607E-10	-0.1899E-08	0.2735E-11
64 TO 70	0.0	0.0	0.1407E-10	-0.8272E-09	-0.2267E-10	0.0	0.0
71 TO 77	-0.1605E-10	-0.5764E-09	-0.2927E-11	0.0	0.0	0.1278E-10	-0.3773E-08
78 TO 84	-0.1538E-09	0.0	0.0	0.0	-0.1419E-11	-0.2230E-10	0.0
85 TO 91	0.0	0.0	0.2225E-10	0.0	0.0	-0.1902E-10	-0.3705E-09
92 TO 98	-0.1394E-10	0.0	0.0	0.0	-0.7339E-12	-0.3880E-08	-0.3161E-11
99 TO 105	0.0	0.0	0.0	-0.7930E-13	-0.2165E-09	-0.1147E-10	0.0
106 TO 112	0.0	0.0	0.1705E-12	-0.3542E-08	-0.1308E-10	0.0	0.0
113 TO 114	0.0	0.2527E-14					

EIGENVECTOR FOR ROOT NO.= 19

Mode 19, Frequency = 0.9049 Hz, Ω = 4 RPM

EIGENVALUE= 0.56854958E 01 (rad./sec.)

REAL PART

1 TO 7	0.1901E-07	-0.2932E-02	0.6762E 00	0.8593E-08	-0.2176E-03	-0.5878E-01	0.9775E-09
8 TO 14	-0.9271E-04	-0.9142E 00	0.1069E-07	-0.8278E-04	-0.5480E-01	0.2914E-07	0.1677E-02
15 TO 21	-0.1167E 00	-0.9381E-09	0.3601E-03	0.5855E-01	0.1389E-07	0.2791E-04	-0.4394E-01
22 TO 28	-0.1608E-09	0.2793E-04	0.2368E-01	-0.1090E-08	-0.7129E-04	-0.5136E 00	0.1348E-07
29 TO 35	-0.7139E-04	-0.2090E-01	-0.3533E-08	0.2142E-03	0.1000E 01	0.1292E-07	0.2143E-03
36 TO 42	0.1769E-02	0.3413E-07	-0.4986E-06	-0.2771E-02	-0.7305E-05	0.2194E-09	-0.3287E-07
43 TO 49	-0.4951E-06	-0.4669E-02	-0.7232E-05	0.2050E-09	0.1731E-07	-0.4963E-06	-0.3296E-02
50 TO 56	-0.7295E-05	0.2619E-09	-0.1701E-07	-0.4951E-06	-0.4148E-02	-0.7254E-05	0.2514E-09
57 TO 63	-0.2213E-07	-0.8477E-08	0.5396E-02	-0.5030E-04	0.1819E-11	0.2271E-07	-0.5404E-09
64 TO 70	-0.1880E-02	-0.4082E-05	0.9428E-11	-0.1738E-07	-0.8405E-08	0.2162E-02	-0.3956E-04
71 TO 77	-0.1598E-09	0.1814E-07	-0.7027E-08	-0.1160E-02	-0.1640E-04	-0.1708E-10	-0.3433E-10
78 TO 84	-0.4955E-06	-0.3723E-02	-0.7281E-05	0.1168E-04	0.3433E-09	-0.8690E-08	0.2025E-01
85 TO 91	-0.6927E-04	0.5011E-13	0.1383E-09	0.1386E-04	0.5011E-13	0.1380E-09	-0.1578E-11
92 TO 98	-0.8341E-08	0.1461E-03	-0.2858E-04	-0.4457E-05	-0.4738E-09	-0.2806E-10	-0.7741E-06
99 TO 105	-0.9361E-03	-0.1199E-04	0.9797E-05	0.1382E-08	-0.9993E-11	-0.6595E-06	0.9528E-03
106 TO 112	-0.2148E-04	-0.1936E-05	-0.3403E-08	-0.2056E-10	-0.1190E-05	0.8611E-03	-0.1673E-04
113 TO 114	0.3687E-05	0.2230E-10					

IMAGINARY PART

1 TO 7	0.2049E-05	-0.1432E-05	0.0	0.8539E-07	0.5488E-06	0.0	0.5534E-07
8 TO 14	0.1400E-07	0.0	0.6538E-07	0.3600E-06	0.0	-0.1088E-05	0.8293E-06
15 TO 21	0.0	-0.2575E-06	0.3071E-06	0.0	0.7574E-07	-0.1106E-05	0.0
22 TO 28	0.7573E-07	0.1309E-06	0.0	0.3246E-07	0.3691E-06	0.0	0.3249E-07
29 TO 35	-0.1148E-06	0.0	-0.9617E-07	0.4331E-06	0.0	-0.9619E-07	0.2303E-07
36 TO 42	0.0	0.1028E-08	0.1823E-10	0.0	0.0	0.6512E-11	0.1056E-08
43 TO 49	0.1825E-10	0.0	0.0	-0.7213E-11	0.6134E-09	0.1841E-10	0.0
50 TO 56	0.0	0.4221E-11	0.6070E-09	0.1839E-10	0.0	0.0	-0.4318E-11
57 TO 63	0.3485E-09	-0.1187E-11	0.0	0.0	0.1839E-11	0.3221E-09	0.1470E-11
64 TO 70	0.0	0.0	-0.1593E-11	0.1517E-09	-0.3716E-12	0.0	0.0
71 TO 77	0.3019E-11	0.1412E-09	0.8566E-12	0.0	0.0	-0.2781E-11	0.4702E-09
78 TO 84	0.1843E-10	0.0	0.0	0.0	0.1030E-12	-0.5313E-12	0.0
85 TO 91	0.0	0.0	-0.3112E-11	0.0	0.0	0.2869E-11	0.3812E-10
92 TO 98	0.3266E-12	0.0	0.0	0.0	0.4107E-13	0.4300E-09	0.4134E-11
99 TO 105	0.0	0.0	0.0	0.8395E-14	0.7160E-09	0.2514E-11	0.0
106 TO 112	0.0	0.0	0.1037E-13	0.3715E-09	0.7293E-11	0.0	0.0
113 TO 114	0.0	0.3785E-15					

EIGENVECTOR FOR ROOT NO.= 20

Mode 20, Frequency = 0.9291 Hz, Ω = 4 RPM

EIGENVALUE= 0.58375244E 01 (rad/sec.)

REAL PART

1	TO	7	-0.3302E-03	0.1200E 01	0.4846E-01	0.3280E-03	0.6205E 00	-0.6421E-01	-0.1456E-03
8	TO	14	0.2506E 00	-0.2579E 00	0.1495E-03	0.4274E 00	-0.2750E-01	-0.5365E-03	-0.6696E 00
15	TO	21	0.2266E-01	0.5236E-03	-0.1030E 00	0.3100E-01	-0.2532E-03	0.8703E-01	0.3993E-02
22	TO	28	0.2540E-03	0.8473E-01	0.3120E-01	-0.1437E-03	-0.2877E 00	-0.6194E-01	0.1457E-03
29	TO	35	-0.2879E 00	0.2564E-01	-0.4837E-04	-0.1471E 00	0.2039E 00	0.5431E-04	-0.2561E 00
36	TO	42	-0.1125E-01	-0.7441E-03	0.6414E-03	-0.7821E-04	-0.5426E-08	-0.5125E-05	0.7298E-03
43	TO	49	0.6564E-03	-0.7835E-04	-0.4911E-08	-0.4932E-05	-0.3510E-03	0.6512E-03	-0.7851E-04
50	TO	56	-0.2140E-08	-0.5712E-05	0.3584E-03	0.6564E-03	-0.7819E-04	0.2263E-08	-0.5611E-05
57	TO	63	0.4893E-04	0.2785E-04	-0.1593E-04	0.1920E-06	-0.2004E-06	-0.4267E-04	0.1770E-04
64	TO	70	0.1329E-05	0.5278E-08	-0.1230E-06	0.5081E-04	0.2758E-04	-0.2214E-05	0.1343E-06
71	TO	77	0.3208E-06	-0.4238E-04	0.2301E-04	0.1110E-05	-0.8774E-08	0.2074E-06	0.1975E-05
78	TO	84	0.6547E-03	-0.7846E-04	0.4107E-08	0.4900E-06	-0.6792E-05	0.2860E-04	-0.3596E-04
85	TO	91	0.3065E-07	0.3970E-11	-0.2074E-06	-0.1138E-07	0.3870E-11	-0.2075E-06	0.1099E-07
92	TO	98	0.2731E-04	0.1555E-05	0.1120E-07	-0.6438E-07	0.1542E-05	0.1600E-06	0.3502E-02
99	TO	105	0.3466E-04	0.2556E-07	0.3628E-06	-0.1215E-04	0.6645E-07	0.2539E-02	0.4578E-04
106	TO	112	0.6149E-07	-0.2322E-06	0.1416E-04	0.1216E-06	0.5115E-02	0.8494E-04	0.4489E-07
113	TO	114	0.2628E-09	0.2386E-05					

IMAGINARY PART

1	TO	7	-0.7737E-03	0.3483E-02	0.0	-0.6296E-03	-0.3614E-02	0.0	-0.3223E-03
8	TO	14	0.1553E-02	0.0	-0.5094E-03	-0.1933E-02	0.0	0.3306E-03	-0.3071E-03
15	TO	21	0.0	-0.7958E-04	0.4515E-03	0.0	-0.1463E-03	-0.2754E-03	0.0
22	TO	28	-0.2030E-03	0.2673E-03	0.0	-0.1735E-04	-0.1075E-02	0.0	-0.1720E-04
29	TO	35	0.1100E-02	0.0	-0.9438E-05	-0.3047E-03	0.0	-0.1448E-04	0.5276E-03
36	TO	42	0.0	-0.3765E-05	-0.3111E-07	0.0	0.0	-0.1346E-07	-0.3414E-05
43	TO	49	-0.7401E-07	0.0	0.0	0.8578E-09	-0.2925E-05	-0.8607E-07	0.0
50	TO	56	0.0	-0.8173E-09	-0.2851E-05	-0.7916E-07	0.0	0.0	0.6003E-08
57	TO	63	-0.1694E-05	-0.6596E-08	0.0	0.0	-0.9858E-08	-0.1591E-05	-0.2135E-08
64	TO	70	0.0	0.0	0.9309E-09	-0.7095E-06	-0.6291E-08	0.0	0.0
71	TO	77	-0.1364E-07	-0.6546E-06	-0.3127E-09	0.0	0.0	0.1270E-07	-0.2652E-05
78	TO	84	-0.9262E-07	0.0	0.0	0.0	-0.3912E-09	-0.8024E-08	0.0
85	TO	91	0.0	0.0	0.1559E-07	0.0	0.0	-0.1468E-07	-0.2345E-06
92	TO	98	-0.4831E-08	0.0	0.0	0.0	-0.2490E-09	-0.2606E-05	-0.2806E-07
99	TO	105	0.0	0.0	0.0	-0.8216E-10	-0.1350E-05	-0.2244E-07	0.0
106	TO	112	0.0	0.0	0.7110E-11	-0.2348E-05	-0.2244E-07	0.0	0.0
113	TO	114	0.0	0.1913E-11					

EIGENVECTOR FOR ROOT NO.= 28 Mode 28, Frequency = 1.051 Hz, Ω = 4 RPM

EIGENVALUE= 0.66011696E 01 (rad/sec.)

REAL PART

1 TO 7	0.1188E-01	-0.1000E 01	-0.2027E-01	-0.1167E-01	-0.9983E 00	-0.3753E-01	0.5562E-02
8 TO 14	-0.9996E 00	-0.2431E-01	-0.5536E-02	-0.9989E 00	-0.3030E-01	0.1651E-01	0.8979E 00
15 TO 21	0.2146E-01	-0.1605E-01	0.8970E 00	0.3314E-01	0.7774E-02	0.3375E 00	0.2486E-01
22 TO 28	-0.7770E-02	0.8971E 00	0.3013E-01	0.6909E-02	0.2784E 00	0.1322E-01	-0.6954E-02
29 TO 35	0.2781E 00	0.2314E-01	0.3172E-02	0.2732E 00	0.1992E-01	-0.3433E-02	0.2736E 00
36 TO 42	0.2210E-01	0.2077E-01	0.1943E 00	-0.1971E-03	0.9071E-07	0.1433E-03	-0.2006E-01
43 TO 49	0.1960E 00	-0.1654E-03	0.7819E-07	0.1391E-03	0.9815E-02	0.1353E 00	-0.1826E-03
50 TO 56	0.8831E-07	0.1590E-03	-0.9632E-02	0.1869E 00	-0.1710E-03	0.7633E-07	0.1544E-03
57 TO 63	0.1805E-02	0.2401E-03	0.3274E-04	-0.2810E-06	0.1093E-04	-0.2127E-02	0.1297E-03
64 TO 70	-0.6294E-05	-0.2760E-07	0.7112E-05	0.7249E-03	0.2182E-03	0.1431E-04	-0.2157E-06
71 TO 77	0.1477E-04	-0.1106E-02	0.1634E-03	-0.2377E-05	-0.8354E-07	0.2723E-04	0.1655E-05
78 TO 84	0.1869E 00	-0.1756E-03	0.8001E-07	0.1084E-05	0.1799E-03	0.3140E-03	0.1043E-03
85 TO 91	-0.3125E-05	0.6652E-11	-0.1691E-04	0.5343E-07	0.6652E-11	-0.1432E-04	0.7463E-07
92 TO 98	0.2008E-03	0.4094E-05	-0.1302E-06	-0.1587E-06	0.1133E-04	0.1237E-05	0.1193E 00
99 TO 105	0.7419E-06	0.7972E-07	0.9002E-06	0.2880E-03	0.4470E-06	0.1273E-01	0.9972E-04
106 TO 112	0.5525E-07	-0.4981E-06	0.1172E-03	0.9130E-06	0.5712E-01	0.1347E-03	0.7073E-07
113 TO 114	0.3731E-09	0.2141E-03					

IMAGINARY PART

1 TO 7	0.2507E-03	-0.6135E-02	0.0	0.2532E-03	0.6133E-02	0.0	0.3455E-03
8 TO 14	-0.3214E-02	0.0	0.3462E-03	0.3247E-02	0.0	-0.1216E-02	0.3706E-02
15 TO 21	0.0	-0.1202E-02	-0.3762E-02	0.0	-0.1073E-02	0.1372E-02	0.0
22 TO 28	-0.1072E-02	-0.1951E-02	0.0	-0.3325E-03	0.4052E-02	0.0	-0.3993E-03
29 TO 35	-0.4004E-02	0.0	-0.3433E-03	0.2457E-02	0.0	-0.3395E-03	-0.2333E-02
36 TO 42	0.0	-0.2979E-03	-0.3327E-05	0.0	0.0	-0.2526E-05	-0.2936E-03
43 TO 49	-0.3693E-05	0.0	0.0	0.2555E-05	-0.1235E-03	-0.3433E-05	0.0
50 TO 56	0.0	-0.1633E-05	-0.1224E-03	-0.3581E-05	0.0	0.0	0.1626E-05
57 TO 63	-0.1552E-04	0.8410E-07	0.0	0.0	-0.3947E-07	-0.1426E-04	-0.1511E-06
64 TO 70	0.0	0.0	0.9135E-07	-0.6873E-05	0.2077E-07	0.0	0.0
71 TO 77	-0.1140E-06	-0.6322E-05	-0.8753E-07	0.0	0.0	0.1027E-06	-0.6961E-04
78 TO 84	-0.3509E-05	0.0	0.0	0.0	-0.7505E-08	0.1255E-07	0.0
85 TO 91	0.0	0.0	0.1419E-06	0.0	0.0	-0.1307E-06	-0.3054E-05
92 TO 98	-0.3446E-07	0.0	0.0	0.0	-0.3071E-08	-0.5761E-04	-0.1733E-05
99 TO 105	0.0	0.0	0.0	-0.3532E-08	-0.1973E-04	-0.1536E-05	0.0
106 TO 112	0.0	0.0	-0.4924E-08	-0.3393E-04	-0.1820E-05	0.0	0.0
113 TO 114	0.0	0.1510E-03					

EIGENVECTOR FOR ROOT NO.= 32

Mode 32, Frequency = 3.841 Hz, Ω =4RPM

EIGENVALUE= 0.24135910E 02 (rad/sec.)

REAL PART								
1	TO 7	0.9977E 00	0.5596E-02	0.4274E-02	0.9985E 00	0.5797E-02	0.4283E-02	0.3553E 00
8	TO 14	0.4765E-02	0.4276E-02	0.3545E 00	0.4845E-02	0.4280E-02	0.9414E 00	0.5596E-02
15	TO 21	0.4724E-02	0.8412E 00	0.5940E-02	0.4477E-02	0.3047E 00	0.4949E-02	0.4658E-02
22	TO 28	0.3043E 00	0.5099E-02	0.4547E-02	0.8573E 00	0.5959E-02	0.4625E-02	0.8685E 00
29	TO 35	0.6052E-02	0.4634E-02	0.3035E 00	0.5091E-02	0.4628E-02	0.3023E 00	0.5123E-02
36	TO 42	0.4632E-02	0.4808E 00	0.8072E-03	-0.1976E-03	0.8096E-06	0.4794E-02	0.4790E 00
43	TO 49	0.7961E-03	-0.9170E-04	0.4412E-04	-0.4742E-02	0.1799E 00	0.7986E-03	-0.1436E-03
50	TO 56	0.6427E-05	0.2955E-02	0.1797E 00	0.7964E-03	-0.1190E-03	0.1904E-06	-0.2945E-02
57	TO 63	0.6654E 00	0.1530E-03	0.5401E-04	-0.2640E-07	0.4449E-02	0.6641E 00	0.6072E-04
64	TO 70	0.5433E-04	-0.5658E-07	-0.4441E-02	0.2256E 00	0.1269E-03	0.5019E-04	-0.4151E-07
71	TO 77	0.6155E-02	0.2250E 00	0.9547E-04	0.5408E-04	0.4649E-07	-0.6142E-02	0.8338E-01
78	TO 84	0.7972E-03	-0.1163E-03	0.2480E-06	0.7128E-05	-0.6658E-06	0.2616E-03	0.6688E-05
85	TO 91	0.3164E-06	0.1814E-09	-0.6409E-02	-0.3135E-06	0.1914E-09	0.6398E-02	0.1037E-01
92	TO 98	0.1057E-03	0.5092E-04	0.4954E-07	-0.2215E-05	0.4271E-05	0.6553E-01	0.1359E-02
99	TO 105	0.1318E-02	0.5926E-07	0.2758E-05	-0.3666E-05	0.2895E-01	0.1261E-02	0.1271E-02
106	TO 112	0.1222E-05	-0.3542E-05	0.4800E-05	0.4736E-01	0.2079E-02	0.1421E-02	0.9960E-07
113	TO 114	0.7936E-07	0.1569E-07					
IMAGINARY PART								
1	TO 7	0.4691E-01	-0.2316E-01	0.0	0.5509E-01	-0.2312E-01	0.0	0.1753E-01
8	TO 14	-0.8190E-02	0.0	0.2032E-01	-0.3158E-02	0.0	0.3564E-01	-0.1892E-01
15	TO 21	0.0	0.5019E-01	-0.1871E-01	0.0	0.1294E-01	-0.6707E-02	0.0
22	TO 28	0.1030E-01	-0.6626E-02	0.0	0.4589E-01	-0.2261E-01	0.0	0.4555E-01
29	TO 35	-0.2247E-01	0.0	0.1759E-01	-0.7855E-02	0.0	0.1688E-01	-0.7816E-02
36	TO 42	0.0	0.1634E-01	-0.1390E-01	0.0	0.0	0.1836E-03	0.3333E-01
43	TO 49	-0.1302E-01	0.0	0.0	-0.3111E-03	0.5430E-02	-0.1392E-01	0.0
50	TO 56	0.0	0.9735E-04	0.1316E-01	-0.1392E-01	0.0	0.0	-0.2180E-03
57	TO 63	0.3634E-01	0.1062E-02	0.0	0.0	0.2356E-03	0.3221E-01	0.6837E-03
64	TO 70	0.0	0.0	-0.2216E-03	0.1282E-01	0.9154E-03	0.0	0.0
71	TO 77	0.3350E-03	0.1049E-01	0.7456E-03	0.0	0.0	-0.3001E-03	0.4309E-02
78	TO 84	-0.1392E-01	0.0	0.0	0.0	-0.6678E-04	0.1061E-02	0.0
85	TO 91	0.0	0.0	-0.3467E-03	0.0	0.0	0.3134E-03	0.5346E-03
92	TO 98	0.7919E-03	0.0	0.0	0.0	0.2222E-04	0.3383E-02	-0.1025E-03
99	TO 105	0.0	0.0	0.0	-0.2477E-04	0.1492E-02	0.2642E-02	0.0
106	TO 112	0.0	0.0	-0.7908E-05	0.2443E-02	0.7906E-06	0.0	0.0
113	TO 114	0.0	0.4629E-12					

EIGENVECTOR FOR ROOT NO.= 1 Mode 1. Frequency = 0.1787 Hz, Ω = 8 RPM

EIGENVALUE= 0.11227112E 01 (rad/sec.)

REAL PART							
1 TO 7	0.1154E-06	0.2978E-02	-0.4598E 00	-0.1376E-07	0.2978E-02	0.9604E 00	0.7224E-07
8 TO 14	0.2978E-02	-0.4296E 00	-0.1730E-08	0.2978E-02	0.4313E 00	0.1030E-06	0.1837E-02
15 TO 21	-0.1000E 01	-0.3138E-07	0.1337E-02	0.9997E 00	0.5594E-07	0.1837E-02	-0.4481E 00
22 TO 28	-0.1127E-07	0.1637E-02	0.4484E 00	0.6980E-07	0.1254E-02	-0.3953E 00	-0.2585E-07
29 TO 35	0.1254E-02	0.3949E 00	0.4543E-07	0.1254E-02	-0.1769E 00	-0.1901E-07	0.1254E-02
36 TO 42	0.1775E 00	0.6424E-07	0.1228E-05	-0.5851E 00	0.4481E-02	0.5361E-09	-0.5344E-07
43 TO 49	0.1292E-05	0.5846E 00	0.4481E-02	0.3909E-09	0.2696E-07	0.1291E-05	-0.2624E 00
50 TO 56	0.4481E-02	0.4931E-09	-0.2476E-07	0.1292E-05	0.2619E 00	0.4482E-02	0.4136E-09
57 TO 63	0.3380E-07	0.1442E-07	-0.1752E-02	0.1414E-04	-0.6723E-10	-0.3487E-07	0.9176E-08
64 TO 70	0.8438E-03	0.2102E-05	-0.5131E-10	0.3023E-07	0.1428E-07	-0.7548E-03	0.1329E-04
71 TO 77	0.2502E-09	-0.3160E-07	0.1193E-07	0.5123E-03	0.7249E-05	0.2699E-09	0.1354E-09
78 TO 84	0.1291E-05	-0.2511E-03	0.4491E-02	0.4556E-06	0.4375E-09	0.1481E-07	-0.5141E-02
85 TO 91	0.1425E-04	0.1629E-12	-0.1739E-09	-0.6389E-05	0.1829E-12	-0.1788E-09	0.6929E-11
92 TO 98	0.1416E-07	-0.3044E-04	0.1124E-04	0.8842E-06	0.8193E-09	0.9758E-10	0.1505E-05
99 TO 105	-0.1534E-03	0.3364E-02	0.2516E-06	-0.3384E-08	0.4001E-10	0.1213E-05	-0.1258E-03
106 TO 112	0.1129E-02	0.6922E-07	0.6579E-08	0.6527E-10	0.2395E-05	-0.1281E-03	0.2247E-02
113 TO 114	0.1884E-08	0.3355E-11					
IMAGINARY PART							
1 TO 7	-0.2470E-05	0.5203E-05	0.0	-0.2470E-05	0.6613E-06	0.0	-0.2469E-05
8 TO 14	0.2346E-05	0.0	-0.2469E-05	0.1942E-06	0.0	-0.1667E-05	0.3315E-05
15 TO 21	0.0	-0.1667E-05	0.3736E-06	0.0	-0.1666E-05	0.1468E-05	0.0
22 TO 28	-0.1665E-05	0.9658E-07	0.0	-0.1132E-05	0.2215E-05	0.0	-0.1132E-05
29 TO 35	0.9057E-07	0.0	-0.1131E-05	0.8814E-06	0.0	-0.1131E-05	-0.1582E-06
36 TO 42	0.0	-0.2337E-08	-0.2152E-11	0.0	0.0	-0.2082E-10	-0.2255E-08
43 TO 49	-0.3895E-11	0.0	0.0	0.1966E-10	-0.1015E-08	-0.8104E-11	0.0
50 TO 56	0.0	-0.1347E-10	-0.5937E-09	-0.8494E-11	0.0	0.0	0.1298E-10
57 TO 63	-0.6354E-09	0.2026E-12	0.0	0.0	-0.3049E-11	-0.6116E-09	-0.2029E-11
64 TO 70	0.0	0.0	0.2533E-11	-0.2825E-09	-0.3380E-12	0.0	0.0
71 TO 77	-0.6027E-11	-0.2715E-09	-0.1602E-11	0.0	0.0	0.5806E-11	-0.5631E-09
78 TO 84	-0.8262E-11	0.0	0.0	0.0	-0.6632E-13	-0.1337E-11	0.0
85 TO 91	0.0	0.0	0.5529E-11	0.0	0.0	-0.5318E-11	-0.4015E-10
92 TO 98	-0.1017E-11	0.0	0.0	0.0	-0.5815E-13	-0.4475E-09	-0.5505E-11
99 TO 105	0.0	0.0	0.0	0.4706E-14	-0.2073E-09	-0.6331E-11	0.0
106 TO 112	0.0	0.0	0.4453E-14	-0.3577E-09	-0.3733E-11	0.0	0.0
113 TO 114	0.0	0.1354E-19					

EIGENVECTOR FOR ROOT NO.= 2

Mode 2. Frequency = 0.1977 Hz, Ω = 8 RPM

EIGENVALUE= 0.12424011E 01 (rad/sec.)

REAL PART							
1 TO 7	0.2047E-09	0.2169E-05	-0.5086E 00	-0.3265E-10	0.2169E-05	-0.6463E 00	0.1286E-09
8 TO 14	0.2439E-05	-0.5463E 00	-0.6307E-11	0.2439E-05	-0.6081E 00	0.1884E-09	0.1562E-05
15 TO 21	-0.6855E 00	-0.6643E-10	0.1562E-05	-0.8734E 00	0.1023E-09	0.1712E-05	-0.7372E 00
22 TO 28	-0.2473E-10	0.1713E-05	-0.6214E 00	0.1218E-09	-0.1083E-06	-0.2843E 00	-0.4964E-10
29 TO 35	-0.1083E-06	-0.3590E 00	0.8534E-10	0.1664E-05	-0.3046E 00	-0.3472E-10	0.1664E-05
36 TO 42	-0.3381E 00	0.1266E-09	0.2346E-08	-0.7836E 00	-0.8276E-03	0.1039E-11	-0.1072E-09
43 TO 49	0.2352E-08	-0.1000E 01	-0.8305E-03	0.7766E-12	0.5392E-10	0.2350E-08	-0.8432E 00
50 TO 56	-0.8279E-03	0.9539E-12	-0.4998E-10	0.2352E-08	-0.9402E 00	-0.8300E-03	0.8292E-12
57 TO 63	0.6131E-10	0.2582E-10	-0.4918E-02	0.1598E-04	-0.1131E-12	-0.6339E-10	0.1643E-10
64 TO 70	-0.1969E-02	0.7382E-05	-0.1404E-12	0.5429E-10	0.2557E-10	-0.3803E-02	0.1460E-04
71 TO 77	0.4546E-12	-0.5694E-10	0.2137E-10	-0.2503E-02	0.7872E-05	0.4929E-12	0.2404E-12
78 TO 84	0.2351E-09	-0.8917E 00	-0.8288E-03	0.1239E-02	0.8894E-12	0.2653E-10	-0.8791E-02
85 TO 91	0.1637E-04	0.3198E-15	-0.3289E-12	0.8691E-05	0.3198E-15	-0.3287E-12	0.1229E-13
92 TO 98	0.2536E-10	-0.3039E-02	0.1102E-04	0.1232E-03	0.1466E-11	0.1734E-12	0.2693E-08
99 TO 105	-0.5846E 00	-0.6189E-03	0.1178E-02	-0.5908E-11	0.7101E-13	0.2163E-08	-0.1019E 00
106 TO 112	-0.1991E-03	0.6343E-03	0.1226E-10	0.1161E-12	0.4267E-08	-0.3091E 00	-0.4090E-03
113 TO 114	0.9835E-03	0.6012E-14					
IMAGINARY PART							
1 TO 7	-0.1317E-08	0.3927E-08	0.0	-0.1317E-08	0.1174E-08	0.0	-0.2783E-08
8 TO 14	0.2151E-08	0.0	-0.2784E-08	0.1008E-08	0.0	-0.1012E-08	0.3117E-08
15 TO 21	0.0	-0.1012E-08	0.6463E-09	0.0	-0.1963E-08	0.1565E-08	0.0
22 TO 28	-0.1963E-08	0.5285E-09	0.0	0.1052E-09	-0.2600E-08	0.0	0.1053E-09
29 TO 35	0.1541E-08	0.0	-0.1672E-08	-0.9982E-09	0.0	-0.1672E-08	0.1521E-08
36 TO 42	0.0	-0.4865E-11	-0.1742E-13	0.0	0.0	-0.4348E-13	-0.4697E-11
43 TO 49	-0.1924E-13	0.0	0.0	0.4108E-13	-0.2104E-11	-0.1740E-13	0.0
50 TO 56	0.0	-0.2815E-13	-0.2073E-11	-0.1833E-13	0.0	0.0	0.2713E-13
57 TO 63	-0.1353E-11	0.4367E-15	0.0	0.0	-0.6500E-14	-0.1305E-11	-0.4217E-14
64 TO 70	0.0	0.0	0.6267E-14	-0.6003E-12	-0.6736E-15	0.0	0.0
71 TO 77	-0.1286E-13	-0.5780E-12	-0.3326E-14	0.0	0.0	0.1241E-13	-0.1160E-11
78 TO 84	-0.1779E-13	0.0	0.0	0.0	-0.1394E-15	-0.2796E-14	0.0
85 TO 91	0.0	0.0	0.1176E-13	0.0	0.0	-0.1135E-13	-0.8289E-13
92 TO 98	-0.2091E-14	0.0	0.0	0.0	-0.1185E-15	-0.9189E-12	-0.1136E-13
99 TO 105	0.0	0.0	0.0	0.7864E-17	-0.4248E-12	-0.1290E-13	0.0
106 TO 112	0.0	0.0	0.1318E-16	-0.7330E-12	-0.7619E-14	0.0	0.0
113 TO 114	0.0	0.2965E-22					

EIGENVECTOR FOR ROOT NO.= 3 Mode 3, Frequency = 0.3524 Hz, Ω = 8 RPM

EIGENVALUE= 0.22144775E 01 (rad/sec.)

REAL PART							
1 TO 7	0.1236E-02	-0.2601E 00	0.4525E-03	0.1315E-02	-0.1500E 00	-0.2957E-02	0.1071E-02
8 TO 14	-0.1713E 00	0.4280E-02	0.1121E-02	-0.4434E-01	0.1507E-01	0.1087E-02	-0.5129E 00
15 TO 21	-0.3375E-02	0.1306E-02	-0.3008E 00	-0.9728E-02	0.9261E-03	-0.2980E 00	0.3774E-02
22 TO 28	0.1049E-02	-0.2245E 00	0.2414E-01	0.7494E-03	-0.2786E 00	-0.2987E-02	0.1093E-02
29 TO 35	-0.2725E 00	-0.1152E-01	0.1048E-02	-0.3192E 00	0.1032E-01	0.1027E-02	-0.2399E 00
36 TO 42	0.3791E-01	-0.5768E-03	-0.3167E-02	-0.2655E-05	0.3071E-07	-0.5869E-05	0.2393E-03
43 TO 49	-0.3163E-02	0.5651E-05	0.3443E-07	-0.1826E-05	-0.1996E-03	-0.3164E-02	-0.4340E-06
50 TO 56	0.3119E-07	-0.3973E-05	0.1089E-03	-0.3162E-02	0.3222E-05	0.3223E-07	-0.1783E-05
57 TO 63	-0.3580E-04	-0.6537E-05	0.1121E-06	-0.8655E-09	-0.4679E-06	0.2816E-05	-0.3674E-05
64 TO 70	0.1049E-08	-0.3154E-10	0.8346E-07	-0.3514E-04	-0.6398E-05	0.2943E-07	-0.8605E-09
71 TO 77	-0.3004E-06	0.6693E-05	-0.4305E-05	0.3857E-08	-0.4215E-10	-0.3820E-07	-0.1198E-04
78 TO 84	-0.3163E-07	0.1395E-05	0.3102E-07	-0.2234E-08	-0.2654E-05	-0.7755E-05	-0.1291E-06
85 TO 91	0.1950E-08	0.5410E-12	0.7736E-06	0.8378E-11	0.5410E-12	-0.2435E-07	-0.9155E-06
92 TO 98	-0.5133E-05	0.7440E-08	-0.1011E-09	-0.6484E-09	-0.1887E-06	-0.9130E-05	-0.1972E-02
99 TO 105	0.9061E-06	0.2164E-07	-0.1641E-08	-0.6019E-05	-0.3526E-05	0.2968E-04	0.6406E-06
106 TO 112	0.6671E-08	-0.1872E-08	-0.4989E-06	-0.6237E-05	-0.5514E-03	0.6855E-06	0.1366E-07
113 TO 114	0.6320E-10	-0.4319E-05					
IMAGINARY PART							
1 TO 7	0.3176E-03	0.4493E 00	0.0	0.9188E-03	0.1769E 00	0.0	0.7844E-03
8 TO 14	0.1211E 00	0.0	0.6462E-03	0.1256E 00	0.0	0.7767E-03	0.8584E 00
15 TO 21	0.0	0.8480E-03	0.5122E 00	0.0	0.6709E-03	0.4354E 00	0.0
22 TO 28	0.6081E-03	0.3948E 00	0.0	0.5136E-03	0.4287E 00	0.0	0.7657E-03
29 TO 35	0.4653E 00	0.0	0.6675E-03	0.5025E 00	0.0	0.6171E-03	0.4468E 00
36 TO 42	0.0	-0.1693E-03	-0.5441E-02	0.0	0.0	-0.2306E-05	0.1717E-03
43 TO 49	-0.5450E-02	0.0	0.0	-0.1866E-05	-0.3169E-04	-0.5446E-02	0.0
50 TO 56	0.0	-0.1145E-05	0.5617E-04	-0.5449E-02	0.0	0.0	-0.1081E-05
57 TO 63	-0.8164E-04	-0.2943E-04	0.0	0.0	-0.1761E-06	0.1320E-03	-0.1817E-04
64 TO 70	0.0	0.0	-0.4125E-06	-0.5328E-04	-0.2829E-04	0.0	0.0
71 TO 77	-0.5955E-06	0.7557E-04	-0.2302E-04	0.0	0.0	-0.1089E-05	0.1158E-04
78 TO 84	-0.5443E-02	0.0	0.0	0.0	-0.5355E-06	-0.3220E-04	0.0
85 TO 91	0.0	0.0	0.6014E-06	0.0	0.0	0.1037E-05	0.1081E-05
92 TO 98	-0.2716E-04	0.0	0.0	0.0	-0.1446E-05	0.9133E-05	-0.5288E-02
99 TO 105	0.0	0.0	0.0	-0.1532E-05	0.3866E-05	-0.1895E-02	0.0
106 TO 112	0.0	0.0	-0.1058E-04	0.6585E-05	-0.4299E-02	0.0	0.0
113 TO 114	0.0	-0.7085E-05					

EIGENVECTOR FOR ROOT NO.= 9, Mode 9, Frequency = 0.5025 Hz, Ω = 8 RPM

EIGENVALUE= 0.31574402E 01 (rad/sec.)

REAL PART							
1 TO 7	0.4196E-06	0.3547E-02	0.6391E 00	-0.5249E-07	0.3547E-02	-0.1352E 00	0.2519E-06
8 TO 14	0.3547E-02	-0.9697E 00	-0.1167E-07	0.3547E-02	0.8027E 00	0.3953E-06	0.3552E-02
15 TO 21	0.4790E 00	-0.1023E-06	0.3552E-02	-0.2821E 00	0.2118E-06	0.3552E-02	-0.1000E 01
22 TO 28	-0.3545E-07	0.3552E-02	0.7443E 00	0.2611E-06	0.3745E-02	-0.5214E 00	-0.9506E-07
29 TO 35	0.3745E-02	-0.4642E 00	0.1650E-06	0.3745E-02	-0.4952E 00	-0.7206E-07	0.3746E-02
36 TO 42	-0.4808E 00	0.2212E-06	0.4230E-05	-0.9223E-01	0.2597E-04	0.1832E-08	-0.1858E-06
43 TO 49	0.4239E-05	-0.8450E-01	0.3040E-04	0.1355E-08	0.9346E-07	0.4236E-05	-0.9030E-01
50 TO 56	0.2835E-04	0.1065E-08	-0.8629E-07	0.4239E-05	-0.8671E-01	0.3124E-04	0.1437E-08
57 TO 63	0.1077E-06	0.4576E-07	-0.1169E-02	0.6014E-05	-0.1889E-09	-0.1130E-06	0.2912E-07
64 TO 70	-0.1154E-03	0.2086E-05	-0.2584E-09	0.9520E-07	0.4542E-07	-0.7857E-03	0.4676E-05
71 TO 77	0.7800E-09	-0.1020E-06	0.3797E-07	-0.3145E-03	0.3397E-05	0.8785E-09	0.4089E-09
78 TO 84	0.4238E-05	-0.8855E-01	0.3109E-04	0.6380E-04	0.1530E-08	0.4701E-07	-0.2986E-02
85 TO 91	0.3417E-05	0.5055E-12	-0.5824E-09	-0.3171E-06	0.5055E-12	-0.5820E-09	0.2081E-10
92 TO 98	0.4520E-07	-0.5346E-03	0.4021E-05	0.2235E-04	0.2631E-08	0.2962E-09	0.4873E-05
99 TO 105	-0.7119E-01	0.2326E-04	0.7870E-04	-0.1063E-07	0.1205E-09	0.3916E-05	-0.1815E-01
106 TO 112	0.7545E-05	0.1058E-03	0.2209E-07	0.1987E-09	0.7690E-05	-0.4733E-01	0.1541E-04
113 TO 114	0.1117E-03	0.9985E-11					
IMAGINARY PART							
1 TO 7	-0.1471E-04	0.1459E-04	0.0	-0.1471E-04	0.6335E-05	0.0	-0.1471E-04
8 TO 14	0.9291E-05	0.0	-0.1471E-04	0.5455E-05	0.0	-0.1284E-04	0.2423E-04
15 TO 21	0.0	-0.1284E-04	0.9834E-05	0.0	-0.1284E-04	0.1516E-04	0.0
22 TO 28	-0.1284E-04	0.7563E-05	0.0	-0.9442E-05	0.1980E-04	0.0	-0.9443E-05
29 TO 35	-0.1198E-06	0.0	-0.9444E-05	0.7367E-05	0.0	-0.9445E-05	-0.1457E-05
36 TO 42	0.0	-0.2577E-08	0.4649E-10	0.0	0.0	-0.1220E-10	-0.2573E-08
43 TO 49	0.4989E-10	0.0	0.0	0.1153E-10	-0.1843E-08	0.4756E-10	0.0
50 TO 56	0.0	-0.6191E-11	-0.1867E-08	0.4935E-10	0.0	0.0	0.6333E-11
57 TO 63	0.3737E-08	0.1582E-10	0.0	0.0	0.1771E-10	0.3818E-08	-0.8543E-12
64 TO 70	0.0	0.0	-0.1829E-10	0.1577E-08	0.1010E-10	0.0	0.0
71 TO 77	0.3951E-10	0.1601E-08	0.3137E-11	0.0	0.0	-0.4024E-10	-0.1668E-08
78 TO 84	0.4850E-10	0.0	0.0	0.0	0.2687E-12	0.2192E-10	0.0
85 TO 91	0.0	0.0	-0.3236E-10	0.0	0.0	0.3319E-10	-0.6980E-10
92 TO 98	0.5895E-11	0.0	0.0	0.0	0.2596E-13	-0.1540E-08	0.7514E-11
99 TO 105	0.0	0.0	0.0	0.7450E-13	-0.7452E-09	0.3044E-11	0.0
106 TO 112	0.0	0.0	-0.1965E-13	-0.1308E-08	0.1468E-11	0.0	0.0
113 TO 114	0.0	0.1278E-19					

EIGENVECTOR FOR ROOT NO.= 10

Mode 10, Frequency = 0.5151 Hz, Ω = 8 RPM

EIGENVALUE= 0.32366943E 01 (rad/sec.)

REAL PART							
1 TO 7	0.7219E-07	0.4532E-02	-0.8736E 00	0.5179E-07	0.3444E-02	0.9168E 00	0.5251E-07
8 TO 14	0.5797E-02	-0.5059E 00	0.2837E-07	0.5796E-02	0.9008E 00	0.7449E-07	0.1786E-02
15 TO 21	0.1123E 00	0.8928E-08	0.1135E-02	-0.1017E 00	0.4157E-07	0.2416E-02	0.5083E-01
22 TO 28	0.7244E-08	0.2415E-02	0.4554E 00	0.5597E-07	0.9913E-03	0.2169E 00	0.1995E-08
29 TO 35	0.9913E-03	-0.1615E 00	0.4052E-07	0.9913E-03	0.4020E-01	-0.7312E-08	0.9913E-03
36 TO 42	-0.6688E-01	0.8856E-07	0.1482E-05	0.9983E 00	-0.7657E-02	0.7474E-09	-0.7318E-07
43 TO 49	0.1481E-05	-0.1000E 01	-0.7657E-02	0.5649E-09	0.3673E-07	0.1481E-05	0.4470E 00
50 TO 56	-0.7657E-02	0.6633E-09	-0.3287E-07	0.1481E-05	-0.4487E 00	-0.7656E-02	0.5526E-09
57 TO 63	0.3733E-07	0.1566E-07	-0.9186E-02	0.7814E-04	-0.5955E-10	-0.3928E-07	0.9960E-08
64 TO 70	0.4053E-02	0.1040E-04	-0.8488E-10	0.3265E-07	0.1554E-07	-0.3831E-02	0.6909E-04
71 TO 77	0.2709E-09	-0.3513E-07	0.1298E-07	0.2414E-02	0.3507E-04	0.3069E-09	0.1385E-09
78 TO 84	0.1481E-05	-0.9101E-03	-0.7655E-02	-0.2188E-05	0.5941E-09	0.1609E-07	-0.2901E-01
85 TO 91	0.8558E-04	0.1678E-12	-0.2049E-09	-0.3069E-04	0.1678E-12	-0.2047E-09	0.7041E-11
92 TO 98	0.1546E-07	-0.1961E-03	0.5377E-04	0.5960E-05	0.8993E-09	0.1004E-09	0.1668E-05
99 TO 105	-0.1409E-02	-0.5729E-02	-0.1554E-05	-0.3531E-08	0.4081E-10	0.1334E-05	-0.1273E-02
106 TO 112	-0.1874E-02	0.2675E-05	0.7518E-08	0.6740E-10	0.2617E-05	-0.1606E-02	-0.3802E-02
113 TO 114	0.1237E-06	0.3376E-11					
IMAGINARY PART							
1 TO 7	-0.9134E-05	-0.3241E-05	0.0	-0.7378E-05	0.1753E-04	0.0	-0.1110E-04
8 TO 14	0.4678E-06	0.0	-0.1110E-04	0.8546E-05	0.0	-0.5584E-05	-0.1924E-05
15 TO 21	0.0	-0.4320E-05	0.5253E-05	0.0	-0.6907E-05	-0.2685E-06	0.0
22 TO 28	-0.6905E-05	0.2062E-05	0.0	-0.3327E-05	-0.2325E-05	0.0	-0.3327E-05
29 TO 35	0.7681E-05	0.0	-0.3327E-05	-0.1640E-05	0.0	-0.3327E-05	0.3403E-05
36 TO 42	0.0	-0.1298E-08	0.1468E-10	0.0	0.0	-0.7981E-11	-0.1300E-08
43 TO 49	0.1512E-10	0.0	0.0	0.7834E-11	-0.8038E-09	0.1470E-10	0.0
50 TO 56	0.0	-0.4624E-11	-0.8114E-09	0.1503E-10	0.0	0.0	0.4684E-11
57 TO 63	0.1186E-08	0.5217E-11	0.0	0.0	0.5617E-11	0.1216E-08	-0.5562E-12
64 TO 70	0.0	0.0	-0.5831E-11	0.4980E-09	0.3253E-11	0.0	0.0
71 TO 77	0.1263E-10	0.5075E-09	0.8215E-12	0.0	0.0	-0.1291E-10	-0.6594E-09
78 TO 84	0.1489E-10	0.0	0.0	0.0	0.8066E-13	0.7069E-11	0.0
85 TO 91	0.0	0.0	-0.1027E-10	0.0	0.0	0.1057E-10	-0.2960E-10
92 TO 98	0.1792E-11	0.0	0.0	0.0	-0.1070E-14	-0.5937E-09	0.1549E-11
99 TO 105	0.0	0.0	0.0	0.2556E-13	-0.2844E-09	-0.5938E-13	0.0
106 TO 112	0.0	0.0	-0.5669E-14	-0.4991E-09	-0.2043E-12	0.0	0.0
113 TO 114	0.0	0.9675E-20					

EIGENVECTOR FOR ROOT NO.= 11 Mode 11, Frequency = 0.6881 Hz; Ω = 8RPM

EIGENVALUE= 0.43236084E 01 (rad/sec.)

REAL PART							
1 TO 7	0.3790E-03	0.9779E-01	0.4139E-01	-0.3194E-03	0.9941E-03	0.1421E-01	0.1335E-03
8 TO 14	0.5181E-02	-0.1174E-01	-0.1828E-03	0.2641E-02	0.1513E-01	0.5535E-03	0.9997E 00
15 TO 21	0.5456E-01	-0.4385E-03	0.4664E 00	0.1965E-01	0.1858E-03	0.4103E 00	-0.4571E-01
22 TO 28	-0.2928E-03	0.3805E 00	0.1264E-01	0.2100E-03	-0.9590E 00	-0.2785E-01	-0.2694E-03
29 TO 35	-0.4435E 00	0.2551E-02	0.1283E-03	-0.3991E 00	0.6560E-01	-0.5577E-04	-0.3866E 00
36 TO 42	0.1009E-01	0.6738E-03	0.3901E-02	-0.3723E-04	0.8558E-07	0.4671E-05	-0.6566E-03
43 TO 49	0.3889E-02	-0.1904E-04	0.6528E-07	0.4465E-05	0.3253E-03	0.3893E-02	-0.3127E-04
50 TO 56	0.7714E-07	0.5180E-05	-0.3211E-03	0.3889E-02	-0.2363E-04	0.6054E-07	0.5051E-05
57 TO 63	0.1067E-03	-0.9475E-05	0.8456E-05	-0.7606E-07	0.8931E-06	-0.1063E-03	-0.6438E-05
64 TO 70	-0.1992E-05	-0.6626E-08	0.8997E-06	0.2467E-04	-0.9876E-05	0.3532E-05	-0.5820E-07
71 TO 77	0.1024E-05	-0.2411E-04	-0.8195E-05	-0.9927E-06	-0.2161E-07	0.1017E-05	-0.6506E-07
78 TO 84	0.3890E-02	-0.2716E-04	0.6348E-07	0.1718E-06	0.6057E-05	-0.7521E-05	0.2933E-04
85 TO 91	-0.9322E-07	0.1663E-11	-0.1118E-05	0.1584E-07	0.1663E-11	-0.1118E-05	-0.6120E-09
92 TO 98	-0.9463E-05	0.7212E-06	-0.3802E-07	-0.2746E-07	-0.3967E-06	-0.3933E-07	0.1256E-02
99 TO 105	0.1255E-04	0.4294E-07	0.1278E-06	0.1256E-04	-0.9051E-08	-0.1070E-02	0.1651E-04
106 TO 112	0.1051E-07	-0.9135E-07	-0.4886E-05	-0.1655E-07	-0.1266E-02	0.3035E-04	0.2557E-07
113 TO 114	0.1152E-09	0.4984E-05					
IMAGINARY PART							
1 TO 7	-0.4048E-03	0.4352E-02	0.0	-0.1394E-03	0.1847E-01	0.0	-0.1234E-03
8 TO 14	-0.1391E-01	0.0	-0.9241E-04	-0.9504E-02	0.0	-0.1612E-02	0.2384E-01
15 TO 21	0.0	-0.7723E-03	0.3733E-01	0.0	-0.6739E-03	-0.3345E-01	0.0
22 TO 28	-0.6096E-03	-0.3339E-01	0.0	0.1074E-02	-0.2754E-01	0.0	0.4967E-03
29 TO 35	-0.3153E-01	0.0	0.4424E-03	0.3017E-01	0.0	0.4329E-03	0.3452E-01
36 TO 42	0.0	0.5512E-04	-0.5119E-04	0.0	0.0	0.1044E-05	-0.7929E-05
43 TO 49	-0.5122E-04	0.0	0.0	0.3890E-06	-0.1452E-05	-0.5121E-04	0.0
50 TO 56	0.0	0.2700E-06	0.9733E-05	-0.5122E-04	0.0	0.0	-0.4184E-07
57 TO 63	0.8387E-05	-0.1656E-06	0.0	0.0	0.5654E-07	0.1217E-04	-0.8711E-07
64 TO 70	0.0	0.0	-0.6804E-07	0.2812E-05	-0.1424E-06	0.0	0.0
71 TO 77	0.7763E-07	0.4851E-05	-0.1066E-06	0.0	0.0	-0.1151E-06	-0.1896E-06
78 TO 84	-0.5121E-04	0.0	0.0	0.0	-0.1996E-06	-0.1645E-06	0.0
85 TO 91	0.0	0.0	-0.8102E-07	0.0	0.0	0.1105E-06	0.2905E-06
92 TO 98	-0.1373E-06	0.0	0.0	0.0	-0.9365E-08	0.1011E-05	-0.7938E-05
99 TO 105	0.0	0.0	0.0	-0.1337E-06	0.1169E-05	0.4408E-05	0.0
106 TO 112	0.0	0.0	0.4069E-07	0.2091E-05	0.1162E-04	0.0	0.0
113 TO 114	0.0	-0.1347E-07					

EIGENVECTOR FOR ROOT NO.= 17 Mode 17, Frequency = 0.7777 Hz, Ω = 8 RPM

EIGENVALUE= 0.48864746E 01 (rad/sec.)

REAL PART							
1 TO 7	-0.3051E-05	-0.2057E-01	0.7159E-01	0.4390E-05	-0.9714E-02	0.1068E-01	-0.1281E-05
8 TO 14	0.4828E-03	-0.1660E-01	0.2200E-05	0.4268E-01	0.3337E-01	-0.5442E-05	0.5827E-01
15 TO 21	0.9227E 00	0.6126E-05	0.4178E-01	0.7425E 00	-0.2405E-05	0.2504E-01	0.9753E 00
22 TO 28	0.3034E-05	-0.4422E-01	0.9665E 00	-0.1286E-05	-0.2508E-01	-0.9513E 00	0.1841E-05
29 TO 35	-0.1013E-01	-0.7580E 00	-0.4919E-06	0.4971E-02	-0.1000E 01	0.7681E-06	0.6786E-01
36 TO 42	-0.9673E 00	-0.7721E-05	-0.4977E-05	-0.2330E-01	0.1331E-04	-0.5256E-07	0.7608E-05
43 TO 49	-0.4908E-05	-0.1961E-01	0.1442E-04	-0.5083E-07	-0.3774E-05	-0.4935E-05	-0.2233E-01
50 TO 56	0.1366E-04	-0.5933E-07	0.3761E-05	-0.4908E-05	-0.2065E-01	0.1469E-04	-0.5862E-07
57 TO 63	0.5041E-06	0.2973E-06	0.1742E-02	-0.1501E-04	-0.2402E-08	-0.4419E-06	0.1909E-06
64 TO 70	-0.4886E-03	-0.1653E-05	-0.1635E-08	0.5453E-06	0.3017E-06	0.7666E-03	-0.1192E-04
71 TO 77	0.3229E-08	-0.4676E-06	0.2486E-06	-0.2426E-03	-0.5269E-05	0.2104E-08	0.2311E-08
78 TO 84	-0.4915E-05	-0.2151E-01	0.1444E-04	0.6864E-04	-0.7144E-07	0.2827E-06	0.6004E-02
85 TO 91	-0.1930E-04	0.2087E-11	-0.1968E-08	0.3900E-05	0.2087E-11	-0.1963E-08	0.1175E-09
92 TO 98	0.2957E-06	0.1620E-03	-0.8636E-05	-0.6150E-05	0.1682E-07	0.1730E-08	0.2621E-04
99 TO 105	-0.5316E-02	0.1046E-04	0.5577E-04	-0.1393E-06	0.6872E-09	0.2635E-04	0.3386E-02
106 TO 112	0.2584E-05	-0.1466E-04	0.1375E-06	0.1167E-08	0.4792E-04	0.4288E-02	0.6507E-05
113 TO 114	0.1567E-04	0.2053E-09					
IMAGINARY PART							
1 TO 7	0.1421E-04	0.7183E-04	0.0	-0.8237E-05	0.7375E-04	0.0	-0.2963E-04
8 TO 14	-0.5061E-05	0.0	-0.1187E-03	0.5517E-04	0.0	-0.8615E-04	-0.1499E-04
15 TO 21	0.0	-0.6708E-04	0.2796E-04	0.0	-0.4766E-04	0.8227E-04	0.0
22 TO 28	0.3239E-04	0.1044E-04	0.0	0.5031E-04	0.3027E-04	0.0	0.2031E-04
29 TO 35	-0.3127E-05	0.0	-0.9985E-05	-0.6754E-04	0.0	-0.1362E-03	-0.2178E-05
36 TO 42	0.0	-0.1486E-07	-0.7726E-09	0.0	0.0	0.2190E-11	-0.1253E-07
43 TO 49	-0.7950E-09	0.0	0.0	-0.2598E-10	-0.1492E-07	-0.7758E-09	0.0
50 TO 56	0.0	-0.2116E-11	-0.1412E-07	-0.7953E-09	0.0	0.0	-0.1444E-10
57 TO 63	-0.9122E-08	-0.1257E-09	0.0	0.0	-0.6926E-10	-0.7661E-08	0.1818E-10
64 TO 70	0.0	0.0	0.6125E-10	-0.3118E-08	-0.1048E-09	0.0	0.0
71 TO 77	-0.6327E-10	-0.2500E-08	-0.1008E-10	0.0	0.0	0.5002E-10	-0.1468E-07
78 TO 84	-0.7856E-09	0.0	0.0	0.0	-0.6005E-11	-0.1052E-09	0.0
85 TO 91	0.0	0.0	0.9199E-10	0.0	0.0	-0.7898E-10	-0.1456E-08
92 TO 98	-0.6188E-10	0.0	0.0	0.0	-0.3113E-11	-0.1507E-07	-0.8907E-10
99 TO 105	0.0	0.0	0.0	-0.4469E-12	-0.8473E-08	-0.1013E-09	0.0
106 TO 112	0.0	0.0	0.5678E-12	-0.1375E-07	-0.1319E-09	0.0	0.0
113 TO 114	0.0	0.8087E-14					

EIGENVECTOR FOR ROOT NO.= 18

Mode 18, Frequency = 0.7911 Hz, Ω = 8 RPM

EIGENVALUE= 0.49705811E 01 (rad/sec.)

REAL PART							
1 TO 7	-0.1562E-05	-0.1275E-01	-0.4999E-01	0.2158E-05	-0.5623E-02	0.7488E-01	-0.6660E-06
8 TO 14	-0.1222E-02	-0.2211E-01	0.1075E-05	0.2016E-01	-0.8530E-01	-0.2733E-05	0.2535E-01
15 TO 21	-0.3924E 00	0.3042E-05	0.1680E-01	0.8343E 00	-0.1225E-05	0.1083E-01	-0.2720E 00
22 TO 28	0.1501E-05	-0.1683E-01	0.7499E 00	-0.6684E-06	-0.9494E-02	0.1000E 01	0.9067E-06
29 TO 35	-0.2154E-02	-0.9491E 00	-0.2454E-06	0.2927E-02	0.3459E 00	0.3736E-06	0.2654E-01
36 TO 42	-0.7533E 00	-0.3888E-05	-0.2177E-05	-0.3355E-01	0.2558E-03	-0.2648E-07	0.3830E-05
43 TO 49	-0.2139E-05	0.3313E-01	0.2551E-03	-0.2560E-07	-0.1900E-05	-0.2154E-05	-0.1514E-01
50 TO 56	0.2556E-03	-0.2988E-07	0.1893E-05	-0.2139E-05	0.1476E-01	0.2554E-03	-0.2950E-07
57 TO 63	0.2672E-06	0.1568E-06	-0.1449E-02	0.1306E-04	-0.1165E-08	-0.2376E-06	0.9899E-07
64 TO 70	0.5654E-03	0.1272E-05	-0.7988E-09	0.2826E-06	0.1573E-06	-0.5903E-03	0.1072E-04
71 TO 77	0.1716E-03	-0.2455E-06	0.1289E-06	0.3471E-03	0.4905E-05	0.1179E-08	0.1170E-08
78 TO 84	-0.2143E-05	-0.1934E-03	0.2555E-03	-0.1483E-06	-0.3596E-07	0.1549E-06	-0.5131E-02
85 TO 91	0.1663E-04	0.9484E-12	-0.1098E-08	-0.4191E-05	0.9484E-12	-0.1095E-08	0.5874E-10
92 TO 98	0.1532E-06	-0.3331E-04	0.8113E-05	0.1005E-05	0.8699E-08	0.8709E-09	0.1352E-04
99 TO 105	-0.2254E-03	0.1941E-03	-0.7423E-07	-0.7009E-07	0.3444E-09	0.1351E-04	-0.1823E-03
106 TO 112	0.7035E-04	0.3010E-06	0.7008E-07	0.5693E-09	0.2444E-04	-0.2255E-03	0.1322E-03
113 TO 114	0.7243E-07	0.1208E-09					
IMAGINARY PART							
1 TO 7	0.1222E-04	0.2859E-04	0.0	-0.2344E-05	0.3425E-04	0.0	-0.1194E-04
8 TO 14	-0.6715E-05	0.0	-0.5611E-04	0.2642E-04	0.0	-0.3662E-04	0.3384E-05
15 TO 21	0.0	-0.2725E-04	0.7264E-05	0.0	-0.2074E-04	0.3713E-04	0.0
22 TO 28	0.9494E-05	0.1268E-05	0.0	0.2055E-04	0.4686E-05	0.0	0.4722E-05
29 TO 35	0.1466E-05	0.0	-0.6345E-05	-0.2848E-04	0.0	-0.5749E-04	0.1162E-05
36 TO 42	0.0	-0.7594E-08	-0.2923E-09	0.0	0.0	0.1270E-10	-0.6278E-08
43 TO 49	-0.2746E-09	0.0	0.0	-0.2704E-10	-0.8380E-08	-0.2856E-09	0.0
50 TO 56	0.0	0.7197E-11	-0.7963E-08	-0.2827E-09	0.0	0.0	-0.1627E-10
57 TO 63	-0.5200E-08	-0.4130E-10	0.0	0.0	-0.3693E-10	-0.4444E-08	0.4224E-12
64 TO 70	0.0	0.0	0.3271E-10	-0.1901E-08	-0.3817E-10	0.0	0.0
71 TO 77	-0.3714E-10	-0.1587E-08	-0.7643E-11	0.0	0.0	0.3024E-10	-0.8546E-08
78 TO 84	-0.2842E-09	0.0	0.0	0.0	-0.2987E-11	-0.3558E-10	0.0
85 TO 91	0.0	0.0	0.5116E-10	0.0	0.0	-0.4439E-10	-0.8424E-09
92 TO 98	-0.2553E-10	0.0	0.0	0.0	-0.1448E-11	-0.8811E-08	0.7717E-10
99 TO 105	0.0	0.0	0.0	-0.2767E-12	-0.4905E-08	0.4666E-10	0.0
106 TO 112	0.0	0.0	0.6122E-12	-0.8064E-08	0.5920E-10	0.0	0.0
113 TO 114	0.0	0.8593E-14					

EIGENVECTOR FOR ROOT NO.= 19 Mode 19, Frequency = 0.9049 Hz, Ω = 8 RPM

EIGENVALUE= 0.56654858E 01 (rad/sec.)

REAL PART

1 TO 7	-0.3135E-06	-0.2118E-02	0.6762E 00	0.3353E-06	-0.5446E-04	-0.5878E-01	-0.1271E-06
8 TO 14	0.1836E-04	-0.9142E 00	0.1552E-06	0.2147E-04	-0.5480E-01	-0.5134E-06	0.1364E-02
15 TO 21	-0.1167E 00	0.5253E-06	0.3416E-03	0.5855E-01	-0.2406E-06	0.3400E-04	-0.4384E-01
22 TO 28	0.2543E-06	0.3215E-04	0.2368E-01	-0.1157E-06	-0.1417E-03	-0.5136E 00	0.1337E-06
29 TO 35	-0.1419E-03	-0.2090E-01	-0.2574E-07	0.1669E-03	0.1000E 01	0.4707E-07	0.1669E-03
36 TO 42	0.1769E-02	-0.7206E-06	-0.1607E-06	-0.2771E-02	-0.7305E-05	-0.4945E-08	0.7047E-06
43 TO 49	-0.1535E-06	-0.4669E-02	-0.7232E-05	-0.4718E-08	-0.3505E-06	-0.1559E-06	-0.3296E-02
50 TO 56	-0.7295E-05	-0.5530E-08	0.3430E-06	-0.1534E-06	-0.4148E-02	-0.7254E-05	-0.5424E-08
57 TO 63	0.7957E-07	0.3362E-07	0.5396E-02	-0.5030E-04	-0.2559E-09	-0.6637E-07	0.2161E-07
64 TO 70	-0.1980E-02	-0.4082E-05	-0.9112E-10	0.7570E-07	0.3351E-07	0.2162E-02	-0.3956E-04
71 TO 77	0.6385E-09	-0.5913E-07	0.2812E-07	-0.1160E-02	-0.1640E-04	0.3987E-09	0.2103E-09
78 TO 84	-0.1541E-06	-0.3723E-02	-0.7281E-05	0.1168E-04	-0.6621E-08	0.3396E-07	0.2025E-01
85 TO 91	-0.6827E-04	0.5011E-13	-0.3724E-09	0.1386E-04	0.5011E-13	-0.3721E-09	0.1055E-10
92 TO 98	0.3341E-07	0.1461E-03	-0.2858E-04	-0.4457E-05	0.1906E-08	0.1606E-09	0.2727E-05
99 TO 105	-0.9361E-03	-0.1199E-04	0.9797E-05	-0.1282E-07	0.6304E-10	0.2665E-05	0.9628E-03
106 TO 112	-0.2148E-04	-0.1936E-05	0.1343E-07	0.1133E-09	0.4711E-05	0.8611E-03	-0.1673E-04
113 TO 114	0.3687E-05	0.4485E-10					

IMAGINARY PART

1 TO 7	0.2961E-05	-0.2440E-05	0.0	-0.1222E-06	-0.2941E-06	0.0	-0.6584E-07
8 TO 14	0.7766E-06	0.0	-0.7021E-07	-0.7474E-07	0.0	-0.1911E-05	0.2538E-05
15 TO 21	0.0	-0.5677E-06	0.3873E-06	0.0	0.8747E-07	-0.1862E-06	0.0
22 TO 28	0.9003E-07	0.1713E-06	0.0	0.1261E-06	0.2201E-06	0.0	0.1264E-06
29 TO 35	0.2609E-06	0.0	-0.1529E-06	0.6100E-06	0.0	-0.1529E-06	0.2994E-06
36 TO 42	0.0	-0.2680E-08	0.5380E-10	0.0	0.0	0.5273E-11	-0.2508E-08
43 TO 49	0.8154E-10	0.0	0.0	-0.9853E-11	-0.3223E-08	0.6227E-10	0.0
50 TO 56	0.0	0.3666E-11	-0.3125E-08	0.7328E-10	0.0	0.0	-0.6107E-11
57 TO 63	-0.1686E-08	0.3350E-11	0.0	0.0	-0.9815E-11	-0.1498E-08	-0.4128E-11
64 TO 70	0.0	0.0	0.8674E-11	-0.7301E-09	-0.5539E-12	0.0	0.0
71 TO 77	-0.1259E-10	-0.6577E-09	-0.2499E-11	0.0	0.0	0.1086E-10	-0.3338E-08
78 TO 84	0.6778E-10	0.0	0.0	0.0	-0.6269E-12	0.5048E-12	0.0
85 TO 91	0.0	0.0	0.1551E-10	0.0	0.0	-0.1377E-10	-0.3115E-09
92 TO 98	-0.2368E-11	0.0	0.0	0.0	-0.2369E-12	-0.3416E-08	0.1386E-09
99 TO 105	0.0	0.0	0.0	-0.1778E-13	-0.1841E-08	0.1015E-09	0.0
106 TO 112	0.0	0.0	0.4405E-12	-0.3165E-08	0.1262E-09	0.0	0.0
113 TO 114	0.0	0.5406E-14					

EIGENVECTOR FOR ROOT NO.= 20 Mode 20, Frequency = 0.9224 Hz, Ω = 8 RPM

EIGENVALUE= 0.57954712E 01 (rad/sec.)

REAL PART							
1 TO 7	0.9832E-05	0.1000E 01	-0.4238E-03	-0.1304E-04	0.4972E 00	0.3067E-02	0.2489E-04
8 TO 14	0.3891E 00	-0.3059E-01	-0.2201E-04	0.4061E 00	0.5652E-02	-0.1396E-03	-0.6969E 00
15 TO 21	0.7206E-02	0.131[illegible]E-03	-0.8146E-01	-0.3295E-02	-0.6191E-04	0.6689E-01	0.3713E-03
22 TO 28	0.6249E-04	0.6719E-01	-0.2281E-02	0.1200E-03	-0.2345E 00	-0.1006E-01	-0.1187E-03
29 TO 35	-0.2347E 00	0.3574E-02	0.9151E-04	-0.2195E 00	0.2544E-01	-0.8650E-04	-0.2318E 00
36 TO 42	-0.3495E-02	-0.2[illegible]7E-03	0.1333E-01	-0.3197E-04	0.3251E-06	-0.1810E-05	0.2743E-03
43 TO 49	0.1335E-01	0.5219E-04	0.3225E-06	-0.1637E-05	-0.1469E-03	0.1334E-01	-0.8594E-05
50 TO 56	0.3239E-06	-0.2201E-05	0.1451E-03	0.1334E-01	0.2901E-04	0.3207E-06	-0.2109E-05
57 TO 63	0.2419E-03	0.7219E-04	0.5334E-04	-0.4950E-06	0.3608E-06	-0.2362E-03	0.4430E-04
64 TO 70	-0.1910E-04	-0.3964E-07	0.4301E-06	0.1630E-03	0.6982E-04	0.2166E-04	-0.3892E-06
71 TO 77	0.1942E-05	-0.1559E-03	0.5731E-04	-0.1185E-04	-0.1687E-06	0.1839E-05	0.4716E-06
78 TO 84	0.1334E-01	0.1028E-04	0.3210E-06	0.8128E-08	-0.2952E-05	0.7872E-04	0.2024E-03
85 TO 91	-0.6900E-06	0.3755E-12	-0.1702E-05	0.1400E-06	0.3768E-12	-0.1701E-05	0.2390E-07
92 TO 98	0.6760E-04	0.1573E-05	-0.2899E-06	-0.4839E-07	0.3697E-05	0.3682E-06	0.1441E-01
99 TO 105	0.1206E-04	-0.1621E-06	0.4631E-08	-0.1009E-05	0.1440E-06	0.5160E-02	0.1075E-04
106 TO 112	-0.1518E-04	-0.2355E-07	0.3023E-04	0.2639E-06	0.1224E-01	0.1255E-04	0.4753E-08
113 TO 114	0.2798E-10	0.2026E-04					
IMAGINARY PART							
1 TO 7	-0.1539E-02	0.5396E-02	0.0	-0.1055E-02	-0.6401E-02	0.0	-0.9293E-03
8 TO 14	0.3232E-02	0.0	-0.9675E-03	-0.3234E-02	0.0	0.7046E-03	-0.7802E-03
15 TO 21	0.0	-0.1928E-03	0.8003E-03	0.0	-0.3623E-03	-0.4715E-03	0.0
22 TO 28	-0.3753E-03	0.4761E-03	0.0	-0.6836E-04	-0.1914E-02	0.0	-0.6774E-04
29 TO 35	0.1923E-02	0.0	-0.4767E-04	-0.9116E-03	0.0	-0.4801E-04	0.9051E-03
36 TO 42	0.0	-0.6415E-04	0.7909E-06	0.0	0.0	-0.5145E-06	-0.6313E-04
43 TO 49	0.7999E-06	0.0	0.0	0.5028E-06	-0.3160E-04	0.7937E-06	0.0
50 TO 56	0.0	-0.3274E-06	-0.3130E-04	0.7972E-06	0.0	0.0	0.3206E-06
57 TO 63	-0.2375E-04	0.1990E-07	0.0	0.0	-0.1380E-06	-0.2326E-04	-0.3111E-07
64 TO 70	0.0	0.0	0.1351E-06	-0.9402E-05	0.3946E-08	0.0	0.0
71 TO 77	-0.2144E-05	-0.9208E-05	-0.1880E-07	0.0	0.0	0.2100E-06	-0.2070E-04
78 TO 84	0.7954E-06	0.0	0.0	0.0	-0.2094E-08	-0.2085E-08	0.0
85 TO 91	0.0	0.0	0.2184E-06	0.0	0.0	-0.2139E-06	-0.1517E-05
92 TO 98	-0.8664E-08	0.0	0.0	0.0	-0.7290E-09	-0.1771E-04	0.1086E-05
99 TO 105	0.0	0.0	0.0	-0.1059E-09	-0.7780E-05	0.2700E-06	0.0
106 TO 112	0.0	0.0	0.2260E-08	-0.1365E-04	0.8483E-06	0.0	0.0
113 TO 114	0.0	0.1890E-08					

EIGENVECTOR FOR ROOT NO.= 28　　Mode 28, Frequency = 1.0454 Hz,　Ω = 8 RPM

EIGENVALUE= 0.65686035E 01 (rad/sec.)

REAL PART

1 TO 7	0.8533E-02	-0.9999E 00	-0.1790E 00	-0.8337E-02	-0.9985E 00	-0.9345E-01	0.3900E-02
8 TO 14	-0.9992E 00	-0.1573E 00	-0.4001E-02	-0.9986E 00	-0.1189E 00	0.1246E-01	0.9446E 00
15 TO 21	0.1758E 00	-0.1206E-01	0.9439E 00	0.9259E-01	0.5845E-02	0.9437E 00	0.1538E 00
22 TO 28	-0.5839E-02	0.9434E 00	0.1165E 00	0.4357E-02	0.3332E 00	0.1107E 00	-0.4393E-02
29 TO 35	0.3319E 00	0.9112E-01	0.1835E-02	0.3327E 00	0.1068E 00	-0.2054E-02	0.3322E 00
36 TO 42	0.9602E-01	0.1608E-01	0.5995E-01	-0.8816E-03	0.8140E-06	0.1143E-03	-0.1547E-01
43 TO 49	0.6004E-01	-0.6956E-03	0.7163E-06	0.1059E-03	0.7641E-02	0.6001E-01	-0.8241E-03
50 TO 56	0.7668E-06	0.1231E-03	-0.7530E-02	0.6004E-01	-0.7456E-03	0.6421E-06	0.1190E-03
57 TO 63	0.7451E-04	-0.1532E-03	0.1517E-03	-0.1313E-05	0.5893E-05	-0.3386E-03	-0.1051E-03
64 TO 70	-0.3022E-04	-0.1259E-06	0.2574E-05	-0.2879E-03	-0.1582E-03	0.6560E-04	-0.1005E-05
71 TO 77	0.5101E-06	-0.4406E-04	-0.1366E-03	-0.1213E-04	-0.3876E-06	0.5312E-05	-0.8254E-06
78 TO 84	0.6002E-01	-0.7822E-03	0.6553E-06	0.4789E-05	0.1411E-03	-0.1363E-03	0.4883E-03
85 TO 91	-0.1461E-05	0.2991E-10	-0.3414E-05	0.2532E-06	0.2991E-10	-0.3423E-05	-0.4282E-07
92 TO 98	-0.1621E-03	0.1796E-04	-0.6479E-06	-0.6942E-06	-0.9123E-05	-0.6507E-06	0.8500E-02
99 TO 105	0.3211E-03	0.4657E-06	0.3535E-05	0.1846E-03	-0.2585E-06	-0.1440E-01	0.4353E-03
106 TO 112	0.2429E-06	-0.2184E-05	-0.5643E-04	-0.4754E-06	-0.1683E-01	0.8098E-03	0.3343E-06
113 TO 114	0.1775E-08	0.3638E-04					

IMAGINARY PART

1 TO 7	0.6149E-03	-0.1037E-01	0.0	0.6166E-03	0.1036E-01	0.0	0.6814E-03
8 TO 14	-0.5331E-02	0.0	0.6816E-03	0.5567E-02	0.0	-0.2183E-02	0.7496E-02
15 TO 21	0.0	-0.2177E-02	-0.7189E-02	0.0	-0.2088E-02	0.3881E-02	0.0
22 TO 28	-0.2087E-02	-0.3723E-02	0.0	-0.7716E-03	0.7784E-02	0.0	-0.7678E-03
29 TO 35	-0.7472E-02	0.0	-0.7384E-03	0.4659E-02	0.0	-0.7370E-03	-0.4460E-02
36 TO 42	0.0	-0.1578E-03	-0.4844E-05	0.0	0.0	-0.1745E-05	-0.1527E-03
43 TO 49	-0.5415E-05	0.0	0.0	0.1673E-05	-0.4788E-04	-0.5016E-05	0.0
50 TO 56	0.0	-0.1092E-05	-0.4692E-04	-0.5241E-05	0.0	0.0	0.1062E-05
57 TO 63	0.5254E-06	-0.2816E-07	0.0	0.0	-0.9625E-08	-0.1407E-07	-0.4528E-07
64 TO 70	0.0	0.0	0.1392E-07	0.1032E-05	-0.1939E-07	0.0	0.0
71 TO 77	0.1372E-08	0.8970E-06	-0.2940E-07	0.0	0.0	0.3713E-08	-0.1184E-04
78 TO 84	-0.5128E-05	0.0	0.0	0.0	-0.5227E-08	-0.1620E-07	0.0
85 TO 91	0.0	0.0	0.1500E-08	0.0	0.0	-0.7123E-08	0.7657E-06
92 TO 98	-0.1641E-07	0.0	0.0	0.0	-0.7535E-09	-0.3269E-06	-0.3253E-05
99 TO 105	0.0	0.0	0.0	-0.4790E-08	0.4604E-05	-0.2298E-05	0.0
106 TO 112	0.0	0.0	-0.9266E-08	0.7475E-05	-0.3136E-05	0.0	0.0
113 TO 114	0.0	0.6712E-09					

EIGENVECTOR FOR ROOT NO.= 32 Mode 32, Frequency = 3.8441 Hz, Ω = 8 RPM

EIGENVALUE= 0.24153320E 02 (rad/sec.)

REAL PART									
1	TO	7	-0.4493E-01	-0.6728E-01	0.8113E-03	-0.3046E-01	-0.6769E-01	0.8130E-03	-0.1015E-01
8	TO	14	-0.2329E-01	0.8117E-03	-0.4440E-02	-0.2339E-01	0.8125E-03	-0.3207E-01	-0.5601E-01
15	TO	21	0.8965E-03	-0.6760E-02	-0.5665E-01	0.8497E-03	-0.8844E-02	-0.1929E-01	0.8840E-03
22	TO	28	[illegible]	-0.1852E-01	0.8630E-03	-0.1629E 00	-0.6432E-01	0.8778E-03	-0.1626E 00
29	TO	35	-0.6449E-01	0.8796E-03	-0.4997E-01	-0.2191E-01	0.8783E-03	-0.5150E-01	-0.2183E-01
36	TO	42	0.8791E-03	-0.4363E-01	-0.2780E-01	-0.3755E-04	0.1540E-06	-0.3976E-03	-0.1335E-01
43	TO	49	-0.2782E-01	-0.1553E-04	0.8387E-07	0.1998E-03	-0.1736E-01	-0.2782E-01	-0.2729E-04
50	TO	56	0.1222E-06	-0.2962E-03	-0.2472E-02	-0.2782E-01	-0.2053E-04	0.3616E-07	0.5680E-04
57	TO	63	-0.3334E-01	0.2182E-02	0.1043E-04	-0.5054E-08	-0.2390E-03	-0.4282E-01	0.1402E-02
64	TO	70	0.1332E-04	-0.1072E-07	0.2769E-03	-0.1018E-01	0.1882E-02	0.9529E-05	-0.7911E-08
71	TO	77	-0.3133E-03	-0.1526E-01	0.1532E-02	0.1027E-04	0.8861E-08	0.3919E-03	-0.4282E-02
78	TO	84	-0.2782E-01	-0.2210E-04	0.4713E-07	0.1354E-05	-0.1315E-03	0.2188E-02	0.1275E-05
85	TO	91	-0.6009E-07	0.3453E-09	0.3292E-03	-0.5955E-07	0.3453E-09	-0.4058E-03	-0.5375E-03
92	TO	98	0.1630E-02	0.9667E-05	0.9227E-08	-0.4207E-06	0.4638E-04	-0.3168E-02	-0.3802E-03
99	TO	105	0.2503E-03	0.1126E-07	0.5228E-06	-0.5123E-04	-0.1314E-02	0.5399E-02	0.2413E-03
106	TO	112	0.2325E-07	-0.6719E-06	-0.1479E-04	-0.2188E-02	0.4987E-03	0.2695E-03	0.1896E-07
113	TO	114	0.1499E-07	-0.6958E-06					
IMAGINARY PART									
1	TO	7	-0.9990E 00	0.4347E-01	0.0	-0.9989E 00	0.4249E-01	0.0	-0.3534E 00
8	TO	14	0.1495E-01	0.0	-0.3529E 00	0.1460E-01	0.0	-0.8360E 00	0.3890E-01
15	TO	21	0.0	-0.8359E 00	0.3724E-01	0.0	-0.3012E 00	0.1371E-01	0.0
22	TO	28	-0.3309E 00	0.1293E-01	0.0	-0.9371E 00	0.3934E-01	0.0	-0.9382E 00
29	TO	35	0.3904E-01	0.0	-0.3260E 00	0.1365E-01	0.0	-0.3259E 00	0.1353E-01
36	TO	42	0.0	-0.4865E 00	0.4743E-03	0.0	0.0	-0.4853E-02	-0.4874E 00
43	TO	49	0.4395E-03	0.0	0.0	0.4862E-02	-0.1818E 00	0.4516E-03	0.0
50	TO	56	0.0	-0.2991E-02	-0.1821E 00	0.4398E-03	0.0	0.0	0.2998E-02
57	TO	63	-0.6749E 00	-0.1916E-03	0.0	0.0	-0.4507E-02	-0.6741E 00	-0.9478E-04
64	TO	70	0.0	0.0	0.4509E-02	-0.2284E 00	-0.1490E-03	0.0	0.0
71	TO	77	-0.6234E-02	-0.2283E 00	-0.1055E-03	0.0	0.0	0.6234E-02	-0.8421E-01
78	TO	84	0.4441E-03	0.0	0.0	0.0	0.1523E-05	-0.2849E-03	0.0
85	TO	91	0.0	0.0	0.6493E-02	0.0	0.0	-0.6494E-02	-0.1048E-01
92	TO	98	-0.1139E-03	0.0	0.0	0.0	-0.1322E-05	-0.6608E-01	0.1895E-02
99	TO	105	0.0	0.0	0.0	-0.6195E-05	-0.2914E-01	0.1768E-02	0.0
106	TO	112	0.0	0.0	0.7764E-05	-0.4770E-01	0.2376E-02	0.0	0.0
113	TO	114	0.0	-0.7634E-07					

EIGENVECTOR FOR ROOT NO.= 1

Mode 1, frequency = 0.1787 Hz, Ω = 12 RPM

EIGENVALUE= 0.11227112E 01 (rad/sec)

REAL PART							
1 TO 7	0.1250E-06	0.1381E-02	-0.9598E 00	-0.2584E-07	0.1381E-02	0.9604E 00	0.7806E-07
8 TO 14	0.1515E-02	-0.4256E 00	-0.6885E-08	0.1515E-02	0.4313E 00	0.1193E-06	0.1003E-02
15 TO 21	-0.1000E 01	-0.4782E-07	0.1003E-02	0.9997E 00	0.6409E-07	0.1080E-02	-0.4481E 00
22 TO 28	-0.1576E-07	0.1080E-02	0.4434E 00	0.7265E-07	-0.2342E-03	-0.3953E 00	-0.3228E-07
29 TO 35	-0.2342E-03	0.3949E 00	0.5059E-07	0.9047E-03	-0.1769E 00	-0.2166E-07	0.9050E-03
36 TO 42	0.1775E 00	0.8480E-07	0.1425E-05	-0.5851E 00	0.4481E-02	0.6831E-09	-0.7316E-07
43 TO 49	0.1429E-05	0.5846E 00	0.4481E-02	0.5252E-09	0.3670E-07	0.1427E-05	-0.2624E 00
50 TO 56	0.4481E-02	0.6405E-09	-0.3436E-07	0.1428E-05	0.2619E 00	0.4482E-02	0.5661E-09
57 TO 63	0.3702E-07	0.1535E-07	-0.1752E-02	0.1414E-04	-0.6110E-10	-0.3841E-07	0.9766E-08
64 TO 70	0.9498E-03	0.2102E-05	-0.7923E-10	0.3235E-07	0.1520E-07	-0.7548E-03	0.1329E-04
71 TO 77	0.2750E-09	-0.3411E-07	0.1269E-07	0.5123E-03	0.7249E-05	0.3006E-09	0.1409E-09
78 TO 84	0.1428E-05	-0.2511E-03	0.4481E-02	0.4556E-06	0.6160E-09	0.1578E-07	-0.5141E-02
85 TO 91	0.1425E-04	0.1829E-12	-0.2022E-09	-0.6389E-05	0.1829E-12	-0.2021E-09	0.7195E-11
92 TO 98	0.1500E-07	-0.3044E-04	0.1124E-04	0.8842E-06	0.8701E-09	0.1017E-09	0.1598E-05
99 TO 105	-0.1534E-03	0.3364E-02	0.2516E-06	-0.3363E-08	0.4161E-10	0.1277E-05	-0.1258E-03
106 TO 112	0.1129E-02	0.6922E-07	0.7226E-08	0.6821E-10	0.2516E-05	-0.1281E-03	0.2247E-02
113 TO 114	0.1884E-08	0.3564E-11					
IMAGINARY PART							
1 TO 7	-0.9711E-06	0.3650E-05	0.0	-0.9709E-06	0.8679E-06	0.0	-0.2253E-05
8 TO 14	0.1967E-05	0.0	-0.2253E-05	0.7741E-06	0.0	-0.7758E-06	0.2899E-05
15 TO 21	0.0	-0.7756E-06	0.4584E-06	0.0	-0.1609E-05	0.1448E-05	0.0
22 TO 28	-0.1609E-05	0.3996E-06	0.0	0.3249E-06	-0.2560E-05	0.0	0.3250E-06
29 TO 35	0.1499E-05	0.0	-0.1269E-05	-0.1053E-05	0.0	-0.1270E-05	0.1377E-05
36 TO 42	0.0	-0.4350E-08	-0.1649E-10	0.0	0.0	-0.3910E-10	-0.4200E-08
43 TO 49	-0.1649E-10	0.0	0.0	0.3699E-10	-0.1865E-08	-0.1659E-10	0.0
50 TO 56	0.0	-0.2535E-10	-0.1837E-08	-0.1759E-10	0.0	0.0	0.2444E-10
57 TO 63	-0.1273E-05	0.3205E-12	0.0	0.0	-0.6128E-11	-0.1232E-08	-0.3767E-11
64 TO 70	0.0	0.0	0.5932E-11	-0.5628E-09	-0.6255E-12	0.0	0.0
71 TO 77	-0.1216E-10	-0.5437E-09	-0.2990E-11	0.0	0.0	0.1178E-10	-0.1014E-08
78 TO 84	-0.1702E-10	0.0	0.0	0.0	-0.1284E-12	-0.2651E-11	0.0
85 TO 91	0.0	0.0	0.1107E-10	0.0	0.0	-0.1072E-10	-0.7303E-10
92 TO 98	-0.1878E-11	0.0	0.0	0.0	-0.1033E-12	-0.7988E-09	-0.1013E-10
99 TO 105	0.0	0.0	0.0	0.4107E-14	-0.3678E-09	-0.1125E-10	0.0
106 TO 112	0.0	0.0	0.1161E-13	-0.6348E-09	-0.6659E-11	0.0	0.0
113 TO 114	0.0	0.2407E-19					

EIGENVECTOR FOR ROOT NO.= 2

Mode 2, frequency = 0.1977 Hz, Ω = 12 RPM

EIGENVALUE= 0.12424011E 01 (rad/sec)

REAL PART									
1	TO	7	0.2325E-09	0.2559E-05	-0.5086E [illegible]	-0.5572E-10	0.2559E-05	-0.6463E 00	0.1580E-09
8	TO	14	.3551E-05	-0.5463E [illegible]	-0.1703E-1[illegible]	0.2764E-05	-0.6081E 00	0.2245E-09	0.1866E-05
15	TO	21	-0.[illegible]55E 00	-0.9787E-10	0.1856E-[illegible]	-0.[illegible]734E 00	0.1299E-09	0.2447E-05	-0.7372E 00
22	TO	28	-0.3960E-10	0.1986E-05	-0.6214E [illegible]	0.1315E-09	-0.5922E-06	-0.2843E 00	-0.6192E-10
29	TO	35	-0.5923E-06	-0.3590E 00	0.1104E-[illegible]	0.9705E-05	-0.3046E 00	-0.4056E-10	0.1532E-05
36	TO	42	-0.3381E 00	0.1659E-04	0.2604E-[illegible]	-0.7836E 00	-0.8276E-03	0.1320E-11	-0.1449E-09
43	TO	49	0.2610E-06	-0.1000E 01	-0.8305E-03	0.1034E-11	0.7254E-10	0.2608E-08	-0.8432E 00
50	TO	56	-0.8279E-03	0.1255E-11	-0.6836E-1[illegible]	0.2610E-08	-0.9402E 00	-0.8300E-03	0.1121E-11
57	TO	63	0.6740E-10	0.2754E-10	-0.4918E-[illegible]	0.1598E-04	-0.1012E-12	-0.7009E-10	0.1755E-10
64	TO	70	-0.1969E-02	0.7392E-05	-0.1363E-1[illegible]	0.5526E-10	0.2724E-10	-0.3803E-02	0.1460E-04
71	TO	77	0.5016E-12	-0.6170E-10	0.2280E-1[illegible]	-0.2503E-02	0.7872E-05	0.5511E-12	0.2507E-12
78	TO	84	0.2609E-08	-0.6917E 00	-0.9288E-03	0.1239E-02	0.1231E-11	0.2837E-10	-0.8791E-02
85	TO	91	0.1637E-04	0.3198E-15	-0.3731E-12	0.8691E-05	0.3198E-15	-0.3729E-12	0.1279E-13
92	TO	98	0.2705E-10	-0.3039E-02	0.1102E-04	0.1232E-03	0.1562E-11	0.1812E-12	0.2867E-08
99	TO	105	-0.5846E 00	-0.6199E-03	0.1178E-[illegible]	-0.5500E-11	0.7403E-13	0.2282E-08	-0.1019E 00
106	TO	112	-0.1991E-03	0.6343E-05	0.1290E-1[illegible]	0.1216E-12	0.4495E-08	-0.3091E 00	-0.4090E-03
113	TO	114	0.9825E-03	0.6409E-14					
IMAGINARY PART									
1	TO	7	-0.1507E-08	0.7830E-08	0.0	-0.1807E-08	0.1533E-08	0.0	-0.1464E-07
8	TO	14	0.5386E-08	0.0	-0.4451E-0[illegible]	0.1436E-08	0.0	-0.1481E-08	0.6223E-08
15	TO	21	0.0	-0.1480E-08	0.7601E-[illegible]	0.0	-0.9837E-08	0.3805E-08	0.0
22	TO	28	-0.3261E-08	0.7201E-09	0.0	0.9251E-09	-0.5701E-08	0.0	0.9254E-09
29	TO	35	0.3382E-08	0.0	-0.1528E-07	0.9964E-08	0.0	-0.2414E-08	0.2956E-08
36	TO	42	0.0	-0.9219E-11	-0.3605E-13	0.0	0.0	-0.8315E-13	-0.8905E-11
43	TO	49	-0.4038E-13	0.0	0.0	0.7873E-13	-0.3935E-11	-0.3644E-13	0.0
50	TO	56	0.0	-0.5395E-13	-0.3875E-11	-0.3981E-13	0.0	0.0	0.5204E-13
57	TO	63	-0.2773E-11	0.7687E-15	0.0	0.0	-0.1337E-13	-0.2689E-11	-0.7985E-14
64	TO	70	0.0	0.0	0.1297E-13	-0.1223E-11	-0.1190E-14	0.0	0.0
71	TO	77	-0.2656E-13	-0.1184E-11	-0.6336E-14	0.0	0.0	0.2578E-13	-0.2124E-11
78	TO	84	-0.3748E-13	0.0	0.0	0.0	-0.2760E-15	-0.5672E-14	0.0
85	TO	91	0.0	0.0	0.2412E-13	0.0	0.0	-0.2342E-13	-0.1535E-12
92	TO	98	-0.3939E-14	0.0	0.0	0.0	-0.2142E-15	-0.1666E-11	-0.2132E-13
99	TO	105	0.0	0.0	0.0	0.4423E-17	-0.7653E-12	-0.2331E-13	0.0
106	TO	112	0.0	0.0	0.2419E-16	-0.1321E-11	-0.1381E-13	0.0	0.0
113	TO	114	0.0	0.5898E-22					

EIGENVECTOR FOR ROOT NO.= 3

Mode 3, frequency = 0.3185, Ω = 12 RPM

EIGENVALUE= 0.20009766E 01 (rad/sec)

REAL PART								
1 TO 7	0.5659E-03	-0.2414E 00	0.1229E-01	0.1406E-03	-0.8988E-01	0.1173E-02	-0.2207E-03
8 TO 14	-0.4207E 00	0.7694E-02	0.1013E-02	-0.3923E 00	0.4517E-02	0.4041E-03	-0.5950E 00
15 TO 21	0.9753E-02	0.2001E-03	-0.4574E 00	-0.1070E-02	-0.3875E-04	-0.9983E 00	0.5896E-02
22 TO 28	0.8463E-03	-0.7658E 00	0.2098E-02	0.5171E-03	-0.6886E 00	-0.6687E-02	0.1698E-03
29 TO 35	-0.5329E 00	0.6375E-03	-0.2247E-03	-0.3633E 00	0.4242E-01	0.7693E-03	-0.7117E 00
36 TO 42	0.1528E-02	-0.4715E-04	0.4562E-02	-0.8103E-05	0.1384E-06	0.4205E-06	0.3944E-04
43 TO 49	0.4566E-02	0.2695E-04	0.1365E-06	0.3099E-06	-0.5524E-04	0.4560E-02	0.1799E-05
50 TO 56	0.1352E-06	-0.5024E-06	-0.4280E-04	0.4563E-02	0.1725E-04	0.1318E-06	-0.4819E-06
57 TO 63	0.8374E-04	0.2206E-04	-0.1227E-06	-0.3849E-08	0.4899E-06	-0.8500E-04	0.1380E-04
64 TO 70	-0.2314E-06	0.3545E-09	0.4261E-06	0.3796E-04	0.2246E-04	-0.3544E-06	-0.1656E-08
71 TO 77	0.5475E-06	-0.4213E-04	0.1731E-04	-0.2977E-06	0.1106E-08	0.5789E-06	-0.5150E-05
78 TO 84	0.4562E-02	0.9633E-05	0.1312E-06	-0.7495E-07	-0.1080E-05	0.2407E-04	0.6389E-06
85 TO 91	-0.2865E-06	0.8560E-12	-0.7716E-06	0.1027E-08	0.8560E-12	-0.7482E-06	-0.5060E-06
92 TO 98	0.2121E-04	-0.3626E-06	0.8674E-09	0.1412E-07	0.1140E-05	-0.3944E-05	0.4915E-02
99 TO 105	-0.7544E-05	0.9484E-07	-0.5559E-07	-0.6166E-06	-0.2062E-05	0.1940E-02	-0.8612E-05
106 TO 112	0.3195E-07	0.4065E-07	0.1110E-04	-0.3025E-05	0.4340E-02	-0.1524E-04	0.6211E-07
113 TO 114	0.4447E-09	0.6276E-05					
IMAGINARY PART							
1 TO 7	0.2244E-02	0.9936E-01	0.0	0.1645E-02	-0.3293E-01	0.0	0.2024E-02
8 TO 14	-0.9746E-01	0.0	0.2644E-02	0.2208E 00	0.0	0.1981E-02	0.1056E 00
15 TO 21	0.0	0.1526E-02	0.6061E-01	0.0	0.2191E-02	0.5837E-01	0.0
22 TO 28	0.2375E-02	0.2674E 00	0.0	0.2066E-02	0.1502E 00	0.0	0.1606E-02
29 TO 35	0.7900E-01	0.0	0.1064E-02	-0.7933E-01	0.0	0.2172E-02	0.2625E 00
36 TO 42	0.0	-0.1508E-04	-0.1798E-02	0.0	0.0	0.4417E-05	-0.2335E-04
43 TO 49	-0.1799E-02	0.0	0.0	0.5679E-06	-0.3175E-04	-0.1798E-02	0.0
50 TO 56	0.0	-0.1899E-06	0.4110E-05	-0.1798E-02	0.0	0.0	0.8095E-08
57 TO 63	-0.1305E-04	-0.9767E-05	0.0	0.0	0.3506E-06	0.3405E-05	-0.6075E-05
64 TO 70	0.0	0.0	0.3020E-06	-0.2877E-04	-0.1064E-04	0.0	0.0
71 TO 77	-0.1803E-06	0.1956E-04	-0.7026E-05	0.0	0.0	-0.6143E-07	-0.9592E-05
78 TO 84	-0.1798E-02	0.0	0.0	0.0	-0.4257E-06	-0.1050E-04	0.0
85 TO 91	0.0	0.0	-0.9326E-07	0.0	0.0	-0.1297E-06	-0.9344E-06
92 TO 98	-0.9399E-05	0.0	0.0	0.0	-0.5269E-06	-0.7058E-05	-0.1618E-02
99 TO 105	0.0	0.0	0.0	-0.1066E-05	-0.3822E-05	-0.5135E-03	0.0
106 TO 112	0.0	0.0	-0.2871E-05	-0.5523E-05	-0.1212E-02	0.0	0.0
113 TO 114	0.0	-0.2305E-05					

EIGENVECTOR FOR ROOT NO.= 9

Mode 9, frequency = 0.5025 Hz, Ω = 12 RPM

EIGENVALUE= 0.3157+402E 01 (rad/sec)

REAL PART									
1	TO	7	-0.4528E-04	0.2549E-01	0.6391E 00	-0.3971E-04	0.2832E-02	-0.1352E 00	0.3528E-04
8	TO	14	0.1011E-01	-0.9597E 00	0.4848E-04	0.2433E-01	0.8027E 00	-0.3269E-04	0.1192E-01
15	TO	21	0.4790E 00	-0.2849E-04	-0.2522E-03	-0.2621E 00	0.2527E-04	0.3855E-02	-0.1000E 01
22	TO	28	0.3512E-04	0.1163E-01	0.7443E 00	0.6068E-05	-0.1215E-02	-0.5214E 00	-0.1787E-05
29	TO	35	-0.1417E-02	-0.4642E 00	-0.1506E-04	-0.9250E-02	-0.4952E 00	0.1238E-04	-0.7894E-02
36	TO	42	-0.4804E 00	-0.4798E-06	0.8451E-06	-0.9223E-01	0.2597E-04	-0.2201E-08	0.4768E-06
43	TO	49	0.8531E-06	-0.8450E-01	0.3040E-04	-0.2228E-08	-0.2800E-06	0.8504E-06	-0.9030E-01
50	TO	56	0.2835E-04	-0.3939E-08	0.2766E-06	0.8532E-06	-0.8671E-01	0.3124E-04	-0.3876E-08
57	TO	63	0.4370E-07	0.3387E-07	-0.1169E-02	0.6014E-05	0.1161E-10	-0.4381E-07	0.2168E-07
64	TO	70	-0.1154E-03	0.2086E-05	0.8178E-11	0.3695E-07	0.3369E-07	-0.7857E-03	0.4676E-05
71	TO	77	0.9681E-10	-0.3918E-07	0.2823E-07	-0.3145E-03	0.3397E-05	0.8942E-10	-0.2011E-11
78	TO	84	0.6510E-06	-0.8855E-01	0.3109E-04	0.6380E-04	-0.5570E-08	0.3443E-07	-0.2986E-02
85	TO	91	0.8417E-05	0.5055E-12	-0.2806E-09	-0.3171E-06	0.5055E-12	-0.2809E-09	-0.3526E-11
92	TO	98	0.3354E-07	-0.5346E-03	0.4021E-05	0.2235E-04	0.1835E-08	0.1807E-10	0.3470E-05
99	TO	105	-0.7119E-01	0.2326E-04	0.7870E-04	-0.1213E-07	0.5130E-11	0.3180E-05	-0.1815E-01
106	TO	112	0.7545E-05	0.1058E-03	0.1544E-07	0.1751E-11	0.5379E-05	-0.4733E-01	0.1541E-04
113	TO	114	0.1117E-03	0.2682E-10					
IMAGINARY PART									
1	TO	7	-0.5235E-04	-0.2112E-01	0.0	0.1617E-05	-0.1630E-01	0.0	0.1418E-04
8	TO	14	0.2005E-01	0.0	-0.2443E-04	0.1637E-01	0.0	-0.3377E-04	-0.1145E-01
15	TO	21	0.0	0.4730E-05	-0.8954E-02	0.0	0.1341E-04	0.1090E-01	0.0
22	TO	28	-0.1442E-04	0.8981E-02	0.0	0.6010E-05	0.1260E-02	0.0	0.6992E-05
29	TO	35	-0.3879E-02	0.0	0.4543E-04	-0.3014E-02	0.0	0.3889E-04	0.2534E-02
36	TO	42	0.0	-0.8079E-08	-0.3931E-08	0.0	0.0	-0.5127E-10	0.4005E-08
43	TO	49	-0.6632E-08	0.0	0.0	-0.8128E-10	-0.4505E-08	-0.5416E-08	0.0
50	TO	56	0.0	-0.4679E-10	-0.7781E-09	-0.5387E-08	0.0	0.0	-0.3377E-10
57	TO	63	0.1390E-05	-0.6377E-09	0.0	0.0	0.1400E-10	0.1656E-08	0.6168E-09
64	TO	70	0.0	0.0	-0.1426E-10	0.2128E-09	-0.8325E-09	0.0	0.0
71	TO	77	0.1295E-10	0.3247E-09	0.8194E-09	0.0	0.0	-0.1584E-10	-0.2168E-08
78	TO	84	-0.5410E-08	0.0	0.0	0.0	-0.2863E-10	-0.6571E-11	0.0
85	TO	91	0.0	0.0	-0.1585E-10	0.0	0.0	0.1883E-10	-0.1541E-09
92	TO	98	0.2998E-11	0.0	0.0	0.0	0.1088E-11	-0.2050E-08	0.4526E-08
99	TO	105	0.0	0.0	0.0	-0.4220E-10	-0.9034E-09	0.5547E-08	0.0
106	TO	112	0.0	0.0	0.3273E-10	-0.1585E-08	0.1108E-07	0.0	0.0
113	TO	114	0.0	-0.3625E-12					

EIGENVECTOR FOR ROOT NO.= 10

Mode 10, frequency = 0.5151 Hz, Ω = 12 RPM

EIGENVALUE= 0.32366943E 01 (rad/sec)

REAL PART							
1 TO 7	-0.1395E-04	0.83[illegible]E-02	-0.673[illegible] 00	-0.1040E-04	0.2972E-03	0.9168E 00	0.1301E-04
8 TO 14	0.2776E-02	-0.5[illegible]	0.1417E-04	[illegible]5941E-02	0.9008E 00	-0.1061E-04	0.4126E-02
15 TO 21	0.1123E 00	-0.7827E-05	-0.4955E-03	-0.1017E 00	0.9941E-05	0.9424E-03	0.5083E-01
22 TO 28	0.1057E-04	0.4266E-02	0.4554E 00	0.4684E-05	-0.5666E-03	0.2169E 00	-0.8190E-06
29 TO 35	-0.6635E-03	-0.1615E 00	-0.5652E-05	-0.3182E-02	0.4020E-01	0.5467E-05	-0.2039E-02
36 TO 42	-0.6698E-01	-0.2751E-07	-0.2772E-06	0.9983E 00	-0.7637E-02	-0.2179E-09	0.1225E-07
43 TO 49	-0.2762E-06	-0.10[illegible]E 01	-0.7657E-02	-0.4818E-10	-0.1219E-07	-0.2765E-06	0.4470E 00
50 TO 56	-0.7657E-02	-0.2251E-09	0.7586E-08	-0.2762E-06	-0.4487E 00	-0.7656E-02	-0.9442E-10
57 TO 63	-0.7885E-08	-0.279[illegible]E-08	-0.9156E-02	0.7514E-04	0.1833E-10	0.7829E-08	-0.1770E-08
64 TO 70	0.4053E-02	0.104[illegible]E-04	0.1829E-10	-0.7016E-08	-0.2767E-08	-0.3831E-02	0.6909E-04
71 TO 77	-0.6642E-10	0.697[illegible]E-08	-0.2309E-08	0.2414E-02	0.3507E-04	-0.6574E-10	-0.7836E-10
78 TO 84	-0.2764E-06	-0.9101E-03	-0.7655E-02	-0.2195E-05	-0.1800E-09	-0.2882E-08	-0.2901E-01
85 TO 91	0.8559E-04	0.1673E-12	0.4037E-10	-0.3069E-04	0.1678E-12	0.4006E-10	-0.4826E-11
92 TO 98	-0.2750E-08	-0.1961E-03	0.5377E-04	0.5960E-05	-0.1633E-09	-0.5359E-10	-0.2893E-06
99 TO 105	-0.1409E-02	-0.5729E-02	-0.1554E-05	0.6105E-09	-0.2080E-10	-0.2278E-06	-0.1273E-02
106 TO 112	-0.1874E-02	0.2675E-05	-0.1345E-08	-0.4059E-10	-0.4681E-06	-0.1606E-02	-0.3802E-02
113 TO 114	0.1237E-06	0.39[illegible]E-11					
IMAGINARY PART							
1 TO 7	-0.1737E-04	-0.7083E-02	0.0	0.2990E-05	-0.3938E-02	0.0	0.6758E-05
8 TO 14	0.7044E-02	0.0	-0.1234E-04	0.3962E-02	0.0	-0.1177E-04	-0.4067E-02
15 TO 21	0.0	0.3534E-05	-0.2272E-02	0.0	0.6092E-05	0.4059E-02	0.0
22 TO 28	-0.7983E-05	0.2291E-02	0.0	0.2381E-05	0.9374E-03	0.0	0.3345E-05
29 TO 35	-0.1661E-03	0.0	0.1605E-04	-0.1106E-02	0.0	0.1030E-04	0.1090E-02
36 TO 42	0.0	-0.2[illegible]E-10	0.1043E-09	0.0	0.0	-0.3681E-11	0.8694E-09
43 TO 49	0.7349E-10	0.0	0.0	-0.1092E-10	0.2106E-09	0.4624E-10	0.0
50 TO 56	0.0	-0.126[illegible]E-11	0.2626E-09	0.4903E-10	0.0	0.0	-0.3211E-11
57 TO 63	-0.2317E-09	-0.275[illegible]E-10	0.0	0.0	-0.1624E-11	-0.2659E-09	0.8799E-11
64 TO 70	0.0	0.0	0.2332E-11	-0.6681E-10	-0.3031E-10	0.0	0.0
71 TO 77	-0.2150E-11	-0.8097E-10	0.1254E-10	0.0	0.0	0.2736E-11	0.2251E-09
78 TO 84	0.4646E-10	0.0	0.0	0.0	0.5156E-12	-0.1438E-10	0.0
85 TO 91	0.0	0.0	0.2228E-11	0.0	0.0	-0.2225E-11	0.8975E-11
92 TO 98	-0.5824E-11	0.0	0.0	0.0	-0.1041E-12	0.1723E-09	-0.9739E-10
99 TO 105	0.0	0.0	0.0	-0.9799E-14	0.8916E-10	-0.8871E-10	0.0
106 TO 112	0.0	0.0	0.6173E-14	0.1513E-09	-0.8722E-11	0.0	0.0
113 TO 114	0.0	0.4151E-16					

EIGENVECTOR FOR ROOT NO.= 11

Mode 11, frequency = 0.6716 Hz, Ω = 12 RPM

EIGENVALUE= 0.42200928E 01 (rad/sec)

REAL PART							
1 TO 7	-0.6773E-03	0.1464E-01	0.2133E-01	0.4698E-04	0.4272E-01	0.1986E-01	-0.2486E-03
8 TO 14	0.3596E-02	-0.1403E-01	0.5235E-05	-0.6420E-02	0.1257E-01	-0.2537E-02	0.3157E-02
15 TO 21	0.2741E-01	-0.8746E-03	0.5678E-01	0.1690E-01	-0.1107E-02	-0.2052E-01	-0.2775E-01
22 TO 28	-0.7250E-03	-0.7814E-01	0.8191E-02	0.1488E-02	0.5340E-02	-0.1237E-01	0.9025E-03
29 TO 35	-0.3338E-01	-0.1193E-02	0.5984E-03	0.3157E-01	0.3723E-01	0.6640E-03	0.9393E-01
36 TO 42	0.6067E-02	-0.1726E-03	-0.6506E-02	-0.6626E-05	0.3499E-07	-0.1675E-06	0.2634E-03
43 TO 49	-0.6506E-02	0.2026E-05	0.3218E-07	-0.1450E-05	-0.1283E-03	-0.6506E-02	-0.4126E-05
50 TO 56	0.3399E-07	-0.1511E-05	0.1404E-03	-0.6506E-02	-0.2890E-06	0.3217E-07	-0.2225E-05
57 TO 63	-0.9234E-04	-0.1601E-04	0.1238E-05	-0.1207E-07	-0.2890E-06	0.9550E-04	-0.9288E-05
64 TO 70	-0.3924E-06	-0.8272E-09	-0.3294E-06	-0.5217E-04	-0.1547E-04	0.4538E-06	-0.9239E-08
71 TO 77	-0.7900E-06	0.5214E-04	-0.1228E-04	-0.2484E-06	-0.3226E-08	-0.8177E-06	-0.4950E-05
78 TO 84	-0.6505E-02	-0.2180E-05	0.3263E-07	0.6951E-08	-0.2600E-05	-0.1887E-04	0.4494E-05
85 TO 91	-0.1444E-07	0.1090E-11	0.7253E-06	0.2882E-08	0.1000E-11	0.7653E-06	-0.2623E-06
92 TO 98	-0.1506E-04	0.1234E-07	-0.5880E-08	-0.2011E-09	-0.9234E-06	-0.3790E-05	-0.5378E-02
99 TO 105	-0.4983E-06	0.2681E-07	0.5375E-08	-0.6410E-05	-0.1489E-05	-0.1191E-02	-0.5062E-07
106 TO 112	0.9892E-08	-0.7825E-09	-0.7538E-05	-0.2710E-05	-0.3379E-02	0.2821E-06	0.1910E-07
113 TO 114	0.1192E-05	-0.8974E-05					
IMAGINARY PART							
1 TO 7	-0.2975E-03	-0.7496E-01	0.0	0.1215E-03	0.1616E-01	0.0	-0.1288E-03
8 TO 14	0.3443E-02	0.0	0.1318E-03	0.1780E-01	0.0	-0.3742E-03	-0.9908E 00
15 TO 21	0.0	0.2447E-03	-0.4604E 00	0.0	-0.1336E-03	-0.4154E 00	0.0
22 TO 28	0.3585E-03	-0.3544E 00	0.0	-0.1805E-03	0.1000E 01	0.0	0.1899E-03
29 TO 35	0.4730E 00	0.0	-0.1189E-03	0.4198E 00	0.0	-0.1115E-03	0.3694E 00
36 TO 42	0.0	-0.4674E-03	-0.1395E-03	0.0	0.0	-0.3109E-05	0.5584E-03
43 TO 49	-0.1260E-03	0.0	0.0	-0.3853E-05	-0.2294E-03	-0.1304E-03	0.0
50 TO 56	0.0	-0.3696E-05	0.2728E-03	-0.1259E-03	0.0	0.0	-0.4197E-05
57 TO 63	-0.6728E-04	0.1913E-04	0.0	0.0	-0.7511E-06	0.2974E-04	0.1209E-04
64 TO 70	0.0	0.0	-0.5323E-06	-0.2245E-05	0.1906E-04	0.0	0.0
71 TO 77	-0.7390E-06	-0.1161E-04	0.1561E-04	0.0	0.0	-0.3615E-06	0.1317E-04
78 TO 84	-0.1272E-03	0.0	0.0	0.0	-0.4741E-05	0.1882E-04	0.0
85 TO 91	0.0	0.0	0.7987E-06	0.0	0.0	0.4527E-06	0.3412E-06
92 TO 98	0.1854E-04	0.0	0.0	0.0	0.9554E-06	0.1037E-04	0.1902E-02
99 TO 105	0.0	0.0	0.0	-0.9037E-05	0.3817E-05	0.1855E-02	0.0
106 TO 112	0.0	0.0	0.9562E-05	0.7210E-05	0.3314E-02	0.0	0.0
113 TO 114	0.0	0.2912E-07					

EIGENVECTOR FOR FOOT NO.= 17 Mode 17, frequency = 0.7777 Hz, Ω = 12 RPM

EIGENVALUE= 0.48364746E 01 (rad/sec)

REAL PART									
1	TO	7	-0.32[illegible]	-0.2[illegible]E-01	0.7159E-01	0.4901E-05	-0.1262E-01	0.1068E-01	-0.1518E-05
8	TO	14	-0.2651E-02	-0.1660E-01	0.2477E-05	0.4449E-01	0.3337E-01	-0.5991E-05	0.5565E-01
15	TO	21	0.9227E 00	0.6727E-05	0.3672E-01	0.7425E 00	-0.2587E-05	0.2399E-01	0.9753E 00
22	TO	28	0.3313E-05	-0.3665E-01	0.9665E 00	-0.1429E-05	-0.2057E-01	-0.9513E 00	0.1986E-05
29	TO	35	-0.4526E-02	-0.7580E 00	-0.6896E-06	0.6354E-02	-0.1000E 01	0.8191E-06	0.5779E-01
36	TO	42	-0.9673E 00	-0.8576E-05	-0.4730E-05	-0.2330E-01	0.1331E-04	-0.5833E-07	0.8448E-05
43	TO	49	-0.4645E-05	-0.1961E-01	0.1442E-04	-0.5639E-07	-0.4195E-05	-0.4679E-05	-0.2233E-01
50	TO	56	0.1366E-04	-0.6590E-07	0.4179E-05	-0.4645E-05	-0.2065E-01	0.1469E-04	-0.6508E-07
57	TO	63	0.6035E-06	0.3495E-06	0.1742E-02	-0.1501E-04	-0.2554E-08	-0.5376E-06	0.2207E-06
64	TO	70	-0.4886E-03	-0.1653E-05	-0.1741E-08	0.6329E-06	0.3506E-06	0.7666E-03	-0.1192E-04
71	TO	77	0.3900E-08	-0.5506E-06	0.2873E-06	-0.2426E-03	-0.5269E-05	0.2709E-08	0.2600E-08
78	TO	84	-0.4695E-05	-0.2151E-01	0.1444E-04	0.6864E-04	-0.7946E-07	0.3454E-06	0.6004E-02
85	TO	91	-0.1930E-04	0.2087E-11	-0.2517E-08	0.3900E-05	0.2087E-11	-0.2512E-08	0.1304E-09
92	TO	98	0.3417E-06	0.1620E-03	-0.8636E-05	-0.6150E-05	0.1940E-07	0.1936E-08	0.3010E-04
99	TO	105	-0.5316E-07	0.1046E-04	0.5577E-04	-0.1557E-06	0.7653E-09	0.3007E-04	0.3386E-02
106	TO	112	0.2584E-05	-0.1456E-04	0.1559E-06	0.1310E-08	0.5436E-04	0.4288E-02	0.6507E-05
113	TO	114	0.1567E-04	0.2672E-09					
IMAGINARY PART									
1	TO	7	0.4093E-04	0.9233E-04	0.0	-0.7116E-05	0.1108E-03	0.0	-0.3776E-04
8	TO	14	-0.2332E-04	0.0	-0.1821E-03	0.8574E-04	0.0	-0.1182E-03	0.1138E-04
15	TO	21	0.0	-0.3778E-04	0.2293E-04	0.0	-0.6739E-04	0.1208E-03	0.0
22	TO	28	0.3010E-04	0.3718E-05	0.0	0.6593E-04	0.1481E-04	0.0	0.1449E-04
29	TO	35	0.4719E-05	0.0	-0.2039E-04	-0.9196E-04	0.0	-0.1854E-03	0.3818E-05
36	TO	42	0.0	-0.2483E-07	-0.9118E-09	0.0	0.0	0.4411E-10	-0.2055E-07
43	TO	49	-0.8483E-09	0.0	0.0	-0.9101E-10	-0.2757E-07	-0.8885E-09	0.0
50	TO	56	0.0	0.2542E-10	-0.2623E-07	-0.8768E-09	0.0	0.0	-0.5490E-10
57	TO	63	-0.1692E-07	-0.1273E-09	0.0	0.0	-0.1180E-09	-0.1445E-07	-0.1347E-11
64	TO	70	0.0	0.0	0.1041E-09	-0.6300E-08	-0.1197E-09	0.0	0.0
71	TO	77	-0.1216E-09	-0.5274E-08	-0.2546E-10	0.0	0.0	0.9898E-10	-0.2819E-07
78	TO	84	-0.8826E-09	0.0	0.0	0.0	-0.9633E-11	-0.1100E-09	0.0
85	TO	91	0.0	0.0	0.1654E-09	0.0	0.0	-0.1432E-09	-0.2767E-08
92	TO	98	-0.8151E-10	0.0	0.0	0.0	-0.4695E-11	-0.2906E-07	0.2717E-09
99	TO	105	0.0	0.0	0.0	-0.8247E-12	-0.1615E-07	0.1645E-09	0.0
106	TO	112	0.0	0.0	0.2011E-11	-0.2660E-07	0.2021E-09	0.0	0.0
113	TO	114	0.0	0.2810E-13					

9

EIGENVECTOR FOR ROOT NO.= 18

Mode 18, frequency = 0.7911 Hz, Ω = 12 RPM

EIGENVALUE= 0.49705811E 01 (rad/sec)

REAL PART									
1	TO	7	-0.9458E-04	-0.7668E-02	-0.4999E-01	0.1626E-05	0.4574E-03	0.7488E-01	-0.2729E-06
8	TO	14	-0.7906E-02	-0.2211E-01	0.6619E-06	-0.7955E-02	-0.8530E-01	-0.1690E-05	0.1410E-01
15	TO	21	-0.8524E 00	0.2143E-05	0.5979E-02	0.5343E 00	-0.8156E-06	0.1549E-01	-0.2720E 00
22	TO	28	0.1079E-05	0.1549E-01	0.7499E 00	-0.1992E-06	0.6741E-02	0.1000E 01	0.4538E-06
29	TO	35	0.6740E-02	-0.9491E 00	0.3790E-07	0.6741E-02	0.3459E 00	0.1963E-06	0.6740E-02
36	TO	42	-0.7533E 00	-0.2147E-05	-0.2547E-05	-0.3355E-01	0.2558E-03	-0.1462E-07	0.2107E-05
43	TO	49	-0.2519E-05	0.3313E-01	0.2551E-03	-0.1383E-07	-0.1050E-05	-0.2529E-05	-0.1514E-01
50	TO	56	0.2556E-03	-0.1649E-07	0.1051E-05	-0.2519E-05	0.1476E-01	0.2554E-03	-0.1632E-07
57	TO	63	0.1712E-06	0.7492E-07	-0.1449E-02	0.1306E-04	-0.1139E-08	-0.1124E-06	0.4839E-07
64	TO	70	0.5654E-03	0.1272E-05	-0.4027E-09	0.1927E-06	0.7490E-07	-0.5903E-03	0.1072E-04
71	TO	77	0.1578E-08	-0.1186E-06	0.6301E-07	0.3471E-03	0.4905E-05	0.5084E-09	0.7077E-09
78	TO	84	-0.2526E-05	-0.1934E-03	0.2555E-03	-0.1483E-06	-0.1989E-07	0.7495E-07	-0.5131E-02
85	TO	91	0.1663E-04	0.9484E-12	-0.5067E-09	-0.4191E-05	0.9484E-12	-0.5059E-09	0.3710E-10
92	TO	98	0.7490E-07	-0.3381E-04	0.8113E-05	0.1005E-05	0.4361E-08	0.5129E-09	0.6049E-05
99	TO	105	-0.2254E-03	0.1941E-03	-0.7423E-07	-0.3646E-07	0.2143E-09	0.6344E-05	-0.1823E-03
106	TO	112	0.7005E-04	0.3010E-06	0.3446E-07	0.3508E-09	0.1203E-04	-0.2255E-03	0.1322E-03
113	TO	114	0.7293E-07	0.9823E-10					
IMAGINARY PART									
1	TO	7	-0.1466E-04	-0.1902E-05	0.0	-0.2410E-04	0.4663E-04	0.0	-0.1561E-04
8	TO	14	0.3286E-04	0.0	-0.1561E-04	0.3594E-04	0.0	-0.4232E-04	-0.3718E-04
15	TO	21	0.0	-0.2249E-04	0.9970E-04	0.0	-0.4572E-04	-0.4292E-04	0.0
22	TO	28	-0.4572E-04	0.4767E-04	0.0	-0.2343E-04	0.4992E-04	0.0	-0.2342E-04
29	TO	35	-0.4910E-04	0.0	-0.2343E-04	0.2934E-04	0.0	-0.2343E-04	-0.2558E-04
36	TO	42	0.0	-0.2070E-08	-0.2652E-09	0.0	0.0	0.5332E-10	-0.1938E-08
43	TO	49	-0.2216E-09	0.0	0.0	-0.5091E-10	-0.5376E-08	-0.2504E-09	0.0
50	TO	56	0.0	0.3139E-10	-0.5186E-08	-0.2358E-09	0.0	0.0	-0.3327E-10
57	TO	63	-0.2011E-08	-0.1806E-10	0.0	0.0	-0.1480E-10	-0.1448E-08	-0.5678E-12
64	TO	70	0.0	0.0	0.1165E-10	-0.8040E-09	-0.2250E-10	0.0	0.0
71	TO	77	-0.1005E-10	-0.5779E-09	-0.5614E-11	0.0	0.0	0.5052E-11	-0.6340E-08
78	TO	84	-0.2431E-09	0.0	0.0	0.0	-0.1899E-11	-0.2108E-10	0.0
85	TO	91	0.0	0.0	0.2006E-10	0.0	0.0	-0.1485E-10	-0.6335E-09
92	TO	98	-0.1734E-10	0.0	0.0	0.0	-0.1041E-11	-0.6800E-08	-0.4174E-10
99	TO	105	0.0	0.0	0.0	-0.2037E-13	-0.3852E-08	-0.4966E-10	0.0
106	TO	112	0.0	0.0	0.7756E-13	-0.6445E-08	-0.7795E-10	0.0	0.0
113	TO	114	0.0	0.9329E-14					

EIGENVECTOR FOR ROOT NO.= 19

Mode 19, frequency = 0.9049 Hz, Ω = 12 RPM

EIGENVALUE= 0.56854858E 01 (rad/sec)

REAL PART

1 TO 7	-0.3572E-06	0.5426E-03	0.6762E 00	0.5683E-06	0.1190E-02	-0.5878E-01	-0.4157E-06
8 TO 14	-0.1184E-02	-0.9142E 00	0.4012E-06	0.9037E-03	-0.5480E-01	-0.1420E-05	-0.2624E-03
15 TO 21	-0.1167E 00	0.1424E-05	0.1453E-03	0.5855E-01	-0.6910E-06	0.1879E-03	-0.4384E-01
22 TO 28	0.6869E-06	0.1879E-03	0.2368E-01	-0.4200E-06	-0.7419E-03	-0.5136E 00	0.4343E-06
29 TO 35	-0.7425E-03	-0.2090E-01	-0.1587E-06	0.9688E-03	0.1000E 01	0.1746E-06	-0.3671E-03
36 TO 42	0.1769E-02	-0.1971E-05	-0.1862E-05	-0.2771E-02	-0.7305E-05	-0.1359E-07	0.1935E-05
43 TO 49	-0.1826E-05	-0.4669E-02	-0.7232E-05	-0.1311E-07	-0.9552E-06	-0.1838E-05	-0.3296E-02
50 TO 56	-0.7295E-05	-0.1513E-07	0.9498E-06	-0.1826E-05	-0.4148E-02	-0.7254E-05	-0.1488E-07
57 TO 63	0.7144E-07	0.5742E-07	0.5396E-02	-0.5030E-04	-0.6505E-09	-0.5528E-07	0.3694E-07
64 TO 70	-0.1880E-02	-0.4082E-05	-0.4498E-09	0.9738E-07	0.5731E-07	0.2162E-02	-0.3956E-04
71 TO 77	0.3609E-09	-0.7712E-07	0.4810E-07	-0.1160E-02	-0.1640E-04	0.8741E-10	0.4235E-09
78 TO 84	-0.1829E-05	-0.3723E-02	-0.7281E-05	0.1168E-04	-0.1794E-07	0.5772E-07	0.2025E-01
85 TO 91	-0.6827E-04	0.5011E-13	-0.1239E-09	0.1386E-04	0.5011E-13	-0.1242E-09	0.2399E-10
92 TO 98	0.5719E-07	0.1461E-03	-0.2858E-04	-0.4457E-05	0.3264E-08	0.3438E-09	0.5769E-05
99 TO 105	-0.9361E-03	-0.1199E-04	0.9797E-05	-0.3344E-07	0.1447E-09	0.5618E-05	0.9628E-03
106 TO 112	-0.2148E-04	-0.1936E-05	0.3101E-07	0.2630E-09	0.1084E-04	0.8611E-03	-0.1673E-04
113 TO 114	0.3687E-05	0.1118E-08					

IMAGINARY PART

1 TO 7	-0.2429E-05	0.1556E-04	0.0	-0.4355E-05	-0.1967E-04	0.0	0.4251E-05
8 TO 14	-0.8027E-06	0.0	-0.3143E-05	-0.1007E-04	0.0	-0.7898E-06	0.2739E-05
15 TO 21	0.0	-0.1651E-05	0.2047E-05	0.0	0.1335E-05	-0.1470E-05	0.0
22 TO 28	-0.1069E-05	0.1279E-05	0.0	-0.5398E-06	-0.5455E-05	0.0	-0.5392E-06
29 TO 35	0.6015E-05	0.0	0.6911E-06	0.5803E-05	0.0	-0.2678E-06	0.3129E-05
36 TO 42	0.0	-0.4495E-08	-0.5322E-09	0.0	0.0	0.9169E-10	-0.2237E-08
43 TO 49	-0.4044E-09	0.0	0.0	-0.1231E-09	-0.1038E-07	-0.4944E-09	0.0
50 TO 56	0.0	0.6113E-10	-0.9932E-08	-0.4428E-09	0.0	0.0	-0.7495E-10
57 TO 63	-0.4052E-08	-0.5207E-10	0.0	0.0	-0.2353E-10	-0.3449E-08	-0.4588E-11
64 TO 70	0.0	0.0	0.2034E-10	-0.1907E-08	-0.4524E-10	0.0	0.0
71 TO 77	-0.2422E-10	-0.1641E-08	-0.1543E-10	0.0	0.0	0.1872E-10	-0.1241E-07
78 TO 84	-0.4686E-09	0.0	0.0	0.0	-0.2250E-11	-0.5493E-10	0.0
85 TO 91	0.0	0.0	0.3724E-10	0.0	0.0	-0.3198E-10	-0.1214E-08
92 TO 98	-0.3085E-10	0.0	0.0	0.0	-0.1452E-11	-0.1319E-07	-0.1461E-09
99 TO 105	0.0	0.0	0.0	-0.5238E-12	-0.7344E-08	-0.1202E-09	0.0
[illegible] TO 112	0.0	0.0	0.1346E-12	-0.1271E-07	-0.1060E-09	0.0	0.0
[illegible] TO 114	0.0	0.1976E-13					

EIGENVECTOR FOR ROOT NO.= 20

Mode 20, frequency = 0.9090 Hz, Ω = 12 RPM

EIGENVALUE= 0.57113647E 01 (rad/sec)

REAL PART

1	TO	7	-0.2936E-03	0.1000E 01	0.1613E 00	0.2908E-03	0.5866E 00	-0.7553E-01	-0.1297E-03
8	TO	14	0.2565E 00	-0.5161E 00	0.1312E-03	0.4209E 00	0.1623E 00	-0.5188E-03	-0.6727E 00
15	TO	21	0.7034E-01	0.5117E-03	-0.9341E-01	0.4378E-02	-0.2464E-03	0.9655E-01	0.2032E-01
22	TO	28	0.2403E-03	[illegible]	-0.2018E-01	-0.1362E-03	-0.2807E 00	-0.2787E 00	0.1381E-03
29	TO	35	-0.2500E 00	0.6666E-01	-0.4494E-04	-0.1554E 00	0.4399E 00	0.5067E-04	-0.2526E 00
36	TO	42	-0.1354E 00	-0.7260E-03	0.8250E-03	-0.1271E-02	0.1410E-04	-0.4990E-05	0.7120E-03
43	TO	49	0.8399E-03	0.2402E-02	0.1406E-04	-0.4803E-05	-0.3526E-03	0.8348E-03	-0.2565E-03
50	TO	56	0.1409E-04	-0.5573E-05	0.3501E-03	0.8399E-03	0.1390E-02	0.1406E-04	-0.5474E-05
57	TO	63	0.5203E-04	0.2831E-04	0.2443E-02	-0.2282E-04	-0.1879E-06	-0.4582E-04	0.1797E-04
64	TO	70	-0.8572E-03	-0.1799E-05	-0.1112E-06	0.5237E-04	0.2801E-04	0.9783E-03	-0.1787E-04
71	TO	77	0.3484E-06	-0.4461E-04	0.2336E-04	-0.5318E-03	-0.7517E-05	0.2359E-06	0.1993E-06
78	TO	84	0.8382E-03	0.5671E-03	0.1407E-04	-0.4348E-06	-0.6643E-05	0.2914E-04	0.9190E-02
85	TO	91	-0.3102E-04	0.3465E-11	-0.2332E-06	0.6291E-05	0.3465E-11	-0.2332E-06	0.1104E-07
92	TO	98	0.2772E-04	0.6685E-04	-0.1300E-04	-0.2023E-05	0.1564E-05	0.1612E-06	0.3631E-02
99	TO	105	0.4619E-03	0.7077E-05	-0.3822E-06	-0.1188E-04	0.6677E-07	0.2556E-02	0.3898E-03
106	TO	112	-0.6879E-05	-0.4940E-06	0.1428E-04	0.1222E-06	0.5177E-02	0.4025E-03	0.9832E-07
113	TO	114	0.3913E-06	0.2626E-05					

IMAGINARY PART

1	TO	7	-0.2238E-02	0.9963E-02	0.0	-0.1776E-02	-0.1031E-01	0.0	-0.9576E-03
8	TO	14	0.4526E-02	0.0	-0.1432E-02	-0.5234E-02	0.0	0.9792E-03	-0.8666E-03
15	TO	21	0.0	-0.2621E-03	0.1246E-02	0.0	-0.4654E-03	-0.7643E-03	0.0
22	TO	28	-0.5937E-03	0.7448E-03	0.0	-0.6434E-04	-0.3053E-02	0.0	-0.6390E-04
29	TO	35	0.3171E-02	0.0	-0.3693E-04	-0.9140E-03	0.0	-0.5477E-04	0.1493E-02
36	TO	42	0.0	-0.1211E-04	-0.2633E-06	0.0	0.0	-0.4926E-07	-0.1109E-04
43	TO	49	-0.2147E-06	0.0	0.0	0.3537E-07	-0.9024E-05	-0.2490E-06	0.0
50	TO	56	0.0	-0.3022E-07	-0.8809E-05	-0.2293E-06	0.0	0.0	0.2389E-07
57	TO	63	-0.5316E-05	-0.1788E-07	0.0	0.0	-0.3090E-07	-0.5011E-05	-0.6975E-08
64	TO	70	0.0	0.0	0.2927E-07	-0.2218E-05	-0.1753E-07	0.0	0.0
71	TO	77	-0.4329E-07	-0.2086E-05	-0.9383E-08	0.0	0.0	0.4051E-07	-0.8017E-05
78	TO	84	-0.2392E-06	0.0	0.0	0.0	-0.1156E-08	-0.2251E-07	0.0
85	TO	91	0.0	0.0	0.4888E-07	0.0	0.0	-0.4621E-07	-0.7017E-06
92	TO	98	-0.1386E-07	0.0	0.0	0.0	-0.6997E-09	-0.7822E-05	-0.7555E-07
99	TO	105	0.0	0.0	0.0	-0.2552E-09	-0.4022E-05	-0.6250E-07	0.0
106	TO	112	0.0	0.0	0.4031E-10	-0.6998E-05	-0.5786E-07	0.0	0.0
113	TO	114	0.0	0.1458E-10					

EIGENVECTOR FOR ROOT NO.= 28

Mode 28, frequency = 1.0331 Hz, Ω = 12 RPM

EIGENVALUE= 0.64909668E 01 (rad/sec)

REAL PART

1	TO	7	0.3920E-02	-0.9999E 00	-0.1595E 00	-0.8729E-02	-0.9983E 00	-0.8040E-01	0.4097E-02
8	TO	14	-0.9985E 00	-0.1595E 00	-0.4203E-02	-0.9978E 00	-0.1040E 00	0.1297E-01	0.9313E 00
15	TO	21	0.1470E 00	-0.1256E-01	0.9305E 00	0.7448E-01	0.6093E-02	0.9294E 00	0.1279E 00
22	TO	28	-0.6089E-02	0.9290E 00	0.9542E-01	0.4677E-02	0.3144E 00	0.9181E-01	-0.4716E-02
29	TO	35	0.3131E 00	0.7139E-01	0.2008E-02	0.3136E 00	0.8751E-01	-0.2232E-02	0.3130E 00
36	TO	42	0.7836E-01	0.1666E-01	0.7604E-01	-0.5670E-03	0.6130E-06	0.1184E-03	-0.1604E-01
43	TO	49	0.7612E-01	-0.4252E-03	0.5470E-06	0.1099E-03	0.7918E-02	0.7609E-01	-0.5237E-03
50	TO	56	0.5805E-06	0.1275E-03	-0.7805E-02	0.7612E-01	-0.4634E-03	0.4956E-06	0.1235E-03
57	TO	63	0.2828E-03	-0.1046E-03	0.9816E-04	-0.8585E-06	0.6474E-05	-0.5509E-03	-0.7617E-04
64	TO	70	-0.1981E-04	-0.7972E-07	0.3103E-05	-0.1644E-03	-0.1117E-03	0.4188E-04	-0.6541E-06
71	TO	77	0.2224E-05	-0.1726E-03	-0.9895E-04	-0.8250E-05	-0.2486E-06	0.7099E-05	-0.5253E-06
78	TO	84	0.7610E-01	-0.4918E-03	0.5040E-06	0.2983E-05	0.1462E-03	-0.8050E-04	0.3164E-03
85	TO	91	-0.9431E-06	0.1955E-10	-0.5015E-05	0.1646E-06	0.1955E-10	-0.5023E-05	-0.2869E-07
92	TO	98	-0.1173E-03	0.1108E-04	-0.4167E-06	-0.4273E-06	-0.6604E-05	-0.4224E-06	0.2220E-01
99	TO	105	0.1956E-03	0.3594E-06	0.2203E-05	0.1985E-03	-0.1736E-06	-0.1103E-01	0.2678E-03
106	TO	112	0.1798E-06	-0.1350E-05	-0.3545E-04	-0.3191E-06	-0.7676E-02	0.5004E-03	0.2555E-06
113	TO	114	0.1351E-08	0.5841E-04					

IMAGINARY PART

1	TO	7	0.9284E-03	-0.1606E-01	0.0	0.9314E-03	0.1604E-01	0.0	0.1049E-02
8	TO	14	-0.8347E-02	0.0	0.1050E-02	0.8576E-02	0.0	-0.3241E-02	0.1116E-01
15	TO	21	0.0	-0.3232E-02	-0.1096E-01	0.0	-0.3067E-02	0.5838E-02	0.0
22	TO	28	-0.3065E-02	-0.5676E-02	0.0	-0.1102E-02	0.1174E-01	0.0	-0.1096E-02
29	TO	35	-0.1142E-01	0.0	-0.1040E-02	0.7060E-02	0.0	-0.1037E-02	-0.6803E-02
36	TO	42	0.0	-0.3102E-03	-0.6938E-05	0.0	0.0	-0.3219E-05	-0.3022E-03
43	TO	49	-0.7811E-05	0.0	0.0	0.3108E-05	-0.1073E-03	-0.7201E-05	0.0
50	TO	56	0.0	-0.2016E-05	-0.1057E-03	-0.7544E-05	0.0	0.0	0.1967E-05
57	TO	63	-0.4558E-05	-0.8076E-08	0.0	0.0	-0.4260E-07	-0.4811E-05	-0.1117E-06
64	TO	70	0.0	0.0	0.4584E-07	-0.9921E-06	-0.1860E-07	0.0	0.0
71	TO	77	-0.3561E-07	-0.9734E-06	-0.6880E-07	0.0	0.0	0.3820E-07	-0.4084E-04
78	TO	84	-0.7372E-05	0.0	0.0	0.0	-0.8910E-08	-0.1807E-07	0.0
85	TO	91	0.0	0.0	0.4995E-07	0.0	0.0	-0.5329E-07	-0.1173E-06
92	TO	98	-0.3360E-07	0.0	0.0	0.0	-0.2045E-08	-0.1964E-04	-0.4520E-05
99	TO	105	0.0	0.0	0.0	-0.6728E-08	-0.8453E-06	-0.3475E-05	0.0
106	TO	112	0.0	0.0	-0.1333E-07	-0.2651E-05	-0.4524E-05	0.0	0.0
113	TO	114	0.0	0.1904E-08					

EIGENVECTOR FOR ROOT NO.= 32

Mode 32, frequency = 3.8462 Hz, Ω = 12 RPM

EIGENVALUE= 0.24166260E 02 (rad/sec)

REAL PART							
1 TO 7	-0.1703E 00	-0.8287E-01	0.5514E-02	-0.1479E 00	-0.3450E-01	0.5525E-02	-0.5193E-01
8 TO 14	-0.2596E-01	0.5517E-02	-0.4262E-01	-0.2638E-01	0.5522E-02	-0.1347E 00	-0.6684E-01
15 TO 21	0.6092E-02	-0.9548E-01	-0.6933E-01	0.5775E-02	-0.4457E-01	-0.1995E-01	0.6007E-02
22 TO 28	-0.2638E-01	-0.2084E-01	0.5865E-02	-0.3406E 00	-0.7957E-01	0.5965E-02	-0.3404E 00
29 TO 35	-0.8032E-01	0.5977E-02	-0.1093E 00	-0.2398E-01	0.5969E-02	-0.1111E 00	-0.2400E-01
36 TO 42	0.5974E-02	-0.1155E 00	-0.4107E-01	-0.2555E-03	0.1048E-05	-0.1095E-02	-0.7017E-01
43 TO 49	-0.4111E-01	-0.1056E-03	0.5705E-06	0.6002E-03	-0.4479E-01	-0.4110E-01	-0.1856E-03
50 TO 56	0.8316E-06	-0.7520E-03	-0.2243E-01	-0.4112E-01	-0.1396E-03	0.2458E-06	0.3934E-03
57 TO 63	-0.1205E 00	0.3278E-02	0.7091E-04	-0.3457E-07	-0.8303E-03	-0.1350E 00	0.2103E-02
64 TO 70	0.7016E-04	-0.7277E-07	0.8896E-03	-0.3913E-01	0.2829E-02	0.6477E-04	-0.5393E-07
71 TO 77	-0.1118E-02	-0.4687E-01	0.2303E-02	0.6981E-04	0.6040E-07	0.1242E-02	-0.1510E-01
78 TO 84	-0.4111E-01	-0.1503E-03	0.3205E-06	0.9211E-05	-0.1979E-03	0.3295E-02	0.8692E-05
85 TO 91	0.4085E-06	0.2352E-08	0.1173E-02	-0.4049E-06	0.2352E-08	-0.1290E-02	-0.1897E-02
92 TO 98	0.2453E-02	0.6571E-04	0.6278E-07	-0.2660E-05	0.7057E-04	-0.1156E-01	0.9981E-03
99 TO 105	0.1702E-02	0.7650E-07	0.3550E-05	-0.8148E-04	-0.4982E-02	0.9366E-02	0.1641E-02
106 TO 112	0.1583E-05	-0.4564E-05	-0.1614E-04	-0.6202E-02	0.2915E-02	0.1831E-02	0.1291E-06
113 TO 114	0.1024E-06	-0.5053E-06					
IMAGINARY PART							
1 TO 7	-0.9853E 00	0.1069E 00	0.0	-0.9871E 00	0.1051E 00	0.0	-0.3499E 00
8 TO 14	0.3729E-01	0.0	-0.3495E 00	0.3640E-01	0.0	-0.8248E 00	0.9479E-01
15 TO 21	0.0	-0.8276E 00	0.9190E-01	0.0	-0.2980E 00	0.3358E-01	0.0
22 TO 28	-0.2986E 00	0.3209E-01	0.0	-0.9012E 00	0.9756E-01	0.0	-0.9042E 00
29 TO 35	0.9714E-01	0.0	-0.3150E 00	0.3386E-01	0.0	-0.3145E 00	0.3368E-01
36 TO 42	0.0	-0.4742E 00	0.5418E-02	0.0	0.0	-0.4734E-02	-0.4799E 00
43 TO 49	0.5344E-02	0.0	0.0	0.4777E-02	-0.1771E 00	0.5370E-02	0.0
50 TO 56	0.0	-0.2910E-02	-0.1797E 00	0.5345E-02	0.0	0.0	0.2955E-02
57 TO 63	-0.6664E 00	-0.5918E-03	0.0	0.0	-0.4455E-02	-0.6659E 00	-0.3570E-03
64 TO 70	0.0	0.0	0.4455E-02	-0.2259E 00	-0.4843E-03	0.0	0.0
71 TO 77	-0.6163E-02	-0.2254E 00	-0.3787E-03	0.0	0.0	0.6159E-02	-0.8264E-01
78 TO 84	0.5354E-02	0.0	0.0	0.0	0.2022E-04	-0.6893E-03	0.0
85 TO 91	0.0	0.0	0.6419E-02	0.0	0.0	-0.6416E-02	-0.1033E-01
92 TO 98	-0.3946E-03	0.0	0.0	0.0	-0.6770E-05	-0.6489E-01	0.4587E-02
99 TO 105	0.0	0.0	0.0	-0.4831E-05	-0.2867E-01	0.3423E-02	0.0
106 TO 112	0.0	0.0	0.1844E-04	-0.4688E-01	0.5222E-02	0.0	0.0
113 TO 114	0.0	-0.7707E-07					